



INTELLI 2013

The Second International Conference on Intelligent Systems and Applications

ISBN: 978-1-61208-269-1

April 21 - 26, 2013

Venice, Italy

INTELLI 2013 Editors

Michael Negnevitsky, University of Tasmania, Australia

Pascal Lorenz, University of Haute Alsace, France

INTELLI 2013

Foreword

The Second International Conference on Intelligent Systems and Applications (INTELLI 2013), held between April 21st-26th, 2013 in Venice, Italy, was an inaugural event on advances towards fundamental, as well as practical and experimental aspects of intelligent and applications.

The information surrounding us is not only overwhelming but also subject to limitations of systems and applications, including specialized devices. The diversity of systems and the spectrum of situations make it almost impossible for an end-user to handle the complexity of the challenges. Embedding intelligence in systems and applications seems to be a reasonable way to move some complex tasks from user duty. However, this approach requires fundamental changes in designing the systems and applications, in designing their interfaces and requires using specific cognitive and collaborative mechanisms. Intelligence became a key paradigm and its specific use takes various forms according to the technology or the domain a system or an application belongs to.

We take here the opportunity to warmly thank all the members of the INTELLI 2013 Technical Program Committee, as well as the numerous reviewers. The creation of such a high quality conference program would not have been possible without their involvement. We also kindly thank all the authors who dedicated much of their time and efforts to contribute to INTELLI 2013. We truly believe that, thanks to all these efforts, the final conference program consisted of top quality contributions.

Also, this event could not have been a reality without the support of many individuals, organizations, and sponsors. We are grateful to the members of the INTELLI 2013 organizing committee for their help in handling the logistics and for their work to make this professional meeting a success.

We hope that INTELLI 2013 was a successful international forum for the exchange of ideas and results between academia and industry and for the promotion of progress in the field of intelligent systems and applications.

We are convinced that the participants found the event useful and communications very open. We also hope the attendees enjoyed the charm of Venice, Italy.

INTELLI Advisory Committee:

Pascal Lorenz, University of Haute Alsace, France

Petre Dini, Concordia University, Canada / China Space Agency Center, China

INTELLI 2013

Committee

INTELLI Advisory Committee

Pascal Lorenz, University of Haute Alsace, France
Petre Dini, Concordia University, Canada / China Space Agency Center, China

INTELLI 2013 Technical Program Committee

Syed Sibte Raza Abidi, Dalhousie University - Halifax, Canada
Witold Abramowicz, The Poznan University of Economics, Poland
Michael Affenzeller, HeuristicLab, Australia
Samir Aknine, Université Lyon 1, France
Jose M. Alcaraz Calero, Hewlett-Packard Laboratories - Bristol, UK
Andreas S. Andreou, Cyprus University of Technology - Limassol, Cyprus
Ngamnij Arch-int, Khon Kaen University, Thailand
Wudhichai Assawinchaichote, Mongkut's University of Technology -Bangkok, Thailand
Pradeep Atrey, University of Winnipeg, Canada
Paul Barom Jeon, Samsung Electronics, Korea
Daniela Barreiro Claro, Federal University of Bahia, Brazil
Rémi Bastide, Université Champollion, France
Bernhard Bauer, University of Augsburg, Germany
Barnabas Bede, DigiPen Institute of Technology - Redmond, USA
Noureddine Belkhatir, University of Grenoble, France
Orlando Belo, University of Minho, Portugal
Petr Berka, University of Economics, Prague, Czech Republic
Félix Biscarri, University of Seville, Spain
Magnus Boman, SICS and KTH/ICT/SCS - Kista, Sweden
Luis Borges Gouveia, University Fernando Pessoa, Portugal
Abdenour Bouzouane, Université du Québec à Chicoutimi, Canada
Stefano Bromuri, University of Applied Sciences Western Switzerland, Switzerland
Rui Camacho, Universidade do Porto, Portugal
Luis M. Camarinha-Matos, New University of Lisbon, Portugal
Longbing Cao, University of Technology - Sydney, Australia
Jose Jesus Castro Sanchez, Universidad de Castilla-La Mancha - Ciudad Real, Spain
Marc Cavazza, University of Teesside - Middlesbrough, UK
Kit Yan Chan, Curtin University - Western Australia, Australia
Chin-Chen Chang, Feng Chia University, Taiwan, R. O. C.
Maiga Chang, Athabasca University, Canada
Yue-Shan Chang, National Taipei University, Taiwan
Naoufel Cheikhrouhou, Ecole Polytechnique Fédérale de Lausanne, Switzerland
Rung-Ching Chen, Chaoyang University of Technology, Taiwan
Li Cheng, BII/A*STAR, Singapore

Been-Chian Chien, National University of Tainan, Taiwan
Sunil Choenni, Ministry of Security and Justice, The Netherlands
Byung-Jae Choi, Daegu University, Korea
Chin-Wan Chung, Korea Advanced Institute of Science and Technology (KAIST), Korea
Antonio Coronato, National Research Council (CNR)& Institute for High-Performance Computing and Networking (ICAR) - Napoli, Italy
Karl Cox, University of Brighton, UK
Sharon Cox, Birmingham City University, UK
Chuangyin Dang, City University of Hong Kong, Hong Kong
Sergio de Cesare, Brunel University - Uxbridge, UK
Juri Luca de Coi, Université Jean Monnet - Saint-Etienne, France
Sara de Freitas, Coventry University, UK
Suash Deb, IRDO, India
Angel P. del Pobil, Universitat Jaume-I, Spain
Vincenzo Deufemia, Università di Salerno - Fisciano, Italy
Kamil Dimililer, Near East University, Cyprus
Tadashi Dohi, Hiroshima University, Japan
Andrei Doncescu, LAAS-CNRS - Toulouse France
Partha Dutta, Rolls-Royce Singapore Pte Ltd, Singapore
Marcos Eduardo Valle, University of Londrina, Brazil
Shu-Kai S. Fan, National Taipei University of Technology, Taiwan
Aurelio Fernandez Bariviera, Universitat Rovira i Virgili, Spain
Edilson Ferneda, Catholic University of Brasília, Brazil
Manuel Filipe Santos, Universidade do Minho, Portugal
Adina Magda Florea, University "Politehnica" of Bucharest, Romania
Juan J. Flores, Universidad Michoacana, Mexico
Gian Luca Foresti, University of Udine, Italy
Rita Francese, Università di Salerno - Fisciano, Italy
Kaori Fujinami, Tokyo University of Agriculture and Technology, Japan
Naoki Fukuta, Shizuoka University, Japan
Matjaž Gams, Jožef Stefan Institute - Ljubljana, Slovenia
Leonardo Garrido, Tecnológico de Monterrey - Campus Monterrey, Mexico
Alexander Gelbukh, Mexican Academy of Sciences, Mexico
David Gil, University of Alicante, Spain
Anandha Gopalan, Imperial College London, UK
Sérgio Gorender, UFBA, Brazil
Manuel Graña, Facultad de Informatica - San Sebastian, Spain
David Greenhalgh, University of Strathclyde, UK
Christophe Guéret, Free University Amsterdam, The Netherlands
Bin Guo, Northwestern Polytechnical University, China
Sung Ho Ha, Kyungpook National University, Korea
Maki K. Habib, The American University in Cairo, Egypt
Sami Habib, Kuwait University, Kuwait
Sven Hartmann, Technische Universität Clausthal, Germany
Fumio Hattori, Ritsumeikan University - Kusatsu, Japan
Jessica Heesen, University of Tübingen, Germany
Benjamin Hirsch, Khalifa University - Abu Dhabi, United Arab Emirates
Didier Hoareau, University of La Réunion, France

Tetsuya Murai Hokkaido, University Sapporo, Japan
Wladyslaw Homenda, Warsaw University of Technology, Poland
Katsuhiro Honda, Osaka Prefecture University, Japan
Tzung-Pei Hong, National University of Kaohsiung, Taiwan
Wei-Chiang Hong, Oriental Institute of Technology - Taipei, Taiwan
Bin Hu, Birmingham City University, UK
Yo-Ping Huang, National Taipei University of Technology - Taipei, Taiwan
Germán Hurtado, University College Ghent & Ghent University, Belgium
Ming Huwi Horng, National PingTung Institute of Commerce, Taiwan
Carlos A. Iglesias, Universidad Politecnica de Madrid, Spain
Fodor János, Óbuda University – Budapest, Hungary
Jayadeva, Indian Institute of Technology - Delhi, India
Antonio Jimeno, NICTA - Melbourne, Australia
Maria João Ferreira, Universidade Portucalense - Porto, Portugal
Janusz Kacprzyk, Polish Academy of Sciences, Poland
Epaminondas Kapetanios, University of Westminster - London, UK
Nikos Karacapilidis, University of Patras - Rion-Patras, Greece
Panagiotis Karras, Rutgers University, USA
Jung-jae Kim, Nanyang Technological University, Singapore
Sunghin Kim, Pusan National University- Busan, Korea
Alexander Knapp, Universität Augsburg, Germany
Ondrej Krejcar, University of Hradec Kralove, Czech Republic
Natalia Kryvinska, University of Vienna, Austria
Satoshi Kurihara, Osaka University, Japan
Bogdan Kwolek, Rzeszow University of Technology, Poland
Kennerd Laviers, Air Force Institute of Technology - Wright-Patterson
Frédéric Le Mouël, INRIA/INSA Lyon, France
Alain Léger, Orange - France Telecom R&D / University St Etienne - Betton, France
George Lekeas, City Universty – London, UK
Daniel Lemire, LICEF Research Center, Canada
Omar Lengerke, Autonomous University of Bucaramanga, Colombia
Carlos Leon, University of Seville, Spain
Haowei Liu, INTEL Corporation, USA
Wei Liu, Amazon.com - Seattle, USA
Ying Liu, KAIST, Korea
Abdel-Badeeh M. Salem, Ain Shams University - Cairo, Egypt
Giuseppe Mangioni, University of Catania, Italy
Yannis Manolopoulos, Aristotle University of Thessaloniki, Greece
Gregorio Martinez, University of Murcia, Spain
George Mastorakis, Technological Educational Institute of Crete, Greece
Eric Matson, Purdue University - West Lafayette, USA
Constandinos X. Mavromoustakis, University of Cyprus, Cyprus
Pier Luigi Mazzeo, Institute on Intelligent System for Automation - Bari, Italy
Michele Melchiori, Università degli Studi di Brescia, Italy
Radko Mesiar, Slovak University of Technology Bratislava, Slovakia
John-Jules Charles Meyer, Utrecht University, The Netherlands
Thomas B. Moeslund, Aalborg University, Denmark
Dusmanta Kumar Mohanta, Birla Institute of Technology - Mesra, India

Felix Mora-Camino, ENAC, Toulouse, France
Fernando Moreira, Universidade Portucalense - Porto, Portugal
Pieter Mosterman, MathWorks, Inc. - Natick, USA
Haris Mouratidis, University of East London, UK
Isao Nakanishi, Tottori University, Japan
Tomoharu Nakashima, Osaka Prefecture University, Japan
Michael Negnevitsky, University of Tasmania, Australia
Filippo Neri, University of Naples "Federico II", Italy
Mario Arrigoni Neri, University of Bergamo, Italy
Hongbo Ni, Northwestern Polytechnical University, China
Hichem Omrani, CEPS/INSTEAD Research Institute, Luxembourg
Frank Ortmeier, Otto-von-Guericke Universitaet Magdeburg, Germany
Jeng-Shyang Pan, Harbin Institute of Technology, Taiwan
Endre Pap, University Novi Sad, Serbia
Marcin Paprzycki, Systems Research Institute / Polish Academy of Sciences - Warsaw, Poland
Dana Petcu, West University of Timisoara, Romania
Leif Peterson, Methodist Hospital Research Institute / Weill Medical College, Cornell University, USA
Alain Pirott, Université de Louvain - Louvain-la-Neuve, Belgium
Agostino Poggi, Università degli Studi di Parma, Italy
Radu-Emil Precup, "Politehnica" University of Timisoara, Romania
Anca Ralescu, University of Cincinnati, USA
Thurasamy A/L Ramayah, Universiti Sains Malaysia - Penang, Malaysia
Fano Ramparany, Orange Labs Networks and Carrier (OLNC) - Grenoble, France
Zbigniew W. Ras, University of North Carolina - Charlotte & Warsaw University of Technology, Poland
José Raúl Romero, University of Córdoba, Spain
Danda B. Rawat, Eastern Kentucky University, USA
David Riaño, Universitat Rovira i Virgili, Spain
Daniel Rodríguez, University of Alcalá - Madrid, Spain
Agos Rosa, Technical University of Lisbon, Portugal
Gunter Saake, University of Magdeburg, Germany
Ozgur Koray Sahingoz, Turkish Air Force Academy, Turkey
Daniel Schang, Groupe Signal Image et Instrumentation - ESEO, France
Ingo Schwab, Karlsruhe University of Applied Sciences, Germany
Amal El Fallah Seghrouchni, University of Pierre and Marie Curie (Paris 6) - Paris, France
Hirosato Seki, Kwansei Gakuin University, Japan
Timothy K. Shi, National Central University, Taiwan
Kuei-Ping Shih, Tamkang University - Taipei, Taiwan
Choonsung Shin, Carnegie Mellon University, USA
Elena Simperl, Karlsruhe Institute of Technology, Germany
Peter Sincák, Technical University of Kosice, Slovakia
Spiros Sirmakessis, Technological Educational Institute of Messolonghi, Greece
Alexander Smirnov, St. Petersburg Institute for Informatics and Automation of Russian Academy of Sciences (SPIIRAS), Russia
Paolo Spagnolo, Italian National Research Council, Italy
Adel Taweel, King's College London, UK
Abdel-Rahman Tawil, University of East London, UK
Jilei Tian, Nokia Research Center Beijing, China
Federico Tombari, University of Bologna, Italy

Anand Tripathi, University of Minnesota Minneapolis, USA
Juan Carlos Trujillo Mondéjar, University of Alicante, Spain
Theodoros Tzouramanis, University of the Aegean, Greece
Gantcho Vatchkov, University of the South Pacific (USP) in Suva, Fiji Island
Jan Vascak, Technical University of Košice, Slovakia
José Vasconcelos, Instituto Superior de Tecnologias Avançadas de Lisboa, Portugal
Mario Vento, Università di Salerno - Fisciano, Italy
Mario Verdicchio, University of Bergamo - Dalmine, Italy
Dimitros Vergados, Technological Educational Institution of Western Macedonia, Greece
Nishchal K. Verma, Indian Institute of Technology Kanpur, India
Mirko Viroli, Università di Bologna - Cesena, Italy
Mattias Wahde, Chalmers University of Technology - Göteborg, Sweden
Yan Wang, Macquarie University - Sydney, Australia
Zihui Wang, Dalian University of Technology, China
Viacheslav Wolfengagen, Institute "JurInfoR-MSU", Russia
Mudasser F. Wyne, National University - San Diego, USA
Guandong Xu, Victoria University, Australia
Songhua Xu, ORNL, USA
WeiQi Yan, Queen's University Belfast, UK
Chao-Tung Yang, Tunghai University - Taichung City, Taiwan, R.O.C.
Motoi Yamagiwa, Toyo University, Japan
Hwan-Seung Yong, Ewha Womans University - Seoul, Korea
Si Q. Zheng, The University of Texas at Dallas, USA
Jose Jacobo Zubcoff Vallejo, University of Alicante, Spain

Copyright Information

For your reference, this is the text governing the copyright release for material published by IARIA.

The copyright release is a transfer of publication rights, which allows IARIA and its partners to drive the dissemination of the published material. This allows IARIA to give articles increased visibility via distribution, inclusion in libraries, and arrangements for submission to indexes.

I, the undersigned, declare that the article is original, and that I represent the authors of this article in the copyright release matters. If this work has been done as work-for-hire, I have obtained all necessary clearances to execute a copyright release. I hereby irrevocably transfer exclusive copyright for this material to IARIA. I give IARIA permission to reproduce the work in any media format such as, but not limited to, print, digital, or electronic. I give IARIA permission to distribute the materials without restriction to any institutions or individuals. I give IARIA permission to submit the work for inclusion in article repositories as IARIA sees fit.

I, the undersigned, declare that to the best of my knowledge, the article does not contain libelous or otherwise unlawful contents or invading the right of privacy or infringing on a proprietary right.

Following the copyright release, any circulated version of the article must bear the copyright notice and any header and footer information that IARIA applies to the published article.

IARIA grants royalty-free permission to the authors to disseminate the work, under the above provisions, for any academic, commercial, or industrial use. IARIA grants royalty-free permission to any individuals or institutions to make the article available electronically, online, or in print.

IARIA acknowledges that rights to any algorithm, process, procedure, apparatus, or articles of manufacture remain with the authors and their employers.

I, the undersigned, understand that IARIA will not be liable, in contract, tort (including, without limitation, negligence), pre-contract or other representations (other than fraudulent misrepresentations) or otherwise in connection with the publication of my work.

Exception to the above is made for work-for-hire performed while employed by the government. In that case, copyright to the material remains with the said government. The rightful owners (authors and government entity) grant unlimited and unrestricted permission to IARIA, IARIA's contractors, and IARIA's partners to further distribute the work.

Table of Contents

Simple and Compact Indexing for Efficient KNN Search in High Dimensional Feature Space <i>Zaher Al Aghbari and Ayoub Al-Hamadi</i>	1
Automated Annotation of Text Using the Classification-based Annotation Workbench (CLAW) <i>R.oy George, Hema Nair, Khalil Shujaae, David Krooks, and Chandler Armstrong</i>	6
Mining Incomplete Data with Many Missing Attribute Values A Comparison of Probabilistic and Rough Set Approaches <i>Patrick G. Clark, Jerzy W. Grzymala-Busse, and Martin Kuehnhausen</i>	12
Identification of Failing Banks Using Clustering with Self-Organising Neural Networks <i>Michael Negnevitsky</i>	18
A Formal Framework for Modeling Topological Relations of Spatial Ontologies <i>Sana Chaabane, Faiez Gargouri, and Wassim Jaziri</i>	23
Requirements and Matching Software Technologies for Sustainable and Agile Manufacturing Systems <i>Daniel Telgen, Leo van Moergestel, Erik Puik, Pascal Muller, and John-Jules Meyer</i>	30
Apriori-with-Constraint for Flexible Association Rule Discovery <i>Kittisak Kerdprasop, Phaichayon Kongchai, and Nittaya Kerdprasop</i>	36
Bayes Net Analysis to Support Database Design and Normalization <i>Nittaya Kerdprasop and Kittisak Kerdprasop</i>	42
Flexible Process Modeling Determined by Existing Human Expert Domain Knowledge Bases <i>Ingo Schwab, Melanie Senn, Susanne Fischer, and Norbert Link</i>	48
Content Adaptation for an Adaptive Hypermedia System <i>Marta Fernandes, Paulo Couto, Constantino Martins, and Luiz Faria</i>	54
Context Processing: A Distributed Approach <i>Penghe Chen, Shubhabrata Sen, Hung Keng Pung, and Wai Choong Wong</i>	58
N-Screen Service Platform based on Location-Awareness <i>Jiho Kim, Dohee Lee, and Ohyoung Song</i>	65
Extendable Dialog Script Description Language for Natural Language User Interfaces <i>Kiyoshi Nitta</i>	69

Classification of Three Negative Emotions based on Physiological Signals <i>Eun-Hye Jang, Byoun-Jun Park, Sang-Hyeob Kim, Myoung-Ae Chung, Mi-Sook Park, and Jin-Hun Sohn</i>	75
Physiological Signals and Classification for Happiness, Neural and Surprise Emotions <i>Eun-Hye Jang, Sang-Hyeob Kim, Chul Huh, and Myoung-Ae Chung</i>	79
Robot Control Using 2D Visual Information Via Database <i>Yutaka Maeda and Hidetaka Ito</i>	83
Incorporating Online Process Mining Based on Context Awareness into Human-Robot-Cooperation Framework <i>Stephan Puls, Benjamin Lotspeich, and Heinz Worn</i>	89
Step Climbing and Descending for a Manual Wheelchair with a Network Care Robot <i>Hikaru Kanda, Nobuyuki Yamashima, and Eiji Nakano</i>	95
On the Analysis of a Swarm-Intelligence Coordination Model for Swarm Robots <i>Caio D. D. Monteiro, Diego M. P. F. Silva, and Carmelo J. A. Bastos-Filho</i>	103
A Multi-Objective Particle Swarm Optimizer Based on Diversity <i>Dennis R. C. Silva and Carmelo J. A. Bastos-Filho</i>	109
A new Heuristic of Fish School Segregation for Multi-Solution Optimization of Multimodal Problems <i>Marcelo G. P. Lacerda and Fernando B. de L. Neto</i>	115
Intelligent Assertions Placement Scheme for String Search Algorithms <i>Ali Alakeel</i>	122
Modeling of Sales Forecasting in Retail Using Soft Computing Techniques <i>Luis Lobo-da-Costa, Susana Vieira, and Joao Sousa</i>	129
Transmission Network Expansion Planning under Uncertainty using the Conditional Value at Risk and Genetic Algorithms <i>Hugo Sardinha, Joao Sousa, Carlos Silva, Daniel Delgado, and Joao Claro</i>	135
General Framework for Context-Aware Recommendation of Social Events <i>Wolfgang Beer, Walter Hargassner, Sandor Herramhof, and Christian Derwein</i>	141
Collective Intelligent Management of Freight Trains' Flow <i>Boris Davydov</i>	147
Infomobility and Vehicle Routing Problem <i>Luigi Sanfilippo and Giuseppe Salvo</i>	153

Overcoming the Condorcets Border in Collective Intelligence Systems <i>Vladislav Protasov, Zinaida Potapova, and Eugene Melnikov</i>	161
Measurement and Calibration System of Arrow's Impact Point using High Speed Object Detecting Sensor <i>Yeongsang Jeong, Hansoo Lee, Jungwon Yu, and Sungshin Kim</i>	167
Vision-based Cattle Detection and Localization System in an RGB Color Space <i>Jieun Kim and Woo Young Jung</i>	173
Evaluation of Machine Learning Methods in a Rain Detection System for Partial Discharge Data Analysis <i>Leandro H. S. Silva, Sergio C Oliveira, and Eduardo Fontana</i>	176

Simple and Compact Indexing for Efficient KNN Search in High Dimensional Feature Space

Zaher Al Aghbari

Department of Computer Science,
College of Sciences, University of Sharjah,
Sharjah, UAE
zaher@sharjah.ac.ae

Ayoub Al-Hamadi

Institute for Electronics, Signal Processing and
Communications, IESK, University Magdeburg,
Magdeburg, Germany
Ayoub.Al-Hamady@ovgu.de

Abstract—In this paper, we propose a technique to find the exact KNN image objects to a given query object in high dimensional space. The proposed technique clusters the images using a self-organizing map algorithm and then it projects these clusters into points in a linear space based on their distances from a selected reference point. The projected points in a linear space are then organized in a simple, compact and yet fast index structure, called array-index. Unlike most indexes that support KNN search, the array-index requires a storage space that is linear in the number of projected points. The experiments show that the proposed technique is more efficient and robust to dimensionality as compared to other well known techniques due to its simplicity and compactness.

Keywords—KNN search; image search; efficient indexing; dimensionality reduction; image clustering.

I. INTRODUCTION

Content-based retrieval of similar objects in a high dimensional feature space is important to many database applications. That is if an application is managing a database of N objects, given a query object q , the application should be able to return the K -Nearest Neighbors (KNN) objects in the database that are most similar to q . Finding KNN objects is one of the most expensive, but essential, operations in high-dimensional database applications.

In large databases, given a query q , finding the KNN answer set by a linear scan method is prohibitively expensive, particularly, if the database objects are high dimensional. Even with the existing indexing structures the response time of finding KNN answer set is equal to, or higher than, that of a linear scan due to a well-known phenomenon called *curse of dimensionality* [6][22]. Therefore, there is an essential need for efficient KNN search techniques. In this paper, we propose a technique that speeds up the KNN search of high-dimensional objects as compared to well-known methods, such as the R*-tree [3], SR-tree [14] and linear scan

Our approach is based on clustering the multi-dimensional objects (e.g., image data) using a self-organizing map (SOM) algorithm and then projecting the clusters into a linear (1-dimensional) distance space in which the projected clusters are ordered based on their similarity to a chosen reference point, R . These projected points in the linear space are inserted into the *array-*

index [1]. Since the points in the array index are sorted, search for similar points to a given query can be achieved by a binary search whose complexity is $O(\log N_c)$, where N_c is the number of indexed points. The search for KNN images start at the most similar cluster, called winning cluster (WC), to a given query and then proceeds to the left and right of the WC. The search continues till checking new clusters do not result in any new KNN images on both sides. This method retrieves exact KNN answer images to a given query image. More details of this technique can be found in [23].

Due to the small size of the index, our method requires a storage space that is linear in the number of generated clusters. As shown by the experiments, the proposed technique requires a search time that is much lower than that of the well known indexing structures R*-tree, SR-tree and linear scan, especially at high dimensions, which are bottlenecks for most KNN search algorithms.

The rest of this paper is organized as follows: Section 2 presents the related work. Section 3 discusses data clustering and the KNN search algorithm. The experiments are discussed in Section 4. Finally, we conclude the paper in Section 6.

II. RELATED WORK

Most works on finding the exact, or approximate, KNN points in a database to a given query point have provided good solutions for the low-dimensionality case, but for the high-dimensionality case there have been very little progress. To project high-dimensional objects to a lower dimensional space, some indexing structures such as the grid-file [18], K-D-tree [4] or LSD-tree [12] partition the data space into disjoint regions regardless of data clusters. On the other hand, data partitioning approaches like R*-tree[3], SR-tree [14] or X-tree [7] divide the data space according to the distribution of points in these data partition trees. Both the space and data partitioning approaches aim at speeding up the KNN search by pruning the irrelevant partitions to the given query. Generally, these approaches work well at low dimensions, but their performance degrades as the dimensionality increases [8].

To reduce the effect of high-dimensionality on KNN search, some methods apply “dimensionality reduction”

techniques on the data and then insert the data into the indexing trees. The QBIC system [11] of IBM uses a bounding method to map the high-dimensional color histograms of images into points in a 3-dimensional space. Faloutsos et. al [9] used the Discrete Fourier Transform (DFT) to map subsequences of a time series into points in a 6-dimensional space.

Space-filling curve methods like the Z-order curve [20] or Hilbert curve [10] map the d -dimensional points into a one-dimensional space, i.e., $\mathcal{R}^d \rightarrow \mathcal{R}^1$. Generally, space-filling curve methods are suitable for approximate KNN search, but not exact KNN search. A filter based approach such as the VA-file [22] divides the data space into 2^b rectangular cells, where b denotes a user specified number of bits. The VA-file is an array of these compact approximations of points.

In summary, the current KNN search approaches, which are classified above, work well in low-dimensional spaces; however, their performance degrades in high-dimensional spaces. In high-dimensional spaces, there has not been a satisfying solution for the KNN search problem. Towards finding a satisfying solution, the proposed technique improves performance of the KNN search by clustering the image data and then projecting those clusters into points in a linear space. From these projected points, a simple index is built that supports efficient KNN search for images.

III. EFFICIENT KNN SEARCH

A. Image Representation

We use a wavelet transform to decompose an image into several frequency bands and then compute a feature vector from the coefficients of the low frequency band. Particularly, we use the Haar wavelets because it is the fastest to compute and simplest to implement as compared to the other wavelet bases. The significant features of the image are concentrated in the low frequency band, thus allowing the image coefficients to be truncated, keeping only a few coefficients that sufficiently represent the image. Moreover, such truncation process improves discrimination power because the process of matching feature vectors is focused on the significant features of images.

B. SOM-based Clustering

SOM is an unsupervised neural network that maps high-dimensional input data \mathcal{R}^n onto a usually two-dimensional output space while preserving the similarities between the data items [16]. The SOM consists of nodes (neurons) arranged in a two-dimensional grid.

Clustering qualities of the self-organizing maps (SOM) are comparable to other clustering methods, and additionally SOMs offer better representation of clustered data [19]. The SOMs are well known for their superiority in clusters' visualization of very large and high dimensional image databases due to the SOM property of preserving the clusters' structure within the data as well as inter-cluster similarity [13]. Due to this property, we chose to cluster the feature vectors of images by a SOM.

C. KNN Search Method

The proposed technique indexes the clusters of images rather than the images themselves. After clustering the images using the SOM method, the array-index [1] is constructed by the following steps:

(i) Select a *reference point* (R): For the image database that is used in our experiments, we found that selecting a center cluster as a reference cluster leads to a slightly faster search time than other selection schemes.

(ii) Compute the distance $D(R, m_i)$ between R and each cluster's representative codebook vector, m_i :

(iii) Project the cluster points into a linear space (array-index) based on the computed distances : The SOM clusters are projected into a linear space by inserting the computed distances $D(R, m_i)$ into the array-index. Along with each distance, a pointer to the best-matching-list of the corresponding cluster is set. The best-matching-list of cluster C_i is a list of the points that are associated with C_i and sorted according to their Euclidean distances from m_i . Hence, the array-index contains a list of clusters sorted based on their distances $D(R, m_i)$ and each cluster contains a pointer to a list of points sorted based on their distances $D(p_j, m_i)$. Also, for every C_i , we compute its radius r_i that reflect the size of C_i . The constructed array-index is very small in size since it only contains three fields (distance, pointer, and radius) for every generated cluster. Therefore, all, or most, of the array-index can be put in main memory; thus, eliminating, or minimizing, (depending on the number of clusters and size of main memory) the disk operations during the search.

D. KNN Search: Flow Control

The proposed KNN search algorithm starts by finding the WC, which is a cluster with the most similar codebook vector to q , by computing $D(R, q)$ and projecting this distance on the array-index. The WC will be the left or right cluster to $D(R, q)$, whichever closer to q , and in case of tie either choice will do. Then, as shown in Fig. 1, the algorithm continues the search for similar clusters on both the left and right directions of WC. During the KNN search we employ 4 conditions to control the flow and speed up the search process [1]:

- Cluster Pruning Condition to prune dissimilar clusters.
- Cluster Ending Condition to end the search as soon as all KNN points are retrieved and further checking of new clusters does not result in new KNN answer points.
- Point Pruning Condition to prune dissimilar points (images) in the currently visited cluster.
- Point Ending Condition to end the search for candidate points in the currently visited cluster if further checking will not result in new KNN candidate points.

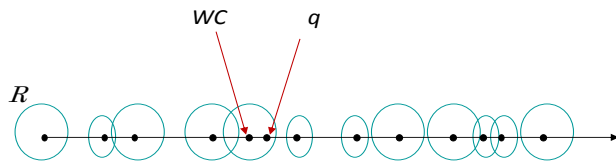


Figure 1. Searching to the left and right of the winner cluster (WC)

E. KNNSearch Algorithm

To find the exact KNN points to a given q , the *KNNsearch* algorithm first finds the *WC*, which is a cluster whose m_i is the most similar to q , within the array-index. Then, the *visitCluster()* function is called to visit the found *WC* and update *KNN_list* with the points associated with the *WC*. L_{ptr} and R_{ptr} are pointers used to traverse the array-index toward the left and the right of *WC*, respectively. Thus, after finding *WC*, the algorithm initializes L_{ptr} and R_{ptr} to point to *WC*.

The *traverseLeft()* and *traverseRight()* functions traverse to the left and right of *WC*, respectively, till one or both traversal paths are ended. If both traversal directions (left and right) are ended, the search stops and then the *KNNsearch* algorithm returns the *KNN_list*, which contains the exact KNN points to the given q . Otherwise, if both traversal direction (left and right) are not ended, the distances $D_L(q, m_{Lptr})$ and $D_R(q, m_{Rptr})$ are computed and the *visitCluster()* function is called to update the *KNN_list* with either the left, or right, current clusters (the one with the smaller distance from q), then the traversal in the opposite direction is blocked temporarily, so that the next iteration of the algorithm fetches the next partition in the direction of the *closer* cluster (the one with the smaller distance). When the left traversal is ended and the search is advancing only in the right direction, the *KNN_Search* algorithm updates the *KNN_list* with the next qualifying cluster on the right direction. Similarly, when the right traversal is ended and the search is advancing only in the left direction, the *KNN_Search* algorithm updates the *KNN_list* with the next qualifying cluster on the left direction. Finally, when the search stops, the *KNN_list* is returned with the exact KNN answer points.

The array-index speeds up the KNN search as follows:

- i) Finding the *WC* takes $\log_2 N_c$ distance comparisons since the proposed technique uses a binary search as compared to a brute force method, which requires N_c distance comparisons.
- ii) In the KNN search, the left and right traversal is ended as soon as the exact KNN answer points have been retrieved by the ending condition without the need to traverse the whole array-index. Thus, normally, only a small portion of the database is traversed to find the exact KNN answer points.
- iii) Since the points associated with a cluster are sorted by their distances from the m_i , the ending condition ends

the search at a certain point p beyond which there will be no KNN candidates.

IV. EXPERIMENTS

We performed our experiments on collected images from publicly available image databases: H^2 Soft image databases and Stanford University database lab. The size of the collected image database is 80,000 artificial and natural images that span the following categories: landscapes, animals, buildings, people, plants, CG, etc. Where 50% of the images (40000 images) are used for training the SOM and the other 50% is used for testing. The image size is fixed at 128x128 pixels. Although the experiments are conducted on image vectors, the proposed algorithm can be applied on any high-dimensional vectors.

We extracted the color feature of each image using the Haar wavelets. The color space used in this paper is the YIQ since it exploits certain characteristics of the human eye, where Y represents the luminance information and I and Q represent the chrominance information [2][17]. The YIQ color feature for each image is represented by a d -dimensional vector. To demonstrate the efficiency of our KNN search algorithm, we generated 3 databases with different dimensionalities: 3, 12, and 48 dimensions by applying a 7-level, 6-level, and 5-level decomposition, respectively, of the Haar wavelet transform on the image data. To show the feasibility of our technique and its tolerance to high dimensions, we chose the 3, 12 and 48 dimensions since they represent a low, medium and high dimensionality, respectively, of the feature space.

From each database (3, 12, and 48 dimensions), we generated different data sets 1000, 5000, 10000, 20000, 30000, 40000 vectors in both the training and test databases. Each of these data sets was clustered by a SOM. The different dimensions were generated via applying Haar wavelets on the images.

To analyze the effect of dimensionality on the KNN search time, we measured the KNN search time of data sets of different sizes and different dimensionalities, as shown in Fig. 2. First, we randomly selected 10 query images from the database and issued a query to retrieve the KNN answer images (where $K=1$ and $K=50$) for each query image from each of the different data sets and different dimensionalities. The KNN search times shown in Fig. 2.left and Fig. 2.right are the average results of 10 queries. It is clear that the KNN search time increases as the dimensionality increases. That is because the volumes of clusters increase as the dimensionality increases causing a greater degree of overlap between clusters; thus, more clusters are visited during the search. Moreover, the KNN search time increases as the value of K increases. That is obvious because larger values of K lead to more clusters' visits; thus, larger percentage of the database is accessed to answer a query.

To prove the above reasoning, we measured the percentage of the non-empty clusters (associated with one or more images) accessed to retrieve the KNN images to each of the randomly selected queries at different

dimensionalities and different values of K (see Fig. 3). Clearly, as the dimensionality increases and/or the value of K increases a bigger percentage of the database is accessed (more clusters are visited).

According to [15][22] and as verified by our experiments (see Fig. 4), most KNN search algorithms are outperformed by a linear scan method especially at high dimensions (≥ 12 dimensions) of real (non-uniformly distributed) databases, such as image databases. We compared the proposed technique with other well known methods (R*-tree, SR-tree

and linear scan), which serve as a stick yard to evaluate the proposed technique, in terms of KNN search time versus the number of dimensions. The KNN search of the R*-tree and SR-tree methods is implemented based on the algorithm presented in [21]. Fig. 4 shows the comparison between the four methods for $K=1$ and $K=50$ using a test database of 40000 images. Notice that the scale of the y-axis of Fig. 10 is logarithmic.

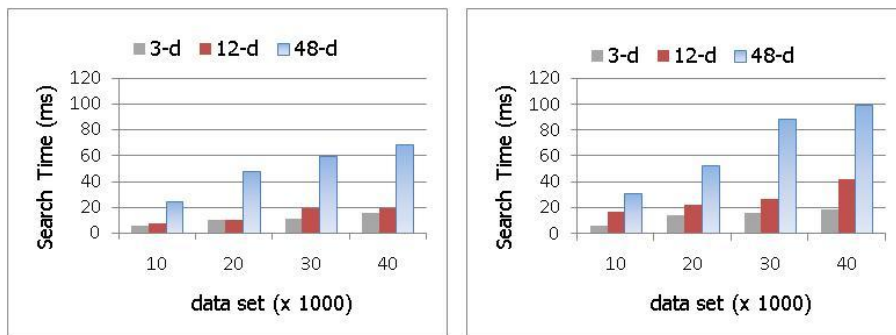


Figure 2. Average KNN time versus database size when (left) $K=1$ and (right) $K=50$.

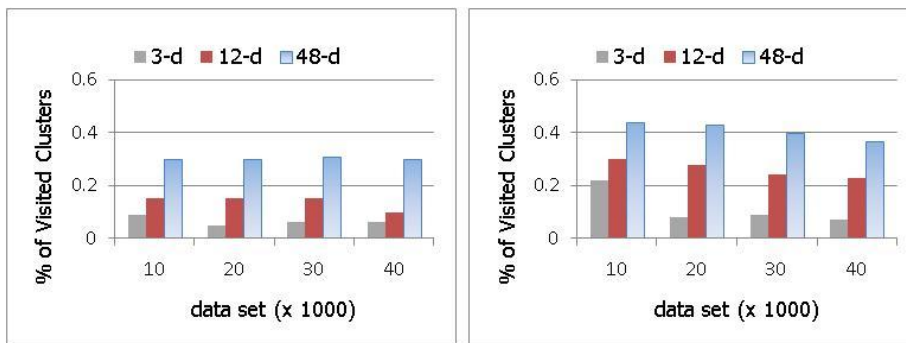


Figure 3. The percentage of the accessed database (visited nodes) versus database size when (left) $K=1$ and (right) $K=50$.

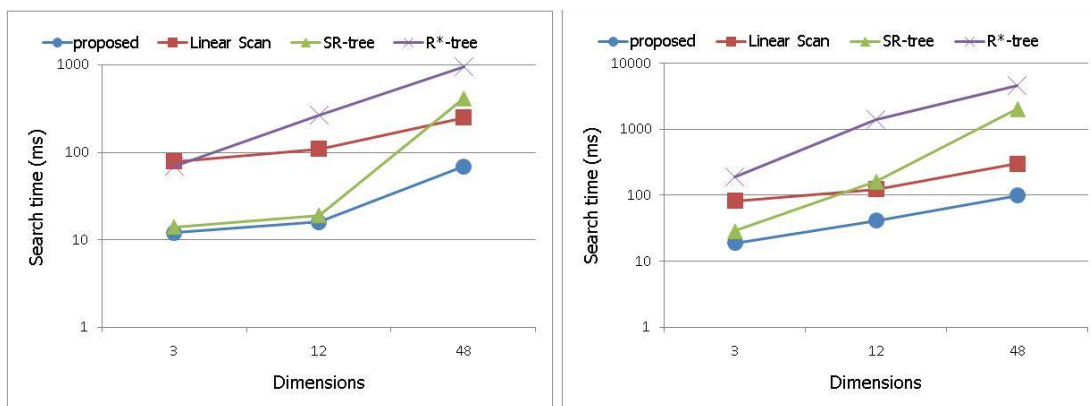


Figure 4. Comparison between the array-index, a linear scan, R*-tree and SR-tree methods in terms of KNN search time versus number of dimensions: (left) for $K=1$ and (right) for $K=50$.

Obviously, the proposed technique outperforms the R*-tree, SR-tree and linear scan methods at all dimensions and all variations of the value of K . At low dimensions and low

values of K (dimensions = 3 and $K = 1$), the R*-tree and SR-tree generate their least disk operations; thus, they outperform the linear scan method. However, as the dimensionality increases and/or the value of K increases the

disk operations of the R*-tree and SR-tree methods increase and hence they are outperformed by a linear scan. Due to the simple and compact structure of the array-index used by our technique, it generates no disk operations and thus it results in a significant performance gain over the R*-tree and SR-tree methods. Also, the proposed technique outperforms the linear scan method, on the average of the value of K , by 81% at 3 dimensions, 77% at 12 dimensions and 70% at 48 dimensions. Notice that the KNN search time of the linear scan methods increases linearly with the number of dimensions and the KNN search time of the R*-tree and SR-tree increase exponentially with the number of dimensions. On the other hand, the proposed technique shows more robustness to the number of dimensions since the KNN search time only increases slightly as the dimensionality increases.

V. CONCLUSION

We presented a simple and efficient technique to retrieve exact KNN points for a given query. The proposed technique is based on clustering the data and then indexing the clusters' representative vectors instead of the data points themselves; thus, reducing the size the index structure. Although, in this paper, we used an image database and a SOM algorithm as examples of a multi-dimensional data and a clustering technique, respectively, the technique can be adapted to any multi-dimensional data and any clustering method. Even though the paper only presents the KNN search algorithm, the range search can be easily implemented. Given q a range query ρ , the search algorithm first finds the WC, next it retrieves all clusters that overlap with this range on both sides of the WC as a candidate set. Finally, the candidate set is refined by retrieving only the points p_i that satisfy the range condition $|D(q, p_i)| \leq \rho$. The projection of clusters into a linear space and the compactness of the index are the main reasons behind the fast KNN search time as compared to other known methods. The experiments show that the proposed technique is faster and more robust to dimensionality as compared to other well known techniques due to its simplicity and compactness.

REFERENCES

- [1] Z. Al Aghbari, "Array-index: A Plug&Search K Nearest Neighbors Methods for High-Dimensional Data," *Journal of Data & Knowledge Engineering*, Vol 52, no.3, pp 333-352, Mar. 2005.
- [2] Z. Aghbari, K. Kaneko, and A. Makinouchi, "New Indexing Method for Content-Based Video Retrieval and Clustering for MPEG Video Database," *International Symposium on Digital Media Information Base (DMIB'97)*, p Nov.1997, pp.140-149.
- [3] N.Beckmann, H.Kriegel, R.Schneider, and B.Seeger, "R*-tree: An Efficient and Robust Access Method for Points and Rectangles," *ACM SIGMOD*, May 1990, pp. 322-331.
- [4] J.L.Bentley, "Multidimensional Binary Search Trees in Database Applications," *IEEE Trans. on Software Engineering*, SE- vol. 5, no. 4, July 1979, pp.333-340.
- [5] S.Berchtold, C.Bohm, D.Keim, and H.P.Kriegel, "A Cost Model for Nearest Neighbor Search in High-Dimensional Data Spaces," *ACM SIGACT-SIGMOD-SIGART*, 1997.
- [6] S.Berchtold, B.Ertl, D.Keim, H.P.Kriegel, and T.Seidl, "Fast Nearest Neighbor Search in High-Dimensional Space," *Int'l conf. on Data Eng. (ICDE)*, 1998.
- [7] S.Berchtold, D.Keim, and H.P.Kriegel, "The X-tree: An Index Structure for High-Dimensional Data," *VLDB* 1996.
- [8] C.Faloutsos, "Searching Multimedia Databases By Content," Kluwer Academic Publishers, Boston, USA, 1996.
- [9] C. Faloutsos, M. Ranganathan, and Y. Manolopoulos, "Fast Subsequence Matching in Time-Series Databases," *ACM SIGMOD*, 1994.
- [10] C.Faloutsos and S.Roseman, "Fractals for Secondary Key Retrieval," 8th *ACM SIGACT-SIGMOD-SIGART Symposium on Principles of Database Systems (PODS)*, March 1989.
- [11] M. Flickner, H. Sawhney, W. Niblack, J. Ashley, Q. Huang, B. Dom, M. Gorkani, J. Hafner, D. Lee, D. Perkovic, D. Steele, and P. Yanker, "Query by Image and Video Content: The QBIC System," *IEEE*, Sept. 1995.
- [12] A.Henrich and H-W.Six, P.Widmayer, "The LSD tree: Spatial Access to multidimensional Point and Non-Point Objects," *Proc. of 15th VLDB*, 1989.
- [13] J.Himberg, "A SOM based cluster visualization and its application for false coloring," *International Joint Conf. in Neural Networks*, 2000.
- [14] N.Katayama and S.Satoh, "The SR-tree: An Index Structure for High-Dimensional Nearest Neighbor Queries," *ACM SIGMOD*, May 1997.
- [15] J.M.Kleinberg, "Two Algorithms for Nearest Neighbor Search in High Dimensions," 29th *ACM Symposium on Theory of Computing*, 1997.
- [16] T.Kohonen, "Self-Organizing Maps," Springer-Verlag, 1997. 2nd extended edition.
- [17] M. Kubo, Z. Aghbari, K-S Oh, and A. Makinouchi, "Content-Based Image Retrieval Technique using Wavelet-Based Shift and Brightness Invariant Edge Feature," *International Journal on Wavelets, Multiresolution and Information Processing (IJWMP)*, vol.1, no.2, 2003, pp. 163-178.
- [18] J.Nievergelt, H.Hinterberger, and K.Sevcik, "The grid file: An Adaptable Symmetric Multikey File Structure," *ACM Transaction on Database Systems*, vol. 9, no. 1, 1984, pp. 38-71.
- [19] K. S. Oh, Z. Aghbari, and P-K. Kim, "Fast k-NN Image Search with Self-Organizing Maps," *CIVR* 2002.
- [20] J.Orenstein, "Spatial Query Processing in an Object-Oriented Database System," *Proc. ACM SIGMOD*, May 1986.
- [21] N.Roussopoulos, S.Kelley, and F.Vincent, "Nearest Neighbor Queries," *ACM SIGMOD*, 1995.
- [22] R.Weber, H-J.Schek, and S.Blott, "A Quantitative Analysis and Performance Study for Similarity-Search Methods in High-Dimensional Spaces," *Proc. of the 24th VLDB*, USA, 1998.
- [23] Z. Al Aghbari and A. Al-Hamadi, "Efficient KNN Search by Linear Projection of Image Clusters," *Wiley International Journal of Intelligent Systems*, Vol. 26, no. 9, 2011, pp. 844-865.

Automated Annotation of Text Using the Classification-based Annotation Workbench (CLAW)

R. George, H. Nair, K. A. Shujaee

Department of Computer and Information Science
Clark Atlanta University
Atlanta, GA, USA
Email: rgeorge@cau.edu

D. A. Krooks, C. M. Armstrong

Construction Engineering Research Laboratory
Champaign, IL, USA

Abstract—Text annotation is used to mark up text using highlights, comments, footnotes, tags, and links. Manual annotation is a human intensive process and is not feasible for a large corpus of text. Classification is a technique that may be used to automate the annotation process. This paper develops a Classification-based Text Annotation Workbench (CLAW), an annotation assistance tool that incorporates automated classification to reduce the difficulty of manual annotation. There are several technical challenges posed by the practical nature of the text corpus and the annotation methodology. The text corpus, is large and consists of numerous reports, lessons learnt and best practices. Complexity is introduced due to the size of the documents, the variety of formats and the range of subject matter. The annotation taxonomy is extensive and unstructured and may be applied to the text body without constraints. Consequently, the search space for the label(s) become prohibitively large and it becomes necessary to adopt strategies that reduce the complexity of the classification process. We introduce a simplification technique to reduce the large classification search space. We improve precision by supplementing these predictive algorithms with similarity based measures and evaluate CLAW for performance using both prediction-based metrics and ranking-based metrics. It is shown that CLAW performs better than a competing algorithm on all evaluation metrics.

Keywords—Text Annotation, Multi-label Classification, Bayes Theorem, Annotation Workbench.

I. INTRODUCTION

Text annotation is the practice of marking up text using highlights, comments, footnotes, tags, and links. This may include notes written for a reader's private purposes, as well as shared annotations written for the purposes of collaborative writing, editing, commentary, social sharing, and learning. Annotation of these documents is the first step in the automation of the processing of such documents with applications such as identification of socio-cultural constructs, and improved methods of query and retrieval.

Manual annotation is a human intensive process and is not feasible for a large corpus of text. Classification is a technique, well-researched in data mining and machine learning that may be used to automate the annotation process. Classification separates data into distinct classes characterized by some distinguishing features and rules relate class labels to these features. Automated classification has

been used in a variety of domains including textual data such as e-mails, web pages, news articles; audio; images and video; medical data; or even annotated genes (Read, 2010). Each example is associated with an attribute vector, which represents data from its domain. Labels represent concepts from the problem domain such as subject categories, descriptive tags, genres, gene functions, and other forms of annotation. The training set is readily available in practical scenarios, usually in the form of human-annotation by a domain expert. A supervised classifier trains its model on these examples and continues the labeling task thereafter automatically. Single-label classification is the task of associating each example with a single class label. Classes may also overlap, in which case, the same data may belong to all of the many classes that overlap. In such instances, it becomes necessary to collect the details or features of all the classes that the data belongs to in order to perform a complete classification that is also accurate. When each example may be associated with multiple labels simultaneously, this is known as multi-label classification. In this paper, the terms class, label and tag are used interchangeably.

This paper presents the Classification-Based Text Annotation Workbench (CLAW), an annotation assistance tool that reduces the difficulty of the annotation process. The area of application for the tool is a large corpus (~1G) supplied by the U.S. Army Corps of Engineers with the objective of annotating the text using a classification taxonomy provided. The purpose of the annotation is to introduce common terminology in order to facilitate an understanding of the dominant themes within the corpus. The corpus consists of numerous reports, lessons learned, and best practices drawn from peace keeping and nation building operations. There are several technical challenges posed by this application domain. The document set is complex with respect to size, variety of formats and range of subject matter. The subject matter in these documents is extensive and includes reports on social and cultural institutions, physical infrastructure, education, agriculture, etc. The annotation taxonomy is large and unstructured with the flexibility of labels being applied orthogonally. Furthermore the annotation is required at the phrase level. Consequently, the search space for the label(s) is large and it becomes necessary

to adopt strategies that reduce the complexity of the classification process. The work reported in this paper is the development of a practical solution to this problem. We investigate the applicability of the Naïve Bayes classification technique to the corpus and compare to a more complex text classification technique, the MLkNN. It is found that the Naïve Bayes provides sufficient accuracy for automating the classification process for the target taxonomy, and text corpus. This evaluation is used to justify the incorporation of the algorithm into the automation workbench, CLAW.

The paper is organized as follows. Section II reviews published literature on text processing and multi-label classification in text. Section III describes the approach to the problem and the architecture of CLAW. Section IV describes the results and compares them with a benchmark algorithm. Section V concludes this paper and points to directions of future research.

II. RELATED WORK

In document classification a large number of attributes are used to characterize the document. The attributes of the examples to be classified are the words in the text phrases, and the number of different words can be quite large. McCallum and Nigam [8] clarify the two different first order probabilistic generative models that are used for text classification, both of which make the Naïve Bayes assumption. The first model is a multi-variate Bernoulli model, which is a Bayesian network with no dependencies between words and binary features. The second model is the multinomial model, which specifies that a document is represented by the set of word occurrences in the document. The probability of a document is a product of the probability of each of the words that occur.

Lauser et al. [6] propose an approach to automatically subject index full-text documents with multiple labels based on binary Support Vector Machines (SVMs). The authors incorporate multilingual background knowledge in the form of thesauri and ontologies in their text document representation. Godbole et al [2] present methods for enhancing and adapting discriminative classifiers for multi-labeled predictions. Their approach exploits the relationship between classes, by combining text features and the features indicating relationship between classes. They also propose enhancements to the margin of SVMs for building better models in the event of overlapping classes. In [3] the authors evaluate the preprocessing combination of feature reduction, feature subset selection, and term weighting is best suited to yield a document representation that optimizes the SVM classification of particular datasets. Ikonomakis et al. [4] describe the text classification process using the vector representation of documents, feature selection, and provide definitions of evaluation metrics.

Tsoumakas and Katakis [13] give a good introduction to multi-label classification using methods such as algorithm adaptation and problem transformation. The different techniques are compared and evaluated using metrics, after

they are applied to classify some benchmarked data sets. Zhang et al. [17] present a multi-label lazy learning approach named MLkNN, which is derived from the traditional k-Nearest Neighbor (kNN) algorithm. Using experiments on three different multi-label learning problems, i.e., yeast gene functional analysis, natural scene classification and automatic web page categorization, the authors show that MLkNN achieves better performance when compared to some well-established multi-label learning algorithms.

Younes et al. [15] describe an adaptation of MLkNN that takes into account dependencies between labels (DMLkNN). The authors use a Bayesian version of kNN. Experiments on simulated and benchmarked datasets show the efficiency of this approach compared to other existing approaches. Tsoumakas et al. [11] describe a new enhancement on the multi-label algorithm called label powerset (LP) that considers each distinct combination of labels that exist in the training set as a different class value in a single-label classification task.

Previous work in work benches for text annotation includes the Koivunen [5] system. This work describes Annotea, a semantic web-based project. Metadata is generated in the form of objects such as web annotations, reply threads, bookmarks, topics etc. Users can easily create RDF metadata that may be queried, merged and mixed with other metadata. In Zeni et al. [16], a software tool (Biblio) is described for automatically generating a list of references and an annotated bibliography, given a collection of published research articles. Finlayson [1] describes the Story Workbench, a software tool that facilitates semantic annotation of text documents. The tool uses Natural Language Processing tools to make a best guess as to the annotation, presenting that guess to the human annotator for approval, correction, or elaboration. This is a semi-automatic process. Annotation is generalized into a “tagging” procedure with parts-of-speech tags as well as general tags for “tooltips” or “infotips” in a GUI.

The problem that we address in this research is unique to the domain in several respects- the need to annotate at an atomic level, i.e., the noun phrase and verb phrase level; the unstructured labeling taxonomy supplied to annotate text; and finally, the need to find a practical solution to automating a supplied corpus and taxonomy. The taxonomy gives rise to a very large labeling search space, which makes accurate classification of text difficult. The algorithms discussed previously are developed for a much smaller set of classifications, and are applicable at a grosser level than that required here (paragraph or document). The software tools in general with the exception of Annotea are not geared towards the annotation process.

III. APPROACH

The first phase of the process is to input previously classified text phrases to the Stanford Parts Of Speech (POS) Tagger [9]. The Text Preprocessor component performs pre-processing on POS Tagged data. Pre-processing includes steps such as the filtering of records that do not contain either noun phrases or verb phrases, and retaining only those features (words) that have appropriate parts-of-speech tags

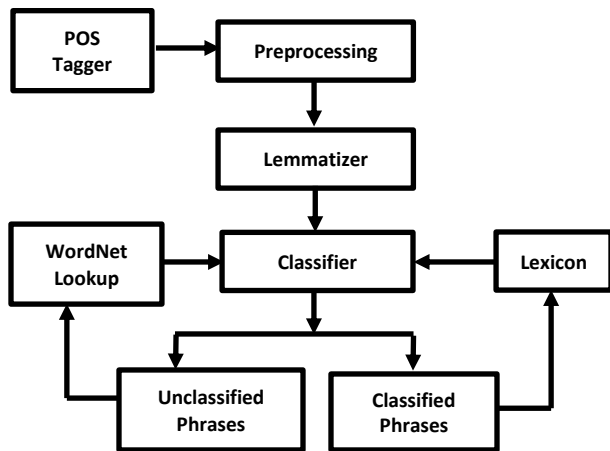


Figure 1. Process Flow Diagram for CLAW

for noun phrases and verb phrases. This component produces as output a delimited ASCII text file for next phase of lemmatizing. The lemmatizer uses WordNet® [14] database to extract synonyms or lemmas of input phrases to build an expanded input set for the next stage of classification. The Java API for WordNet Searching (JAWS, 2012) interface to WordNet is utilized in the lemmatizer. The lemmatized phrases are input into the Naïve Bayes classifier. Unclassified phrases are passed into a WordNet Lookup component to extract synonyms and returned to the Naïve Bayes Classifier for another attempt at classification. The lexicon is stored in a SQLite database [10] that stores the data. The process flow diagram for *CLAW* is shown in Figure 1.

Naïve Bayes is a standard algorithm for learning to classify text. Naïve Bayes classifiers are faster than other algorithms discussed in literature such as SVMs, since they learn a probabilistic generative model in just one pass of the training data even though they may sacrifice some classification accuracy. Bayes' Theorem finds the probability of an event occurring given the probability of another event that has already occurred. If *B* represents the dependent event and *A* represents the prior event, Bayes' theorem is stated as follows.

$$Prob(B \text{ given } A) = Prob(A \text{ and } B) / Prob(A) \quad (1)$$

i.e., the probability of classification, *B*, given a phrase *A*, is the probability of *A* classified as *B* in the training data, divided by the probability of *A* occurring in the training data. The Training data consists of text phrases classified /annotated by human annotator, which is input into the *CLAW* system as discussed previously.

The labels or tags for this domain are verb phrase tags (*task*, *state*, *role*, and *other*) and noun phrase tags. Noun phrase tags are further subdivided into Level 1 (*L1*), and Level 2 (*L2*) tags shown in TABLE 1 and TABLE 2 respectively. $L2^{(i)}$ denotes the i^{th} most frequent *L2* tag.

As previously noted, we have a very large search space of labels, which could be used to tag noun phrases, since the *L1*

TABLE 1. LEVEL 1 TAGS

L1 Tags
entity/agents
entity/events
entity/info
entity/institutions
entity/materials
entity/organizations
entity/physical_behaviors
entity/physical_infrastructures
entity/places
entity/services
entity/social_behaviors
entity/social_infrastructures
entity/technical_capabilities
entity/time

and *L2* tags may be orthogonally applied multiple number of times (depending on the context that we are annotating), with the only condition that every NP has at least one L1 tag. In the case of the verb phrases the process is simpler since there are only four possible tags to be applied. A simplification strategy is used to reduce the search space in the case of noun phrases. We calculate the frequency count of the labels to isolate and replace L1 labels with the most frequent ten classes and L2 labels in a particular instance with $L2^{(i)}$ where $i=1..4$, in the data set (if present in that string) to create particular models to be learnt by the Bayesian classifier. This selection strategy transforms the multi-label learning problem to a single label learning problem. Thus, based on frequency counts of labels, different models are learnt by the Naïve Bayes classifier. The instances that correspond to the top ten Level 1 Tags alone are also tested separately, and a model corresponding to L1 tags is learnt.

There is only one learning model for Verb Phrases (VP) test data since there are only four possible VP tags. Rare classes with percentage frequency less than 1% in the data set are matched using simple string matching. In the final step the individually predicted labels are composed together. This approach avoids the need to learn a combinatorial number of classes directly by simplifying the problem, however restoring the complexity of the labeling by composition in the final step.

IV. RESULTS AND COMPARISONS

Prediction-based metrics and Ranking-based metrics are standard measures used to evaluate performance of text classification. Ranking based metrics (TABLE 3) evaluate the label ranking quality depending on the ranking or scoring function. Hamming Loss is used as the basis for Ranking Function in our classification. Lower Hamming Loss implies

TABLE 2. LEVEL 2 TAGS

L2 Tags		
administrative	global	private
agreement	governance	psychological
agriculture	health	public
authority	Illicit	public opinion
civilian	indigenous	purpose
communication	labor	relationships
conditions	language	relief
conflicting	liaison	religion
contractor	licit	requirements
criminal	local_governance	return
definition	military	routine
dislocated	negotiation	security
economy	oversight	social
education	perspective	transition
environment	pets	transportation
extremism	political	utilities
food		

TABLE 3. DEFINITIONS OF RANKING-BASED METRICS

<p>Hamming Loss = # of misclassified records in Test Data/(# of records of Test Data* Size of Label Set)</p> <p>Subset Accuracy = (No. of Exact Matched records with True Predicted Classes)/(No. of Test Records)</p> <p>Average Precision: Average fraction of labels ranked above a particular label (Best value is 1)</p> <p>Coverage: Average # of steps needed to move down the ranked label list in order to cover all the labels assigned to a test instance. Smaller value of this metric is desirable.</p> <p>One-Error: Calculates how many times the top-ranked label i.e., the label with highest ranking score, is not in the set of labels for the appropriate instance. Smaller value of this metric is desirable.</p> <p>Ranking loss: Average fraction of label pairs that are reversely ordered i.e., number of times irrelevant labels are ranked higher than relevant labels for an instance. This does not happen in our case. Smaller value of this metric is desirable.</p>

higher rank for a label. The most relevant label has highest rank of 1.

The MULAN [12] package has implemented the MLkNN (Multi-label lazy learning k-NN) and provides a good comparison metric for the approach taken in this paper. The software generates classification metrics automatically when supplied with train-test data.

TABLE 4. RANKING METRICS FOR NOUN AND VERB PHRASES.

Classification Algorithm	Ranking Metrics	L1 Tags only for Noun Phrases	Verb Phrase Tags only
Naïve Bayes	Hamming Loss	0.03	0.05
	Subset Accuracy	0.7	0.8
	Average Precision	0.78	0.5
	Coverage	2	1
	One Error	0.0023	0.005
	Ranking Loss	0	0
MULAN MLkNN	Hamming Loss	0.1	0.25
	Subset Accuracy	< 0.01	< 0.01
	Avg. Precision	0.53	0.5454
	Coverage	2.1336	1.255
	One Error	0.6889	0.76
	Ranking Loss	0.2371	0.4183

For the experiments we used a training set of approximately 1000 classified phrases, with 200 phrases as the test set. In the first part of the experiments, we consider L1 Noun Phrase (NP) tags alone and in a separate experiment Verb Phrases alone. The results of this experiment are shown in TABLE 4.

From TABLE 4 it may be seen that, while the MLkNN has marginally better Average Precision for Verb Phase test data, all other evaluation metrics are considerably better for the Naïve Bayes classifier used in this work. TABLE 5 establishes this for a series of L1L2⁽ⁱ⁾ models tested. It should be noted that these conclusions are specific to the annotation taxonomy and the domain of application used here.

A. Integrating the Learning Component into CLAW

The learning component described in the previous section is integrated into the software tool, to develop the Classification-based Text Annotation Workbench (CLAW). CLAW uses the learning component, and the corpus database to provide hints for annotation to the user. SQLite is chosen as the database for the work bench because of its light weight footprint. The workbench is developed using the .NET framework, with the learning components constructed as Java services.

TABLE 5. RANKING METRICS FOR L1L2⁽¹⁾ MODELS

	Ranking Metrics	L1L2 ⁽¹⁾	L1L2 ⁽²⁾	L1L2 ⁽³⁾	L1L2 ⁽⁴⁾
Naïve Bayes	Hamming Loss	0.026	0.027	0.0236	0.05
	Subset Accuracy	0.59	0.65	0.72	0.55
	Average Precision	0.91	0.92	0.75	0.89
	Coverage	4	3	3	2
	One Error	0.0043	0.0055	0.0024	0
	Ranking Loss	0	0	0	0
MULAN MLKNN	Hamming Loss	0.0625	0.0769	0.1	0.1111
	Subset Accuracy	< 0.01	<0.01	<0.01	<0.01
	Average Precision	0.4448	0.4863	0.4883	0.5208
	Coverage	4.2735	3.1209	2.4633	2.2038
	One Error	0.6795	0.7005	0.7267	0.6943
	Ranking Loss	0.2849	0.2601	0.2737	0.2755

V. CONCLUSIONS AND FUTURE WORK

This work approached the problem of text annotation in two phases. In the first phase we annotated the text manually based on a taxonomy provided, and in the second phase we used the annotations to develop algorithms to perform automated annotation. There were several challenges to developing the automated annotation component- the text corpus is wide ranging encompassing a broad range of topics; the taxonomy is unstructured and large; and finally the annotations may be applied combinatorially. We introduced a multi-modal approach that reduces the combinatorial nature of the problem, making the automation feasible. The resulting model was validated against a benchmark algorithm for text classification. Finally, we integrated the approach into a novel system, Classification-based Text Annotation Workbench (CLAW) that facilitates both manual annotation and incorporates supervised annotation (based on automated classification) to reduce the complexity of annotating text. CLAW provides a flexible environment with the ability to change the taxonomy depending on the domain of application. The CLAW tool also has the capability to ensure a consistent basis to annotation, since it generates annotations based on the deterministic learning component. Processing times within the tool are fairly reasonable, but this could change as the repository gets larger.

While the CLAW tool provides a good infrastructure for annotation of text, there are several possible enhancements to the tool that can improve the quality and repeatability of the annotation process.

- Automated generation of learning models. The quality of the automated annotations provided by CLAW depends on the learning model used (refer the CLAW user guide). While the learning model is generated manually, the corpus database could provide a mechanism for the automated creation of models. Multiple models may be created and used within CLAW. The use of multiple models would improve the recall of the classification process. A further possibility might be the application of active learning into this component.
- Qualitative evaluation of model outputs. In the current version of CLAW every model output is treated identically. A quantitative approach that evaluates each model independently, and ranks the outputs could provide the user with greater confidence in the results. This would also help the user select annotation suggestions based on quantitative measures.
- Traceability of CLAW suggestions. In the current version of CLAW, the annotation suggestions are provided to the user, however there is no mechanism that informs the user as to how the suggestion was being made. Providing traceability of the model outputs would improve confidence in the system.

ACKNOWLEDGMENT

This research is funded in part by the Construction Engineering Research Laboratory, Engineering Research and Development Center (ERDC-CERL) under Contract No: W913T-12-C-007, ARL under Grant No: W911NF-12-2-0067 and ARO under Grant Number W911NF-11-1-0168. Any opinions, findings, conclusions or recommendations expressed here are those of the author(s) and do not necessarily reflect the views of the sponsor.

REFERENCES

- [1] M.A. Finlayson. "The Story Workbench: An Extensible Semi-Automatic Text Annotation Tool," *AAAI Technical Report WS-11-18*. Copyright 2011.
- [2] S. Godbole and S.Sarawagi. "Discriminative Methods for Multi-labeled Classification," *PAKDD 2004*, LNAI 3056, pp. 22–30.
- [3] T. Gonçalves and P. Quaresma. "Evaluating preprocessing techniques in a text classification problem," *XXV Congresso da Sociedade Brasileira de Computação*, July 2005, pp. 841-850
- [4] M. Ikonomakis, S. Kotsiantis, and V. Tampakas. "Text Classification: A Recent Overview," *ICCOMP'05. Proceedings of the 9th WSEAS International Conference on Computers*. Article no: 125. In *ESWC 2005, UserSWeb workshop*
- [5] M.R. Koivunen. "Annotea and semantic web supported collaboration," Downloaded from http://ceur-ws.org/Vol-137/01_koivunen_final.pdf, November 2012.
- [6] B., Lauser, A. Hotho, T. Koch, and I.T. Solvberg, (Eds.). "Automatic Multi-label Subject Indexing in a Multilingual Environment," *ECDL 2003*, LNCS 2769, pp. 140–151.
- [7] Machine Learning Group at University of Waikato, 2012. <http://www.cs.waikato.ac.nz/ml/weka/>

- [8] A. McCallum, and K. A. Nigam. "Comparison of Event Models for Naive Bayes Text Classification," In *AAAI-98 Workshop on 'Learning for Text Categorization'*, 1998, 41-48, WS-98-05
- [9] POSTagger, <http://nlp.stanford.edu/software/tagger.shtml>
- [10] SQLite. <http://www.sqlite.org/>
- [11] G. Tsoumakas, I. Katakis, and I. Vlahavas. "Random k-Labelsets for Multilabel classification," *IEEE Transactions on Knowledge and Data Engineering*, July 2011, Vol 23, No. 7.
- [12] G. Tsoumakas, E. Spyromitros-Xioufis, J. Vilcek, and I. Vlahavas. "MULAN: A Java library for Multi-Label Learning," *Journal of Machine Learning Research*, 12, 2411-2414.
- [13] G. Tsoumakas and I. Katakis. "Multi-Label Classification: An Overview," *International Journal of Data Warehousing and Mining*, 3(3), July-Sept 2007, p.1-13.
- [14] WordNet. <http://wordnet.princeton.edu/>
- [15] Z. Younes, F. Abdallah, T. Denoeux, and H. Snoussi. "A Dependent Multilabel Classification Method Derived from the k-Nearest Neighbor Rule," In *Proceedings of EURASIP J. Adv. Sig. Proc.* 2011.
- [16] N. Zeni, N. Kiyavitskaya, L. Mich, J. Mylopoulos, and J. R. Cordy. "A Lightweight Approach to Semantic Annotation of Research Papers," In *Proceedings of NLDB.* 2007, 61-72.
- [17] M.L. Zhang and Z. H. Zhou. "MI-knn: A lazy learning approach to multi-label learning," *Pattern Recognition*, 40, 2038-2048.

Mining Incomplete Data with Many Missing Attribute Values

A Comparison of Probabilistic and Rough Set Approaches

Patrick G. Clark, Jerzy W. Grzymala-Busse, and Martin Kuehnhausen
 Department of Electrical Engineering and Computer Science
 University of Kansas
 Lawrence, KS 66045, USA
 E-mail: pclark@ku.edu, jerzy@ku.edu, mkuehnhausen@ku.edu

Abstract—In this paper, we study probabilistic and rough set approaches to missing attribute values. Probabilistic approaches are based on imputation, a missing attribute value is replaced either by the most probable known attribute value or by the most probable attribute value restricted to a concept. In this paper, in a rough set approach to missing attribute values we consider two interpretations of such value: *lost* and “do not care”. Additionally, we apply three definitions of approximations (*singleton*, *subset* and *concept*) and use an additional parameter called α . Our main objective was to compare probabilistic and rough set approaches to missing attribute values for incomplete data sets with many missing attribute values. We conducted experiments on six incomplete data sets with as many missing attribute values as possible. In these data sets an additional incremental replacement of known values by missing attribute values resulted with the entire records filled with only missing attribute values. Rough set approaches were better for five data sets, for one data set probabilistic approach was more successful.

Keywords—Data mining; probabilistic approaches to missing attribute values; rough set theory; probabilistic approximations; parameterized approximations

I. INTRODUCTION

In this paper, we compare two methods handling missing attribute values based on probability theory with a rough set approach to missing attribute values represented by two interpretations of missing attribute values (*lost* and “do not care”), three definitions of approximations (*singleton*, *subset* and *concept*) and on a parameter called α .

In probabilistic methods for missing attribute values, the most frequently used in data mining practice, in our first method called Most Common Value for Symbolic Attributes and Average Value for Numerical Attributes (MCV-AV), for symbolic attributes a missing attribute value was replaced by the most probable known attribute value (the most frequent). For numerical attributes, a missing attribute value was replaced by the average of known attribute values. In the second probabilistic method, called Concept Most Common Value for Symbolic Attributes and Concept Average Values for Numerical Attributes (CMCV-CAV), for symbolic attributes a missing attribute value was replaced by the most common value restricted to the concept that contains the missing attribute value. A *concept* is the set of all cases

(records) with the same decision value (labeled the same way by an expert). Thus, for symbolic attributes a missing attribute value was replaced by a known attribute value with the largest conditional probability given the concept to which the case belongs. For numerical attributes, a missing attribute value was replaced the average of known attribute values restricted to the corresponding concept.

Using a rough set approach to missing attribute values, we may distinguish two interpretations of missing attribute values: *lost* and “do not care”. The former interpretation means that an attribute value was originally given, however, currently we have no access to it (e.g., the value was forgotten or erased). For data sets with *lost* values we try to induce the rule set from known data. The latter interpretation represents, e.g., a refusal to answer a question. For example, patients suspected of having flu may refuse to tell the value of the attribute *Eye color* since they may consider it irrelevant. For data mining from data sets affected by such missing attribute values we replace a “do not care” condition by all possible attribute values.

An idea of lower and upper approximations is a basic idea of rough set theory [1], [2]. For incomplete data sets there exist many definitions of approximations. In this paper, we use three types of approximations: singleton, subset and concept [3]. A probabilistic (or parameterized) approximation, associated with a probability (parameter) α , is a generalization of lower and upper approximations. For very small α , the probabilistic approximation becomes the upper approximation. For $\alpha = 1$, the probabilistic approximation is a lower approximation [4]. Probabilistic approximations for complete data sets were studied for years, the idea was introduced in [5] and further developed in [6]–[15]. Such approximations were explored from a theoretical view point. The first paper on experimental validation of such approximations, for complete data sets, was [16]. For incomplete data sets probabilistic approximations were generalized in [4]. Results of experiments on probabilistic approximations for incomplete data sets were presented in [16]–[21]. In all of these papers, rough set approaches to mining incomplete data were not compared with any other approaches to missing attribute values.

TABLE I. An incomplete decision table

Case	Attributes			Decision
	Temperature	Headache	Cough	Flu
1	high	?	no	yes
2	normal	no	yes	yes
3	?	yes	no	yes
4	high	no	yes	yes
5	high	?	yes	yes
6	very-high	no	no	yes
7	*	no	*	no

The main objective of this paper was to compare (experimentally) probabilistic and rough set approaches to missing attribute values for incomplete data sets with many missing attribute values. Our main result is that a rough set approach to missing attribute values was successful on five out of six data sets since it provides smaller error rates, a result of ten-fold cross validation. Our data sets had as many missing attribute values as possible. With an additional incremental replacement of known values by missing attribute values, the entire records were filled with only missing attribute values.

Section II describes the formal foundation of characteristic sets that form the basis of the probabilistic approximations we explore in Section III. Furthermore, we consider the problem of definability and its relationship to probabilistic approximations in Section IV. The results of our experiments are analyzed in Section V and further examined in the conclusion of this paper.

II. CHARACTERISTIC SETS

We assume that the input data sets are presented in the form of a *decision table*. An example of a decision table is shown in Table I (a similar table was presented in [22]). Rows of the decision table represent *cases*, while columns are labeled by *variables*. The set of all cases is denoted by U . In Table I, $U = \{1, 2, 3, 4, 5, 6, 7\}$. Some variables are called *attributes* while one selected variable is called a *decision* and is denoted by d . The set of all attributes will be denoted by A . In Table I, $A = \{\text{Temperature}, \text{Headache}, \text{Cough}\}$ and $d = \text{Flu}$.

An important tool to analyze data sets is a *block of an attribute-value pair*. Let (a, v) be an attribute-value pair. For *complete* decision tables, i.e., decision tables in which every attribute value is specified, a block of (a, v) , denoted by $[(a, v)]$, is the set of all cases x for which $a(x) = v$, where $a(x)$ denotes the value of the attribute a for the case x . For incomplete decision tables the definition of a block of an attribute-value pair is modified.

- If for an attribute a there exists a case x such that $a(x) = ?$, i.e., the corresponding value is *lost*, then the

case x should not be included in any blocks $[(a, v)]$ for all values v of attribute a ,

- If for an attribute a there exists a case x such that the corresponding value is a “do not care” condition, i.e., $a(x) = *$, then the case x should be included in blocks $[(a, v)]$ for all specified values v of attribute a .

A special block of a decision-value pair is called a *concept*. In Table I, $[(\text{Flu}, \text{yes})] = \{1, 2, 3, 4, 5, 6\}$. Additionally, for Table I

$$\begin{aligned} [(\text{Temperature}, \text{normal})] &= \{2, 7\}, \\ [(\text{Temperature}, \text{high})] &= \{1, 4, 5, 7\}, \\ [(\text{Temperature}, \text{very-high})] &= \{6, 7\}, \\ [(\text{Headache}, \text{no})] &= \{2, 4, 6, 7\}, \\ [(\text{Headache}, \text{yes})] &= \{3\}, \\ [(\text{Cough}, \text{no})] &= \{1, 3, 6, 7\}, \\ [(\text{Cough}, \text{yes})] &= \{2, 4, 5, 7\}. \end{aligned}$$

For a case $x \in U$ the *characteristic set* $K_B(x)$ is defined as the intersection of the sets $K(x, a)$, for all $a \in B$, where the set $K(x, a)$ is defined in the following way:

- If $a(x)$ is specified, then $K(x, a)$ is the block $[(a, a(x))]$ of attribute a and its value $a(x)$,
- If $a(x) = ?$ or $a(x) = *$ then the set $K(x, a) = U$.

Characteristic set $K_B(x)$ may be interpreted as the set of cases that are indistinguishable from x using all attributes from B and using a given interpretation of missing attribute values. Thus, $K_A(x)$ is the set of all cases that cannot be distinguished from x using all attributes.

For Table I and $B = A$,

$$\begin{aligned} K_A(1) &= \{1, 4, 5, 7\} \cap U \cap \{1, 3, 6, 7\} = \{1, 7\}, \\ K_A(2) &= \{2, 7\} \cap \{2, 4, 6, 7\} \cap \{2, 4, 5, 7\} = \{2, 7\}, \\ K_A(3) &= U \cap \{3\} \cap \{1, 3, 6, 7\} = \{3\}, \\ K_A(4) &= \{1, 4, 5, 7\} \cap \{2, 4, 6, 7\} \cap \{2, 4, 5, 7\} = \{4, 7\}, \\ K_A(5) &= \{1, 4, 5, 7\} \cap U \cap \{2, 4, 5, 7\} = \{4, 5, 7\}, \\ K_A(6) &= \{6, 7\} \cap \{2, 4, 6, 7\} \cap \{1, 3, 6, 7\} = \{6, 7\}, \text{ and} \\ K_A(7) &= U \cap \{2, 4, 6, 7\} \cap U = \{2, 4, 6, 7\}. \end{aligned}$$

The characteristic relation $R(B)$ is a relation on U defined for $x, y \in U$ as follows

$$(x, y) \in R(B) \text{ if and only if } y \in K_B(x).$$

The characteristic relation is reflexive but—in general—it does not need to be symmetric or transitive. In our example, $R(A) = \{(1, 1), (1, 7), (2, 2), (2, 7), (3, 3), (4, 4), (4, 7), (5, 4), (5, 5), (5, 7), (6, 6), (6, 7), (7, 2), (7, 4), (7, 6), (7, 7)\}$. For Table I the relation $R(A)$ is neither symmetric nor transitive. A relation $R(A)$ that is an equivalence relation is called an *indiscernibility* relation [1], [2].

III. PROBABILISTIC APPROXIMATIONS

The singleton probabilistic approximation of X with the threshold α , $0 < \alpha \leq 1$, denoted by $\text{appr}_\alpha^{\text{singleton}}(X)$, is defined as follows

$$\{x \mid x \in U, Pr(X|K_B(x)) \geq \alpha\}, \quad (1)$$

where $Pr(X|K_B(x)) = \frac{|X \cap K_B(x)|}{|K_B(x)|}$ is the conditional probability of X given $K_B(x)$.

A subset probabilistic approximation of the set X with the threshold α , $0 < \alpha \leq 1$, denoted by $appr_\alpha^{subset}(X)$, is defined as follows

$$\cup\{K_B(x) \mid x \in U, Pr(X|K_B(x)) \geq \alpha\}. \quad (2)$$

A concept probabilistic approximation of the set X with the threshold α , $0 < \alpha \leq 1$, denoted by $appr_\alpha^{concept}(X)$, is defined as follows

$$\cup\{K_B(x) \mid x \in X, Pr(X|K_B(x)) \geq \alpha\}. \quad (3)$$

For Table I, all distinct probabilistic approximations (singleton, subset and concept) for [(Flu, yes)] are

$$appr_{0.5}^{singleton}(\{1, 2, 3, 4, 5, 6\}) = U,$$

$$appr_{0.667}^{singleton}(\{1, 2, 3, 4, 5, 6\}) = \{3, 5, 7\},$$

$$appr_{0.75}^{singleton}(\{1, 2, 3, 4, 5, 6\}) = \{3, 7\},$$

$$appr_1^{singleton}(\{1, 2, 3, 4, 5, 6\}) = \{3\},$$

$$appr_{0.5}^{subset}(\{1, 2, 3, 4, 5, 6\}) = U,$$

$$appr_{0.667}^{subset}(\{1, 2, 3, 4, 5, 6\}) = \{2, 3, 4, 5, 6, 7\},$$

$$appr_{0.75}^{subset}(\{1, 2, 3, 4, 5, 6\}) = \{2, 3, 4, 6, 7\},$$

$$appr_1^{subset}(\{1, 2, 3, 4, 5, 6\}) = \{3\},$$

$$appr_{0.5}^{concept}(\{1, 2, 3, 4, 5, 6\}) = U,$$

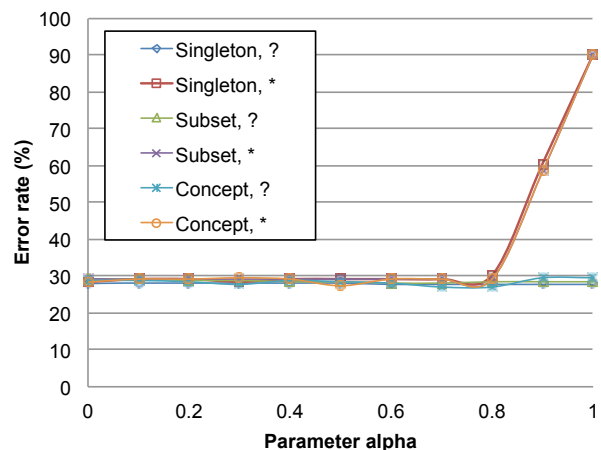
$$appr_{0.667}^{concept}(\{1, 2, 3, 4, 5, 6\}) = \{3, 4, 5, 7\},$$

$$appr_{0.75}^{concept}(\{1, 2, 3, 4, 5, 6\}) = \{3\},$$

As follows from our example, all three probabilistic approximations, in general, are distinct, even for the same value of the parameter α . If a characteristic relation $R(B)$ is an equivalence relation, all three types of probabilistic approximation: singleton, subset and concept are reduced to the same probabilistic approximation. Additionally, if α is small but greater than 0 (in our experiments such α was equal to 0.001), a probabilistic approximation is called *upper* [4]. For $\alpha = 1$, a probabilistic approximation is called *lower* [4].

TABLE II. Data sets used for experiments

Data set	Number of		Percentage of
	cases	attributes	missing attribute values
Breast cancer	277	9	44.81
Echocardiogram	74	7	40.15
Hepatitis	155	19	60.27
Image segmentation	210	19	69.85
Lymphography	148	18	69.89
Wine recognition	178	13	64.65


 Figure 1. Results of experiments with *Breast cancer* data set

IV. DEFINABILITY

Let B be a subset of the set A of all attributes. For incomplete decision tables, a union of some intersections of attribute-value pair blocks, where such attributes are members of B and are distinct, will be called *B-locally definable* sets. A union of characteristic sets $K_B(x)$, where $x \in X \subseteq U$ will be called a *B-globally definable* set. Any set X that is *B-globally definable* is *B-locally definable*, the converse is not true [4].

Singleton probabilistic approximations—in general—are not even locally definable. For example, the singleton probabilistic approximation of [(Flu, yes)] with the threshold $\alpha = 0.667$, i.e., the set $\{3, 5, 7\}$, is not *A-locally definable*. Indeed, in all attribute blocks which contain the case 5 (there are two such blocks, [(Temperature, high)] and [(Cough, yes)], 5 is in the same block with cases 4 and 7. Thus, any definable case containing 5 must contain cases 4 and 7. The set $\{3, 5, 7\}$ does not contain case 4.

On the other hand, both subset and concept probabilistic approximations are *A-globally definable*. Obviously, if a set is not *B-locally definable* then it cannot be expressed by rule sets using attributes from B .

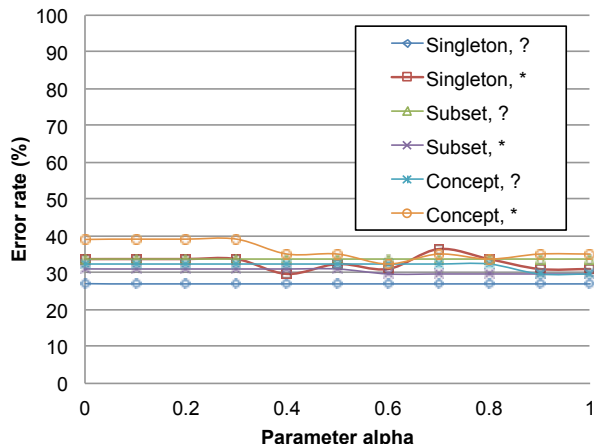


Figure 2. Results of experiments with *Echocardiogram* data set

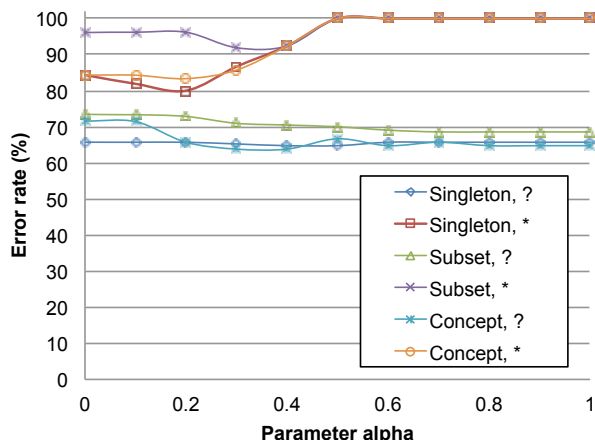


Figure 4. Results of experiments with *Image segmentation* data set

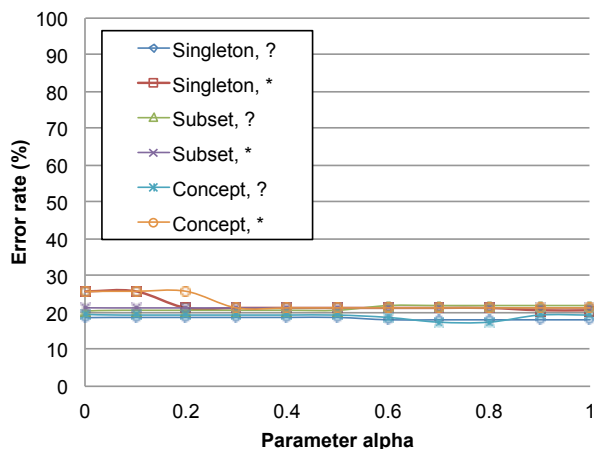


Figure 3. Results of experiments with *Hepatitis* data set

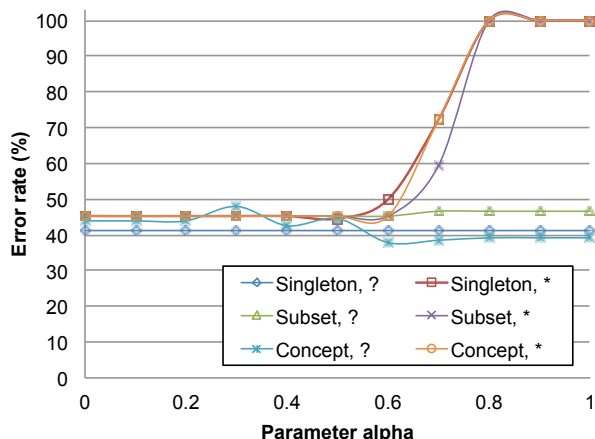


Figure 5. Results of experiments with *Lymphography* data set

V. EXPERIMENTS

For our experiments we used six real-life data sets that are available on the University of California at Irvine *Machine learning Repository*, see Table II. For every data set a set of templates was created. Templates were formed by replacing incrementally (with 5% increment) existing specified attribute values by *lost* values. Thus, we started each series of experiments with no *lost* values, then we added 5% of *lost* values, then we added additional 5% of *lost* values, etc., until at least one entire row of the data sets was full of *lost* values. Then three attempts were made to change configuration of new *lost* values and either a new data set with extra 5% of *lost* values were created or the process was terminated. Additionally, the same formed templates were edited for further experiments by replacing question marks, representing *lost* values by “*”s, representing “do not care” conditions.

For any data set there was some maximum for the percentage of missing attribute values. For example, for the *Breast cancer* data set, it was 44.81%.

For rule induction we used the Modified Learning from Examples Module version 2 (MLEM2) rule induction algorithm, a component of the Learning from Examples based on Rough Sets (LERS) data mining system [23], [24].

VI. CONCLUSIONS

A comparison of two probabilistic approaches to missing attribute values is presented on Table III. This table shows that for incomplete data with many missing attribute values, the MCV-AV method is better for four data sets (*Echocardiogram*, *Hepatitis*, *Lymphography* and *Wine recognition*) while the CMCV-CAV method is better for two data sets (*Breast cancer* and *Image segmentation*).

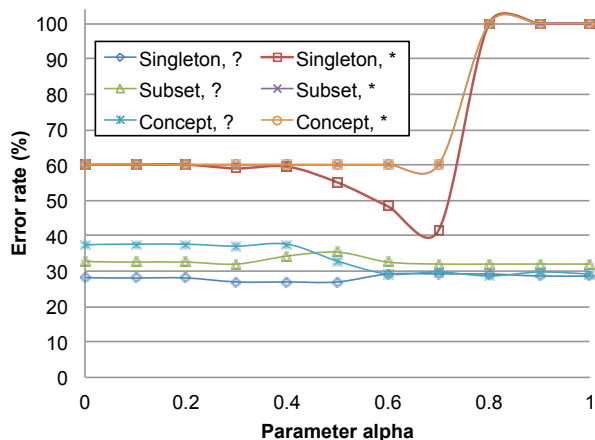


Figure 6. Results of experiments with Wine recognition data set

TABLE III. Error rate for MCV-AV and CMCV-CAV

Data set	Error rate in percent	
	MCV-AV	CMCV-CAV
Breast cancer	30.69	29.96
Echocardiogram	22.97	27.03
Hepatitis	19.35	21.29
Image segmentation	72.86	64.76
Lymphography	41.22	47.97
Wine recognition	31.46	44.38

Similarly, Figures 1–6 show that for four data sets (*Breast cancer*, *Hepatitis*, *Image segmentation* and *Lymphography*) the best rough set approach is based on concept approximations. For remaining two data sets (*Echocardiogram* and *Wine recognition*) the best rough set approach is based on singleton approximations. For all six data sets the smallest error rate is always associated with missing attribute values interpreted as *lost*. Note that with the exception of the

TABLE IV. Error rate for the better of MCV-AV and CMCV-CAV and the best rough set approach

Data set	Error rate in percent	
	better of MCV-AV and CMCV-CAV	best rough set approach
Breast cancer	29.96	27.08
Echocardiogram	22.97	27.03
Hepatitis	19.35	17.42
Image segmentation	64.76	63.81
Lymphography	41.22	37.84
Wine recognition	31.46	26.97

Echocardiogram data set (where the best value is associated with any alpha, between 0.001 and 1), for remaining five data sets the smallest error rate occurs always for some alpha larger than 0.001 and smaller than 1. Moreover, for the parameter α close to one, error rate associated with “do not care” conditions is close to 100% due to small probabilistic approximations, as exemplified by *Breast cancer*, *Image segmentation* and *Wine recognition* data sets.

Finally, a comparison of the best of the two probabilistic approaches to missing attribute values (MCV-AV and CMCV-CAV) is presented in Table IV. This table shows the best results accomplished using rough set theory with three parameters: kind of approximation (singleton, subset and concept), two interpretations of missing attribute values (*lost* and “do not care” condition) and α (0.001, 0.1, 0.2, ..., 1). The better results for five of the data sets is the rough set approach, while for only one data set (*Echocardiogram*) the better approach is achieved by the MCV-AV method. However, statistically, the superiority of a rough set approach is insignificant. Clearly, more experiments are needed to compare probabilistic and rough set approaches to missing attribute values.

Theoretically, we should not use singleton probabilistic approximations for data mining, see Section IV. Nevertheless, our experiments show that—in practice—singleton approximations are worth considering, since rule sets induced from such approximations classify unknown cases using the sophisticated LERS classification system [23], [24].

REFERENCES

- [1] Z. Pawlak, “Rough sets,” *International Journal of Computer and Information Sciences*, vol. 11, pp. 341–356, 1982.
- [2] Z. Pawlak, *Rough Sets. Theoretical Aspects of Reasoning about Data*. Dordrecht, Boston, London: Kluwer Academic Publishers, 1991.
- [3] J. W. Grzymala-Busse, “Rough set strategies to data with missing attribute values,” in *Workshop Notes, Foundations and New Directions of Data Mining, in conjunction with the 3-rd International Conference on Data Mining*, 2003, pp. 56–63.
- [4] J. W. Grzymala-Busse, “Generalized parameterized approximations,” in *Proceedings of the RSKT 2011, the 6-th International Conference on Rough Sets and Knowledge Technology*, 2011, pp. 136–145.
- [5] S. K. M. Wong and W. Ziarko, “INFER—an adaptive decision support system based on the probabilistic approximate classification,” in *Proceedings of the 6-th International Workshop on Expert Systems and their Applications*, 1986, pp. 713–726.
- [6] J. W. Grzymala-Busse and W. Ziarko, “Data mining based on rough sets,” in *Data Mining: Opportunities and Challenges*, J. Wang, Ed. Hershey, PA: Idea Group Publ., 2003, pp. 142–173.

- [7] Z. Pawlak and A. Skowron, "Rough sets: Some extensions," *Information Sciences*, vol. 177, pp. 28–40, 2007.
- [8] Z. Pawlak, S. K. M. Wong, and W. Ziarko, "Rough sets: probabilistic versus deterministic approach," *International Journal of Man-Machine Studies*, vol. 29, pp. 81–95, 1988.
- [9] D. Ślęzak and W. Ziarko, "The investigation of the bayesian rough set model," *International Journal of Approximate Reasoning*, vol. 40, pp. 81–91, 2005.
- [10] S. Tsumoto and H. Tanaka, "PRIMEROSE: probabilistic rule induction method based on rough sets and resampling methods," *Computational Intelligence*, vol. 11, pp. 389–405, 1995.
- [11] Y. Y. Yao, "Probabilistic rough set approximations," *International Journal of Approximate Reasoning*, vol. 49, pp. 255–271, 2008.
- [12] Y. Y. Yao and S. K. M. Wong, "A decision theoretic framework for approximate concepts," *International Journal of Man-Machine Studies*, vol. 37, pp. 793–809, 1992.
- [13] Y. Y. Yao, S. K. M. Wong, and P. Lingras, "A decision-theoretic rough set model," in *Proceedings of the 5th International Symposium on Methodologies for Intelligent Systems*, 1990, pp. 388–395.
- [14] W. Ziarko, "Variable precision rough set model," *Journal of Computer and System Sciences*, vol. 46, no. 1, pp. 39–59, 1993.
- [15] W. Ziarko, "Probabilistic approach to rough sets," *International Journal of Approximate Reasoning*, vol. 49, pp. 272–284, 2008.
- [16] P. G. Clark and J. W. Grzymala-Busse, "Experiments on probabilistic approximations," in *Proceedings of the 2011 IEEE International Conference on Granular Computing*, 2011, pp. 144–149.
- [17] P. G. Clark and J. W. Grzymala-Busse, "Rule induction using probabilistic approximations and data with missing attribute values," in *Proceedings of the 15-th IASTED International Conference on Artificial Intelligence and Soft Computing ASC 2012*, 2012, pp. 235–242.
- [18] P. G. Clark and J. W. Grzymala-Busse, "Experiments using three probabilistic approximations for rule induction from incomplete data sets," in *Proceedings of the MCCSIS 2012, IADIS European Conference on Data Mining ECDM 2012*, 2012, pp. 72–78.
- [19] P. G. Clark and J. W. Grzymala-Busse, "Experiments on rule induction from incomplete data using three probabilistic approximations," in *Proceedings of the 2012 IEEE International Conference on Granular Computing*, 2012, pp. 90–95.
- [20] P. G. Clark, J. W. Grzymala-Busse, and Z. S. Hippe, "How good are probabilistic approximations for rule induction from data with missing attribute values?" in *Proceedings of the RSCTC 2012, the 8-th International Conference on Rough Sets and Current Trends in Computing*, 2012, pp. 46–55.
- [21] P. G. Clark, J. W. Grzymala-Busse, and M. Kuehnhausen, "Local probabilistic approximations for incomplete data," in *Proceedings of the ISMIS 2012, the 20-th International Symposium on Methodologies for Intelligent Systems*, 2012, pp. 93–98.
- [22] J. W. Grzymala-Busse and W. Rzasa, "Local and global approximations for incomplete data," *Transactions on Rough Sets*, vol. 8, pp. 21–34, 2008.
- [23] J. W. Grzymala-Busse, "LERS—a system for learning from examples based on rough sets," in *Intelligent Decision Support. Handbook of Applications and Advances of the Rough Set Theory*, R. Slowinski, Ed. Dordrecht, Boston, London: Kluwer Academic Publishers, 1992, pp. 3–18.
- [24] J. W. Grzymala-Busse, "MLEM2: A new algorithm for rule induction from imperfect data," in *Proceedings of the 9th International Conference on Information Processing and Management of Uncertainty in Knowledge-Based Systems*, 2002, pp. 243–250.

Identification of Failing Banks Using Clustering with Self-Organising Neural Networks

Michael Negnevitsky
School of Engineering
University of Tasmania
Hobart, Australia

Michael.Negnevitsky@utas.edu.au

Abstract—This paper presents experimental results of cluster analysis using self-organising neural networks for identifying failing banks. The paper first describes major reasons and likelihoods of bank failures. Then it demonstrates an application of a self-organising neural network and presents results of the study. Findings of the paper demonstrate that a self-organising neural network is a powerful tool for identifying potentially failing banks. Finally, the paper discusses some of the limitations of cluster analysis related to understanding of the exact meaning of each cluster.

Keywords—cluster analysis, self-organising neural network; Kohonen layer; likelihood of bank failure

I. INTRODUCTION

In 2008, a series of bank failures triggered a financial crisis. By any historical standard, this crisis was the worst since the Great Depression of the 1930s. The immediate cause of the crisis was the bursting of the United States housing bubble. This, in turn, caused the values of securities tied to real estate pricing to nose-dive, damaging financial institutions worldwide. Bank insolvencies and lack of credits reduced the investor confidence and, as a result, the stock market plummeted. In 2009, the global economy contracted by 1.1%, while in advanced countries, the contraction reached 3.4%. After intervention by central banks and governments of an unprecedented scale, the global economy began to recover. However, the global financial system remains at risk.

The danger of cascading failures of major banks would be reduced significantly if we could identify banks with potential problems before they face solvency and liquidity crises. There are many reasons for bank failures. These include high risk-taking, interest rate volatility, poor management practices, inadequate accounting standards, and increased competition from non-depository institutions. Since the crisis, bank regulators have been increasingly concerned with reducing the size of deposit insurance liabilities. It has even been suggested that the best regulatory policy is to close banks before they become undercapitalised.

Therefore, identifying potentially failing banks as early as possible is essential for avoiding another major financial crisis.

Over the last thirty years many tools have been developed to identify problem banks. While early models mostly relied on statistical techniques [1], [4], [6], most recent developments are based on fuzzy logic and neural networks [2], [7], [9]. Most of these models use a dichotomous classification – bankruptcy versus non-bankruptcy. In real world, however, banks are ranked in terms of their *likelihood* of bankruptcy. What regulators really need is an early warning system that can “flag” potentially failing banks. Once such banks are identified, different preventive programs tailored to each bank’s specific needs can be put in place, thereby avoiding a major banking failure.

In this paper, we “flag” potentially failing banks using cluster analysis. First, we introduce bank rating system used in the U.S., select 100 banks and obtain their financial data. Then, we use a self-organising map with a 5-by-5 array of 25 neurons in the Kohonen layer to cluster the selected banks. We demonstrate how to determine the number of clusters in a multidimensional data set. Finally, we analyse the results and discuss challenges related to applications of self-organising maps to real life problems.

II. CLUSTER ANALYSIS

Cluster analysis is an exploratory data analysis technique that divides different objects into groups, called *clusters*, in such a way that the degree of association between two objects is maximised if they belong to the same cluster and minimised otherwise.

The term “cluster analysis” was first introduced over 70 years ago by Robert Tryon [8]. Since then, cluster analysis has been successfully applied in many fields including medicine, archeology, astronomy, etc. In clustering, there are no predefined classes – objects are grouped together only on the basis of their similarity. For this reason, clustering is often referred to as unsupervised classification. There is no distinction between

independent and dependent variables, and when clusters are found the user needs to interpret their meaning.

We can identify three major methods used in cluster analysis. These are based on statistics, fuzzy logic and neural networks. In this case study, we will apply a self-organising neural network.

In this paper, we “flag” potentially failing banks are identified using cluster analysis.

III. BANK RATING SYSTEM

Our goal is to cluster banks using their financial data. The data can be obtained from annual reports of the Federal Deposit Insurance Corporation (FDIC). The FDIC is an independent agency created by the Congress of the United States. It insures deposits, examines and supervises financial institutions, and manages receiverships. To assess the overall financial state of a bank, regulators use the CAMELS (Capital adequacy, Asset, Management, Earnings, Liquidity, and Sensitivity to market risk) rating system. The CAMELS ratings have been applied to 8,500 banks in the U.S. It was also used by the United States government in selecting banks for the capitalisation program of 2008.

For our case study, we select 100 banks and obtain their financial data from the FDIC annual report for the last year. We adapt the following five ratings based on the CAMELS system:

1. NITA – Net Income divided by Total Assets. NITA represents return on assets. Failing banks have very low or even negative values of NITA.
2. NLLAA – Net Loan Losses divided by Adjusted Assets. Adjusted assets are calculated by subtracting the total loans from the total assets. Failing banks usually have higher NLLAA values than healthy banks.
3. NPLTA – Non-Performing Loans divided by Total Assets. Non-performing loans consist of loans that have past their due dates by 90 days and non-accrual loans. Failing banks usually have higher values of NPLTA than healthy banks.
4. NLLTL – Net Loan Losses divided by Total Loans. Failing banks have higher loan losses as they often make loans to high-risk borrowers. Thus, failing banks usually have higher values of NLLTL than healthy banks.
5. NLLPLLNI – Sum of Net Loan Losses and Provision for Loan Losses divided by Net Income. The higher the NLLPLLNI value, the poorer the bank performance.

Preliminary investigations of the statistical data can reveal that a number of banks may experience some financial difficulties. Clustering should help us to identify groups of banks with similar problems.

IV. SELF-ORGANISING MAP

Fig. 1 shows a self-organising map (SOM) with a 5-by-5 array of 25 neurons in the Kohonen layer. Note that

neurons in the Kohonen layer are arranged in a hexagonal pattern.

The input data are normalised to be between 0 and 1. The network is trained for 10,000 iterations with a learning rate of 0.1. After training is complete, the SOM forms a semantic map where similar input vectors are mapped close together while dissimilar apart. In other words, similar input vectors tend to excite either the same neuron or neurons closely located to each other in the Kohonen layer. This SOM property can be visualised using the weight distance matrix, also known as the *U-matrix*.

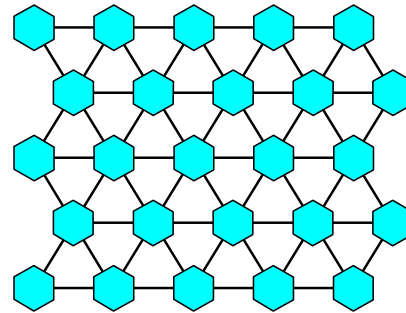
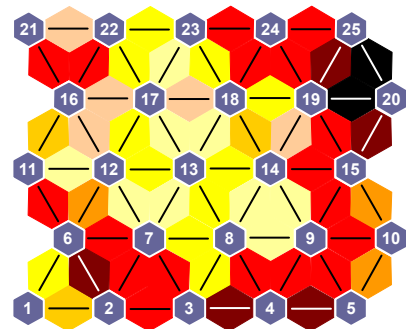
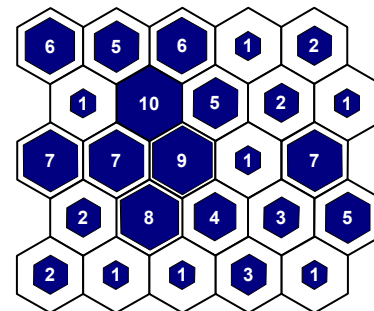


Figure 1. The SOM structure.

Fig. 2 shows the U-matrix and the SOM sample hit plot for the bank financial data. In the U-matrix, the hexagons represent the neurons in the Kohonen layer. The colours in the regions between neighbouring neurons indicate the distances between them – the darker the colour the greater the distance. The SOM sample hit plot reveals how many input vectors are attracted by each neuron of the Kohonen layer.



(a)



(b)

Figure 2. The 5-by 5 SOM after training: (a) the U-matrix; (b) the sample hit plot.

Typically, a SOM identifies fewer clusters than the number of neurons in the Kohonen layer, and thus several input vectors attracted by close neighbouring neurons may, in fact, represent the same cluster. For instance, in Fig. 2(a), we can observe that distances between neurons 3 – 8, 7 – 8, 7 – 12, 7 – 13, 8 – 9, 8 – 13, 8 – 14, 9 – 14, 11 – 12, 12 – 13, 12 – 16, 12 – 17, 13 – 14, 13 – 17, 13 – 18, 14 – 19, 16 – 17, 17 – 18, 17 – 22, 17 – 23, 18 – 19, 18 – 23, 21 – 22 and 22 – 23 are relatively short (the colours in the regions between neighbouring neurons are lighter, so the distances are shorter). Thus, we can reasonably assume that neurons 3, 7, 8, 9, 11, 12, 13, 14, 16, 17, 18, 19, 21, 22 and 23 form a single cluster. At the same time, we should also notice that the distance between neurons 3 and 7 is much greater than the distances between neurons 3 and 8, and 7 and 8. Therefore, it might be useful to examine what makes the input vectors associated with neuron 3 so different from these attracted by neuron 7. Table I shows results of clustering. Interpreting the meaning of each cluster is often a difficult task. Unlike classification where the number of classes is decided beforehand, in SOM-based clustering the number of clusters is unknown, and

assigning a label or interpretation to each cluster requires some prior knowledge and domain expertise.

For a start, we need a way to compare different clusters. As we discussed in Case Study 6, the centre of a cluster often reveals features that separate one cluster from another. Therefore, determining the average member of a cluster should enable us to interpret the meaning of the entire cluster. In Table I, the last column “Financial profile of the cluster” contains mean, median and standard deviation (STD) values of the CAMELS ratings utilised in this study. Using these values an expert can identify groups of banks that exhibit similar patterns of behaviour or experience similar problems.

Let us begin our analysis by identifying problem banks with negative returns on their assets. As can be seen in Table I, three clusters, E, F and G, have negative values of NITA. For example, banks included in Cluster E have mean net losses of 0.06% of their total assets. On the other hand, healthy banks usually report a positive return on their assets. Thus, banks included in Cluster A, which has the highest value of NITA, could be considered healthy.

TABLE I. CLUSTERING RESULTS OF THE 5-BY-5 SOM

Cluster	Size	Neuron number	Financial profile of the cluster								
			NITA			NLLAA			NPLTA		
			Mean	Median	STD	Mean	Median	STD	Mean	Median	STD
A	4	1 6	0.0369	0.0369	0.0043	-0.1793	-0.1340	0.2516	0.0125	0.0100	0.0055
B	1	2	0.0121	0.0121	0	-0.4954	-0.4954	0	0.0323	0.0323	0
C	75	3 7 8 9 11 12 13 14 16 17 18 19 21 22 23	0.0101	0.0094	0.0097	-0.0899	-0.0701	0.1646	0.0153	0.0144	0.0102
D	3	4	0.0066	0.0041	0.0064	0.4448	0.4528	0.0672	0.0190	0.0185	0.0058
E	13	5 10 15	-0.0006	-0.0010	0.0044	0.0363	0.0357	0.0257	0.0205	0.0166	0.0144
F	1	20	-0.0092	-0.0092	0	0.0089	0.0089	0	0.0215	0.0215	0
G	1	24	-0.0060	-0.0060	0	0.0199	0.0199	0	0.0198	0.0198	0
H	2	25	0.0014	0.0015	0.0019	0.0225	0.0225	0.0048	0.0164	0.0164	0.0029

Cluster	Size	Neuron number	Financial profile of the cluster					
			NLLTL			NLLPLLNI		
			Mean	Median	STD	Mean	Median	STD
A	4	1 6	0.0050	0.0057	0.0036	0.2839	0.2839	0.0164
B	1	2	0.0006	0.0006	0	1.1522	1.1522	0
C	75	3 7 8 9 11 12 13 14 16 17 18 19 21 22 23	0.0143	0.0121	0.0093	0.8399	0.6973	0.7252
D	3	4	0.0133	0.0145	0.0068	0.1894	0.1676	0.1617
E	13	5 10 15	0.0388	0.0376	0.0108	8.0965	7.1786	3.9200
F	1	20	0.0055	0.0055	0	9.4091	9.4091	0
G	1	24	0.0662	0.0662	0	0.3612	0.3612	0
H	2	25	0.0740	0.0740	0.0052	10.9785	10.9785	1.2720

Regarding the NLLAA rating, Cluster D has the highest mean value, followed by Cluster E. Note that although banks in Cluster E are problem banks, their NLLAA values are at least 12 times lower than these of Cluster D (a 3.63% mean against 44.48%). This could be a clear indication that the three banks associated with Cluster D experience severe difficulties with their loans (even though they still have a positive return on their assets). Banks in Clusters A, B and C show negative NLLAA values, which is normal for healthy banks.

The value of NPLTA is highest for Cluster B, followed by the problem banks in Clusters E, F and G. This may indicate that the bank in Cluster B (Cluster B is a solitary cluster) experiences difficulties in recovering its loans. In fact, the situation with this particular bank could be even worse than with the problem banks associated with Clusters E, F and G.

Finally, the values of NLLTL and NLLPLLNI are highest for the two banks in Cluster H, followed by the problem banks. Because higher values of NLLTL indicate higher loan losses, we may find that banks in Cluster H are involved in providing loans to high-risk borrowers. High risk-taking also contributed to the poor performance of these banks, reflected by the high NLLPLLNI values.

An important part of cluster analysis is to identify outliers, objects that do not naturally fall into any larger cluster. As can be seen in Table I, there are three banks that are viewed as solitary clusters – Cluster B, Cluster F and Cluster G. These banks are outliers, and each of them has a unique financial profile. While conventional clustering algorithms, such as K-means clustering, do not handle outliers well, a SOM can easily identify them.

It is difficult, however, to determine the number of clusters in a multidimensional data set. In fact, when a clustering algorithm attempts to create larger clusters, outliers are often forced into these clusters. This may result not only in poorer clustering but, even worse, in failing to distinguish unique objects.

As an example, let us cluster the same set of banks using a 2-by-2 SOM. The SOM is trained for 1,000 iterations. Fig. 3 shows the U-matrix and the SOM sample hit plot. Obviously, now we have only four clusters. Further investigation reveals that based on their average values, banks associated with neurons 1, 2 and 3 can be classified as healthy, while 13 banks attracted by neuron 4 as failing. Two failing banks and two banks with unusually high values of NLLPLLNI, previously identified by the 5-by-5 SOM, are now absorbed by the “healthy” cluster.

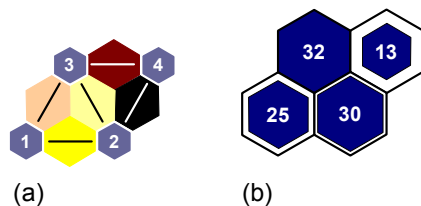


Figure 3. The 2-by 2 SOM after training: (a) the U-matrix; (b) the sample hit plot.

V. SOM TESTING

In order to test a neural network, including a SOM, we need a test set. From the FDIC Annual Report we can obtain a list of failed banks, and collect appropriate financial statement data. Several studies of bank failures suggest that failed banks could be detected between six and 12 months before the call date, and in some cases as early as four years before a bank fails [2], [5]. Although solvency and liquidity are the most important predictors of failure close to the call date, asset quality, earnings and management practices become increasingly significant as the time before failure increases. To test the SOM performance, we select 10 banks that failed last year, and collect their one-year-prior financial statement data. Table II contains mean, median and standard deviation (STD) values of their CAMELS ratings. Now we can apply 10 input vectors to see the SOM response.

As expected, in the 2-by-2 SOM, all 10 input vectors are attracted by neuron 4. In the 5-by-5 SOM, the situation is more complicated. Six input vectors are attracted by neuron 5, two by neuron 10, one by neuron 20 and two by neuron 24. Thus, in both cases, failing banks are clustered correctly.

Finally, a word of caution. Although a SOM is a powerful clustering tool, the exact meaning of each cluster is not always clear, and a domain expert is usually needed to interpret the results. Also a SOM is a neural network, and any neural network is only as good as the data that goes into it. In this case study, we have used only five financial variables. However, to identify problem banks well in advance of their failure, we might need many more variables that hold additional information about bank performance (researchers in the industry use up 29 financial variables based on the CAMELS rating system).

A good example of challenges associated with clustering is given in [3]. A large bank decided to increase its market share in home equity loans. It gathered data on 5,000 customers who had home equity loans and 5,000 customers who did not have them. The data included appraised value of a house, amount of credit available, amount of credit granted, customer age, marital status, number of children and household income. The data was then used to train a SOM. It identified five clusters. One of the clusters was particularly interesting. It contained customers who took home equity loans. These customers were in their forties, married with children in their late teens. The bank assumed that they were taking loans to pay college tuition fees for their children. Thus, the bank organised a marketing campaign to offer home equity loans as a means to pay for college education. However, results of the campaign were disappointing.

Further investigation revealed that the problem was in the interpretation of the clusters identified by the SOM. Consequently, the bank decided to include more information about its customers such as type of accounts, deposit system, credit card system, etc. After retraining the SOM, it was discovered that customers who took home equity loans in addition to being in their forties

TABLE II. FINANCIAL PROFILE OF THE FAILING BANKS

NITA			NLLAA			NPLTA			NLLTL			NLLPLLNI		
Mean	Median	STD	Mean	Median	STD	Mean	Median	STD	Mean	Median	STD	Mean	Median	STD
-0.0625	-0.0616	0.0085	0.0642	0.0610	0.0234	0.0261	0.0273	0.0065	0.0341	0.0339	0.0092	7.3467	6.9641	3.8461

with college-age children often also had business accounts. So, the bank concluded that when children left home to go to college, parents took out home equity loans to start new businesses. The bank organised a new marketing campaign targeting this group of potential customers, and this time the campaign was successful.

VI. CONCLUSIONS

A very large number of bank failures in 2008 triggered a financial crisis. Although unprecedented intervention of central banks and governments helped economies to recover, the global financial systems remains at risk. As a result, identifying failing banks as early as possible is essential. This paper has clearly demonstrated a great potential of a self-organising neural network as a tool for performing this task. The results show that self-organising maps can successfully carry out bank clustering tasks and identify banks that require immediate attention from the regulatory bodies.

REFERENCES

[1] Abrams B. A. and Huang, C. J., 1987. Predicting bank failures: the role of structure in affecting recent failure experiences in the USA, *Applied Economics*, 19, 1291–1302.

[2] Alam, P., Booth, D., Lee K. and Thordarson, T., 2000. The use of fuzzy clustering algorithm and self-organizing neural networks for identifying potentially failing banks: an experimental study, *Expert Systems with Applications*, 18(3), 185–199.

[3] Berry, M. and Linoff, G., 2004. *Data Mining Techniques For Marketing, Sales, and Customer Relationship Management*, 2nd edn., John Wiley & Sons, New York.

[4] Booth D. E., Alam, P., Ahkam, S. N. and Osyk, B., 1989. A robust multivariate procedure for the identification of problem savings and loan institutions, *Decision Sciences*, 20, 320–333.

[5] Eichengreen, B., 2002. *Financial Crises and What to Do About Them*, Oxford University Press.

[6] Espahbodi, P., 1991. “Identification of problem banks and binary choice models”, *Journal of Banking and Finance*, 15(1), 53–71.

[7] Ozkan-Gunay, E. N. and Ozkan, M., 2007. Prediction of bank failures in emerging financial markets: an ANN approach, *Journal of Risk Finance*, 8(5), 465–480.

[8] Tryon, R. C., 1939. *Cluster Analysis*, McGraw-Hill, New York, NY.

[9] Zhang, G., Hu, M. Y., Patuwo, B. E. and Indro, D. C., 1999. Artificial neural networks in bankruptcy prediction: general framework and cross-validation analysis, *European Journal of Operation Research*, 116, 16–32.

A Formal Framework for Modeling Topological Relations of Spatial Ontologies

Sana Châabane, Wassim Jaziri, Faïez Gargouri
 MIRACL Laboratory, ISIM Sfax
 University of Sfax, Tunisia
 {sana.chaabane, jaziri.wassim, faiez.gargouri}@gmail.com

Abstract— A spatial ontology adds to the components of a domain ontology spatial relations and spatial aspects of its concepts. Spatial relations are of two types: the metric relations and topological relations, expressing a link of interconnection between two spatial concepts. In this paper, we propose a formal modeling of topological relations of a spatial ontology. This formal model is called "meta-OntologicalOnto" which is a set of rules written in description logic. The "meta-OntologicalOnto" is used as a reference during the construction of the spatial ontology. The field of application of our work is the road domain whose ultimate goal is to obtain a road ontology named "OntoRoad".

Keywords- Spatial Ontology; topological relations; road domain; formal rules; meta-OntologicalOnto; OntoRoad.

I. INTRODUCTION

A geographical object is an object modeling a real-world phenomenon. It is described by semantic data and geometric data. The building of spatial ontologies should allow modeling of all properties of spatial objects to meet users' needs. This makes the problem of constructing spatial ontologies more complex than those of other domain ontologies.

The most known definition of ontology [1] is: ontology is a specification of a conceptualization of a knowledge domain. This definition shows that domain ontology must have a formal aspect. Spatial domain ontology consists of concepts with a spatial aspect and spatial relations. Spatial aspect of a concept means its graphic shape: Point, Line or Polygon. Spatial relations are of two types: the metric relations expressing a value of distance or proximity between two objects, as beside, near, etc.... between two objects, and topological relations expressing a link of interconnection between two spatial objects. Topological relations are characterized by the property to be preserved under topological transformations and describe whether features intersect or not, how they intersect, and concepts of overlap, neighborhood and inside. They are important for numerous practical applications that involve spatial query, spatial analysis and spatial reasoning. Referring to the ontology definition, it is essential to use formal methods to identify and define topological relations in spatial ontologies.

The formalization of spatial relations is an active research field and numerous works deal with the recognition of pertinent topological relations. The core models in this domain are the Calculus Based Model (CBM) [2], the 9-Intersections Model (9IM) [3] and the Region Connection Calculus (RCC) [4]. All these approaches satisfy the

requirements that they provide a sound and complete set of topological relations between two spatial objects.

In N-intersection models, a mathematical model, called Four-Intersection Model (4IM) [5] that classifies topological relations based on the content of the four intersections between the boundaries and interiors of the two simple geometric features, was derived. A number of variants of this model were derived, including Dimension Extended Method (DEM) [2] that takes the dimension of the intersection components into account, Nine-Intersection Model (9-IM) [3] that categorizes binary topological relations based on the comparison of nine intersections between the interiors, boundaries and exteriors of the two features and finally Dimensionally Extended Nine-Intersection model (DE-9IM) [6] that introduces the dimension of the intersections into 9IM.

The binary topological relation between two objects (A and B) in [5], is based upon the intersection of A's interior (A°), boundary (∂A), and exterior (A^-) with B's interior (B°), boundary (∂B), and exterior (B^-). The nine intersections between the six object parts describe a topological relation that can be concisely represented by a 3-3 matrix, called the 9-intersection model.

$$\begin{pmatrix} \partial A \cap \partial B & \partial A \cap B^\circ & \partial A \cap B^- \\ A^\circ \cap \partial B & A^\circ \cap B^\circ & A^\circ \cap B^- \\ A^- \cap \partial B & A^- \cap B^\circ & A^- \cap B^- \end{pmatrix} \emptyset \text{ or } \neg \emptyset \tag{1}$$

By considering the values empty (\emptyset) and non empty ($\neg \emptyset$), one can distinguish between $2^9=512$ binary topological relations. Only a small subset of them can be realized when the objects of concern are embedded [7] [19]. There is a set which provides a mutually exclusive and complete coverage of topological relations between two regions (Fig. 1), termed {Disjoint, Meet, Overlap, equal, Contains, Inside, Covers and coveredBy} [8].

			
$\begin{pmatrix} 0 & 0 & 1 \\ 0 & 0 & 1 \\ 1 & 1 & 1 \end{pmatrix}$	$\begin{pmatrix} 1 & 1 & 1 \\ 0 & 0 & 1 \\ 0 & 0 & 1 \end{pmatrix}$	$\begin{pmatrix} 1 & 0 & 0 \\ 1 & 0 & 0 \\ 1 & 1 & 1 \end{pmatrix}$	$\begin{pmatrix} 1 & 0 & 0 \\ 0 & 1 & 0 \\ 0 & 0 & 1 \end{pmatrix}$
disjoint	contains	inside	equal
			
$\begin{pmatrix} 0 & 0 & 1 \\ 0 & 1 & 1 \\ 1 & 1 & 1 \end{pmatrix}$	$\begin{pmatrix} 1 & 1 & 1 \\ 0 & 1 & 1 \\ 0 & 0 & 1 \end{pmatrix}$	$\begin{pmatrix} 1 & 0 & 0 \\ 1 & 1 & 0 \\ 1 & 1 & 1 \end{pmatrix}$	$\begin{pmatrix} 1 & 1 & 1 \\ 1 & 1 & 1 \\ 1 & 1 & 1 \end{pmatrix}$
meet	covers	coveredBy	overlap

Figure 1. The eight topological relations between two spatial regions and their corresponding 9-intersection matrices [2].

The RCC8 model [4] is composed of 8 Jointly Exhaustive and Pairwise Disjoint (JEPD) base topological relations between two spatial regions A and B. These relations are based on the binary primitive $C(A,B)$, which means A is connected to B. In the RCC8 context, $C(A,B)$ is interpreted as being true when the closure of A and B share a point, where A and B are viewed as sets of points. The only requirement for the relation C is that it is reflexive and symmetric. Using $C(A,B)$ a large number of relations can be defined [4]. The set of eight relations {DC, EC, PO, EQ, TPP, NTPP, TPPi, NTPPi} constitutes the set of the RCC8 relations (see Table 1). They are invariant with respect to geometric transformations. It is possible to add more expressiveness to the RCC relations by introducing additional primitives. In [4], 23 relations are defined by adding the convex hull as another primitive. This extension allows distinguishing different types of “inside” a region. In the context of [4], a region is said to be inside another one when it is connected to its convex hull, but the regions do not overlap.

TABLE I. : SOME OF THE RELATIONS DEFINED BY $C(A,B)$.

Relation	Interpretation	Definition of $R(A,B)$
$DC(A,B)$	A is disconnected from B	$\neg C(A,B)$
$P(A,B)$	A is a part of B	$\forall D[C(D,A) \rightarrow C(D,B)]$
$PP(A,B)$	A is a proper part of B	$P(A,B) \wedge \neg P(B,A)$
$EQ(A,B)$	A is identical with B	$P(A,B) \wedge P(B,A)$
$O(A,B)$	A overlaps B	$\exists D[P(D,A) \wedge P(D,B)]$
$DR(A,B)$	A is discrete from B	$\neg O(A,B)$
$PO(A,B)$	A partially overlaps B	$O(A,B) \wedge \neg P(A,B) \wedge \neg P(B,A)$
$EC(A,B)$	A is externally connected to B	$C(A,B) \wedge \neg O(A,B)$
$TPP(A,B)$	A is a tangential proper part of B	$PP(A,B) \wedge \exists D[EC(D,A) \wedge EC(D,B)]$
$NTPP(A,B)$	A is a non-tangential proper part of B	$PP(A,B) \wedge \exists D[EC(D,A) \wedge EC(D,B)]$
$TPPi(A,B)$	B is a tangential proper part of A	$PP(B,A) \wedge \exists D[EC(D,B) \wedge EC(D,A)]$
$NTPPi(A,B)$	B is a non-tangential proper part of A	$PP(B,A) \wedge \exists D[EC(D,B) \wedge EC(D,A)]$

The CBM [2] offers a small set of topological relations with high expressiveness: { Touch, In, Cross, Overlap, Disjoint} and three boundary operators, which are proved to be mutually exclusive and complete. The capability of CBM is equivalent to DE-9IM [6].

Through the analysis of literature, it can be found that the numbers of topological relations differentiated by these models can only indicate the capacities of the models but nothing about a complete spectrum of all possible topological relations. For example, there should be infinite number of topological relations for a line and a region. To overcome the deficiency of these general models, efforts have also been made to develop dedicated models to specific types of features, e.g., line-line relations [9, 10], region-region relations [11, 12] and Line-region relations [13].

The field of our works is the road domain; we are therefore interested in topological relations supposed being relevant in this domain. This paper presents the topological relations considered by our approach of building spatial ontologies and formally defines these relations.

In the first part of this paper, we present an approach of building spatial ontologies which defines a process of building adding a new step of spatialization [18] to the process of building domain ontologies [14]. In the second part of this paper, we present the formal definitions of topological relations written in descriptive logic. We

end this paper with a conclusion and future works we intend to achieve.

II. APPROACH OF BUILDING A SPATIAL ONTOLOGY

Several studies have been carried on methods for building ontologies [21]. We propose an approach for building spatial ontologies that defines a process of building with two application phases: meta-modeling phase and modeling phase. The first phase of meta-modeling defines, for each step, a meta-model that will serve as a reference then during the second phase of modeling of the process. The proposed process is based on the steps of the building process of domain ontology [14] and adds an intermediate step of definition and explanation of spatial relations within geographic applications. To this end, our approach is based on the following four steps: conceptualization, Spatialization, ontologization and Operationalization. (Fig. 2) presents the process of building spatial ontologies.

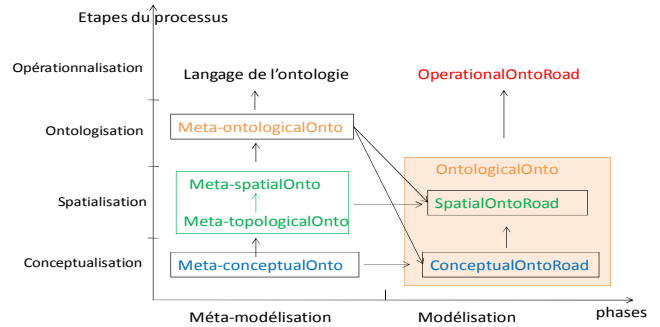


Figure 2. Process of building spatial ontologies.

The first phase of meta-modeling is to define, for every step of ontology construction, a meta-model that will serve as reference in the subsequent phase. The conceptualization step is to identify a body in the knowledge domain and to clarify the conceptual nature (concepts, relations, properties and relations of concepts, rules, constraints, etc.) of extracted knowledge from the corpus. The use of object-oriented paradigm for the conceptualization of the geographical world has been widely discussed in the literature [17]. It consists of definition of geographical object, their attributes and their relations. We proceeded to study the nature of knowledge may exist in a spatial ontology and we considered that it is important that a spatial ontology consists of a set of concepts characterized by their names and relations between concepts. Relations are those supported by the Unified Modeling Language (UML) [23] namely association, aggregation, composition and generalization.

The spatialization step is to give tow points: a spatial dimension to the concepts of ontology and to clarify the spatial relations between them. The spatial aspect of a concept is reflected in the graphic form of this concept: Line, Point or Polygon. Then we classify the ontology concepts according to their graphic shapes. A Point

is characterized by a name, an abscissa and an ordinate. A Line is characterized by a name, two points: an initial section (is) and an end section (es), a direction, a length and a height. A Polygon is characterized by a name and at least three points which form its extremities. Spatial relations are of two types: metric relations and topological relations. Metric relations fall into two classes: distance relations that express a value of distance and unit of measure; and proximity relations that express an approximate distance between two spatial objects. We characterize a topological relation between two spatial concepts by the graphic form of the intersection of these two concepts. To represent these relations we use the formalism of connection to express that two geographical entities share a geographical space. Each topological relation is modeled graphically in [15] to show the graphic shape of the intersection of two spatial objects. (Table 2) lists all topological relations supported supported by our approach.

TABLE II. SUPPORTED TOPOLOGICAL RELATIONS.

Graphic Form Topological relation	Point /Point t	Point /Line	Point/ Polygon	Line/ Line	Line/ Polygon	Polygon/ Polygon
Equality	x			x		x
Extremity		x				
Inclusion		x	x	x	x	x
Connection			x		x	x
Junction				x		
Joint				x		
Meet				x	x	
Adjacency				x	x	
Superposition				x		
Partial-Recovery						x

These relations are represented as a graph called "Meta-topologicalOnto" (Fig. 3). In this meta-model, classes represent the graphic shapes of one concept including: Point, Line or Polygon; and relations represent the topological relations considered in our ontology. After considering the spatial relations of our ontology we proceeded to define the spatial meta-model "meta-SpatialOnto" which extends the conceptual model [16] with spatial relations.

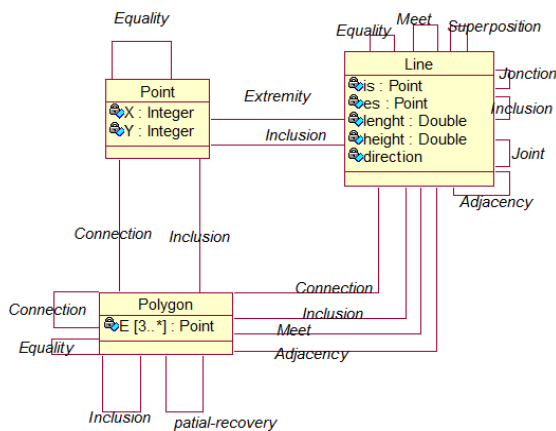


Figure 3. Topological meta-model of a spatial ontology: "Meta-topologicalOnto".

The third step of the process of building a spatial ontology is the ontologization step. It consist to model in a formal language the domain properties, the objective is to obtain a model in which almost all the ambiguities inherent in natural language are lifted. Finally, the operationalization is to make operational or functional ontology. First, must select the ontology language and the tool to build the ontology.

The modelling phase depends on the domain of the ontology and consists to define, for each step of the process of building, a model containing the concepts and relations of the domain. The result of this phase is a model of a spatial ontology instantiable depending on the user data. We chose the road domain as field of application of our work. The result ontology is called "OntoRoad".

We focus in this paper on the metamodeling phase of the ontologization step of process of building a spatial ontology, especially we focus on topological relations of spatial ontology. Next section will present the formal definitions of supported topological relations.

III. FORMAL DEFINITIONS OF TOPOLOGICAL RELATIONS

Various studies have formally defines topological relations between spatial objects [19] [20] [22]. However, new needs of expressing these relations otherwise have arisen, including the need to express the type of the graph entity resulting of the intersection of the objects involved in the topological relation.

We define usage rules and we formally written topological relations of the ontology using the descriptive logic, the set of these rules and these formal definitions is called a formal meta-model of a spatial ontology "meta-OntologicalOnto".

We define the graphical shapes of a spacial object namely: Point, Line and Polygon as structures of objects. Thus we write:

Rule 1: a Point is characterized by a name of string and an x and y coordinates of integer:

$$\text{Point: } \left\{ \begin{array}{l} \text{name: String} \\ x: \text{entier} \\ y: \text{entier} \end{array} \right\} \tag{1}$$

Rule 2: A Line is characterized by a name of string, by the properties ds: start of section and fs: end of section of Point, a height of integer and a direction that takes a value of the Direction Set which is defined by:

Direction = {East, Weast, North, South, North-East, North-Weast, South-East, South-Weast}

$$\text{Line: } \left\{ \begin{array}{l} \text{Name: String} \\ \text{ds: Point} \\ \text{fs: Point} \\ \text{direction: Direction} \\ \text{heigt: Integer} \end{array} \right\} \tag{2}$$

Rule 3: A Polygon is characterized by a name of string and five extremities of Point: e1, e2, e3, e4 and e5.

$$\text{polygon: } \left\{ \begin{array}{l} \text{name : String} \\ \text{e1 : Point} \\ \text{e2 : Point} \\ \text{e3 : Point} \\ \text{e4 : Point} \\ \text{e5 : Point} \end{array} \right\} \quad (3)$$

To define the formal definitions of spatial relations we consider: C1, C2: two spatial concepts; P1, P2: two variables of Point; G1, G2: two variables of Polygon; L1, L2: two variables of Line. We also consider the sets: E1 and E2, where E1 = {e1, e2, e3, e4, e5} representing the extremities of G1 and E2 = {e'1, e'2, e'3, e'4, e'5} representing the extremities of G2.

Rule 4: Equality (C1, C2) is a relation which holds between two spatial concepts C1 and C2 if and only if the intersection of C1 and C2 is equal to the concept itself. Then, we write:

$$\text{Equality}(C1, C2) \Leftrightarrow (C1 \cap C2 = (C1 \vee C2)) \wedge \left(\begin{array}{l} C1, C2: \text{Point} \wedge C1.\text{name} = C2.\text{name} \wedge \\ C1.x = C2.x \wedge C1.y = C2.y \\ C1, C2: \text{Ligne} \wedge C1.\text{name} = C2.\text{name} \wedge \\ C1.\text{ds} = C2.\text{ds} \wedge C1.\text{fs} = C2.\text{fs} \\ C1, C2: \text{Polygone} \wedge C1.\text{name} = C2.\text{name} \wedge \\ C1.E1 = C2.E2 \end{array} \right) \vee \quad (4)$$

Equality(C1, C2) is transitive :

$$\text{Equality}(C1, C2) \wedge \text{Equality}(C2, C3) \Rightarrow \text{Equality}(C1, C3) \quad (5)$$

Equality(C1, C2) is symmetric:

$$\text{Equality}(C1, C2) \Leftrightarrow \text{Equality}(C2, C1) \quad (6)$$

Rule 5: Extremity(P1, L1) is a relation which holds between two concepts P1 and L1 of respective graphic shapes Point and Line, if and only if the intersection of P1 and L1 is equal to P1 and P1 is one extremity of L1. Then, we write:

$$\text{Extremity}(P1, L1) \Leftrightarrow L1 \cap P1 = P1 \wedge (\text{Equality}(L1.\text{ds}, P1) \vee \text{Equality}(L1.\text{fs}, P1)) \quad (7)$$

Extremity(P1, L1) is not transitive.

Extremity(P1, L1) is not symmetric.

Rule 6: Inclusion (P1, L1) is a relation which holds between two spatial concepts P1 and L1 of respective graphic shapes Point and Line if and only if the intersection of P1 and L1 is equal to P1 and the function Linear(P1, L1.ds, L1.fs) is satisfied. Linear() is a mathematical function which checks that three points are linear. This function is defined as follows:

considering P1, P2 and P3 three points with respective coordinates (x, y), (x', y') and (x'', y'');

$$\text{Linear}(P1, P2, P3) \Leftrightarrow (x - x'') * (y' - y'') - (x' - x'') * (y - y'') = 0 \quad (8)$$

Then, we write:

$$\text{Inclusion}(P1, L1) \Leftrightarrow P1 \cap L1 = P1 \wedge \text{Linear}(P1, L1.\text{ds}, L1.\text{fs}) \quad (9)$$

Inclusion(P1, L1) isn't transitive.

Inclusion(P1, L1) is not symmetric.

Rule 7: Connection(P1, G1) is a relation which holds between two spatial concepts P1 and G1 of respective graphic shapes point and Polygon if and only if the intersection of P1 and G1 is equal to P1 and P1 belongs to the extremities of G1. Then, we write:

$$\text{Connexion}(P1, G1) \Leftrightarrow (P1 \cap G1 = P1) \wedge P1 \in G1.E \quad (10)$$

Connection(P1, G1) isn't transitive.

Connection(P1, G1) isn't symmetric.

Rule 8: Inclusion(P1, G1) is a relation which holds between two spatial concepts P1 and G1 of respective graphic shapes point and Polygon if and only if the intersection of P1 and G1 is equal to P1 and the relation Inclusion (P1, Rect(G1)) is true.

In order to check if a point belongs to a polygon G1, we use the concept of the minimum bounding rectangle which is defined as the smallest rectangle containing the geometry of an object. The sides of the rectangle can be oriented parallel to the x axis and the y axis, we obtain the minimum bounding rectangle x, y. The bounding polygon of G1 is named Rect(G1) defined by [Xmin, Xmax, Ymin, Ymax] Then we write:

$$\text{Inclusion}(P1, G1) \Leftrightarrow P1 \cap G1 = P1 \wedge (Xmin < P1.x < Xmax) \wedge (Ymin < P1.y < Ymax) \quad (11)$$

Inclusion(P1, G1) is not transitive.

Inclusion(P1, G1) is not symmetric.

Rule 9: Inclusion (L1, L2) is a relation which holds between two spatial concepts L1 and L2 of line graphic shapes is verified if and only if the intersection of L1 and L2 is equal to L1; and the extremities of L1 admit an Inclusion () relation with L2. Then, we write:

$$\text{Inclusion}(L1, L2) \Leftrightarrow (L1 \cap L2 = L1) \wedge \text{Inclusion}(L1.\text{ds}, L2) \wedge \text{Inclusion}(L1.\text{fs}, L2) \quad (12)$$

Inclusion(L1, L2) is transitive.

$$Inclusion(L1, L2) \wedge Inclusion(L2, L3) \Rightarrow Inclusion(L1, L3) \quad (13)$$

Inclusion(L1, L2) is not symmetric.

Rule 10: Joint(L1, L2) is a relation which holds between two spatial concepts L1 and L2 of Line graphic shapes is satisfied if and only if the intersection of L1 and L2 is equal to a point P1 which is the extremity of both L1 and L2. Then, we write:

$$Joint(L1, L2) \Leftrightarrow (L1 \cap L2 = P1) \wedge Extremity(P1, L1) \wedge Extremity(P1, L2) \quad (14)$$

Joint(L1, L2) isn't transitive.
Joint(L1, L2) is symmetric :

$$Joint(L1, L2) \Leftrightarrow Joint(L2, L1) \quad (15)$$

Rule 11: Junction (L1, L2) is a relation which holds between two spatial concepts L1 and L2 of line graphic shapes is verified if and only if the intersection of L1 and L2 is equal to a point P1 which is neither an extremity of L1 nor of L2. Then, we write:

$$Junction(L1, L2) \Leftrightarrow (L1 \cap L2 = P1) \wedge Inclusion(P1, L1) \wedge Inclusion(P1, L2) \wedge \neg Extremity(P1, L1) \wedge \neg Extremity(P1, L2) \quad (16)$$

Junction(L1, L2) isn't transitive.
Junction(L1, L2) is symmetric :

$$Junction(L1, L2) \Leftrightarrow Junction(L2, L1) \quad (17)$$

Rule 12: Meet(L1, L2) is a relation which holds between two spatial concepts L1 and L2 of Line graphic shapes is satisfied if and only if the intersection of L1 and L2 is equal to a point which is equal to one extremity of L1. Then, we write:

$$Meet(L1, L2) \Leftrightarrow (L1 \cap L2 = P1) \wedge Extremity(P1, L1) \wedge Inclusion(P1, L2) \quad (18)$$

Meet(L1, L2) isn't transitive.
Meet(L1, L2) isn't symmetric.

Rule 13: Adjacency (L1, L2) is a relation which holds between two spatial concepts L1 and L2 of line graphic shapes is verified if and only if the intersection of L1 and L2 is equal to a line L3 and the L3 extremities are equal to L1 or L2 extremities. Then, we write:

$$Adjacency(L1, L2) \Leftrightarrow L1 \cap L2 = L3 \wedge \{L3. ds, L3. fs\} \equiv (\{L1. ds, L1. fs\} \vee \{L2. ds, L2. fs\}) \quad (19)$$

Adjacency (L1, L2) isn't transitive.
Adjacency (L1, L2) is symmetric:

$$Adjacency(L1, L2) \Leftrightarrow Adjacency(L2, L1) \quad (20)$$

Rule 14: Superposition (L1, L2) is a relation which holds between two spatial concepts L1 and L2 of line graphic shapes is verified if and only if L1 has a height different to zero and L1 extremities belong to L2. Then, we write:

$$Superposition(L1, L2) \Leftrightarrow (L1. height \neq 0 \wedge Inclusion(L1. ds, L2) \wedge Inclusion(L1. fs, L2)) \quad (21)$$

Superposition(L1, L2) isn't transitive.
Superposition(L1, L2) isn't symmetric.

Rule 15: Inclusion (L1, G1) is a relation which holds between two spatial concepts L1 and G1 of respective graphic shapes line and polygon is satisfied if and only if the intersection of L1 and G1 is equal to L1 and L1 extremities admit Inclusion() relation with G1. Then, we write:

$$Inclusion(L1, G1) \Leftrightarrow L1 \cap G1 = L1 \wedge Inclusion(L1. ds, G1) \wedge Inclusion(L1. fs, G1) \quad (22)$$

Inclusion(L1, G1) is not transitive.
Inclusion(L1, G1) is not symmetric.

Rule 16: Meet(L1, G1) is a relation which holds between two spatial concepts L1 and G1 of respective graphic shapes Line and polygon is satisfied if and only if the intersection of L1 and G1 is equal to a point which is one of the extremities of L1 and the other extremity of L1 does not admit Inclusion() relation with G1. Then, we write:

$$Meet(L1, G1) \Leftrightarrow L1 \cap G1 = P1 \wedge ((L1. ds = P1 \wedge \neg Inclusion(L1. fs, G1)) \vee (L1. fs = P1 \wedge \neg Inclusion(L1. ds, G1))) \quad (23)$$

Meet (L1, G1) is not transitive.
Meet (L1, G1) is not symmetric.

Rule 17: Adjacency (L1, G1) is a relation which holds between two spatial concepts L1 and G1 of respective graphic shapes line and polygon is satisfied if and only if the intersection of L1 and G1 is equal to a line L2 which extremities belong to G1 extremities and the extremities of L1 do not admit Inclusion() relation with G1. Then, we write:

$$Adjacency(L1, G1) \Leftrightarrow L1 \cap G1 = L2 \wedge \exists \{e1, e2\} \subset E1 \wedge \{L2. ds, L2. fs\} = \{e1, e2\} \wedge \neg Inclusion(L1. ds, G1) \wedge \neg Inclusion(L1. fs, G1) \quad (24)$$

Adjacency (L1, G1) is not transitive.
Adjacency (L1, G1) is not symmetric.

Rule 18: Connection(L1, G1) is a relation which holds between two spatial concepts L1 and G1 of respective graphic shapes line and polygon is satisfied, if and only if the intersection of L1 and G1 is equal to a line L2 and at least one of the extremities of L1 doesn't admit *Inclusion()* relation with G1. Then, we write:

$$\begin{aligned} \text{Connection}(L1, G1) &\Leftrightarrow L1 \cap G1 \\ &= L2 \wedge \text{Inclusion}(L2. ds, G1) \\ &\wedge \text{Inclusion}(L2. fs, G1) \wedge \exists P: \text{Point} (P \\ &\in \{L1. ds, L1. fs\} \wedge \neg \text{Inclusion}(P, G1)) \end{aligned} \quad (25)$$

Connection(L1, G1) is not transitive.
Connection(L1,G1) is not symmetric.

Rule 19: Inclusion (G1, G2) is a relation which holds between two spatial concepts G1 and G2 of polygon graphic shapes if and only if the intersection of the two concepts G1 and G2 is equal to G1 and all the extremities of G1 admit an *Inclusion()* relation with G2. Then, we write:

$$\begin{aligned} \text{Inclusion}(G1, G2) &\Leftrightarrow G1 \cap G2 = G1 \wedge \forall e \in \\ E1 \text{ Inclusion}(e, G2) \end{aligned} \quad (26)$$

Inclusion(G1,G2) is transitive :

$$\text{Inclusion}(G1, G2) \wedge \text{Inclusion}(G2, G3) \Rightarrow \text{Inclusion}(G1, G3) \quad (27)$$

Inclusion(G1,G2) is not symmetric.

Rule 20: *Connection*(G1, G2) is a relation which holds between two spatial concepts of polygon graphic shapes if and only if the intersection of G1 and G2 is equal to a point belonging to the extremities of both G1 and G2, the other extremities of G1 do not belong to G2 and other extremities of G2 do not belong to G1. Then, we write:

$$\begin{aligned} \text{Connection}(G1, G2) &\Leftrightarrow G1 \cap G2 = P1 \wedge (P1 \in G1. E \wedge \\ P1 \in G2. E) \wedge (\forall e \in E1 - P1, \neg \text{Inclusion}(e, G1)) \wedge \\ (\forall e \in E2 - P1, \neg \text{Inclusion}(e, G2)) \end{aligned} \quad (28)$$

Connection (G1, G2) is not transitive.
Connection (G1, G2) is symmetric:

$$\text{Connection}(G1, G2) \Leftrightarrow \text{Connection}(G2, G1) \quad (29)$$

Rule 21: Adjacency (G1, G2) is a topological relation which is satisfied between two spatial concepts G1 and G2 of polygon graphic shapes if and only if the intersection of G1 and G2 is equal to a line L1 and the extremities of L1 belong to the extremities of both G1 and G2. Then, we write:

$$\text{Adjacency}(G1, G2) \Leftrightarrow G1 \cap G2 = L1 \wedge \exists \{e1, e2\} \subset E1, \{e1, e2\} \subset E2 \wedge \{L1. ds, L1. fs\} = \{e1, e2\} \quad (30)$$

Adjacency(G1,G2) is not transitive.
Adjacency(G1,G2) is symmetric:

$$\text{Adjacency}(G1, G2) \Leftrightarrow \text{Adjacency}(G2, G1) \quad (31)$$

Rule 22: Partial-Recovery(G1, G2) is a topological relation which holds between two spatial concepts G1 and G2 of polygon graphic shapes if and only if the intersection of G1 and G2 is equal to a polygon G3 and there is at least one extremity e1 of G1 admitting *Inclusion()* relation with G2 and there is at least one extremity e'1 of G2 admitting an *Inclusion()* relation with G1 and $\{e1, e'1\} \subset E3$ (Extremities of G3). Then, we write:

$$\begin{aligned} \text{Partial - Recovery}(G1, G2) &\Leftrightarrow G1 \cap G2 = G3 \wedge \exists e1 \in \\ E1, e1 \in E2, \{e1, e'1\} \subset E3, \text{Inclusion}(e1, G2) \wedge \\ \text{Inclusion}(e1, G1) \end{aligned} \quad (32)$$

Partial-Recovery (G1,G2) isn't transitive.
Partial-Recovery (G1,G2) is symmetric:

$$\text{Partial - Recovery}(G1, G2) \Leftrightarrow \text{Partial - Recovery}(G2, G1) \quad (33)$$

IV. CONCLUSION AND FUTURE WORK

In this paper, we presented an approach of building spatial ontologies, which defines a process of building realised in two phases: the meta-modelling phase and the modelling phase. Then, we detailed, the meta-modeling phase of the ontologization step of the process of building a spatial ontology. The result of this step is an ontological meta-model "meta-OntologicalOnto" representing the formal definitions of topological relations of the ontology using description logic. In future work, we will define the modeling phase of the building process of a spatial ontology. This phase depends on the field of study and refers to the meta-modeling phase to define the models of the ontology. Our approach is applied to the road domain to give as a result a road ontology named "OntoRoad" which will be instantiated with data from several geographic areas of Sfax city in Tunisia in purposes of geo-localization.

REFERENCES

- [1] T. Gruber, "A translation Approach to portable ontology specification". Knowledge Acquisition, vol. 5, pp. 199-220, 1993.
- [2] E. Clementini, P. Di Felice, and P. van Oosterom, "A Small Set of Formal Topological Relationships Suitable for End-User Interaction," in Advances in Spatial Databases - Third International Symposium, SSD '93. vol. 692, D. Abel and B. C. Ooi, Eds. Berlin: Springer-Verlag, 1993, pp. 277-295.
- [3] Max J. Egenhofer, "Reasoning about binary topological relations", in Proceedings of the 2^{ed} Symposium on Large Spatial Databases, Lecture Notes in Computer Science, No.523, pp.143-160, Springer-Verlag, 1991.

- [4] Cohn, A. G. B. Bennett, J. Gooday, and N. M. Gotts, "Qualitative spatial representation and reasoning with the region connection calculus." *GeoInformatica* 1, 1997, pp. 275–316.
- [5] Max J. Egenhofer, "A formal definition of binary topological relationships," 3rd International Conference, FODO 1989 on Foundations of Data Organization and Algorithms. New York, NY, USA: Springer-Verlag New York, Inc. pp. 457–472, 1989.
- [6] Eliseo Clementini and Paolino Di Felice, "A comparison of methods for representing topological relationships," *Information Sciences—Applications: An International Journal archive* Volume 3 Issue 3, pp. 149 – 178, May 1995.
- [7] Max J. Egenhofer, and J. Herring, "A mathematical framework for the definition of topological relationships," Fourth International Symposium on Spatial Data Handling, pp. 803–813, 1990.
- [8] Max J. Egenhofer, and R. D. Franzosa, "Point-set topological spatial relations." *International Journal of Geographical Information Science* 5, 1991, pp. 161–174.
- [9] Eliseo Clementini, and Paolino Di Felice, "Topological invariants for lines," *IEEE Transactions on Knowledge and Data Engineering*, 10(1), pp. 38-54, 1998.
- [10] Z. L. Li, and M. Deng, "A hierarchical approach to the line-line topological relations," *Progress in Spatial Data Handling*, Springer-Verlag Berlin Heidelberg, pp. 365-382, 2006.
- [11] M. Deng, T. Cheng, X. Chen and Z. L. Li, "Multi-level topological relations between spatial regions based upon topological invariants". *GeoInformatica*, 11(2), 2007, pp. 239-267.
- [12] Max J. Egenhofer, and R. Franzosa, "On the equivalence of topological relations," *International Journal of Geographical Information Systems*, 9(2), 1995, pp. 133-152.
- [13] M. Deng "A hierarchical representation of line-region topological relations," *The International Archives of the Photogrammetry, Remote Sensing and Spatial Information Sciences*. Vol. VII. Part B2. Beijing 2008.
- [14] N. Noy, D. McGuinness, "Ontology Development: A Guide to Creating Your First Ontology," Stanford Medical Informatics Report, SMI-2001.
- [15] Sana Châabane, Wassim Jaziri, Faïez Gargouri, "OntoRoad: Spatial Ontology for the Road Domain," *Journées Francophones sur les Ontologies (JFO'2008)* Lyon, France, pp. 135-144, Décembre 2008.
- [16] Sana Châabane, Faïez Gargouri, « Toward the foundation of building spatial ontologies»: *International Journal Of Metadata, Semantics and Ontologies* 2013. Copyright 2013 Inderscience Enterprises Ltd, unpublished.
- [17] F. Fonseca, Max J. Egenhofer and G. Câmara, "Using Ontologies in Integrated Geographic Information Systems". *Transactions in GIS* Vol 6, N° 3, 2002.
- [18] Sana Châabane and Wassim Jaziri, "Meta-modélisation du processus de construction d'ontologies géographiques Application au domaine routier »; *International Conference on Web and Information Technologies (ICWIT 09)*, Kerkennah Islands, Tunisia, pp. 653-661, 2009.
- [19] D. V. Pullar and Max J. Egenhofer, "Toward formal definitions of topological relations among spatial objects", *The third International Symposium on Spatial Data Handling*, Sydney, Australia, pp. 225-241, 1988.
- [20] T. Ubeda, "Contrôle de la qualité spatiale dans les bases de données géographiques : Cohérence topologique et corrections d'erreurs", Thesis supported at INSA of Lyon, 1997.
- [21] Fléty Yann, Sède-Marceau and Marie-Hélène, "Vers une géo-ontologie pour les Systèmes Énergétiques Territoriaux », *Ontologie et dynamique des systèmes complexes*, XVIème rencontres de Rochebrune, January 2009, Megève.
- [22] V. M. Zurita, "Semantic-based Approach to Spatial Data Sources Integration", Thesis supported at Universitat Politècnica de Catalunya, Juin 2004.
- [23] James Rumbaugh, Ivar Jacobson, Grady Booch. "The Unified Modeling Language", Reference Manual. Addison-Wesley, 1998.

Requirements and Matching Software Technologies for Sustainable and Agile Manufacturing Systems

Daniël Telgen, Leo van Moergestel, Erik Puik, and Pascal Muller
 Dept. of Micro Systems Technology and Embedded Systems,
 HU University of Applied Sciences Utrecht
 Nijenoord 1, 3552AS Utrecht, The Netherlands
 {Daniel.Telgen, Leo.vanMoergestel, Erik.Puik,
 Pascal.Muller}@hu.nl

John-Jules Meyer
 Dept. of Information and Computing Sciences
 Utrecht University
 Princetonplein 5, 3584 CC Utrecht, The Netherlands
 J.J.C.Meyer@uu.nl

Abstract—Sustainable and Agile manufacturing is expected of future generation manufacturing systems. The goal is to create scalable, reconfigurable and adaptable manufacturing systems which are able to produce a range of products without new investments into new manufacturing equipment. This requires a new approach with a combination of high performance software and intelligent systems. Other case studies have used hybrid and intelligent systems in software before. However, they were mainly used to improve the logistic processes and are not commonly used within the hardware control loop. This paper introduces a case study on flexible and hybrid software architecture, which uses prototype manufacturing machines called *equiplets*. These systems should be applicable for the industry and are able to dynamically adapt to changes in the product as well as changes in the manufacturing systems. This is done by creating self-configurable machines which use intelligent control software, based on agent technology and computer vision. The requirements and resulting technologies are discussed using simple reasoning and analysis, leading to a basic design of a software control system, which is based on a hybrid distributed control system.

Keywords—Sustainable Manufacturing; Agile Manufacturing; Agent Technology; Hybrid Systems; Multi Agent Systems.

I. INTRODUCTION

Sustainability and flexibility are growing more important by the day. A changing economy, technological progress and a decline of world resources fuel these needs. At the same time, consumer expectations are rising. A new phone is bought almost every year and of course preferably in the color and coating of your choice. To make this possible there is a need for more flexibility in manufacturing and a shorter time to market. The term used for this fast and flexible type of production is *Agile Manufacturing* [7]. Agile Manufacturing calls for automated flexible production which is still cost-effective. To achieve this, a change is required from original Dedicated Manufacturing Systems (DMS), i.e., classic production lines [1]. Sustainability is another important consideration in addition to agility. Not only should the products be more sustainable for the new generation of manufacturing systems, but the manufacturing systems themselves are required to be sustainable as well. This is achieved by developing machines which can build generations of different product families on small to medium scale rather than just one product. This will require a new and more flexible approach for manufacturing, hence it is necessary to create manufacturing systems that can be reconfigured for the latest demand. To be able to produce small to medium quantities and still be cost-effective, these

machines should be scalable [5]. Reconfiguration should also be possible on every layer: from adding or removing entire systems for scalability towards changing a specific module or device on a single production machine to give it new capabilities. Hardware should be either changed by hand or by another machine; the software and necessary variables should automatically configure itself. This flexibility through reconfiguration is an important step towards sustainable and agile manufacturing [1]. However, the main problem is that while the flexibility of such systems increases its possibilities, it also increases the complexity of the software. For this reason there is a need to limit dependency between software systems. This requires an analysis of current platforms and architectures to move towards a new approach of the software which controls flexible manufacturing systems.

This research project focuses on a case study on flexible manufacturing systems for sustainable and agile manufacturing purposes [2]. A manufacturing machine is introduced that is not only modular from a hardware point of view, but also from a software perspective. This system should have some intelligence to be able to recognize its own environment. It needs to identify and configure the modules and capabilities automatically, or with limited support from a mechanic rather than an expert or engineer.

In this research project all systems and products have a virtual counterpart. These counterparts should be autonomous entities [8]. This led to a research project on an architecture that makes use of agent technology. The word agent comes from the Latin word *agere*, meaning: to act. Software agents are autonomous entities [3] with their own goals and the ability to communicate with other agents. Agent technology provides a way to deal with a dynamic, unpredictable environment and it enforces a system design with distributed control. There are many types of agents, for example a Belief Desire Intention (BDI) agent, see Fig. 1. A BDI agent has its background in the philosophies of Dennett [14] and Bratman [13]. The BDI agent uses its sensors to build a set of beliefs, its desires consist of goals, which lead to an intention of the agent, which characterizes the desire the agent has selected to work on. The BDI agent is also equipped with a set of plans and it will deliberately choose a plan to achieve its goals. Agents in manufacturing systems and products have been proposed before in several other research projects, like Ellis (recycle of rare earth elements) [16] and Kovacs (agent technology in car-recycling) [17]. Also Paolucci and Sacile [18] give an extensive overview of related work. Agents are used in

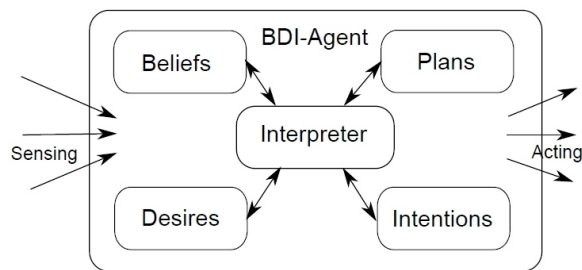


Figure 1. BDI-agent.

these systems for various reasons: scheduling, replacing human operators and control support. However, our research focuses on a production paradigm where every physical entity has a virtual agent counterpart, where all systems are distributed, and where the agents are essential for all processes: from scheduling and product logging towards direct control to the machine and module layer.

At the HU University of Applied Sciences Utrecht, the project HUniversal production was started to look at the current level of technology and use this to research and develop new modular and self-configuring machines, which are called equiplets [2]. Equiplets are meant to be low cost and have multi-purpose properties, offering generic services to any product which requires a production step that falls within its capabilities. An equiplet can be configured with a variety of modules necessary for manufacturing purposes, e.g., pick and place modules, grippers, (3D) printers, etc.

Fig. 2 shows three schematics of prototype equiplets with several modules. The particular equiplet on the left has a pick and place module (based on a delta robot), in the middle a gripper module is added to pick and place parts. On the right a camera module is added to get the location parameters of the objects it interacts with. While the hardware is changed manually or by another equiplet, software agents are used to automatically start the appropriate control software entities and set up the variables for the correct configuration of the system. This is what we call 'automatic reconfiguration'.

To deal with several equiplets, *Grid Manufacturing* [2] is introduced to show that production is not done anymore by production lines, but by flexible grids, which provide services to virtual products called *product agents* [8]. A grid is a set of equiplets. There are several agents on the grid layer. Hence the software of this manufacturing paradigm is based on a Multi Agent System (MAS). MAS consists of several interacting autonomous agents that should cooperate, coordinate and negotiate to achieve their goals. In a multi-agent system several abstract concepts are specified, for instance what the role, permission, responsibility and possible interactions are between each agent. In the concept of grid manufacturing these specifications are set for all entities. The product agent is a virtual (software) representative of the real product, which holds the requirements and knowledge that is needed to build it. There are also equiplet agents that represent the equiplets. The equiplet agents will interact with the product agents and other entities in the environment. The grid provides a flexible setup with a range of equiplets which uses modular tooling and hardware so that a large range of services can be provided

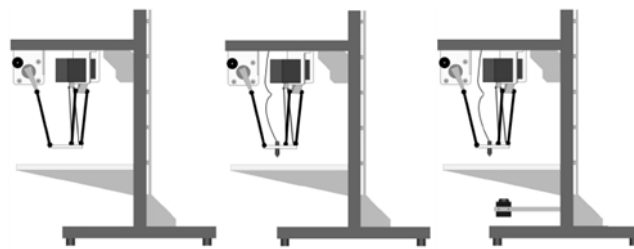


Figure 2. This particular equiplet has (from left to right) a pick and place module (based on a delta robot), a gripper module to pick and place parts and finally a camera module to get the location parameters of the objects it interacts with.

to the products. This makes it possible to create a range of different products on a single grid. Products can be produced dynamically using this concept. Intelligent agents also ease the processes on the grid layer; coordinating and configuring modules when necessary and providing the cognitive abilities that are necessary for the communication between equiplets and the products.

The paper shows the problems involved in the software of agile manufacturing systems and gives an example of how such a system could function. Next it states what is required to create such a flexible architecture for reconfigurable systems. The requirements, feasible for future use in industry, are discussed and matched. Also, a software hierarchy and basic architecture is presented that can be developed using these technologies. Finally, the conclusion states the potential for the combination of these technologies and discusses future work based on the analysis in this paper.

II. PROBLEM DESCRIPTION

The goal of HUniversal production is to create a grid of manufacturing machines which is fully flexible, meaning it can create any product at any scale which falls within the sum of capabilities that are determined by the parameters and configurations of all equiplets in the grid. These capabilities can change at any time, since the grid is designed as such that it can be reconfigured at runtime. Equiplets can manually be added or removed with limited interference to other systems. As a result, software systems have to act autonomously, since they are unaware of all the systems and their capabilities in the environment. Giving them all the information of every system in the grid would make the software too complex and inflexible. This implies that a distributed control system is required, which uses autonomous software entities, where every entity can have unknown abilities. Since these systems still need to interact, it is required that they communicate in a more abstract manner. This way each system can interpret the abstract communication according to its knowledge. In such a system it is not possible to program beforehand which methods to call. To achieve cooperation, there is a need for dynamic behavior.

Fig. 3 shows an example of a simplified functional design of the architecture that is currently under development [9]. The example shows one product within a grid and two modular manufacturing systems (equiplets). Since these equiplets are configured with several modules they have to acquire the right information to be able to function. In Fig. 3, six steps are

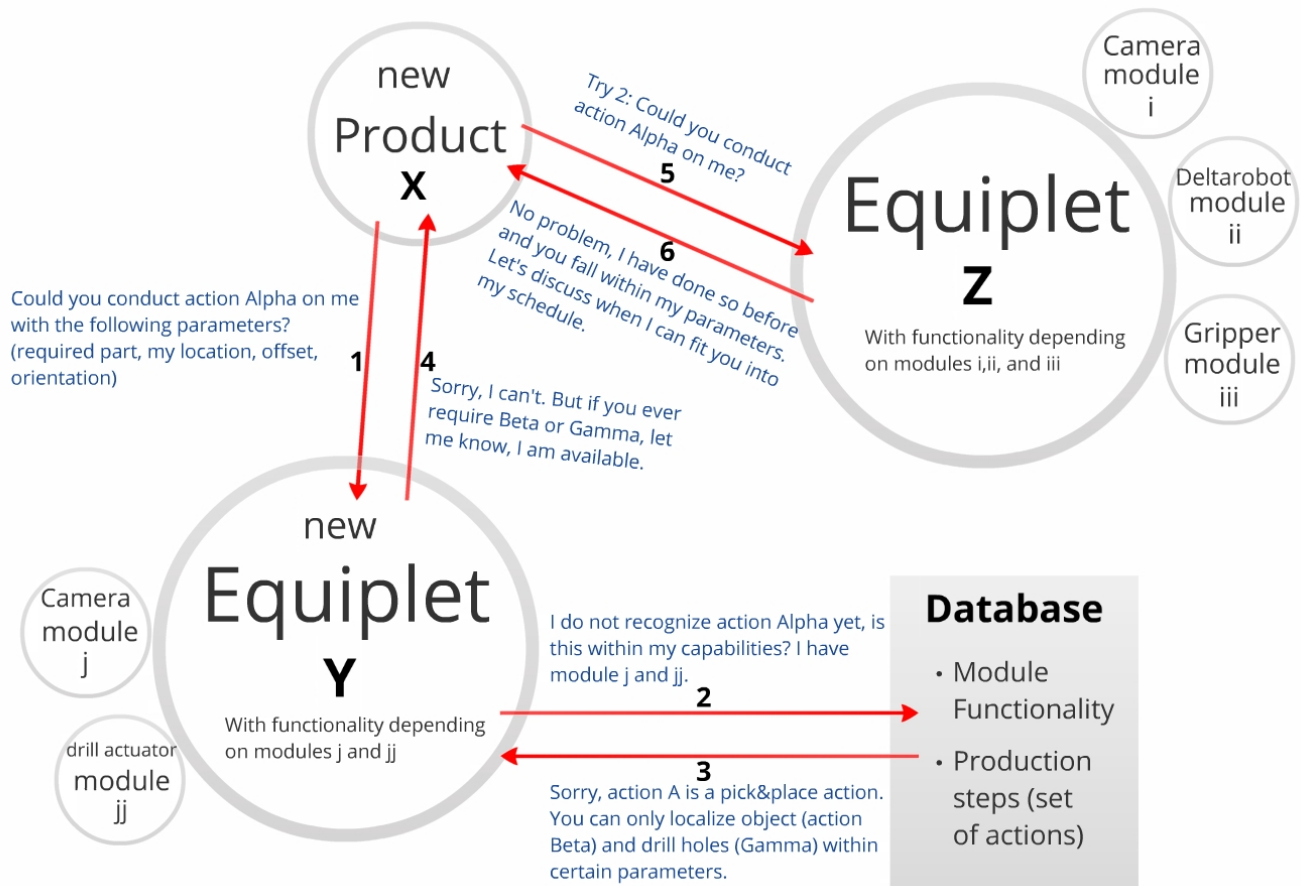


Figure 3. Simplified example of how a product communicates with equiplets in a grid where equiplets offer services within certain parameters.

presented when a product requires a pick and place action. In this example, equiplet Y is just added within the grid and has been configured with two modules. Equiplet Y has just been reconfigured with these modules and is therefore not yet aware of all its capabilities. Because the environment is completely flexible, it is possible that new equiplets, products or modules, and therefore new functionality and production steps, can be added at any time in a running system. This makes it necessary for the equiplets to inquire at the central database whether they are able to perform this specific action. To "know" the capabilities of the equiplet we look towards the research of Järvenpää [6] who has developed a rule-based matching system for requirements and capabilities in production systems. Equiplet Z already has done several pick and place actions. Since it has not been reconfigured it can immediately answer to product X that its demands fall within the possibilities.

The largest problems that need to be overcome are the high software complexity which is a result of the flexible automation and the different requirements of the software on different levels within the software architecture. While the direct control of the hardware requires high performance, stability and real-time capabilities, the flexible agents require cognitive abilities, which are inherently slow and not real-time. These cognitive abilities are necessary for automatically reconfiguring the systems. The agents have to load the necessary software and

setup the correct variables that it needs to function. Hence the modules and machines have to be able to recognize their capabilities, necessary parameters for their configuration, and dependencies. This requires an entirely new hybrid architecture, whereof the requirements and the hierarchy design are presented in this paper. The scope will be limited to the decisions on the requirements and necessary specifications of the technologies that are required to develop a proof of concept system using the current equiplet prototypes. The problem description brings us to the main research questions which are important at this phase:

- What are the requirements for the software architecture of an equiplet, using agents and MAS?
- Which technologies are available at this time that could be used in a proof of concept system and fit the requirements?
- What architecture can be used for industrial applications which works within a dynamic environment?

III. REQUIREMENTS AND MATCHING TECHNOLOGIES

The system is meant to become applicable in industry. The system is also reconfigurable and should work in a dynamic, non-deterministic environment. Hence, the logistics, i.e., where are the product parts that are necessary and the parts

it interacts with, should be dynamic as well. The equiplet has to be able to find the component and important objects within the environment to interact with on a visual level. Since systems, objects and therefore functionality can be added at any moment in runtime, the system needs to have distributed control, where dependencies between systems have to be kept to a minimum [10]. It is unlikely that the dependencies between different systems and modules can be nil. Take for example a system that transports the product between equiplets. If such a system is in an error state, this will directly influence the equiplets it is connected to. It is important to decouple the depending systems as much as possible. This is done by using a data driven system. The different systems, e.g., 'higher' logistic systems and 'lower' control systems, are decoupled by data that can be influenced from both sides. This way an error in one autonomous system will not block another, also the performance of several systems will only be influenced by interdependent systems. Finally it is important that the abstraction of the system is as high as possible, for the hardware, as well as the software, interfaces and communication between systems.

Summarizing the requirements:

- Since the configuration and the logistics are flexible, every equiplet system should be visually aware of objects it needs to interact with within its working environment.
- There should be a minimum amount of dependencies between systems, since not all systems are aware of each other's existence, hence distributed control is necessary.
- To further decouple systems and be able to change and update information, the system should have some properties of a data driven software design. This way, it is easier to add new functionality for new products without directly interfering with the running systems. Required data for new actions could be requested from the database when necessary.
- There should be a high level of abstraction for the communication between the software entities themselves and the hardware. By using a higher abstraction level, communication can be made less specific which makes the system more flexible. Systems can use their own beliefs to interpret the messages they receive and act according to their own design goals and capabilities.
- Manufacturing machines interact within the environment. While most objects (products and modules) in the environment have an agent as virtual representative, there are also (very) simple hardware devices and software objects that only have to be used and as such are not depicted as a (software) entity. These objects in the environment should also be as abstract as possible such that all entities can interact with them when necessary.

This brings us to some specific requirements that are set to be the basis of an architecture that will be researched and

developed in the next phases:

- Hardware systems should be able to communicate as abstract as possible with the higher order intelligent agents in the software. Therefore there is the need for a hardware abstraction layer where modules can be added in runtime.
- An adaptive system is required based on computer vision that can interpret the environment in which the manufacturing machine operates to distinguish production parts and their position.
- A higher level abstract architecture is necessary that can communicate with other unknown entities in the system and can deal with a dynamic and changing environment.

To apply all these requirements and to limit the scope of the research, we have decided to use the following technologies:

- 1) ROS - Robot Operating System is a software framework and provide tools and libraries. ROS can be used as an abstraction layer for the hardware in modular machines and robots. ROS utilizes the C++ program language and can be used directly to control hardware systems in real-time.
- 2) MAS - Multi Agent Systems [4] are the most likely option for the higher layer systems. Since a dynamic environment is used with many reconfigurable modules, it is important to decouple dependencies and lower the overall complexity by defining specific entities that each have their own responsibilities. Agents can act independently and have flexible behavior. Especially the Java Agent DEvelopment framework (JADE) seems of interest because of its low learning curve (based on the Java programming language), negotiation abilities, and its ability to migrate, terminate and add agents in runtime [15], the Jade platform has been in development since 2001 and has matured enough to be thrustworthy for industrial application.
- 3) OpenCV - Open Computer Vision is included with ROS, as such it is logical to choose for the OpenCV library that is integrated in this system. The computer vision is used to identify and localize parts within the working space of the equiplet and is used for other logistic processes necessary for configuration and calibration of the systems, e.g., identification of a new gripper.
- 4) Environment Programming - As mentioned in the requirements, the MAS system needs to interact with parts of the environment that might not be directly part of the MAS. Ricci introduced environment programming that considers the environment as an explicit part of the MAS and clearly distinguishes responsibilities between the agents and the environments. [11]. In Environment Programming there are agents and artifacts. Artifacts are non-autonomous, function-oriented entities that operate as a first level abstraction of usable objects in the environment.

IV. DISCUSSION

The requirements and matching technologies provide the possibility to start the design of an architecture for control

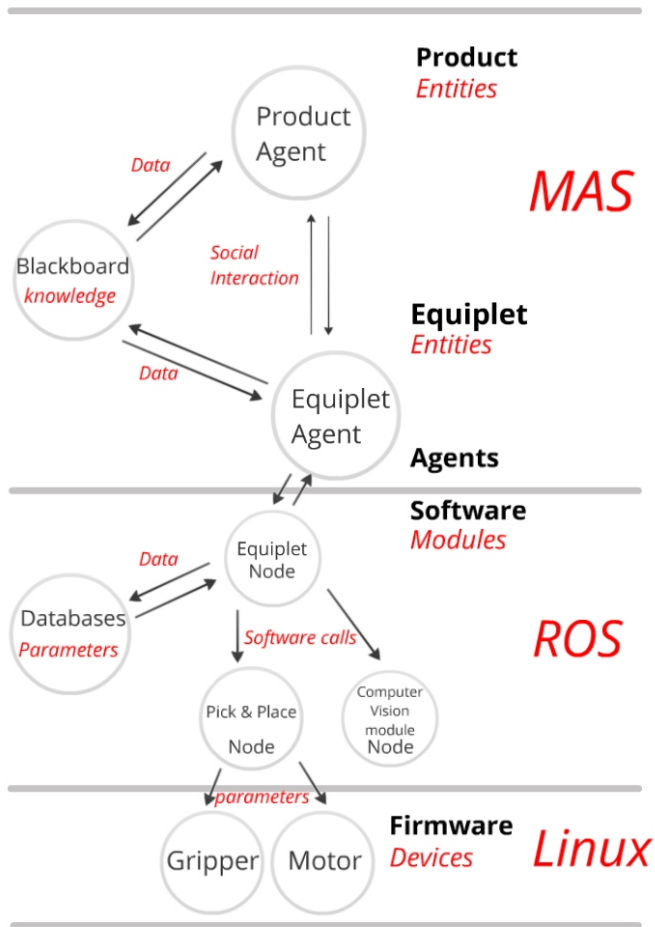


Figure 4. An example of the software hierarchy showing a single product and equiplet with several modules and the ROS, MAS and Linux layers.

of all systems within the equiplet and grid layer. To be able to create a system based on industrial specifications, it is necessary to combine these systems, hence to create a hybrid system [12]. The hybrid system is based on an architecture where the real-time capabilities with the physical abilities and cognitive abilities are split in two. In practice this means that real time capabilities like the direct control of sensors and actuators are managed by ROS, which runs on the Linux operating system and is especially tailored to interface with modular hardware. Cognitive abilities, like reasoning, are to determine if an equiplet has the capability to perform a new action on request by a product. This is handled by the MAS platform based on the JADE platform. The equiplets and grids have a modular design and are configurable in real-time, hence the system should be able to change the software when necessary. Both MAS and ROS platforms have these capabilities. Several MAS platforms are able to start new agent entities at runtime. ROS also works with entities that can interface with each other and it calls these software entities nodes. Nodes can be launched and stopped in runtime, but do not have the autonomous and cognitive capabilities like an agent. In other words, they are less intelligent.

In Fig. 4 the hierarchy is shown. On the MAS layer there is social interaction using the abstract communication



Figure 5. A QR code is used to identify items and modules in the environment, this particular QR code leads to a demonstration of an older prototype showing its flexible adaptation to the environment.

on the equiplet and product layers between several entities. Note that there can be any number of equiplet and product agents and every entity represents a physical counterpart. The knowledge that is required by the data driven environment is stored on Blackboards, which can also be used to decouple the data from the agents that needs to be shared amongst the agents. On a lower layer ROS also uses (autonomous) entities. However, these are called nodes. Nodes are usually programmed on the ROS platform using the program language C++. While they are autonomous entities, they do not offer the abstract level of communication that is common among agents. However, ROS is designed to be used for Robot or Industrial Machine applications and does provide better performance and a more rigid and stable platform that is required for industrial applications. Also ROS provides a large amount of libraries, making it easier to develop new functionality. Therefore ROS provides a more robust method of the essential control of hardware systems. Finally at the lowest layer of the hierarchy there is the firmware layer, where devices are shown that are connected to the control system using an Industrial bus.

A. Reconfiguration

As determined, MAS and ROS can be configured with new software in runtime. However, how does any system know that it has been reconfigured? In other words, what is the trigger to start or update a node with the necessary software to use it? For this a system is designed that uses QR codes to "scan" items. Every module or device has its own QR code, see Fig. 5, which uniquely identifies this module. This way the machine can be configured just by scanning a configuration QR code and a specific QR code that belongs to the new module that is being added or removed. When the Computer Vision system detects a reconfiguration code it will inform the ROS control system, which will in turn message the MAS system to find the appropriate software, either on the cognitive (MAS) or physical (ROS) layer. While Computer Vision is used to trigger changes in the hardware it is also used to provide other parameters. The environment is monitored by the system, providing information of the working field and objects within sight. By communicating with product agents and other equiplets also objects and systems are identified. This way the physical configuration of systems can also be determined automatically. If necessary, QR codes are also used to help with the identification. The QR codes can be identified

accurately without the usual margin of error that is common in computer vision applications.

V. CONCLUSION AND FUTURE WORK

The analysis shows that a proof of concept of a combination of ROS (using C++), MAS (using Java) and Computer Vision has potential for an industrial environment. Problems like stability and performance of the agent platforms are minimized by using the hybrid system with a combination of JADE and ROS. The more stable and performant ROS is used for critical systems that should be running at all times and MAS provides the cognitive abilities that are necessary in a dynamic distributed system. The hierarchy of these systems also lowers the overall complexity, because of the decoupling of systems and the distributed (autonomous) architecture. The distributed nature of the systems lowers the complexity of the software and makes it possible to address problems with a black box approach, focusing on the interfacing behaviour between the entities. The software auto configuration is made possible by using the MAS and ROS architecture, that are both based on autonomous entities, which can be added and configured in runtime. In combination with the computer vision systems based on OpenCV the parameters of the environment are used to quickly determine the state of the environment, identifying objects of interest and making it easy to configure new hardware systems when necessary.

Currently, due to the analysis in this paper, the research group has decided to start the development of the software architecture as presented. The functional design of the software has been completed and the hardware of several modules is in its beta phase. Progress has also been made on the hardware, in Fig. 6 the newest (4th generation) equiplot prototype is shown. This prototype uses the distributed system as proposed, including the suggested hybrid architecture using agents and nodes coupled by blackboards. The programming of various subprojects are in progress, like research on the lifecycle of a product [8], which is used to acquire information on the product for (sustainable) goals like recycling and repairs. Several other projects are planned for the future, for example how grid agents can be used for optimisation, intelligent behavior within an equiplot and the development of more hardware and software modules.

REFERENCES

- [1] Y. Koren et al., Reconfigurable Manufacturing Systems, CIRP Annals - Manufacturing Technology, vol. 48, no. 2, 1999, pp. 527-540.
- [2] E. Puik and L.J.M. van Moergestel, Agile multi-parallel micro manufacturing using a grid of equiplots, IPAS 2010 proceedings, 2010, pp. 271-282.
- [3] M. Wooldridge and N. Jennings, "Intelligent Agents: Theory and practice", The Knowledge Engineering Review, 1995, pp. 115-152.
- [4] M. Wooldridge, "An Introduction to Multi Agent Systems", Second Edition, Wiley, 2009.
- [5] E. Puik, L. van Moergestel, and D. Telgen, Cost Modeling for Micro Manufacturing Logistics when using a Grid of equiplots, ISAM2011, IEEE, Finland, 2011.
- [6] E. Järvenpää, P. Luostarinen, M. Lanz, and R. Tuokko, "Development of a Rule-base for Matching Product Requirements against Resource Capabilities in an Adaptive Production System", FAIM2012 proceedings, Helsinki, 2012, pp. 449-456.
- [7] A. Gunasekaran, Agile manufacturing: the 21st century competitive strategy, 2001.



Figure 6. One of the new prototype equiplots currently under assembly.

- [8] L. van Moergestel, E. Puik, D. Telgen, H. Folmer, M. Grnbauer, R. Proost, H. Veringa and J.-J. Meyer, "Monitoring Agents in Complex Products - Enhancing a Discovery Robot with an Agent for Monitoring, Maintenance and Disaster Prevention", ICAART2013 proceedings, volume 2, 2013, pp. 5-13.
- [9] D. Telgen, L. van Moergestel, E. Puik, and J.-J. Meyer, "Agent Manufacturing Possibilities with Agent Technology", FAIM2012 proceedings, Helsinki, Finland, 2012, pp. 341-346.
- [10] L. van Moergestel, E. Puik, D. Telgen, and J.-J. Meyer, Decentralized autonomous-agent-based infrastructure for agile multiparallel manufacturing, ISADS 2011 Japan, 2011, pp. 281-288.
- [11] A. Ricci, M. Piunti, and M. Viroli, "Environment Programming in Multi-Agent Systems - An Artifact-Based Perspective" Autonomous Agents and Multi-Agent Systems journal 23(2), September 2011, pp. 158-192.
- [12] R.C. Arkin, "Behaviour-Based Robotics", MIT press, Hybrid Systems, 1998, pp. 205-234.
- [13] M.E. Bratman, "Intention, Plans, and Practical Reason", Harvard University Press, Cambridge, Mass, 1987.
- [14] D.C. Dennett, "The Intentional Stance", MIT Press, Cambridge, Mass, 1987.
- [15] N.R. Bordini, M. Dastani, J. Dix, and A. E. F. Seghrouchni, "Multi-Agent Programming", Springer, 2005.
- [16] T.W. Ellis, F.A. Smith, and L.L. Jones. "Methods and opportunities in the recycling of rare earth based materials", The Metallurgical Society (TMS) conference on high performance composites, (IS-M796), 1994.
- [17] G. Kovacs and G. Heidegger, "Car-recycling sme network with agent-based solutions", European Research Consortium for Informatics and Mathematics, (73), 2008, pp. 53-54.
- [18] M. Paolucci and R. Sacile, "Agent-based manufacturing and control systems: new agile manufacturing solutions for achieving peak performance", CRC Press, Boca Raton, Fla., 2005.

Apriori-with-Constraint for Flexible Association Rule Discovery

Kittisak Kerdprasop, Phaichayon Kongchai, Nittaya Kerdprasop

Data Engineering Research Unit,

School of Computer Engineering,

Suranaree University of Technology, Thailand

kerdpras@sut.ac.th, zaguraba_ii@hotmail.com, nittaya@sut.ac.th

Abstract—Association rule discovery, or association mining, is one of the major data mining tasks that has gained much interest from researchers and general users. The knowledge obtained from association mining can be used to benefit business in many aspects such as recommend new products, design catalogs, manage sales promotion, and so on. But data processing for association rule discovery has expensive computing time because the relationships induced from data can be tremendously many more than those induced from other data mining tasks such as classification. As a consequence, most association mining software generally create so many rules from the association mining process and some of these rules are not beneficial to any users. To solve this useless rule mining problem, we propose to incorporate Apriori algorithm with constraint function for users to specify subset of association rules containing only interesting items. Besides specific items, users can also identify length of the association rules. Our two Apriori-with-constraint algorithms, called Association rule discovery with Constraints In Frequent itemset mining (ACIF) and Association rule discovery with Constraints After Frequent itemset mining (ACAF), are experimentally proven to be able to reduce processing time and also pruning a great number of useless rules.

Keywords-association rules; frequent itemset mining; data mining; association analysis; constraint logic programming.

I. INTRODUCTION

Data mining aims at extracting hidden knowledge from data [8]. Knowledge is known to be a valuable asset to most organizations as a substantial source to enhance understanding of relationships among data instances and support better decision making to increase organizational competency. Automatic knowledge acquisition can be achieved through the availability of the knowledge induction component. The induced knowledge can facilitate various knowledge-related activities ranging from expert decision support, data exploration and explanation, estimation of future trends, and prediction of future outcomes based on present data. The methodology of knowledge induction is known as knowledge discovery in databases, or data mining.

Data mining methods are broadly defined depending on the specific research objective and involve different classes of mining tasks including regression, classification, clustering, identifying meaningful associations between data attributes. The later mining task refers to association mining,

or market basket analysis [9] in the retail business domain, which is the main focus of our research.

Association mining is a popular method for discovering relations between features or variables in large databases [11], [12], [15], [20] and then presenting the discovered results as a set of if-then rules, such as {milk, bread} => {butter} to indicate that if a customer buys milk and bread, he or she is more likely to buy butter as well. Association rule generation process is composed of two major phases: frequent itemset mining and rule generation. Frequent itemset mining is to find all items or features that are frequently occurred together [13], [22]. It is an important phase of association mining because it is a difficult task to search all possible itemsets.

We thus pay attention to the design and implementation of frequent itemset discovery by applying the constraint concepts in this step. We propose two algorithms: Association rule discovery with Constraints In Frequent itemset mining (ACIF) and Association rule discovery with Constraints After Frequent itemset mining (ACAF). The first algorithm considers constraints during the frequent itemset mining phase, whereas the later one applies constraints after the frequent itemset mining steps. Constraints in our proposed method include items of interest, items to be excluded from the mining results, and desired rule length of the final association mining. Our implementation is based on the ECLiPSe constraint system (www.eclipseclp.org).

This paper is the extension of our previous work [14] on association rule discovery with constraint logic programming that was the proposal of extending Apriori [1] with more domain-specific constraints. The work presented here explains in more details the idea of incorporating domain-specific constraints both during and after the frequent itemset mining stage (ACIF and ACAF algorithms, respectively). Applicability of the proposed idea and its implementation have also been demonstrated in this paper.

The organization of this paper is as follows. The problem of association rule discovery and main concepts of logic and constraint logic programming are reviewed in Section 2. Then the design of association mining with constraint algorithms is explained in Section 3. The implementation of the two algorithms, ACIF and ACAF, together with their experimental results are presented in Section 4. Finally, Section 5 concludes the paper with discussion of our future research direction.

II. PRELIMINARIES

A. Frequent Patterns and Association Mining

Frequent patterns are common occurrences such as sets of features or items that appear in data frequently. Frequent pattern mining focuses on the discovery of relationships or correlations between items in a dataset. In frequent itemset mining, we are interested in analyzing connections among items. A collection of zero or more items is called an itemset. The discovery of interesting relationships hidden in large datasets is the objective of frequent pattern mining. The uncovered relationships can be represented in the form of association rules. An association rule is an inference of the form $X \rightarrow Y$, where X and Y are non-empty disjoint itemsets. An itemset is called a *frequent itemset* if its support, i.e., the number of transactions that contain a particular itemset, is greater than or equal to user-specified support threshold (called *MinSup*). It is the *MinSup* constraint that helps reducing the computational complexity of frequent itemset generation. If the itemset is infrequently occurred, all supersets of this itemset are also infrequent and they can be pruned to reduce the search space.

This pruning strategy is called an anti-monotone property and has been applied as a basis for searching frequent patterns in the well-known algorithm Apriori [1], [2]. The algorithms find all frequent itemsets by generating supersets of previously found frequent itemsets. This generate-and-test method is computational expensive. Han et al [10] proposed a different divide-and-conquer approach based on the prefix-tree structure that consumes less memory space. Toivonen [21] employed sampling techniques to deal with frequent pattern mining from large databases. Zaki et al [23] tackled the problem by means of parallel computation.

Some researchers [4], [7], [17], [18], [19] consider the issue of search space reduction through the concept of constraints. Our research is in the same direction as De Raedt et al [7]. We consider the problem of mining frequent patterns within a setting of constraint logic programming using the ECLiPSe constraint system [3]. Constraints can play an important role in improving the performance of mining algorithm. The problem of constraint-based pattern mining can therefore be formulated as the discovery of all patterns in a given dataset that satisfy the specified constraints.

B. Constraint Logic Programming

Constraint logic programming, or CLP, is a declarative programming style that combines the features of logic programming [16] and constraint propagation to solve combinatorial and optimization problems. Common structure of a constraint program is consisted of the part to define variables and constraints on variables and the part to search for a valid value on each variable. This is the style of constraint-and-search. The structure of constraint logic program is as follows:

```

solve(Variables) :-
    setup_constraints(Variables),
    search(Variables).
    
```

A constraint logic program to solve inequality $A > B$, in which both variables are integers in the range 1..5 can be shown as follows:

```

:- lib(ic).           % include library
solve(R) :-
    R = [A,B],        % define variables
    R :: 1..5,        % define constraint
    A #> B,           % constraint over variables
    alldifferent([B]),
    labeling(R).
    
```

The predicate “labeling” is responsible for searching all possible values of A and B that comply with the constraints $A > B$ and $A \neq B$.

III. APRIORI-WITH-CONSTRAINT ALGORITHMS

Apriori algorithm [1], [2] is a general method that can efficiently generate all association rules satisfying minimum support and minimum confidence constraints. We argue that besides these basic constraints, users should specify their item of interest constraint over the method. We thus design two algorithms to support the extension of Apriori that takes into account user-specified constraints. The first algorithm, called Association rule discovery with Constraints In Frequent itemset mining (ACIF), applies constraints during the phase of frequent itemset mining. The second algorithm is called Association rule discovery with Constraints After Frequent itemset mining (ACAF) in which constraints are considered after all frequent itemsets are generated. The design frameworks of both algorithm are presented in Fig. 1. Detailed steps of ACIF and ACAF algorithms are shown in Fig. 2 and Fig. 3, respectively.

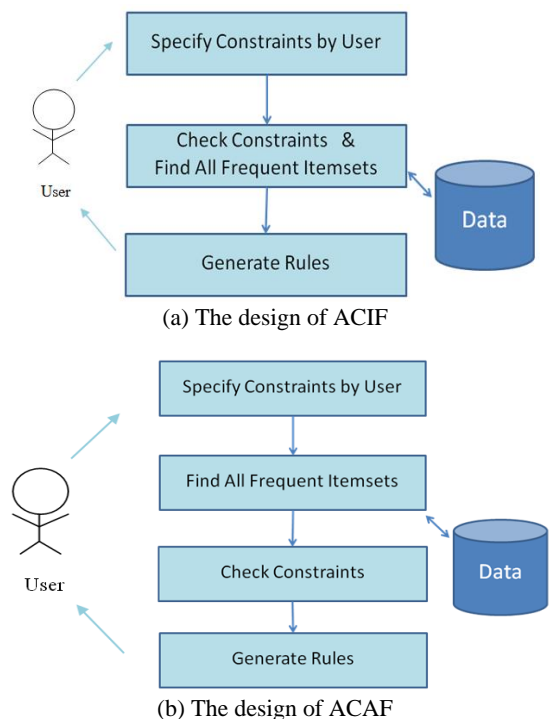


Figure 1. Design frameworks of Apriori-with-constraint

```

Algorithm ACIF
//Input : Database D,
        Constraints: Length, Subset, NotSubset,
                RHS_items, Mincon, Minsup.
//Output : Rules.

(1) L1 = find_frequent_itemset(D)
(2) for (k=2; Lk-1 ≠ ∅; k++) {
(3)   Ck = apriori_gen(Lk-1, Minsup)
(4)   for each transaction t ∈ D { // scan D for counts
(5)     C1 = subset(Ck, t)
(6)     for each candidate c ∈ C1 { c.count++ }
(7)     C2 = checkcondition(Length, Subset,
                            NotSubset, C1)
(8)     Lk={c ∈ C2 | c.count ≥ Minsup}
(9)   }
(10) }
(11) FreqSet = ∪k Lk
(12) For each l ∈ FreqSet // l is frequent-itemset.
(13)   k = |l| // size of frequent itemset
(14)   m = |Hm| // size of right hand side Items
(15)   For each hm+1 ∈ Hm+1 {
(16)     If hm+1 = RHS_items {
(17)       conf = support(fk) / support(fk - hm+1)
(18)       If conf ≥ Mincon {
(19)         Rules = rule(fk - hm+1) ⇒ hm+1
(20)       } Else
(21)         delete hm+1 from Hm+1
(22)     }
(23)   }
(24) return Rules
    
```

Figure 2. Pseudocode of ACIF algorithm

```

Algorithm ACAF
//Input : Length, Subset, NotSubset, Minimum_support,
//        Min_conf (Minimum confidence), RHS (right hand side Items).
//Output : Rules.

(1) L = find_all_frequent_itemset(Minimum_support)
(2) For each l ∈ L { //l = frequent_itemset
(3)   If l.length > 1 {
(4)     Lk = checkcondition(Length, Subset, NotSubset, L)
(5)   }
(6) }
(7) Rules = generate_rule(Lk, Min_conf, RHS)
(8) return Rules
    
```

Figure 3. Pseudocode of ACAF algorithm

IV. IMPLEMENTATION AND EXPERIMENTAL RESULTS

A. CLP Implementation

Program and data in the constraint logic programming style are both in the same format, that is, a Horn clause. In our implementation, declaration of items and transactional database are in the list structure within the predicate “data” (as shown in Fig. 4). To run the program, user calls the predicate “association” and the running result will appear as shown in Fig. 5.

```

data([
[beer],[cannedmeat],[cannedveg],[confectionery],[dairy],[fish],
[freshmeat],[frozenmeal],[fruitveg],[softdrink],[wine]]
-
[
[beer,cannedmeat,confectionery,wine],
[softdrink,fruitveg,wine,confectionery],
[dairy,cannedmeat,fish],
[dairy,freshmeat],
[wine,softdrink,fruitveg,confectionery],
[frozenmeal,confectionery,fish],
[confectionery,wine],
[fruitveg,frozenmeal,dairy,freshmeat],
[softdrink,cannedmeat,dairy,cannedveg],
[cannedveg,beer],
[softdrink,cannedmeat,beer,cannedveg],
[softdrink,dairy,beer]
]
).
    
```

Figure 4. Predicate data containing lists of items and transactions

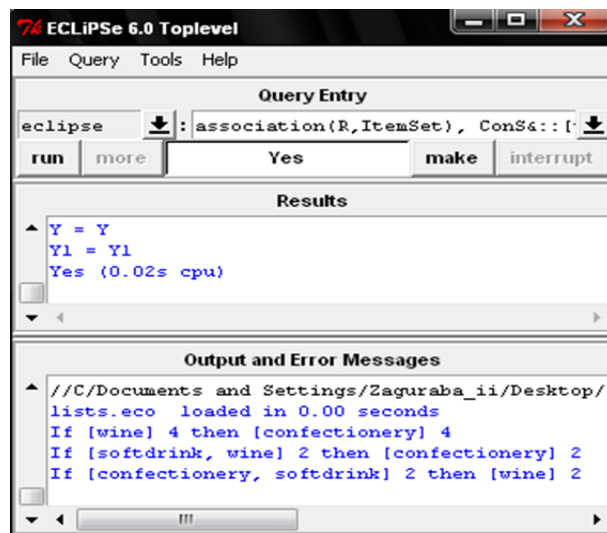


Figure 5. Running result of association rule mining

A program source code of ACAF algorithm that was implemented with the constraint logic programming language using ECLiPSe constraint system is given as follows:

```

% User calls: association(R,0,2,100)
:- compile("filename.txt"). % load file.
:- lib(sd).
:- lib(ic).
:- lib(ordset).
    
```

```

association(R,LengthI,MinSup,Conf) :-
  writeln('Please specify member in [[_] :)',read(Subset),
  writeln('Please specify member do not need in [[_] :)',
  read(NotSubset),
  writeln('Please specify member in [[_] :)',read(Goal),
  data(Data),Data=_-,
  ( count(I,2,6), fromto(Data,
  S0,S1,R),param(LengthI,Subset,NotSubset,Conf,MinS
  up,Goal) do
    ( S0=A-B,
      findCL(A-B-MinSup,R-_-
      _,LengthI,Subset,NotSubset,Conf,Goal),
      allUnion(I,R,NewItemSet),
      S1=NewItemSet-B,! ).
  findCL(ItemSet-Items-MinSup,R-Items-MinSup,LengthI,
  Subset,NotSubset,Conf,Goal) :-
  (foreach(X,ItemSet), fromto(R,S1,S0,[]),
  param(Items,MinSup) do
    (supOK(X,Items,MinSup,LenItem) ->
      S1=[X-LenItem | S0], ! ; S1=S0
    ),
    not1Item(R,Re1),
    findLength(LengthI,Re1,Re),
    findSubset(Subset,Re,R1),
    findNotSubset(NotSubset,R1,R2),
    findRule(R2-Items-Conf,Goal).
% Check Item set length > 1
not1Item(R,Re) :- R=[H-_|_],length(H,LenItem),
  LenItem = 1 -> Re = [] ; Re = R .
% findLength(0,[[a,b]-2,[a,c]-2],R).
findLength(Cons,Re,R) :-
  (foreach(I,Re), fromto(R,S1,S0,[]), param(Cons) do
    I = X-_, length(X,LenItem),LenItem > Cons ->
    S1 = [ I | S0 ], ! ; S1=S0 ).
% findSubset([[b],[c]],[[a,b]-2,[b,c]-2,[b,c,d]-2],R1).
findSubset([],X, X).
findSubset([Subset | Tr],Re,R1) :-
  Subset = [] -> R1 = Re ;
  (foreach(I,Re), fromto(R,S1,S0,[]), param(Subset) do
    I = X-_,
    Subset1&::Subset, Y&::X, Subset1&=Y
    -> S1 = [ I | S0 ], ! ; S1=S0 ),
  findSubset(Tr,R,R1).
% findNotSubset([[b],[c]],[[a,b]-2,[b,c]-2,[b,c,d]-2],R1).
findNotSubset([],X, X).
findNotSubset([NotSubset | Tr],Re,R1) :-
  NotSubset = [] -> R1 = Re ;
  (foreach(I,Re), fromto(R,S1,S0,[]), param(NotSubset) do
    I = X-_,
    NotSubset1&::NotSubset, Y&::X, \+NotSubset1&=Y
    -> S1 = [ I | S0 ], ! ; S1=S0 ),
  findNotSubset(Tr,R,R1).
% findGoal([[a],[a,b],R).
findGoal([],X, X).
findGoal([Subset | Tr],Re,R1) :-
  Subset = [] -> R1 = Re ;
  Subset1&::Subset, Y&::Re, Subset1&=Y -> R1 = Re,
  findGoal(Tr,Re,R1).
supOK(X,Items,MinSup,LenItem) :-
  (foreach(I,Items), fromto(R,S1,S0,[]), param(X) do
    (my_subset(X,I) -> S1 = [ I | S0 ], ! ; S1=S0 ),
    length(R,LenItem),
    LenItem >= MinSup.
% findRule
findRule(ItemSet-Items-MinConf,Goal) :-
  (foreach(Set,ItemSet), param(Items,MinConf,Goal) do
    Set = X-LenItem,
    findall(Re,powerset(X,Re),PwSet),
    (foreach(ItemX,PwSet),
    param(X,Items,LenItem,MinConf,Goal) do
      ( ItemX = X ; ItemX = [] -> ! ;
      createRule(ItemX,X,Re),findGoal(Goal,Re,R1) ->
      supOK(ItemX,Items,0,LenItemX),
      conOk(LenItem-LenItemX-MinConf,ItemX,R1),! ; !
      ) ) ).
% createRule([a],[a,b,c],Result).
createRule([],X,X).
createRule([H | Tr],X,Result) :-
  delete(H,X,Re),createRule(Tr,Re,Result).
% Check Confident
conOk(LenItem-LenItemX-MinConf,ItemX,Re) :- Re11 is
  (LenItem/LenItemX)*100,Re11 >= MinConf -> write('If
  '),
  write(ItemX),write(' '),write(LenItemX),write(' then '),
  write(Re),write(' '),writeln(LenItem) ; ! .
% my_subset compare([1],[1,2]) return T or F
my_subset(Sub,S) :- toSet(Sub,OrdSub), toSet(S,OrdS),
  ord_subset(OrdSub,OrdS).
allUnion(I,ItemSet,NewItemSet) :- combi(ItemSet,R_),
  flatten(R_,R),
  (foreach(X,R), fromto(NewItemSet_,S1,S0,[]), param(I)
  do First-Sec=X,
  (unionN(I,First-Sec,Out) -> S1=[Out | S0], !;S1=S0) ),
  toSet(NewItemSet_,NewItemSet).

unionN(N,First-Sec,Out) :- toSet(First,F), toSet(Sec,S),
  ord_union(F,S,Out),
  length(Out,Len),Len=N.

combi([],[]).
combi([H | T],[HR | TR]) :- (foreach(X,T), foreach(Y,HR),
  param(H) do
  X = Set2-_,H = Set1-_, Y=Set1-Set2 ),
  combi(T,TR).
toSet(X,S) :- list_to_ord_set(X,S).
% powerset([a,b],X).
powerset([],[]).
powerset([_ | Rest],L) :- powerset(Rest,L).
powerset([X | Rest],[X | L]) :- powerset(Rest,L).
% ===== End of ACAF program =====

```

B. Experimentation with Chess data

To test correctness and effectiveness of ACIF and ACAF programs, we use the Chess dataset obtained from the website <http://fimi.ua.ac.be/data/>. The dataset contains 3196 records, each record has 37 attributes, or items in the context of association mining. The first and last records of Chess data can be shown as follows:

```

data([[1],[2],[3],[4],[5],[6],[7],[8],[9],[10],[11],[12],[13],[14],[
  15],[16],[17],[18],[19],[20],[21],[22],[23],[24],[25],[26],[27],[
  28],[29],[30],[31],[32],[33],[34],[35],[36],[37],[38],[39],[40],[
  41],[42],[43],[44],[45],[46],[47],[48],[49],[50],[51],[52],[53],[
  54],[55],[56],[57],[58],[59],[60],[61],[62],[63],[64],[65],[66],[
  67],[68],[69],[70],[71],[72],[73],[74],[75]
]-[[1,3,5,7,9,11,13,15,17,19,21,23,25,27,29,31,34,36,38,40,42,
  44,46,48,50,52,54,56,58,60,62,64,66,68,70,72,74],
...
[2,4,5,8,9,11,13,16,17,19,21,23,26,27,30,31,35,36,38,40,42,44,
  46,48,51,52,54,56,58,61,62,64,67,68,71,73,74] ] ).

```

In our CLP implementations of association rule mining with constraints, users can specify three kinds of constraints: (1) items that must appear in the association rules, (2) items that must not appear in the rules, and (3) items that must appear in the consequence part of the rule. Constraints on items can use a conjunction (AND), a disjunction (OR), and an empty list of items to identify no constraint. These constraints have to be specified prior to the generation of association rules. We test the performance of ACIF and ACAF programs against the original Apriori (which is also implemented with the CLP paradigm for a fair comparison), and then compare the results in terms of computation time and number of association rules. Figs. 6 and 7 demonstrates the running time and number of rule comparisons, respectively. For the case of no further constraint (except the basic minimum support and confidence) are identified, the three programs can discover the same set of association rules, but ACIF and ACAF take more time to find such rules.

For the search of rules with constraints on rule length and items to appear/exclude, Apriori cannot perform such association mining because the algorithm does not support constraints on specific items. It can be noticed that ACIF may run faster than ACAF, but it is incomplete in the sense that there are some rules that should be appeared in the final result but are excluded during the phase of frequent itemset mining. We thus can conclude that ACIF and ACAF are correct, but ACAF is better than ACIF in terms of completeness.

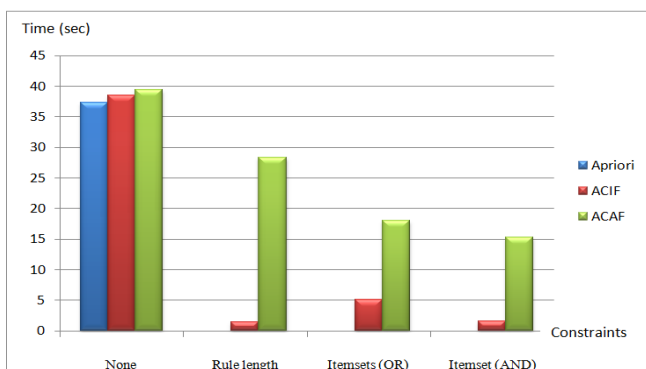


Figure 6. Running time comparison of ACIF and ACAF programs against Apriori program

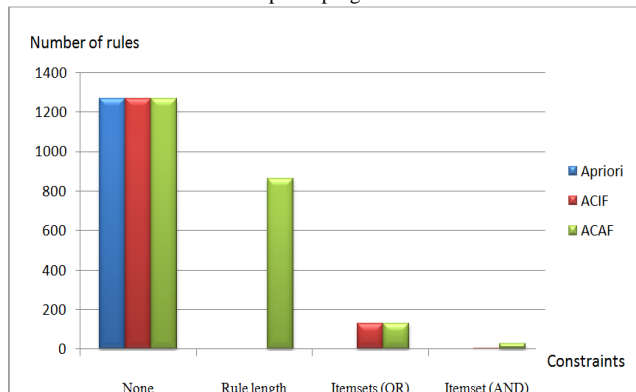


Figure 7. ACIF, ACAF, and Apriori comparison in terms of number of association rules discovered by the program

C. Experimentation with Customer Churn data

To test effectiveness of ACAF program over various constraints, we use the Customer Churn dataset obtained from the website <http://www.sgi.com/tech/mlc/db/>. The dataset contains information of 3333 customers. In the original data set, each record has 21 features (or attributes) in which the last one is the label churn/non-churn customer. The first step of our experimentation is feature selection; the selected 12 features are state, account length, area code, international plan, voice mail plan, number vmail messages, total day calls, total eve calls, total night calls, total intl calls, number customer service calls, and churn. The other nine features are removed because of their insignificance in inducing the association model.

We performed a series of eight experiments with the customer churn data set. Minimum support threshold in each experiment is 50 (that means there must be at least 50 records satisfying the rule’s content), whereas the minimum confidence is 80%. Additional constraints are as follows:

- Exp. 1: No other constraint.
- Exp. 2: The results must contain the feature churn_False.
- Exp. 3: The results must contain rules that has at least three features.
- Exp. 4: The results must NOT contain the feature ‘churn_False’.
- Exp. 5: The results must contain the feature ‘churn_False’ at the then-part of the rule.
- Exp. 6: The results must contain either the feature ‘churn_False’, or ‘churn_True’.
- Exp. 7: The results must contain both the feature ‘churn_True’ and ‘vMailPlan_no’.
- Exp. 8: The results must contain rules that has at least three features, must contain both ‘churn_False’ and ‘vMailPlan_no’, the results must NOT contain either the feature ‘vMailMessage_0’, or ‘intlCalls_2’, and the target clause of the rules must be ‘churn_False’.

(Running result is shown in Fig. 8.)

Running time in each experiment and number of rules reported as the association mining results after constraining with different conditions are varied. We comparatively illustrate the experimental results in Fig. 9.

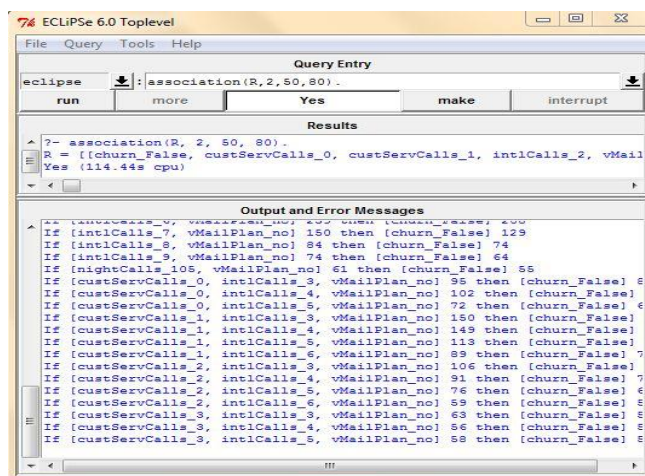


Figure 8. Running result of experiment 8

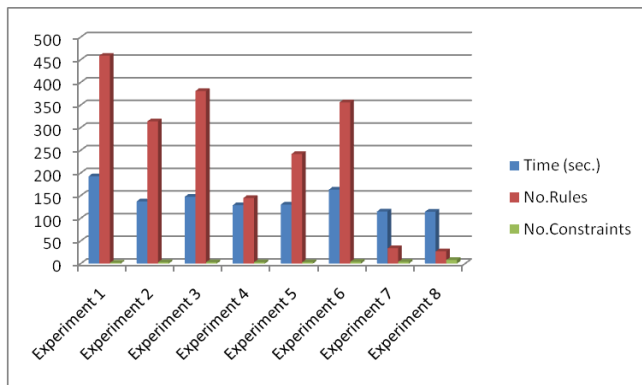


Figure 9. A comparison of computational time usage and number of rules received from varying constraints in each of the eight experiments

V. CONCLUSION AND FUTURE WORK

Association rule discovery is one major problems in the areas of data mining, statistical learning, and business intelligence. The problem concerns finding frequent patterns, or itemsets, hidden in a large database. Finding such frequent itemsets has become an important task because it reveals associations, correlations, and many other interesting relations among items in the transactional databases. We suggest that the problem of frequent itemset and association rule mining can be efficiently implemented with the incorporation of constraints.

We design the two versions of association mining with constraint algorithms called Association rule discovery with Constraints In Frequent itemset mining (ACIF) and Association rule discovery with Constraints After Frequent itemset mining (ACAF). We demonstrated that the proposed algorithms can be concisely implemented with high-level declarative language using ECLiPSe, a constraint logic language. Coding in declarative style takes less effort because pattern matching is a fundamental feature supported by most logic-based languages. Experimentation to verify effectiveness of the proposed methods has been performed and compared against the well-known Apriori method. The results confirm the correctness of the ACIF and ACAF programs and also reveal the power of constraints that have been applied over the frequent itemsets. We focus our future research on the design of constraint formulating and processing to optimize the speed and storage requirement.

ACKNOWLEDGMENT

This research work has been funded by grants from the National Research Council of Thailand (NRCT) and Suranaree University of Technology.

REFERENCES

- [1] R. Agrawal, T. Imielinski, and A. Swami, "Mining association rules between sets of items in large databases," in Proc. ACM SIGMOD, 1993, pp. 207-216.
- [2] R. Agrawal and R. Srikant, "Fast algorithms for mining association rules," in Proc. VLDB, 1994, pp. 487-499.

- [3] K. R. Apt and M. Wallace, Constraint Logic Programming using ECLiPSe, Cambridge University Press, 2007.
- [4] S. Bistarelli and F. Bonchi, "Soft constraint based pattern mining," Data and Knowledge Engineering, vol. 62, 2007, pp. 118-137.
- [5] I. Bratko, Prolog Programming for Artificial Intelligence, 3rd ed., Pearson, 2001.
- [6] A. Cegler and J. Roddick, "Association mining," ACM Computing Surveys, vol.38, no.2, 2006.
- [7] L. De Raedt, T. Guns, and S. Nijssen, "Constraint programming for itemset mining," in Proc. KDD, 2008, pp. 204-212.
- [8] W. J. Frawley, G. Piatetsky-Shapiro, and C. J. Matheus, "Knowledge discovery in databases: an overview," AI Magazine, vol. 13, no. 3, 1992, pp. 57-70.
- [9] J. Han and M. Kamber, Data Mining: Concepts and Techniques, 2nd ed., Morgan Kaufmann, 2006.
- [10] J. Han, J. Pei, and Y. Yin, "Mining frequent patterns without candidate generation," in Proc. ACM SIGMOD, 2000, pp. 1-12.
- [11] J. Hu and X. Li, "Association rules mining including weak-support modes using novel measures," WSEAS Trans. on Computers, vol. 8, no. 3, 2009, pp. 559-568.
- [12] M.C. Hung, S.Q. Weng, J. Wu, and D.L. Yang, "Efficient mining of association rules using merged transactions," WSEAS Trans. on Computers, vol. 5, no. 5, 2006, pp. 916-923.
- [13] N. Kerdprasop and K. Kerdprasop, "Recognizing DNA splice sites with the frequent pattern mining technique," Int. J. of Mathematical Models and Methods in Applied Science, vol.5, no. 1, 2011, pp. 87-94.
- [14] P. Kongchai, K. Kerdprasop, and N. Kerdprasop, "Association rule discovery with constraint logic programming," in Proc. 11th WSEAS Int. Conf. on Computational Intelligence, Man-Machine Systems and Cybernetics, 2012, pp. 135-140.
- [15] R. Kuusik and G. Lind, "Algorithm MONSA for all closed sets finding: basic concepts and new pruning techniques," WSEAS Trans. on Information Science & Applications, vol. 5, no. 5, 2008, pp. 599-611.
- [16] S.-H. Nienhuys-Cheng and R.D. Wolf, Foundations of Inductive Logic Programming, Springer, 1997.
- [17] J. Pei and J. Han, "Can we push more constraints into frequent pattern mining?" in Proc. ACM SIGKDD, 2000, pp. 350-354.
- [18] J. Pei, J. Han, and L. Lakshmanan, "Pushing convertible constraints in frequent itemset mining," Data Mining and Knowledge Discovery, vol. 8, 2004, pp. 227-252.
- [19] R. Srikant, Q. Vu, and R. Agrawal, "Mining association rules with item constraints," in Proc. KDD, 1997, pp. 67-73.
- [20] H. Sug, "Discovery of multidimensional association rules focusing on instances in specific class," Int. J. of mathematics and Computers in Simulation, vol. 5, no. 3, 2011, pp. 250-257.
- [21] H. Toivonen, "Sampling large databases for association rules," in Proc. VLDB, 1996, pp. 134-145.
- [22] G. Yu, S. Shao, and X. Zeng, "Mining long high utility itemsets in transaction databases," WSEAS Trans. on Information Science & Applications, vol. 5, no. 2, 2008, pp. 202-210.
- [23] M. J. Zaki, S. Parthasarathy, M. Ogihara, and W. Li, "Parallel algorithm for discovery of association rules," Data Mining and Knowledge Discovery, vol. 1, 1997, pp. 343-374.

Bayes Net Analysis to Support Database Design and Normalization

Nittaya Kerdprasop

Data Engineering Research Unit,
School of Computer Engineering,
Suranaree University of Technology, Thailand
nittaya@sut.ac.th

Kittisak Kerdprasop

Data Engineering Research Unit,
School of Computer Engineering,
Suranaree University of Technology, Thailand
kerdpras@sut.ac.th

Abstract—Knowledge discovery, also known as data mining, has gained much interest from diverse sectors due to their great potential on revealing potentially useful relationships. Among many possible applications, we focus our research on the database design and analysis application. Functional dependency plays a key role in database normalization, which is a systematic process of verifying database design to ensure the nonexistence of undesirable characteristics. Bad design could incur insertion, update, and deletion anomalies that are the major cause of database inconsistency. In this paper, we propose a novel technique to discover functional dependencies from the database table. The discovered dependencies help the database designers covering up inefficiencies inherent in their design. Our discovery technique is based on the structure analysis of Bayesian network. Most data mining techniques applied to the problem of functional dependency discovery are rule learning and association mining. Our work is a novel attempt of applying the Bayesian network to this area of application. The proposed technique can reveal functional dependencies within a reduced search space. Therefore, computational complexity is acceptable.

Keywords-functional dependency; knowledge discovery; data mining; Bayesian network; database design; normalization

I. INTRODUCTION

Database design methodology normally starts with the first step of conceptual schema design in which users' requirements are modeled as the entity-relationship (ER) diagram. The next step of logical design focuses on the translation of conceptual schemas into relations or database tables. The later step of physical design concerns the performance issues such as data types, indexing option, and other parameters related to the database management system. Conceptual schema and logical designs are two important steps regarding correctness and integrity of the database model. Database designers have to be aware of specifying thoroughly primary keys of tables and also determining extensively relationships between tables. Data normalization is a common mechanism employed to support database designers to ensure the correctness of their design.

Normalization transforms unstructured relation into separate relations, called normalized ones [9]. The main purpose of this separation is to eliminate redundant data and reduce data anomaly (i.e., data inconsistency as a result of insert, update, and delete operations). There are many different levels of normalization depending on the purpose of

database designer. Most database applications are designed to be either in the third, or the Boyce-Codd normal forms in which their dependency relations [3] are sufficient for most organizational requirements.

The main condition to transform from one normal form to the next level is the dependency relationship, which is a constraint between two sets of attributes in a relation. Functional dependency constrains the determination uniqueness from one set of attribute values to the others.

Experienced database designers are able to elicit this kind of dependency information. But in some applications in which the business process and operational requirements are complex, this task of dependency analysis is tough even for the experienced ones. We thus propose to use the data mining technique called Bayesian network learning or Bayes net to help analyzing the database structure and then report the underlying functional dependencies. This work can also support the automatic induction of functional dependencies from legacy databases that design documents are no longer available. The rest of this paper is organized as follows. We discuss related work regarding the functional dependency discovery problem in Section 2. Then propose our methodology in Section 3. Running examples and experimentation appear in Sections 4 and 5, respectively. Finally, the last section concludes this paper with the mention of our future work.

II. RELATED WORK

The main objective of our study is the induction of functional dependency relationships from the database instances. It has long been the problem of interest among database researchers [16], [22], [23], [26], [29], [32], [33] because such relationships are abstract in their nature and hence can be easily missed out in the database design.

Silva and Melkanoff [29] was the first team attempting to discover functional dependencies (FDs) through the data mining technique. The complexity of discovering FDs from existing database instances has been studied by Mannila and Raiha [22], [23]. Early work on FD discovery handled the complexity problem by means of partitioning the set of rows according to their attribute values and perform a level-wise search for desired solution [15], [17], [26], [33]. The later work of Wyss et al. [33] and Atoum et al. [4] applied the minimal cover concept on equivalent classes.

Researchers in the application area of database reverse engineering are also interested in the same objective. Lee and

Yoo [20] proposed a method to derive a conceptual model from object-oriented databases. The final products of their method are the object model and the scenario diagram describing a sequence of operations. The work of Perez et al. [28] emphasized on relational object-oriented conceptual schema extraction. Their technique is based on a formal method of term rewriting. Rules obtained from term rewriting are then generated to represent the correspondences between relational and object-oriented elements. Researchers that focus their study on a particular issue of semantic understanding including Lammari et al. [19] who proposed a method to discover inter-relational constraints and inheritances embedded in a relational database. Chen et al. [7] also based their study on entity-relationship model. They proposed to apply association rule mining to discover new concepts leading to a proper design of relational database schema. They employed the concept of fuzziness to deal with uncertainty inherited with the association mining process. The work of Pannurat et al. [27] and Alashqur [1] are also in the line of association mining technique application to the database design.

Besides functional dependencies, other kinds of database relationships are also explored. De Marchi et al. [11] studied the problem of inclusion dependencies. Fan et al. [12] proposed the idea to capture conditional FDs. Calders et al. [6] introduced a notion of roll-up dependency to be applied to the OLAP context. Approximate FDs concept has been recently applied to different subfield of data mining such as decision tree building [18], data redundancy detection [2], and data cleaning [8], [24].

Our work is different from those in the literature in that our method of discovering FDs is based on the analysis of Bayes net structure [13], [14], [21], [30]. The work of Mayfield et al. [24] also consider applying Bayesian network but for a different purpose of correcting missing information. They perform stochastic process to simulate and estimate missing values. Our work does not require simulation; we instead base our discovery task solely on the existing database instances. Therefore, from the literature review we can state that our work is original in this area of problem.

III. PROPOSED METHODOLOGY

Functional dependencies between attributes of a relation express a constraint between two sets of attributes. For instance, the constraint $X \rightarrow Y$ states that the values of attributes in a set Y are fully determined by values of attributes in a set X . The obvious example is given the social security number, there is at most one individual associated with that number.

Discovering such constraints from the database instances requires extensive search over each pair of attribute values. We propose a methodology of employing Bayesian networks learning [5], [25] at this step. Bayesian network or Bayes net is a graphical model representing correlations among variables in the network structure. Relation attributes correspond to variables, which appear as nodes in the Bayes net. A Bayes net is a directed acyclic graph whose edges represent statistical dependencies.

Input: a set of database instances
Output: functional dependency rules
Steps:

/ Learning Phase */*

1. Apply Bayesian learning algorithm to the set of database instances to form a network structure
2. Identify conditional independency with ICS search algorithm [26] and assign direction to the edges
3. Output causal Bayes net with additional conditional probability table associated with each node

/ FDs Detection Phase */*

4. For an effect node (E) linking from a single causal node (C) or at most two causal nodes
5. Check conditional probability table of the effect node
6. If for each value of E there exists distinct value of C related to E with probability not less than 0.5 (regarding to existing values in the database instances),
Then add a rule $C \rightarrow E$ to the FD rule set
7. If C contains two nodes (C1 and C2),
Then repeat step 6 with $C1 \rightarrow E$ and $C2 \rightarrow E$
8. For an effect node (E) linking from multiple causal nodes (Cs)
9. Examine each edge linking from each C in Cs
10. If the criterion in steps 5-6 is satisfied by each and every edge,
Then add a rule $Cs \rightarrow E$ to the FD rule set
11. Return the FD rule set as the output

Figure 1. Algorithm BayesFD for discovering functional dependencies from the database instances

With the proper search procedure, such as the ICS algorithm [31], and the use of conditional dependencies associated with each node, we can turn dependence relations between variables into causal relationship among nodes in the Bayes net.

We also apply heuristics on the consideration over each conditional dependency table associated with the child node to select proper functional dependencies from the Bayes net. For a strong dependency requirement, the minimum conditional probability can be set greater than 0.5. Our algorithm of FDs discovery, named BayesFD, is presented in Fig. 1.

IV. RUNNING EXAMPLES AND ANALYSIS RESULTS

We demonstrate the mechanism of our proposed method via the two examples.

Example 1. The database instances are given as shown in Table I.

TABLE I. EXAMPLE DATABASE

A	B	C	D
a1	b1	c1	d1
a1	b2	c1	d2
a2	b2	c2	d2
a2	b3	c2	d3
a3	b3	c2	d4

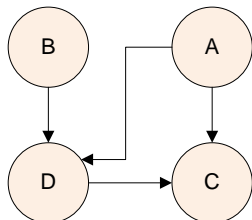


Figure 2. Bayesian network structure of the example database

Learning Phase (steps 1-3)

Perform causal Bayesian learning (illustration of Bayesian learning is given in Appendix) to the database instances in Table I to obtain the network structure as illustrated in Fig. 2.

There are two effect nodes in Bayes net of Fig. 2, that are, node D and node C. Both of them have two causal nodes. Therefore, the FDs detection phase follows the steps 4-7.

FDs Detection Phase (steps 4-7)

Check conditional probability tables for each causal edge, that is, $AB \rightarrow D$ and $AD \rightarrow C$. Details of conditional probability values in each relation are shown in Tables II and III (combinations of attribute values that do not exist in the database table have been removed). Both dependency relationships hold. But they are composed of two causal nodes. We thus have to check other four dependencies: $A \rightarrow D$, $B \rightarrow D$, $A \rightarrow C$, and $D \rightarrow C$. The only dependency that holds is $A \rightarrow C$, and its conditional probability table is shown in Table IV.

TABLE II. CONDITIONAL PROBABILITY FOR DEPENDENCY $AB \rightarrow D$

	D=d1	D=d2	D=d3	D=d4
A=a1, B=b1	0.5	0.167	0.167	0.167
A=a1, B=b2	0.167	0.5	0.167	0.167
A=a2, B=b2	0.167	0.5	0.167	0.167
A=a2, B=b3	0.167	0.167	0.5	0.167
A=a3, B=b3	0.167	0.167	0.167	0.5

TABLE III. CONDITIONAL PROBABILITY FOR DEPENDENCY $AD \rightarrow C$

	C=c1	C=c2
A=a1, D=d1	0.75	0.25
A=a1, D=d2	0.75	0.25
A=a2, D=d2	0.25	0.75
A=a2, D=d3	0.25	0.75
A=a3, D=d4	0.25	0.75

TABLE IV. CONDITIONAL PROBABILITY FOR DEPENDENCY $A \rightarrow C$

	C=c1	C=c2
A=a1	0.833	0.167
A=a2	0.167	0.833
A=a3	0.25	0.75

Therefore, we can conclude that with the given example database as shown in Table I, the three discovered functional dependencies are: $AB \rightarrow D$, $AD \rightarrow C$, and $A \rightarrow C$.

Example 2. The customer database instances are given as shown in Table V.

TABLE V. CUSTOMER DATABASE

A1	A2	A3	A4	A5	A6	A7
1	c1	Kitty	21000	Honda	31	Dang
1	c8	Kitty	21000	Toyota	41	Dum
1	c6	Kitty	21000	Nissan	51	Ple
2	c2	Somsak	20111	Mitsubishi	41	Dum
2	c5	Somsak	20111	Toyota	31	Dang
3	c4	Siri	19999	Toyota	31	Dang

Learning Phase (steps 1-3)

Perform causal Bayesian learning to the database instances in Table V to obtain the network structure as illustrated in Fig. 3.

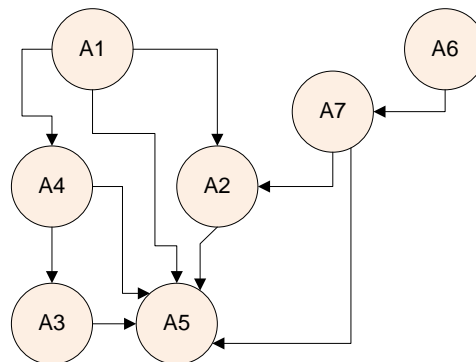


Figure 3. Bayesian network structure of customer database

There are five effect nodes in Bayes net of Fig. 3, that are, nodes A2, A3, A4, A5, and A7. Nodes A3, A4, and A7 have a single causal node, and A2 has two causal nodes. Thus, the FDs detection phase follows the steps 4-7, whereas the node A5 has to follow steps 8-10 because it has multiple causal nodes.

FDs Detection Phase (steps 4-7)

Single causal nodes (A3, A4, and A7) are easy to examine the dependencies as shown in Tables VI-VIII.

TABLE VI. CONDITIONAL PROBABILITY FOR DEPENDENCY A4 → A3

	A3=Kitty	A3=Somsak	A3=Siri
A4=21000	0.778	0.111	0.111
A4=20111	0.143	0.714	0.143
A4=1999	0.2	0.2	0.6

TABLE VII. CONDITIONAL PROBABILITY FOR DEPENDENCY A1 → A4

	A4=21000	A4=21000	A4=21000
A1=1	0.778	0.111	0.111
A1=2	0.143	0.714	0.143
A1=3	0.2	0.2	0.6

TABLE VIII. CONDITIONAL PROBABILITY FOR DEPENDENCY A6 → A7

	A7=Dang	A7=Dum	A7=Ple
A6=31	0.778	0.111	0.111
A6=41	0.143	0.714	0.143
A6=51	0.2	0.2	0.6

TABLE IX. CONDITIONAL PROBABILITY FOR DEPENDENCY A1A7 → A2

	A2=c1	A2=c2	A2=c4	A2=c5	A2=c6	A2=c8
A1=1, A7=Dang	0.375	0.125	0.125	0.125	0.125	0.125
A1=1, A7=Dum	0.125	0.125	0.125	0.125	0.125	0.375
A1=1, A7=Ple	0.125	0.125	0.125	0.125	0.375	0.125
A1=2, A7=Dang	0.125	0.125	0.125	0.375	0.125	0.125
A1=2, A7=Dum	0.125	0.375	0.125	0.125	0.125	0.125
A1=3, A7=Dang	0.125	0.125	0.375	0.125	0.125	0.125

It can be noticed from the conditional probability tables that the three dependencies A4→A3, A1→A4, and A6→A7 hold. The node A2 has two causal nodes: A1 and A7. The conditional probability of A1A7 → A2 is given in Table IX. It can be seen that all probability values are less than 0.5. Therefore, the dependency A1A7 → A2 does not hold, so do the dependencies A1 → A2 and A7 → A2.

The last examination is the dependency with multiple causal nodes A1A2A3A4A7 → A5. The steps 8-10 have to be applied. We then split the dependency relation into five cases: A1→ A5, A2→ A5, A3→ A5, A4→ A5, and A7→ A5. Conditional probabilities of the five cases are shown altogether in Table X. It is obviously seen that the only relation that holds is A2→ A5.

The discovered functional dependencies of database 2 are as follows:
 A4→A3,
 A1→A4,
 A6→A7, and
 A2→A5.

TABLE X. CONDITIONAL PROBABILITY FOR DEPENDENCY A1 → A5, A2 → A5, A3 → A5, A4 → A5, A7 → A5

	A5= Honda	A5= Toyota	A5= Nissan	A5= Mitsubishi
A1=1	0.3	0.3	0.3	0.1
A1=2	0.125	0.375	0.125	0.375
A1=3	0.167	0.5	0.167	0.167

A2=c1	0.5	0.167	0.167	0.167
A2=c2	0.167	0.167	0.167	0.5
A2=c4	0.167	0.5	0.167	0.167
A2=c5	0.167	0.5	0.167	0.167
A2=c6	0.167	0.167	0.5	0.167
A2=c8	0.167	0.5	0.167	0.167

A3=Kitty	0.3	0.3	0.3	0.1
A3=Somsak	0.125	0.375	0.125	0.375
A3=Siri	0.167	0.5	0.167	0.167

A4=21000	0.3	0.3	0.3	0.1
A4=20111	0.125	0.375	0.125	0.375
A4=1999	0.167	0.5	0.167	0.167

A7=Dang	0.3	0.3	0.3	0.1
A7=Dum	0.125	0.375	0.125	0.375
A7=Ple	0.167	0.5	0.167	0.167

V. EXPERIMENTATION

This section explains experimentation including steps in data preparation and parameter setting to learn Bayesian network structure with the WEKA software (<http://www.cs.waikato.ac.nz/ml/weka>). For data preparation, the customer database (Table V in example 2) has to be transformed into the *arff* format as follows:

```
@relation CustomerDatabase
@attribute A1 {1, 2, 3}
@attribute A2 {c1, c2, c4, c5, c6, c8}
@attribute A3 {kitty, somsak, siri}
@attribute A4 {21000, 20111, 1999}
@attribute A5 {honda, toyota, nissan, mitsubishi}
@attribute A6 {31, 41, 51}
@attribute A7 {dang, dum, ple }
@data
1, c1, kitty, 21000, honda, 31, dang
1, c8, kitty, 21000, toyota, 41, dum
1, c6, kitty, 21000, nissan, 51, ple
2, c2, somsak, 20111, mitsubishi, 41, dum
2, c5, somsak, 20111, toyota, 31, dang
3, c4, siri, 1999, toyota, 31, dang
```

After invoking WEKA and selecting the explorer task, click the classify tab and choose the ‘BayesNet’ algorithm for learning the Bayesian network structure. The default setting of this algorithm is inappropriate for learning the cause and effect structure, as required by this specific functional dependency application. We thus have to set the

right parameter by clicking at the frame in which the name BayesNet appears (as pointed by the arrow in Fig. 4). A small window will be popped up. Then click the 'searchAlgorithm' option to choose the ICS search algorithm, and then click the OK button.

The Bayesian network structure can be visualized by right-clicking at the algorithm name below the 'Result list' panel (as shown in Fig. 5). Then choose 'Visualize graph.' A new pop-up window will appear as shown in Fig. 6.

Each node in the Bayesian network is associated with the conditional probability table. This table does not automatically display in the network structure, but it can be viewed by clicking at the node. The example of conditional probability table associated with node A7 is shown in Fig. 7.

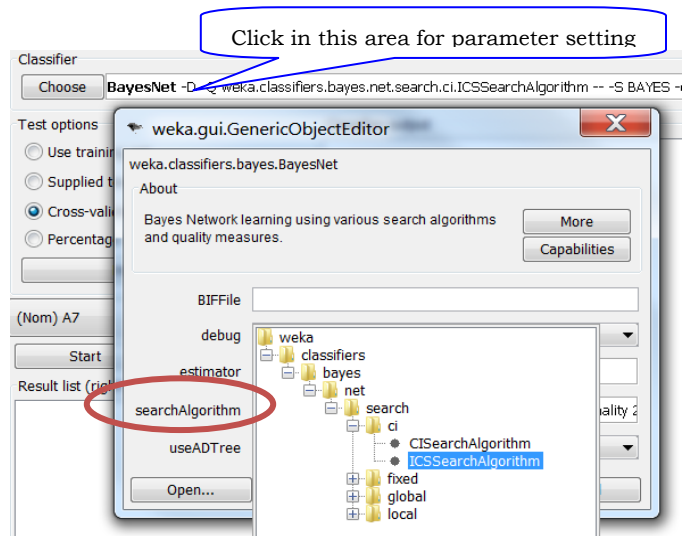


Figure 4. set the 'searchAlgorithm' parameter

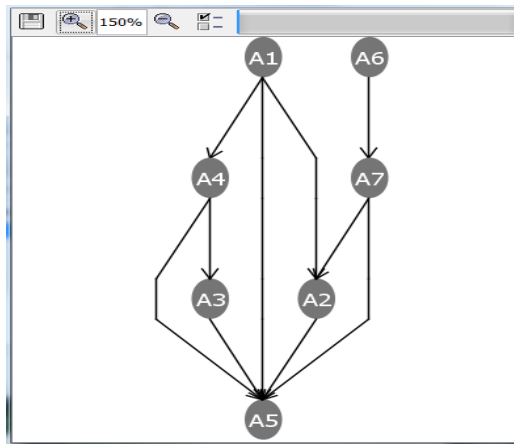


Figure 6. a Bayesian network structure for customer database

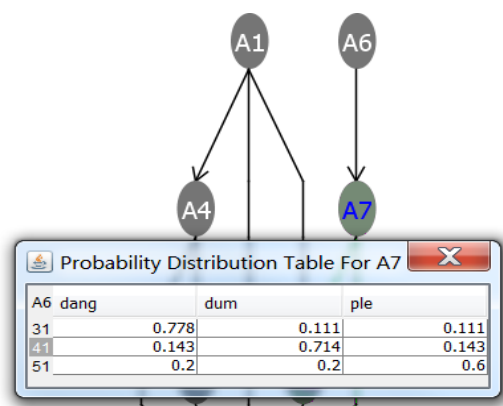


Figure 7. a conditional probability associated with each node

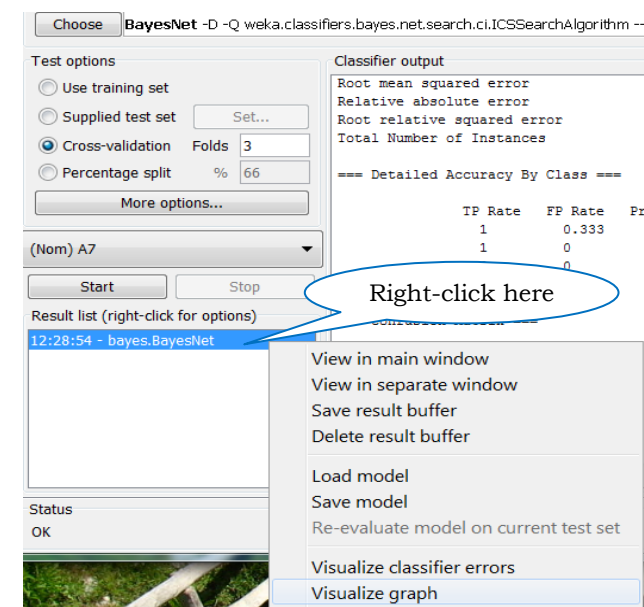


Figure 5. select 'Visualize graph' to view the Bayesian network

VI. CONCLUSION

The design of a complete database starts from the high-level conceptual design to capture detail requirements of the enterprise. Common tool normally used to represent these requirements is the entity-relationship, or ER, diagram and the product of this design phase is a conceptual schema. Typically, the schema at this level needs some adjustments based on the procedure known as normalization in order to reach a proper database design. Then, the database implementation moves to the lower abstraction level of logical design in which logical schema is constructed in a form of relations, or database tables.

In this paper, we propose a method to discover functional dependencies inherent in the conceptual schema from the database relation containing data instances. The discovering technique is based on the structure analysis of learned Bayes net. Heuristics are also applied on the relationship selection over the network structure.

The results from the proposed method are the same as the design schema obtained from the database designer. We plan to improve our methodology to discover a conceptual schema up to the level of multi-relations.

ACKNOWLEDGMENT

This research work has been funded by grants from the National Research Council of Thailand (NRCT) and Suranaree University of Technology through the full support of Data Engineering Research Unit, in which both authors are principal researchers.

REFERENCES

- [1] A. Alashqur, "Expressing database functional dependencies in terms of association rules," *European Journal of Scientific Research*, vol. 32, no. 2, 2009, pp. 260-267.
- [2] P. Andritsos, R. J. Miller, and P. Tsaparas, "Information-theoretic tools for mining database structure from large data sets," in *Proc. SIGMOD*, 2004, pp. 731-742.
- [3] W. W. Armstrong, "Dependency structures of database relationships," *Information Processing*, vol.74, 1974, pp. 580-583.
- [4] J. Atoum, D. Bader, and A. Awajan, "Mining functional dependency from relational databases using equivalent classes and minimal cover," *Journal of Computer Science*, vol. 4, no. 6, 2008, pp. 421-426.
- [5] R. R. Bouckaert, *Bayesian Network Classifiers in Weka for Version 3-5-5*, The University of Waikato, 2007.
- [6] T. Calders, R. T. Ng, and J. Wijsen, "Searching for dependencies at multiple abstraction levels," *ACM Transactions on Database Systems*, vol. 27, no. 3, 2002, pp. 229-260.
- [7] G. Chen, M. Ren, P. Yan, and X. Guo, "Enriching the ER model based on discovered association rules," *Information Sciences*, vol. 177, 2007, pp. 1558-1556.
- [8] F. Chiang and R. J. Miller, "Discovering data quality rules," in *Proc. VLDB*, 2008, pp. 1166-1177.
- [9] E. F. Codd, "A relational model of data for large shared data banks," *Communications of the ACM*, vol.13, no.6, 1970, pp. 377-387.
- [10] C. J. Date and R. Fagin, "Simple conditions for guaranteeing higher normal forms in relational databases," *ACM Transactions on Database Systems*, vol.17, no.3, 1992, pp. 465-476.
- [11] F. De Marchi, S. Lopes, and J. M. Petit, "Efficient algorithms for mining inclusion dependencies," in *Proc. EDBT*, 2002, pp. 464-476.
- [12] W. Fan, F. Geerts, X. Jia, and A. Kementsietsidis, "Conditional functional dependencies for capturing data inconsistencies," *ACM Transactions on Database Systems*, vol. 33, no. 2, 2008, pp. 6:1-6:48.
- [13] A. Heni, M.N. Omri, and A.M. Alimi, "Fuzzy knowledge representation based on possibilistic and necessary Bayesian networks," *WSEAS Transactions on Information Science and Applications*, vol.3, issue 2, 2006, pp. 224-231.
- [14] T.Y. Hsieh and B.C. Kuo, "Information-based item selection with blocking strategy based on Bayesian network," *WSEAS Transactions on Information Science and Applications*, vol.7, issue 9, 2010, pp. 1160-1169.
- [15] Y. Huhtala, J. Karkkainen, P. Porkka, and H. Toivonen, "Efficient discovery of functional and approximate dependencies using partitions," in *Proc. ICDE*, 1998, pp. 392-401.
- [16] T. Hussain, "Schema transformations and dependency preservation," in *Proc. 7th WSEAS Int. Conf. on Applied Informatics and Communications*, Athens, Greece, August 24-26, 2007, pp. 313-318.
- [17] R. S. King and J. J. Legendre, "Discovery of functional and approximate functional dependencies in relational databases," *Journal of Applied Mathematics and Decision Sciences*, vol. 7, no. 1, 2003, pp. 49-59..
- [18] K. Lam and V. Lee, "Building decision trees using functional dependencies," in *Proc. Int. Conf. Information Technology: Coding and Computing*, 2004, p. 470.
- [19] N. Lammari, I. Comyn-Wattiau, and J. Akoka, "Extracting generalization hierarchies from relational databases: A reverse engineering approach," *Data & Knowledge Engineering*, vol.63, 2007, pp. 568-589.
- [20] H. Lee and C. Yoo, "A form driven object-oriented reverse engineering methodology," *Information Systems*, vol.25, no.3, 2000, pp. 235-259.
- [21] J. Ma and K. Sivakumar, "Privacy-preserving Bayesian network parameter learning," *WSEAS Transactions on Information Science and Applications*, vol.3, issue 1, 2006, pp. 1-6.
- [22] H. Mannila and K. J. Raiha, "Dependency inference," in *Pro. VLDB*, 1987, pp. 155-158.
- [23] H. Mannila and K. J. Raiha, "On the complexity of inferring functional dependencies," *Discrete Applied Mathematics*, vol. 40, 1992, pp. 237-243.
- [24] C. Mayfield, J. Neville, and S. Prabhakar, "ERACER: A database approach for statistical inference and data cleaning," in *Proc. SIGMOD*, 2010, pp. 75-86.
- [25] R. E. Neapolitan, *Learning Bayesian Networks*, Pearson Education, 2004.
- [26] N. Novelli and R. Cicchetti, "Functional and embedded dependency inference: a data mining point of view," *Information Systems*, vol. 26, 2001, pp. 477-506.
- [27] N. Pannurat, N. Kerdprasop, and K. Kerdprasop, "Database reverse engineering based on association rule mining," *International Journal of Computer Science Issues*, vol. 7, no 2, March 2010, pp. 10-15.
- [28] J. Perez, I. Ramos, V. Anaya, J. M. Cubel, F. Dominguez, A. Boronat, and J. A. Carsi, "Data reverse engineering for legacy databases to object oriented conceptual schemas," *Electronic Notes in Theoretical Computer Science*, vol.72, no.4, 2003, pp. 7-19.
- [29] A. M. Silva and M. A. Melkanoff, "A method for helping discover the dependencies of a relation," in H. Gallaire, J. Minker, J. M. Nicolas (eds.), *Advances in Data Base Theory*, Plenum Press, 1981, pp. 115-133.
- [30] M. Tuba and D. Bulatovic, "Design of an intrusion detection system based on Bayesian networks," *WSEAS Transactions on Computers*, vol.8, issue 5, 2009, pp. 799-809.
- [31] T. Verma and J. Pearl, "An algorithm for deciding if a set of observed independencies has a causal explanation," in *Proc. Conf. Uncertainty in Artificial Intelligence*, 1992, pp. 323-330.
- [32] C. Wyss, C. Giannella, and E. Robertson, "FastFDs: A heuristic-driven, depth-first algorithm for mining functional dependencies from relational instances," in *Proc. DaWaK*, 2001, pp. 101-110.
- [33] H. Yao and H. J. Hamilton, "Mining functional dependencies from data," *Data Mining and Knowledge Discovery*, vol. 16, 2008, pp. 197-219.

Flexible Process Modeling Determined by Existing Human Expert Domain Knowledge Bases

Ingo Schwab
Karlsruhe University of
Applied Sciences
Karlsruhe, Germany
Ingo.Schwab@hs-
karlsruhe.de

Melanie Senn
Karlsruhe University of
Applied Sciences
Karlsruhe, Germany
Melanie.Senn@hs-
karlsruhe.de

Susanne Fischer
Karlsruhe University of
Applied Sciences
Karlsruhe, Germany
Susanne.Fischer@hs-
karlsruhe.de

Norbert Link
Karlsruhe University of
Applied Sciences
Karlsruhe, Germany
Norbert.Link@hs-
karlsruhe.de

Abstract— The evaluation of final workpiece properties at process end can be realized by process modeling instead of destructive testing methods. In this paper, we give an overview about different modeling strategies. They are focused on the amount of available domain knowledge. White box models try to model the reality by physical principles and black box models are mainly data driven. Grey box models are hybrid variants. The different strategies are applied to the domain of resistance spot welding. The proposed approaches are able to improve the quality of resistance spot welding.

Keywords- *Intelligent Systems; Machine Learning Manufacturing.*

I. INTRODUCTION

Several methods exist to model the dynamics of nonlinear complex systems [1]. Conceptually, they can be split into two classes. The first class includes prior domain knowledge from human experts. For example, numerical simulations like finite elements or phase field methods describe the behavior of systems with domain knowledge from human experts. The second class is characterized by the use of phenomenological or general basis function models, which try to fit the observed behavior of the systems as good as possible. The latter approach includes many Machine Learning, Data Mining and statistical methods.

The second class can be further refined in modeling via symbolic [2, 3] (e.g., general formula expressions) and subsymbolic (e.g., dedicated base function class, support vector machines or neural networks) representations. Symbolic learning representations can be interpreted by human domain experts and they can help to understand the process in a more formal way. Therefore, this class does not only aim to model the system behavior. Sometimes the human experts are able to identify previously unknown facts of the observed process.

In contrast, subsymbolic representations are black box models. In most cases, it is very difficult or impossible to interpret the behavior of the learnt representation [3].

The proposed methods in this paper can be interpreted as modeling the dynamic of processes. A generic process model is depicted in Fig. 1 with an observer and a controller. This representation enables a universal process description by means of the observable quantities, the characteristic process state and the process parameters that allow manipulating the process purposefully. The observer can predict the characteristic state and the workpiece properties for quality evaluation from static or dynamic observable quantities. The observer model depends on the embedded domain knowledge (white, grey or black box). Independently from this, the observer model that represents the process dynamics might be of static or dynamic model type. The controller can then determine the optimal process parameters from the evolution of the characteristic state by solving a multi-stage optimization problem compensating the process noise.

The purpose of this paper is twofold. It can be used as a guideline and introduction for the creation of a model for system processes with different constraints on the amount of existing prior domain knowledge and/or insufficient experimental data. On the other hand, it attempts to give an overview of our developments concerning intelligent systems. The application domain is resistance spot welding. To this end, we decided to summarize the results of some of our projects, give some background information and refer to some of our already published papers. This article is organized as follows. We start in Section II by giving a brief overview of different modeling strategies, which are predetermined by the amount of existing prior system knowledge and the amount of observed experimental system data. These approaches include in general white box and black box models. Grey box models represent a compromise between both ideas. Section III gives a brief overview on resistance spot welding. Section IV reviews some basic ideas of the used Machine Learning, Data Mining and parameter fitting techniques and section V summarizes how we use them. We conclude with a discussion of open questions and future steps of our project. Most of the results and conducted

experiments have been published elsewhere, but this paper focuses on an comprehensive overview.

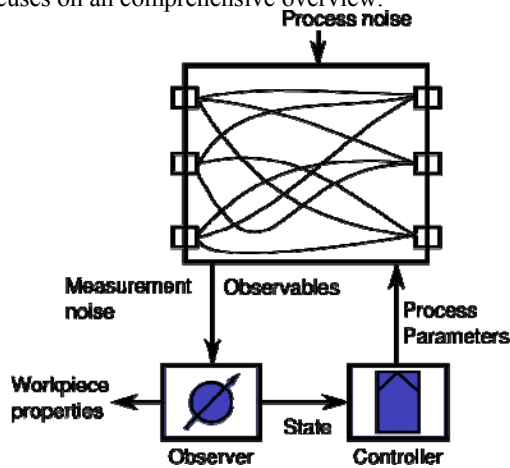


Figure 1. A generic process model.

II. PROCESS MODELING

The basis of system identification is always a model illustrating an idea of the physical reality. In principle, two major modeling approaches can be identified. They are different in terms of the used structure and the free parameters of the model. The structure determines the general behavior and the complexity of the model (qualitative model description) and the parameters determine the specific behavior of a given structure (quantitative model description). Generally, the approaches depend on the existing prior knowledge about the modeled system.

White box models: White box models result from complete understanding of the system behavior and theoretical analysis. This analysis is performed by formulating physical or geometric equations. The predefined model structure and the precise match of the internal model parameters and known physical parameters (e.g., from textbooks) are characteristic for white box models. From this point of view, the parameters are interpretable in a symbolic way which includes a predefined semantic. The model parameters can be compared and fitted to measurements. White box models usually have a high accuracy. However, they assume that the system behavior was analyzed in great detail, which can often be very time-consuming or even impossible. White box models are from this point of view parametric models and the parameters are interpretable by human experts.

Black box models: Sometimes the complicated and time consuming theoretical analysis is not possible. The lack of knowledge of the underlying system principles requires alternative approaches. Most of them make use of the experimental observation data and thus the learning process is mainly data driven. This means that the free parameters of the model are optimized to reproduce the observations of the system as good as possible. The optimized model is a so-

called black box model or grey box model. The difference between the two model types is determined by the amount of prior knowledge which is integrated into the model. The characteristic property of black box models is that there is no or very limited prior knowledge about the behavior and structure of the observed system. Typically, the free parameters of the model have no direct link to the physical meaning of the system. In this case, we refer to non-parametric models (aka subsymbolic knowledge representation). It reflects only the input and output of the system and the physical parameters are represented implicitly by the values of the weighting functions (e.g., the basis functions in neural networks). The parameters of a black box model are not interpretable by a human expert.

Grey box models: Grey box models are a mixture of white box and black box models. They generally involve information from physical equations and data as well as qualitative information in form of rules. Grey box models often judge on the basis of assumptions about the structure of the system and the process. In this case, the free parameters of the system have a physical meaning of the system and we refer to parametric models (aka symbolic representation).

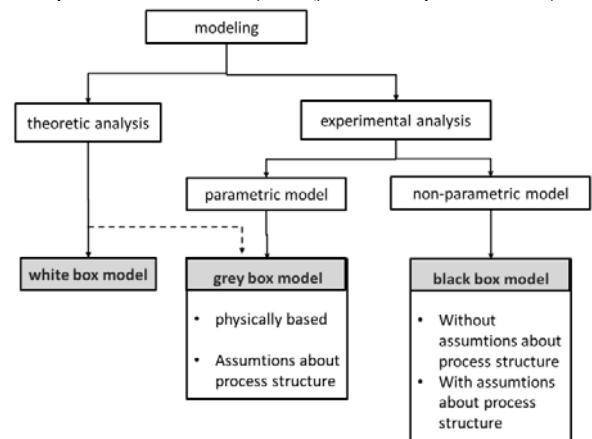


Figure 2. Process modeling.

TABLE I. PROCESS MODEL AND PROPOSED METHODS

	Proposed Methods
white box model	Simulations (e.g., Sorpas)
grey box model	Phenomonologic Model, Symbolic Regression
black box model	SVR

Which type of model is chosen depends on the amount of prior knowledge about the system and the intended use of the extracted model. From a control theory standpoint [4, 5], internal system states are mandatory. This includes white and grey box models. The dynamics of the system (e.g., the behavior of resistance spot welding proposed in this paper) are modeled and the internal states are used to (re-)adjust the parameters in order to optimize the parameters of a goal function. This goal function can be of completely diverse nature, but in most cases it involves reducing costs.

In some use cases, a mapping from the input of a system to its output is sufficient. In these cases, black box models can be applied and experimental data can be used for the

learning process. In this case, the dynamics of the system are not modeled. Consequentially, readjusting parameters during operational time is not possible. Even though, the goal function can also be optimized since a mapping from the starting parameters to the final states is constructed and a good starting point from the parameters can be chosen.

Table I summarizes the methods which we elaborated in the course of our projects. Support Vector Regression (see Section IV) is a black box model and is able to map the starting parameters to the final states in an efficient way. Phenomonologic models (which are also expanded by a correction term found by Symbolic Regression) are used to model the system dynamics in a sense of control theory. That means, that the parameters can be readjusted during the service time to further improve the quality of the process.

In the following section, we will introduce the application of resistance spot welding following by a brief introduction to the used methods (Section IV).

III. RESISTANCE SPOT WELDING

In resistance spot welding (RSW, see [8, 9] for more details), two metal sheets are joined together by means of an evolving welding spot that results from local melting of the sheet material. The melting is caused by the electrical current flow and an associated temperature increase through the application of an electrode force and an electrical current. The experimental RSW environment with its tools, namely the electrodes, the two sheets and the individual resistance components that describe the combined dynamic resistance is depicted in Fig. 3. The temporal evolution of the dynamic resistance is shown in Fig. 4. The diameter of the welding spot serves as a visual, nondestructive quality indicator for the processed experiments. During RSW, quantities such as the electrical current, the voltage, the electrode force and the electrode displacement can be measured. The electrical resistance can then be calculated from the current and the voltage.

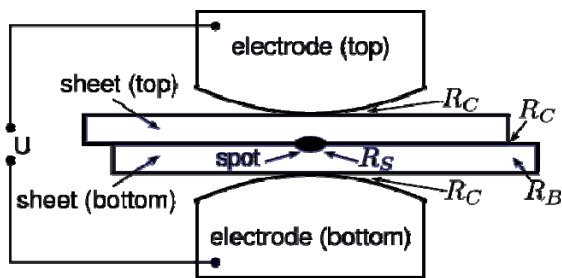


Figure 3. Experimental resistance spot welding environment: tools, sheets and resistance components.

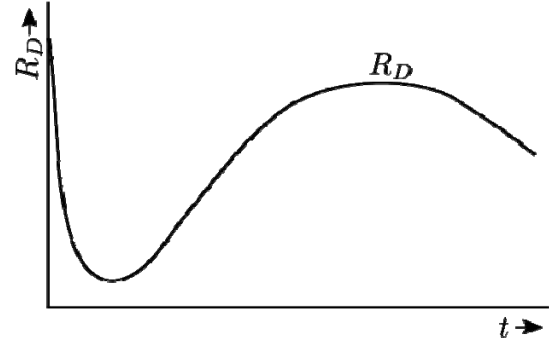


Figure 4. Temporal evolution of the dynamic resistance during resistance spot welding.

Analytical resistance model

In our previous work [6, 7], we have formulated an analytical model of the dynamic resistance that is composed of the individual resistance components as indicated in Fig. 1. The combined dynamic resistance $R_D(t)$ is composed of the bulk resistance $R_B(t)$, the contact resistance $R_C(t)$, the spot resistance $R_S(t)$ and the static resistance $R_0(t)$:

$$R_D(t) = R_0(t) + R_B(t) + R_C(t) + R_S(t). \quad (1)$$

The bulk resistance

$$R_B(t) = \alpha_{BL} \cdot (1 - \exp(-\alpha_{BC} \cdot t)) \quad (2)$$

describes the rising resistivity in the bulk material with increasing temperature. The contact resistance

$$R_C(t) = R_{CF}(t) + R_{CC}(t) = \alpha_{CFD} \cdot \exp(-\alpha_{CFC} \cdot t) + \alpha_{CCD} \cdot \exp(-\alpha_{CCC} \cdot t) \quad (3)$$

consists of the contact film resistance $R_{CF}(t)$ caused by contaminations on the sheet surface and the contact constriction resistance $R_{CC}(t)$. The contact resistance decreases with increasing contact area. The spot resistance

$$R_S(t) = -\alpha_{SH} \cdot \frac{1}{1 + \exp(-\alpha_{SC} \cdot (t - \alpha_{SD}))} \quad (4)$$

drops with the evolution of the welding spot. The static resistance

$$R_0(t) = \alpha_O = const. \quad (5)$$

comprises the constant percentages of all previously introduced resistance components. The meaningful features of the dynamic resistance can then be represented by the model parameters

$[\alpha_O, \alpha_{BL}, \alpha_{BC}, \alpha_{CCD}, \alpha_{CCC}, \alpha_{CFD}, \alpha_{CFC}, \alpha_{SC}, \alpha_{SH}, \alpha_{SD}]$ which can be determined by fitting the model to experimental data. A fitted model instance from [2, 7] is depicted in Fig. 5.

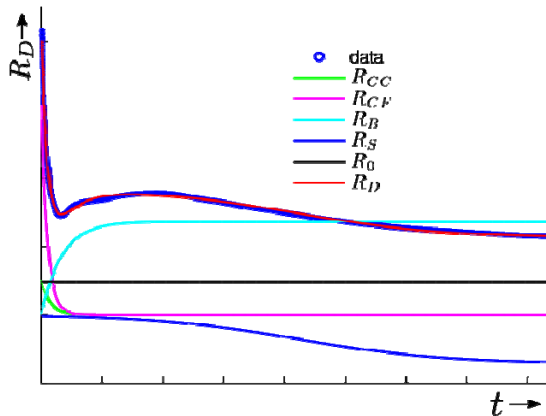


Figure 5. Analytical resistance model fitted to data.

IV. MODELING APPROACHES

This section provides a brief overview of the used methods. Due to a lack of space of this paper, we have to limit the explained methods. For example, the proposed Support Vector Machines should be reread in the literature (see [1] for more details)

A. Nonlinear Curve Fitting + Partial Least Squares

A grey box model for predicting the welding spot diameter as a quality measure from the meaningful features of the dynamic resistance has been introduced in [8, 9]. In a first step, the analytical resistance model described in the previous section is fitted to experimental data for each sample by Nonlinear Curve Fitting (NCF). This results in a low-dimensional feature representation for each individual experiment. In a second step, a Partial Least Squares Regression (PLS) is performed with the features as regression input and the welding spot diameter as regression output.

In NCF, the free model parameters are determined by nonlinear optimization. The objective function is formulated by means of the deviation between the model and the data, e.g., the Sum of Squared Errors (SSE) which is to be minimized. Then, the model represents the real process given by the experimental data in an optimal manner.

PLS combines linear regression with dimension reduction in regression input and output. The dimension reduction is performed similarly as in Principal Component Analysis (PCA) which finds orthogonal directions of largest variance in the data and projects the data to a lower-dimensional space of only the selected components. In PLS, the single steps of dimension reduction in input and output as well as the linear regression are interconnected by an iterative procedure, such that the covariance between the input and the output is maximized. As a result, PLS does not solely provide an efficient regression method to establish a

model for the prediction of a target quantity. It additionally reveals the influences of the input on the target quantity.

B. Classical Regression Analysis and Symbolic Regression

Regression analysis [10] is one of the basic tools of scientific investigation. It enables the identification of functional relationships between independent and dependent variables and the general task is defined as the estimation of a functional relationship between the independent variables $\mathbf{x} = [x_1, x_2, \dots, x_n]$ and dependent variables $\mathbf{y} = [y_1, y_2, \dots, y_m]$, where n is the number of independent variables in each observation and m is the number of dependent variables.

The task is often reduced from the identification of an arbitrary functional relationship f to the estimation of the parameter values of a predefined (e.g., linear) function. That means that the structure of the function is predefined by a human expert and only the free parameters are adjusted. From this point of view, Symbolic Regression goes much further.

Like other statistical and machine learning regression techniques, Symbolic Regression also tries to fit experimental data. But unlike the well-known regression techniques in statistics and machine learning, Symbolic Regression is used to identify an analytical mathematical description and it has more degrees of freedom in building it. Therefore, a set of predefined (basic) operators is defined (e.g., add, multiply, sin, cos) and the algorithm is mostly free in concatenating them. In contrast to the classical regression approaches, which optimize only the parameters of a predefined structure, here also the structure of the function is free and the algorithm both optimizes the parameters and the structure of the basis functions.

Since Symbolic Regression operates on discrete representations of mathematical formulas, non-standard optimization methods are needed to fit the data. The main idea of the algorithm is to focus the search on promising areas of the target space while abandoning unpromising solutions (see [11, 12] for more details). In order to achieve this, the Symbolic Regression algorithm uses the main mechanisms of Genetic and Evolutionary Algorithms. In particular, these are mutation, crossover and selection [12] which are applied to an algebraic mathematical representation.

The representation is encoded in a tree [12] (see Fig. 6). Both the parameters and the form of the equation are subject to search in the target space of all possible mathematical expressions of the tree. The operations are nodes in the tree (Fig. 6 represents the formula $6x+2$) and can be expressed by mathematical operations such as additions (add), multiplications (mul), abs, exp and others. The terminal values of the tree consist of the function's input variables and real numbers. The input variables are replaced by the values of the training dataset.

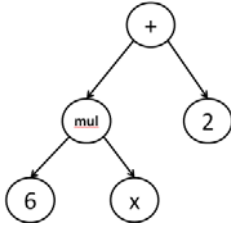


Figure 6. Tree representation of the equation $6x+2$.

In Symbolic Regression, many initially random symbolic equations compete to model experimental data in the most promising way. Promising are those solutions, which are a good compromise between correct prediction quality of the predicted data and the length of the computed mathematical formula.

Mutation in a symbolic expression can change the mathematical type of formula in different ways. For example, a div is changed to an add, the arguments of an operation are replaced (e.g., change $2*x$ to $3*x$), an operation is deleted (e.g., change $2*x+1$ to $2*x$), or an operation is added (e.g., change $2*x$ to $2*x+1$).

The fitness objective in Symbolic Regression, like in other machine learning and data mining mechanisms, is to minimize the regression error on the training set. After an equation reaches a desired level of accuracy, the algorithm returns the best equation or a set of good solutions (the pareto front). In many cases, the solution reflects the underlying principles of the observed system.

V. EXPERIMENTS AND RESULTS

In this section we summarize the basic ideas of the used methods. For more details we refer to the literature.

A. Support Vector Regression

In [13], we describe and evaluate the use of Support Vector Regression to determine a statistical model for a welding spot function associated with a resistance spot welding process (see section III). Based on the training data a Support Vector Regression is used to extract a welding spot diameter function (our goal function) of five variables: current, welding time, force, sheet thickness of material. According to this diameter function, we developed a description of our optimized method needed by an intelligent welding machine.

The SVR represents a black box model (subsymbolic representation), which incorporates no prior domain knowledge. The results were very promising (see [13] for more details). A maximum error value of 0.29mm in the welding spot diameter in a typical range of 2.5 and 6.5mm indicates a good model quality.

B. Nonlinear Curve Fitting + Partial Least Squares

A model for the welding spot diameter based on the meaningful features of the dynamic resistance has been created in [7]. Domain knowledge is embedded through an analytical resistance model, which is fitted to experimental data by NCF. Then, the welding spot diameter is determined

from the fitted model parameters as the features of the dynamic resistance by a PLS model. The prediction quality is characterized by a mean relative error value of 8%.

C. Improving a Phenomenological Model by Symbolic Regression

In [6, 7] the process dynamics are modeled by a parameterized phenomenological base model with fixed structure (see Section III). Additionally, Symbolic Regression is used to add a flexible correction term [6], which reflects process effects not considered in the base model. The full model is formed by simultaneous parameter fitting and adding a correction term found by Symbolic Regression. While the phenomenological model covers the major effects that occur in the Resistance Spot Welding process, the correction term can explain further hidden procedures in the residuals of the former. The phenomenological model has been created by use of expert knowledge and the formation of a grey box model. The symbolic correction term found by Symbolic Regression might be interpretable by a human expert again. In the paper, it has been shown that the phenomenological model yields good results, which are further improved by the correction term added by Symbolic Regression.

VI. CONCLUSIONS AND FUTURE WORK

Different approaches have been proposed in this paper that try to improve the quality of resistance spot welding by modeling the process dynamics. Throughout the last years different approaches have been evaluated. In this paper, we propose a scheme to select an adequate model based on the prior domain knowledge.

The different approaches have been successfully applied to the domain of resistance spot welding. Our next step is to demonstrate that this approach is general enough to be applied to other domains.

Future work includes modeling the system dynamics. That means, the described methods will utilize the measured process inputs and outputs to construct static process model components. Therefore we use system information of time step t to predict time step $t+1$. In the future, we will use time series to model the system information as continuous process dynamics. Instead of using measured output data of the previous time step as input for the current time step, the output is represented as a function of the previous time step. Thus, the process output can be modeled as a function of the previous input and model output: $\hat{y} = f(u(k-1), \dots, u(k-1), \dots, \hat{y}(k-1), \dots, \hat{y}(k-1))$ where $\hat{y}(k-i)$ is the previous model output and $u(k-i)$ the past values of the input. Hence, the output of the dynamic model is connected with the input in terms of recurrent structures. At the current stage of our project, one consideration is to use recurrent neural networks. The connections of a recurrent neural network form a directed

circle, allowing the modeling of dynamic behavior. Examples of recurrent networks are the Elman Network [14] or the Hopfield Network [15], these or extended versions of these architectures are often found in publications to identify dynamic systems. Our future research targets the creation of a dynamic model, integrating knowledge of structural features of the desired function (grey box) and minimizing the complexity of the model. Dimension reduction will be applied to realize an efficient process control (based on an observer, see Fig. 1) to improve the quality of the welding process.

the National Academy of Sciences of the USA, vol. 79 no. 8 , April 1982, pp. 2554–2558.

REFERENCES

- [1] R. O. Duda, P. E. Hart, and D. G. Stork, "Pattern Classification," 2nd ed., Wiley Interscience, 2000.
- [2] I. Schwab and N. Link, "Reusable Knowledge from Symbolic Regression Classification," Genetic and Evolutionary Computing (ICGEC 2011), 2011.
- [3] P. Smolensky, "On the Proper Treatment of Connectionism," in Behavioral and Brain Sciences, 11, 1988, pp. 1-74.
- [4] J. Lunze, "Regelungstechnik 2: Mehrgrößensysteme, Digitale Regelung," Bd. 6. Springer, 2010.
- [5] O. Nelles, "Nonlinear System Identification: From Classical Approaches to Neural Networks and Fuzzy Models," Springer, 2001.
- [6] I. Schwab, M. Senn, and N. Link, "Improving Expert Knowledge in Dynamic Process Monitoring by Symbolic Regression," (ICGEC 2012).
- [7] M. Senn and N. Link, "Revealing Effects of Dynamic Characteristics in Process Monitoring and Their Influences on Quality Prediction," Proceedings of the 8th International Conference of Numerical Analysis and Applied Mathematics (ICNAAM 2010), 2012, pp. 1306-1309.
- [8] H. Zhang and J. Senkara, "Resistance Welding: Fundamentals and Applications," CRC Press, 2005, 1 edn.
- [9] D. W. Dickinson, J. E. Franklin, and A. Stanya, "Welding Journal," 59, pp. 170–176, 1980.
- [10] D. A. Freedman, "Statistical Models: Theory and Practice," Cambridge University Press, 2005.
- [11] R. E. Steuer, "Multiple Criteria Optimization: Theory, Computations, and Application". New York: John Wiley & Sons, 1986.
- [12] J. R. Koza, "Genetic Programming: On the Programming of Computers by Means of Natural Selection," Cambridge, MA, USA: MIT Press, 1992.
- [13] J. Pollak, A. Sarveniazi, and N. Link, "Retrieval of process methods from task descriptions and generalized data representations", The International Journal of Advanced Manufacturing Technology, March 2011, Volume 53, Issue 5-8, pp. 829-840.
- [14] J. L. Elman, "Finding Structure in Time", Cognitive Science 14 (2), 1990, pp. 179–211.
- [15] J. J. Hopfield, "Neural networks and physical systems with emergent collective computational abilities", Proceedings of

Content Adaptation for an Adaptive Hypermedia System

Marta Fernandes, Paulo Couto, Constantino Martins, Luiz Faria
 GECAD – Knowledge Engineering and Decision Support Group
 Institute of Engineering – Polytechnic of Porto
 Porto, Portugal
 mamaf@isep.ipp.pt

Abstract— The aim of this paper is presenting the recommendation module of the Mathematics Collaborative Learning Platform (PCMAT). PCMAT is an Adaptive Educational Hypermedia System (AEHS), with a constructivist approach, which presents contents and activities adapted to the characteristics and learning style of students of mathematics in basic schools. The recommendation module is responsible for choosing different learning resources for the platform, based on the user's characteristics and performance. Since the main purpose of an adaptive system is to provide the user with content and interface adaptation, the recommendation module is integral to PCMAT's adaptation model.

Keywords- *adaptive educational hypermedia; user model; adaptation model; learning objects; recommendation module*

I. INTRODUCTION

E-learning has been gaining prominence in the past few years, but 2012 has seen some significant changes due to the rapid spread of massive online open courses (MOOCs).

MOOCs are free online courses aimed at large scale participation. They have existed for a few years [1], but after more than a hundred and sixty thousand students in over a hundred and ninety countries enrolled in Sebastian Thrun and Peter Norvig's "Introduction to Artificial Intelligence" in September 2011 [3], several free online learning platforms have launched that now offer courses on various subjects. Currently, Coursera, a social entrepreneurship company that partners with top US universities and was founded in January 2012, has had almost two million students enroll in its courses [2]. Udacity, founded by Sebastian Thrun and two colleagues after the success of "Introduction to Artificial Intelligence", has enrolled more than seven hundred and fifty thousand students [4]. And edX, a nonprofit start-up from Harvard University and the Massachusetts Institute of Technology, whose first courses started this fall, already has close to four hundred thousand students [2].

MOOCs are not massive in the number of students alone, there is also great diversity in the people enrolling. Students of these courses include both men and women from all over the world, with varying levels of education and ranging from preadolescents to senior citizens. As can be expected, these students do not all learn in the same way or with the same ease, yet MOOCs, as is the case with most e-learning, offer a one-size-fits-all solution.

Unlike traditional e-learning approaches, Adaptive Educational Hypermedia Systems adapt interface, content presentation, link navigation and so on, to the specific characteristics, needs and interests of different users. As these goals and characteristics change, so does the content presented by the system [5]. The aim of these systems is to help users achieve their learning goals, therefore characteristics such as previous knowledge and learning style are particularly important [5, 7].

AEHSs offer an educational experience that is tailored to each individual student and as e-learning continues to evolve and grow, they are a solution to a problem that is particularly noticeable in large-scale e-learning projects such as MOOCs: the absence of a teacher that will guide students and provide them with individual explanations, adapted to their specific abilities, knowledge and personality. A student who already possesses a doctorate will learn in a very different way than someone who is still in high school. AEHSs can adapt content presentation to suit each student's different level of knowledge and in that way improve their learning experience.

Adaptive Hypermedia Systems (AHSs), of which AEHSs are a subset, have been the subject of much research but more development, experimentation and implementation are necessary to conclude about the adequate features and effectiveness of these systems [5]. Some examples of Adaptive Educational Hypermedia Systems are AHA! [7], OntoAIMS [8] and WINDS [9].

In this paper, we introduce the adaptation model of the Mathematics Collaborative Learning Platform [10], and present an in-depth analysis of its recommendation module. PCMAT is an AEHS with a constructivist approach, which assesses the user's knowledge and presents contents and activities adapted to the characteristics and learning style of students of mathematics in basic schools. This adaptation is achieved by means of the recommendation module, which is responsible for choosing different learning resources for the platform. With the development of PCMAT, our main objective is to help drive AHS research forward, but we also hope to assist Portuguese students, who are still significantly below the OECD average in mathematics performance [11], improve their knowledge of the subject.

In SECTION II we make brief descriptions of the User Model and the Adaptation Model. In SECTION III we describe in more detail the platform's recommendation

module and in SECTION IV we take some conclusions and talk about future work.

II. ADAPTATION

A. User Modelling

AHSs change several aspects of the system based on the user's characteristics, such as goals and preferences. These characteristics, which can be provided by the user or inferred by the system, are stored in the User Model [12]. In the case of AEHSs, the User Model, or Student Model, also stores the user's knowledge. The purpose of AEHSs is helping users achieve their learning goals. When one goal is reached, the system re-adapts to the newly acquired knowledge [12, 13, 14]. This means that the Student Model is of particular importance for AEHSs because the information it contains about the user's knowledge is crucial for a properly adapted learning experience.

The Student Model includes Domain Dependent Data and Domain Independent Data. The first consists of the user's subject knowledge, learning goals and a complete description of the user's navigation through the course. Domain Independent Data consists of personal information, demographic data, academic background, qualifications, learning style, cognitive capacities, etc. Depending on the system being developed, some of these features are relevant for the User Model and some are not [12, 14, 15]. Determining which of the user's characteristics should be used is an important step in the creation of an AHS [13].

PCMAT's Student Model stores several characteristics, but the most relevant one is the user's learning style. Learning differs from individual to individual and depends on many unique and personal factors [16]. Learning styles attempt to be representations of how an individual learns. It is now known most people are multimodal, meaning they have more than one learning style [17, 18], as opposed to having only one learning style as was previously believed. The Learning Styles theory has been subject to criticism [19, 20, 21], but it is also supported by several studies [22, 23, 24]. There does not seem to be, however, any evidence suggesting the use of learning styles is detrimental. Moreover, it is the personal opinion of the mathematics teachers working on this project that learning styles might indeed be useful and facilitate the user's learning process. One of the objectives of this project is assessing the usefulness of learning styles as a feature of the User Model of Adaptive Educational Hypermedia Systems.

B. Adaptation Model

The development of PCMAT takes into account the constructivist learning theory. The system sets up a path into the subject, using the information obtained from assessing the user's previous knowledge. It adapts content and activities to the user's characteristics and performance, and is capable of automatic feedback and support, through pedagogical strategies and educational activities explored in a constructivist manner.

PCMAT uses the features contained in the User Model to create a specific domain concept graph, adapted from the

domain model, and uses it to provide adaptation that will respond to the student's needs. The initial scheme is set by the teacher, but the path each student takes in the graph is determined by the interaction with the system using progressive assessment, the student's knowledge and the user's characteristics in the user model. Adaptation occurs through changes in content presentation, in the structure of links and in the links annotation [29].

Changes to content presentation are achieved by showing or omitting each of the multiple fragments a course page is composed of. These fragments consist of different learning objects such as exercises, figures and narrative text, among others. Changes in the structure of links and the links' annotation serve the purpose of guiding the student through the course, towards the most relevant information and away from knowledge that is not appropriate yet [5].

III. RECOMMENDATION MODULE

Choosing the most appropriate learning object for a student, for a given section of his learning path, implies defining the relationship between specific student characteristics and the parameters of a learning object. The recommendation module takes as input data from the User Model and uses a Fuzzy Logic system to output a set of parameters the learning object must comply with. These parameters are based on elements of the IEEE LOM's general and educational categories [27].

The system takes as input both domain dependent data, such as the student's subject knowledge, and domain independent data, namely the student's learning style and learning rate. The Fuzzy Logic engine then maps these characteristics into the following parameters [25]:

difficulty - indicates the level of ease associated with the learning resource.

resource type - indicates the potential educational use(s) or type(s) of content associated with the learning resource.

semantic density - indicates the degree of concision or brevity of expression in a resource.

interactivity level - indicates the degree to which the learning resource is able to respond to the actions and input of the user.

interactivity type - indicates whether the resource requires action on the part of the user.

The relationships established between User Model characteristics and Learning Object parameters are the following:

knowledge + learning rate -> difficulty

learning style + learning rate -> resource type

knowledge + learning rate -> semantic density

learning style -> interactivity level

learning style -> interactivity type

Both knowledge level and learning rate contribute to the choice of a learning object's difficulty level because, in our view, a student that learns at a faster pace should more easily be able to understand the contents of a more difficult learning object than a student that learns at a slower pace.

The resource type depends on the learning style for obvious reasons. If the student tends toward the visual learning style, a diagram will be a more appropriate learning

object than a block of text. The learning rate is also taken into account because certain resource types, such as exercises, might at some point in the course be appropriate for faster learning students, whereas slower learning students might need more learning time before being presented with a learning object of that type. The semantic density of a learning object can be determined in two different ways. It might refer to the ratio between the number of written or spoken words and the total number of words, or it may be determined by the total length of the learning object [25]. We take into consideration the student's knowledge level and learning rate when determining the appropriate semantic density of a learning object because not only will it be easier for a more knowledgeable student to understand a learning object of greater semantic density, but a student who learns faster is one who understands content more rapidly and therefore should be able to deal with greater semantic density more easily. As for the interactivity level and interactivity type of a learning object, we have chosen to only factor in the student's learning style because we believe neither knowledge nor learning rate must influence the interactivity of a learning object. A student's learning style, on the other hand, should be taken into consideration because a highly interactive object seems more appropriate to a student with a kinesthetic learning style, than to a student with an auditory learning style.

The mapping between student characteristics and learning object parameters is performed using Fuzzy Logic. The recommendation module takes the numeric values, which represent the input data and, after fuzzifying them, uses the specified Fuzzy rules to determine the output parameters the learning object must be in accordance with. An example of a Fuzzy rule is: if learning_rate is slow and knowledge_level is low then difficulty is very_easy.

These parameters, as well as a set of context-dependent keywords, are then used by PCMAT's search and retrieval module to retrieve a list of compliant learning objects.

After obtaining the list, the recommendation module verifies in the Student Model if the object at the top of the list has already been presented to the student. If there is a record of that object in the Student Model, the system checks the following objects until it cannot find a match. If all the learning objects in the list have already been shown to the student, the recommendation module asks the search and retrieval module for more learning objects that comply with the parameters specified. It then checks the Student Model again until it finds an object in the list that has not been shown to the student yet. If, after asking the search and retrieval module for learning objects a given number of times, no such object can be found, the system searches the Student Model for the learning object with the oldest timestamp. Once the system finds a learning object that can be presented to the student, be it a brand new one or one retrieved from the Student Model, that object is processed for inclusion in one of the fragments that make up the course's pages.

The courses pages are created using XHTML, which means that the recommendation module must process the learning object so that it will extend the Web page

seamlessly. Learning objects can be of many different types, such as images, videos, text documents, and so on. Integrating these different types of objects in a seamless manner is achieved by using JQuery to determine some of the object's parameters (height and width, for example) and adjust the fragment's own parameters accordingly.

IV. CONCLUSION

The PCMAT platform is being developed in an attempt to contribute to the progress of AHSs, in particular AEHSs. As e-learning systems become more commonplace and grow in prominence, the usefulness of adaptive systems becomes more apparent. Our work on PCMAT intends to show the advantages of such systems, as well as perform more experimentation on User Modeling.

This project is still a work-in-progress, but has already helped define new strategies for the implementation of an AEHS to support and improve mathematics in the context of basic schools. It has also contributed to the definition of a student model describing the personal information, knowledge, preferences, and learning style of the user, the definition of a process and tools needed to produce learning objects aligned with the IEEE LOM standard, and the implementation of a set of adaptive and dynamic pedagogical strategies [26].

In this paper, we have presented PCMAT's recommendation module. This module is responsible for defining the parameters of a learning object, based on the user's characteristics and performance. The proper choice of learning objects is crucial to the system's adaptability and the individualization of the learning process.

PCMAT has already undergone some preliminary tests in two basic schools and achieved good results. After the testing phase, students from both the experimental and control groups had to answer a written test set up by their teachers. The results show the average student scores, from both schools, in the experimental group was higher than the average student scores in the control group, 59,1% ($\sigma = 19,7$) against 44,2% ($\sigma = 21,8$). The differences observed are statistically significant ($p=0,010$). Students from the experimental groups also performed better in the knowledge acquisition of individual concepts. The two groups were statistically compared using a two sided, independent samples t test with a 0.05 (5%) critical level of significance [28].

These results are very positive, and a strong indicator that PCMAT's architecture is viable and appropriate for AEHSs used in the context of basic schools. They also allow us to conclude that AEHSs, by adapting to the different needs and characteristics of a student, contribute indeed to the effectiveness and efficiency of the learning process. In addition, students perceived this tool as being relevant to their learning experience, and as a self-operating application to be integrated in a more global learning strategy that also includes tutoring (direct contact with the teacher) and peer learning. The teachers that participated in this experiment agreed with these definitions of the platform as well.

PCMAT will enter a new testing phase in the coming months, with a larger sample size. We hope to confirm the results previously obtained in order to conclude about the adequate features and true effectiveness of the PCMAT system. We will continue working on the system in order to improve its adaptability. Our current and future work also focuses on a Natural Language Processing module, which is capable of analyzing and assessing the answers given by students to open-ended questions.

ACKNOWLEDGMENT

The authors would like to acknowledge FCT, FEDER, POCTI, POSI, POCI and POSC for their support to GECAD unit, and the project PCMAT (PTDS/CED/ 108339/2008).

REFERENCES

- [1] K. Masters, "A brief guide to understanding MOOCs", *The Internet Journal of Medical Education*, vol. 1, number 2, 2011, doi: 10.5580/1f21, <http://www.ispub.com/journal/the-internet-journal-of-medical-education/volume-1-number-2/a-brief-guide-to-understanding-moocs.html#sthash.bngD45s5.dpbs>, retrieved: February 2013.
- [2] L. Pappano, "The Year of the MOOC", http://www.nytimes.com/2012/11/04/education/edlife/massive-open-online-courses-are-multiplying-at-a-rapid-pace.html?pagewanted=all&_r=0, retrieved: February 2013.
- [3] Udacity, <http://www.udacity.com/us>, retrieved: February 2013.
- [4] K. M. Heussner, "Udacity nabs another \$15M to bring more interactivity to online education", <http://gigaom.com/2012/10/25/udacity-nabs-another-15m-to-bring-more- interactivity-to-online-education/>, retrieved: February 2013.
- [5] M. Fernandes, P. Couto, C. Martins, L. Faria, C. Bastos, and F. Costa, "Learning objects recommendation in an adaptive educational hypermedia system", *Proc. 8th WSEAS International Conference on Educational Technologies (EDUTE '12)*, 2012, pp. 123-128.
- [6] V. Chepegin, L. Aroyo, P. De Bra, and D. Heckman, "User modeling for modular adaptive hypermedia", *SWEL'04 Workshop at the AH2004 Conference, TU/e Computing Science Report 04-19*, 2004, pp. 366-371.
- [7] P. De Bra, "Web-based educational hypermedia", in *Data Mining in E-Learning*, C. Romero and S. Ventura, Eds. Universidad de Cordoba, Spain, WIT Press, 2006, pp. 3-17.
- [8] L. M. Aroyo, R. Mizoguchi, and C. K. Tzolov, "OntoAIMS: ontological approach to courseware authoring", in *The Second Wave of ICT in Education: from Facilitating Teaching and Learning to Engendering Education Reform*, 2003, pp. 2-5.
- [9] M. Kravcik and M. Specht, "Flexible navigation support in the Winds learning environment for architecture and design", *Proc. Third International Conference AH2004*, Eindhoven, The Netherlands, August 23-26, 2004, pp. 156-165.
- [10] C. Martins, P. Couto, M. Fernandes, C. Bastos, C. Lobo, L. Faria, and E. Carrapatoso, "PCMAT - mathematics collaborative learning platform", *Highlights in Practical Applications of Agents and Multiagent Systems, AISC 89*, Springer-Verlag, Berlin Heidelberg, 2011, pp. 93-100.
- [11] "OECD, PISA 2009 Results: Learning Trends: Changes in Student Performance Since 2000 (Volume V)", 2010.
- [12] P. Brusilovsky, "Adaptive hypermedia, user modeling and user adapted interaction", *Ten Year Anniversary Issue, Alfred Kobsa*, Ed. 11 (1/2), 2001, pp. 87-110.
- [13] C. Martins, L. Faria, and E. Carrapatoso, "Constructivist approach for an educational adaptive hypermedia tool", *Proc. ICALT, IEEE*, 2008, pp. 303-305.
- [14] C. Martins, L. Faria, C. V. Carvalho, and E. Carrapatoso, "User modeling in adaptive hypermedia educational systems", *Educational Technology & Society*, 11(1), 2008, pp. 194-207.
- [15] P. Brusilovsky, "Adaptive hypermedia: an attempt to analyze and generalize", in *Multimedia, Hypermedia, and Virtual Reality, Lecture Notes in Computer Science*, Vol. 1077, P. Brusilovsky, P. Kommers and N. Streitz, Eds. 1996, pp. 288-304.
- [16] D. Ritu and M. Sugata, "Learning styles and perceptions of self", *International Education Journal*, Vol. 1, No 1, 1999, pp. 61-71.
- [17] N. D. Fleming, "VARK, a review of those who are multimodal", 2007, http://www.vark-learn.com/english/page_content/multimodality.htm, retrieved: February 2013.
- [18] P. Miller, "Learning styles: the multimedia of the mind", *Educational Resources Information Center ED 451 140*, 2001.
- [19] E. Brown, T. Fisher, and T. Brailsford, "Real users, real results: examining the limitations of learning styles within AEH", *Proc. 18th Conf. Hypertext and Hypermedia*, 2007, pp. 57-66.
- [20] D. Hargreaves, "About learning: report of the learning working group", *Demos*, 2005.
- [21] S. A. Stahl, "Different strokes for different folks?", in *Taking sides: Clashing on controversial issues in educational psychology*, L. Abbeduto, Ed. Guilford, CT, USA: McGraw-Hill, 2002, pp. 98-107.
- [22] A. Kolb, "Learning styles and learning spaces: enhancing experiential learning in higher education", *Academy of Management Learning and Education*, 4 (2), 2005, pp.193-212.
- [23] S. Montgomery and L. N. Groat, "Student learning styles and their implications for teaching", *Occasional Paper, Center for Research on Learning and Teaching, University of Michigan*, 1998, http://www.eecs.umich.edu/cse/cs_connections/cs4hs_presentations_09/Student_Learning_Styles.pdf, retrieved: February 2013.
- [24] A. S. Richmond and R. Cummings, "Implementing Kolb's learning styles into online distance education", *International Journal of Technology in Teaching and Learning*, 1(1), 2005, pp. 45-54.
- [25] N. Friesen, S. Fisher, and A. Roberts, *CanCore Guidelines Version 2.0: Educational Category*, 2004, http://cancore.tru.ca/guidelines/CanCore_Guidelines_Educational_2.0.pdf, retrieved: February 2013.
- [26] C. Martins, L. Faria, M. Fernandes, P. Couto, C. Bastos, and E. Carrapatoso, "PCMAT - mathematics collaborative educational system", *Intelligent and Adaptive Educational-Learning Systems: Achievements and Trends, Smart Innovation, Systems and Technologies*, Vol. 17, A. Peña-Ayala, Ed. Springer, 2013, pp. 183-212.
- [27] IEEE 1484.12.1-2002, *Standard for learning object metadata*, The Institute of Electrical and Electronics Engineers, Inc., New York, 2002.
- [28] M. Bland, *An introduction to medical statistics*, 3rd ed., Oxford: Oxford University Press, 2000.
- [29] P. Brusilovsky, "Efficient Techniques for Adaptive Hypermedia", *Intelligent Hypertext: Advanced Techniques for the World Wide Web*, Charles K. Nicholas and James Mayfield (Eds.), Springer-Verlag, London, 1997, pp. 12-30.

Context Processing: A Distributed Approach

Penghe Chen
NUS Graduate School for Integrative Sciences and Engineering
National University of Singapore (NUS)
 Singapore
 g0901858@nus.edu.sg

Hung Keng Pung
 School of Computing (SOC)
 National University of Singapore (NUS)
 Singapore
 dcsphk@nus.edu.sg

Shubhabrata Sen
 School of Computing (SOC)
 National University of Singapore (NUS)
 Singapore
 g0701139@nus.edu.sg

Wai Choong Wong
 Department of Electrical & Computer Engineering
 National University of Singapore (NUS)
 Singapore
 elewwcl@nus.edu.sg

Abstract—Context processing refers to the operation of processing different types of context data and/or information using different kinds of operators. These operators are applied according to some conditions or constraints given in context queries. Existing context aware systems process context data in a centralized fashion to answer context queries and generate context information. However, this method can cause scalability issues and give poor system throughput. In this paper, we aim to address this issue by proposing a distributed context data processing mechanism in which the context data processing computations of different context queries will be distributed to different computing devices. Relying on the developed prototype, a performance evaluation was conducted with centralized context data processing method as benchmark.

Keywords—Context; context-aware; ubiquitous computing; data management; distributed; context processing; query plan

I. INTRODUCTION

The advances in the field of ubiquitous computing have resulted in the proliferation of context aware applications that are flexible, adaptable and capable of acting autonomously on behalf of users (1). Context is any information that can be used to characterize the situation of an entity (2), and context awareness dictates the state in which devices or software programs are aware of the situation and adapt changes automatically, without requiring explicit user intervention (1). In order to truly realize context awareness, various kinds of context aware systems are developed to utilize context information about the situation of its users, the environment, or the state of the system itself to adapt their behavior (3).

An important part of a context aware system is a context data management system which takes charge of gathering, processing, managing, evaluating and disseminating context information. Among these different operations of context data management, context processing is the process in which different context data and/or information is processed with different kinds of operators or operations applied according

to some conditions or constraints given in context queries. Context processing is the operation where lower level data is converted to higher level context information that is more meaningful and useful for users, so it is very important for a well developed context aware system. A centralized context data processing approach is usually adopted due to its simplicity in development and management.

However, as the demand for context information grows with the advent of advanced context aware applications a centralized data processing approach may not be adequate. One of the issues is that the central point will become a bottleneck when handling large scale context queries which will cause a scalability issue. Also, it severely affects the system throughput which we define as the number of context queries handled in a unit time interval.

Motivated by this, we proposed a distributed context processing mechanism through which context processing computations of different context tasks will be distributed and executed on different computing devices automatically. As a result, system performance upon system throughput and resource utilization can be improved. The contribution of this paper can be highlighted in two aspects. Firstly, we propose a way to build context processing plan automatically in runtime, and divide context processing operations into several independent parts. Secondly, leveraging on the context processing plan, we propose a way to process context data for different tasks automatically in a distributed manner.

The rest of the paper is organized as follows. A system overview of our context aware system Coalition is given in Section 2. Section 3 will illustrate the details of distributed context processing mechanism and its work flow. Performance evaluation is demonstrated in Section 4. Section 5 discusses the related work and the whole paper is concluded in Section 6.

II. SYSTEM OVERVIEW

Coalition (Fig. 1) is a four layer based context aware system: physical operating space layer, data management layer, service management layer and application layer. The physical operating space layer includes all physical entities such as sensors, actuators and computing devices that provide the actual context data. The context data management layer aims to provide effective and efficient context data organization, lookup and storage. The service management layer manages context-aware services to handle the consolidated applications. Application layer supplies interfaces that are used to invoke services or acquire data from lower layers. The work of this paper focuses on the data management layer.

Coalition utilizes two main concepts to manage context sources - physical space and context space. A physical space is a person, object or place and provides a software module for managing context data and communicating with other components named as physical space gateway (PSG). Context spaces are defined as domains of physical spaces with similar context attributes, and the software module is context space gateway (CSG). Leveraging on these two concepts, Coalition could supports SQL-based context queries through the query processor component. More details of Coalition can be found in (4).

III. DISTRIBUTED CONTEXT PROCESSING

As discussed in the introduction, context processing is the process by which context data and/or information is processed using different kinds of operators or operations applied according to some conditions or constraints given in context queries. The previous version of Coalition utilizes a centralized context processing method to handle context queries and process context data. However, this can lead to a scalability issue in handling large number of context queries and affect system throughput. The proposed distributed context processing mechanism will handle these issues through decoupling the computations of context processing of queries from the other operations. As a result, context data processing of different queries can be executed independently and in parallel to improve system scalability and throughput.

In this section, we first discuss the basic concepts related to a context query language. We then proceed to discuss the details of the context processing operation and introduce the notion of a query plan. Finally, we illustrate how these concepts can be utilized to decouple the context processing computation from other operations in order to realize a distributed context processing mechanism.

A. Context Query Language

A context query language (CQL) is the language with specific syntax used by a context aware system to query context information. Context query language is crucial for querying

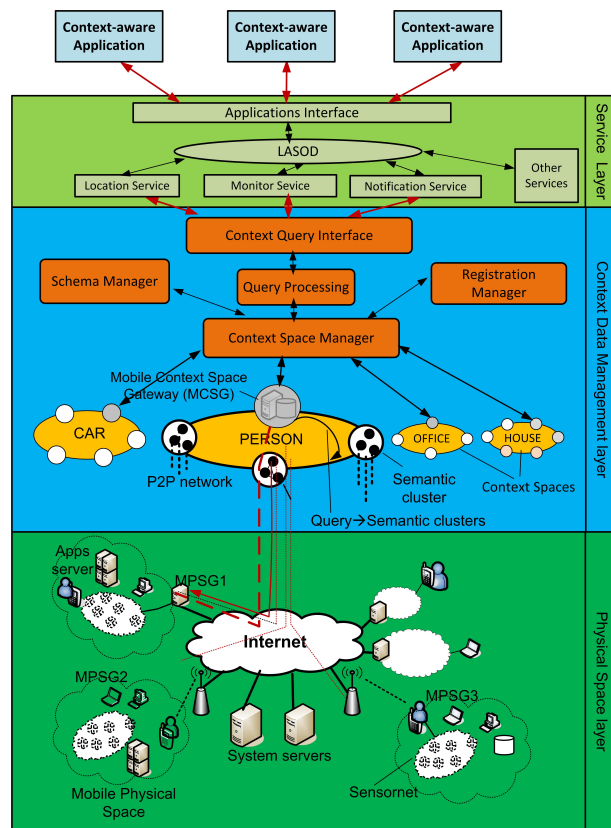


Figure 1. Coalition Architecture

context as it defines the way of query represented and context information required (5). Also, a good CQL should consider heterogeneity of context sources and different types of operations like reasoning, filtering and aggregating (6).

Many different types of context query languages have been proposed and designed in previous work, such as RDF-based, XML-based, SQL-based and Graph-based CQL. An evaluation work done by (5) indicates that SQL -based and RDF -based query languages are better than others. In our work, we will leverage on SQL-based Query Language to represent context queries. The basic structure of context query is as following:

```

SELECT (context attribute)
FROM (context domain)
[WHERE (constraints)]
    
```

The design of this CQL is inspired by normal SQL, so the syntax and format is quite similar to normal SQL, and that is why we call it SQL-based CQL. Due to the specialties of context data management, we have to admit that, comparing with normal SQL, this CQL has less query handling capability. This CQL cannot handle complex queries containing more context attributes and context domains, and it does not support the functionalities of "HAVE" and

”SORT BY”. Additionally, the actual query analysis and processing operations are different from normal relational database management system. Other than the key words, the semantics of the queries are restricted by the concepts inside this context aware management system. A typical example of context query in our system likes – SELECT preference FROM PERSON WHERE location = ”Shop A”.

B. Context Processing Operation

An important aspect of context processing is the context processing operation (CPO) which represents the specific methods that transform low level context data into high level context information. For example, an aggregation operation can represent a summarized view of several low level context data items. Context processing operations are closely related to context query language. Based on the CQL defined in previous subsection, we can outline the different types of context processing operations as follows

- **Filtering** - operations that aim to retrieve a piece or a set of context information leveraging on certain constraints to filter out unnecessary context information.
- **Aggregating** - operations that mainly include functions of SUM, AVG, COUNT, MAX, and MIN of a set of context information, and it is utilized together with filtering operations.
- **Reasoning** - operations that aim to generate higher level context information by applying certain user defined rules or methods on a set of context data.
- **Matching** - operations that aim to match two or more different pieces of context information based on certain constraints.
- **Sorting** - operations that aim to sort a set of context information in certain order based on certain context information or certain constraints.
- **Merging** - operations that aim to consolidate a set of context information together based on certain constraints.

C. Query Plan

Based on the notions of CQL and CPOs discussed previously, we propose the concept of query plan which aims to provide a generic representation of context query information. Query plan is defined as an object that contains a list of attributes to represent context query information and a list of methods for retrieving these attribute values. As per the current design, the query plan contains the information about the query issuer, context domains, context attributes, context processing operations and the query constraints. An important piece of information is the details of the query issuer that represents the address of the PSG that issues a context query. The inclusion of this piece of information in the query plan lets the PSGs holding the relevant answers reply to the query issuer directly instead of going through the query processor as an intermediary. As a result,

```

QUERY PLAN
Query Issuer – http://172.29.34.204:13001/xmlrpc
Query String
  – SELECT location FROM PERSON WHERE name = "Ivan"
Context Domain -- PERSON
Context Attribute -- location
Context Processing Operation -- filter
Constraint
  Context Attribute – "name"
  Operator – "="
  Constant – "Ivan"
Error Message – null

```

Figure 2. Example of Query Plan

the context processing operations can now be carried out independently. This query plan is generated from parsing the query according to the CQL and CQOs defined previously. Any subsequent operations in query processing can easily get the query information directly from the query plan object without parsing the original query. As a result, the query information becomes independent from CQL. We utilize this observation to develop a decentralized approach to perform the context processing operation. A diagrammatic illustration of query plan is shown in Fig. 2.

D. Details of Previous Query Processing Operation

Based on the previous discussion, we observe that there is a possibility of implementing a distributed context processing mechanism to solve the scalability issue and improve system throughput. The previous query processing operation utilized in the middleware can be roughly divided into the following phases as follows:

Query Parsing: parse the context query based on specified CQL syntax and extract corresponding information of context query. This phase processes context queries at syntax level.

Query Analysis: based on the information obtained during query parsing, further analysis is applied to extract more information, like required context information, context domain involved and constraints of the query. This phase interprets the context query.

Query Distribution: based on information extract in query analysis phase, we further identify the context sources involved in each context query and distribute the query to the relevant PSGs to collect the necessary context data.

PSG Context Data Collection: after receiving the query, each PSG will parse the query and check whether its context data satisfies the constraints stated in the query and report the result to the query processor.

Context Processing: consolidate the required context information by applying the context processing operation extracted from the query in the analysis phase on context

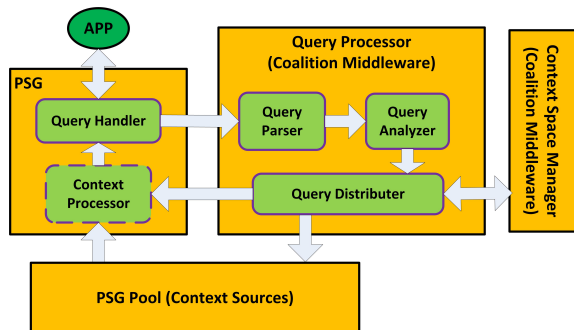


Figure 3. Architecture of Distributed Context Processing

data collected from different PSGs. This work is done in query processor of Coalition middleware, and all queries utilize this single context processor to generate required context information.

In the subsequent sections, we illustrate how the proposed distributed processing approach modifies and improves the aforementioned query processing operation to realize better scalability and throughput performance.

E. Distributed Context Data Processing

The new architecture design of query processing based on proposed distributed context processing mechanism is shown in Fig. 3. Different from previous design, in this architecture, Context Processor resides in PSG side rather than the query processor in Coalition middleware. Additionally, instead of utilizing a single context processor for all context queries, this new design creates an individual context processor for each PSG. As a result, those context processors can work simultaneously for different context queries to improve system performance.

The design of the distributed context processing mechanism includes two tasks. A major task is to decouple the context processing phase from the other phases. The next one is to shift and distribute the context processing computations of different context queries among different PSGs. These two tasks are solved leveraging on the design of query plan which enables the five phases of query processing to be loosely coupled by recording query parsing results. The other phases can retrieve any query information directly from this query plan object. As a result, the PSG context data processing phase does not need to re-parse the query and can execute independently from other phases.

Query plan can also help to distribute computations of context data processing into different PSGs. In the centralized context processing mechanism, all data is processed in the query processor where each PSG reports a matching query answer to. However, in the proposed distributed context processing mechanism, the PSGs need to be informed the place where to report their context data and a PSG processing the context data needs to know the relevant

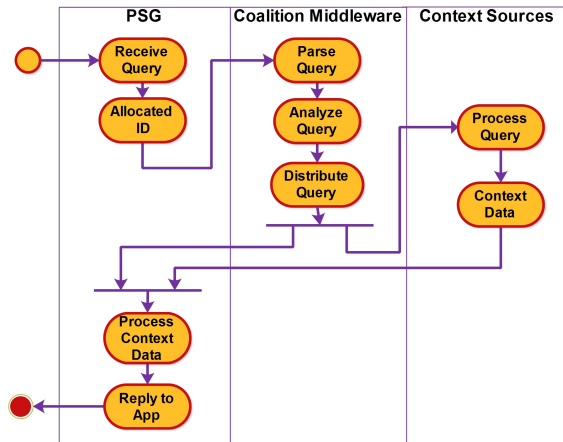


Figure 4. Work Flow Diagram

operations to be applied on the data. These functionalities can be provided using the query plan. The PSGs can utilize the query issuer information to identify where the data needs to be sent. Also, the PSGs can utilize the context processing operation information to identify the operations to be applied on the data.

F. Work Flow of Distributed Context Processing Mechanism

In order to better demonstrate how this distributed context processing mechanism handles context queries, we describe the operational work flow in this subsection. A diagrammatical illustration of the work flow leveraging on UML activity diagram is given in Fig. 4.

At the beginning, an application issues a context query to its host PSG which will generate a unique ID for the query. Also, PSG forwards the query to the query processor in Coalition middleware. After receiving the query, the query parser of query processor will generate a query plan for this query by parsing it based on SQL-base CQL syntax. Also, this query parser will check the validity of context domain and context attribute information wrapped inside the query. Leveraging on the query plan object, query analyzer will extract out information of context domain and context attribute, and then identify the group of PSGs of context sources involved. Subsequently, query distributor retrieves a random PSG reference from Coalition middleware utilizing on extracted context domain and context attribute information. Query distributor forwards query plan to host PSG to create context processor. Meanwhile, it also forwards query plan to the random PSG which will then flood query plan to all PSGs involved leveraging on P2P network. Query handler residing on each PSG of context source will check their context data fulfills the requirements stated in query plan and reports to corresponding context processor if it is. Context processor created in host PSG applies context processing operation stated in query plan on all the collected context

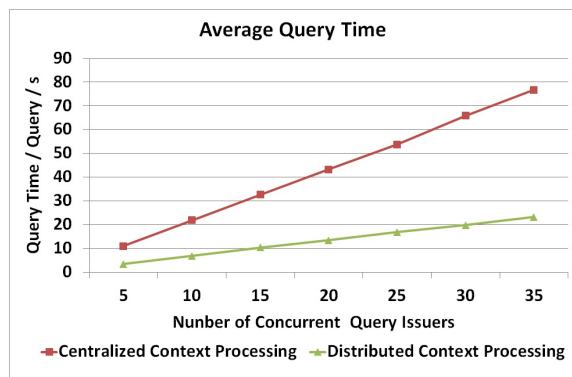


Figure 5. Average Query Time

data to generate the required context information and then reply the context information to application.

IV. PERFORMANCE EVALUATIONS

We have implemented a prototype of this distributed context processing mechanism and integrated with our context aware system Coalition (4). A Dell PowerEdge T300 server with four 2.83 Ghz quad-core Intel Xeon CPU was used as the server. PSG instances are simulated by desktop PCs where each PC had an Intel Core 2 Duo 2.83 GHz CPU and runs the Windows XP OS.

Several hundreds of PSGs from five different context domains were simulated: PERON, HOME, OFFICE, SHOP and CLINIC. Queries of different domains and different context information were continuously issued to test the average query time and system throughput. A range cluster based mechanism is used to restrain the number of PSGs to be flooded for each query (7). The centralized context processing method utilized by previous version of Coalition is used as a benchmark to evaluate the performance of this proposed distributed context processing algorithm.

A. Average Query Time

We first studied the average query time in case of different number of users issuing queries concurrently. The query time is measured as the interval between the issuing of a query and the reception of the context information. Average query time is measured by letting all users issue 100 queries simultaneously and continuously. The measurements of the currently utilized centralized context processing method are utilized as a benchmark. The results are illustrated in Fig. 5. The results indicate that our proposed distributed context processing provides a significant improvement on the average query time. The average query time is an important indicator of system scalability because a system can easily be break down if average query time increase so rapidly to overtake the responding time threshold with the number of user increasing. By observing the results, we can say that

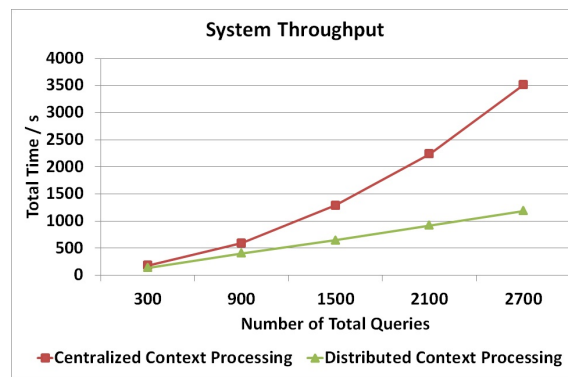


Figure 6. System Throughput

our proposed mechanism makes the system more scalable now.

B. System Throughput

Another performance indicator studied is system throughput which measures the maximum number of queries that can be processed within a unit time interval. Since counting the maximum number of queries handled is not easy especially for a distributed system, we measure the time consumed for certain number of queries. Methods with shorter total responding time means they can handle more queries in a given time period and have a higher throughput. Fig. 6 illustrates the total response time in case of different number of total queries issued with the condition that 30 users concurrently issue queries. Compared with centralized method, our proposed distributed context processing method requires shorter time to process the same number of context queries. This reflects that our proposed distributed context processing method can increase the throughput of the middleware with regards to the number of queries processes within a certain time period.

C. Query Time Breakdown

We also analyzed the time breakdown for the operations included in context query processing namely the following - query preprocessing, query distribution and context processing. The query preprocessing event refers to the operations involved in query processing including query parsing and query analyzing. The query distribution process refers to the flooding of the query to PSGs and local query processing in each PSG. This also includes the queuing time for issuing queries and reporting context data to query processor. The context processing operation refers to the task of processing context data to generate context information. Due to space constraints, we only present one example here in which 20 users issue queries concurrently and continuously. Table 1 illustrates time spent of each operation in query processing. We observe that the query preprocessing and context processing time does not change too much but query distribution

TABLE I. QUERY TIME BREAKDOWN

	Centralized Context Processing (/s)	Distributed Context Processing (/s)
Query Preprocessing	2.3	2.4
Query Distribution	38.9	8.8
Context Processing	2.1	2.2

is significantly improved. This is consistent with the design of distributed context processing mechanism which relieves the work load and communication congestion of Coalition middleware. As a result, the PSGs do not need to wait longer to issue queries and report context data.

V. RELATED WORK

There is little previous work in context aware computing that explores specifically on how to process context data. Most of existing work focuses on either single domain with centralized context processing or multiple domains but centralized context processing. This state of the art demonstrates the proposal of this distributed context processing algorithm is novel and promising.

Some of existing systems managing context data in single space or domain utilize centralized context processing method. CoBra (8), which is an agent based context aware system in smart spaces, utilizes a specialized component called Context Broker as the central point to reason and store context information on behalf of applications. Semantic Space (9) leverages on semantic web technologies to manage context data in smart spaces. Context aggregator gathers various context markups from different context sources and reports to context knowledge base which takes charge of answering context queries, but both context aggregator and context knowledge are centralized. The heart of CMF (10) is a centralized black-board based context manager which collects context data from all participating services or notes and processes those context data to generate proposer context information for querying. Trimmed to mobile devices, Hydrogen (11) leverages on various adaptors to collection context data. Meanwhile, it replies a centralized Context Server in management layer stores all the context information to handle context retrieval and subscription.

Some systems manage context data in multiple spaces or domains, but utilize centralized context processing method. SOCAM (12) can manage context data from different domains and is efficient in reasoning higher level context information leveraging ontology based context modeling technique. However, the data management and reasoning relies on pulling all context data into a central semantic space. CASS (13) utilizes a server based mechanism to abstract higher level context information and support SQL

based queries. The server serves as a central point to collect various context data from sensor notes and derive higher context information leveraging on rule engines. Toolkit (14) designs various types of widgets to manage context data. Context aggregators and context interpreters are built to aggregate context data and derive context information. These aggregators and interpreters are distributed and executed for different purpose, but it lacks a systematic interface to handle context query but let the developers specify all required context sources in higher level. Solar (15) utilizes operators to produce various kinds of context information, in which computations are done in a distributed manner like our mechanism. However, Solar requires application developers manually define and create those operators, while our mechanism can automatically generate the processing operators and produce the final context information in runtime. As a result, application developers will not be decoupled from details of lower level context data management.

VI. CONCLUSION AND FUTURE WORK

We propose a distributed context processing mechanism in this paper that aims to handle large scale context queries. Leveraging on the design of query plan, we decouple context processing from the other query processing operations. As a result, the proposed mechanism can execute context processing part in separate computing devices; thereby improving the system scalability and throughput. Additionally, a performance evaluation is done by taking previous centralized context processing method as benchmark. The experimental results demonstrate that the proposed technique performs better in terms of system scalability and throughput. As part of our future work, we plan to extend the query capability in handling more complex context queries which may include more complicated context processing operations with different conditions and more context data from different context domains.

REFERENCES

- [1] M. Baldauf, S. Dustdar, and F. Rosenberg, "A survey on context-aware systems," *International Journal of Ad Hoc and Ubiquitous Computing*, vol. 2, no. 4, pp. 263–277, 2007.
- [2] A. Dey, "Understanding and using context," *Personal and ubiquitous computing*, vol. 5, no. 1, pp. 4–7, 2001.
- [3] C. Bettini, O. Brdiczka, K. Henricksen, J. Indulska, D. Nicklas, A. Ranganathan, and D. Riboni, "A survey of context modelling and reasoning techniques," *Pervasive and Mobile Computing*, vol. 6, no. 2, pp. 161–180, 2010.
- [4] H. Pung, T. Gu, W. Xue, P. Palmes, J. Zhu, W. Ng, C. Tang, and N. Chung, "Context-aware middleware for pervasive elderly homecare," *Selected Areas in Communications, IEEE Journal on*, vol. 27, no. 4, pp. 510–524, 2009.

- [5] P. Haghghi, A. Zaslavsky, and S. Krishnaswamy, "An evaluation of query languages for context-aware computing," in *17th International Conference on Database and Expert Systems Applications*, 2006, pp. 455–462.
- [6] R. Reichle, M. Wagner, M. Khan, K. Geihs, M. Valla, C. Fra, N. Paspallis, and G. Papadopoulos, "A context query language for pervasive computing environments," in *Proceedings of the 2008 Sixth Annual IEEE International Conference on Pervasive Computing and Communications*, ser. PERCOM '08, 2008, pp. 434–440.
- [7] S. Sen and H. Pung, "A mean-variance based index for dynamic context data lookup," *Mobile and Ubiquitous Systems: Computing, Networking, and Services*, pp. 101–112, 2012.
- [8] H. Chen, T. Finin, and A. Joshi, "An intelligent broker for context-aware systems," Ph.D. dissertation, 2003.
- [9] X. Wang, J. Dong, C. Chin, S. Hettiarachchi, and D. Zhang, "Semantic space: an infrastructure for smart spaces," *Pervasive Computing, IEEE*, vol. 3, no. 3, pp. 32–39, 2004.
- [10] P. Korpipaa, J. Mantyjarvi, J. Kela, H. Keranen, and E. Malm, "Managing context information in mobile devices," *Pervasive Computing, IEEE*, vol. 2, no. 3, pp. 42–51, 2003.
- [11] T. Hofer, W. Schwinger, M. Pichler, G. Leonhartsberger, J. Altmann, and W. Retschitzegger, "Context-awareness on mobile devices - the hydrogen approach," in *Proceedings of the 36th Annual Hawaii International Conference on System Sciences (HICSS'03)*, 2003.
- [12] T. Gu, H. Pung, and D. Zhang, "A service oriented middleware for building context aware services," *Journal of Network and Computer Applications*, vol. 28, no. 1, pp. 1–18, 2005.
- [13] P. Fahy and S. Clarke, "Cass - middleware for mobile context-aware applications," in *Workshop on Context Awareness, MobiSys 2004*, 2004.
- [14] A. Dey, G. Abowd, and D. Salber, "A conceptual framework and a toolkit for supporting the rapid prototyping of context-aware applications," *Human-Computer Interaction*, vol. 16, no. 2-4, pp. 97–166, 2001.
- [15] G. Chen, M. Li, and D. Kotz, "Data-centric middleware for context-aware pervasive computing," *Pervasive and Mobile Computing*, vol. 4, no. 2, pp. 216–253, 2008.

N-Screen Service Platform based on Location-Awareness

Jiho Kim, Dohee Lee and Ohyoung Song
 School of Electrical and Electronics Engineering
 Chung-Ang University
 Seoul, Korea
 {jihokim, dynamic85}@wm.cau.ac.kr, song@cau.ac.kr

Abstract—We propose a location-aware multimedia delivery platform for N-Screen service. Our architecture allows the content providers to enable consistent LBS and seamless multimedia service for adaptive source multi device (ASMU).

Keywords- LBS; N-Screen; Multimedia delivery platform

I. INTRODUCTION

Location Based Services (LBS) can reach useful and convenience lifestyle of users. As the advance of wireless network technologies and the accuracy of the location/positioning technologies accelerate, many LBS will appear to be realizing more efficient and reliable services. Recently, multimedia service has become one of popular applications, which users take advantage of spare time at a smart home/hotspot, as smart home/hotspot services plays an important role in providing entertainment for the user. Therefore, smart home users require supporting mobility of multimedia service because it needs to be served seamlessly at any place [1].

With extensive use of smart phones and with development of smart television, the necessity for the seamless display among various devices, so called ‘N-Screen’, becomes apparent [2]. N-Screen service can be perceived as the essential multimedia service by providing one-source multi-use (OSMU). Seamless N-Screen services are an emerging killer application in personal wireless devices. Seamless services in the heterogeneous networks require smooth automation person by person. In order to provide intelligent services, we manage location of the mobile user. By location information, the proposed platform makes adaptively modifying the multimedia contents according to heterogeneous networks as well as devices.

We propose a location-aware multimedia platform for N-Screen service. Our architecture allows the content providers to enable seamless multimedia service with location-awareness for adaptive-source multi-device (ASMD).

The rest of the paper is organized as follows. In the section 2, we describe related works on seamless multimedia services. In section 3, we propose a location-aware multimedia platform for N-Screen service. The section 4 concludes the paper.

II. RELATED WORKS ON SEAMLESS MULTIMEDIA SERVICES

There have been researches related to seamless multimedia services. Content adaptation framework for Heterogeneous Devices utilizes information about devices, network, interaction, social activities and users in order to adapt digital content and SNS activities [3]. Functional architecture and mechanism for mobile station to provide seamless multimedia services offer continuous and bandwidth-adaptive IPTV service while switching the mobile terminals [4]. Method models for the multimedia service adapt the interfaces and interaction processes of heterogeneous devices [5]. A multimedia service platform includes session mobility management and adaptive streaming to manage video streaming sessions on heterogeneous networks and devices [14].

N-screen is a technology aimed to provide seamless computing environment by supporting synchronized data or program or display [2]. Classification of N-Screen service introduces various kinds of N-screen service scenarios and technologies based on overall scenario model [6]. One of N-Screen deals with token-sharing mechanism among media for guarantying synchronization and continuity of playing contents [7]. Another is new control architecture of group communication that delivers contents to available devices added or deleted dynamically by users in N-Screen service architecture [8]. Some of them are at the level of automated data synchronization such as Dropbox [9], uCloud [10], and others are focusing on ceaseless displaying covering from mobile device to personal computer and television [11].

Several studies have been made on context/location-aware service that can be considered as the decisive application by accomplishing the pervasive intelligence. Context-aware middleware provide an automatic service based on a user’s preference inside a smart home [12]. A flexible context-sensitive user profile model gathers static and dynamic data characterizing the user and his operational context in order that Services, especially the multimedia ones, must perform automatically actions/operations to adapt the delivered content to the user expectations and his environment capabilities [13]. A context-aware scalable media delivery for heterogeneous devices has shown good context-aware use cases with video streaming for best possible quality under the constraints of client device capability, network conditions [15].

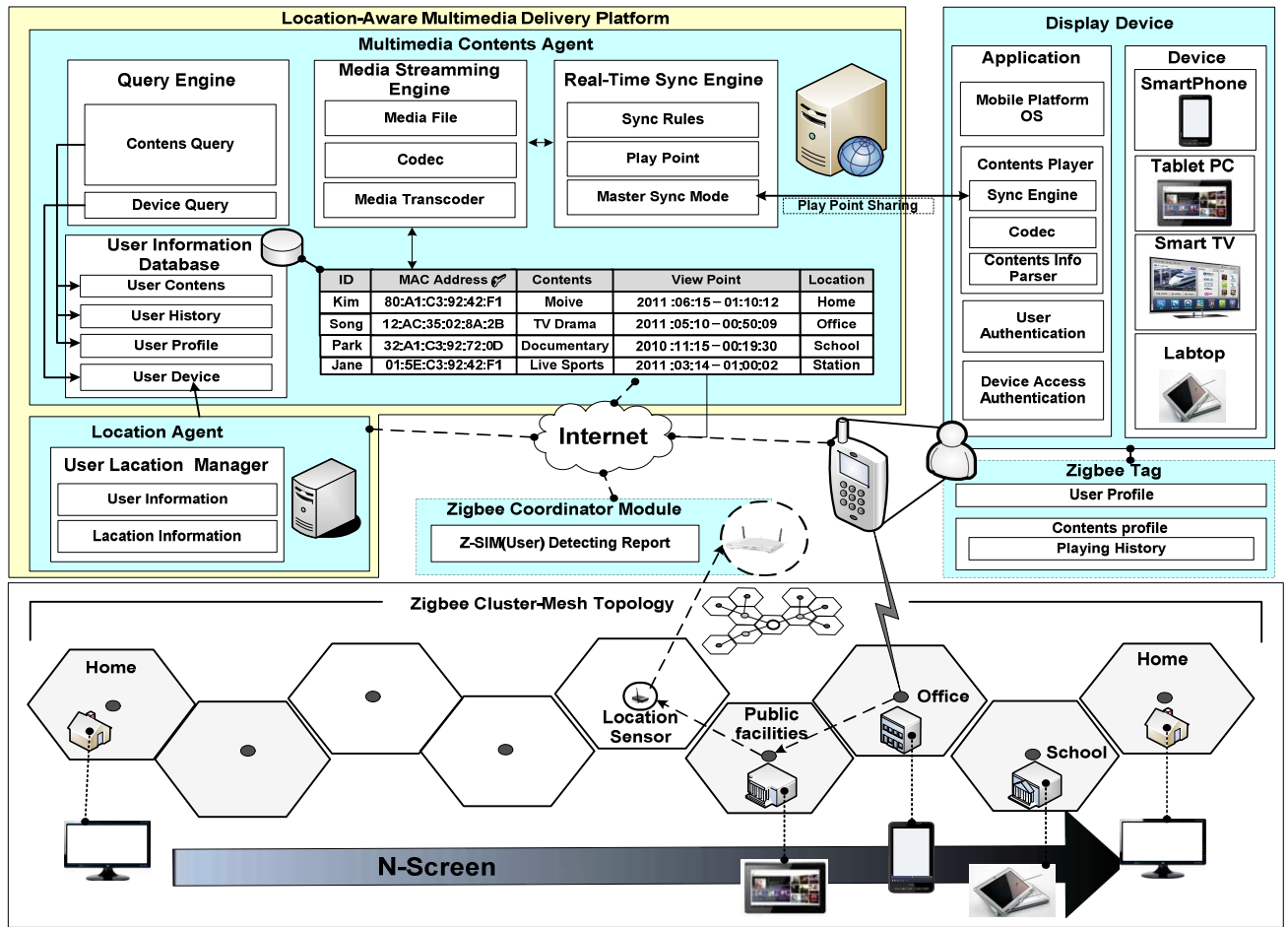


Figure 1. Location-aware multimedia delivery platform architecture

Mobile nodes (MNs) for multimedia services must support seamlessly the service roaming in the heterogeneous devices and networks. Our schemes manage user profile information that should be registered and managed by the servers which are located in the remote space. For location-aware intelligent services, we use the location agent with location/position surveillance and tracking in each spot. Location agent play essential role in assigning location aware intelligence in wireless networks. The smart and ubiquitous computing is dynamic providing the wireless access for seamless multimedia service.

III. LOCATION-AWRE MULTIMEDIA PLATFORM

By location information, we can increase application with the enhanced intelligence by providing seamless services and automatic contents adaptation. For seamless multimedia service, the location information will play an important role in defining context-awareness. In order to provide intelligent services we use smart techniques for location management of the user. The proposed multimedia

platform makes autonomously modifying the multimedia contents according to heterogeneous devices as well as networks.

Fig. 1 shows the proposed architecture which consists of several two components - Location Agent and Multimedia Contents Agent. The Multimedia Contents Agent is an agent that administrates various services. It decides proper services with profile information such as the user's preference and the device's type. The Location Agent that is able to detect the accurate location will play the major role. Intuitively, it is clear that successful location detection can lead to fully automated activation of roaming services while minimizing the service latencies. The mobility prediction is possible by validating location history, by the profiles. The widest existing deployments for positioning are WPAN networks based on ZigBee, which is particularly suited for indoor applications, especially at home, in office building. Location Agent and Location Tag support our fine-grained location recognition using wireless networks.

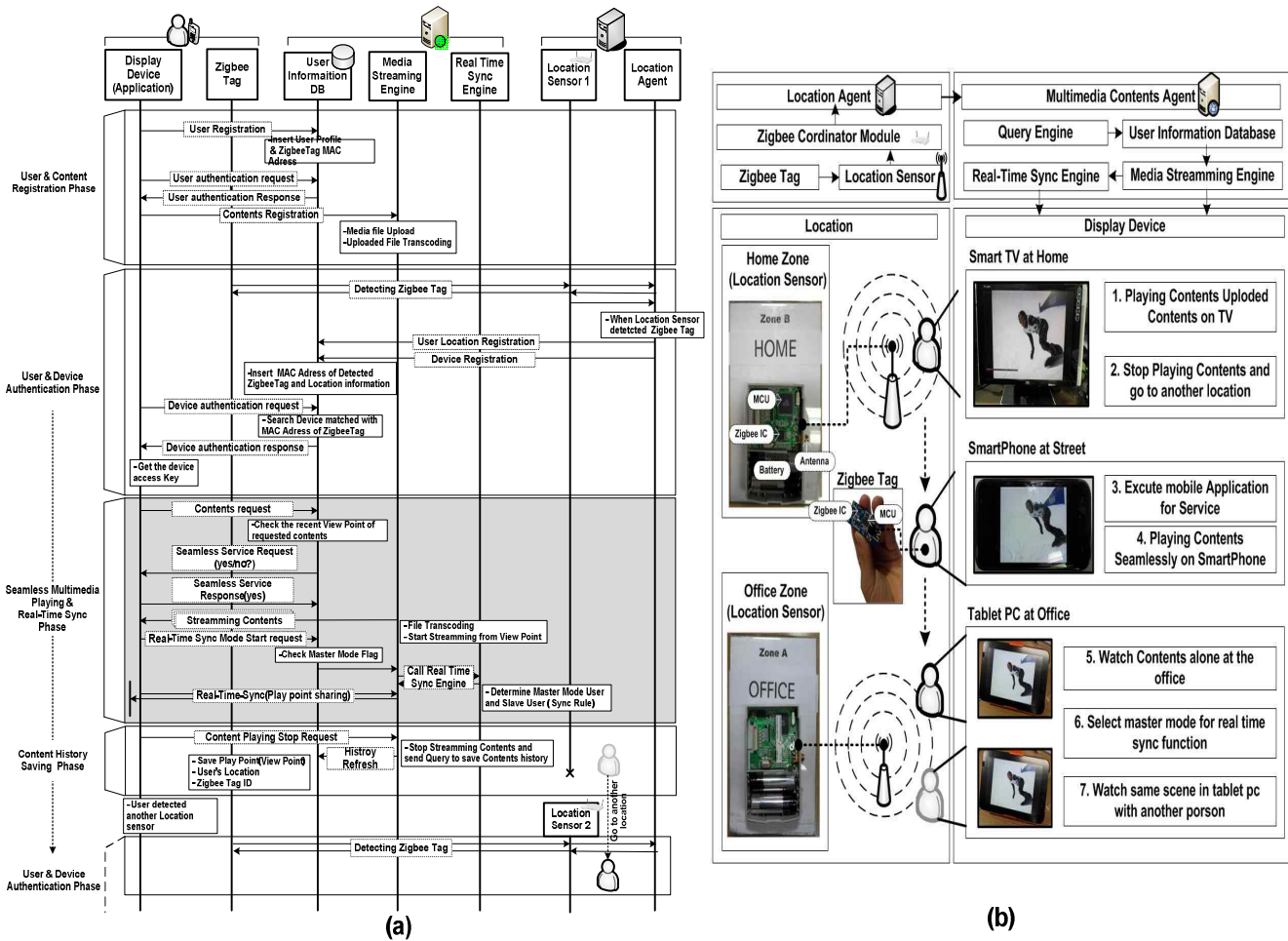


Figure 2. Protocol design (a) and service flow (b) for location-aware seamless multimedia push service

The Location Agent detects when user have Location Tag enters the ZigBee network. Typical ZigBee tag exist two types: The Location Agent detects when user have Location Tag enters the ZigBee network. Typical ZigBee tag exist two types: the integrated USIM with ZigBee transceiver in the smartphone and stand-alone ZigBee dongle. The motion detector senses any movement around the sensor. Hybrid positioning scheme due to two types of measurements from different sensors (IR, ZigBee) enhances location accuracy of the user. Also, an advantage of ZigBee zoning is that ZigBee tag store the user's profile. User profile contains user information, schedule and preferred services. A crucial benefit of the profile is that flexible multimedia push services can be customized to adjust user's specific needs. If there is person present, service appliances are turned on. When a user moves into a different spot, location is the significant contexts in order to determine which types of devices are available and how communication should be conducted to fit the user's needs. The platform enforces fast location detection as well as provides service roaming for wireless network where various display environments.

In the platform of our architecture several information are managed by context based protocol as shown in Fig. 2. The procedure includes initiate, request and response of service, multimedia and location information. Figure 2 shows the procedures in order to register user's current location as well as service profile in the platform and acquire user's service profile from the platform. First, in the case of

user's service initiation, a user accesses the Location Agent, which gets the User ID using WPAN and requests User Registration to the platform. In the case of user's service roaming, the user accesses the Location Sensor#2 from Location Sensor#1. The Location Sensor #2 recognizes the User using ZigBee. New intelligent applications will combine the characteristics of location-aware, device-aware and multimedia applications in varying degrees and forms. As shown in Fig 2(b), if a user move into the office, automatic recognizance of the presence of other devices through sensing the presence of neighboring beacons, allows the transfer of the current content seamlessly from the smart phone to the tablet.

IV. CONCLUUION

Our platform architecture integrates location-aware scheme for seamless mobility with multimedia services by the cooperation of Location Agent and Multimedia Contents Agent. We expect that the proposed location-aware a multimedia delivery platform can be applied as intelligent to existing multimedia applications for N-screen service.

ACKNOWLEDGMENT

This research was supported by a grant (SS10020) from the Seoul R&BD program funded by the Seoul Development Institute of the Korean government and supported by the Ministry of Knowledge Economy (10041725), Republic of Korea.

REFERENCES

- [1] Younghun Yoo, Byung Chul Shin, Seong Gon Choi, Sang Kwon Kim, "User Mobility Mechanism for Seamless Multimedia Service in Home Networks," ICACT 2008, Feb 2008.
- [2] K. Ha, K. Kang, and J. Lee, "N-screen service using I/O Virtualization technology", 2010 International Conference on Information and Communication Technology Convergence (ICTC), pp. 525-526, 2010
- [3] Jun Lee, HyungSeok Kim, Jee-In Kim, "A Framework for Adapting Content of Social Network Services for Heterogeneous Devices," IEEE International Conference on Consumer Electronics (ICCE), pp506-507, 2012
- [4] Kam Yong Kim, Seong Gon Choi, "Functional Architecture for User-Centric Multimedia Service on Mobile Station," 13th International Conference on Advanced Communication Technology (ICACT), pp.93-98, 2011
- [5] S.J. Kim, K.J. Gil, H.S. Kim, S.B. Lim, and J.I. Kim, "Adaptive interactions in shared virtual environments for heterogeneous devices", *Journal of Visualization and Computer Animation* 21(5): 531-543 , 2010.
- [6] Taiwon Um, Hyunwoo Lee, "Classification of N-Screen Services and its Standardization," 14th International Conference on Advanced Communication Technology (ICACT), pp.592-602, 2012
- [7] Jong-Hyoun Kim, Soo Hong Kim, "N-Screen Convergence Services Applied Hands and Objects Tracking in Educational Environment," 5th International Conference on New Trends in Information Science and Service Science (NISS), pp.412-415, 2011
- [8] Ullah, F., Sung Chang Lee, Seng Kyoun Jo, Hyun Woo Lee, "Dynamic Addition and Deletion of Device in N-Screen Environment," Fourth International Conference on Ubiquitous and Future Networks (ICUFN), pp.118-122, 2012
- [9] 2012 Dropbox, <https://www.dropbox.com/>, Dropbox Service
- [10] Korea Telecommunication, <http://ucloud.com/main.kt>, uCloud Service
- [11] Goo Jun, "Home media center and media clients for multi-room audio and video applications," Consumer Communications and Networking Conference, 2005. CCNC. 2005 Second IEEE, 2005, pp. 257-260.
- [12] J. Choi, D.K. Shin, and D. Shin, "Research and Implementation of the Context-Aware Middleware for Controlling Home Appliances", *IEEE Transaction on Consumer Electronics*, 51-1. pp.301-306, 2005.
- [13] Soraya Ait Chellouche, Julien Arnaud, Daniel Négru, "Flexible User Profile Management for Context-Aware Ubiquitous Environment," Consumer Communications and Networking Conference (CCNC), 2010 7th IEEE, 2010.
- [14] Chung-Ming Huang, Chung-Wei Lin, and Chia-Ching Yang, "Mobility Management for Video Streaming on Heterogeneous Networks," *Multimedia, IEEE*, 2010.
- [15] Kwong Huang Goh, Jo Yew Tham, Tianxi Zhang, Timo Laakko, "Context-Aware Scalable Multimedia Content Delivery Platform for Heterogeneous Mobile Devices," *The Third International Conferences on Advances in Multimedia*, 2011

Extendable Dialog Script Description Language for Natural Language User Interfaces

Kiyoshi Nitta
Yahoo Japan Research
Tokyo, Japan
Email: knitta@yahoo-corp.jp

Abstract—Natural language user interfaces are expected to be useful and provide a friendly atmosphere for human users working with intelligent human-computer interaction systems. Building correct and consistent large-scale script data for such interfaces requires large costs for construction and maintenance. Scripts written by many end-users in thoroughly flexible script languages might be a practical solution to this problem. We propose a dialog script description language and its framework. Two versions of script execution engines have been developed in C++ and Erlang programming languages. An example dialog script processed by one of these engines shows that a script editing function can be successfully represented by the script language. Because the script language has self-extending flexibility and ability to represent several versions of scripting languages, it increases the opportunity for end-users to accumulate and share a large amount of script data.

Index Terms—natural language user interface; conversational agent; chat bot; chatter-bot; ontology extension

I. INTRODUCTION

Constructing large-scale dialog script databases is one of the most critical issues for building practical natural language user interfaces that interact with users via typed text messages or voice utterances. Two major approaches can be considered to perform the task. The first approach is to apply machine learning technology to user operation or conversation logs for constructing dialog scripts. While the machine learning approach has an advantage in constructing large-scale scripts for reducing editorial operations of human staff, it might be difficult to achieve high precision adequateness of automatically generated scripts. The second approach is to accumulate dialog scripts created by many individual users. Script editing through natural language user interfaces might allow users to create their own dialog scripts. Because each user may have different preferences for editing scripts, such interfaces should be flexibly customized to maximize the opportunity.

With the second approach, we should address two technical challenges to operate a service in which many users safely customize natural language user interfaces for editing dialog scripts:

- dialog script languages and engines that are flexible for extending their description capability and modifying scripts by some types of script executions,
- load regulation methods for handling large-scale conversational transactions of many users.

We devised a knowledge representation framework [1] on which flexible dialog script languages can be represented. We developed several versions of flexible dialog script languages called *Graphical Language for Dialog Scripts (GLDS)* and two versions of GLDS execution engines coded in C++ and Erlang programming languages. In this paper, we explain a GLDS that address the first challenge by using the framework that can flexibly extend ontology. GLDS and its engines provide language elements that can modify operating dialog scripts. The Erlang version of the dialog script execution engine address the second challenge by using the parallel processing capability of Erlang language; however, this will be addressed in another study.

The main contributions of this paper can be summarized as follows:

- design of a flexible dialog script language (GLDS),
- implementation of GLDS execution engines, and
- evaluation of conversational operations for modifying dialog scripts.

The rest of this paper is organized as follows. Section II introduces the devised framework, execution engine algorithm, and GLDS dialog script language designed using the framework. Section III explains a self extendable example dialog script successfully executed using a system developed using the framework. Section IV describes the self-extending flexibility and ability of representing several versions of scripting languages. In Section V, several relevant studies on natural language user interface systems, graph-based knowledge representation methods, and semantic web technologies are summarized. This paper is concluded in Section VI.

II. GLDS FRAMEWORK

The framework described in this section consists of a data structure having basic semantics of dialog scripts and a dialog script execution engine that interprets the semantics. The data structure offers an extensible basis for GLDS. Dialog scripts executed by the engine are represented by *GLDS dialog scripts* based on this data structure.

A. Graph Structure and Semantics

The data structure of the framework is based on an augmented directed graph $ADG(E)$ [1] that permits edges to

connect to other edges as well as vertexes.

$$E_v = \{e(e_s, e_d) | e_s = \mathbf{null}, e_d = \mathbf{null}\} \quad (1)$$

$$E_{hoe} = \{e(e_s, e_d) | e_s \in E, e_d = \mathbf{null}\} \quad (2)$$

$$E_{toe} = \{e(e_s, e_d) | e_s = \mathbf{null}, e_d \in E\} \quad (3)$$

$$E_e = \{e(e_s, e_d) | e_s, e_d \in E\} \quad (4)$$

$$E = E_v \cup E_{hoe} \cup E_{toe} \cup E_e \quad (5)$$

Here, e means an *element*. Element e has a binomial structure (e_s, e_d) , which is either an element of set E or an empty element **null**. An element of E_v is called a *vertex* and an element of E_e is called an *edge*. An element of $E_{hoe} \cup E_{toe}$ is called an *open edge*. Element set E is the union of sets of vertexes, edges, and open edges.

The semantics of the framework consists of three layers. The bottom layer semantics gives the meaning of the relationship to the edge set. If an element $e(e_s, e_d)$ is an edge, then e expresses the relationship from element e_s (source) to element e_d (destination). The ADG-based data structure permits element e_d to become an edge. That is, edge e can express the relationship to edge element e_d .

The middle layer semantics gives the class-instance structure by defining a vertex set $E_{apriori}$.

$$E_{apriori} = \{v_{class}, v_{ins}\} \subset E_v \quad (6)$$

The vertex v_{class} means that its instance elements are *classes*, and vertex v_{ins} means that its instance edges are *instance relations*. Consider the following element sets:

$$E_{ii} = \{e(v_{ins}, e_d) | \exists e_d \in E\} \quad (7)$$

$$E_{ins} = \{e | \exists e_{ii}(v_{ins}, e) \in E_{ii}\} \subset E_e \quad (8)$$

$$E_{class} = \{e | \exists e_i(v_{class}, e) \in E_{ins}\} \subset E_v \quad (9)$$

Element set E_{ii} includes all edges starting from the a priori vertex v_{ins} . Each element $e(v_{ins}, e_d) \in E_{ii}$ means that its destination element e_d is an instance relation. Edge set E_{ins} includes all these instance relation edges. Set E_{ins} is called an *instance relation set*. Each instance relation edge $e(e_c, e_d) \in E_{ins}$ means that its source vertex e_c is a class and that its destination e_d is an instance of the class. Vertex set E_{class} contains instance vertexes of the class v_{class} and is called a *class set*. Any set tuple (E_{ins}, E_{class}) should satisfy the following condition:

$$\forall e_i(e_c, e) \in E_{ins}, \exists e_c \in E_{class} \quad (10)$$

The top-level layer semantics defines the meaning of some vertex elements in class set E_{class} . Consider the following instance element set $\text{ins}(e_c)$ for an arbitrary class vertex $e_c \in E_{class}$:

$$\text{ins}(e_c) = \{e | \exists e_i(e_c, e) \in E_{ins}\} \subset E \quad (11)$$

Each element of set $\text{ins}(e_c)$ inherits the meaning from class e_c . All functional definitions are combined to each element of class set E_{class} . Dialog scripts based on the framework are

TABLE I
CLASS DEFINITIONS REQUIRED BY DIALOG SCRIPT TRACER (DST)

class	type	meaning
SRL	vertex	root of dialog script
SRK	vertex	matching keyword
REL	edge	transitional relation
RM	vertex	reply message
SEL	vertex	select action

represented by the instance data of these classes. The data set is expressed as E_{data} :

$$E_{data} = \bigcup_{e_c \in E_{class}} \text{ins}(e_c) \quad (12)$$

The data structure part of the framework is denoted as ADG_F :

$$ADG_F = (E_{apriori}, E_{ii}, E_{ins}, E_{class}, E_{data}) \quad (13)$$

In this graph structure, every element of the sets, except for $E_{apriori}$ and E_{ii} , has at least one edge that connects from a semantically defined vertex to the element. This characteristic ensures that the meanings of all elements can always be resolved by checking source nodes of incoming instance edges.

B. Dialog Script Tracer

Dialog scripts are executed by a dialog controller called a *dialog script tracer* (DST). It requires the definitions of the classes in Table I. The ‘class’ column lists the mnemonic symbols of these classes, the ‘type’ column lists the vertex or edge type of the instance element of each class, and the ‘meaning’ column gives brief semantic explanations of these classes.

These classes are represented as class vertexes in the graph structure of the framework.

$$E_{class} = \{c_{srl}, c_{srk}, c_{rel}, c_{rm}, c_{sel}\} \quad (14)$$

Dialog scripts are expressed by instance elements I_{srl} , I_{srk} , I_{rel} , I_{rm} , and I_{sel} , where

$$\begin{aligned} I_{srl} &= \text{ins}(c_{srl}), I_{srk} = \text{ins}(c_{srk}), I_{rel} = \text{ins}(c_{rel}), \\ I_{rm} &= \text{ins}(c_{rm}), I_{sel} = \text{ins}(c_{sel}) \end{aligned} \quad (15)$$

There is no class of which an instance element can become both types.

$$I_{srl}, I_{srk}, I_{rm}, I_{sel} \subseteq E_v \cap E_{data} \quad (16)$$

$$I_{rel} \subseteq E_e \cap E_{data} \quad (17)$$

Only one instance element of the SRL class must be registered in a dialog script. When a new conversational session starts, the DST sets its context status to the vertex element. The DST can set its context status to one of the vertex set $V_{context}$ in an executing dialog script.

$$I_{srl} = \{\text{root}\} \quad (18)$$

$$V_{context} = I_{srl} \cup I_{sel} \quad (19)$$

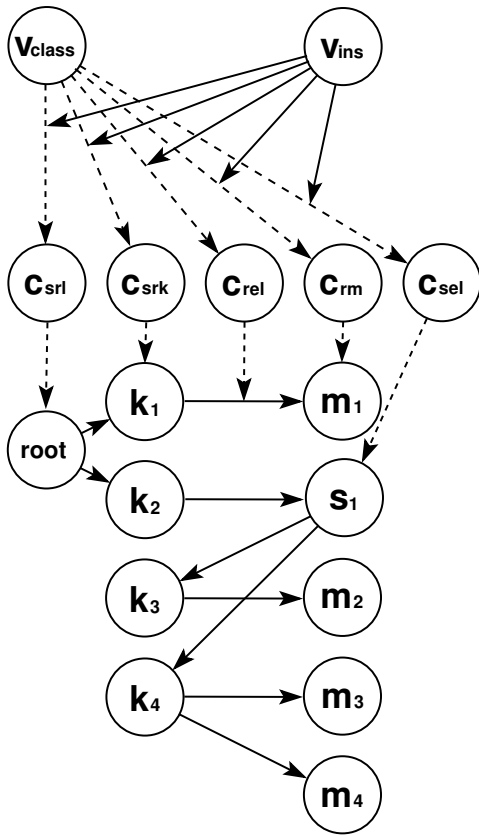


Fig. 1. Simple example of DST-consistent dialog script

At least one instance element of the SRK class must be connected to each element of $V_{context}$ using REL instance elements. When the context status is v_c and the DST receives a user input message, the DST attempts to find a v_c -related SRK instance element whose label matches the input message.

$$\forall v_c \in V_{context}, \exists k \in I_{srk}, \exists r(v_c, k) \in I_{rel} \quad (20)$$

At least one instance element of action type classes must be connected to each element of SRK.

$$\forall k \in I_{srk}, \exists a \in V_{action}, \exists r(k, a) \in I_{rel} \quad (21)$$

where

$$V_{action} = I_{rm} \cup I_{sel} \quad (22)$$

When an SRK instance element k is found to be a matched keyword, the DST randomly selects an action instance element a and executes it. If the element a is an instance of the RM class, the DST replies to the user with the text label of a and sets the context to $root$. If element a is an instance of the SEL class, the DST sets the context to a .

A simple example dialog script that can be executed by the DST is shown in Fig. 1. The dashed lines represent instance relations corresponding edge elements E_{ins} . Some are omitted for simplifying the diagram, e.g., relations between c_{srk} and k_2 or c_{rm} and m_2 . In this example, $V_{context} = \{root, s_1\}$ and

 TABLE II
SOME DEFINED CLASSES IN GLDS

	class	type	meaning
1	SM	edge	selection message relation
2	WCK	vertex	match a wild card keyword
	CFM	vertex	confirm an element
	CFA	vertex	confirm an array
	FMT	edge	format a relation
	NOP	vertex	no operation (dummy)
	SVC	vertex	save the context
	SLS	vertex	save the last selection
	SLR	vertex	save the last reply
	SVT	vertex	save a token
	QUI	vertex	quit
3	SUC	edge	success attribute
	FAI	edge	failure attribute
	IMM	edge	immediate attribute
4	VAR	edge	first argument
	VR2	edge	second argument
	VR3	edge	third argument
5	CTX	edge	variable (context)
	LSK	edge	variable (last selected keyword)
	LRP	edge	variable (last reply)
	MSG	edge	variable (message)
6	LET	vertex	set literal
	COP	vertex	copy
	ISN	vertex	check null
	CLR	vertex	clear
7	CSMS	vertex	search selection message
	CSMD	vertex	delete selection message
	CSMP	vertex	replace selection message

$V_{action} = \{s_1, m_1, m_2, m_3, m_4\}$. The diagram illustrates that the DST processes elements in I_{srk} and V_{action} alternatively.

C. Graphical Language for Dialog Scripts

The meanings of dialog scripts are resolved through the meanings of all the elements in vertex set E_{class} of the framework data structure explained in Subsection II-A. We added class vertexes required by dialog scripts for describing practical conversational applications. Their meanings are written in program codes, which are almost separated from DST implementations. Their major classes are listed in TABLE II.

Classes are divided into seven categories: 1) those required to implement simple replies, 2) those accessing functions of the dialog controller, 3) those modifying transitional relations, 4) those specifying variable arguments, 5) those identifying variable entities, 6) those operating on variables, and 7) those accessing the data structure of the GLDS framework. Due to the space limitation of this paper, detailed description of each class is omitted. Some are explained in Section III.

III. EXAMPLE

GLDS dialog scripts can be modified through the execution of another GLDS dialog script that uses action instances to modify the data structure of the GLDS framework. An example of such a GLDS dialog script is shown in Fig. 2. The script modifies a selection message of an existing script. The selection messages are replied to the user when the DST change its context.

TABLE III
STRING DATA OF SCRIPT FOR CHANGING A SELECTION MESSAGE

symbol	class	string
<i>kw</i>	SRK	change selection message
<i>str</i>	RM	selection message: '%s'
<i>sry_x</i>	SRK	yes
<i>srn_x</i>	SRK	no
<i>sra</i>	SRK	abandon
<i>m₁</i>	RM	Move to any context.
<i>m₂</i>	RM	Specify a selection message to change.
<i>m₃</i>	RM	No matching selection message found.
<i>m₄</i>	RM	Do you want to change this selection message?
<i>m₅</i>	RM	Abandon changing the selection message.
<i>m₆</i>	RM	Specify a selection message again.
<i>m₇</i>	RM	Do you want to delete it?
<i>m₈</i>	RM	Really delete?
<i>m₉</i>	RM	Deleted.
<i>m₁₀</i>	RM	Could not delete the last selection message.
<i>m₁₁</i>	RM	Specify a new selection message.
<i>m₁₂</i>	RM	Do you want to replace the selection message with this?
<i>m₁₃</i>	RM	Specify a new selection message again.
<i>m₁₄</i>	RM	Replaced.

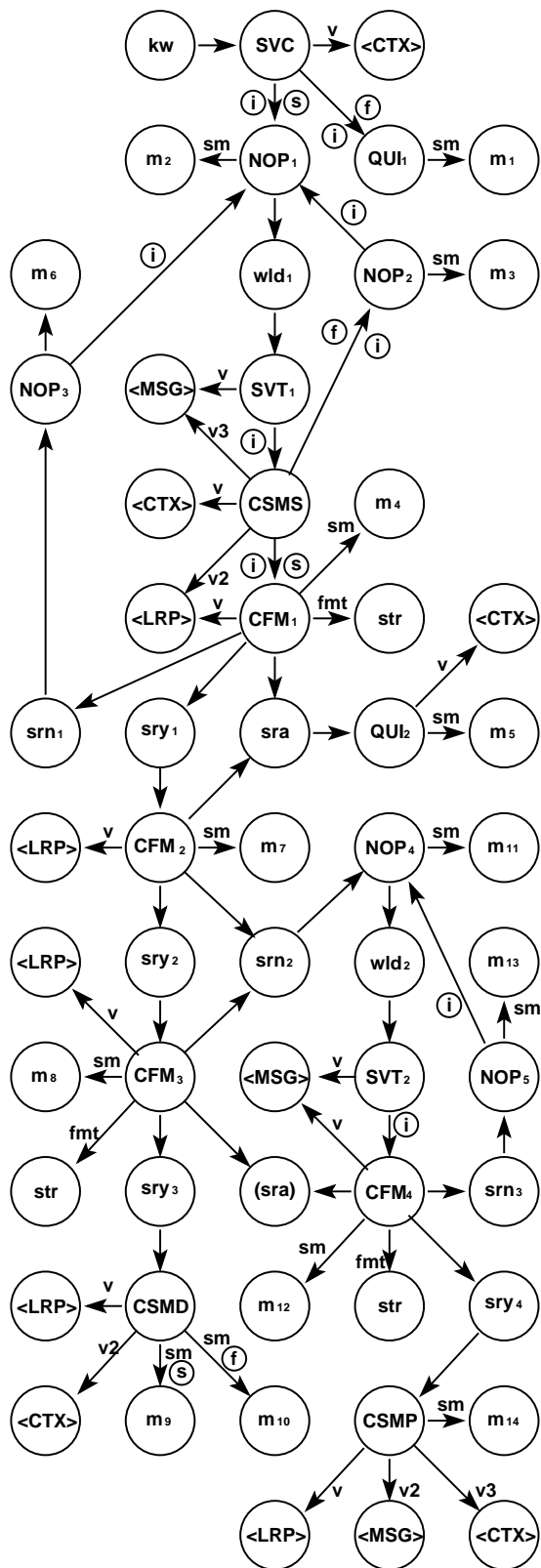


Fig. 2. Example GLDS dialog script for changing selection message

Instance edges and vertexes are represented by arrows and large circles in the diagram. A label consisting of capital letters in a circle indicates that the labeled vertex is an instance of the class whose name is indicated by the label. The number suffix of such a label identifies an instance from among those of the same class. A capital-letter label surrounded by angle brackets indicates that the vertex is a class vertex. This notation is used to represent variable references. A label consisting of lowercase letters in a circle indicates a vertex bound with string data (see TABLE III), except that the label “wld” indicates an instance vertex of the WCK class (see TABLE II), which is not bound with any string data.

String labels aligned with arrows indicate to which class each edge instance belongs. An arrow with no string label represents an instance edge of the transitional relation (REL) class. An arrow with the label “sm” represents an instance edge of the selection message relation (SM) class. An arrow with the label “v”, “v2”, or “v3” represents an instance edge of the argument variable relation (VAR, VR2, or VR3) class. An arrow with the label “fnt” represents an instance edge of the format relation (FMT) class. A small circle surrounding the characters “s”, “f”, or “i” indicates that the aligned edge has success, failure, or immediate attributes, respectively.

Fig. 3 shows an example of a dialog between a user (U) and the system (A) executing the script depicted in Fig. 2. It is assumed that the dialog began during the execution of another script. When *kw* string (see TABLE III) is detected, DST execution engine process SVC vertex that saves the current context pointer into variable <CTX>. Because this script

```

U: Change selection message
A: Specify a selection message to change.
U: Source
A: Do you want to change this selection message?
  selection message: 'source?'
  yes, no, abandon.
U: Yes
A: Do you want to delete it?
  yes, no, abandon.
U: No
A: Specify a new selection message.
U: What source do you have in mind?
A: Do you want to replace the selection message with this?
  selection message: 'What source do you have in mind?'
  yes, no, abandon.
U: Yes
A: Replaced.

```

Fig. 3. Example of dialog when changing selection message

was invoked during the execution of another script, the SVC process succeeds. DST follows the edge having immediate and success attributes, processes NOP_1 and m_2 that replies m_2 string to the user, and waits for user input. DST accepts any user input string, because wld_1 is connected to NOP_1 by a REL edge. Then DST proceeds to process SVT_1 that saves the user input string into variable $\langle MSG \rangle$. Vertex CSMS searches a RM vertex that is connected from the vertex stored in variable $\langle CTX \rangle$ and has a text label matching the string stored in variable $\langle MSG \rangle$. If the search task is succeeded, it stores the result into variable $\langle LRP \rangle$. The explanations for the rest processes are omitted because of the space limitation of this paper.

IV. DISCUSSION

GLDS has been developed by extending script description language specifications. We experimented with at least three internal versions: $GLDS_0$, $GLDS_1$, and $GLDS_2$. The basic finite-state-based dialog scripts are represented by $GLDS_0$, which contains the class vertexes in Equation (14). We extended $GLDS_0$ to $GLDS_1$ for representing dialog scripts that have script editing functions. $GLDS_1$ contains action classes, each of which performs a set of complex operations for a specific script editing task. $GLDS_1$ provides a safe environment in which inconsistent dialog scripts cannot be generated by any script editing operation. However, $GLDS_1$ must append class definitions with executable codes when a user requires new editing tasks. After such classes have been developed, we found that they can be represented by GLDS graphs connecting more reduced granularity of commonly reusable functions. We extended $GLDS_1$ to $GLDS_2$ by reducing complex classes to simple classes. Each $GLDS_1$ -introduced class can be replaced by an adequate combination graph structure using $GLDS_2$ -introduced classes. Some of these classes are listed in TABLE II. The ‘changing a selection

message’ example explained in Section III and depicted in Fig. 2 is written in $GLDS_2$, which permits the representation of dialog scripts that may generate inconsistent dialog scripts due to their executions. This problem should be resolved in future studies.

The polymorphic framework holds executable script data written in these three GLDS versions. This makes it easier for the developer to try a new script description language even if the amount of accumulated legacy script data is huge. Our experimental system even permits the execution of dialog scripts that connect different versions of GLDS class instances. Although there is not enough space to show concrete examples in this paper, we can note that this benefit is derived by the graph structure design. As explained in Section II, the graph structure maintains an element set E_{class} that defines a kind of ontology giving the semantics of each dialog script element. The class set E_{class} can be extended by just adding classes that have new meanings, when a new version of GLDS is introduced. Therefore, no conflict occurs by resolving semantics of script elements, even if they are instances of different versions of GLDS classes.

The change selection message script example shown in Fig. 2 modified another GLDS dialog script through a conversation between the user and the system. It shows that GLDS and its framework provides a script modification function. We also implemented a GLDS dialog script that dynamically generates GLDS graph data and executes them. Although this was not efficient, it might be a solution to the problem of finite-state-based dialog control methods requiring a huge amount of scripts to achieve the conversational flexibility that can be provided using frame-based methods [2]. GLDS and its framework offer a kind of programming environment rather than a built-in customization language. Its specifications can increase in tandem with extensions of the system.

While the modification made by the change selection message script was applied to element set E_{data} , it is possible to modify element set E_{class} . If a class is created dynamically and its semantics defined, it means that the GLDS specifications are dynamically extended. A serious limitation of the current dialog script execution engines is that the semantics of classes is defined only by code written in a programming language (C++ or Erlang). Rich variations of E_{class} elements and a synthetic definition feature of an extended GLDS will overcome this restriction in the future. We hope to implement frame-based and agent-based dialog controllers [2] that cooperatively work with existing and extended DST/GLDS specifications. We believe that this infrastructure might help in the development of Minsky’s emotional models [3] by using different types of dialog controllers and a polymorphic application of the knowledge model.

V. RELATED WORK

Many natural language user interface systems have been developed. The earliest system, Weizenbaum’s ELIZA [4], was reported in 1966. It was equipped with a reply function that repeated user messages with suitable pronouns substituted for

pronouns. To some degree, it gave users the impression they were conversing with a human psychiatrist. Colby's PARRY [5] acted as a psychiatric patient, and it was not required to reply with answers that were correct for its users. This showed that it is possible to implement a natural language user interface system that cannot be distinguished from a human psychiatric patient. The CONVERSE agent [5] integrated a commercial parser, query interface for accessing a parse tree, large-scale natural language resources like Wordnet, and other natural language processing technologies commonly available in 1997. It achieved a high percentage of completion, and won the 1997 annual medal of the Loebner prize [6]. Wallace's ALICE (<http://alicebot.org/articles/wallace/dont.html> [retrieved: February 2013]) promoted the XML-based script description language AIML. Wallace developed the AIML processor and the ALICE subset knowledge data in the AIML format as open source resources, and several chat bots [7], [8] have subsequently been developed based on these ALICE resources. ALICE has won the annual medal of the Loebner prize three times. While AIML provides one of the most customizable notations for natural language user interfaces, dialog scripts can only be authorized manually or externally. GLDS and its execution engines provide a dialog script notation, which has an ability to express the dialog scripts for authorizing other dialog scripts.

A semantic network is a well known graph structure having specific semantics. Griffith [9] defined it universally by dividing the net into a conveying net and an abstract net. The conveying semantic network corresponds to the whole data structure ADG_F that represents the expression system. The abstract semantic network corresponds to the element set E_{data} that represents the meanings of graph data. Griffith had no intention of extending the description capability of the abstract net, which is often the case, because semantic networks are used in natural language processing, where the semantics is considered to be stable. GLDS and its framework uses the net to represent dialog scripts, so we extended the net to be as extensible and flexible as an augmented semantic network [1].

Graph-based network data are commonly distributed using the resource description framework (RDF), which is a fundamental component of Semantic Web technology. In principle, ADG graph data can be expressed by the RDF. It is additionally required to provide a semantic basis like our GLDS framework to express GLDS script data using the RDF. The OWL Web Ontology Language can provide such a basis that partially represents the GLDS semantics. GLDS scripts expressed by OWL are convenient to port. It becomes more convenient to assume syntactical consistency if the scripts are expressed by OWL-DL, which is a subset of OWL, and can be processed by description logic (DL) [10] inference engines. Ontology extending issues are discussed in the linked data community [11] and large-scale ontology development [12]. Results of these studies might be used to improve the design of our framework.

VI. CONCLUSION AND FUTURE WORK

To advance the research being done on natural language user interface systems, we have focused on methodologies that enable dialog script execution engines to preserve the consistency of their dialog scripts while using different types of dialog control methods simultaneously. We have also focused on technologies for implementing script editing functions by dialog scripts. We proposed and implemented a script description language (GLDS) and its framework that meet these requirements. We developed two versions of GLDS execution engines. A GLDS dialog script example was presented to show that a script editing function can be represented by $GLDS_2$ and executed successfully. Because GLDS and its engines have self-extending flexibility and ability to execute several versions of scripting languages, they increase the opportunity for end-users to accumulate and share a large amount of script data.

This framework has affinity for RDF-represented knowledge bases that increase their content rapidly via the semantic web and linked data activities. Integrating such knowledge bases and dialog scripts to increase the intelligence of natural language user interfaces is left for future work.

REFERENCES

- [1] K. Nitta, "Building an autopoietic knowledge structure for natural language conversational agents," in RuleML '08: Proceedings of the International Symposium on Rule Representation, Interchange and Reasoning on the Web. Berlin, Heidelberg: Springer-Verlag, 2008, pp. 211–218.
- [2] M. F. McTear, "Spoken dialogue technology: enabling the conversational user interface," ACM Comput. Surv., vol. 34, no. 1, 2002, pp. 90–169.
- [3] M. Minsky, The Emotion Machine: Commonsense Thinking, Artificial Intelligence, and the Future of the Human Mind. Simon & Schuster, 2006.
- [4] J. Weizenbaum, "ELIZA — a computer program for the study of natural language communication between man and machine," Commun. ACM, vol. 9, no. 1, 1966, pp. 36–45.
- [5] Y. Wilks, Machine Conversations. Norwell, MA, USA: Kluwer Academic Publishers, 1999.
- [6] H. G. Loebner, "In response," Commun. ACM, vol. 37, no. 6, 1994, pp. 79–82.
- [7] A. M. Galvao, F. A. Barros, A. M. M. Neves, and G. L. Ramalho, "Persona-aiml: An architecture developing chatterbots with personality," in AAMAS '04: Proceedings of the Third International Joint Conference on Autonomous Agents and Multiagent Systems. Washington, DC, USA: IEEE Computer Society, 2004, pp. 1266–1267.
- [8] G. O. Sing, K. W. Wong, C. C. Fung, and A. Depickere, "Towards a more natural and intelligent interface with embodied conversation agent," in CyberGames '06: Proceedings of the 2006 international conference on Game research and development. Murdoch University, Australia, Australia: Murdoch University, 2006, pp. 177–183.
- [9] R. L. Griffith, "Three principles of representation for semantic networks," ACM Trans. Database Syst., vol. 7, no. 3, 1982, pp. 417–442.
- [10] F. Baader, D. Calvanese, D. L. McGuinness, D. Nardi, and P. F. Patel-Schneider, Eds., The description logic handbook: theory, implementation, and applications. New York, NY, USA: Cambridge University Press, 2003.
- [11] C. Bizer, T. Heath, K. Idehen, and T. Berners-Lee, "Linked data on the web (ldow2008)," in Proceedings of the 17th international conference on World Wide Web, ser. WWW '08. New York, NY, USA: ACM, 2008, pp. 1265–1266.
- [12] J. Hoffart, F. M. Suchanek, K. Berberich, E. Lewis-Kelham, G. de Melo, and G. Weikum, "Yago2: exploring and querying world knowledge in time, space, context, and many languages," in Proceedings of the 20th international conference companion on World wide web, ser. WWW '11. New York, NY, USA: ACM, 2011, pp. 229–232.

Classification of Three Negative Emotions based on Physiological Signals

- Classification of fear, surprise and stress

Eun-Hye Jang, Byoun-Jun Park, Sang-Hyeob Kim,
Myoung-Ae Chung

IT Convergence Technology Research Laboratory & IT
Convergence Services Future Technology Research Dept.
Electronics and Telecommunications Research Institute
Daejeon, Republic of Korea
{cleta4u, bj_park, shk1028, machung}@etri.re.kr

Mi-Sook Park, Jin-Hun Sohn

Department of Psychology & Brain Research Institute
Chungnam National University
Daejeon, Republic of Korea
{peaceful1026, jhsohn}@cnu.ac.kr

Abstract—Physiological signal is one of the most commonly used emotional cues. In recent emotion classification research, the one of main topics is to recognize human's feeling or emotion using multi-channel physiological signals. In this study, we discuss the comparative results of emotion detection using several classification algorithms, which classify negative emotions (fear, surprise and stress) based on physiological features. Physiological signals, such as skin temperature (SKT), electrodermal activity (EDA), electrocardiogram (ECG), and photoplethysmography (PPG) were recorded while participants were exposed to emotional stimuli. Twenty-eight features were extracted from these signals. For classification of negative emotions, four machine learning algorithms, namely, Linear Discriminant Analysis (LDA), Classification And Regression Tree (CART), Self Organizing Map (SOMs), and Naïve Bayes were used. The 70% of the whole datasets were selected randomly for training and the remaining patterns are used for testing purposes. Testing accuracy by using the 30% datasets ranged from 32.4% to 46.9% and, consequently the selected physiological features didn't contribute to classify the three negative emotions. In the further work, we intend to improve emotion recognition accuracy by applying the selected significant features, such as NSCR, SCR, SKT, and FFTap_HF.

Keywords-emotion classification; physiological signals; negative emotions; machine learning algorithm

I. INTRODUCTION

Emotion detection is one of the core factors for implementing emotional intelligence in human computer interaction research [1]. In particular, it is important to recognize negative emotions (e.g., anger, fear, etc.) because they have direct or indirectly effects gradual deviance or interruption of our normal thinking process, they are essential for our natural (unforced) survival or struggle for existence. Emotion recognition has been done using by facial expression, gesture, voice, and physiological signals. In particular, physiological signals have advantages; they are less affected by social and cultural difference as well as signal acquisition by non-invasive sensors is relatively simple and is possible to observe user's state in real time. They aren't robust to social masking or factitious emotion expression and are related to emotional state [2]. Recently, emotion recognition based on physiological signals has been performed by using various machine learning algorithms,

e.g., Fisher Projection (FP), k-Nearest Neighbor algorithm (kNN), and Support Vector Machine (SVM). Previous results that have showed the over 80% accuracy on average seems to be applicable in real world settings [3-8]. We have already reported the recognition accuracy on the three emotions, i.e., fear, surprise, and stress, derived from only training data [9]. As a follow-up work, we performed supplementary analysis by using machine learning algorithms for these emotions based on physiological signals. We performed each classifier by 10 fold cross-validation for solution of the overfitting problem and divided the dataset into 70% training and 30% testing subsets for testing purposes. The results were compared with the previous result that used the only training dataset. To classify three negative emotions, four well-known machine learning algorithms, i.e., were Linear Discriminant Analysis (LDA), Classification And Regression Tree (CART), Self Organizing Map (SOMs), and Naïve Bayes, were used. For dataset of physiological signals, twenty-eight features were extracted from physiological signals, i.e., skin temperature (SKT), electrocardiogram (ECG), electrodermal activity (EDA), and photoplethysmography (PPG).

II. PHYSIOLOGICAL SIGNALS OF EMOTIONS

Twelve male and female college students (mean age: 21 ± 1.48 yrs) participated in this study. They reported that they had not any medical illness or psychotropic medication and any kind of medication due to heart disease, respiration disorder, or central nervous system disorder. They participated in an experimental session for 10 weeks on a weekly basis over 10 times. A written consent was obtained prior to the study from the participants and they were paid \$20 USD per session to compensate for their participation.

Thirty emotional stimuli (3 emotions x 10 sessions), which are the 2-4 min long audio-visual film clips captured originally from movies, documentary, and TV shows, were used to successfully induce emotions (fear, surprise, and stress) in this study (Figure 1). Audio-visual film clips have widely used because they have a relatively high degree of ecological validity as well as they have the desirable properties of being readily standardized and being dynamic rather than static [10-13].

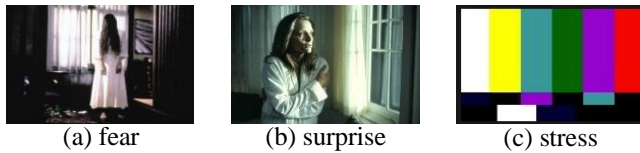


Figure 1. Examples of emotional stimuli

The appropriateness and effectiveness of the stimuli were examined through a preliminary study. The appropriateness of emotional stimulus means the consistency between emotion intended by experimenter and participants’ experienced emotion (e.g., scared, surprise, and annoying). The effectiveness was determined by the intensity of emotions reported and rated by the participants on a 1 to 11 point Likert-type scale (e.g., 1 being “least surprising” or “not surprising” and 11 being “most surprising”). The result showed that emotional stimuli had the appropriateness of 92% and the effectiveness of 9.4 points on average. The appropriateness and effectiveness of each emotional stimuli were as follows; appropriateness and effectiveness of fear were 89.0% and 9.6 points, 89% appropriateness and 9.5 points effectiveness in surprise. Stress had the appropriateness of 98% and the effectiveness of 9.1 points.

Prior to the experiment, participants were introduced detailed experiment procedure. They had an adaptation time to feel comfortable in the laboratory’s environment and then, an experimenter attached electrodes on the participants’ wrist, finger, and ankle for the measurement of physiological signals. Physiological signals were measured for 60 sec as baseline prior to the presentation of emotional stimulus and for 2 to 4 min as emotional state during the presentation of the stimulus, then for 60 sec as recovery term after presentation of the stimulus. Participants reported the emotion that they had experienced during the presentation of the film clips and the intensities of experienced emotions on the emotion assessment scale. This procedure was repeated 3 times in three different emotion conditions.

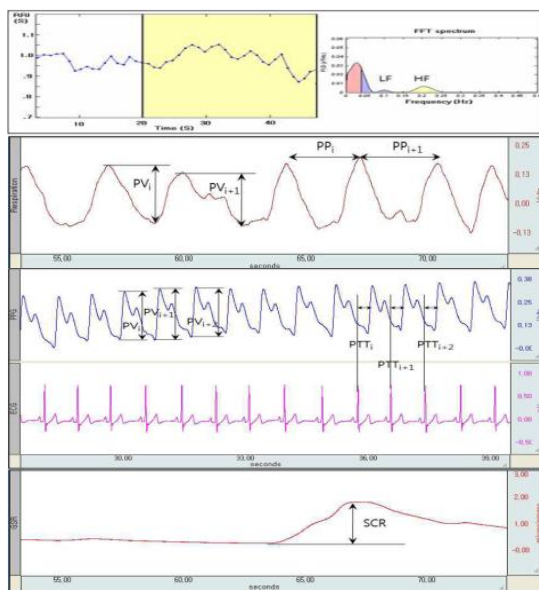


Figure 2. Analysis of physiological signals

The dataset of physiological signals were collected using MP150 (Biopac system Inc., USA). SKT electrode was attached on the first joint ring finger of non-dominant hand and EDA was measured with the use of 8 mm AgCl electrodes placed on the volar surface of the distal phalanges of the index and middle fingers of the non-dominant hand. Electrodes were filled with a 0.05 molar isotonic NaCl paste to provide a continuous connection between the electrodes and the skin. ECG electrodes were placed on both wrists and one left ankle with two kinds of electrodes, sputtered and AgCl ones. The left-ankle electrode was used as a reference. PPG electrode was attached on the first joint of the thumb of the non-dominant hand. To extract features, the obtained signals for 30 seconds from the baseline and the each emotional state are analyzed by AcqKnowledge (Ver. 3.8.1) software (USA) as shown in Fig. 2. Twenty-eight features were firstly extracted from the physiological signals, which have been used for emotion recognition in the study (shown in Table I).

TABLE I. FEATURES EXTRACTED FROM PHYSIOLOGICAL SIGNALS

Signals		Features	
EDA		SCL, NSCR, meanSCR	
SKT		meanSKT, maxSKT	
PPG		meanPPG	
ECG	Time domain	Statistical parameter	meanRRI, stdRRI, meanHR, RMSSD, NN50, pNN50
		Geometric parameter	SD1, SD2, CSI, CVI, RRtri, TINN
	Frequency domain	FFT	FFT_apLF, FFT_apHF, FFT_nLF, FFT_nHF, FFT_LF/HF ratio
		AR	AR_apLF, AR_apHF, AR_nLF, AR_nHF, AR_LF/HF ratio

Two hundred-seventy physiological signal data (3 emotions x 10 sessions x 9 cases) were used for emotion classification except for data having severe artifacts by movements, noises, etc. To classify three negative emotions by the twenty-eight physiological features, four machine learning algorithms, namely, LDA, which is one of the oldest classification systems, CART, which is a robust classification and regression tree, unsupervised SOM, and Naïve Bayes classifier based on density were used in data analysis.

III. CLASSIFICATION OF EMOTIONS

In this study, we have used LDA, which is one of the oldest mechanical classification systems and linear models, CART which is a robust classification and regression tree, unsupervised SOM, and Naïve Bayes classifier based on density for three emotion classifications. LDA is a method used in statistics, pattern recognition and machine learning to find a linear combination of features, which characterizes or separates two or more classes of objects or events. It is a technique for dimensionality reduction that projects the data onto a subspace that satisfies the requirement of maximizing the between-class variance (SB) and minimizing the within-class variance (SW). It then offers a linear transformation of

the predictor variables, which provides a more accurate discrimination. In LDA, the measurement space is transformed allowing the separability between the emotional states to be maximized. The separability between the emotional states can be expressed through several criteria [14]. SW is proportional to the sample covariance matrix for the pooled d-dimensional data. It is symmetric and positive semidefinite, and it is usually nonsingular if $n > d$. Likewise, SB is also symmetric and positive semidefinite, but because it is the outer product of two vector, its rank is at most one. In terms of SB and SW, the criterion function J is written as

$$J(\mathbf{w}) = (\mathbf{w}^T \mathbf{S}_B \mathbf{w}) / (\mathbf{w}^T \mathbf{S}_W \mathbf{w}) \quad (1)$$

This expression is well known in mathematical physics and the generalized Rayleigh quotient. It is easy to show that a vector \mathbf{w} that maximizes J must satisfy

$$\mathbf{S}_B \mathbf{w} = \lambda \mathbf{S}_W \mathbf{w}, \quad (2)$$

for some constant λ , which is a generalized eigenvalue problem.

CART [14-15] is a non-parametric decision tree technique that produces either classification or regression trees, depending on whether the dependent variable is categorical or numeric, respectively. Given the data represented at a node, either declare that node to be a leaf (and state what category to assign to it), or find another property to use to split the data into subsets. In the generic tree-growing methodology known as CART, the basic principle underlying a tree creation is simplicity. We prefer decisions that lead to a simple, compact tree with few nodes. In formalizing this notion, the most popular measure is the entropy impurity (or occasionally, information impurity)

$$i(N) = - \sum_j P(\omega_j) \log_2 P(\omega_j) \quad (3)$$

where, $P(\omega_j)$ is the fraction of patterns at node N that are in class ω_j . By the well-known properties of entropy, if all the patterns are of the same category, the impurity is 0; otherwise it is positive, with the greatest value occurring when the different classes are equally likely.

SOMs called Kohonen map, is a type of artificial neural networks in the unsupervised learning category and generally present a simplified, relational view of a highly complex data set [14, 16]. This is called a topology-preserving map because there is a topological structure imposed on the nodes in the network. A topological map is simply a mapping that preserves neighborhood relations. The goal of training is that the “winning” unit in the target space is adjusted so that it is more like the particular pattern. Others in the neighborhood of output are also adjusted so that their weights more nearly match that of the input pattern. In this way, neighboring points in the input space lead to neighboring points being active. Given the winning unit i , the weight update is

$$\mathbf{w}_i(\text{new}) = \mathbf{w}_i + h_{ci} (\mathbf{x} - \mathbf{w}_i) \quad (4)$$

$$h_{ci} = h_0 \exp(- \|\mathbf{r}_i - \mathbf{r}_c\|^2 / \sigma^2) \quad (5)$$

where, h_{ci} is called the neighborhood function that has value 1 for $i=c$ and smaller for large value of the distance between units i and c in the output array. h_0 and σ are suitable decreasing functions of time. Units close to the winner as well as the winner itself, have their weights updated appreciably. Weights associated with far away output nodes do not change significantly. It is here that the topological information is supplied.

The Naïve Bayes algorithm is a classification algorithm based on Bayes rule and particularly suited when the dimensionality of the inputs is high [14]. When the dependency relationships among the features used by a classifier are unknown, we generally proceed by taking the simplest assumption, namely, that the feature are conditionally independent given the category, that is,

$$p(\omega_k | \mathbf{x}) \propto \prod_{i=1}^d p(x_i | \omega_k) \quad (6)$$

This so-called naïve Bayes rule often works quite well in practice, and it can be expressed by a very simple belief net.

The machine learning algorithms were evaluated by only training and the repeated random subsampling validation. The former uses the whole emotional patterns in order to build a classifier model using machine learning algorithms and measure the classification accuracy of those. The repeated random subsampling validation is used to consider overfitting problem for only trained model. This builds and evaluates a classification model using training and testing datasets, respectively. The 70% of the whole emotional patterns are selected randomly for training and the remaining patterns are used for testing purposes. It was repeated 10 times in this study.

Table II summarizes the classification results for the only training dataset and the repeated random subsampling validation (RRSV). The results of RRSV denote the average \pm standard deviation for 10 times. The results of emotion classification by only training dataset had range of 43.1% to 87.2% when all emotions are recognized and in similar results, 70% training dataset had range of 43.0% to 87.4%. However, in recognition using 30% of datasets for testing, accuracy of all emotions had only 32.4% to 46.9% and according to orders of Naive Bayes (Kernel Density), LDA, CART, and supervised SOMs, recognition rates were obtained 46.9%, 44.0%, 42.9% and 35.5%.

TABLE II. CLASSIFICATION RESULTS BY ONLY TRAINING DATASET AND THE REPEATED RANDOM SUBSAMPLING VALIDATION (RRSV)

Methods	Only TR Acc	RRSV		
		TR Acc	TE Acc	
LDA	57.3	58.9±1.7	44.0±3.7	
CART	87.2	87.4±1.9	42.9±4.2	
SOMs	Supervised	43.1	43.0±1.8	35.5±4.5
	Unsupervised	59.5	60.5±1.6	32.4±5.5
Naive Bayes	General	51.0	53.7±2.8	43.7±6.7
	Kernel Density	80.9	81.9±2.9	46.9±4.8

TR : Training, TE : Testing, Acc : Accuracy (%)

TABLE III. THE RESULT ON REPEATED ONE-WAY ANOVA TOWARD EACH FEATURES

ANOVA	SS	df	MS	F
dNSCR	100.398	2	50.199	20.886***
dmeanSCR	7.363	2	3.681	6.242**
dmeanSKT	94.884	2	47.442	5.827**
dmaxSKT	91.563	2	45.781	5.744***
FFTap_HF	2,322.00	2	1,161.00	3.833*

$p < .05$, ** $p < .01$, *** $p < .001$

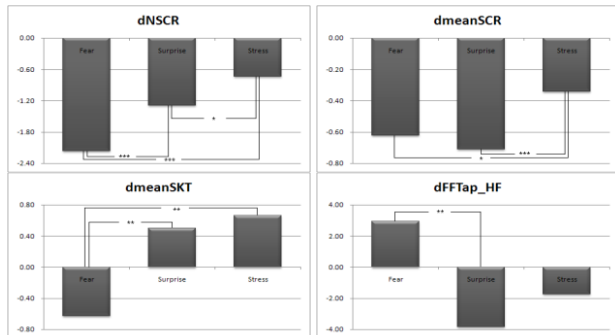


Figure 3. The results of LSD post-hoc test (* $p < .05$, ** $p < .01$, *** $p < .001$)

IV. CONCLUSION

The aim of this study was to classify three negative emotions, fear, surprise, and stress from physiological signals. We performed each classifier by 10 fold cross-validation for solution of the overfitting problem and divided the dataset into 70% training and 30% testing subsets for testing purposes. We compared this result with the previous result by the only training dataset and our results found no significant differences between the accuracies by the training datasets. However, recognition results by 30% of datasets for testing were lower than that of training dataset and had range of 32.4% to 46.9%. This means that consequently the selected physiological features didn't contribute to classify the three negative emotions. Also, these findings suggest that the given dataset by physiological signals has high nonlinear characteristic and reflects the individual variability of physiological property in emotions. The more or less unique and person-independent physiological response among these emotions may fall off the recognition rate with the number of emotion categories [17].

The values of testing performance are good indicators of the generalization capabilities of the constructed models. As selecting a model, if the approximation capability of a trained model is considered only, the selected model has great recognition accuracy; however, it has deteriorated generalization (prediction) capability and cannot apply to a real system. Especially, this is conspicuous in nonlinear problem. This important question arises, too, as to the selection of the proper structure of the emotion recognition in this study. To overcome these limitation, additional works for the verification of our dataset's statistical distribution and for performance of features' normalization those might be able to reduce large variability should be conducted. Also, for improvement of emotion classification, we have already

selected the meaningful features, such as NSCR, SCR, and SKT, which are significantly different among emotions by statistical analysis shown in the Table III and Figure 3 [9]. In the follow-up work, we intend to improve recognition accuracy by applying these features in our classifiers.

ACKNOWLEDGMENT

This research was supported by the Converging Research Center Program funded by the Ministry of Education, Science and Technology (No. 2012K001330 & 2012K001339).

REFERENCES

- [1] J. Wagner, J. Kim, and E. Andre, "From physiological signals to emotions: Implementing and comparing selected methods for feature extraction and classification," IEEE International Conference on Multimedia and Expo., vol. 7, 2005, pp. 940-943.
- [2] P. D. Drummond, and S.-H. Quah, "The effect of expressing anger on cardiovascular reactivity and facial blood flow in Chinese and Caucasians," Psychophysiology, vol. 38, 2001, pp.190-196.
- [3] R. W. Picard, E. Vyzas, and J. Healey, "Toward machine emotional intelligence: Analysis of affective physiological state," IEEE Transaction on Pattern Analysis and Machine Intelligence, vol. 23, 2001, pp. 1175-1191.
- [4] R. Cowie, E. Douglas-Cowie, N. Tsapatsoulis, G. Votsis, S. Kollias, W. Fellenz, J. G. Taylor, "Emotion recognition in human computer interaction," IEEE Signal Processing Magazine, vol. 18, 2001, pp. 32-80.
- [5] A. Haag, S. Goronzy, P. Schaich, J. Williams, "Emotion recognition using bio-sensors: First steps towards an automatic system," Affective Dialogue Systems, vol. 3068, 2004, pp. 36-48.
- [6] J. A. Healey, Wearable and automotive systems for affect recognition from physiology, Doctor of Philosophy, Massachusetts Institute of Technology, Cambridge, MA., 2000.
- [7] F. Nasoz, K. Alvarez, C. L. Lisetti, N. Finkelstein, "Emotion recognition from physiological signals for user modelling of affect," International Journal of Cognition, Technology and Work-Special Issue on Presence, vol. 6, 2003, pp. 1-8.
- [8] R. Calvo, I. Brown, S. Scheduling, "Effect of experimental factors on the recognition of affective mental states through physiological measures," AI 2009: Advances in Artificial Intelligence, vol. 5866, 2009, pp. 62-70.
- [9] E.H. Jang, B.J. Park, S.H. Kim, C. Huh, Y. Eum, J.H. Sohn, "Emotion Recognition Through ANS Responses Evoked by Negative Emotions," ACHI 2012 : The Fifth International Conference on Advances in Computer-Human Interactions, 2012, pp. 218-223.
- [10] J.J. Gross, and R.W. Levenson, "Emotion elicitation using films," Cognition and Emotion, vol. 9, 1995, pp. 87-108.
- [11] R.S. Lazarus, J.C. Speisman, A.M. Mordkoff, and L.A. Davidson, "A Laboratory study of psychological stress produced by an emotion picture film," Psychological Monographs, vol. 76, 1962, pp. 553.
- [12] M.H. Davis, J.G. Hull, R.D. Young, and G.G. Warren, "Emotional reactions to dramatic film stimuli: the influence of cognitive and emotional empathy," Journal of personality and social psychology, vol. 52, 1987, pp. 126-133.
- [13] D. Palomba, M. Sarlo, A. Angrilli, A. Mini, and L. Stegagno, "Cardiac responses associated with affective processing of unpleasant film stimuli," International Journal of Psychophysiology, vol. 36, 2000, pp. 45-57.
- [14] R. O. Duda, P. E. Hart, and D. G. Stork, Pattern Classification, 2nd edn. 2000.
- [15] L. Breiman, J. H. Friedman, R. A. Olshen, and C. J. Stone, Classification and Regression Trees, Monterey, Calif., U.S.A.: Wadsworth, Inc., 1984.
- [16] T. Kohonen, Self-Organizing Maps, Springer Series in Information Sciences, Vol. 30, Springer, Berlin, Heidelberg, New York, Third Extended Edition, 2001.
- [17] K. H. Kim, S. W. Bang, S. R. Kim, "Emotion recognition system using short-term monitoring of physiological signals," Medical & Biological Engineering & Computing, vol. 42, 2004, pp.419-427.

Physiological Signals and Classification for Happiness, Neural and Surprise Emotions

Three emotion classification

Byoung-Jun Park, Eun-Hye Jang, Sang-Hyeob Kim,
Chul Huh

IT Convergence Technology Research Laboratory
Electronics and Telecommunications Research Institute
Daejeon, Republic of Korea
{bj_park, cleta4u, shk1028, chuh}@etri.re.kr

Myoung-Ae Chung

IT Convergence Services Future Technology Research Dept.
Electronics and Telecommunications Research Institute
Daejeon, Republic of Korea
machung@etri.re.kr

Abstract—In this study, we discuss the comparative results of emotion classification by several algorithms, which classify three different emotional states (happiness, neutral, and surprise) using physiological features. 300 students participated in this experiment. While three kinds of emotional stimuli are presented to participants, physiological signal responses (EDA, SKT, ECG, RESP, and PPG) were measured. Participants rated their own feelings to emotional stimuli on emotional assessment scale after presentation of emotional stimuli. The emotional stimuli had 96% validity and 5.8 point efficiency on average. There were significant differences of autonomic nervous system responses among three emotions by statistical analysis. The classification of three differential emotions was carried out by Fisher's linear discriminant (FLD), Support Vector Machine (SVM), and Neural Networks (NN) using difference value, which subtracts baseline from emotional state. The result of FLD showed that the accuracy of classification in three different emotions was 77.3%. 72.3% and 42.3% have obtained as the accuracy of classification by SVM and NN, respectively. This study confirmed that the three emotions can be better classified by FLD using various physiological features than SVM and NN. Further study may need to get those results to obtain more stability and reliability, as comparing with the accuracy of emotions classification by using other algorithms.

Keywords—emotion classification; physiological signals; machine learning

I. INTRODUCTION

Recent emotion recognition studies have tried to detect a human emotion by using physiological signals. It is important to detect emotions for applying on human-computer interaction system. Various physiological signals have been widely used to recognize a human's emotion and feeling because signal acquisition using non-invasive sensors is relatively simple and physiological responses are less sensitive in social and cultural difference [1]. Physiological signal may happen to artifact due to motion, and have difficulty mapping emotion-specific responses pattern, but this has some advantages, which are less affected by environment than any other modalities as well as possible to observe user's state in real time. In addition, those can be

acquired spontaneous emotional responses and not caused by responses to social masking or factitious emotion expressions. Finally, measurement of emotional responses by multi-channel physiological signals offers more information for emotion recognition, because physiological responses are related to emotional state [2]. Various physiological signals offer a great potential for the recognition of emotions in computer systems. In order to fully exploit the advantages of physiological measures, standardizations of experimental methods have to be established on the emotional model, stimulus used for the identification of physiological patterns, physiological measures, parameters for analysis, and model for pattern recognition and classification [3].

The objective of this study is to achieve emotion dataset including physiological signals for three emotions (happiness, neutral, and surprise) induced by emotional stimuli and to classify three differential emotions using physiological signals. Electrodermal activity, skin temperature, electrocardiac activity, respiration and photoplethysmography are recorded from 300 people; during they are exposed to visual-acoustic emotional stimuli. And participants classified their present emotion and assessed its intensity on the emotion assessment scale. As the results of emotional stimulus evaluation, emotional stimuli were shown to mean 93.3% of appropriateness and 5.71 of effectiveness; this means that each emotional stimulus caused its own emotion quite effectively. In addition that, we used Fisher's linear discriminant, which is one of the linear models as a statistical method and Support Vector Machine and Neural Networks as a machine learning algorithm [4]-[7] for classifying three emotions. The comparative analysis results by those algorithms showed that the FLD exhibits higher accuracy.

This paper is organized as follows. Section II describes emotion stimuli and physiological signals of emotions. Section III deals with the classification of emotions and presents the results of classification. Finally, some conclusions are contained in Section IV.

II. PHYSIOLOGICAL SIGNALS OF EMOTIONS

300 students (140 males, 160 females and 21.6 ± 3.5 years) have participated in this study. They reported that they have not any history of medical illness or psychotropic

medication and any kind of medication due to heart disease, respiration disorder, or central nervous system disorder. A written consent was obtained before the beginning of the study from the participants.

The emotional stimuli, which are the 2-4 min long audio-visual film clips captured originally from movies, documentary, and TV shows, were used to successfully induce emotions (happiness, neutral, and surprise) in this study as shown in Fig. 1. Audio-visual film clips have widely used because these have the desirable properties of being readily standardized, involving no deception, and being dynamic rather than static. [8]-[11].

The audio-visual film clips that had been tested their appropriateness and effectiveness were used to provoke emotion. The appropriateness of emotional stimuli means a consistency between the intended emotion by experimenter and the participants' experienced emotion. The effectiveness is an intensity of emotions that participants rated on a 1 to 7 point Likert-type scale, that is, 1 being "least boring" and 7 being "most boring". The appropriateness and effectiveness of these stimuli were as follows; appropriateness and effectiveness of happiness were 88.0% and 5.36±1.21, 97% appropriateness and 6.06±1.05 effectiveness in surprise. In Neutral has 94.8% appropriateness.

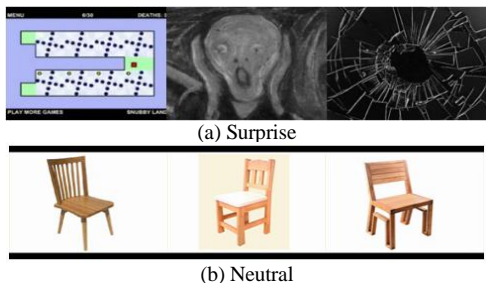


Figure 1. Example of a stimulus for inducing an emotion.

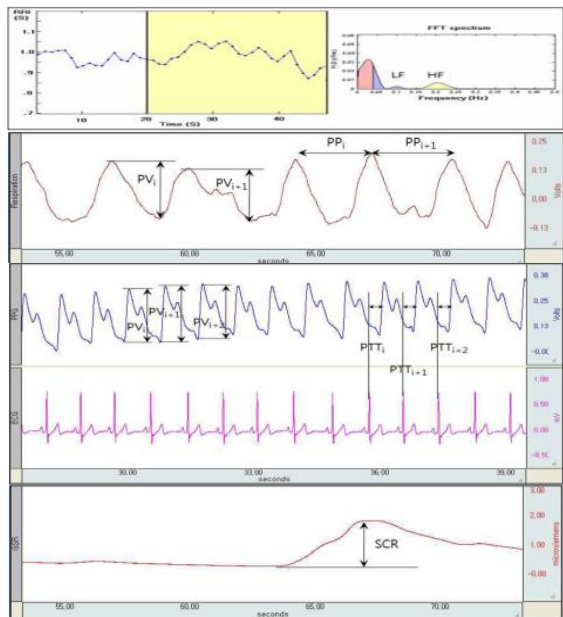


Figure 2. Analysis of physiological signals.

Prior to the experiment, we introduced detail experiment procedure to participants. They had an adaptation time to feel comfortable in the laboratory's environment and then an experimenter attached electrodes on the participants' wrist, finger, and ankle for measurement of physiological signals. Physiological signals were measured for 60 sec prior to the presentation of emotional stimulus (baseline) and for 2 to 4 min during the presentation of the stimulus (emotional state), then for 60 sec after presentation of the stimulus as recovery term. Participants rated the emotion that they experienced during presentation of the film clip on the emotion assessment scale. This procedure was repeated 3 times for elicitation of 3 differential emotions. To collect physiological signals for three emotions, the laboratory is a room with 5m x 2.5m size having a sound-proof (lower than 35dB) of the noise level where any outside noise are completely blocked.

The dataset of physiological signals such as skin temperature (SKT), electrodermal activity (EDA), photoplethysmography (PPG), respiration (RESP), and electrocardiogram (ECG) are collected by MP150 Biopac system Inc. SKT electrodes are attached on the first joint of non-dominant ring finger and on the first joint of the non-dominant thumb for PPG. EDA is measured with the use of 8 mm AgCl electrodes placed on the volar surface of the distal phalanges of the index and middle fingers of the non-dominant hand. Electrodes are filled with a 0.05 molar isotonic NaCl paste to provide a continuous connection between the electrodes and the skin. ECG electrodes are placed on both wrists and one left ankle with two kinds of electrodes, sputtered and AgCl ones. The left-ankle electrode is used as a reference.

The signals are acquired for 1 minute long baseline state prior to presentation of emotional stimuli and 1-2 minutes long emotional states during presentation of the stimuli as emotional state. To extract features, the obtained signals are analyzed for 30 seconds from the baseline and the emotional state by AcqKnowledge (Ver. 3.8.1) software (USA) as shown in Fig. 2. 10 features, namely, SCL and SCR features from EDA signal, meanSKT from SKT, HR and RRI from ECG, RESPrate, RESTamplitude, RESP_Rsd and RESP_Asd from RESP, and BVP from PPG are extracted from the obtained emotional physiological signals.

III. CLASSIFICATION OF EMOTIONS

In this study, we have used Fisher's linear discriminant (FLD), which is one of the linear models as a statistical method and Support Vector Machine (SVM) and Neural Networks (NN) for three emotion classifications.

We have carried out the related research with the same emotions (happiness, neutral, and surprise) and the same methods (FLD, SVM and NN) as an earlier work [12]. In [12], the result of LDA (FLD) showed that the accuracy of classification was 83.4%. 75.5% and 55.6% have obtained as the accuracy of classification by SVM and MLP (NN), respectively. However, the results of the previous research were obtained by only training set. Namely, the methods used the whole emotional patterns in order to build a classifier model and measure the classification accuracy of those. This approach cannot have effectiveness because of realistic and overfitting problems.

For the effectiveness verification of the previous research, we embrace more participants, which have increased by 300 people, and 10-fold cross-validation, which is a statistical method of evaluating models. In typical cross-validation, the training and validation sets must cross-over in successive rounds such that each data point has a chance of being validated against. The three algorithms were evaluated by 10-fold cross validation and the results of this study are reported for those. These values will offer a criteria index for assessing how the results of a statistical analysis will generalize to an independent dataset.

In addition those, we reduced the number of features. We used 10 features, removed LF, HF, and HRV, whereas 13 features were used in the previous work [12].

Firstly, FLD is a method used in statistics, pattern recognition and machine learning to find a linear combination of features, which characterizes or separates classes of objects or events. In FLD, the measurement space is transformed so that the separability between the emotional states is maximized. FLD finds the direction to project data on so that between-class variance (S_B) is maximized and within-class variance (S_W) is minimized, and then offers a linear transformation of predictor variables, which provides a more accurate discrimination [4]. S_W is proportional to the sample covariance matrix for the pooled d-dimensional data. It is symmetric and positive semidefinite, and it is usually nonsingular if $n > d$. Likewise, S_B is also symmetric and positive semidefinite, but because it is the outer product of two vector, its rank is at most one.

In terms of S_B and S_W , the criterion function J is written

$$J(\mathbf{w}) = (\mathbf{w}^T S_B \mathbf{w}) / (\mathbf{w}^T S_W \mathbf{w}). \tag{1}$$

This expression is well known in mathematical physics and the generalized Rayleigh quotient. It is easy to show that a vector \mathbf{w} that maximizes J must satisfy

$$S_B \mathbf{w} = \lambda S_W \mathbf{w}, \tag{2}$$

for some constant λ , which is a generalized eigenvalue. In analysis of FLD, accuracy of all emotions was 77.3 % and accuracy of each emotion had range of 69% to 89%. Happiness was recognized by FLD with 69.1%, neutral 88.6 % and Surprise 75.5% as shown in TABLE I.

TABLE I. RESULT OF THREE EMOTION DISCRIMINANT BY FLD

	Happiness	Neutral	Surprise	Total
Happiness	69.1	30.3	0.5	100.0
Neutral	10.3	88.6	1.1	100.0
Surprise	18.5	6.0	75.5	100.0

TABLE II. RESULT OF THREE EMOTION DISCRIMINANT BY SVM

	Happiness	Neutral	Surprise	Total
Happiness	59.0	29.8	11.2	100.0
Neutral	23.4	73.7	2.9	100.0
Surprise	12.0	6.0	82.0	100.0

TABLE III. RESULT OF THREE EMOTION DISCRIMINANT BY NN

	Happiness	Neutral	Surprise	Total
Happiness	0.5	13.8	85.6	100.0
Neutral	0.6	14.3	85.1	100.0
Surprise	0	3.0	97.0	100.0

SVM is non-linear model, which are used the well-known emotion algorithms and support vector classifier separates the emotional states with a maximal margin. The advantage of support vector classifier is that it can be extended to nonlinear boundaries by the kernel trick. SVM supervised learning models with associated learning algorithms that analyze data and recognize patterns, used for classification and regression analysis. SVM is designed for two class classification by finding the optimal hyperplane where the expected classification error of test samples is minimized and has utilized as a pattern classifier to overcome the difficulty in pattern classification due to the large amount of within-class variation of features and the overlap between classes [13].

SVM finds a hyperplane based on support vector to analyze data and recognize patterns. The complexity of the resulting classifier is characterized by the number of support vectors rather than the dimensionality of the transformed space. The goal in training SVM is to find the separating hyperplane with the largest margin [4]. We expect that the larger the margin, the better generalization of the classifier. The distance from any hyperplane to a pattern \mathbf{y} is $|g(\mathbf{y})|/||\mathbf{a}||$, and assuming that a positive margin b exists

$$z_k g(\mathbf{y}_k) / ||\mathbf{a}|| \geq b, k = 1, \dots, n; \tag{3}$$

The goal is to find the weight vector \mathbf{a} that maximizes b . Here, z_k is the class of k -th pattern, b is margin and $g(\mathbf{y})$ is a linear discriminant in an augmented \mathbf{y} space,

$$g(\mathbf{y}) = \mathbf{a}^T \mathbf{y} \tag{4}$$

SVM provided accuracy of 72.3% when it classified all emotions. In happiness, accuracy of 59.0% was achieved with SVM, 73.7% in neutral, and 82.0% in surprise, refer to TABLE II.

NN is a computational intelligence model inspired by the structure and functional aspects of biological neurons [4]. NN has been widely used to deal with pattern recognition problems. The generic topology of NN consists of three layers as shown in Fig. 3. A neuron in the input layer is connected to a layer of hidden neuron, which is connected to output neuron. The activity of the input neurons represents the raw information that is fed into the network, the activity of each hidden neuron is determined by the activities of the input neuron and the weights on the connections between the input and the hidden, and the behavior of the output depends on the activity of the hidden neurons and connection weights between the hidden and the output layer.

It is realized by connecting neurons and each neuron processes information using activation function,

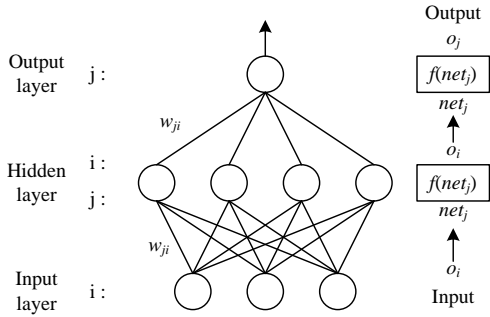


Figure 3. General structure of neural networks.

$$f_j(net_j) = 1 / (1 + e^{-net_j}) \quad (5)$$

where, net_j is input of j -th neuron and computed by,

$$net_j = \sum_i w_{ji} f_i + \theta_j \quad (6)$$

where, w_{ji} is the connection weight between j -th and i -th neurons and adjusted by

$$w_{ji} (\text{new}) = w_{ji} (\text{old}) + \Delta w_{ji} \quad (7)$$

Δw_{ji} is calculated by back-propagation algorithm.

In TABLE III, the result of emotion recognition using NN showed that accuracy to recognize all emotions was 42.3%. NN have lower classification for happiness and neutral because of the overfitting problem for surprise. We need more research about advanced networks.

IV. CONCLUSION

This study was to identify the difference among happiness, neutral, and surprise emotions using physiological responses induced by these emotional stimuli and to find the optimal emotion recognition algorithm for classifying these three emotions. The emotion stimuli used to induce a participant's emotion were evaluated for their suitability and effectiveness. The result showed that emotional stimuli have the appropriateness of 92.5% and the effectiveness of 5.4 point (7 point Likert scale) on average.

Our result showed that FLD is the best algorithm being able to classify three emotions. FLD provides extremely fast evaluations of unknown inputs performed by distance calculations between a new sample and mean of training data samples in each class weighed by their covariance matrices. The FLD shows a recognition ratio much higher chance probability, i.e. 77.3% for three emotion categories, when applied to physiological signal databases.

The values of performance (criteria index) by 10-fold cross validation are good indicators of the generalization capabilities of the constructed models. As selecting a model, if the approximation capability of a trained model is considered only, the selected model has greatly recognition accuracy; however, it has deteriorated generalization (prediction) capability and cannot apply to a real system. Especially, this is conspicuous in nonlinear problem. This

important question arises, too, as to the selection of the proper structure of the emotion recognition in this study.

Although some algorithm showed lower accuracy of emotion classification for the criteria index, the results led to better chance to recognize human emotions and to identify the optimal emotion recognition algorithm by using physiological signals. For example, this will be applied to the realization of emotional interaction between man and machine and play an important role in several applications, e.g., the human-friendly personal robot or other devices. However, for more accurate and realistic applications, a novel method to identify not only basic emotions but also more various emotions such as boredom, frustration, and love, etc. must be devised before it is mentioned that emotion recognition based on physiological signals is a practicable and reliable way of enabling HCI with emotion-understanding capability.

ACKNOWLEDGMENT

This research was supported by the Converging Research Center Program funded by the Ministry of Education, Science and Technology (No. 2012K001330).

REFERENCES

- [1] J. Wagner, J. Kim, and E. Andre, "From physiological signals to emotions: Implementing and comparing selected methods for feature extraction and classification," IEEE International Conference on Multimedia and Expo., vol. 7, 2005, pp. 940-943.
- [2] P. D. Drummond, and S.-H. Quah, "The effect of expressing anger on cardiovascular reactivity and facial blood flow in Chinese and Caucasians," Psychophysiology, vol. 38, 2001, pp.190-196.
- [3] R. W. Picard, E. Vyzas, and J. Healey, "Toward machine emotional intelligence: Analysis of affective physiological state," IEEE Transaction on Pattern Analysis and Machine Intelligence, vol. 23, 2001, pp. 1175-1191.
- [4] R. O. Duda, P. E. Hart, and D. G. Stork, Pattern Classification, 2nd edn. 2000.
- [5] M. Murugappan, R. Nagarajan, and S. Yaacob, "Classification of human emotion from EEG using discrete wavelet transform," Journal of Biomedical Science and Engineering, vol. 3, 2010, pp. 390-396.
- [6] K. Takahashi, "Remarks on emotion recognition from bio-potential signals," 2nd International Conference on Autonomous Robots and Agents, 2004, pp. 186-191.
- [7] C. Lee, and M.-G. Jang. "A Prior Model of Structural SVMs for Domain Adaptation," ETRI Journal, vol. 33, 2011, pp. 712-719.
- [8] J.J. Gross, and R.W. Levenson, "Emotion elicitation using films," Cognition and Emotion, vol. 9, 1995, pp. 87-108.
- [9] R.S. Lazarus, J.C. Speisman, A.M. Mordkoff, and L.A. Davidson, "A Laboratory study of psychological stress produced by an emotion picture film," Psychological Monographs, vol. 76, 1962, pp. 553.
- [10] M.H. Davis, J.G. Hull, R.D. Young, and G.G. Warren, "Emotional reactions to dramatic film stimuli: the influence of cognitive and emotional empathy," Journal of personality and social psychology, vol. 52, 1987, pp. 126-133.
- [11] D. Palomba, M. Sarlo, A. Angrilli, A. Mini, and L. Stegagno, "Cardiac responses associated with affective processing of unpleasant film stimuli," International Journal of Psychophysiology, vol. 36, 2000, pp. 45-57.
- [12] B.-J. Park, E.-H. Jang, Sang-Hyeob Kim, C. Huh and J.-H. Sohn, "Three Differential Emotions and Classification Using Physiological Signals," IPCSIT, vol. 25, 2012, pp. 55-59.
- [13] P.D. Wasserman, "Advanced Methods in Neural Computing," New York, Van Nostrand Reinhold, 1993, pp. 35-55.

Robot Control Using 2D Visual Information Via Database

Yutaka Maeda and Hidetaka Ito
 Faculty of Engineering Science
 Kansai University
 Suita, Japan
 maedayut@kansai-u.ac.jp

Abstract—This paper proposes a control scheme for a robot system via a database using two-dimensional (2D) visual images. Generally speaking, when we use visual images by cameras to control a robot, three-dimensional (3D) calibration for the position information acquisition is necessary. Moreover, we calibrate the 3D camera coordinate and the robot coordinate. However, these processes are complicated. In addition, especially for hand-eye systems, the calibration is required for every movement of the robot. Thus, the situation is more difficult. In this work, we propose a calibration-free robot system via a database which gives 3D quantity of deviation for the robot arm from 2D image data by two cameras. We also explain a method to establish and update the database effectively using the simultaneous perturbation optimization method. As a result, the hand-eye robot arm system with the proposed control scheme based on visual information can work well without the calibration.

Index Terms—2D Visual Information; Calibration-free; Hand-eye system; Database; Simultaneous Perturbation; Tracking Control;

I. INTRODUCTION

Recently, system control is very important in many industrial fields. There are many methods to control actual systems using certain sensors. It is crucial to establish robust and flexible systems from many aspects [1]. Control using visual information is one of promising approaches in the sense that the system can recognize and adapt to changing or new environment [2], [3], [4]. Robot systems are typical. Visual information has an important role, and thus, research on robot control systems based on the visual information is getting important.

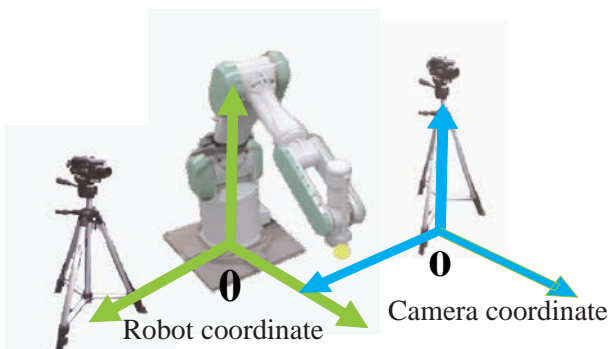


Figure 1. Calibration for robot system.

Now we can assume a robot system controlled by camera vision (see Fig. 1). When we think about control of a robot by the information given by cameras, we generally require three-dimensional (3D) recognition for the position information acquisition.

Using image data from the two CCD cameras like human eyes, the robot can establish 3D coordinates by a camera calibration. However, the calibration is complicated process, because it requires initial setting such as a direct measurement of outside and internal parameters of camera or geometry of the robot [5]. On the other hand, a robot system has its own coordinate. We have to adjust the robot coordinate and the camera one.

Moreover, in case of hand-eye systems in which the robot carries cameras, the calibration is required for every movement, since relation of the robot coordinates and the camera coordinates changes for every movement of the camera in such a system. Therefore the robot control system becomes more complicated and difficult to realize.

In this paper, we solved this problem with a database using two-dimensional (2D) visual image information. That is, we built a calibration-free robot system using the database based on the visual information. The database is established by distance optimization control using the the simultaneous perturbation method. The database converts the image data of the tip of the robot arm and the objective from two CCD cameras into moving quantity.

There are many various complicated tracking control methods by using visual feedback [6]. However, many of them are basically using geometry of robots, cameras or environment of the system. In this work, we do not require such a prior information.

An uncalibrated visual hand-eye system is reported [7]. However, the system contains complicated calculations for Gauss-Newton method with partitioned Broyden's method. On the other hand, our proposed method does not contain such a complex procedure. Instead of the calculation, the database can tell us a moving direction of the robot.

Graefe [8], [9] proposed a system without calibration using a database as well. However, the database does not memorize 3D moving quantities directly.

Section II describes control scheme based on a database. Next section explains meaning of the database. Section IV

shows details of the overall system and how to establish the database using the simultaneous perturbation method. Concrete task using the proposed scheme is demonstrated in Section V. Section VI is conclusion.

II. ROBOT CONTROL USING DATABASE

Instead of the calibration, we utilize a database. The database realizes a relation of 2D coordinates of two camera images and 3D coordinates of the robot arm. It memorizes proper derivation of movement against the target position.

When we use a single camera for visual control system, the camera converts 3D world into 2D image. Then some information of 3D world disappears. In other words, there is an ambiguity by loss of information in 2D image when using a single camera [10]. The system cannot determine a position of an object in 3D space by this ambiguity of sight if we use a single camera.

Of course, we can remove the ambiguity by using two cameras. Then the system can determine a position of the object in 3D space by 3D calibration. In this work, we realize the relation as the database without the calibration.

Fig. 2 and Table 1 show two 2D images and the database of this study. For camera images, we divided them into 13×20 area (see Fig. 2). This resolution depends on capability of the image processing equipment and size of goal object. The database consists of two camera's 2D coordinates and 3D quantity of movement of the robot arm. The 3D quantity of movement means a deviation between the tip of the robot and the goal position. The database memorizes the moving quantity for every combinations of two 2D coordinates (see Table 1). For examples, we consider the point "a" shown in Fig. 1. In camera A and B, the point "a" is located in (1, 8) and (-3, 6) respectively. Then in order to move the robot arm to the goal point, the 3D deviation ΔX , ΔY and ΔZ is (-10, 20, 55) (see Table 1). Similar to this, when we have the point "b", then locations in camera A and B are (-5, 6) and (3, 8) respectively, corresponding 3D moving quantity is (30, 35, 45). Using this method, we can obtain the 3D deviation via the database.

If the cameras are equipped with the robot arm and move with the robot arm, the system is called hand-eye system. The cameras have to always catch the tip of the robot arm. We set up the camera position to satisfy this condition. As a result, the robot arm can move without loss of operability of the hand-eye system [10].

The 2D coordinate (0, 0) in the two cameras denotes the robot arm tip, and it is the original point on the display, and this relation of the cameras and the robot arm tip does not change, even if the robot moves.

III. DATABASE FOR ROBOT CONTROL

First of all, we have to establish the proper database. At the initial stage, we do not know 3D moving quantities in the database. Fig. 3 shows two cameras images. d_1 and d_2 is distance on a straight line between the tip of the robot and its object on two camera images. The sum of the distance D is

TABLE I. DATABASE

		Camera A		Camera B		Deviation
		x	y	x	y	$(\Delta X, \Delta Y, \Delta Z)$
...	
a point		1	8	-3	6	(-10, 20, 55)
b point		-5	6	3	8	(30, 35, 45)
...	

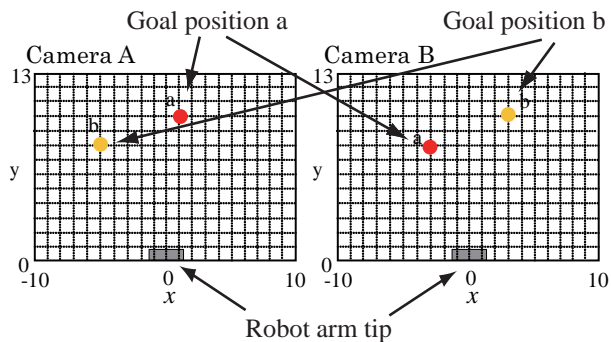


Figure 2. 2D images from two cameras.

a clue if the tip arrives at the target.

$$J(\mathbf{w}_t) = D = d_1 + d_2 \quad (1)$$

If the evaluation D is 0, the tip of the robot arm has arrived at the goal point. Then we can find out how the tip has to move. Memorizing the moving deviation for different positions of the goal, we can establish the database.

We can find the moving quantity for a target position by trial and error. That is, moving the tip of the arm randomly may give the optimal moving quantity by chance. However, this method is extremely ineffective and actually difficult to realize. Then we adopt a distance optimization using the simultaneous perturbation method.

The simultaneous perturbation optimization method was introduced by J. C. Spall [11], [12]. J. Alespector et al. [13] and G. Cauwenberghs [14] describe the same method. Y. Maeda also independently proposed a learning rule using the simultaneous perturbation and reported a feasibility of the learning rule for neural networks [15], [16], [17]. At the same time, the merit of the learning rule was demonstrated in the implementation of neural networks [18], [19], [20], [21]. Convergence conditions of the method in framework of the stochastic approximation is also described [22].

We consider a simple optimization problem. We would like to find a minimum point of a function $J(\mathbf{w})$ with the parameter \mathbf{w} . The simultaneous perturbation recursion using sign vector is described as follows [17], [18], [20], [21];

$$\mathbf{w}_{t+1} = \mathbf{w}_t + \Delta \mathbf{w}_t \quad (2)$$

$$\Delta \mathbf{w}_t = -\alpha \frac{J(\mathbf{w}_t + c\mathbf{s}_t) - J(\mathbf{w}_t)}{c} \mathbf{s}_t \quad (3)$$

Where, $\mathbf{w}_t \in \mathcal{R}^n$ and $\Delta \mathbf{w}_t$ are an adjustable parameter vector and its modifying quantity at the t -th iteration. $c(> 0)$

is a perturbation. s_t is a sign vector whose elements are +1 or -1.

The simultaneous perturbation estimates gradient of the function J using a kind of finite difference, effectively. The most important advantage of the simultaneous perturbation method is its simplicity. The simultaneous perturbation can estimate the gradient of a function using only the two values of the function. Therefore, it is relatively easy to implement for many optimization problems. Moreover even if the function is not differentiable partly, we can apply the method. In our research, we applied the simultaneous perturbation method to obtain optimal value of moving quantity of the robot arm.

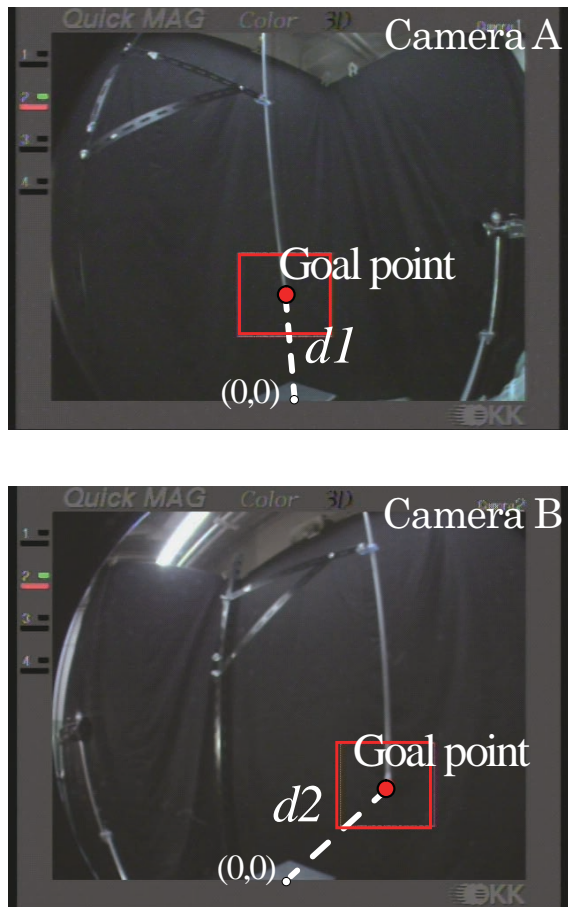


Figure 3. Two camera images.

Now, we explain details of the distance optimization control via the simultaneous perturbation. Fig. 4 shows the flowchart of the distance optimization control via the simultaneous perturbation.

At first, we set a value of learning coefficient α , perturbation c and the other as an initial setting. After the setting, we obtain image data from the two cameras and have the evaluation $J(w_t)$. Where $w_t=(x_t, y_t, z_t)$ denotes 3D position of the tip in the robot coordinate at the t -th time. $J(w_t)$ is the evaluation function defined by (1).

After that, we add the perturbation to the tip of the robot arm. That is, the tip moves by the perturbation $c s_t$. s_t denotes

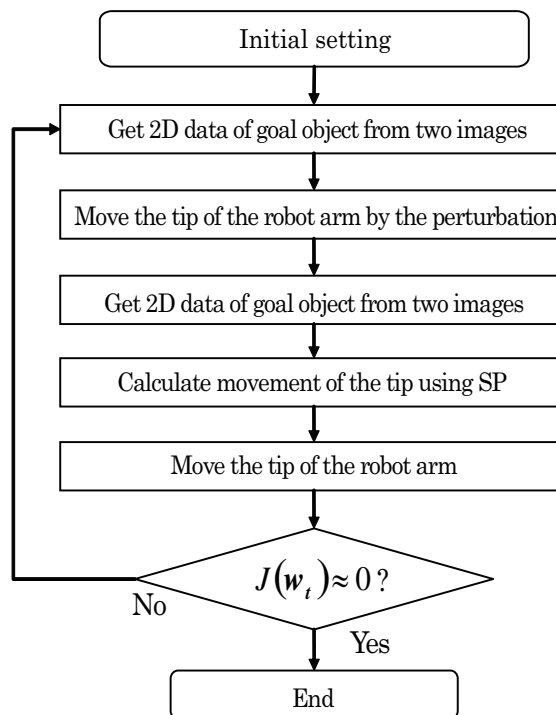


Figure 4. Distance optimization control via simultaneous perturbation.

the 3D sign vector whose elements are +1 or -1, and c is a scalar perturbation. Therefore the perturbation vector $c s_t$ takes value of $+c$ or $-c$ and the sign is decided randomly.

Afterward we obtain image data again and have the evaluation $J(w_t + c s_t)$. Then we can estimate a gradient of the evaluation function based on two values of the evaluation functions with the perturbation and without the perturbation. This corresponds to the first term of the right hand side of (4). Then we calculate a quantity of movement q_t of the robot arm as follows;

$$q_t = -\alpha \frac{J(w_t + c s_t) - J(w_t)}{c} s_t - c s_t \quad (4)$$

The robot arm moved by $c s_t$ from the position w_t in order to obtain the perturbed evaluation $J(w_t + c s_t)$. The second term of the right hand side of the above equation $-c s_t$ is for compensation of the perturbed procedure.

The tip of the robot arm moves according to the quantity calculated by (4). At last, we observe evaluation function after the movement.

When the evaluation function $J(w_t)$ is minimized in this observation, in other words, when $J(w_t)$ is in the neighborhood of 0, the tip of the robot arm arrived at goal point. If the evaluation function is still large, we repeat this process until the evaluation function converges to 0.

Obtained moving deviation is memorized in the database. Repeating the series of procedure for different positions of the target establishes the proper database.

IV. EXPERIMENTAL SYSTEM

A. Experiment equipments

Fig. 5 shows the experimental system in this study. The robot arm PA-10 (Mitsubishi Heavy Industry) is a control object in this system. The tip of the robot arm has a metal plate in Fig. 6. The controller consists of a servo driver, a personal computer (PC) and an image processing equipment (Quick MAG). Two CCD cameras that are equipped on the robot arm take images of color marker of the target. Quick MAG produces 2D coordinate data of the color marker of two image data. The data is sent to PC, and it calculates quantity of movement of the robot arm based on the proposed scheme. Servo driver receives the calculated value and converts it into an actuating signal of the robot arm. The robot arm tip moves to a certain direction of the robot coordinate by the signal.

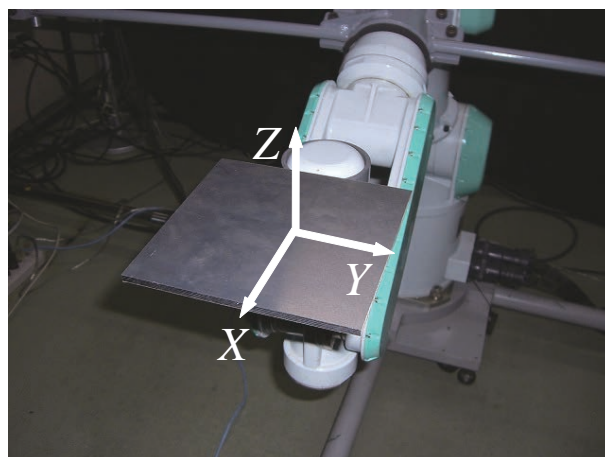


Figure 6. Tip of the robot arm.

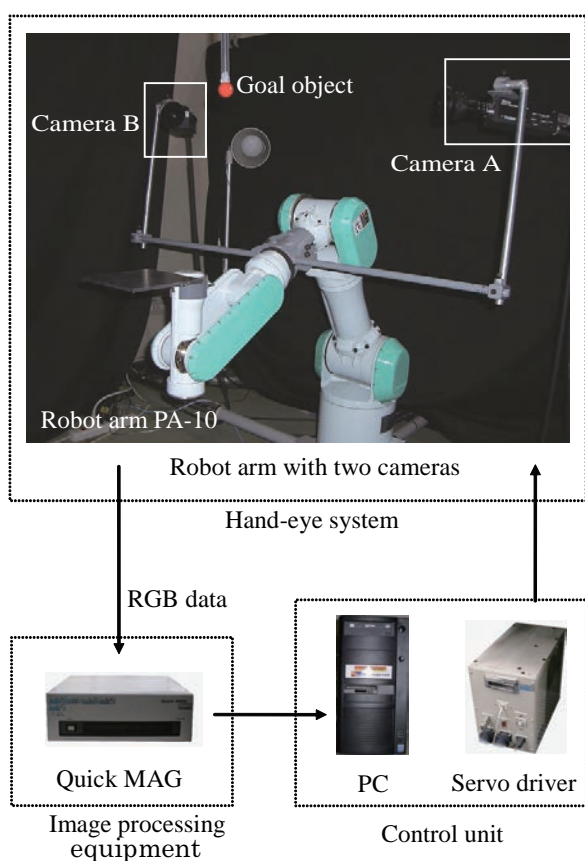


Figure 5. Calibration-free robot system.

This system uses only 2D image data to calculate quantity of movement of the robot arm without 3D calibration. In this sense, this system is a calibration free robot system.

B. Establishment of database via simultaneous perturbation

Fig. 7 shows the flowchart of a process to establish the database. By this process, the robot arm moves and the database is also redeemed for every movement.

In this operation, there are three movement patterns. If there is a datum for a goal position in the database, then the robot

arm obtains 3D quantity of deviation from the database. The tip of the robot arm can move quickly to the goal point. Then the database does not modified.

If the database does not contain a datum for the goal position, the system searches data in the search area, that is, the neighbor area(see Fig. 8). If there is a datum in the search area, then the robot arm can obtain 3D quantity of deviation for a neighborhood position and moves to the neighborhood point.

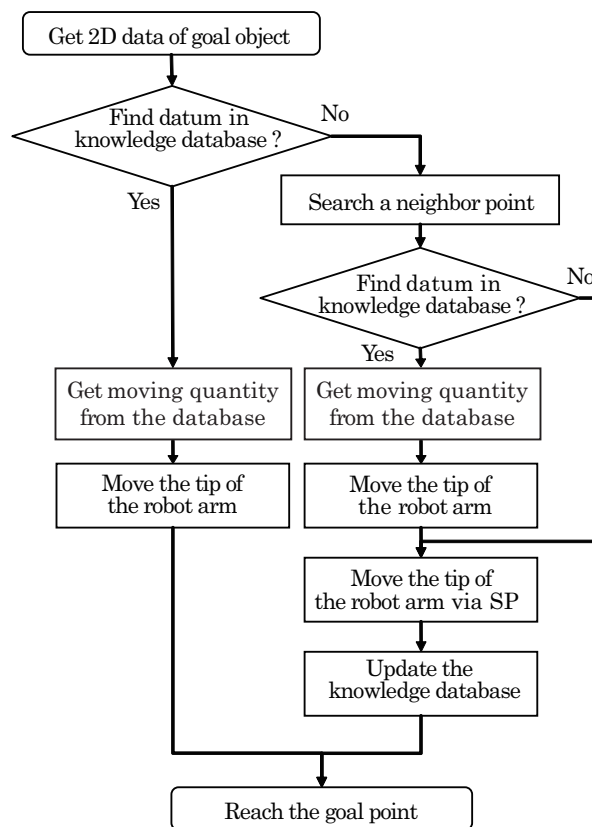


Figure 7. Flowchart of establishing database.

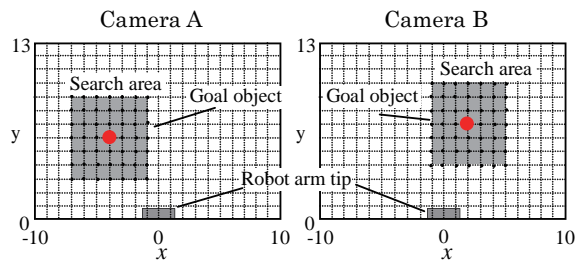
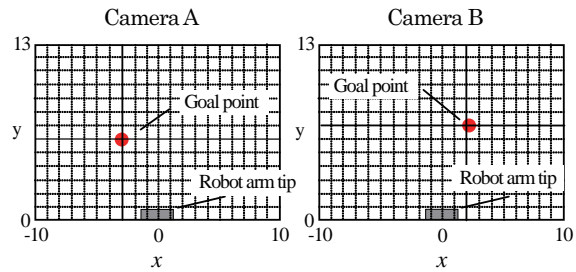
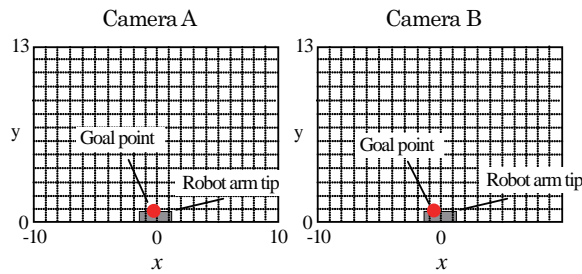


Figure 8. Search of the neighbor area.



Camera A		Camera B		Robot arm
x	y	x	y	($\Delta X, \Delta Y, \Delta Z$)
-3	6	2	7	No data

(a) Before update



Camera A		Camera B		Robot arm
x	y	x	y	($\Delta X, \Delta Y, \Delta Z$)
-3	6	2	7	(-25,30,75)

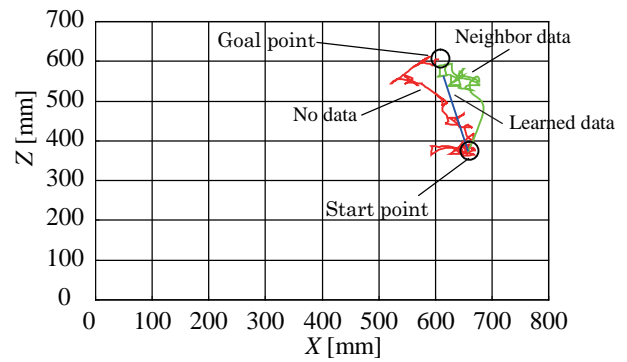
(b) After update

Figure 9. Update of the database.

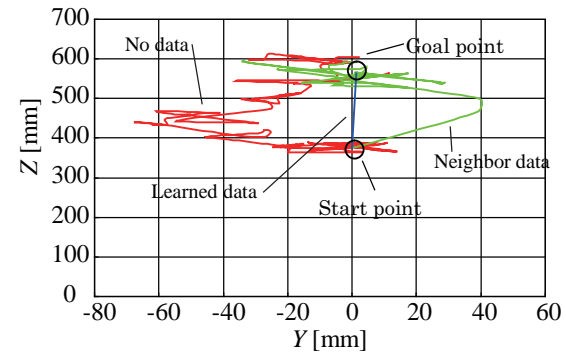
After the movement, the robot arm searches the goal object by the distance optimization control via the simultaneous perturbation. As the robot arm can obtain 3D quantity of the deviation from the initial point to the goal point, the database is updated(see Fig. 9).

Provided that there is no datum in the neighborhood area for the goal position, the robot arm searches the goal object by the distance optimization control via the simultaneous perturbation from the beginning. When the arm arrived at the goal, we updates the database(see Fig. 9).

Totally, the database is effectively established. That is, we can construct the precise database through this procedure. The database contains about 1000 data. Especially, main area is



(a) X-Z plane



(b) Y-Z plane

Figure 10. Locus of the robot arm.

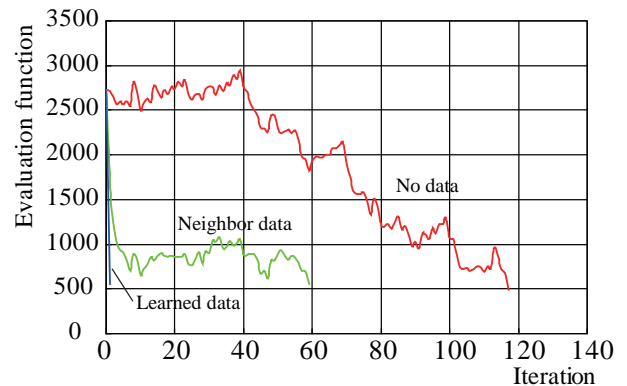


Figure 11. Change of evaluation function.

covered by these data.

Fig. 10 shows loci of the arm tip on Robot X-Y plane and Y-Z plane for this process. Notice that the locus of the robot arm tip moves to the goal object quickly, provided that there is a datum in the database(see blue line in Fig. 10). If the database does not have corresponding datum and has data for neighbor area, the arm moves to the nearest point first and moves to the goal point from the point by the simultaneous perturbation method. Therefore, the robot arm moves to a certain position first as straight as a line, then the distance optimization process is carried out(see green line in Fig. 10). If the database has no

datum, the arm tip moves to the goal point from start point using the distance optimization(see red line in Fig. 10).

The more the system moves, the more the accuracy of the database increases. The robot arm becomes to move quickly based on the database(see Fig. 11).

Fig. 11 shows typical changes of the evaluation function. If there exists a datum in the database, the robot can move to the objective position immediately, that is, the evaluation is zero at this moment. If there exists a datum in neighbor area, value of the evaluation started a certain value and decreases gradually. If there is no datum, the evaluation function decreases via the distance optimization gradually. We set that end condition for the evaluation function is 500.

V. MOVING TASKS FOR REAL-TIME CONTROL

In order to confirm feasibility of the proposed control scheme, we tried real time robot control task. The task is that the tip of the robot arm attached a white marker pursue a target red ball. The system controls the robot with $c = 30$, $\alpha = 2.0$.

The system is monitoring the target object constantly. If the database contains a datum for the present position of the target, the robot arm moves to the target position using deviation in the database. Since we have enough data around assumed space, the system works well.

It is interesting that real-time robot control is carried out using the database approach.

VI. CONCLUSION

Calibration is crucial but troublesome for robot control only using visual information. In this paper, we propose a calibration free robot control system using 2D camera images via a database. Moreover, we described a method to construct a proper database effectively. This scheme is unsuitable for precise robot control. However, it is relatively easy for rough control. We confirmed feasibility and effectiveness of the proposed real-time control scheme for the hand-eye robot system through moving task.

ACKNOWLEDGMENT

This work is financially supported by Grant-in-Aid for Scientific Research (No.23500290) of the Ministry of Education, Culture, Sports, Science and Technology(MEXT) of Japan, and Nonverbal Communication Technology and Media Information Communication Technology Research group of ORDIST, Kansai University.

REFERENCES

- [1] E. Kiyak and F. Caliskan, "Design of Fault Tolerant Flight Control System," WSEAS Transactions on Systems and Control, 5, 2010, pp. 454 – 463.
- [2] K. Hashimoto, T. Ebine, and H. Kimura, "Visual servoing with hand-eye manipulator-optimal control approach," IEEE Transactions on Robotics and Automation, 12, 1996, pp.766 – 774.
- [3] G.D. Hager, Wen-Chung Chang, and A.S. Morse, "Robot hand-eye coordination based on stereo vision," IEEE Control Systems, 15, 1995, pp.30 – 39.
- [4] G.D. Hager, "A modular system for robust positioning using feedback from stereo vision," IEEE Transactions on Robotics and Automation, 13, 1997, pp.582 – 595.

- [5] Sang De Ma, "A self-calibration technique for active vision systems," IEEE Transactions on Robotics and Automation, 12, 1996, pp.114 – 120.
- [6] J.A. Piepmeier and H. Lipkin, "Uncalibrated Eye-in-Hand Visual Servoing," The International Journal of Robotics Research, 22, 2003, pp.805–819.
- [7] Q. Xie, V. Graefe, and K. Vollmann, "Using a Knowledge Base in Manipulator Control by Calibration-Free Stereo Vision," IEEE International Conference on Intelligent Processing System, 1997, pp.1307–1311.
- [8] V. Graefe and A. Maryniak, "The Sensor-Control Jacobian as a Basis for Controlling Calibration-Free Robots," IEEE International Symposium on Industrial Electronics, 1998, pp.420–425.
- [9] A. Satou, Computer vision - Geometry of sight -, Corona publishing, 1999 (in Japanese).
- [10] S. Matsuda and Y. Maeda, "Hand-eye System Via Knowledge Base Using Image Data," Proceedings of 2006 International Symposium on Flexible Automation, 2006, pp.942–945.
- [11] J.C. Spall, "A stochastic approximation technique for generating maximum likelihood parameter estimates," Proceedings of the 1987 American Control Conference, 1987, pp. 1161–1167.
- [12] J.C. Spall, "Multivariable stochastic approximation using a simultaneous perturbation gradient approximation," IEEE Transactions on Automatic Control, 37, 1992, pp.332–341.
- [13] J. Alespector, R. Meir, B. Yuhua, A. Jayakumar, and D. Lippe, "A parallel gradient descent method for learning in analog VLSI neural networks," in: S. Hanson, J. Cowan, C. Lee (Eds.), Advances in neural information processing systems, Vol. 5, Morgan Kaufmann Publisher, Cambridge, MA, 1993, pp. 836–844.
- [14] G. Cauwenberghs, "A fast stochastic error-descent algorithm for supervised learning and optimization," in: S.J.Hanson, J.D.Cowan, C. Lee (Eds.), Advances in neural information processing systems, Vol. 5, Morgan Kaufmann Publisher, Cambridge, MA, 1993, pp. 244–251.
- [15] Y. Maeda and Y. Kanata, "A learning rule of neural networks for neuro-controller," Proceedings of the 1995 World Congress of Neural Networks, 2, 1995, pp.402–405.
- [16] Y. Maeda and R.J.P.de Figueiredo, "Learning rules for neuro-controller via simultaneous perturbation," IEEE Transaction on Neural Networks, 8, 1997, pp.1119–1130.
- [17] Y. Maeda, Y. Fukuda, and T. Matsuoka, "Pulse Density Recurrent Neural Network Systems with Learning Capability Using FPGA," WSEAS Transactions on Circuits and Systems, 7, 2008, pp.321–330.
- [18] Y. Maeda, H. Hirano, and Y. Kanata, "A learning rule of neural networks via simultaneous perturbation and its hardware implementation," Neural Networks, 8, 1995, pp.251–259.
- [19] G. Cauwenberghs, "An analog VLSI recurrent neural network learning a continuous-time trajectory," IEEE Transactions on Neural Networks, 7, 1996, pp.346–361.
- [20] Y. Maeda, A. Nakazawa, and Y. Kanata, "Hardware implementation of a pulse density neural network using simultaneous perturbation learning rule," Analog Integrated Circuits and Signal Processing, 18, 1999, pp.153–162.
- [21] Y. Maeda and T. Tada, "FPGA implementation of a pulse density neural network with learning ability using simultaneous perturbation," IEEE Transactions on Neural Networks, 14, 2003, pp.688–695.
- [22] J.C.Spall, Introduction to Stochastic Search and Optimization, John Wiley & Sons, Inc., 2003.

Incorporating Online Process Mining Based on Context Awareness into Human-Robot-Cooperation Framework

Stephan Puls, Benjamin Lotspeich, and Heinz Wörn

Institute of Process Control and Robotics (IPR)

Karlsruhe Institute of Technology (KIT)

Karlsruhe, Germany

{puls, lotspeich, woern}@ira.uka.de

Abstract—The framework, in which this work is embedded, focuses on the cooperation of humans and robots in productive scenarios. Based on action recognition and situation awareness, conclusions about human behavior can be drawn. The presented work utilizes an online process mining method based on the Heuristic Miner in order to identify a process model regarding context and recognized actions. The process model represents temporal and spatial dependencies of events and is used for detecting recurring behavior sequences.

Keywords – cognitive robotics; online process mining; heuristic miner; ambient intelligence; context awareness; situation and action recognition; human-robot-cooperation.

I. INTRODUCTION

Assistance through technology can be found in many areas of daily living. Nowadays, many, mostly trivial, work processes are conducted by machinery and robots. Due to their strength, dependability and accuracy, there is a wide variety of uses for robots. Nevertheless, human labor is still more flexible, dynamic and robust due to cognitive abilities to identify processes and errors and react accordingly. Bringing these strengths together in human and robot cooperation is an important research field.

Industrial robotics is a challenging domain for cognitive systems, especially when close interactions between solid machinery and human intelligence is wanted. We are conducting research on recognition of and reasoning about human actions, situations and spatio-temporal context in a human centered productive environment, in order to enable interactive and cooperative scenarios. For this purpose a framework for human-robot-cooperation (MAROCO) was introduced [1, 2], in which human pose reconstruction and context awareness is achieved (see Fig. 1).

This paper focuses on using this extracted information for online process mining based on the Heuristic Miner [3]. Process mining aims at extracting knowledge from event logs consisting of process events and their respective temporal order. Thus, the framework is extended by identifying a sequence model of performed human actions and detecting recurring sequences.

The remainder of this paper is organized as follows. In Section II, some related research work on process mining and sequence detection will be presented. In Section III, the framework will be introduced, which enables the sensor data processing and subsequent knowledge based reasoning. Also

the modeled situations, activities and context are explained. In Section IV, the Heuristic Miner will be briefly introduced and the module realizing the online process mining will be presented in detail. Section V discusses experimental results which have been carried out for both, predetermined test cases and under real-life conditions. In Section VI, a summary is given. Finally, some hints for future work are also mentioned.

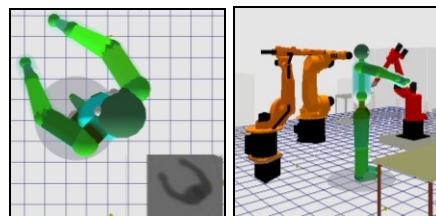


Figure 1. Human kinematics reconstruction based on depth information from time-of-flight camera (left) and the overall scene (right).

II. RELATED WORKS

For identifying work sequences in complex processes, patterns of variable length need to be recognized in a time series of discrete state variations. Many fundamental methods in the area of artificial intelligence are devised to recognize sequences. In this context, Sun and Giles distinguish between recognition and detection of patterns and present some possible solutions [4].

One such solution can be inductive logical programming (ILP). In [5], ILP is used learn and recognize symbols. Based on positive and negative examples, rules are learned, which enable a subsequent classification of images.

In [6], temporal logics are used to detect frequent patterns in temporal databases by using temporal operators and constructing temporal logic programs. These programs were specific to the pattern and the overall system performance was argued to be too slow for practical applications by the authors.

Hidden Markov Models (HMMs) are a widely used means for learning and recognizing temporal patterns (e.g., [7, 8, 9]). For detecting unknown patterns this method cannot be used, due to its supervised learning strategy. That is also the case for the above mentioned procedures. On the contrary, discovering unknown patterns in a time series is an unsupervised task. In [10], an approach is presented which

uses HMMs for the pattern discovery task. The length of the patterns and structure of the HMMs has to be known a priori, which modifies the task of discovery of unknown patterns to a distinguishing task of similar patterns.

The research field of process mining (PM) wants to extract knowledge from event logs, which are comprised of process events including their temporal order. PM is mainly used to identify and optimize business processes. Different methods have been devised to identify processes, their internal structure and to model them in so called Workflow-Nets [11, 12].

The Alpha-Algorithm is one of the first developed methods for process modeling [13]. It models temporal relationships of events based on their occurrence in the event log. In [14], it is shown that the Alpha-Algorithm is prone to incomplete or noisy event logs and produces erroneous process models. The Tsinghua-Alpha-Algorithm is a further development of the Alpha-Algorithm and takes the duration of activities into account and allows the modeling of parallelism [15]. It also requires complete and noise-free data logs [14].

The Heuristic Miner models a process based on frequency and order of events [3]. In contrast to the Alpha and Tsinghua-Alpha Algorithms, it can deal with noisy data sets, which is a prerequisite in sensor based cognitive systems, hence, its adoption in the research framework MAROCO (see Section IV).

The basic methods for process mining mentioned above are offline algorithms due to their main application in analyzing business processes. Thus, data logs are recorded over some period of time and analyzed afterwards. Accordingly, for the use of process mining in human-robot-cooperation scenarios the adaption to online data analysis is necessary.

III. THE MAROCO FRAMEWORK

The process mining presented in this paper is embedded into a general human robot cooperation software framework. In this section, an overview of the framework is given. Also, the generated information, which is processed during mining, is presented.

A. Overview

In our previous research a framework for human-robot-cooperation (MAROCO) was developed [1]. The goal is to realize a comprehensive cognition cycle, which consists of (1) sensing, (2) cognition, and (3) acting. The sensing is done by a photon mixer device (PMD) camera, which captures directly a 3D point cloud of the scene. Through 3D image sequence analysis the work space of an industrial robot is observed and the kinematics of a human worker is reconstructed (see Fig. 1).

The reconstruction of the human kinematics is based purely on depth image analysis and does not require markers attached to the human agent [16]. During the process of reconstruction many parameters of the human kinematics are estimated, e.g., head orientation, upper body orientation, arm configurations, etc. Due to the position of the camera above

the work cell some parameters, like leg configurations, cannot be identified.

The camera fixation at the ceiling is mandatory in respect to safety concerns. Dirt, which is inevitable in a production environment, is less prone to stick to the lens system of the camera. Furthermore, manipulation of the camera position is difficult to achieve. Thus, its calibration in the environment is constant. Also, occlusions of the human through movement of the robots and production materials are avoided.

In order to achieve seamless interaction and an intuitive human-machine interface an activity recognition and situation awareness system based on the combination of HMMs and Description Logics (DLs) was implemented [2, 17]. Fast action recognition is implemented based on HMMs, whereas higher cognitive reasoning about situations and activities is accomplished with the slower DL-based reasoning system. Also, due to the sensing of the human kinematics in the scene, a localization module identifies the current semantic position of the human co-worker in the scene. The overall system regarding action recognition and situation awareness is depicted in Fig. 2.

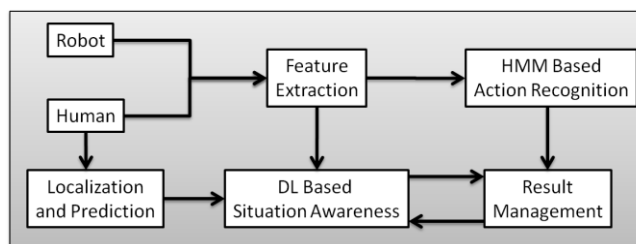


Figure 2. System overview of the different components involved regarding action recognition and situation awareness.

B. Actions, Places, and Situations

The generated information from the scene analysis is used as input for the online process mining. So far, there are 33 modeled activities and actions, 9 modeled situations and 5 different places. Some examples are shown in Table I.

For the process mining, each occurring action, situation or place information is handled as an event.

Based on the behavior of the human co-worker different events and combinations thereof are recognized and made available through the result management module (see Fig. 2).

TABLE I. EXAMPLES FOR MODELED ACTIONS, PLACES, AND SITUATIONS

Actions and Activities	Places	Situations
Taking Tool	Cooperative Workplace A/B	Monitoring
Putting Tool Away	Manual Workplace C	Distraction
Sitting	Outside of Working Area	Communication
Crouching	Place in Between	Cooperation
Walking		Partially Attentive

IV. THE PROCESS MINING MODULE

This section is dedicated to discuss the online process mining module incorporated into the framework after a very short introduction to the underlying Heuristic Miner.

A. Heuristic Miner

The Heuristic Miner analyses a data log based on frequency and order of occurring events. Thus, temporal relations and dependencies are modeled depending on how often events occur after one another (see Fig.3).

According to [3], different temporal relations can be distinguished:

- $A > B$ – Event B is direct successor of A,
- $A \rightarrow B$ – Event A comes generally before B,
- $A >> B$ – There is a cycle of the form A-B-A,
- $A >>> B$ – Marks *long-distance-dependencies*.

The norm, given as $|\cdot|$, marks the number of instances that conform to the specified relation.

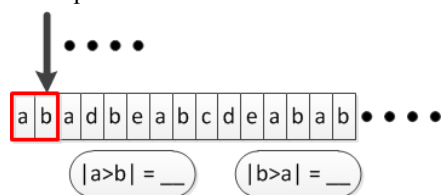


Figure 3. Frequency and temporal order analysis of occurring events.

Using these relations a dependency-graph is extracted. For each relation and combination of event pairs a coefficient based on the data log L is computed, for example:

$$a \Rightarrow b = \frac{|a >_L b| - |b >_L a|}{|a >_L b| + |b >_L a| + 1} \quad (1)$$

$$a \Rightarrow_2 b = \frac{|a >>_L b| + |b >>_L a|}{|a >>_L b| + |b >>_L a| + 1} \quad (2)$$

The value of the coefficient, similarly to a correlation coefficient, is in the interval $[-1, 1]$, where 1 shows complete direct dependency and -1 complete inverse dependency. Using a threshold for the coefficient, the dependency-graph can be determined.

The advantage of this method is that a small amount of noise does not lead to significant changes in the process model. The role and influence of noise is closely examined in Section V.

In [3], the information of the dependency-graph is augmented by further analyzing different parameters in order to identify causal dependencies, which are modeled in a *Causal Net*. In the here presented work, only temporal dependency is assumed for occurring events. Thus, necessary computations to identify a causal net are left aside.

B. The Online Mining Module

The recognition and situation awareness results are stored as a triple: (Timestamp, Descriptor, Class). The descriptor is a string containing the identifier of the event, e.g., "Taking Tool". The class value represents if the event is an action,

situation, location, etc. Based on the timestamp, the temporal order can be defined.

In order to accelerate computations during comparisons of events, a look-up table is defined to map descriptors onto integer identifiers. This mapping is done bidirectional before invocation of the mining algorithm and afterwards.

Also, the isolated analysis or combination of different event classes leads to either one-dimensional or multi-dimensional data logs. For the online analysis three different sets of event classes are considered:

- Actions alone,
- Actions and situations,
- Actions in combination with their occurring location.

The first two sets are considered one-dimensional, due to their subsequent occurrences. The third set is two-dimensional because actions are related to locations. Thus, the same action can occur at different places and the combination can characterize a sequence.

Another adaptation lies in the amount of analyzed data. It is not wanted to collect an event log of a week or day and perform process mining afterwards. Thus, a smaller amount of data needs to be accumulated. The actual number of logged events is dependent on the complexity of the process and can influence the process model significantly, which is shown in Section V.

The presented approach uses a sliding window to extract a current log from the history of recorded events. Events that are too old are discarded from the history. Also, if the event log is large enough the Heuristic Miner is triggered to analyze the new data. Afterwards, part of the event log is freed-up to allow accumulation of new events (see Fig. 4).

The mining algorithm is running in its separate thread in parallel to the overall framework. Thus, new events can be recognized and the event log buffer can be filled.

It would also be possible to invoke the mining algorithm with each new event but the computation load would increase drastically. Hence, the buffered approach is incorporated into this work. Details on runtime are presented in Section V.

In Fig. 5, an example of a process model is depicted. The visualization is done with the software library GraphViz. In order to reduce the complexity of the process model graph a graph-cycle search is used to extend the mining algorithm. As can be seen in Fig. 6, the extracted cycles ease the examination of the overall process model. This enables subsequent process analysis, e.g., for detecting production faults or inefficiencies.

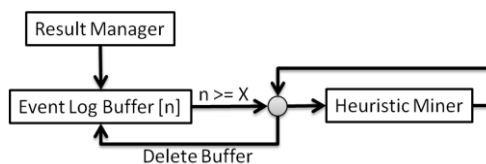


Figure 4. Online implementation of Heuristic Miner: Parallel to the framework the buffer is filled and subsequently analyzed.

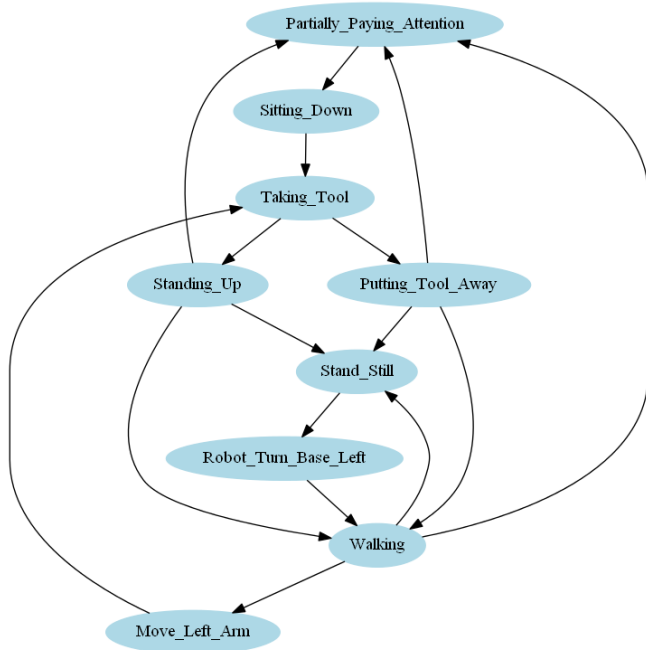


Figure 5. Example of a process model regarding recognized actions and activities only.

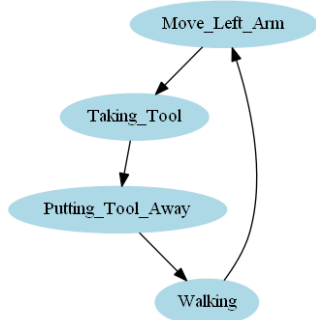


Figure 6. Example of extracted process cycle for better analysis of the overall process.

V. EXPERIMENTAL RESULTS

For experimental analysis of the online process mining module, different courses of actions were executed and results were recorded.

The evaluation was divided into two parts. Firstly, for analyzing different parameter influences efficiently means of automated event presetting were implemented. Secondly, actual recognition results based on sensor data processing were used during online execution to determine online behavior of the mining module. Thus, sensor noise resulting in recognition errors influences the mining procedure.

In Fig. 7, the overall setup of the working area is depicted, which is used throughout the experimental evaluation of the mining module. The figure shows the different work places, the reconstructed human kinematics

and the robot. As mentioned in Section III.B the robots' movements and actions are not included into the event log.

In this section, analyzed parameters and mining result are illustrated and discussed.

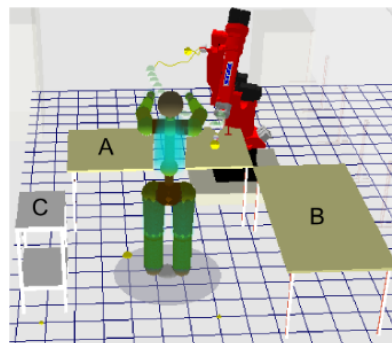


Figure 7. The overall setup of the working area.

A. Quality Criterion

For benchmarking the mining results a quality criterion was devised. Based on the comparison of mining results and expected outcome it tries to answer the following questions:

- Are the correct transitions identified?
- Are there too many nodes identified?
- Are all correct nodes identified?

Thus, the overall criterion Q is assessed by three different criteria:

$$C_1 = \frac{\text{Correct Number of Transitions}}{\text{Number of Found Transitions}} \Rightarrow Q_1 = |C_1 - 1|$$

$$C_2 = \frac{\text{Number of Correctly Identified Nodes}}{\text{Number of Identified Nodes}} \Rightarrow Q_2 = |C_2 - 1|$$

$$C_3 = \frac{\text{Number of Correctly Identified Nodes}}{\text{Correct Number of Nodes}} \Rightarrow Q_3 = |C_3 - 1|$$

$$\Rightarrow Q = \max(Q_1, Q_2, Q_3) \quad (3)$$

Using the maximum of the separate criteria defines the value which influences the outcome most negatively. Thus, a Q value of 0 is defined to be optimal.

B. Analysis Based on Synthetic Data

For efficiently analyzing different parameters a set of cyclic event log presets were defined. They included different courses of actions in different situations and at different places. Depending on the analyzed parameter, these presets could be tested in an isolated manner or in arbitrary combination.

The following parameters were evaluated using synthetic event logs:

- Number of different cycles in the event log,
- Length of the cycles,
- Influence of noise in the event log,
- Number of events in the event log buffer.

The variation of the number of different cycles in the event log resulted in a more complex process model. As expected, the value of the quality criterion stayed optimal. The same effect is also true for the variation of cycle lengths.

Robustness against noise is an important property when dealing with sensor based systems. For evaluation purposes, noise was added to the defined event log presets in two ways: (1) addition of random events after a complete event cycle, marked as R_1 , and (2) addition of a random event in a cycle, marked as R_2 . These two noise processes were also analyzed in combination. In Table II, results are presented. When using a combined noise ratio of 13% or greater the quality of the identification of temporal relations is insufficient. Also, the noise R_2 has generally a lower impact on the quality of the process model.

When considering an online process mining, it is important to know how much data needs to be processed. In Table III, results are shown for varying the event log buffer size regarding noisy event logs. Thus, using a buffer size of about 800 event entries yields acceptable results. Due to the greater influence of R_1 the impact of R_2 is discarded.

TABLE II. VARIATION OF ADDITIONAL NOISE. THE QUALITY CRITERION WAS EVALUATED FOR DIFFERENT NOISE VALUES.

$R_2 \setminus R_1$	0%	3%	5%	8%	12%	20%
0%	0	0.05	0.12	0.19	x	x
3%	0	0.12	0.19	0.12	x	x
5%	0.05	0.05	0.12	x	x	x
8%	0.05	0.12	x	0.26	x	x
12%	x	x	x	x	0.26	x
20%	x	x	x	x	x	0.46

TABLE III. VARIATION OF EVENT LOG BUFFER SIZE. THE QUALITY CRITERION WAS EVALUATED FOR DIFFERENT SIZES AND NOISE VALUES.

$R_1 \mid R_2 \setminus$ Buffer Size	100	200	400	800
0% 0%	8.5	0.72	0.35	0
3% 0%	8.5	0.72	0.58	0.19
5% 0%	8.5	0.9	0.9	0.19

C. Analysis Based on Sensor Data Processing

For experimental analysis using actual recognition results from sensor data processing different courses of action were defined (see Fig. 8). Different scenarios of differing complexity were used. Also, each scenario consists of sequences of varying complexity. Moreover, to simulate process faults and unexpected events, deliberately executed defined actions were introduced into the scenarios at random time (see Fig. 8 bottom row).

The result of the process mining for the second sequence of the second scenario (see Fig. 8 middle column and row) is shown in Fig. 9. The overall structure of the sequence is clearly visible and well captured.

Similar to synthetic event logs, the size of the event log buffer is of interest. In contrast, the buffer size resulting in best quality criterion is 400 log entries (see Table IV).

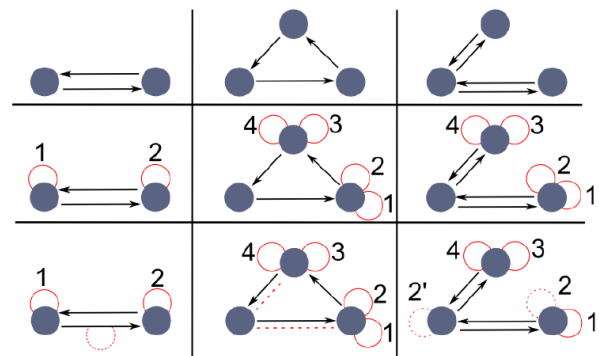


Figure 8. Different courses of action. Each column depicts a scenario, which is extended with each row. Full dots represent places, black arrows place changes, red circles actions, and dotted red lines deliberately executed noise.

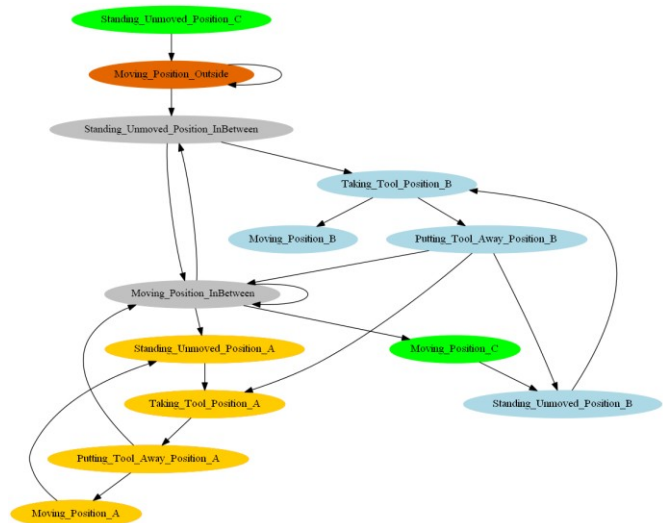


Figure 9. Identified process model of the second sequence of the second scenario. Different colors represent different places: Yellow – A, Blue – B, Green – C, Grey – In Between, and Red – Outside.

TABLE IV. VARIATION OF EVENT LOG BUFFER SIZE. THE QUALITY CRITERION WAS EVALUATED FOR DIFFERENT SIZES AND SCENARIOS.

Scenario \ Buffer Size	100	200	400	800	1200
1 2	4	0.5	0.29	0.29	0.4
4 3 2 1	x	4	0.25	0.55	0.63
4 3 2 1 (with noise)	x	1.5	0.2	0.42	0.47

Also of interest is the threshold for the dependency coefficient (see Section IV.A). In Table V, the corresponding results are presented listing the quality criterion for a buffer size of 400 event log entries. Q_1 represents the quality criterion for the first sequence and Q_2 of the second sequence of the second scenario. A threshold of 0.9 yields best results. This might change with varying complexity of the process but allows best results so far. Moreover, using a lower threshold allows for faster adaptation when the underlying process changes. Thus, using dynamic threshold adaption needs to be further investigated.

TABLE V. VARIATION OF COEFFICIENT THRESHOLD.

Threshold	0.85	0.875	0.9	0.925
Q_1	0.5	0.29	0.285	1
Q_2	0.55	0.36	0.25	0.43

The runtime behavior is another important characteristic for online processing methods. In Table VI, some results of the runtime measurements are shown. In tested scenarios, the needed computation time is well below one second. Thus, fast process mining is possible. Still, invocation of the mining with each new recognition result is not feasible so far. Considering that processes are not subject to change frequently and rapidly, this result is very promising.

TABLE VI. VARIATION OF COEFFICIENT THRESHOLD.

# Events	100-500	500-1000	1000-1500
Runtime [ms]	~ 300	~ 450	~ 650

VI. CONCLUSION

In this paper, an online process mining method was incorporated into a human-robot-cooperation framework. It is capable of identifying recurring event sequences, which consist of recognized actions, situations and locations.

Temporal relations of events are extracted and a process model is generated. In order to ease model analysis the mining algorithm is extended with a subsequent process cycle search. Thus, complex and unclear models are split into connected cyclic components.

The online mining method was experimentally evaluated regarding different parameters using defined event log presets and actual recognition results from sensor data processing. It was shown that the identified processes resemble the structure of the test scenarios. Also, a quality criterion was proposed for allowing comparison of different results.

The next steps will be the exploitation of the identified process model. Extracted cycles can be generalized and used for concept learning in the Description Logics based reasoning system. Thus, the foundation for action plan identification and recognition is laid.

The mining results are thus far only represented as dependency graphs. This does not allow for discrimination of major work cycles and processes that occur only eventually. There is further research needed to remedy that constraint.

Moreover, investigation of using an adaptive dynamic dependency coefficient threshold might allow faster adoption of changing work processes.

REFERENCES

- [1] S. Puls, J. Graf, and H. Wörn, "Cognitive Robotics in Industrial Environments," Human Machine Interaction – Getting Closer, InTech, I. Murtua(Ed.), Rijeka, Croatia, 2012, pp. 213-234.
- [2] S. Puls and H. Wörn, "Combining HMM-Based Continuous Human Action Recognition and Spatio-Temporal Reasoning for Augmented Situation Awareness," Proc. of Int. Conf. on Interfaces and Human Computer Interaction, 2012, pp. 133-140.
- [3] A.J.M.M. Weijters, W.M.P. van der Aalst, and A.K.A. de Medeiros, "Process mining with the Heuristics Miner algorithm," Report, Technische Universiteit Eindhoven, 2006.
- [4] R. Sun and C.L. Giles, "Sequence Learning: From Recognition and Prediction to Sequential Decision Making," IEEE Intelligent Systems, 16(4), 2001, pp. 67-70.
- [5] K.C. Santosh, B. Lamiroy, and J.-P. Ropers, "Inductive Logic Programming for Symbol Recognition," 10th Int. Conf. on Document Analysis and Recognition, 2009, pp. 1330-1334.
- [6] B. Padmanabhan and A. Tuzhilin, "Pattern Discovery in Temporal Databases: A Temporal Logic Approach," Proc. of the Int. Conf. on Knowledge Discovery and Data Mining (KDD), 1996, pp. 351-354.
- [7] F. Niu and M. Abdel-Mottaleb, "HMM-Based Segmentation and Recognition of Human Activities from Video Sequences," IEEE Int. Conf. on Multimedia and Expo, 2005, pp. 804-807.
- [8] J. Krajcovic, M. Hrncar, and L. Muzikarova, "Hidden Markov Models in Speech Recognition," Advances in Electrical and Electronic Engineering, 7(1-2), 2011.
- [9] N. Arica and F.T. Yarman-Vural, "An overview of character recognition focused on off-line handwriting," IEEE Trans. on Systems, Man, and Cybernetics, Part C: Applications and Reviews, 2001, pp. 216-233.
- [10] D. Chudova and P. Smyth, "Pattern discovery in sequences under a Markov assumption," Proc. of the 8th Int. Conference on Knowledge Discovery and Data Mining (KDD), 2002, pp. 143-162.
- [11] W.M.P. van der Aalst, "Process Mining – Discovery, Conformance and Enhancement of Business Processes," Springer, 2011.
- [12] W.M.P. van der Aalst, "Process Mining: Discovering and Improving Spaghetti and Lasagna Processes," IEEE Symposium on Computational Intelligence and Data Mining (CIDM), 2011, pp. 1-7.
- [13] W.M.P. van der Aalst, A.J.M.M. Weijters, and L. Maruster, "Workflow mining: discovering process models from event logs," IEEE Transactions on Knowledge and Data Engineering, 16(9), 2004, pp. 1128-1142.
- [14] M. Waimer, "Integration Adaptiver Prozess-Management-Technologie und Process Mining," Diploma Thesis, University Ulm, 2006.
- [15] L. Wen, J. Wang, W. van der Aalst, B. Huang, and J. Sun, "A novel approach for process mining based on event types," Journal of Intelligent Information Systems, 2009, pp.163-190.
- [16] J. Graf and H. Wörn, "Safe Human-Robot Interaction using 3D Sensor," Proc. of VDI Automation, 2009, pp. 1-12.
- [17] S. Puls, J. Graf, and H. Wörn, "Design and Evaluation of Description Logics based Recognition and Understanding of Situations and Activities for Safe Human-Robot Cooperation," International Journal on Advances in Intelligent Systems, Vol. 4, 2011, pp. 218-227.

Step Climbing and Descending for a Manual Wheelchair with a Network Care Robot

Hidetoshi Ikeda, Hikaru Kanda and Nobuyuki Yamashima
 Department of Mechanical Engineering
 Toyama National College of Technology (Hongou campus)
 13 Hongou-chou, Toyama-shi, Japan
 E-mail: ikedah@nc-toyama.ac.jp

Eiji Nakano
 Robofesta Org.
 Narashino-shi, Japan
 E-mail: nakanoeni@gmail.com

Abstract—Realization of step climbing or descending for a heavy cart or a wheelchair using human-friendly robot with manipulators is a technical issue. This paper describes cooperative step climbing and descending tactics for a manual wheelchair and a partner robot that is equipped with manipulators driven by small direct current motors. When the wheelchair and robot climb or descend a step, these vehicles are linked together by the robot hands, and some of the manipulator joints are allowed to move passively. Thus, the manipulators motors do not need to exert major torque to support the vehicles. The velocity differences between the two vehicles is used to pass over the step. When the wheelchair is climbing or descending, the upper links of the manipulators are pressed against the robot's chest to stabilize the wheelchair's movements. In addition, the forearm links of the robot are pressed against, or fixed to, the back of the wheelchair. The robot equipped with manipulators driven by small motors allows the wheelchair to overcome a step, and then the robot itself is able to overcome the step by using the wheelchair. In an experiment, we connected a teleoperation system for the robot through an intranet and confirmed that these vehicles could cooperatively climb and descend steps.

Keywords—step climbing; wheelchair; robot; cooperation

I. INTRODUCTION

Without a human assistant, most wheelchair users are not able to enter an area that has steps. Thus, they need a special wheelchair equipped with a step climbing or descending mechanism. Wheelchairs with such special mechanisms have been widely researched and include, for example, a wheelchair with additional legs [1], a wheelchair with multiple wheels [2] [3], a wheelchair with multiple wheels connected by active linkages [4], a wheelchair with an adjustable center of gravity [5], a wheelchair with a combination of an adjustable center of gravity and multiple wheels [6], a wheelchair with special wheels [7], and a tracked vehicle [8]. These mechanisms can provide the wheelchair with the ability to climb stairs or surmount other obstacles. The research group of the present report achieved cooperative step climbing of a wheelchair connected to a wheeled robot by passive links [9] and, separately, of a wheelchair and a wheeled robot with manipulators [10]. This report presents the step climbing and descending method for a wheelchair and a care robot having dual manipulators that allow the wheelchair user to overcome many of the obstacles encountered in daily life. Because most of the human-friendly robots that are used in homes or offices have small motors due to their limited body size, it is difficult for such robots to lift heavy vehicles. In addition, precisely controlling the axes'

angles of the manipulators according to the processes related to pushing and pulling, and in relation to the vehicle's incline is very difficult. In such cases slippage of driving wheels can occur or the vehicles can tip over. Thus, mobile robots with manipulators have not previously been used to assist heavy carts or wheelchairs in step climbing and descending. In the method used in this study, some of manipulator joints and the upper links or forearm links of manipulators press passively against the robot or wheelchair when these vehicles climb or descend a step. Thus, the motors do not need to exert major torque to support with vehicles.

The wheelchair users considered in the present study were assumed to have the upper-body capability of an able-bodied person. Based on preliminary measurements, the friction coefficients of the vehicles and the ground surface in this research were assumed to be in the range of 0.6 to 0.9, and the target step height was set at a maximum of 0.12 [m] (More than 80% of the observed step heights were lower than 0.12 [m]).

This paper is organized as follows. Section II describes the cooperative step-climbing system and Section III describes the step climbing and descending procedures. Section IV provides the theoretical analysis. Section V describes an experiment and presents the experimental results, and Section VI is the conclusion.

II. ROBOT AND WHEELCHAIR

The robot used in this research is the wheeled "Tateyama" developed in this laboratory (Figure 1). TABLE I lists the specifications. When passing over a step, the wheelchair and robot are deployed in a forward-and-aft configuration (Figure 2). This robot has three sets of wheels consisting of front, middle, and rear pairs on the left and right sides. The front and rear pairs are casters whose positions can be shifted, while the middle pair are the driving wheels. The robot has manipulators attached to the left and right sides of its upper half: each arm has 5 degrees of freedom (DOF) and each hand has 1 DOF for a total of 6 DOF (Figs. 1 and 3). In this study, the length from Joint 2 (shoulder) to Joint 4 (elbow) is called "Link 2" (length l_2), from Joint 4 (elbow) to Joint 5 (wrist) is called "Link 4" (length l_4), and from Joint 5 (wrist) to the tip of the hand is called "Link 6" (length l_6). The length from Joint 4 (elbow) to Joint 6 (the location of the connection between the wheelchair and the robot) is designated l_{4C} . The manipulator joint angles are -90 [deg] $\leq \phi_2 \leq +90$ [deg] and 0 [deg] $\leq \phi_4 \leq +100$

TABLE I. ROBOT SPECIFICATIONS.

Overall length	0.230–0.800 [m]
Overall height	0.747 [m]
Radius of front wheels (r_{Bf})	0.025 [m]
Radius of middle wheels (R_B)	0.145 [m]
Radius of rear wheels (r_{Br})	0.019 [m]
Wheelbase (WB_r)	0.190–0.440 [m]
Wheelbase (WB_f)	0.270 [m]
Mass position from the rear axes (l_{rB})	0.093 [m]
Height of the mass from the rear axes (h_{mB})	0.286 [m]
Position of Joint 2 from the rear axes (l_{LB})	0.090 [m]
Height of Joint 2 from the rear axes (h_{LB})	0.532 [m]
Mass of the robot body	55 [kg]
Mass of link 2 (from Joints 2 to 4)	2.55×2 [kg]
Mass of link 4 (from Joint 4 to hand)	0.8×2 [kg]
Length of link 2 (l_2)	0.330 [m]
Length of link 4 (l_4)	0.300 [m]
Length of the hand (l_6)	0.105 [m]
Length from Joint 4 to the connecting position (l_{4c})	0.370 [m]
Mass position of link 2 (L_2)	0.067 [m]
Mass position of link 4 (L_4)	0.169 [m]
Mass position of link 6 (hand mechanism) (L_6)	0.035 [m]

TABLE II. SPECIFICATIONS OF THE MANUAL WHEELCHAIR.

Overall length	1.060 [m]
Overall height	0.985 [m]
Radius of front wheels (r_A)	0.063 [m]
Radius of rear wheels (R_A)	0.300 [m]
Wheelbase (l_A)	0.430 [m]
Handrim position (l_{LA})	0.250 [m]
Mass position from the rear wheel axes (l_{rA})	0.149 [m]
Height of mass from rear wheel axes (h_{mA})	0.371 [m]
Mass (wheelchair + driver) (M_A)	92.7 [kg]

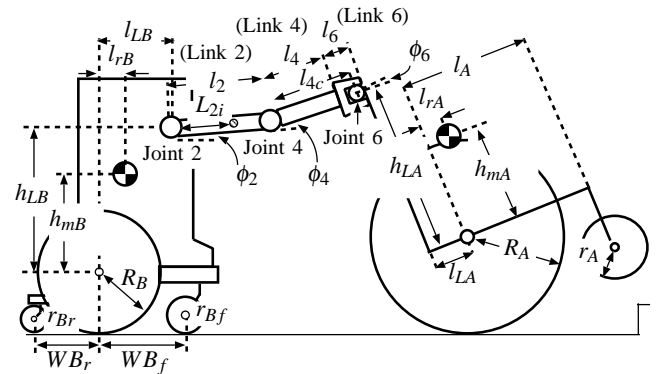


Figure 2. Model of the wheelchair and robot.

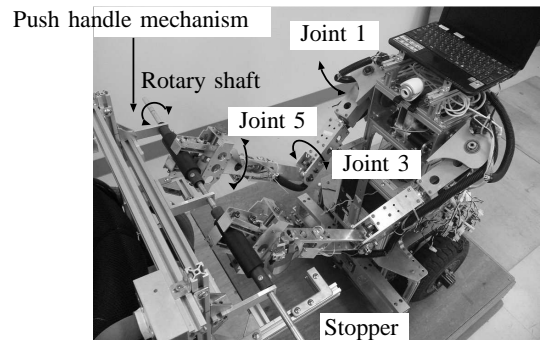


Figure 3. Push handle mechanism of the wheelchair.

[deg]. The hands consist of two fingers that open and close in order to grasp items (Figure 3). These axes and the hands are driven by small direct current (DC) motors (Joints 1, 2: 20 [W], Joints 3, 4: 6 [W], Joint 5: 2.5 [W], 1.5 [W]). The robot also has a stopper mounted on the front part of its body (Figs. 4 (a) and 5 (a)). The stopper limits the passive rotational travel of the robot manipulators and thus enables the robot to imitate the operation of a human pushing an object by limiting the passive rotation about the shoulder joint as the upper arm is pushed into the chest of the robot when the wheelchair climbs (Figure 5 (a)) and descends a step (Figure 5 (b)).

The wheelchair (NOVA Integral-ME) has a shape typical of wheelchairs currently available in the market (Figure 1). TABLE II provides the specifications. This is a manually operated chair to which an electric drive unit was added. In

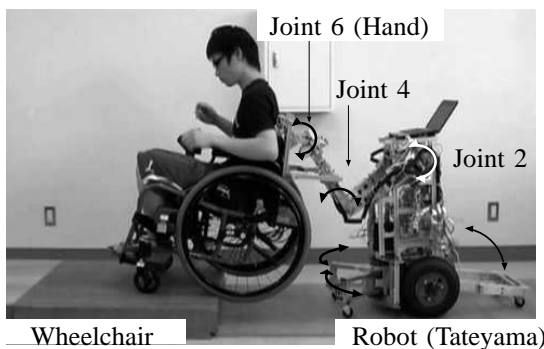


Figure 1. The wheelchair and the robot.

this study, the wheelchair is operated manually by the user, but it is also equipped a push handle mechanism on the back that is held by the robot hands (Figure 3). This system needs 2.07 [m] step length. The push handle mechanism is composed of a rotary shaft that allows passive rotation and a stopper for use when the robot is climbing or descending. The hand mechanism grasps the shaft to connect the two vehicles. The angle ϕ_6 is formed by the wheelchair with Link 4 (Figure 2). The stopper of the wheelchair is composed of front and rear bars (Figs. 6 (a) and (b)), and is mounted on the rear side. When the robot is climbing or descending, the sides of the robot are opened, and the two manipulators are inserted into the stopper (Figure 6 (a)). The robot pushes the front bars to lift its front wheels (Figure 6 (a)). The rear bars are used to prevent it from tipping over backward when the robot's mass position shifts behind the contact point between the center wheels and the ground (Figure 6 (b)).

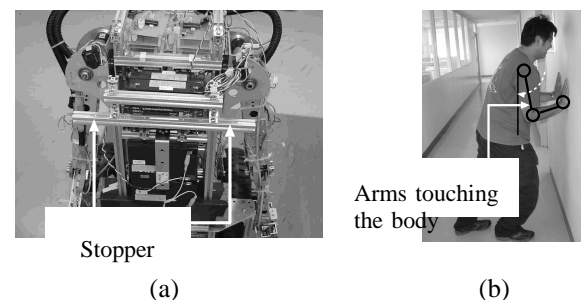


Figure 4. Control of rotary motions of the robot shoulder is performed by using the body. (a) The front body of the robot. (b) A human pushing an object.

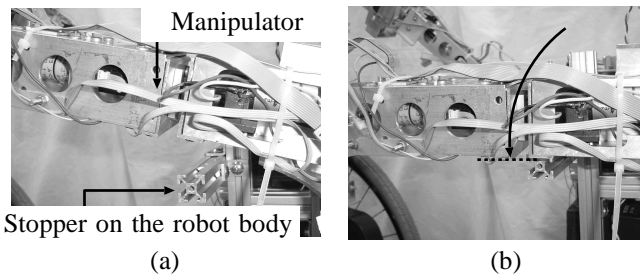


Figure 5. Stopper details. (a) Pulling the wheelchair. (b) Pushing the wheelchair.

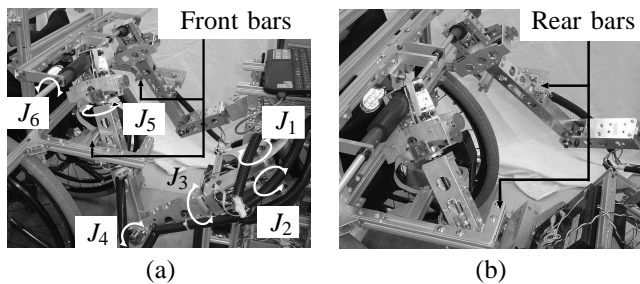


Figure 6. Action of the stopper. (a) Lifting the wheels of the robot. (b) Preventing the robot from falling down.

Figure 7 is a diagram of the system configuration. The motors mounted on the robot are connected to Faulhaber motion controllers (Faulhaber MCDC3006-S, MCDC3003-S). In turn, these are connected to a notebook PC mounted on the robot. The motors are controlled via commands issued using the Faulhaber Motion Manager 4 software package. The robot employs a camera built into the PC, and the moving images from that camera and the Motion Manager 4 operating window are displayed on the notebook PC mounted on the robot. This notebook PC uses RealVNC remote access and control software and data is transmitted over the intranet as-is to the display of the PC used by the caregiver in a different location. The caregiver and the wheelchair user both wear headsets and use Skype telecommunication software to communicate verbally. The caregiver’s headset is connected to the caregiver’s PC, and the wheelchair user’s headset is connected to the PC on the robot. The caregiver controls the robot by operating Motion Manager 4 from his PC. The keyboard commands for Motion Manager 4, which are issued using JoyToKey software, correspond to the manipulation by the caregiver to operate the robot. The robot has internal and external sensors (encoders and touch sensors). Thus, the robot is moved by the information integrated in the sensors’ signals with the commands from the caregiver.

III. PROCESS OF MOVING OVER A STEP

When encountering a step, the robot hands grasp the rotary shaft of the wheelchair push handle mechanism, thus linking itself to the wheelchair. The chair is then controlled to raise first its front wheels, and then its back wheels, onto the upper level of the step. The ascent and descent processes are described below. The stages shown in Figs. 8–11 correspond to (1)–(32) below; “Forward” or “Backward” and signifies the robot or the wheelchair’s motion ahead or behind, respectively.

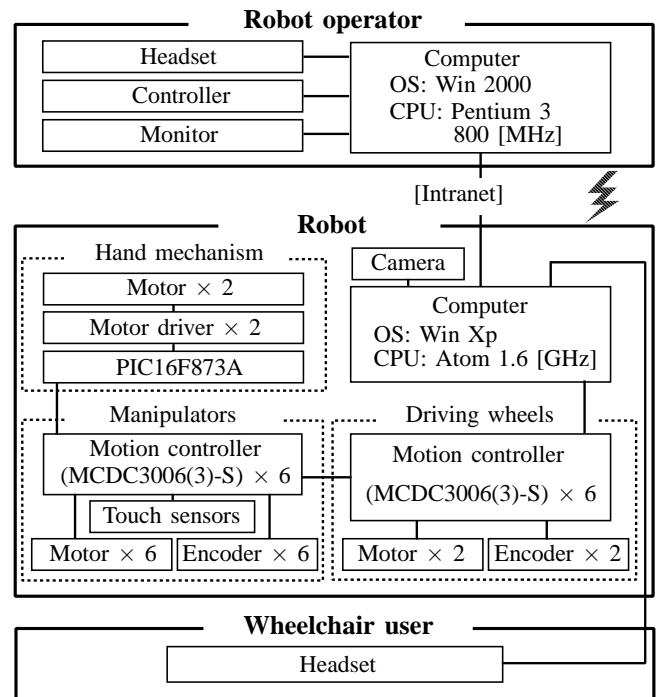


Figure 7. Diagram of the robot system.

“Free” is the state in which the vehicle does not do anything. “Stop” is the state in which the vehicle does not move.

[Stage 1]

(1) The robot hand grasps the wheelchair push handle to link the two vehicles. Joints 2, 4, and 6 are allowed to rotate passively until the ascent of the wheelchair has been completed. (2) The robot controller stops the robot. The wheelchair user manipulates the handrims as if to move forward, lifting the front wheels. (3) As the wheelchair tilt increases, if the location of the wheelchair’s center of mass shifts behind the contact point between the back wheels and the ground, the chair exerts forces on the manipulators, causing passive rotation about Joint 2 (Figure 5 (b)). In this case, the bottom part of the manipulator upper-arm link comes into contact with the stopper and limits the extent of the rotation (Figure 5 (b)). Thus, the robot supports the wheelchair from behind to prevent the wheelchair from tipping over backward. (4) The robot moves forward and the wheelchair user manipulates the handrims to adjust the difference between the speeds of the two vehicles, so that the front wheels of the wheelchair are placed on the upper level of the step. After completion of stage 1, the wheelchair user does not perform any operations until the end of stage 2.

[Stage 2]

(5) The robot continues to move forward while pushing the wheelchair from behind. (6) The back wheels of the wheelchair then come into contact with the step. (7) The robot continues to push on the wheelchair so that the rear wheels of the wheelchair climb up onto the step. The robot supports the wheelchair during this process to prevent the wheelchair from tipping over backward. (8) Once the wheelchair rear wheels have reached the upper level of the step, the robot stops.

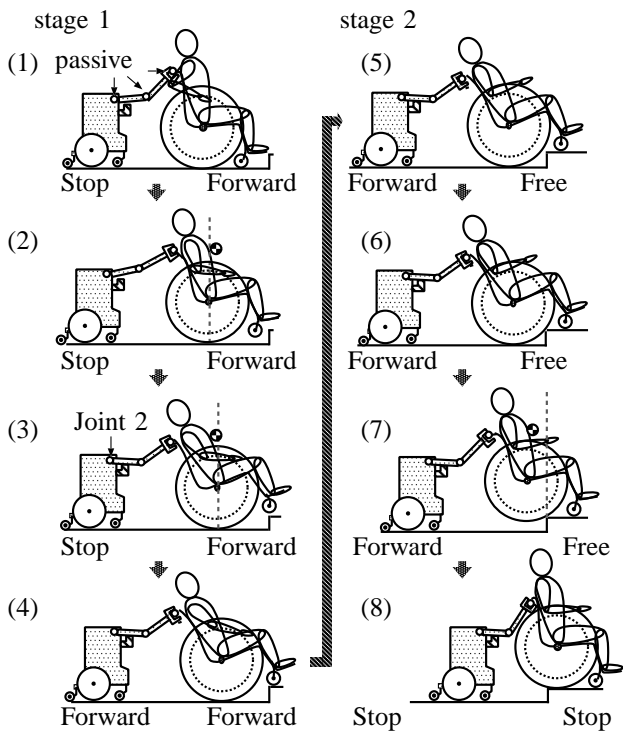


Figure 8. Step-climbing process of the wheelchair (stages 1, 2).

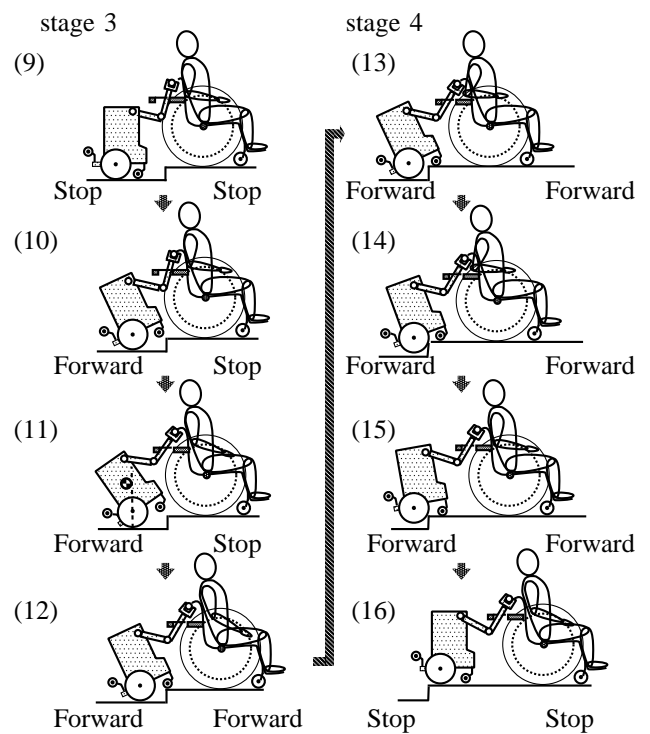


Figure 9. Step-climbing process of the robot (stages 3, 4).

[Stage 3]

(9) After stage 2, the rear wheels of the robot are folded upward. The sides of the robot are opened, and the two manipulators are inserted into the stopper (Figure 6 (a)). The wheelchair user holds the handrims and maintains the position of the wheelchair. The robot moves forward, the manipulator forearm link comes into contact with the stopper of the wheelchair (Figure 6 (a)). (10) The robot continues to push on the wheelchair and the front wheels of the robot are lifted. (11) As the robot tilt increases, if the location of the center of mass of the robot shifts behind the contact point between its middle wheels and the ground, the robot begins to tip over backward, but part of the manipulator forearm link comes into contact with the stopper of the wheelchair and limits the extent of rotation (Figure 6 (b)). Thus, the wheelchair supports the robot and prevents it from tipping over backward. (12) The robot then moves forward and the wheelchair user manipulates the handrims, thereby adjusting the difference between the speeds of the two vehicles so that the front wheels of the robot are placed on the upper level of the step.

[Stage 4]

(13) Both vehicles move forward. (14) The middle wheels of the robot come into contact with the step. The wheelchair pulls the robot, and the value of the normal reaction from the step on the robot middle wheels (driving wheels) is increased. Consequently, the force of the manipulators prevent the robot from falling down. The middle wheels of the robot then start to climb the step. (15) Both vehicles continue to move forward. (16) The center wheels of the robot are able to climb the step. Once the robot middle wheels have reached the upper level of the step, both vehicles are stopped.

[Stage 5]

(17) The robot hand grasps the wheelchair push handle to link the two vehicles. The sides of the robot are opened, and the two manipulators are inserted into the wheelchair stopper (Figure 6 (a)). Joint 1 is fixed. Joints 2 to 6 are allowed to rotate passively until the descent of the robot has been completed. In the robot descending process (stages 5, 6), the front wheels of the robot are closed and the rear wheels are folded upward. Both vehicles move backward. (18) After the rear wheel axes of the robot reach the corner of the step, the robot tilt increases and the robot begins to tip over backward. However, at this stage the forearm link comes into contact with the wheelchair stopper and limits the extent of rotation (Figure 6 (b)). (19) Thus, the wheelchair supports the robot and prevents it from tipping over backward. (20) As a result, the middle wheels of the robot are able to descend the step.

[Stage 6]

(21) Both vehicles continue to move backward. (22) The wheelchair moves faster than the robot, and thus the wheelchair front stopper pushes on the manipulator forearm link. The front wheel axes of the robot reach the corner of the step. (23) The wheelchair stops, and the robot continues to move. (24) As a result, the front wheels of the robot are able to descend the step.

[Stage 7]

(25) In the wheelchair descent process (stages 7, 8), the front wheels of the robot are opened and the rear wheels are lowered. The sides of the robot are closed (Figure 3). Joints 2, 4, and 6 are allowed to rotate passively until the descent of

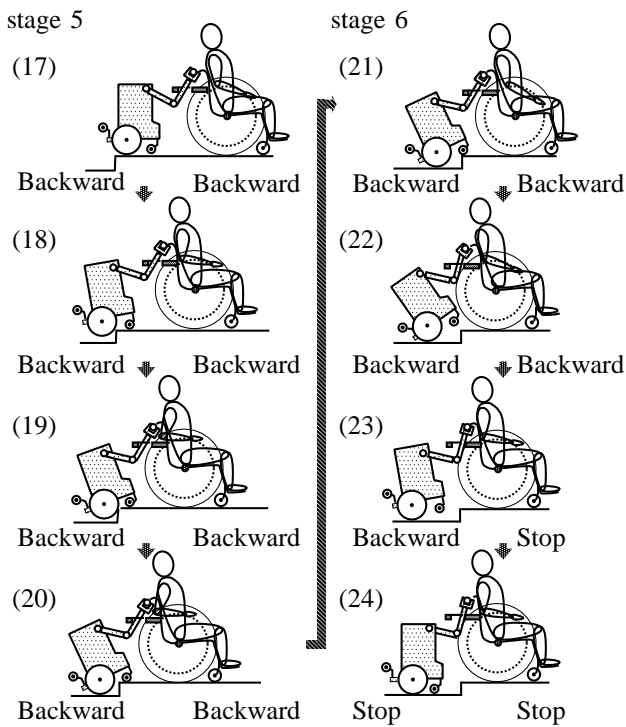


Figure 10. The step descending process (stages 5, 6).

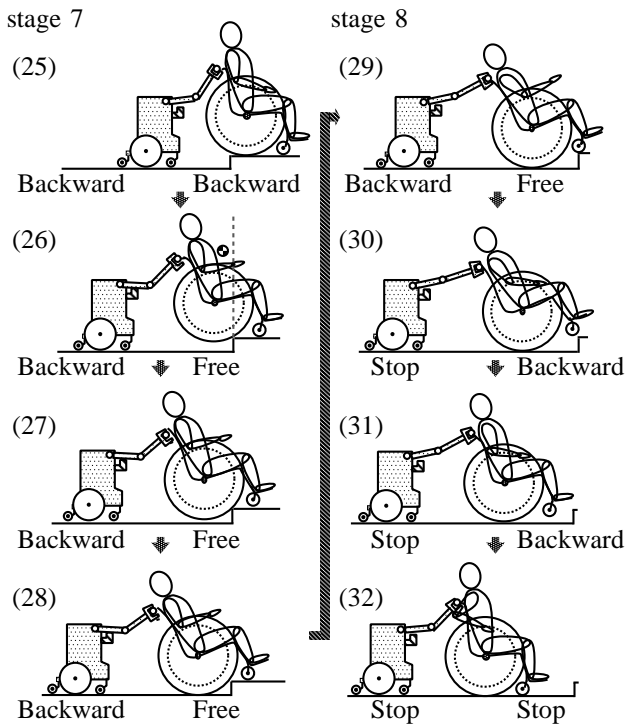


Figure 11. The step descending process (stages 7, 8).

the wheelchair has been completed. (26) As the robot moves backward, the wheelchair user does not perform any operations until the end of stage 7, and the wheelchair is pulled by the robot. The rear wheels of the wheelchair begin to descend the step. (27) The upper arm pushes against the chest (robot stopper) to limit the passive rotation about the shoulder axes.

Thus, the robot supports the wheelchair during this process to prevent the wheelchair from tipping over backward. (28) The rear wheels of the wheelchair descend the step.

[Stage 8]

(29) Both vehicles continue to move backward. (30) After the front wheel axes of the wheelchair reach the corner of the step, the wheelchair user manipulates the handrims as if to lift the front wheels. (31) The wheelchair user increases the wheelchair speed with both hands, and the incline of the wheelchair begin to decrease. (32) As a result, the rear wheels of the wheelchair are able to descend the step.

IV. THEORETICAL ANALYSIS

The requirements of preventing slippage in stage 1 are listed below. Figs. 12, 13 show $f_{1x}, f_{2z}, \dots, f_{6z}$.

- (i) $\mu > |f_{5x}|/f_{6z} (\phi_2 + \phi_4 + \phi_6 = 0)$
- (ii) $\mu > |f_{1x}|/f_{2z} (\phi_2 + \phi_4 + \phi_6 = 0)$
- (iii) $\mu > |f_{5x}|/f_{6z} (\phi_2 + \phi_4 + \phi_6 = 24.54 \text{ [deg]})$
- (iv) $\mu > |f_{1x}|/f_{2z} (\phi_2 + \phi_4 + \phi_6 = 24.54 \text{ [deg]})$

(i) and (ii) are the requirements to lift the front wheels of the wheelchair from the ground (Figure 8 (1)–(2)). (iii) and (iv) are the requirements to prevent the wheelchair from tipping over backward (Figure 8 (3)–(4)). Here, 24.54 [deg] is the maximum incline of the wheelchair when the wheelchair operator climbs a step, and the height between the lowest point on the front wheel tread surface and the ground surface below the step is $h_t = 0.200 \text{ [m]}$ (Figure 12). It was observed that people tend to raise the front wheels higher than the step they intend to traverse when actually operating a wheelchair. Thus, h_t was measured for five participants and the results were used when specifying a maximum tilt angle.

Figure 12 shows the stage 1 state in which the wheelchair center of mass is forward of the contact point between the rear wheels and the ground (Figure 8 (1)–(2)). At this time point, the robot is stopped, the wheelchair is propelled, and the robot exerts a backward force by pulling on the wheelchair. Figure 13 shows the state when the tilt of the wheelchair is increasing, and the wheelchair center of mass is behind the contact point between the rear wheel and the ground (Figure 8 (3)–(4)). When the situation shown in Figure 12 changes to that shown in Figure 13, the manipulators rotate passively. In this procedure, the stoppers limit the amount of passive rotation about the robot shoulder joint (Figure 5 (b)).

Σ_B is the basic coordinate system for the robot, where contact point B is between the robot middle (driving) wheels and the ground is the origin (Figure 13). Joints 2 (shoulder), 4 (elbow), and 6 (location where the hands hold the push handle) are controlled passively. The position vectors for these joints in system Σ_B are expressed as ${}^B p_{2i} = [x_{2i} \ z_{2i}]^T$ ($i = 1 \sim 3$), where ${}^B p_2 = [x_2 \ z_2]^T = [l_{LB} \ R_B + h_{LB}]^T$, ${}^B p_4 = [x_4 \ z_4]^T = [l_{LB} + l_2 \cos \phi_2 \ R_B + h_{LB} + l_2 \sin \phi_2]^T$, and ${}^B p_6 = [x_6 \ z_6]^T = [l_{LB} + l_2 \cos \phi_2 + l_{4c} \cos(\phi_2 + \phi_4) \ R_B + h_{LB} + l_2 \sin \phi_2 + l_{4c} \sin(\phi_2 + \phi_4)]^T$ (Figure 2).

In the same way, the position vectors for the contact points between the robot front and rear wheels and the ground are

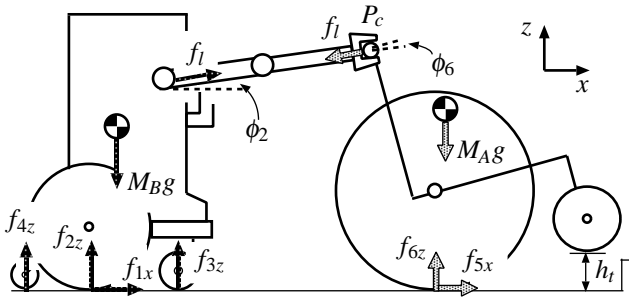
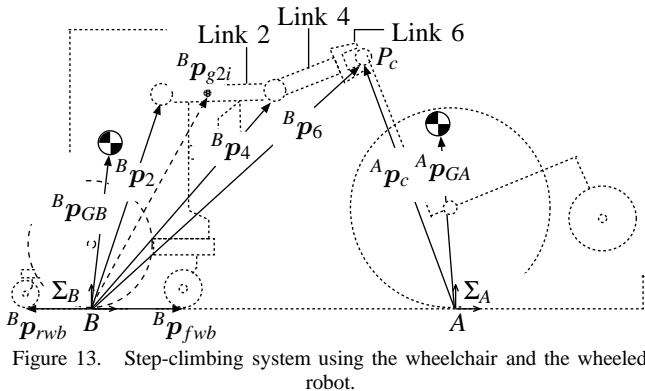
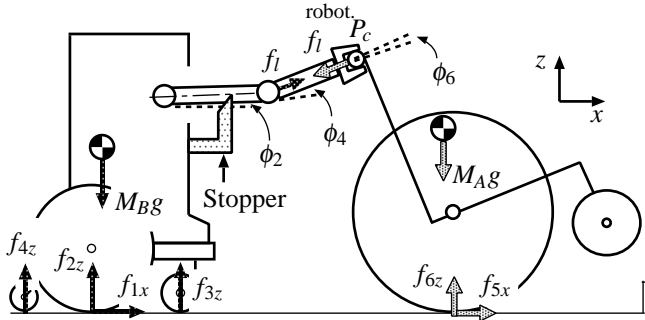


Figure 12. The step-climbing system using the wheelchair and the wheeled



expressed as ${}^B\mathbf{p}_{fwb} = [WB_f \ 0]^T$ and ${}^B\mathbf{p}_{rwb} = [-WB_r \ 0]^T$, respectively. The body of the robot, neglecting the manipulators, is Link 0 with mass m_0 . If the centers of mass of the robot body and each manipulator link (Links 2, 4, and 6) are denoted by ${}^B\mathbf{p}_{gj} = [x_{g2j} \ z_{g2j}]^T$ (where $j = 0-3$), then the center of mass of the entire robot ${}^B\mathbf{p}_{GB} = [x_{GB} \ z_{GB}]^T$ is given by ${}^B\mathbf{p}_{GB} = (\sum_{j=0}^3 m_{2j}^B \mathbf{p}_{g2j}) / \sum_{j=0}^3 m_{2j}$. The driving force vector for the robot middle wheels is $\mathbf{f}_1 = [f_{1x} \ 0]^T$, and the resistance force from the ground surface is $\mathbf{f}_2 = [0 \ f_{2z}]^T$. Additionally, the resistance force at the robot front wheels is $\mathbf{f}_3 = [0 \ f_{3z}]^T$, and that at the rear wheels is $\mathbf{f}_4 = [0 \ f_{4z}]^T$. The reaction force from the linked wheelchair is given by $\mathbf{f}_L = [f_l \cos(\phi_2 + \phi_4) \ f_l \sin(\phi_2 + \phi_4)]^T$.

Σ_A for the wheelchair is the coordinate system fixed at the point of contact between the wheelchair rear wheels and the ground, A. In Σ_A , the wheelchair center of mass is located at ${}^A\mathbf{p}_{GA} = [x_{GA} \ z_{GA}]^T = [l_r \cos(\phi_2 + \phi_4 + \phi_6) - h_m \sin(\phi_2 + \phi_4 + \phi_6) \ l_r \sin(\phi_2 + \phi_4 + \phi_6) + h_m \cos(\phi_2 + \phi_4 + \phi_6) + R_A]^T$, and the push handle location (where it is held by the robot hand) P_c is ${}^A\mathbf{p}_c = [x_c \ z_c]^T = [-l_{LA} \cos(\phi_2 + \phi_4 + \phi_6) - h_{LA} \sin(\phi_2 + \phi_4 + \phi_6) \ -l_{LA} \sin(\phi_2 + \phi_4 + \phi_6) + h_{LA} \cos(\phi_2 + \phi_4 + \phi_6) + R_A]^T$.

The driving force at the wheelchair rear wheels is $\mathbf{f}_5 = [f_{5x} \ 0]^T$, and the resistance force felt at the ground surface is $\mathbf{f}_6 = [0 \ f_{6z}]^T$. Furthermore, the reaction force from the linked

robot is given by $\mathbf{f}'_L = [-f_l \cos(\phi_2 + \phi_4) \ -f_l \sin(\phi_2 + \phi_4)]^T$.

Summing the total forces on the wheelchair exerted by the ground surface (resistance) and by the linked robot for $\mathbf{f}_{\Sigma A} \in \mathbf{R}^2$, we find that $\mathbf{f}_{\Sigma A} = [f_{5x} - f_l \cos(\phi_2 + \phi_4) \ f_{6z} - f_l \sin(\phi_2 + \phi_4)]^T$. When the linked vehicles are moving together in static equilibrium, the equilibrium for both the x and z axes yields (1), while the equilibrium of moments about the point of contact between the wheelchair rear wheels and the ground yields (2). Here, $\mathbf{g} = [0 \ -g]^T$ is gravitational acceleration.

$$\mathbf{f}_{\Sigma A} + M_A \mathbf{g} = 0 \quad (1)$$

$${}^A\mathbf{p}_{GA} \times M_A \mathbf{g} + {}^A\mathbf{p}_c \times \mathbf{f}'_L = 0 \quad (2)$$

We obtain (3) and (4) from (1).

$$f_{5x} = f_l \cos(\phi_2 + \phi_4) \quad (3)$$

$$f_{6z} = M_A g + f_l \sin(\phi_2 + \phi_4) \quad (4)$$

Then, from (2), we find

$$f_l = \frac{x_{GA} M_A g}{z_c \cos(\phi_2 + \phi_4) - x_c \sin(\phi_2 + \phi_4)} \quad (5)$$

Next, from the z -coordinate of ${}^B\mathbf{p}_6$ and ${}^A\mathbf{p}_c$, we obtain

$$h_{LA} = \frac{z_6 + l_{LA} \sin(\phi_2 + \phi_4 + \phi_6) - R_A}{\cos(\phi_2 + \phi_4 + \phi_6)} \quad (6)$$

where $z_6 = R_B + h_{LB} + l_2 \sin \phi_2 + l_{4c} \sin(\phi_2 + \phi_4)$). When the robot acts statically in stage 1, (7) holds, and the equilibrium in the x and z axes gives us

$$\mathbf{f}_{\Sigma B} + M_B \mathbf{g} = 0 \quad (7)$$

Here, $\mathbf{f}_{\Sigma B} \in \mathbf{R}^2$ is the sum of forces on the robot due to resistance at the ground surface and from the linked wheelchair, and $\mathbf{f}_{\Sigma B} = [f_{1x} + f_l \cos(\phi_2 + \phi_4) \ \sum_{k=2}^4 f_{kz} + f_l \sin(\phi_2 + \phi_4)]^T$.

From (7), we obtain (8) and (9).

$$f_{1x} = -f_l \cos(\phi_2 + \phi_4) \quad (8)$$

$$f_{2z} = M_B g - f_l \sin(\phi_2 + \phi_4) - f_{3z} - f_{4z} \quad (9)$$

During the process of moving over a step, while the manipulators are pulling the robot wheelchair (Figure 12), the manipulators and stoppers do not come into contact. By the equilibrium of moments about the contact point between the robot driving wheel and the ground during this time, we obtain

$${}^B\mathbf{p}_{GB} \times M_B \mathbf{g} + {}^B\mathbf{p}_2 \times \mathbf{f}_L + {}^B\mathbf{p}_{fwb} \times \mathbf{f}_3 + {}^B\mathbf{p}_{rwb} \times \mathbf{f}_4 = 0 \quad (10)$$

from which is obtained

$$x_{GB} M_B g - f_l \{x_2 \sin(\phi_2 + \phi_4) - z_2 \cos(\phi_2 + \phi_4)\} + W_B f_{4z} - W_B f_{3z} = 0 \quad (11)$$

When the robot is supporting the wheelchair from behind (Figure 13), passive rotation about Joint 2 (shoulder) is limited by the stopper. At such times, Link 2 (the upper arm of the manipulator) can be treated as a part of the robot body and the equilibrium of moments about the contact point between the robot driving wheels is represented as

$${}^B\mathbf{p}_{GB} \times M_B \mathbf{g} + {}^B\mathbf{p}_4 \times \mathbf{f}_L + {}^B\mathbf{p}_{fwb} \times \mathbf{f}_3 + {}^B\mathbf{p}_{rwb} \times \mathbf{f}_4 = 0 \quad (12)$$

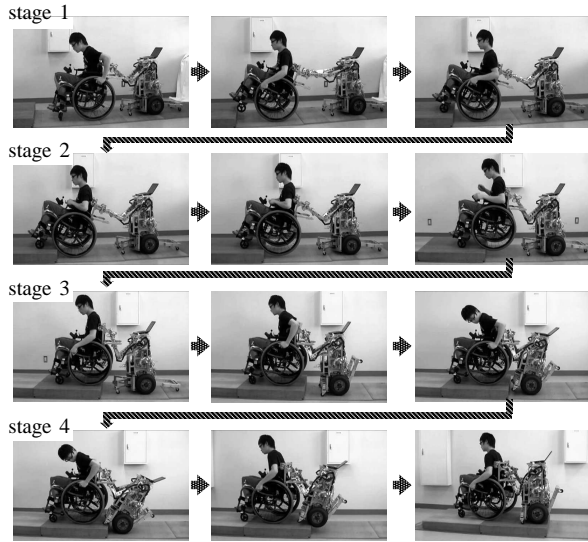


Figure 14. Experiment (Step climbing)

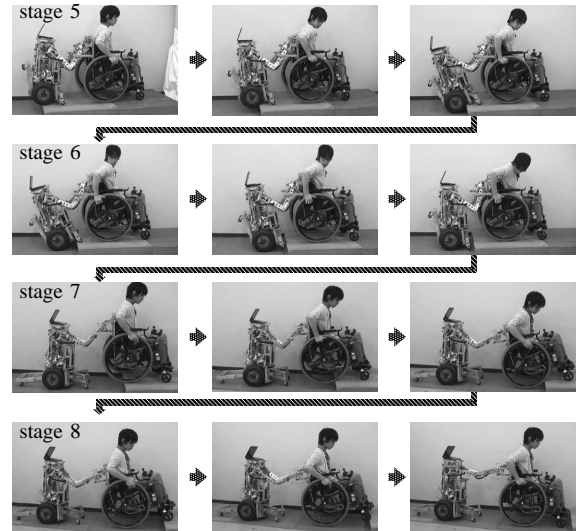


Figure 15. Experiment (Step descending)

from which is obtained

$$x_{GB}M_{BG} - f_1\{x_4 \sin(\phi_2 + \phi_4) - z_4 \cos(\phi_2 + \phi_4)\} + WB_r f_{4z} - WB_f f_{3z} = 0 \quad (13)$$

We obtain f_{3z} and f_{4z} from (10) and (12). In addition, $\mu > |f_{1x}|/f_{2z}$ or $\mu > |f_{5x}|/f_{6z}$ can be calculated from (3)–(6), (8), and (9).

V. EXPERIMENT

An experiment was carried out using this system under an environment of step height 0.12 [m] and friction coefficient $\mu = 0.72$ (Figure 14). The wheelchair user and robot operator were both able-bodied adult males. The wheelchair user and the robot were placed on one floor of the Toyama National College of Technology, and the robot operator was on another floor of the same building. The robot operator performed his task over the intranet while observing the situation via a camera and communicating with the wheelchair user over a voice link.

If the wheelchair was too close to the step in stage 1, the front wheels bumped into the vertical riser of the step. However, following instructions from the wheelchair user, the robot controller was able to back up the two linked vehicles together and re-start the ascent. It was then possible for the front wheels of the wheelchair to climb the step with ease.

Subsequently, during stage 2, the user never needed to push the wheels. More specifically, it was possible to lift the chair onto the upper level of the step by following the procedure proposed above and using only the forward operation of the robot. Stages 3 and 4 were then executed.

Stages 5–8 were performed similarly. In these processes, the wheelchair user twisted his upper body to visually verify the position of the step behind the wheelchair. It should be noted that this system is intended for wheelchair users who can freely move their upper bodies, and one can anticipate

that this movement and posture would be difficult for users with certain physical limitations.

In the climbing or descending processes, both vehicles incline in turn. However, because this system only has one camera installed on the robot, the visual information provided was limited and the robot operator experienced some difficulty controlling the robot. Thus, it is clear that the construction of a system to support the robot operator and the wheelchair operator based on exterior and perhaps other sensors would be required in the future.

VI. CONCLUSION

This report describes the tactics of cooperative step climbing and descending for a manual wheelchair using a robot that imitates the motion of the upper arms of a human pushing his/her chest against a heavy object to move it. We constructed the robot system and an experiment was carried out that incorporated teleoperation of the robot over an intranet. The effectiveness of the handling method for a heavy object was demonstrated by using a robot with manipulators driven by small motors. During the climbing or descending processes, these vehicles incline in turn. However, because this system only has one camera installed on the robot, the visual information supplied to the robot operator was limited. Thus, it is clear that the robot operator will need an enhanced support system that can indicate the distance from the step and show other situations related to the vehicle. It is also clear that the construction of a system to support the wheelchair operator based on exterior and perhaps other sensors would be required in the future.

Despite the above observation, it is worthwhile to demonstrate that mobile manipulators, which are driven by the small motors, are capable of handling a heavy cart (wheelchair) by the method of pressing the manipulator links against the vehicles in addition to the robot hands. In the future, we will verify the force necessary to operate the wheelchair using

this method and an autonomous control system to assist the wheelchair user and robot operator will be built.

ACKNOWLEDGMENT

This work was supported in part by a grant from the Daiwa Securities Health Foundation (2007, Grant No. 19) and the Okawa Foundation for Information and Telecommunications (2008, Grant No. 08-18).

REFERENCES

- [1] V. Kumar and V. Krovi, "Optimal traction control in a wheelchair with legs and wheels," Proc. of 4th National Applied Mechanisms and Robotics Conference, December 1995, pp. 95-030-01-95-030-07.
- [2] N. Yanagihara, F. Sugawara, N. Suzuki, T. Ikeda, and Y. Kanaumi, "Mechanical analysis of a stair-climbing wheelchair using rotary cross arm with wheels," Proc. 17th Annual Conference of the Robotics Society of Japan, September 1999, pp. 1143-1144.
- [3] G. Quaglia, W. Franco, and R. Oderio, "Wheelchair motorized wheelchair with stair climbing ability," Mechanism and Machine Theory, vol. 46, 2011, pp. 1601-160.
- [4] M. Lawn and T. Ishimatsu, "Modeling of a stair-climbing wheelchair mechanism with high single step capability," IEEE Transactions on Neural Systems and Engineering, vol. 11, no. 3, 2003, pp. 323-332.
- [5] Y. Takahashi, S. Ogawa, and S. Machida, "Human assist robot (1st report: Prototype of wheelchair which can fly up and run)," Proc. JSME ROBOMECH'99 1999, Tokyo, pp. 1A1-75-106.
- [6] Independence Technology, L.L.C., iBOT, [Online, retrieved: February 2013] <http://www.ibotnow.com/>, 2008.
- [7] K. Taguchi and H. Sato, "A study of the wheel-feet mechanism for stair climbing," Journal of Robotics Society of Japan, vol. 15, 1997, pp. 118-123.
- [8] K. Sugiyama, T. Ishimatsu, T. Shigechi, and M. Kurihara, "Development of stair-climbing machines at Nagasaki," Proc. of 3rd International Workshop on Advanced Mechatronics, Berlin, Jun - July 1999, pp. 214-217.
- [9] H. Ikeda, Y. Katsumata, M. Shoji, T. Takahashi, and E. Nakano, "Cooperative strategy for a wheelchair and a robot to climb and descend a step," Advanced Robotics, 2008, vol. 22, pp. 1439-1460.
- [10] H. Ikeda, H. Kanda, N. Yamashima, and E. Nakano, "Cooperative step-climbing method using a wheelchair and a partner robot," Proceedings of the International Conference on Future Trends in Automation and Robotics - FTAR 2012, Kuala Lumpur, August 2012, pp. 1-6.

On the Analysis of a Swarm-Intelligence Coordination Model for Swarm Robots

Caio D. D. Monteiro, Diego M. P. F. Silva and Carmelo J. A. Bastos-Filho
Polytechnic School of Pernambuco, University of Pernambuco
{cddm,dmpfs,carmelofilho}@ecom.poli.br

Abstract—In this paper, we propose three specific scenarios in order to allow one to analyze the performance of swarm-intelligence based coordination models for swarm of robots. The specific scenarios aim to assess some features presented on swarm robots: (i) contraction and expansion; (ii) self-segregation and self-aggregation; and (iii) the capacity to change abruptly the fly direction whenever it is necessary. We also propose a metric to analyze the cohesion (COE) of the swarm during a mission. We analyzed a recently proposed model based on the Particle Swarm Optimization technique designed to coordinate automatically swarms of robots in terms of Collision (CL) rate and COE. We performed simulations varying all the parameters in the three scenarios and we observed that the main problem is related to collisions when the width of the passageway is not much more higher than the UAVs collision radius. The proposed model can assist and support the implementation of a system of swarm robots.

Keywords—Unmanned Aerial Vehicles; Swarm Robots; Swarm intelligence; Particle Swarm Optimization; Specific Scenarios.

I. INTRODUCTION

The interest in Unmanned Aerial Vehicles (UAVs) has grown in the last years. UAVs have been applied to perform complex and sophisticated tasks, such as for agricultural applications in order to reduce the agrochemicals [1] or for search and surveillance operations [2].

Swarm intelligence have appeared in the 1990's inspired by swarms of simple creatures, such as ants, bees, birds, fireflies and fish [3] [4]. In this case, an entity is too simple to solve complex tasks, but the emergent behavior of the swarm can tackle such problems. Swarm intelligence algorithms have been successfully applied for the coordination of mobile robots [5] [6]. The application of the swarm intelligence concepts and algorithms to control and/or to coordinate mobile robots is often called swarm robotics [7] and suggests that the coordination of multiple robots does not necessarily need to be performed by means of a multi-agent system.

One of the most used swarm intelligence algorithms is the Particle Swarm Optimization (PSO), proposed by Kennedy and Eberhart in 1995 [4].

Some previous works proposed to tackle the coordination issues in swarm of robots by means of distributed models. In 2011, Wang *et al.* [6] used the PSO to coordinate multiple robots aiming to perform territorial exploration in a collaborative manner. Varela *et al.* [2] used the PSO to coordinate multiple UAVs equipped with sensors aiming to find pollutants in the atmosphere. There are other proposals to tackle some UAVs coordination issues [8] [9], however

these works considered a global positioning systems (GPS). Considering this, Zhu *et al.* [10] developed a search algorithm for swarm robots that does not need necessarily the GPS signal. Qu and Zhang [11] proposed a fault-tolerant collaborative algorithm to address the loss of the GPS signal. Shames *et al.* [12] proposed a self-localization mechanism for mobile agents that uses a cooperative strategy. There are other recent works that aims to contribute in other aspects, such as energy consumption and errors generated by the sensors [8] [9] [13] [14] [15] [16].

Meanwhile, the previous works did not investigate their model effectiveness in specific scenarios. In 2012, La and Sheng [17] investigated the contraction and expansion capability of a swarm of robots. They assessed the capability of the swarm to avoid obstacles, but other required features were not analyzed, such as (i) self-segregation and self-aggregation capabilities and (ii) the capacity to change abruptly the fly direction whenever it is necessary. In 2012, Bentes and Saotome [18] proposed a dynamic swarm formation based on artificial potential fields in order to control the swarm formation and to avoid obstacles when traveling the planned path. The proposal is interesting, but needs the GPS signal.

In 2012, Pinheiro Silva and Bastos-Filho [5] proposed a distributed coordination model for swarms of UAVs with local ad hoc communication based on the PSO. In their model, the swarm robots present the following objectives: (i) allow the locomotion through an environment; (ii) avoid obstacles and collisions; (iii) patrol the entire environment; and (iv) detect and track targets. They analyzed communication issues and energy consumption [5], but some practical required features were not assessed in the proposed model.

In this paper, we propose specific scenarios that allow one to analyze the following capabilities of the swarm: (i) contraction and expansion; (ii) segregation and aggregation; and (iii) abrupt changes of direction. Besides, we assessed an PSO-based UAV coordination model recently proposed in [5] in these specific scenarios. We also propose in this paper a metric to analyze the cohesion of the swarm during a mission.

The remainder of the paper is organized as follows: the previous swarm based coordination model of UAVs is presented in Section II; the improvements in the model are presented in Section III; the simulation results are presented in Section IV; and some conclusions and future works are presented in Section V.

II. PSO-BASED COORDINATION MODEL FOR SWARMS OF UAVS

The previous PSO-based coordination model proposed in [5] presents the following features: (i) locomotion mechanism, in which the UAVs obtain their localization within the environment, $\vec{x}_{uav}(t)$. This information can be acquired by a GPS; (ii) perception mechanism, in which each UAV has a perception sensor in order to detect targets; (iii) anti-collision mechanism, in which each UAV has an anti-collision sensor to avoid obstacles and to ensure a safety locomotion; (iv) and communication mechanism, in which every UAV owns a wireless communication device and acts as a routing bridge in to build a 2-connected ad hoc communication network.

The locomotion mechanism is guided by physical dynamical variables and parameters, such as horizontal acceleration (\vec{a}), maximum horizontal acceleration (a_{max}), horizontal speed (\vec{v}), and maximum horizontal speed (v). The \vec{a} vector is composed by other vectors: synchronism (\vec{a}_{syn}); avoiding collisions (\vec{a}_{col}); avoiding losing communication (\vec{a}_{com}); cognitive (\vec{a}_{cog}); and social (\vec{a}_{soc}).

The Synchronism vector is given by:

$$\vec{a}_{syn} = \vec{a}_{col} + \vec{a}_{com}, \quad (1)$$

in which \vec{a}_{col} and \vec{a}_{com} are calculated by using the information provided by the collision and the communication sensors, respectively.

The Cognitive (related to the UAV) and Social (related to the UAV neighbor) vectors compose the swarm vector, which is given by:

$$\vec{a}_{swm} = \vec{a}_{cog} + \vec{a}_{soc}, \quad (2)$$

where \vec{a}_{cog} and \vec{a}_{soc} are calculated by the PSO algorithm at each iteration. Since the PSO algorithm needs a fitness function, we adopted the euclidean distance to the detected target as the quality metric for the PSO, which is given by:

$$fitness_{uav}(t) = |\vec{x}_{tar}(t) - \vec{x}_{uav}(t)|, \quad (3)$$

in which the information about target position, $\vec{x}_{tar}(t)$, is provided by the perception sensor.

The resultant acceleration is the sum of the Synchronism and the Swarm vectors.

Finally, the new UAV resultant velocity is calculated by:

$$\vec{v}(t+1) = \vec{v}(t) \cdot \omega + \vec{a}(t+1), \quad (4)$$

in which $\vec{v}(t+1)$ is the new speed, $\vec{v}(t)$ is the current speed and ω is the inertia factor.

III. IMPROVEMENTS IN THE MODEL

Improvements were made in the previous model to allow one to assess the effects of specific scenarios in the coordination of multiple UAVs.



Fig. 1. α angle used to determine the distance from an UAV to an obstacle.

A. Initialization of positions of targets, obstacles and UAVs.

The previous model does not present any mechanisms that allow the precise initialization of the position of the targets and UAVs. The positions of the targets and the UAVs were initialized randomly by a uniform density function related to all environment area. A mechanism was developed to initialize the targets in desired pre-defined positions, *i.e.* the user can indicate explicitly the position of each target, obstacle and UAV.

B. Definition of trajectories of the targets

In order to assess the behavior of the swarm of robots in specific scenario, we included a tool to define the trajectories of the targets based on the definition of waypoints. This mechanism guides the targets, which attract the UAVs through the desired passageway.

C. Obstacles construction improvement

In the previous model, the obstacle were modeled as a circle with a position (p) and a radius (r). Then, the area of influence a specific obstacle is a circle centered in p with radius r . In order to allow the definition of more complex obstacles, we implemented a new tool. In this new tool, an obstacle is composed by a set of line segments. The user provides an initial and a final position and, thereupon, the line segment is created. The equation for the line segment is given by:

$$Ax + By + C = 0, \quad (5)$$

in which A and B are the linear coefficients and C is the independent term.

When the UAV is out of the closest line segment ends, the distance between UAV and obstacle is given by Eq. (6):

$$D = \sqrt{(x_a - x_b)^2 + (y_a - y_b)^2}, \quad (6)$$

in which (x_a, y_a) are the coordinates of closest obstacle to the UAV and (x_b, y_b) are the coordinates of the UAV.

When the UAV is within the line segment, the distance between UAV and obstacle is given by:

$$D = \frac{|Ax_o + By_o + C|}{\sqrt{A^2 + B^2}}, \quad (7)$$

in which (x_o, y_o) are the UAV coordinates, and A, B and C are the coefficients and independent term of a line segment that belongs to the obstacle.

The α angle presented in Fig. 1 distinguishes the two cases aforementioned. We use Eq. (6) when $\cos(\alpha) < 0$, and Eq. (7), otherwise.

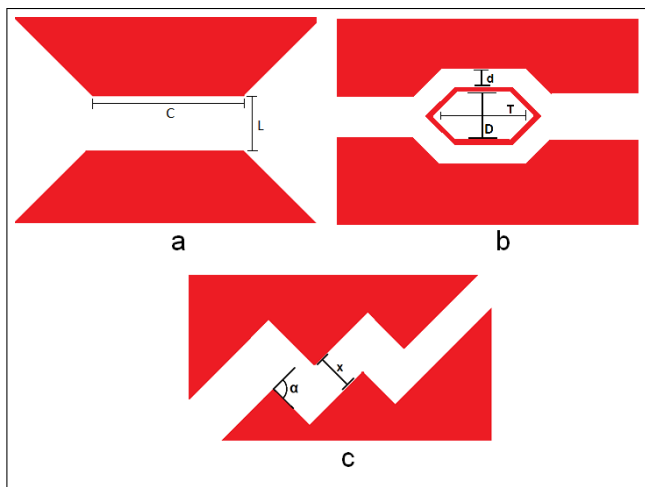


Fig. 2. The three specific scenarios: (a) contraction and expansion, (b) segregation and aggregation and (c) abrupt changes of direction.

D. Cohesion metric

A collision metric (CL) was already implemented in the previous model in order to measure the collision rate of the swarm during the mission. The collision metric is given by Eq. (8):

$$CL = \frac{1}{t_{max} \cdot uav_{num}} \sum_{t=1}^{t_{max}} uav_{crt}(t), \quad (8)$$

where t_{max} is the maximum number of iterations, uav_{num} is the total number of UAVs and $uav_{crt}(t)$ is the current number of UAVs at time t .

However, a cohesion metric (COE) is also required to assess the effects of different specific scenarios in the connection degree of the swarm. Because of this, we propose here a cohesion metric, which is given by Eq. (9):

$$COE = \frac{1}{t_{max} \cdot uav_{num}} \sum_{t=1}^{t_{max}} uav_{con}(t), \quad (9)$$

where t_{max} is the maximum number of iterations, uav_{num} is the total number of UAVs and $uav_{con}(t)$ is the number of 2-connected UAVs at time t . This 2-connected requirement is necessary to guarantee the functionality of the ad-hoc communication network.

IV. SIMULATION RESULTS OF SPECIFIC SCENARIOS

Three specific scenarios were developed in order to assess important features of the swarm robots coordination model. Fig. 2 presents the three scenarios. The first scenario (Fig. 2a) evaluates the contraction and expansion capability of the robot swarm. The second scenario (Fig. 2b) assesses the segregation and aggregation capability of the robot swarm. The third scenario (Fig. 2c) assesses the capability of the swarm to do tight turns on their movement.

A. Contraction and expansion results

The Scenario 1 (Fig. 2a) is used to assess the contraction and expansion swarm capability. C and L represent the length

TABLE I. COHESION AND COLLISION RESULTS FOR SCENARIO 1 WITH $v = 5m/s$, $a = 1,5m/s^2$.

	Cohesion	Collision
Length 20 m, Width 200 m		
Mean	63,20%	62,67%
Standard Deviation	7,06%	7,85%
Length 20 m, Width 400 m		
Mean	84,91%	24,67%
Standard Deviation	9,20%	5,07%
Length 20 m, Width 800 m		
Mean	99,89%	0,00%
Standard Deviation	0,00%	0,00%
Length 2000 m, Width 200 m		
Mean	49,41%	71,00%
Standard Deviation	4,85%	10,29%
Length 2000 m, Width 400 m		
Mean	79,12%	25,34%
Standard Deviation	13,75%	5,71%
Length 2000 m, Width 800 m		
Mean	99,89%	0,00%
Standard Deviation	0,00%	0,00%

TABLE II. COHESION AND COLLISION RESULTS IN SCENARIO 1 WITH $v = 15m/s$ and $a = 4,5m/s^2$.

	Cohesion	Collision
Length 20 m, Width 200 m		
Mean	63,41%	51,67%
Standard Deviation	6,94%	11,97%
Length 20 m, Width 400 m		
Mean	84,13%	20,67%
Standard Deviation	13,06%	8,68%
Length 20 m, Width 800 m		
Mean	99,66%	0,00%
Standard Deviation	0,00%	0,00%
Length 2000 m, Width 200 m		
Mean	47,35%	72,00%
Standard Deviation	2,54%	12,70%
Length 2000 m, Width 400 m		
Mean	77,70%	20,67%
Standard Deviation	15,42%	9,80%
Length 2000 m, Width 800 m		
Mean	99,67%	0,00%
Standard Deviation	0,00%	0,00%

and width of the narrowed path, respectively. It is important to evaluate the swarm behavior in scenarios that require contraction and expansion because it probably occurs in the environment during real missions.

We performed analysis in this scenario varying the width and the length of the path. We used width values equal to 200 m, 400 m and 800 m, and length values equal to 20 m or 2000 m. We also assessed the coordination model performance in two different situations: maximum velocity and maximum acceleration equal to 5 m/s and 1,5 m/s², and 15 m/s and 4,5 m/s².

Table I and Table II show the mean and standard deviation values for Collisions (CL) and Cohesion (COE). Fig. 3 and Fig. 4 show the boxplot of CL and COE as a function of the width and length of the path, for (5m/s, 1,5m/s²) and (15m/s, 4,5m/s²), respectively.

One can observe that the coordination model did not present a good performance for widths equal 200 m and 400 m. The model presented high values for CL, specially for the narrower path. As a consequence, the cohesion of the swarm was affected. On the other hand, the length of the path does not seem to affect the performance of the model, obtaining

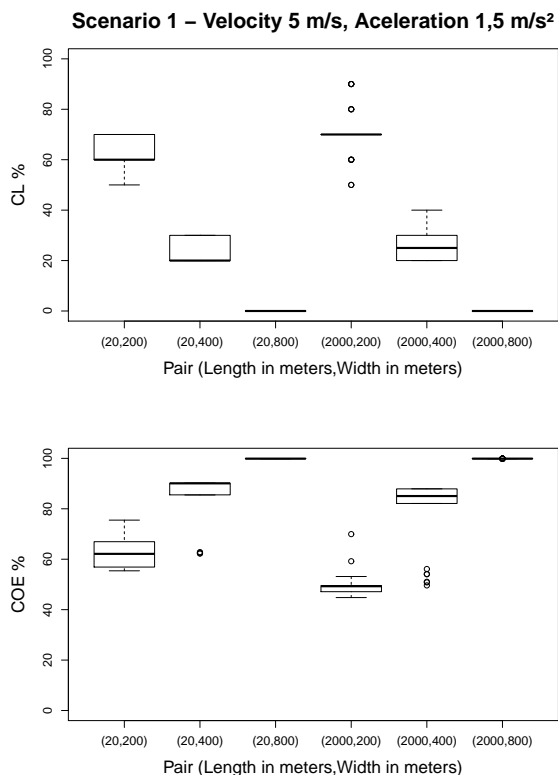


Fig. 3. Analysis of CL and COE as a function of the width and length of the path, for the velocity of 5 m/s and acceleration of 1,5 m/s².

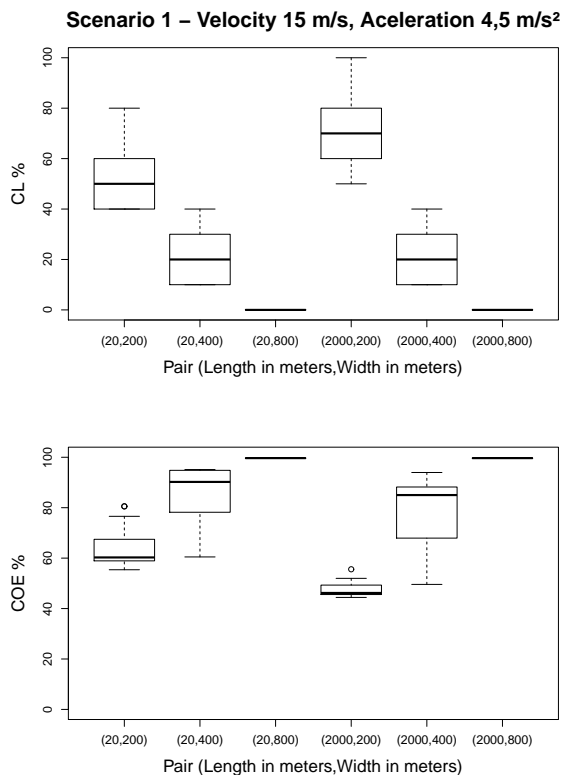


Fig. 4. Analysis of CL and COE as a function of the width and length of the path, for the velocity of 15 m/s and acceleration of 4,5 m/s².

TABLE III. COHESION AND COLLISION RESULTS FOR SCENARIO 2 FOR WIDTH OF THE PATH 200 m.

	Cohesion	Collision
Length of bifurcation 200 m Width of bifurcation 200 m		
Mean	52,22%	95,00%
Standard deviation	2,20%	6,82%
Length of bifurcation 1000 m Width of bifurcation 200 m		
Mean	51,65%	90,00%
Standard deviation	1,48%	7,43%
Length of bifurcation 200 m Width of bifurcation 1000 m		
Mean	46,59%	99,67%
Standard deviation	0,59%	1,82%
Length of bifurcation 1000 m Width of bifurcation 1000 m		
Mean	48,72%	94,00%
Standard deviation	2,42%	4,99%

TABLE IV. COHESION AND COLLISION RESULTS FOR SCENARIO 2 FOR WIDTH OF THE PATH 400 m.

	Cohesion	Collision
Length of bifurcation 200 m Width of bifurcation 200 m		
Mean	63,38%	51,33%
Standard deviation	4,77%	6,81%
Length of bifurcation 1000 m Width of bifurcation 200 m		
Mean	68,59%	44,00%
Standard deviation	9,83%	11,01%
Length of bifurcation 200 m Width of bifurcation 1000 m		
Mean	56,10%	76,00%
Standard deviation	2,54%	9,68%
Length of bifurcation 1000 m Width of bifurcation 1000 m		
Mean	52,20%	81,33%
Standard deviation	1,34%	14,56%

fairly similar results for the same width. One can observe that it did not occur any single collision for width equal to 800 m.

B. Segregation and aggregation results

Scenario 2 (Fig. 2b) was developed to assess the segregation and aggregation swarm capability. *d* is the width of the path, *D* is the width of the bifurcation and *T* is the length of the bifurcation. For this scenario, we analyzed the width and length of the bifurcation alongside with the width of the path. We used the values of 20 m and 2000 m for the width and length of the bifurcation, and 200 m, 400 m and 800 m for the width of the path.

Table III, Table IV and Table V present the results for COE and CL for the width of path equal to 200 m, 400 m and 800 m, respectively. The boxplots for COE and CL are shown in Fig. 5 and Fig. 6, respectively.

One can observe that the swarm coordination was impaired for path width of 200 m. Besides, the presence of a bifurcation mitigates CL and COE. These effects are more evident when the bifurcation width increases. One can observe that the increase on the bifurcation width has more impact on the swarm coordination than the bifurcation length. It might occur because the obstacles are not modeled to block communication signals. This means that a bifurcation width of 200 m is not enough to break the communication among the two sub-swarms.

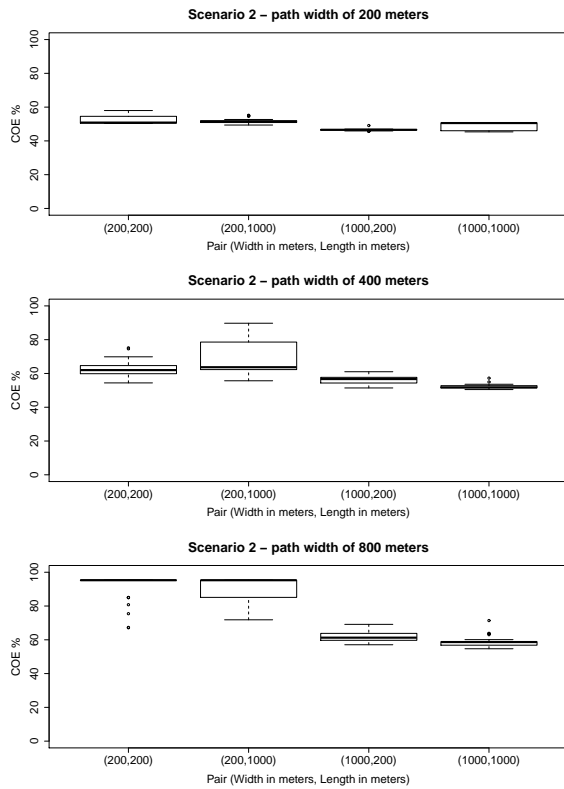


Fig. 5. Analysis of COE on the scenario 2 for each configuration set.

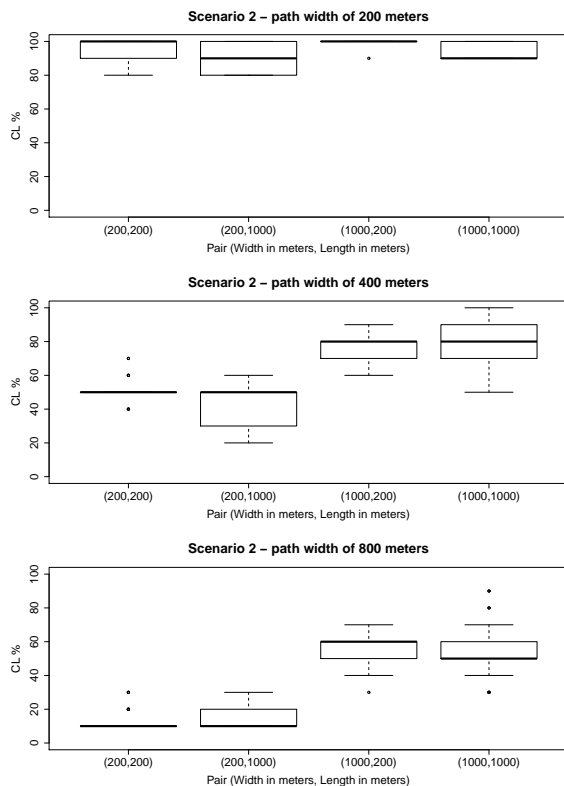


Fig. 6. Analysis of CL on the scenario 2 for each configuration set.

TABLE V. COHESION AND COLLISION RESULTS FOR SCENARIO 2 FOR WIDTH OF THE PATH 800 m.

	Cohesion	Collision
Length of bifurcation 200 m Width of bifurcation 200 m		
Mean	91,24%	13,33%
Standard deviation	8,31%	6,61%
Length of bifurcation 1000 m Width of bifurcation 200 m		
Mean	89,54%	14,67%
Standard deviation	8,95%	7,30%
Length of bifurcation 200 m Width of bifurcation 1000 m		
Mean	61,88%	57,33%
Standard deviation	2,78%	10,15%
Length of bifurcation 1000 m Width of bifurcation 1000 m		
Mean	59,02%	54,67%
Standard deviation	3,33%	16,13%

TABLE VI. COHESION AND COLLISION RESULTS FOR SCENARIO 3.

	COE	CL
Angle 90°, Width 400 m		
Mean	17,90%	94,33%
Standard deviation	6,80%	5,04%
Angle 90°, Width 800 m		
Mean	55,31%	29,33%
Standard deviation	21,52%	9,07%
Angle 90°, Width 1600 m		
Mean	92,96%	0,34%
Standard deviation	19,56%	1,86%
Angle 45°, Width 400 m		
Mean	21,12%	71,67%
Standard deviation	12,36%	6,48%
Angle 45°, Width 800 m		
Mean	92,38%	5,33%
Standard deviation	19,94%	5,07%
Angle 45°, Width 1600 m		
Mean	92,81%	0,33%
Standard deviation	21,33%	1,83%

C. Abrupt changes of direction results

The Scenario 3 (Fig. 2c) was developed to assess the swarm capability to react to tight turns presented along the trajectory. α angle is the curve inclination and x is the width of each segment of the path.

We analyzed two curve inclinations: α equal to 45° and 90°. Since we have already observed problems in narrow paths on previous scenarios, we used widths equal to 400 m, 800 m and 1600 m.

Table VI presents the results for scenario 3 and the boxplots for COE and CL are shown in Fig. 7. One can observe that the results for 45° are better than the ones for $\alpha = 90^\circ$, specially for the broader paths. The effects of the curve inclination could be easily observed comparing the points (45°, 800) and (90°, 800) in Fig. 7.

V. CONCLUSION AND FUTURE WORK

In this paper, we proposed specific scenarios in order to allow one to analyze the performance of swarm-intelligence distributed based coordination models with local ad hoc communication for swarm of robots. The specific scenarios aim to assess some features presented on swarm robots: (i) contraction and expansion; (ii) segregation and aggregation; and (iii) abrupt changes of direction. We also propose a

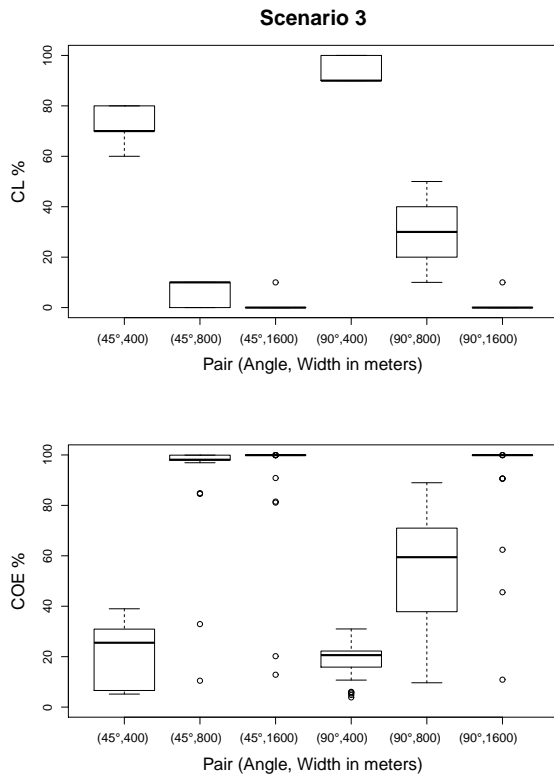


Fig. 7. Analysis of COE and CL in the scenario 3.

metric to analyze the cohesion of the swarm during a mission. We analyzed a recently proposed model based on the Particle Swarm Optimization technique for UAVs coordination regarding Collision and Cohesion. We observed that the main problem is related to collisions when the width is not much more higher than the UAVs collision radius. However, it is important to reanalyze the aforementioned specific scenarios in a three-dimensional model. The proposed model, simulation and prior analysis in this work could assist and support the implementation of system of swarm robots, aiming to identify, verify and validate the previously simulated system behavior.

For future work, we intend to: (i) analyze the behavior of the swarm under different types of scenarios; (ii) improve the current coordination model by including some collaborative skills in the UAVs; (iii) include mechanisms to diminish the energy consumption; (iv) add a health monitoring mechanism in order to allow UAVs to recharge in long missions; and (v) implement more realistic fluid dynamics.

REFERENCES

[1] F. G. Costa, J. Ueyama, T. Braun, G. Pessin, F. S. Osório, and P. A. Vargas, "The use of unmanned aerial vehicles and wireless sensor network in agricultural applications," in *Proceedings of IEEE International Geoscience and Remote Sensing Symposium*. Munich, Alemanha: IEEE, 2012, pp. 5045–5048.

[2] G. Varela, P. Caamamo, F. Orjales, A. Deibe, F. Lopez-Pena, and R. Duro, "Swarm intelligence based approach for real time uav team coordination in search operations," in *Nature and Biologically Inspired Computing (NaBIC), 2011 Third World Congress on*, Oct. 2011, pp. 365–370.

[3] C. J. A. Bastos-Filho, F. B. de Lima Neto, A. J. C. C. Lins, A. I. S. Nascimento, and M. P. Lima, "A novel search algorithm based on fish school behavior," in *2008 IEEE International Conference on Systems, Man, and Cybernetics*. Cingapura: IEEE, Oct. 2008, pp. 2646–2651.

[4] J. Kennedy and R. Eberhart, "Particle swarm optimization," in *Proceedings of IEEE International Conference on Neural Networks*, vol. 4. Perth, Austrália: IEEE, Nov. 1995, pp. 1942–1948.

[5] D. M. P. F. Silva, L. F. F. de Oliveira, M. G. M. Macedo, and C. J. A. B. Filho, "On the analysis of a swarm intelligence based coordination model for multiple unmanned aerial vehicles," in *Robotics Symposium and Latin American Robotics Symposium (SBR-LARS), 2012 Brazilian*, Oct. 2012, pp. 208–213.

[6] Y. Wang, A. Liang, and H. Guan, "Frontier-based multi-robot map exploration using particle swarm optimization," in *Proceedings of IEEE Symposium on Swarm Intelligence*, 2011, pp. 1–6.

[7] A. J. C. Sharkey, "The application of swarm intelligence to collective robots," in *Advances in Applied Artificial Intelligence*. John Fulcher, Idea Group Publishing, 2006, pp. 157–185.

[8] A. Shaw and K. Mohseni, "A fluid dynamic based coordination of a wireless sensor network of unmanned aerial vehicles: 3-d simulation and wireless communication characterization," *Sensors Journal, IEEE*, vol. 11, no. 3, pp. 722–736, Mar. 2011.

[9] J. Riehl, G. Collins, and J. Hespanha, "Cooperative search by uav teams: A model predictive approach using dynamic graphs," *Aerospace and Electronic Systems, IEEE Transactions on*, vol. 47, no. 4, pp. 2637–2656, Oct. 2011.

[10] Q. Zhu, A. Liang, and H. Guan, "A pso-inspired multi-robot search algorithm independent of global information," in *Proceedings of IEEE Symposium on Swarm Intelligence*, 2011, pp. 1–7.

[11] Y. Qu and Y. Zhang, "Cooperative localization against gps signal loss in multiple uavs flight," *Systems Engineering and Electronics, Journal of*, vol. 22, no. 1, pp. 103–112, Feb. 2011.

[12] I. Shames, B. Fidan, B. Anderson, and H. Hmam, "Cooperative self-localization of mobile agents," *Aerospace and Electronic Systems, IEEE Transactions on*, vol. 47, no. 3, pp. 1926–1947, Jul. 2011.

[13] S. Kernbach and O. Kernbach, "Collective energy homeostasis in a large-scale microrobotic swarm," *Robot. Auton. Syst.*, vol. 59, no. 12, pp. 1090–1101, Dec. 2011.

[14] C. Antal, O. Granichin, and S. Levi, "Adaptive autonomous soaring of multiple uavs using simultaneous perturbation stochastic approximation," in *Proceedings of the 49th IEEE Conference on Decision and Control*, Hilton Atlanta Hotel, Atlanta, GA, USA, 2010.

[15] S.-W. Kim and S.-W. Seo, "Cooperative unmanned autonomous vehicle control for spatially secure group communications," *Selected Areas in Communications, IEEE Journal on*, vol. 30, no. 5, pp. 870–882, Jun. 2012.

[16] I. H. Makhdoom and Q. Shi-Yin, "Simultaneous arrival of multiple uavs under imperfect communication," *Aircraft Engineering and Aerospace Technology*, vol. 84, no. 1, pp. 37–50, 2012.

[17] H. M. La and W. Sheng, "Dynamic target tracking and observing in a mobile sensor network," *Robotics and Autonomous Systems*, vol. 60, no. 7, pp. 996–1009, Jul. 2012.

[18] C. Bentes and O. Saotome, "Dynamic swarm formation with potential fields and a* path planning in 3d environment," in *Robotics Symposium and Latin American Robotics Symposium (SBR-LARS), 2012 Brazilian*, Oct. 2012, pp. 74–78.

A Multi-Objective Particle Swarm Optimizer Based on Diversity

Dennis R. C. Silva and Carmelo J. A. Bastos-Filho

University of Pernambuco

Recife, Brazil

Email: carmelofilho@ieee.org

Abstract—This paper presents a novel multi-objective optimization algorithm based on Particle Swarm Optimization (MOPSO-DFR), which uses a global density estimator mechanism called Diversity Factor (DF) to select the cognitive and the social leaders. MOPSO-DFR also uses DF to update and to prune the external archive, whenever it is necessary. We used well known metrics to evaluate the results generated by our proposal in seven widely used benchmark functions. We also compared our approach to other four multi-objective optimization algorithms called MOPSO-CDR, SMPSO, NSGA-II and SPEA-2. The results showed that MOPSO-DFR outperforms the other approaches in most cases.

Keywords—swarm intelligence; particle swarm optimization; multi-objective optimization

I. INTRODUCTION

Multi-objective optimization refers to the simultaneous optimization of two or more conflicting objective functions. For Multi-Objective Optimization Problems (MOPs), it is expected to obtain a set of trade-off solutions in a single run of an optimization algorithm. Besides, MOP with multiple decision variables are often difficult to tackle. Because of this, many approaches have been recently proposed for solving MOP in a faster and more efficient way. Meta-heuristics have been successfully applied to solve MOPs in the last years and most of the recent interesting approaches are based on evolutionary computation or swarm intelligence.

Particle Swarm Optimization (PSO) is one of the most used swarm intelligence algorithms. PSO was proposed by Kennedy and Eberhart in 1995 [1] and it was inspired by the behavior of flocks of birds. In general, PSO is used for solving single objective optimization problems in hyper-dimensional spaces with continuous variables. Due to the simplicity and fast convergence, some approaches based on PSO have been proposed to tackle MOPs. The first Multi-Objective Particle Swarm Optimizer (MOPSO) was proposed in 2002 by Coello Coello *et al* [2]. Since then, many other MOPSO approaches have been proposed. All of them propose to change the policy to select the cognitive and social leaders, that are used to update the velocity of the particles, and/or to define a criterion to update the External Archive (EA), which is used to store the non-dominated solutions obtained along the search process. Santana *et. al* [3] presented the MOPSO-CDR and successfully showed that one can use *Crowding distance* (CD) to select the leaders and to update the EA. They also showed that MOPSO-CDR outperforms some previous approaches, such as *m*-DNPSO [4] and CSS-MOPSO [5]. Nebro *et. al* [6] also

proposed an interesting speed-constrained approach which is also useful for many-objective optimization.

Although there are many proposals presented in the literature, the policies to select the leaders and to update the EA are based on measures that evaluate local features within the EA, such as CD [3]. Recently, Zhan *et al* [7] proposed a global measure to assess the diversity of the whole swarm. We propose here to use this global measure, renamed in this paper as *Diversity factor* (DF), to evaluate the diversity of the solutions within the EA in order to properly select the leaders and to update the EA.

This paper is organized as follow. In Section II, we present some basic concepts on Particle Swarm Optimization and Multi-Objective Optimization. In Section III, we briefly describe some approaches for tackling MOPs. We present our novel MOPSO approach based on the DF in Section IV. In Sections V, we present the simulation setup and some results in well known benchmark functions, including a comparison with MOPSO-CDR, SMPSO and two widely used multi-objective evolutionary computation optimizers (NSGA-II and SPEA-2). In Section VI, we give our conclusions and present some future works.

II. BASIC CONCEPTS

In this section we present basic concepts regarding Particle Swarm Optimization and Multi-objective optimization.

A. Particle Swarm Optimization

Particle Swarm Optimization (PSO) is a stochastic, bio-inspired, population-based global optimization technique [1]. The population is called swarm and the individuals are called particles. Each particle moves within the search space with an adaptive velocity looking for promising regions. Each particle i has four main attributes: the current position in the d -dimensional space $\vec{x}_i = (x_{i1}, x_{i2}, \dots, x_{id})$, the best position found so far in the search process $\vec{p}_i = (p_{i1}, p_{i2}, \dots, p_{id})$, the best position found by its neighborhood so far $\vec{n}_i = (n_{i1}, n_{i2}, \dots, n_{id})$ and the velocity $\vec{v}_i = (v_{i1}, v_{i2}, \dots, v_{id})$. The velocity and the position of every particle are updated iteratively according to the following equations:

$$\vec{v}_i(t+1) = \vec{v}_i(t) + c_1 \cdot r_1 \cdot (\vec{p}_{best} - \vec{x}_i) + c_2 \cdot r_2 \cdot (\vec{n}_{best} - \vec{x}_i), \quad (1)$$

$$\vec{x}_i(t+1) = \vec{x}_i(t) + \vec{v}_i(t+1), \quad (2)$$

where i is the label of the particle, c_1 and c_2 are the cognitive and the social acceleration coefficients, respectively. r_1 and r_2 are two random numbers generated by a uniform distribution in the interval $[0, 1]$.

B. Multi-Objective Optimization

A minimization MOP can be stated as:

$$\text{minimize } \vec{f}(\vec{x}) := [f_1(\vec{x}), f_2(\vec{x}), \dots, f_k(\vec{x})] \quad (3)$$

subject to:

$$g_i(\vec{x}) \leq 0 \quad i = 1, 2, \dots, m, \quad (4)$$

$$h_i(\vec{x}) = 0 \quad j = 1, 2, \dots, p, \quad (5)$$

where $\vec{x} = (x_1, x_2, \dots, x_n) \in \mathbb{R}$ is the vector on the decision search space; and $g_i(\vec{x})$ and $h_j(\vec{x})$ are the constraint functions of the problem.

The best solutions that solves a MOP are called non-dominated solutions. The concept of dominance is given by: given two vectors \vec{x} and \vec{y} , \vec{x} dominates \vec{y} (denoted by $\vec{x} \prec \vec{y}$) if \vec{x} is better than \vec{y} in at least one objective and \vec{x} is not worse than \vec{y} in any objective. \vec{x} is not dominated if does not exist another solution \vec{x}_i in the current population such that $\vec{x}_i \prec \vec{x}$. The set of non-dominated solutions in the objective space found by a particular algorithm trying to solve a MOP is known as Pareto Front.

In order to measure the quality of the Pareto Front obtained by the algorithms, several metrics have been proposed. The following metrics will be used in this paper.

1) *Coverage Set (C)*: is used in order to evaluate the convergence reached by the algorithm [8]. Equation (6) presents how to calculate C using two different Pareto Fronts A and B :

$$C(A, B) = \frac{|\{b \in B; \exists a \in A : a \succ b\}|}{|B|}, \quad (6)$$

where $|B|$ represents the amount of solutions belonging to the Pareto Front B .

If the value $C(A, B) = 1$, all solutions of B are dominated by the solutions of A . On the other hand, if $C(A, B) = 0$, none of the solutions of B are dominated by A .

2) *Spacing (S)*: is used in order to evaluate the distribution of the non-dominated solutions within the Pareto Front. S is calculated according to Equation (7) [9].

$$S = \sqrt{\frac{1}{n-1} \sum_{i=1}^n (\bar{d} - d_i)^2}, \quad (7)$$

where $d_i = \min_j (|f_1^i(\vec{x}) - f_1^j(\vec{x})| + |f_2^i(\vec{x}) - f_2^j(\vec{x})|)$, $i, j = 1, \dots, n$, \bar{d} represents the average distance between all adjacent solutions and n is the number of non-dominated solutions. $S = 0$ means that all non-dominated are equidistant.

3) *Maximum Spread (MS)*: measures the Euclidian distance between the two farthest solutions within the Pareto Front. MS is calculated using Equation (8) [10]:

$$MS = \sqrt{\sum_{m=1}^M (\max_{i=1}^n f_m^i - \min_{i=1}^n f_m^i)^2}, \quad (8)$$

where n is the label of the non-dominated solutions and M is the number of objectives of the problem. High values for MS means that the Pareto Front covers a significant area of the objective space.

4) *Hypervolume (HV)*: is defined by the hypervolume in the objective space covered by the Pareto Front [8]. It is calculated by summing the area formed by the union of all hypercubes, where each hypercube is generated by one of the non-dominated solutions and a reference point in the objective space.

III. RELATED WORK

This section aims to present a brief review of some related work.

A. APSO - Adaptive PSO

APSO was proposed by Zhan *et al* [7] in 2009. APSO is a variation of the PSO that self-adapts the acceleration coefficients and the inertia factor depending on the diversity of the swarm at the current iteration. They proposed to define an evolutionary state for the swarm based on Evolutionary Factor. There are four possible states: Convergence, Escape, Exploration and Exploitation. We used the Evolutionary Factor to define the *Diversity Factor (DF)*, which is used in our proposal (MOPSO-DFR).

B. MOPSO-CDR: Multi-objective PSO Using Crowding Distance and Roulette Wheel

MOPSO-CDR was proposed by Santana *et al* in 2009 [3]. In MOPSO-CDR, particles select the social leaders by using a Roulette Wheel based on CD . The strategy used to update the cognitive leader also uses the dominance criterion and CD when the current position and the current social leader are incomparable. A similar mechanism is used to prune the EA . Non-dominated solutions that present higher CD values, *i.e.* particles in less crowded regions, have more chances to be selected as social leaders.

C. SMPSO: Speed-constrained Multi-objective PSO

SMPSO [6] incorporates a constriction mechanism in order to limit the maximum velocity of particles and enhance the search capability of the algorithm. SMPSO also have an EA , but does not use roulette wheel to select the social leaders. The cognitive leader is just updated if it dominates the current position. Moreover, SMPSO uses a speed-constriction approach proposed originally by Clerc and Kennedy [11] and bounds the accumulated velocity [6].

D. NSGA-II - Nondominated Sorting Genetic Algorithm II

NSGA-II is a very well known and widely used evolutionary algorithm for tackling multi-objective problems proposed by Deb *et al* in 2002 [12]. The most important feature of NSGA-II is that it uses a fast non-dominated sorting mechanism and *CD* for comparing the quality of the solutions. NSGA-II uses dominance ranking to classify the population into a number of layers, since NSGA-II does not use an *EA*. The truncation of the population for the next generation uses *CD* to define which individuals are better within the same layer.

E. SPEA-2 - Strength Pareto Evolutionary Algorithm

SPEA-2 is a multi-objective evolutionary algorithm proposed by Zitzler *et al* in 2001 [13]. SPEA2 uses elitism and *EA*. The non-dominated solutions in the *EA* are ranked according to a strength rule based on dominance. It presents a good performance since it differentiates the quality of the solution within the *EA*.

IV. MOPSO-DFR: MULTI-OBJECTIVE PSO USING DIVERSITY FACTOR AND ROULETTE WHEEL

In this section we introduce our contribution, which aims to obtain a better convergence in MOPs. We name our proposal as Multi-objective Particle Swarm Optimization using Diversity Factor and Roulette Wheel (MOPSO-DFR).

We propose here a diversity estimator, called *Diversity Factor (DF)*. *DF* is used to select the cognitive and social leaders, and to update and prune the *EA* as well. *DF* is based on the Evolutionary Factor used in the APSO algorithm [7]. In order to calculate the *DF*, one needs to calculate the average distance from the particle *i* to the other particles within the Pareto Front using Equation (9).

$$d_i = \frac{1}{N-1} \sum_{j=1, j \neq i}^N \sqrt{\sum_{k=1}^M (x_i^k - x_j^k)^2}, \quad (9)$$

where *N* is the number of the particles of the Pareto Front and *M* is the number of objectives of the problem.

After this, one can calculate *DF* for each particle within the *EA* by using Equation (10).

$$DF_i = \frac{d_i - d_{min}}{d_{max} - d_{min}}, \quad (10)$$

where *DF_i* is the *DF* of the particle *i*, *d_i* is the average distance of particle *i* to the other particles, *d_{max}* and *d_{min}* are, respectively, the maximum and minimum average distances. One can observe that *DF* is a global estimator of diversity within the Pareto Front.

A. Cognitive Leader Selection

The cognitive leader selection process is crucial for the convergence and efficiency of the algorithm. We propose here a similar strategy to the one used in MOPSO-CDR. In our approach we use *DF*, instead of *CD*. We update \vec{P}_{best} if the current position of the particle dominates \vec{P}_{best} . If they are

non-dominated, the selection is performed using the *EA*. The two nearest solutions from the current position and \vec{P}_{best} are found in the *EA*. After this, we check which one presents the higher *DF*. If the nearest solution from the current position has the higher *DF* value, \vec{P}_{best} is updated to the current position, otherwise \vec{P}_{best} remains.

B. Social Leader Selection

The social leader selection mechanism affects the convergence capability and the distribution of the solutions along the Pareto Front. The MOPSO-DFR algorithm selects the social leader from the *EA* using a roulette wheel with the *DF* of each particle as the sorting criterion.

C. External Archive Pruning

In each iteration we include all new non-dominated solutions in the *EA* and remove the solutions that became dominated. It is common to limit the number of solutions in the *EA*. In order to avoid to exceed the maximum number of solutions in the *EA*, we sort the solutions according to the *DF* value and discard the worst non-dominated.

D. Novel Update Velocity Equation

We proposed to include a fourth term in the equation used in the MOPSO-CDR [3] to update the velocity of the particles. The modified equation is given by:

$$\begin{aligned} \vec{v}_i(t+1) = & \vec{v}_i(t) + c_1 \cdot r_1 \cdot (\vec{p}_{best} - \vec{x}_i) \\ & + c_2 \cdot r_2 \cdot (\vec{n}_{best_{DF}} - \vec{x}_i) + c_3 \cdot r_3 \cdot (\vec{n}_{best_{CD}} - \vec{x}_i), \end{aligned} \quad (11)$$

where $\vec{n}_{best_{DF}}$ is selected based on *DF* and $\vec{n}_{best_{CD}}$ is selected based on *CD* as in [3]. *c₃* is the acceleration coefficient associated to this new leader, *r₃* is a random number generated in the interval [0, 1].

V. SIMULATION SETUP, RESULTS AND DISCUSSION

A. Simulation setup

For MOPSO-DFR and MOPSO-CDR, we used a constant mutation rate equal to 0.5 and the inertia factor linearly decreasing from 0.4 to 0. For the SMPSO, the acceleration coefficients are randomly chosen in the interval [1.5, 2.5] and the mutation rate is equal to 0.166. For NSGA-II and SPEA-2, we used the crossover rate and the mutation rate equal to 1.0 and 0.05, respectively. We used 100 particles (or individuals) for all algorithms and the maximum number of non-dominated solutions in the *EA* equal to 100. We run 300,000 fitness function evaluations.

We used a widely used set of benchmark functions called DTLZ, which was proposed by Deb *et al* [14] in 2005. We used the following functions: DTLZ-1, DTLZ-2, DTLZ-3, DTLZ-4, DTLZ-5, DTLZ-6 and DTLZ-7.

All tables presented in the paper shows the average value and the (standard deviation) after 30 trials. The best results are bolded to facilitate the visualization.

B. Parametric analysis

Since we are proposing to include a fourth term in the equation used to update the velocity, it is necessary to perform a parametric analysis. Thus, we executed simulations using several different sets of configurations for the acceleration coefficients. These configurations for the acceleration coefficients are shown in Table I. One can observe that we almost do not vary the values of c_1 . We decided to not vary it significantly since the major change in the algorithm regards on the social leaders selection. For the values of c_2 and c_3 , we considered the combination of fractions of the original value of c_2 used for the MOPSO-CDR.

TABLE I. ACCELERATION COEFFICIENT CONFIGURATIONS ASSESSED FOR THE MOPSO-DFR.

	c_1	c_2	c_3
MOPSO-DFR-A	1, 49445	1, 49445	1, 49445
MOPSO-DFR-B	1, 49445	1, 49445	0, 0
MOPSO-DFR-C	0, 9963	0, 9963	0, 9963
MOPSO-DFR-D	1, 49445	0, 74722	0, 74722
MOPSO-DFR-E	1, 49445	0, 96966	0, 48483
MOPSO-DFR-F	1, 49445	0, 48483	0, 96966
MOPSO-DFR-G	1, 49445	1, 93932	0, 96966
MOPSO-DFR-H	1, 49445	0, 96966	1, 93932

Table II shows the simulation results for all MOPSO-DFR configurations for the DTLZ-1 problem. One can observe that the Coverage for MOPSO-DFR-A outperformed the other configurations (the results are slightly better when compared to MOPSO-DFR-G and MOPSO-DFR-H). This means that the Pareto Front generated by configuration MOPSO-DFR-A dominates the Pareto Fronts obtained by the other configurations.

We also analyzed one case without the CD -based social leader (MOPSO-DFR-B), *i.e.* $c_3 = 0$. MOPSO-DFR-B obtained good results, but MOPSO-DFR-A outperformed it. Therefore, it indicates that it might be useful to use both CD and DF in the equation to update the velocity of the particles.

One can also observe that MOPSO-DFR-F achieved a better S , but MOPSO-DFR-A achieved better results than MOPSO-DFR-F for MS and HV . MOPSO-DFR-G achieved a better HV , but MOPSO-DFR-A achieved better results than MOPSO-DFR-G for S and MS .

We observed for DTLZ-2 and DTLZ-3 functions a similar behavior when compared to DTLZ-1. Thus, we selected the MOPSO-DFR-A configuration for further simulations. From this point, we will call MOPSO-DFR-A as MOPSO-DFR.

C. Comparison with other Multi-objective algorithms

This subsection aims to compare MOPSO-DFR to previous proposed multi-objective optimizers, MOPSO-CDR, SMPSO, NSGA-II and SPEA-2. Table III, IV, V, VI, VII, VIII and IX show the results for DTLZ-1, DTLZ-2, DTLZ-3, DTLZ-4, DTLZ-5, DTLZ-6 and DTLZ-7, respectively, in terms of C , S , MS and HV .

One can observe that our proposal obtained better results in terms of C for most cases. For the DTLZ-3, the MOPSO-CDR achieved slightly better results in terms of coverage when compared to MOPSO-DFR, but one must observe that the difference is small when compared to the standard deviation. For the DTLZ-6, the MOPSO-CDR achieved the best results

TABLE II. COMPARISON OF DIFFERENT VERSIONS OF MOPSO-DFR FOR DTLZ-1 WITH 300,000 FITNESS EVALUATIONS.

Alg.	S	MS	HV	C(DFR-A,*)	C(*,DFR-A)
MOPSO-DFR-A	7.326 (2.860)	121.205 (10.559)	0.411 (0.104)	-	-
MOPSO-DFR-B	4.153 (4.115)	63.030 (45.028)	0.425 (0.134)	0.791 (0.104)	0.070 (0.123)
MOPSO-DFR-C	6.314 (5.411)	79.263 (46.465)	0.512 (0.149)	0.811 (0.266)	0.092 (0.151)
MOPSO-DFR-D	4.351 (4.406)	64.6481 (45.310)	0.556 (0.121)	0.898 (0.190)	0.042 (0.091)
MOPSO-DFR-E	4.879 (3.675)	75.744 (45.903)	0.596 (0.107)	0.845 (0.250)	0.074 (0.150)
MOPSO-DFR-F	4.147 (5.329)	59.542 (42.085)	0.514 (0.124)	0.897 (0.213)	0.045 (0.122)
MOPSO-DFR-G	8.852 (4.313)	117.67 (12.874)	0.341 (0.134)	0.406 (0.224)	0.321 (0.234)
MOPSO-DFR-H	8.828 (4.959)	119.67 (14.010)	0.361 (0.121)	0.378 (0.266)	0.370 (0.247)

TABLE III. SIMULATION RESULTS FOR DTLZ-1 WITH 300.000 FITNESS FUNCTION EVALUATIONS.

Alg.	S	MS	HV	C(DFR,*)	C(*,DFR)
MOPSO-DFR	7,326 (2,859)	121,205 (10,559)	0,411 (0,105)	-	-
MOPSO-CDR	6,962 (4,717)	91,745 (35,343)	0,458 (0,139)	0,753 (0,248)	0,090 (0,151)
SMPSO	0,002 (0,001)	2,0 (0,002)	0,494 (9,1E-05)	1,0 (0,0)	0,0 (0,0)
NSGA-II	0,007 (0,001)	2,004 (0,004)	0,494 (3E-04)	1,0 (0,0)	0,0 (0,0)
SPEA-2	0,113 (0,493)	3,526 (6,870)	0,533 (0,119)	1,0 (0,0)	0,0 (0,0)

in terms of coverage when compared to MOPSO-DFR. Again for the DTLZ-6, the NSGA-II achieved slightly better results in terms of coverage when compared to MOPSO-DFR, but one must observe that the difference is small when compared to the standard deviation.

It is also important to notice that the MOPSO-DFR did not achieve the best results for the S , but it achieved the best results for the MS in most of the cases. This indicates that our approach is reaching more extreme solutions and converging for the optimum Pareto simultaneously when compared to the other algorithms.

VI. CONCLUSION AND FUTURE WORK

This paper proposed a novel multi-objective particle swarm-based optimizer based on a measure of diversity of the whole swarm. The selection of the cognitive and social leaders is performed using a new measure called Diversity Factor (DF). DF is also used to update and prune the External Archive (EA), which is used to store the non-dominated solutions found during the search process so far.

TABLE IV. SIMULATION RESULTS FOR DTLZ-2 WITH 300.000 FITNESS FUNCTION EVALUATIONS.

Alg.	S	MS	HV	C(DFR,*)	C(*,DFR)
MOPSO-DFR	0.041 (0.009)	1.017 (0.005)	0.187 (0.006)	-	-
MOPSO-CDR	0.001 (1E-04)	1.0 (4E-08)	0.211 (1E-05)	0.961 (0.037)	0.0 (0.0)
SMPSO	0.002 (2E-04)	1.0 (4E-05)	0.210 (6E-05)	0.960 (0.036)	0.0 (0.0)
NSGA-II	0.007 (6E-04)	1.001 (0.005)	0.211 (0.008)	0.953 (0.048)	0.0 (0.0)
SPEA-2	0.003 (3E-04)	1.001 (0.001)	0.212 (0.002)	0.953 (0.049)	0.0 (0.0)

TABLE V. SIMULATION RESULTS FOR DTLZ-3 WITH 300.000 FITNESS FUNCTION EVALUATIONS.

Alg.	<i>S</i>	<i>MS</i>	<i>HV</i>	C(DFR,*)	C(*,DFR)
MOPSO DFR	42.289 (12.110)	187.997 (10.405)	0.127 (0.044)	-	-
MOPSO CDR	33.916 (22.403)	208.675 (19.646)	0.174 (0.067)	0.276 (0.294)	0.451 (0.299)
SMPSO	3.793 (5.758)	18.498 (26.729)	0.335 (0.279)	1.0 (0.0)	0.0 (0.0)
NSGA-II	0.028 (0.043)	1.489 (0.608)	0.263 (0.112)	1.0 (0.0)	0.0 (0.0)
SPEA-2	0.069 (0.158)	1.473 (0.590)	0.298 (0.168)	1.0 (0.0)	0.0 (0.0)

TABLE VI. SIMULATION RESULTS FOR DTLZ-4 WITH 300.000 FITNESS FUNCTION EVALUATIONS.

Alg.	<i>S</i>	<i>MS</i>	<i>HV</i>	C(DFR,*)	C(*,DFR)
MOPSO DFR	0.116 (0.031)	1.020 (0.007)	0.131 (0.018)	-	-
MOPSO CDR	0.002 (3E-04)	1.0 (2E-07)	0.210 (2E-04)	0.804 (0.140)	0.0 (0.0)
SMPSO	0.0018 (4E-04)	1.0 (3E-04)	0.211 (5E-04)	0.808 (0.136)	0.0 (0.0)
NSGA-II	0.0064 (0.002)	0.801 (0.40)	0.169 (0.085)	0.846 (0.140)	0.002 (0.010)
SPEA-2	0.0032 (0.001)	0.733 (0.442)	0.170 (0.104)	0.833 (0.155)	0.0 (0.0)

TABLE VII. SIMULATION RESULTS FOR DTLZ-5 WITH 300.000 FITNESS FUNCTION EVALUATIONS.

Alg.	<i>S</i>	<i>MS</i>	<i>HV</i>	C(DFR,*)	C(*,DFR)
MOPSO DFR	0.034 (0.008)	1.026 (0.005)	0.186 (0.006)	-	-
MOPSO CDR	0.001 (2E-04)	1.008 (3E-08)	0.211 (2E-05)	0.962 (0.051)	0.0 (0.0)
SMPSO	0.002 (3E-04)	1.008 (2E-05)	0.210 (7E-05)	0.961 (0.053)	0.0 (0.0)
NSGA-II	0.007 (6E-04)	1.009 (0.003)	0.211 (0.004)	0.953 (0.064)	0.0 (0.0)
SPEA-2	0.003 (3E-04)	1.009 (0.005)	0.213 (0.007)	0.954 (0.065)	0.0 (0.0)

TABLE VIII. SIMULATION RESULTS FOR DTLZ-6 WITH 300.000 FITNESS FUNCTION EVALUATIONS.

Alg.	<i>S</i>	<i>MS</i>	<i>HV</i>	C(DFR,*)	C(*,DFR)
MOPSO DFR	0.029 (0.008)	1.012 (0.009)	0.191 (0.005)	-	-
MOPSO CDR	0.196 (0.097)	1.638 (0.232)	0.180 (0.056)	0.0 (0.0)	0.993 (0.037)
SMPSO	0.001 (2E-04)	1.008 (4E-16)	0.211 (3E-05)	0.843 (0.064)	0.002 (0.005)
NSGA-II	0.011 (0.003)	1.040 (0.035)	0.494 (3E-04)	0.361 (0.350)	0.406 (0.388)
SPEA-2	0.013 (0.019)	1.086 (0.119)	0.278 (0.103)	0.541 (0.325)	0.205 (0.260)

TABLE IX. SIMULATION RESULTS FOR DTLZ-7 WITH 300.000 FITNESS FUNCTION EVALUATIONS.

Alg.	<i>S</i>	<i>MS</i>	<i>HV</i>	C(DFR,*)	C(*,DFR)
MOPSO DFR	0.018 (0.012)	0.637 (0.045)	0.290 (0.054)	-	-
MOPSO CDR	0.001 (2E-04)	0.745 (5E-04)	0.335 (8E-04)	0.458 (0.103)	0.0 (0.0)
SMPSO	0.001 (1E-04)	0.745 (4E-04)	0.334 (4E-04)	0.665 (0.104)	0.0 (0.0)
NSGAI	0.005 (5E-04)	0.745 (0.001)	0.334 (0.002)	0.657 (0.106)	0.0 (0.0)
SPEA2	0.004 (4E-04)	0.745 (4E-04)	0.334 (7E-04)	0.698 (0.091)	0.0 (0.0)

Simulation results showed that MOPSO-DFR converged to Pareto Fronts that dominate Pareto Fronts obtained by well known multi-objective optimization algorithms in most of the functions of a widely used set of benchmark functions. The results shows that our proposal can reach more extreme solutions while converging for the optimum Pareto simultaneously.

We believe that we achieved better results because the *DF* is a global density estimator that helps to properly select the leaders and to prune the *EA*.

We did not achieve the best result for the DTLZ-6 function. Our hypothesis for this case is that MOPSO-DFR converges too fast to a local optimum and gets trapped at this local minimum. We intend to analyze in details what happened for the DTLZ-6 function in order to propose improvements for the MOPSO-DFR. We believe it can help to improve the spacing (*S*) of the non-dominated solutions.

ACKNOWLEDGMENT

The authors would like to thank the Polytechnic School of the University of Pernambuco, FACEPE, CNPq and FINEP.

REFERENCES

- [1] J. Kennedy and R. C. Eberhart, "Particle swarm optimization," in *Proceedings of IEEE International Conference on Neural Networks*. IEEE, 1995, pp. 1945–1948.
- [2] C. A. C. Coello and M. S. Lechuga, "MOPSO: A proposal for multiple objective particle swarm optimization," in *Proceedings of the Congress on Evolutionary Computation (CEC 2002)*, vol. 2. Honolulu, HI, EUA: IEEE, 2002, pp. 1051–1056.
- [3] R. A. Santana, M. R. Pontes, and C. J. A. Bastos-Filho, "A multiple objective particle swarm optimization approach using crowding distance and roulette wheel," in *ISDA '09: Proceedings of the 2009 Ninth International Conference on Intelligent Systems Design and Applications*. IEEE, 2009, pp. 1–5.
- [4] X. Hu, R. Eberhart, and Y. Shi, "Particle swarm with extended memory for multiobjective optimization," in *Swarm Intelligence Symposium, 2003. SIS'03. Proceedings of the 2003 IEEE*, 2003, pp. 193–197.
- [5] S.-Y. Chiu, T.-Y. Sun, S.-T. Hsieh, and C.-W. Lin, "Cross-searching strategy for multi-objective particle swarm optimization," in *IEEE Congress on Evolutionary Computation*. IEEE, 2007, pp. 3135–3141.
- [6] A. J. Nebro, J. J. Durillo, J. García-Nieto, C. A. Coello Coello, F. Luna, and E. Alba, "SMPSO: A New PSO-based Metaheuristic for Multi-objective Optimization," in *IEEE Symposium on Computational Intelligence in Multicriteria Decision-Making (MCDM 2009)*, 2009, pp. 66–73.
- [7] Z.-H. Zhan, J. Zhang, Y. Li, and H. S.-H. Chung, "Adaptive particle swarm optimization," *IEEE Transactions on Systems, Man and Cybernetics, Part B*, vol. 39, no. 6, pp. 1362–1381, Dec. 2009. [Online]. Available: <http://dx.doi.org/10.1109/TSMCB.2009.2015956>
- [8] E. Zitzler, "Evolutionary algorithms for multiobjective optimization: Methods and applications," PHD Thesis, ETH Zurich, Switzerland, 1999.
- [9] J. L. Risco-Martín, S. Mittal, D. Atienza, J. I. Hidalgo, and J. Lanchares, "Optimization of dynamic data types in embedded systems using devts/soa-based modeling and simulation," in *InfoScale '08: Proceedings of the 3rd international conference on Scalable information systems*. ICST (Institute for Computer Sciences, Social-Informatics and Telecommunications Engineering), 2008, pp. 1–11.
- [10] E. Zitzler and L. Thiele, "Multiobjective evolutionary algorithms: a comparative case study and the strength Pareto approach," *IEEE transactions on Evolutionary Computation*, vol. 3, no. 4, pp. 257–271, 1999.
- [11] M. Clerc and J. Kennedy, "The particle swarm - explosion, stability, and convergence in a multidimensional complex space," *IEEE Transactions on Evolutionary Computation*, vol. 6, no. 1, pp. 58–73, 2002. [Online]. Available: <http://dx.doi.org/10.1109/4235.985692>

- [12] K. Deb, A. Pratap, S. Agarwal, and T. Meyarivan, "A fast and elitist multiobjective genetic algorithm: NSGA-II," *IEEE Transactions on Evolutionary Computation*, vol. 6, no. 2, pp. 182–197, 2002.
- [13] E. Zitzler, M. Laumanns, and L. Thiele, "SPEA2: Improving the strength pareto evolutionary algorithm for multiobjective optimization," in *Evolutionary Methods for Design Optimization and Control with Applications to Industrial Problems*. International Center for Numerical Methods in Engineering, 2001, pp. 95–100.
- [14] K. Deb, L. Thiele, M. Laumanns, and E. Zitzler, "Scalable test problems for evolutionary multiobjective optimization," in *Evolutionary Multiobjective Optimization*, ser. Advanced Information and Knowledge Processing, A. Abraham, L. Jain, and R. Goldberg, Eds. Springer London, 2005, pp. 105–145.

A new Heuristic of Fish School Segregation for Multi-Solution Optimization of Multimodal Problems

Marcelo Gomes Pereira de Lacerda, Fernando Buarque de Lima Neto
 Polytechnic School of Pernambuco
 University of Pernambuco
 Recife, Brazil
 mgpl@ecom.poli.br, fbln@ecom.poli.br

Abstract—This work presents a new heuristic for fish school segregation applied to the Fish School Search algorithm (FSS), aiming to serve as a basis for the creation of a new multi-solution optimization method for multimodal problems. In this new approach, the weight of the fish is used as a population segregation element, allowing the heaviest fishes, i.e. the most successful ones, to swim, i.e. to move in the search space, more independently and the lightest ones to be guided by the heaviest ones. The obtained results showed that this new approach is able to find a good amount of solutions in the search space, overcoming the three techniques used for comparison in 6 of 7 benchmark functions. Moreover, it can be seen that the new approach requires less computational effort to obtain excellent results. Another advantage of the new approach is that there is no need for an addition of operators in the original FSS. Even though this new version of multimodal FSS does not have an ideal coverage, which causes the return of many “extra” solutions, the sole use of the weight of the fishes, i.e. a readily available information, as a population segregation operator is an economical and good alternative to be considered upon multi-solution problems. This specially taking into account the expediency of the method and that the detected candidate solutions are mostly false-positives, which can be more easily pruned than the addition of false-negatives.

Keywords—Heuristic Search; Multi-Solution Optimization; Multimodal Problems; Fish School Search.

I. INTRODUCTION

Optimization tasks are present in many situations where information technology is required. Managers, for example, must take decisions aiming to maximize the company’s income, but there are multiple ways for that to be achieved. Racing car teams use their resources in a way which the car endures the least damaged possible, and this can be pursued by various different ways. These are just simple real life examples where multi-model optimization tasks are required. Formally, optimization is defined as a system adjustment aiming to obtain the best possible output. However, in many cases, a “good” result is fair enough [1], not alone, the only possible.

Optimization problems can be classified in many different ways: according to the number of variables and their types, according to the linearity level of the objective function, the dynamicity of this function, the existence or not of constraints, the number of objective function and, finally, the number of optimal solutions. According to the number of optimal solutions, optimization problems can be classified as unimodal or multimodal. Unimodal problems are characterized as problems with only one global optimal solution. Multimodal

problems are, thus, characterized by the existence of more than one global optimal solution, the objective function. Considering only minimization cases, multimodal optimization problems can be defined as the search process for all the local optimum x_L^* (solutions) in the function f as defined by (1), where L is the closest region to x_L^* and \mathbb{R}^n is an n-dimensional real numbered search space [1].

$$f(x_L^*) \leq f(x), \forall x \in L, L \subset \mathbb{R}^n \quad (1)$$

Multimodal problems occur in many different fields, such as geophysics, electromagnetism, climatology and logistics [2].

Optimization algorithms are computational techniques that search for solutions for a certain problem, this represented by an objective function. Several nature inspired methods have been developed in order to tackle the multitude of available problems. A successful set of these techniques are known as population based algorithms (PBA), due to their characteristics of using a group of artificial entities to collectively and in a coordinated way perform the search.

Swarm Intelligence (SI), the most prominent of PBA for searching, can be viewed as a system in which the interaction between the very simple particles of the population generates complex functional patterns [3]. Some of the best known algorithms within SI are: Particle Swarm Optimization (PSO) [4], Ant Colony Optimization (ACO) [5], Artificial Bee Colony (ABC) [6], Bacterial Foraging Algorithm (BFA) [7] and Fish School Search (FSS) [8].

Fish School Search (FSS), which was proposed by Bastos et al. [8], is, in its basic version, an unimodal optimization algorithm inspired on the collective behavior of fish schools. The mechanisms of feeding and coordinated movement, which provides protection to every fish within the swarm against external predators, were used as inspiration to create the collective search mechanism. The main idea is to make the fishes (individuals) to swim toward the direction of the positive gradient in order to gain weight. Collectively, the heavier fishes are more influent in the search process as a whole as the barycenter of the school gradually moves towards better places in the search space.

Niching algorithms are a special member of the SI family that were developed in order to solve multimodal problems, finding multiple solutions at the same time. Some of the

existent niching techniques are the CPSO (Craziness PSO) [9], Multi_PSOer (Multi_Optimizer PSO) [10], NichePSO [11], GSO (Glowworm Swarm Optimization), the latter an SI algorithm based on the social behavior of the glowworms [12].

Density based Fish School Search (dFSS) is another niching algorithm based on the FSS proposed by Madeiro et al. [2]. It tackles multimodal problems elegantly using the concept of food sharing, rather than single fish foraging. The nearby fishes influence and group up around each other along the search process, which leads to the splitting of the whole swarm into sub-swarms. This makes possible the sought detection of multiple solutions. The major problem of that approach is the addition of two new operators onto the original FSS and, consequently, a substantial additional computational cost to the search process.

The current paper proposes another heuristic for the original FSS as an attempt to create a new multimodal version of the algorithm, trying to overcome the necessity of additional operators. In this new approach, the weight of the fishes themselves determine the relations between fishes and consequent strength of the mutual influence among each other. The rationale is simple yet creative: the higher is the difference between the weights of two fishes, the higher is the probability of existing a relation between them and the stronger is the influence from the heavier onto the lighter. This devised mechanism leads to school segregation fulfilling the scope of multiple optimization tasks.

In Section II and Section III, FSS and dFSS Algorithms are detailed, respectively. Section IV introduced the new segregation method based on the weight of fishes. Section V details the experiments whose results are presented in Section VI. And in Section VII conclusions and future works are presented.

II. FISH SCHOOL SEARCH

Fish School Search is inspired by the collective behavior of natural fish schools. In nature, many species live in groups, in order to increase their chances to survive to external threats and also to forage more effectively. In fish schools, the individuals work collectively as a single organism but do possess some local freedom. This combination accounts for fine as well as greater granularities during their search for food.

In FSS, the success of the search process is represented by the weight of each fish. In other words, the heavier is an individual, the better is its represented solution. The weight of the fish is updated throughout the feeding process. A second means to encode success in FSS is the radius of the school. The mechanism to update this is explained in the following subsections together with the other operators. But in advance it is noteworthy to mention that by contracting or expanding the radius of the school FSS can automatically switches between exploitation and exploration, respectively. The pseudo-code of FSS is provided in Fig. 1. Other details such as stopping conditions and minor variations to increase performance are left out as they are not important here.

```

P: Fish population;
while Stopping condition is not met do:
  for each fish in P do:
    Run the individual movement;
  for each fish in P do:
    Run the feeding process;
  for each fish in P do:
    Run the collective instinctive movement;
    Calculate the fish school's barycenter;
  for each fish in P do:
    Run the collective volitive movement;
Return the best solution found;

```

Figure 1. Pseudo-code of FSS.

A. Individual Movement Operator

In the Individual Movement Operator, each fish moves randomly and independently, but toward the positive gradient. In other words, this operator is executed only if the new position is better than the previous one, with regards to the objective function. This movement is described by (2), where $x_{ij}(t+1)$ is the new value of the dimension j in the position vector of the individual i , $x_{ij}(t)$ is the old value, r is a random value between 0 and 1 and $step_{ind}(t)$ is the step size on time t . The new step size is calculated through (3), where $step_{ind_{init}}$ and $step_{ind_{final}}$ are the initial and final step sizes and $iterations$ is the maximum number of iterations.

$$x_{ij}(t+1) = x_{ij}(t) + r \cdot step_{ind}(t), \quad (2)$$

$$step_{ind}(t+1) = step_{ind}(t) - \frac{step_{ind_{init}} - step_{ind_{final}}}{iterations}. \quad (3)$$

B. Feeding Operator

As mentioned before, the feeding operator is responsible for the weight update of all fishes, which is made accordingly with the *fitness* increase obtained after the individual movement. This update process is defined by (4), where Δf_i is the fitness variation after the Individual Movement of the fish i , and $\max(\Delta f)$ is the maximum fitness variation in the whole population.

$$W_i(t+1) = W_i(t) + \frac{\Delta f_i}{\max(\Delta f)}. \quad (4)$$

C. Collective Instinctive Movement Operator

The Collective Instinctive Movement Operator is the first collective movement in the algorithm. A single vector is computed as a vectorial average of all individual movements and added to the position vector of all fish. This operator is defined by (5), where N is the population size, Δx_k and $\Delta f(x_k)$ is the position variation and the fitness variation of the individual of index k in the Individual Movement.

$$x_{ij}(t+1) = x_{ij}(t) + \left(\frac{\sum_{k=1}^N \Delta x_{kj} \Delta f(x_k)}{\sum_{k=1}^N \Delta f(x_k)} \right). \quad (5)$$

D. Collective Volitive Movement Operator

In this step, the population must contract or expand, using as reference the barycenter of the fish school, which is calculated according to (6), where $W_i(t)$ is the weight of the fish i on time t . The total weight of the whole population must be calculated in order to decide if the fish school will contract or expand. If the total weight increased after the last Individual Movement, the school as a whole will contract in order to execute a finer search, as it means that the search process has been successful. Otherwise, the population will expand, meaning that the search process is not qualitatively improving. This could be due to a bad region of the search space or the school is trapped in a local minimum (hence, it should try to scape from it). The contraction and expansion processes are defined by (7) and (8), respectively, where

$$B_j(t) = \frac{\sum_{i=1}^N x_{ij} W_i(t)}{\sum_{i=1}^N W_i(t)}, \quad (6)$$

$$x_{ij}(t+1) = x_{ij}(t) - step_{vol} rand(0,1) \frac{(x_{ij}(t) - B_j(t))}{distance(x_i(t), B_j(t))}, \quad (7)$$

$$x_{ij}(t+1) = x_{ij}(t) + step_{vol} rand(0,1) \frac{(x_{ij}(t) - B_j(t))}{distance(x_i(t), B_j(t))}. \quad (8)$$

III. DENSITY BASED FISH SCHOOL SEARCH

The dFSS is an FSS based multi-solution optimization algorithm for multimodal problems. In it, the food found by any fish during the search process is shared among "peers". Moreover, each fish stores the amount of food given by others. Using this information, each fish decides to which ones it will be linked in order to establish sub-populations. In dFSS the operator resemble FSS, but the collective movements are made in a way that the sub-populations explore in parallel many different niches [2]. The pseudo-code of dFSS is provided in Fig. 2.

Two operators were added to the ones existing in the original FSS in order to create the multimodal version. They are: the Memory Operator and the Operator for Partitioning the Main Fish School. Some adjustments were made to all the already existent operators of the FSS to account for the various sub-swarm (and not only one anymore). The operators are described next.

A. Individual Movement

The Individual Movement mechanism remains almost the same, but individual step size update method was changed. It is calculated by (9), (10), (11) and (12), where $step_{ind_i}(t)$ is the individual step of the fish i , $decay_{min}$ is the minimum decay rate, $decay_{max_{final}}$ and $decay_{max_{ini}}$ are the final and initial max decay rate, respectively, T_{max} is the maximum number of iterations, q_{ij} is the number of fishes that lie between the fishes i and j , including the fish i and $d_{R_{jk}}$ is the relative distance between the fishes j and k . In other words, $d_{R_{jk}} = \frac{d_{jk}}{\min(d_{ij})}$, where j represents any other fish different from i .

$$step_{ind_i}(t+1) = decay_i(t) * step_{ind_i}(t), \quad (9)$$

$$decay_i = decay_{min} - \left(\frac{R_i(t) - \min(R_j(t))}{\max(R_j(t)) - \min(R_j(t))} \right) (decay_{min} - decay_{max}(t)), \quad (10)$$

$$decay_{max}(t) = decay_{max_{ini}} \left(\frac{decay_{max_{final}}}{decay_{max_{ini}}} \right)^{\frac{t}{T_{max}}}, \quad (11)$$

$$R_i(t) = \sum_{j=1}^Q \frac{\Delta f_i}{(d_{R_{ij}})^{q_{ij}} \sum_{k=1}^N \frac{1}{(d_{R_{jk}})^{q_{jk}}}}. \quad (12)$$

```

The fishes are initialized;
The fitnesses of the fishes are calculated;
The distances between the fishes are calculated;
while Stopping criteria is not met:
    for each Fish in the population do:
        Run the Individual Movement;
        if The fish's fitness increased then:
            for each Fish in the population do:
                Run the feeding operator;
                Update the fish's weight;
                Run the memory operator;
            for each Fish in the population do:
                Run the Collective Instinctive Movement;
                Determine the most influent fish for the given fish;
                Run the division of the main population process;
            for each Generated sub-population do:
                Calculate the barycenter;
            for each Fish in the population do:
                Update the Individual Movement step size;
                Run the Volitive Collective Movement of the fish;
                Calculate the fitness for each fish in the population;
                Calculate the distances between the fishes;
                Update the value of the variable decay_max(t);
    Returns the best individual of each sub-population formed
    in the last iteration as the solutions located by the
    algorithm;
    
```

Figure 2. Pseudo-code of dFSS.

B. Feeding Operator

In the dFSS, the fishes share their food. The amount of food shared by the fish i to the fish j is defined by (13), which is very similar to (12).

$$C(i, j) = \frac{\Delta f_i}{(d_{R_{ij}})^{q_{ij}} \sum_{k=1}^N \frac{1}{(d_{R_{jk}})^{q_{jk}}}}. \quad (13)$$

C. Memory Operator (new to original FSS)

The memory for all fishes has the role of storing with which ones they have shared more food in the past. For fish i , the bigger is the amount of food M_{ij} shared by the fish j , the bigger is the influence of j upon i . The memory of an individual i is represented by a vector $M_i = \{M_{i1}, M_{i2}, \dots, M_{iN}\}$, where N is the number of fishes in the population. In (14), the food sharing process is defined, where $\rho \in [0, 1]$.

$$M_{ij}(t+1) = (1 - \rho)M_{ij}(t) + C(j, i). \quad (14)$$

D. Collective Instinctive Movement

In the Collective Instinctive Movement of the original FSS, all the fishes move to the same direction. In the dFSS, each fish calculates its own direction according to the most influential fishes within its own sub-swarm (the fishes connected to it), as described by (15).

$$x_{ij}(t+1) = x_{ij}(t) + \left(\frac{\sum_{k=1}^N \Delta x_{kj} M_{ik}(t)}{\sum_{k=1}^N M_{ik}(t)} \right). \quad (15)$$

E. Operator for Partitioning the School (new to original FSS)

This operator is responsible for the partitioning of the main fish school into smaller ones. A fish i is part of the same fish school of the fish j if and only if i is the most influent fish for j or j is the most influent one for i . Moreover, if i is part of the same fish school of j , the contrary is also true.

Before starting with the operator, there must be a reference for each individual in the fish school, because this operator includes removing operations. The process of definition of sub-populations begins with the random choice of a fish i from the fish school. The selected fish must be removed. Then, the fishes which will be in the same fish school as the fish i must be defined and a link between them and i must be created. After this, these fishes must be also removed. The same process must happen for the fishes that had been just removed: the fishes that must be in the same fish school of a given removed fish must be removed as well and a link between them must be created. When there is no fish that can be in the same fish school as a given fish, a new fish must be randomly chosen among all the fishes that is still in the main fish school, so that the process can start again. This procedure must be executed until the main fish school is empty.

F. Collective Volitive Movement

This operator has the role to drive the produced fish schools to the found niches. Differently from the original FSS, in the dFSS, the volitive movement occurs inside each fish school. This movement is defined by (16), where $decay_{max}(t)$ is defined by (11) and $B_{kj}(t)$ is the barycenter of the fish school of which the fish i is part.

$$x_{ij}(t+1) = x_{ij}(t) + (1 - decay_{max}(t))(B_{kj}(t) - x_{ij}(t)). \quad (16)$$

IV. USING THE WEIGHT OF THE FISH AS A SEGREGATION ELEMENT

In this paper, we propose a new approach for a multi-resolution optimization version of multimodal problems for the FSS algorithm as an alternative for the dFSS. A new operator is included in the original algorithm, in addition to some changes in the already existent operators that were needed.

The main flow of this new approach is the same as in the FSS, except for the addition of the new operator right before the Individual Movement. This new operator is responsible for defining the links between the fishes, which defines the "guide-guided" relationship. This relationship defines a dependency relationship between the fishes which is directly proportional to the difference between the weights of the fishes. The bigger is this difference, the bigger is the dependency from the lighter to the heavier one. From these relationships, a desirable and fair independent behavior of the heaviest fishes in the main fish school emerges. The heavier is a fish relatively to the others, the more independent it is. The lighter is the fish, the more dependent it is as it is understandable, given that its light weight suggests lack of success.

In the next sections, the new approach is described. It is important to point out that the individual movement and the feeding operator have not suffered any changes, hence no explanation for them are needed (again).

A. "Guide-Guided" Relationship Links Definition Operator

As mentioned before, this operator has the role of defining links between fishes. These links define "guide-guided" relationships. Fishes which are linked to each other are called *partners*. In this relationship, the lighter fish is guided by the heavier one.

In (17), $W_i(t)$ and $W_r(t)$ are the weight of the fishes i and r , respectively and C_r and C_i are the number of fishes already linked to the fishes r and i , respectively, right before the probability calculation.

$$p_{ir}(t) = \frac{W_i(t)}{W_r(t)C_r C_i}. \quad (17)$$

```

S: Set of fishes from the main fish school;
T: Temporary set of fishes from the main fish school;
Removes every old links between the fishes;
while S is not empty do:
    Choose randomly a fish i in S and remove it from this
    set;
    Restart T with all the fishes from the population;
    while T is not empty do:
        Choose randomly a fish r from T and remove the
        individual from this set;
        if i is different from r then:
            if  $p_{ir}(t)$ , which is calculated through (17), is
            bigger or equal to a random value generated in the
            interval [0,1] and there is not any already created link
            between r and i then:
                i becomes partner of r, where i guides r;

```

Figure 3. Pseudo-code of the new guide-guided operator.

The variables C_r and C_i were included to avoid the monopolization of too-heavy fishes. The semantics for that is: the greater is the number of connections of a fish, the lower is the probability of creating a new link. This mechanism was created in order to make the search process execute wider searches in the given search space.

Considering a fix indexation of the array of individuals in the main fish school, if the choice of fishes for link formation was made sequentially, the fishes with lower index would have a higher probability of being chosen, because, in the beginning, there is almost no links between the give fish and the other ones. Moreover, the first fishes in the queue to choose partners would have more chances create links, since there is almost no links between the fishes in the main fish school. In order to obtain a fair link formation process between fishes, the process of choosing fishes to find new partners is made randomly, as occurs with the choice of fishes to decide if the link between the given fish and the chosen fish must be created. In this way, any dependency of the indexation of the fishes within the array of individuals is completely avoided.

B. Collective Instinctive Movement

In this operator, the algorithm inherited the basic rationale from the same operator in the FSS. The difference in the new approach is that a given fish must calculate its own movement vector based only on its guiders and itself. The operator is defined by (18), where k is the index of the guiders of i and Ng_i is the number of guiders of i .

$$x_{ij}(t+1) = x_{ij}(t) + \left(\frac{\Delta x_{ij} \Delta f(x_i) + \sum_{k=1}^{Ng_i} \Delta x_{kj} \Delta f(x_k)}{\Delta f(x_i) + \sum_{k=1}^{Ng_i} \Delta f(x_k)} \right). \quad (18)$$

C. Collective Volitive Movement

The Collective Volitive Movement also inherited the basics from the FSS algorithm. However, each fish must calculate its own reference point to work as the barycenter of the original FSS. These personal reference points are calculated using solely the partners of each fish. The barycenter calculation is described by (19), where k is the index of the partners of i and $Npart_i$ is the number of partners of i . The mechanism of expansion and contraction is the same as the FSS.

$$B_i(t) = \frac{x_{ij} W_i(t) + \sum_{k=1}^{Npart_i} x_{kj} W_k(t)}{W_i(t) + \sum_{k=1}^{Npart_i} W_k(t)}. \quad (19)$$

IV. EXPERIMENTS DESCRIPTION

Three multi-solution optimization algorithms were used for comparison purposes: NichePSO, GSO and dFSS. We will refer to the approach proposed in this paper as thisFSS. The parameters setup is described in Table I.

Four metrics were used to evaluate and compare the performance of thisFSS with the other algorithms: (i) the number of solutions found by the algorithm; (ii) configuration with the lowest computational cost able to find 95% of the correct solutions or more; (iii) amount of solutions returned by the algorithm; and (iv) amount of solutions returned by the algorithm that is not part of the objective function's solution set. However, in the last two metrics, the algorithm GSO was not used for comparison.

Seven objective functions were used for benchmarking. These functions are detailed in [2], including their domains and number of peaks (correct solutions). Notice that here they are numbered differently: Equal Peaks A as F1; Equal Peaks B as F2; Griewank as F3; Himmelblau as F4; Peaks as F5; Random peaks as F6; Rastrigin as F7. It is important to highlight that these functions were not taken from real-world scenarios

The performance of the algorithms was analyzed varying the size of the population and the number of iterations. The values used for the population size are defined depending on the objective function. They are defined on Table II. The values for the number of iterations are the same for all the functions: 50,100,150,...,500. However, for the dFSS and thisFSS, just the half of each value is used: 25,50,75,...,250. This is due to the double call of the fitness function per iteration made by the FSS, what was inherited by both versions. This way, it is possible to make fair comparisons. 30 simulations for each algorithm (for each objective function) were made for each possible combination between population size and number of iterations. The average value of each metric for each combination is calculated.

It is important to define what is considered as a returned solution. For thisFSS, the best individual of a fish school is one solution. However, in the end of the last iteration, a different method for defining links between fishes is used. According to this method, two fishes must be linked if the

distance between them is lower than 0.01. This value was defined empirically.

TABLE I. PARAMETERS SETUP

Algorithm	Parameters					
	C1	C2	ω	δ	μ	ϵ
NichePSO	1.2	1.2	Linear decreasing from 0.7 to 0.2.	10^{-4}	10^{-2}	0.1
GSO	ρ	γ	β	n_t	s	l_0
	0.4	0.6	0.08	5	0.03	5
dFSS	ρ	$step_{init}$	$decay_{min}$	$decay_{max_{init}}$	$decay_{max_{final}}$	
	0.3	0.05	0.999	0.99	0.95	
thisFSS	$step_{ind}$			$step_{vol}$		
	Linear decreasing from 0.4 to 0.			Linear decreasing from 0.025 to 0.		

TABLE II. VALUES FOR THE POPULATION SIZE

Functions	Values
Equal Peaks A, Equal Peaks B, Himmelblau, Peaks and Random Peaks.	5, 10, 15, ..., 200, 210, 220, ..., 350
Griewank	5, 10, 25, 50, 100, 150, 200, 250, ..., 1300, 1400
Rastrigin	5, 10, 25, 50, 100, 150, 200, 250, ..., 1000

Among the returned solutions, it must be defined which ones correspond to the correct solutions of the objective function. One solution \vec{k} was successfully found if the normalized distance between the solution returned by the function and \vec{k} is lower than 0.005. Moreover, a solution returned by the algorithm of which distance to the closest solution of the objective function is higher than 0.01 is considered as a wrong solution. (20) and (21) explains the normalized distance calculation between the points \vec{i} and \vec{j} , where D is the number of dimensions of the objective function.

$$d_N(\vec{i}, \vec{j}) = \sqrt{\frac{(x_N^i - x_N^j)(x_N^i - x_N^j)}{D}}, \quad (20)$$

$$x_N = \left(\frac{x_1}{x_{1max}}, \frac{x_2}{x_{2max}}, \dots, \frac{x_D}{x_{Dmax}} \right). \quad (21)$$

V. RESULTS AND DISCUSSION

In Table III, the superiority of thisFSS in comparison with the other algorithms can be noticed in five out of seven objective functions. In Random Peaks, none of the methods were able to find 95% of the correct solutions or more in none of the combinations between the values for population size and the values for the number of iterations. For this function, the comparison results can be analyzed in Table IV. As it can be noticed, thisFSS overcame all other algorithms in every interval defined in the first column.

In Table V, the configuration of the lowest computational cost which is able to find 95% of the correct solutions or more for each algorithm in each objective function is shown. Contents of each cell in this table are represented as x/y(z); 'x' is the number of calls to the fitness function; 'y' is the population size and 'z'= $\sqrt{x^2 + y^2}$. In other words, 'z' is the

Euclidian distance between a given configuration represented as a bi-dimensional vector [x,y] and the theoretical configuration with the lowest cost possible, [0,0]. Obviously, a configuration with 0 calls to the fitness function and 0 individuals is not feasible. According to this table, thisFSS was able to find 95% of the correct solutions or more with less computational effort in five out of the six functions used for comparison.

Regarding to the absolute value of the difference between the number of solutions returned by the algorithm and the number of solutions of the objective functions (Table VI and Table VII), thisFSS obtained lower values than the NichePSO in six out of seven functions, but in all the functions obtained a higher value than the dFSS algorithm. Moreover, regarding to the percentage of wrong solutions relative to the total amount of solutions returned by the algorithms, thisFSS overcame the NichePSO in five out of seven functions and lost for the dFSS in all the functions.

TABLE III. PERCENTAGE OF CONFIGURATIONS THAT ARE ABLE TO FIND 95% OF THE CORRECT SOLUTIONS.

Objective Function	NichePSO	GSO	dFSS	thisFSS
Equal Peaks A	68.18%	72.55%	74%	82.18%
Equal Peaks B	34.55%	52%	64.55%	82.18%
Griewank	0.67%	9.33%	34.67%	50%
Himmelblau	80.09%	73.09%	86.91%	88.36%
Peaks	82.73%	78.18%	83.45%	82.54%
Random Peaks	0%	0%	0%	0%
Rastrigin	0%	0%	23.48%	56.52%

TABLE IV. PERCENTAGE OF CONFIGURATIONS THAT ARE ABLE TO FIND THE NUMBER OF SOLUTIONS OF THE FUNCTION RANDOM PEAKS DEFINED IN THE FIRST COLUMN.

Number of Solutions	NichePSO	GSO	dFSS	thisFSS
≥ 7.6	0%	0.18%	0.18%	3.09%
≥ 6.65 and < 7.6	7.6	31.82%	16.36%	38.55%
≥ 5.7 and < 6.65	6.65	42%	32.91%	38.82%
Total ≥ 5.7	73.82%	49.45%	77.55%	91.63%

TABLE V. CONFIGURATION WITH THE LOWEST COST ABLE TO FIND 95% OF THE CORRECT SOLUTION OF THE OBJECTIVE FUNCTIONS OR MORE.

Objective Function	NichePSO	GSO	dFSS	thisFSS
Equal Peaks A	100/95 (137.93)	100/80 (128.06)	100/130 (164.01)	100/40 (107.70)
Equal Peaks B	100/210 (232.59)	150/125 (195.25)	150/110 (186.01)	100/50 (111.80)
Griewank	100/1400 (1403.57)	150/1150 (1202.08)	400/600 (721.11)	150/550 (570.09)
Himmelblau	100/60 (116.62)	100/110 (148.66)	100/75 (125)	100/45 (109.66)
Peaks	50/70 (86.02)	100/80 (128.06)	100/90 (134.53)	100/25 (103.08)
Random Peaks	-	-	-	-
Rastrigin	-	-	400/500 (640.31)	150/400 (427.2)

These results show that the thisFSS is able to find more correct solutions than the other ones in almost all the objective

functions used as benchmark, but is not able to satisfactorily attract the individuals of the population to the peaks that represent these solutions without decreasing the number of correct solutions found. This leads to a big amount of different returned solutions and a high percentage of false-positive solutions. Even though the results of thisFSS are much better than the results of the NichePSO and GSO; comparing to dFSS using the last two metrics, thisFSS did not obtain good results, although in the first two metrics, the new approach overcame the first one in six out of seven functions. Some attempts to speed up the convergence of the fish schools in the peaks of the search space without losing the number of correct solutions were made, such as the addition of memory for the links of each fish, instead of removing every link in the beginning of each iteration, but the results did not improve as expected. Moreover, different probability functions for creation of links between fishes were tested, but, still, the results did not improve and, in some cases, worsened. So, the results showed in this paper were the best ones found so far.

VI. CONCLUSIONS AND FUTURE WORK

In this paper, we proposed the sole use of FSS fish weight as the segregation factor for producing a new multimodal version of the original algorithm. The obtained results showed that the new approach is able to find a bigger amount of correct solutions in most of the functions, when compared to the NichePSO, GSO and even dFSS. However, the technique also returns false-positives which is a disadvantage if compared to the dFSS. However, the proposed version here does require only one economical operator on top of FSS (and not two as in dFSS). This is a highlight, as computing resources can be a problem in high dimensional problems .

TABLE VI. ABSOLUTE VALUE OF THE DIFFERENCE BETWEEN THE NUMBER OF SOLUTIONS FOUND BY THE ALGORITHM AND THE NUMBER OF SOLUTIONS OF THE OBJECTIVE FUNCTIONS.

Objective Function	NichePSO	dFSS	thisFSS
Equal Peaks A	45.73	0.29	16.5
Equal Peaks B	42.42	0.31	28.3
Griewank	109.38	28.82	138.3
Himmelblau	54.52	0.59	37
Peaks	59.05	3.31	29.2
Random Peaks	51.64	1.87	25.7
Rastrigin	70.66	25.74	53.5

TABLE VII. PERCENTAGE OF WRONG SOLUTIONS RELATIVE TO THE TOTAL AMOUNT OF SOLUTIONS RETURNED BY THE ALGORITHMS IN EACH OBJECTIVE FUNCTION (FALSE-POSITIVES).

Objective Function	NichePSO	dFSS	thisFSS
Equal Peaks A	86.27%	4.94%	27.77%
Equal Peaks B	82.71%	13.65%	48.39%
Griewank	2.68%	0.81%	36.29%
Himmelblau	98.51%	16.34%	77.56%
Peaks	97.50%	55.47%	87.81%
Random Peaks	95.07%	19%	65.83%
Rastrigin	3.86%	1.09%	24.30%

From all presented results, it is possible to conclude that the use of the weight of the fishes is indeed a good alternative to the concept of density used in the dFSS, but one needs to consider the trade-offs in both ways. Another advantage of the algorithm proposed here when compared to the dFSS is that in the latter, a shared memory was added to all fishes in order to make it possible the definition of relations between them. This is no longer necessary here because the weights are already existent in all fishes of the original FSS. And they are used to define these links, what makes the new approach simpler than the first one. Moreover, the calculation of food sharing in dFSS uses topological information, such as the calculation of Euclidian distances, what makes it highly sensitive to dimensional explosion , i.e. high dimensional problems. And this does not happen at all in the new approach since the weight is independent of the number of dimensions of the objective function.

As future work, different mechanisms will be tested in order to reduce the number of returned false-positives. The new approach will also be tested for a higher number of dimensions. Moreover, a computational cost evaluation will be performed.

REFERENCES

- [1] A. P. Engelbrecht, , Computational Intelligence, An Introduction, 1st ed., Wiley & Sons, 2007.
- [2] S. S. Madeiro, F. B. Lima Neto, C.J.A.B Filho , and E. M. N Figueiredo, , "Density as the segregation mechanism in fish school search for multimodal optimization problems", Advances in Swarm Intelligence. ICSI 2011. International Conference on, vol. 2, 2011, pp. 563-572.
- [3] E. Bonabeau, M. Dorigo, and G. Theraulaz, Swarm Intelligence: from natural to artificial systems. Oxford University Press, Inc., 1999.
- [4] J. Kennedy. and, R. Eberhart., "A new optimizer using particle swarm theory", Micro Machine and Human Science, International Symposium on, 1995, pp. 39-43.
- [5] M. Dorigo. Optimization, learning and natural algorithms. PhD Thesis – Politecnico di Milano, 1992.
- [6] D. Karaboga, and B. Basturk "A powerful and efficient algorithm for numerical function optimization: artificial bee colony (abc) algorithm.", Journal of Global Optimi-zation, 2006, pp. 459–471.
- [7] K. M. Passino., "Biomimicry of bacterial foraging for distributed optimization and control.", IEEE Control Systems Magazine, v. 22, n. 3, 2002, pp. 52–67.
- [8] C. J. A. B Filho., F. B. de Lima Neto, A. J. C. C. Lins, A. I. S. Nascimento., and M. P. Lima, , "A novel search algorithm based on fish school behavior," Systems, Man and Cybernetics, SMC 2008. IEEE International Conference on, 2008, pp. 2646-2651.
- [9] E. Ozcan., and, M. Yilmaz., "Particle swarms for multimodal optimization." Lecture Notes in Computer Science, v. 4431, 2007, pp. 366–375.
- [10] L. Li, L. Hong-Qi, and X. Shao-Long., "Particle swarm multi_optimizer for locating all local solutions.", Evolutionary Computation. IEEE Congress on, 2008, pp. 1040–1046.
- [11] R. Brits., A. P. Engelbrecht, and F. van der Bergh., "Locating multiple op-tima using particle swarm optimization.", Applied Mathematics and Computation, v. 2, n. 189, 2007, pp. 1859–1883..
- [12] K. Krishnanand., and D. Ghose., "Glowworm swarm optimization for simultaneous capture of multiple local optima of multimodal functions.", Swarm Intelligence, v. 3, n. 2, 2009, pp. 87–124.

Intelligent Assertions Placement Scheme for String Search Algorithms

Ali M. Alakeel

College of Computers and Information Technology
University of Tabuk
Tabuk, Saudi Arabia
alakeel@ut.edu.sa

Abstract— String search algorithms are found within the internal structure of most Information Retrieval Systems in military applications, aircraft software, medical applications, and commercial applications. Like any software, different errors may occur during the implementation of string search algorithms. Because of the wide range of applications that use string search algorithms, the consequences of these programming errors may be disastrous or fatal. This paper presents an intelligent assertions placement scheme for string search algorithms with the objective to enhance the testability of these algorithms during their testing phase. Instead of placing assertions randomly or after each statement of the program, our proposed method inserts assertions intelligently in a set of selected locations of the string search algorithm that are considered to be error prone or essential to the correctness of the program. The results of a small case study show that applying the proposed method may significantly increase the chances of detecting programming errors associated with string search algorithms that may go undetected using only traditional black-box and white-box testing methods.

Keywords-assertions placement; string search algorithms; assertion-based software testing; software testing

I. INTRODUCTION

String search algorithms are found within the internal structure of most Information Retrieval Systems in military applications, aircraft software, medical applications, and commercial applications. The main function of a string search algorithm is to identify all instances of a given pattern p with size m characters that may exist in a text t with size n characters, such that $m \ll n$ [1]. Like any software, different errors may occur during the implementation of string search algorithms. Because of the wide range of applications that use string search algorithms, the consequences of these programming errors may be disastrous or fatal. For example, if a medical information retrieval system fails to return the exact prescribed medicine, this action may jeopardize the patient's life. Also, if a military missile control system fails to retrieve the target's exact coordinates, the results could be disastrous [2]. Therefore, the correctness of the implementation of any string search algorithm is crucial.

Software correctness may be improved by applying thorough and rigorous software testing methods [16]. Program assertions are recognized as a supporting aid in detecting faults during software testing, debugging and

maintenance [17-22]. Also, assertions have been shown to increase software testability [23-25]. Therefore, assertions may be inserted into software code in those positions that are considered to be error prone or have the potential to lead to software crash or failure.

Most string search algorithms, e.g., [3-15], share a common programming internal structure which may make them susceptible to the same type of errors during their implementations. For example, most string search algorithms are composed of two main parts: checking and skipping. These two major parts are considered the heart of any string matching algorithm where they involve the dealings and manipulations of certain elements. Some of these elements are the starting point of checking, the direction of checking, the skipping strategy, the number of static or dynamic reference characters, and different shift distances. For example, a common programming error that may occur during the implementation of a string search algorithm is that the shift distance might become zero. Also, it is possible that the number of occurrences of the pattern p in text t found by the algorithm might be less than or greater than the actual occurrences of p in t . Therefore, the placement of programming assertions in the *proper* locations within string search algorithms may enhance the testability of these programs and leads to the detection of programming faults during the testing stage. It should be noted that the use of assertions for testing purpose should only be used as a complementary and an extra step after traditional testing methods such as black-box and white-box testing methods [3] have been applied to the software.

This paper presents an intelligent assertions placement scheme for string search algorithms with the objective to enhance the testability of these algorithms during their testing phase. Instead of placing assertions randomly or after each statement of the program, our proposed method inserts assertions intelligently in a set of selected locations of the string search algorithm that are considered to be error prone or essential to the correctness of the program. The results of a small case study show that applying the proposed method may increase the chances of detecting programming errors associated with string search algorithms that may go undetected using only traditional black-box and white-box testing methods.

The rest of this paper is organized as follows. Sections II and III provide a brief introduction to assertions-based

software testing and string search algorithms, respectively. Our proposed method for assertions placement in string search algorithms is presented in Section IV. In Section V, a case study is presented. Conclusions are presented in Section VI.

II. ASSERTION-BASED SOFTWARE TESTING

Software testing is a very labor intensive task and cannot by any means guarantee the correctness of any software or that the software is error-free. However, rigorous software testing may increase the confidence in the software under test. There are two main approaches to software testing: Black-box and White-box [3]. Test data generation is the process of finding program input data that satisfies a given criteria, e.g., [30, 31]. Test generators that support black-box testing create test cases by using a set of rules and procedures; the most popular methods include equivalence class partitioning, boundary value analysis, cause-effect graphing. White-box testing is supported by coverage analyzers that assess the coverage of test cases with respect to executed statements, branches, paths, etc. Programmers usually start by testing their software using black-box methods against a given specification. By their nature black-box testing methods might not lead to the execution of all parts of the code. Therefore, this method may not uncover all faults in the program. To increase the possibility of uncovering program faults, white-box testing is then used to ensure that an acceptable coverage has been reached, e.g., branch coverage.

Program assertions are recognized as a supporting aid in revealing faults during software testing, debugging and maintenance [17-22]. Also, assertions have been shown to increase software testability [23-25]. An Assertion specifies a constraint that applies to some state of computation. The state of an assertion is represented by two possible values: *true* or *false*. For example, `assert(0<index<=100)`, is an assertion that constraints the values of some variable "index" to be in the range of 1 and 100 inclusive. As long as the values of "index" is within the allowed range the state of this assertion is *true*. Any other values beyond this range, however, will cause the state of this assertion to become *false* which indicates the violation of this assertion. Many programming languages support assertions by default, e.g., Java and Perl. For languages without built-in support, assertions can be added in the form of annotated statements. For example, [18] presents assertions as commented statements that are pre-processed and converted into Pascal code before compilation. Many types of assertions can easily be generated automatically such as boundary checks, division by zero, null pointers, variable overflow/underflow, etc. Beyond simple assertions that can easily be generated automatically, a method to generate more complex assertions for Pascal programs is presented in [18]. For this reason and to enhance their confidence in their software, programmers may be encouraged to write more programs with assertions. It should be noted, however, that writing the proper type of assertions and choosing the proper locations to inject them into the software is very important to the effectiveness of this methodology. Inserting assertions after every statement of

the program is an extreme case scenario which can make the whole process of assertions processing very costly and prohibitive [28]. Therefore it is imperative to devise a scheme for assertion's placement within the software under test such that assertions are only inserted in *selected* location within the program's code. Assertion-Based software testing [18, 19, 21], has been shown to be effective in detecting program faults as compared to traditional black-box and white-box software testing methods. Given an assertion *A*, the goal of Assertion-Based testing is to identify program input for which *A* will be violated. The main aim of Assertion-Based Testing is to increase the developer confidence in the software under test. Assertion-Based Testing is intended to be used as an extra and complimentary step *after* all traditional testing methods have been performed to the software. Assertion-Based Testing gives the tester the chance to think deeply about the software under test and to locate positions in the software that are very important with regard to the functionality of the software. After locating those important locations, assertions are added to guard against possible errors with regard to the functionality performed in these locations.

The process of writing program assertions may depend heavily on the tester's experience and knowledge of the program under test. To aid in this process a simple tool may be used to automatically generate assertions in certain locations of the program, which guard against errors, such as division by zero, array boundary violations, uninitialized variables, stack overflow, null pointer assignment, pointer out of range, out of memory (heap overflow), and integer / float underflow and overflow [18]. However, there are application-specific locations in the program itself that may need to be guarded by assertions depending on the importance of these locations to the correctness of the application. For example, in string search algorithms, computing the location of the pattern in the input string and index manipulation during the checking and skipping process are very important to the correctness of these algorithms.

III. STRING SEARCH ALGORITHMS

The problem of string searching may be stated as follows. Given a text string *t* of size *n* and a pattern string *p* of size *m* (where $n \gg m$), find all occurrences of *p* in *t* [1]. During our investigation of string matching algorithms, we noticed that most of the proposed algorithms are usually compared against classical exact string searching algorithm such as Naïve (brute force) algorithm and Boyer-Moore-Horspool (BMH) algorithm [5]. Some of these algorithms preprocess both the text and the pattern, e.g., [3], while others need only to preprocess the pattern, e.g., [4, 5]. In all cases, the exact string searching problem consists of two major steps: checking and skipping. The checking step itself consists of two main stages. In the first stage main objective is to search along the text for a reasonable candidate string, while the second stage goal is to perform a detailed comparison of the candidate string, found in the first stage, against the pattern to verify the potential match. Some characters of the candidate string must be selected carefully in order to avoid the problem of repeated examination of

each character of text when patterns are partially matched. Intuitively, the fewer the number of character comparisons in the checking step the better the algorithm is.

Different string search algorithms may differ in the way they implement the checking process, e.g., [4, 5]. After the checking step, the skipping step shifts the pattern to the right to determine the next position in the text where the substring text can possibly match with the pattern. The reference character is a character in the text chosen as the basis for the shift according to the shift table. Some string search algorithms may use one or two reference characters and the references might be static or dynamic [18, 19]. Additionally, some algorithms focus on the performance of the checking operation while others focus on the performance of the skipping operation [10]. The shift distance used may differ from one string search algorithm to another; it ranges from only one position in the Naïve algorithm, up to m positions in Boyer-Moore-Horspool algorithm [5], $m+1$ positions in Raita's algorithm [4], and up to $3m+1$ positions in CSA algorithm [11]. The following text provides a detailed description of the CSA string search algorithm as reported in [11].

A. Checking and Skipping Algorithm (CSA)

A string search algorithm is a succession of checking and skipping, where the aim of a good algorithm is to minimize the work done during each checking and to maximize the length distance during the skipping. Most of the string matching algorithms preprocess the pattern before the search phase to help the algorithm to maximize the length of the skips, the preprocessing phase in the CSA algorithm helps in both increases, the performance of the checking step by converting some of the character-comparison into character-access and maximizes the length of the skips. At each attempt during the checking steps the CSA compares the character at *last_mismatch* (the character that causes the mismatch in the previous checking step) with the corresponding character in *Text*. If they match, the comparison goes from right to left, including the compared character at *last_mismatch*. The idea here is that the mismatched character must be given a high priority in the next checking operation. After a number of checking steps, this leads to start the comparison at the least frequent character without counting the frequency of each character in the text.

For the skipping step, CSA has five reference characters, including three static references and two dynamic references. The *Text* pointer *TextIx* always points to the character, which is next to the character corresponding to the last character in *Pat* and the reference character *ref* always points to the character that corresponds to the last character in *Pat* i.e. $ref = TextIx - 1$. Now let $ref1 = TextIx$, then the reference character $ref2$ can be calculated from ref or $ref1$, where $ref2$ can be found as " $ref2 = TextIx + m - 1$ " or " $ref2 = TextIx + m$ " depending on the existence of ref or $ref1$ in *Pat*, where $ref2 = TextIx + m - 1$ during the checking step if the character at ref doesn't exist in *Pat*, or $ref2 = TextIx + m$ after the checking step if the character at $ref1$ doesn't exist in *Pat*. In addition to that, CSA pre-processes the pattern to produce

two different arrays, namely *skip* and *pos*. Each array has a length equals to the alphabet size. The *skip* array is used when the reference character $ref1$ exists in *Pat*, it expresses how much the pattern is to be shifted forward after the checking step. While the *pos* array defines where each one of the different reference characters $ref1$, $ref2$, ref_ref1 , or ref_ref2 is located in *Pat*, if any one of them exists in *Pat*, where the two dynamic pointers ref_ref1 and ref_ref2 can be calculated from two static pointers $ref1$ and $ref2$, respectively. The CSA algorithm is designed to scan the characters of both the text and the pattern from right to left.

```

1,2,3  #include <iostream>; #include <iomanip>; #include <cstring>
4,5,6  using std::cout; using std::cin; #define ASIZE 256
7      void PreProcessPat(char *, int, int *, int *);
8      void CSA(char *, int, char *, int, int *, int *);
9      int main(){
10     char Text[] = "test This is a test for string test";
11,12,13 char Pat[] = "test"; int PatLength = 4; int TextLength = 35;
14,15,16 int pos[1000]; int skip[1000]; cout<<Text;
17,18,19 getchar(); cout<<Pat; getchar();
20     PreProcessPat(Pat, PatLength, pos, skip);
21     CSA(Pat, PatLength, Text, TextLength, pos, skip);
22,23,24 cout<<Text; getchar(); return 0; }
25 void PreProcessPat(char *Pat, int PatLength, int *pos, int *skip){
26     char c;
27     for(int j = 0; j<ASIZE; j++) {
28,29     pos[j]=0; skip[j] = 2*PatLength; }
30     for(int j=0; j<PatLength; j++) {
31,32,33     c = Pat[j]; pos[c]=j + 1; skip[c] = 2 * PatLength - j - 1; }
34 void CSA(char *Pat, int PatLength, char *Text, int TextLength, int
    *pos, int *skip){
35     int TextIx, PatIx, last_mismatch, z;
36     int pt, pt1, ref, ref1, ref_ref1, ref2, ref_ref2;
37     int infix[ASIZE] = {0};
38,39,40 infix[Pat[0]] = 1; last_mismatch=0; TextIx = PatLength;
41     while(TextIx<=TextLength+1) {
42 if(Text[TextIx - PatLength + last_mismatch] == Pat[last_mismatch])
43     if(infix[Text[TextIx - PatLength]]) {
44     for( z = 0, PatIx = PatLength - 1; PatIx; PatIx-- )
45     if(Text[TextIx - ++z] != Pat[PatIx]){
46     last_mismatch = PatIx;
47     goto next; }
48 cout<<"\nAn occurrence at location "<<TextIx-PatLength<<" to
    "<<TextIx - 1<<"\n"; }
49     next:
50,51     ref = TextIx - 1; ref1 = TextIx;
52     if ( !pos[Text[ref]] ){
53,54,55     ref2 = ref + PatLength; pt1 = pos[Text[ref2]]; ref_ref2 = ref2
    + PatLength - pt1;
56 TextIx += 3 * PatLength - pt1 - pos[Text[ref_ref2]];
    } else {
57     pt = pos[Text[ref1]];
58     if( !pt){
59,60,61 ref2 = TextIx + PatLength; pt1 = pos[Text[ref2]]; ref_ref2 =
    ref2 + PatLength - pt1;
62 TextIx += 3 * PatLength + 1 - pt1 - pos[Text[ref_ref2]]; } else {
63     ref_ref1 = ref1 + PatLength - pt;
64 TextIx += skip[Text[ref_ref1]] - pt + 1;
    } }
65     return;
    }

```

Figure 1. C++ implementation of CSA algorithm.

At each attempt, it first compares the character at *last_mismatch* with the corresponding character in *Text*; if they match, it compares the first character of *Pat* with the corresponding characters in *Text*, and if they match CSA compares the other characters from right to left including the character at *last_mismatch* and excluding the first character of *Pat*. Whether there is an occurrence of *Pat* in *Text* or not, the existence of the character at *ref* in *Pat* will be checked first, so there are two cases:

1) The character at *ref* exists in *Pat*: In this case, the existence of *Pat* in *Text* will be checked. After the checking step, the existence of *ref1* in *Pat* will be examined. Hence, there are two cases:

1.1) the character at *ref1* doesn't exist in *Pat*. Then *ref2* and *ref_ref2* will be calculated. Next, the pointer *TextIx* will be moved forward to align with the character at *ref_ref2*.

1.2) the character at *ref1* exists in *Pat*. Then *ref_ref1* will be calculated. Afterwards, the pointer *TextIx* will be moved forward to align with the character at *ref_ref1*.

2) The character at *ref* doesn't exist in *Pat*: In this case, *ref2* and *ref_ref2* will be calculated according to the pointer *ref*, then the pointer *TextIx* will be moved forward to align with the character at *ref_ref2*. Fig. 1 shows a C++ implementation of the CSA algorithm.

IV. INTELLIGENT ASSERTIONS PLACEMENT SCHEME FOR STRING SEARCH ALGORITHMS

In this section, we will describe in more details our proposed approach for intelligent assertions placement in string search algorithms.

A. Related Work

Assertions placement methods reported previously in the literature, e.g., [24, 26, 27], are mostly dependent on the intervention of the programmer and involves the analysis of all of the programs' code. In [24], a software tool is developed which assist the programmer in inserting assertions in a previously selected locations of C programs. There is no real placement strategy proposed by [24] other than what is proposed manually by the programmer. The usefulness of this tool is in converting assertions specified in pseudo-code into real programming code. Also, an assertion placement scheme designed specifically for embedded systems is proposed in [27]. Given a program *P* with a set of statements *S*, a heuristic presented in [26] that is based on propagation analysis [28] of each statement $s_k \in S$ found in the program, estimates the probability that a program fault at any statement, $s_k \in S$, will propagate to affect *negatively* the output of the program *P*. Based on this probability, this scheme selects those statements of the program that should be guarded by assertions. Although this heuristic is simple it is impractical for large commercial programs because most of its steps require human intervention. Additionally, this heuristic may ends with placing assertions after every statement of the program which makes it very expensive in terms of additional execution time. Our proposed method presented in this paper, only places assertions to guard those parts of the program that are considered to be *vital* to its

functionality, therefore, minimizing the overhead that may be introduced by assertions processing.

B. Motivation

During our investigation of a set of string matching algorithms reported in the literature, e.g., [3-15], we found out that most of these algorithms share a common programming structure which makes them are susceptible to the same types of programming errors that may occur during their implementations. For example, it can be noticed that there are different factors and elements of string matching algorithms that may lead to program errors during the implementations of these algorithms into real program's code. Some of these elements are the starting point of checking, the direction of checking, the skipping strategy, the number of static or dynamic reference characters, and different shift distances. Therefore, like any software, it is possible that program errors may occur during the implementation of any string matching algorithm. For instance, the shift distance might become zero or the number of occurrences of the pattern *p* in text *t* found by the algorithm might be less than or greater than the actual occurrences of *p* in *t*. Moreover, it has been notice during this study that these types of errors are not easily detected by traditional black-box and white box software testing methods [16].

Based on the properties of the internal structure of string search algorithms, this paper proposes an assertions placement strategy that *intelligently* guides the programmer to the locations in which assertions should be placed. As will be described shortly, our proposed method employs data dependency analysis [29] on those parts of the program that are *vital* to its functionality. Through our investigation of string matching algorithms, the checking and skipping components are the most important parts. Data dependency analysis is described as follows. Given a program *P* with as set of statements, $S = \{s_1, s_2, s_3, \dots, s_n\}$ and a set of variables, $V = \{v_1, v_2, v_3, \dots, v_m\}$, form which any statement, $s_k \in S$, may be composed, data dependency analysis defines the relationships between the elements of the set of program statements *S* with respect to the usage and modifications of the set of variables *V*. Formally, there exists a data dependency between two statements s_i and s_j such that $j > i$ in their order of appearance in the program, with respect to a variable, $v_t \in V$, if the following three conditions holds. (1) The statement s_i assigns a value to v , and (2) the variable v_t is used at the statement s_j , and (3) there exists a program control path between s_i and s_j , in which the variable v_t is not modified. For example, in the program of Fig. 1, there exists a data dependency between nodes 57 and 63 because the variable "pt" is assigned a value at node 57, node 63 uses variable "pt", and there exists a program control path, from node 57 to node 63, in which "pt" is not modified. This program control path is: (57, 58, 63). The data dependencies in the program may be represented by data dependency graph [31], such that the nodes of the graph represent program statements and the directed arcs represent data dependencies.

```

1,2,3 #include <iostream>; #include <iomanip>; #include <cstring>
4,5,6 using std::cout; using std::cin; #define ASIZE 256
7 void PreProcessPat(char *, int , int *, int *);
8 void CSA(char *, int , char *, int , int *, int *);
9 int main(){
10 char Text[] = "test This is a test for string test";
11 char Pat[] = "test";
12,13,14 int PatLength = 4; int TextLength = 35; int pos[1000];
15 int skip[1000];
16,17,18,19 cout<<Text; getchar(); cout<<Pat; getchar();
20 PreProcessPat(Pat, PatLength, pos, skip);
21 CSA(Pat, PatLength, Text, TextLength, pos, skip);
22,23 cout<<Text; getchar();
24 return 0; }
25 void PreProcessPat(char *Pat, int PatLength, int *pos, int *skip){
26 char c;
27 for(int j = 0; j<ASIZE; j++) {
/* A1: (j>=0)and(j<ASIZE) */ // Assertion No. 1
28,29 pos[j]=0; skip[j] = 2*PatLength; }
30 for(int j=0; j<PatLength; j++) {
/* A2: (j>=0)and(j<PatLength) */ // Assertion No. 2
31,32,33 c = Pat[j]; pos[c]=j + 1; skip[c] = 2 * PatLength - j - 1; } }
34 void CSA(char *Pat, int PatLength, char *Text, int TextLength, int
*pos, int *skip){
35 int TextIx, PatIx, last_mismatch, z;
36 int pt, pt1, ref, ref1, ref_ref1, ref2, ref_ref2;
37 int infix[ASIZE] = {0};
/* A3: (Pat[0]>=0)and(Pat[0]<ASIZE) */ // Assertion No. 3
38,39,40 infix[Pat[0]] = 1; last_mismatch = 0; TextIx = PatLength;
41 while(TextIx<=TextLength+1) {
/* A4: ((TextIx - PatLength + last_mismatch)>=0)and((TextIx - PatLength +
last_mismatch)<TextLength) * // Assertion No. 4
42 if(Text[TextIx - PatLength + last_mismatch] ==
Pat[last_mismatch])
/* A5: ((Text[TextIx - PatLength])>=0)and((Text[TextIx - PatLength])<ASIZE)
*/ // Assertion No. 5
43 if(infix[Text[TextIx - PatLength]]) {
// Check the occurrence of Pat in Text from right to left excluding first
character
44 for( z = 0, PatIx = PatLength - 1; PatIx; PatIx-- )
/* A6: ((TextIx - ++z)>=0)and((Text[TextIx - tLength])<TextLength) */ //
Assertion No. 6
45 if(Text[TextIx - ++z] != Pat[PatIx]){
46,47 last_mismatch = PatIx; goto next; }
48 cout<<"\nAn occurrence at location "<<TextIx-PatLength <<"
to "<<TextIx - 1<<"\n"; }
49 next:
50,51 ref = TextIx - 1; ref1 = TextIx;
/* A7: ((Text[ref])>=0)and((Text[ref])<1000) */ // Assertion No. 7
52 if ( !pos[Text[ref]] ) {
/* A8: ((Text[ref2])>=0)and((Text[ref2])<1000) */ // Assertion No. 8
53,54 ref2 = ref + PatLength; pt1 = pos[Text[ref2]];
55 ref_ref2 = ref2 + PatLength - pt1;
/* A9: ((Text[ref_ref2])>=0)and((Text[ref_ref2])<1000) */ // Assertion No. 9
56 TextIx += 3 * PatLength - pt1 - pos[Text[ref_ref2]];
} else {
/* A10: ((Text[ref1])>=0) and ((Text[ref1])<1000) */ // Assertion No. 10
57,58 pt = pos[Text[ref1]]; if ( !pt ) {
/* A11: ((Text[ref2])>=0) and ((Text[ref2])<1000) */ // Assertion No. 11
59,60 ref2 = TextIx + PatLength; pt1 = pos[Text[ref2]];
61 ref_ref2 = ref2 + PatLength - pt1;
/* A12: ((Text[ref_ref2])>=0) and ((Text[ref_ref2])<1000) */ //Assertion No. 12
62 TextIx += 3 * PatLength + 1 - pt1 - pos[Text[ref_ref2]]; }
else {
63 ref_ref1 = ref1 + PatLength - pt;
/* A13: ((Text[ref_ref1])>=0) and ((Text[ref_ref1])<1000) */ // Assertion No. 13
64 TextIx += skip[Text[ref_ref1]] - pt + 1; }
} }
65 return; }

```

Figure 2. CSA string search algorithm with assertions.

C. Proposed Intelligent Assertions Placement Scheme

Given a program P that represents an implementation of a string matching algorithm, our proposed method for intelligent assertions placement in string matching algorithms, proceeds in three main stages as follows. In the first stage, the checking and skipping components are identified. Also, the boundaries statements of each part are marked. Note that this step is performed manually. Giving these marked points, the second stage performs, automatically, a data dependency analysis of every statement within the marked boundaries of the checking and skipping components. The outcome of the first stage is a set of data dependency sub-graphs of every statement in the checking and skipping parts of the program P. For every statement sk , that lies within the marked boundaries of the checking and skipping boundaries, each data dependency sub-graphs will be composed of the program statements and data dependencies of the program's data dependence graph for which there exists a path that leads to the statement, sk . Finally, data dependency sub-graphs are then used, in the third stage, to produce a road map that will guide the process of our assertions placement strategy. For example, after applying the proposed method on the CSA program shown previously in Fig. 1, thirteen assertions were placed in selected locations. Fig. 2 shows a new version of the CSA algorithm after assertions have been placed within its code according to the proposed method in this research.

V. A CASE STUDY

The goal of this small case study is to show that applying the proposed method for assertions placement may significantly enhances the testability of string search algorithms, therefore, increasing the chances of detecting programs errors that may exist in these programs. In this case study, the CSA string search algorithm [11], is implemented by three different programmers with 3-5 years of experience. This stage produced three different versions of the CSA algorithm. Each of these versions is subjected to traditional black-box and white-box software testing methods. Specifically, the following software testing methods were used: black-box testing as represented by boundary value analysis and equivalence class partitioning while white-box testing is represented by branch coverage. Errors detected during these tests were fixed and this process is repeated until these methods fail to uncover to detect any faults.

In order to increase our confidence in these programs, our proposed scheme for assertions placement, described previously in Section IV, is applied to the three versions of the CSA string search algorithm. For each version, the outcome of this stage is a modified copy with assertions placed at selected location recommend by the proposed method to be error prone or crucial to the correctness of the CSA algorithm. For example, in the version of the CSA algorithms shown in Fig. 1, thirteen assertions were inserted in this version as shown in Fig. 2.

TABLE I. RESULTS OF CASE STUDY

#Violations	#Assertions Inserted	Program Name
1	13	CSA version#1
2	15	CSA version#2
0	10	CSA version#3

Note that some assertions are inserted automatically without the intervention of the programmer, while more complex assertions are developed manually by the programmer and inserted in the recommended locations as proposed method. Assertions that are generated automatically are array boundary checks, division by zero, null pointers and variable overflow/underflow. In the final stage of this case study, Assertion-Based software testing [18] is performed on each version of the CSA with assertions. Assertion-Based software testing main objective is to generate program's input data for which a given assertion is violated. If this assertion is violated, then a program fault has been uncovered [18]. As stated in [18], Assertion-Based software testing is intended to be used as an extra and complimentary step *after* all traditional testing methods, such as black-box and white-box [16], have been performed on each original copy of each program used in this case study. The result of this case study is shown in Table I. It should be noted that the result of this experiment may be different for different programs with different types of assertions.

As reported in Table I, using our proposed method for assertions placement together with Assertion-Based software testing, we were able to uncover program faults in two out of the three versions of the CSA string search algorithm used in this case study. This is encouraging results considering that all of these faults were not detected by traditional black-box and white-box software testing methods during the first stage of this study. Also, notice that each assertion's violation means that at least *one* fault has been uncovered.

VI. CONCLUSIONS AND FUTURE WORK

This research proposed a new method for intelligent assertions placement in string search algorithms. The proposed method main objective is to increase the testability of string search algorithms and to enhance the delectability of program faults during their testing phase. The proposed method is intended to be used as a pre-step before Assertion-Based software testing is performed on string search algorithms. The result of a case study, conducted to evaluate the proposed method, shows that using this method may significantly enhances the chances of detecting program faults associated with string search algorithms that may go undetected by applying only traditional software testing methods. Our future research concentrates on conducting an experimental study to evaluate the proposed method in wider range of string search algorithms and to investigate the applicability of this method in other applications software.

REFERENCES

- [1] G. Stephen, "String Searching Algorithms", World Scientific, Singapore, 1994.
- [2] [http://www.pcworld.com/article/110035/software_bug_may_cause_missile_errors.html]. Retrieved: March 6, 2013.
- [3] P. Fenwick, "Fast string matching for multiple searches", Software-Practice and Experience, Vol. 31, No. 9, pp. 815-833, 2001.
- [4] T. Raita, "Tuning the Boyer-Moore-Horspool String Searching Algorithm", Software Practice and Experience, Vol. 22, No. 10, pp. 879-844, 1992.
- [5] R.S. Boyer and J.S. Moore, "A fast string searching algorithm", Communications of the ACM, Vol. 20, No. 10, pp. 762-772, 1977.
- [6] M. S. Ager, O. Danvy, and H. K. Rohde, "Fast partial evaluation of pattern matching in strings", ACM/SIGPLAN Workshop Partial Evaluation and Semantic-Based Program Manipulation, San Diego, California, USA, pp. 3 - 9, 2003.
- [7] K. Fredriksson and S. Grabowski, "Practical and Optimal String Matching", Proceedings of SPIRE'2005, Lecture Notes in Computer Science 3772, pp. 374-385, Springer Verlag, 2005.
- [8] P. Smith, "On Tuning the Boyer-Moore-Horspool String Searching Algorithm", Short Communication, Software Practice and Experience, Vol. 24, No. 4, pp. 435-436, 1994.
- [9] M. Mhashi, "The Effect of Multiple Reference Characters on Detecting Matches in String Searching Algorithms," Software Practice and Experience, Vol. 35, No. 13, pp. 1299 -1315, 2005.
- [10] Mhashi, M., "The Performance of the Character-Access On the Checking Phase in String Searching Algorithms", Transactions on Informatica, Systems Sciences and Engineering, Vol. 9, pp. 38 -43, 2005.
- [11] M. Mhashi and M. Alwakeel, "New Enhanced Exact String Searching Algorithm" IJCSNS International Journal of Computer Science and Network Security, Vol. 10, No. 4, pp. 13 - 20, 2010.
- [12] R. N. Horspool, "Practical fast searching in strings," Software - Practice & Experience, Vol. 10, No. 6, pp. 501-506, 1980.
- [13] R. M. Karp and M. O. Rabin, "Efficient randomized pattern-matching algorithms," IBM J. Res. Dev., Vol. 31, No. 2, pp. 249-260, 1987.
- [14] A. Apostolico and M. Crochemore, "Optimal canonization of all substrings of a string," Information and Computation, Vol. 95, No. 1, pp. 76-95, 1991.
- [15] L. Colussi, "Correctness and efficiency of the pattern matching algorithms," Information and Computation, Vol. 95, No. 2, pp. 225-251, 1991.
- [16] G. Myers, "The Art of Software Testing," John Wiley & Sons, New York, 1979.
- [17] D. Rosenblum, "A Practical Approach to Programming With Assertions," IEEE Trans. on Software Eng., Vol. 21, No. 1, pp. 19-31, January, 1995.
- [18] B. Korel and A. Al-Yami, "Assertion-Oriented Automated Test Data Generation," Proc. 18th Intern. Conference on Software Eng., Berlin, Germany, pp. 71-80, 1996.
- [19] A. Alakeel, "An Algorithm for Efficient Assertions-Based test Data Generation," Journal of Software, vol. 5, No. 6, pp. 644-653, 2010.
- [20] K. Shrestha and M. Rutherford, "An Empirical Evaluation of Assertions as Oracles," Proceedings of IEEE Inter. Conference on Software Testing, Verification and Validation, pp. 110-119, 2011.
- [21] A. Alakeel, "A Framework for Concurrent Assertion-Based Automated Test Data Generation," European Journal of Scientific Research, Vol. 46, No. 3, pp. 352-362, 2010.
- [22] S. Khalid, J. Zimmermann, D. Corney, and C. Fidge, "Automatic Generation of Assertions to Detect Potential Security Vulnerabilities in C Program That Use Union and Pointer Types," Proceedings of Fourth Inter. Conference on Network and System Security, pp. 351-356, 2010.
- [23] J. Voas, "How Assertions Can Increase Test Effectiveness," IEEE Software, , pp. 118-122, March 1997.

- [24] H. Yin and J.M. Bieman, "Improving Software Testability with Assertion Insertion," Proceedings of International Test Conference, pp. 831-839 October 1994.
- [25] T. Tsai, C. Huang C., and J. Chang, "A Study of Applying Extended PIE Technique to Software Testability Analysis," Proceedings of IEEE Inter. Computer Software and Application Conf., pp. 89-98, 2009.
- [26] J. Voas, "Software Testability Measurement for Intelligent Assertion Placement," Software Quality Journal (6), pp. 327-335, 1997.
- [27] V. Izosimov, et. al., "Optimization of Assertion Placement in Time-Constrained Embedded Systems," Proceedings of The Sixteenth IEEE European Test Symposium, pp. 171-176, 2011.
- [28] J. Voas, "PIE: A Dynamic Failure-Based Technique," IEEE Trans. on Software Eng., Vol. 18, No. 8, pp. 717-727, August, 1992.
- [29] B. Korel, et. al., "Data Dependence Based Testability Transformation in Automated Test Generation," Proceedings of The 16th IEEE Inter. Symposium on Software Reliability Engineering, pp. 245-254, 2005.
- [30] P. McMinn, "Search-Based Software Test Data Generation: A Survey," Software Testing, Verification and Reliability, Vol. 14, pp. 105-156, 2004.
- [31] M. Harman and P. McMinn, "A theoretical and empirical study of search based testing: Local, global and hybrid search," IEEE Transactions on Software Engineering, Vol. 36, No. 2, pp. 226-247, 2010.

Modeling of Sales Forecasting in Retail Using Soft Computing Techniques

Luís Lobo da Costa, Susana M. Vieira and João M. C. Sousa

Center of Intelligent Systems - IDMEC-LAETA

Instituto Superior Técnico, Technical University of Lisbon

Lisbon, Portugal

Email:susana.vieira@ist.utl.pt

Abstract—This paper addresses the problem of aggregate daily sales forecasting in retail. Soft computing modeling techniques were applied to this problem.

A methodology on how to select the three forecasting periods is presented. The different forecasting horizons consist of a stationary period, a stationary period with disturbances, and a non-stationary period. It is also presented a methodology on how to construct the models' features. These are the weekly and monthly seasonality, the macroeconomic environment translated into the purchasing power, the major promotions and holidays. Further, each model's parameter is developed. The models that presented accurate training performances are finally tested over the forecasting periods, allowing the obtention of reasonably accurate forecasts for the three periods.

Keywords—Sales forecasting, Modeling, Soft computing techniques, Retail.

I. INTRODUCTION

This paper addresses the problem of sales forecasting in retail. The problem was approached using soft computing techniques for three forecasting periods. In order to allow the obtention of accurate performances, the features that have a strong effect on sales had to be determined.

Due to the strong and growing competition existing nowadays, the majority of retailers are in a continuous effort for increasing profits and reducing costs [1]. In addition, the variations in consumers demand contribute to a fluctuating market behavior [2]. In that sense, an accurate sales forecasting system is an efficient way to achieve higher profits and lower costs, by improving customers satisfaction, reducing product destruction, increasing sales revenue and designing production plans efficiently [1]. Sales forecasting refers to the prediction of future sales based on past historical data. Owing to competition and globalization, sales forecasting plays an even more important role as part of the commercial enterprise [3].

From a historical perspective, exponential smoothing methods and decomposition methods were the first forecasting approaches to be developed back in the mid-1950s. During the 1960s, as computer power became more available and cheaper, more sophisticated forecasting methods appeared [4]. Box-Jenkins [5] methodology gave rise to the ARIMA models [4]. Later on, during the 1970s and 1980s, even more sophisticated forecasting approaches were developed including econometric methods and Bayesian methods [6].

Intelligent or softcomputing algorithms, which combined fuzzy theory with neural network has found a variety of applications in various fields [7]. One of the major limitations of the traditional methods compared to soft computing is that they are essentially linear methods [8].

The idea of using neural networks (NNs) for forecasting is not new. The first application dates back to 1964 [9]. Research efforts on NNs for forecasting are considerable. The literature is vast and growing [10]. Applications goes from time series [11], to financial applications [12]; electric load consumption [13], and others [14]. Most studies use the straightforward multilayer perceptron (MLP) networks [15], [16], while others employ some variants of MLP. It should be pointed out that recurrent networks also play an important role in forecasting. In [17], the use of nonlinear autoregressive exogenous model (NARX) is studied. There are also some fuzzy systems applied to forecasting [18], [19]. Most of fuzzy systems are applied in a neuro-fuzzy structure [20],[21].

In Section II, soft computing techniques are presented. Further, in Section III the periods of forecasting are selected as well as the inputs are constructed. In Section IV the models are obtained and in Section V, the results are presented and discussed. Finally, in Section VI, the conclusions are drawn.

II. MODELING

In this work five types of models were developed: Fuzzy classification models, fuzzy NARX models, feedforward classification neural networks, NARX networks and adaptive neuro fuzzy inference system (ANFIS) models. Rule-based fuzzy models describe relationships between variables by means of if-then rules, and in a Takagi-Sugeno model take the form,

$$R_i : \text{If } \mathbf{x} \text{ is } A_i \text{ then } \mathbf{y}_i = \mathbf{f}_i(\mathbf{x}), \quad i = 1, 2, \dots, K, \quad (1)$$

where $\mathbf{x} \in \mathbb{R}^n$ is the multidimensional input (antecedent) variable and $\mathbf{y}_i \in \mathbb{R}^p$ is the also multidimensional output (consequent) variable. R_i denotes the i th rule, and K is the number of rules in the rule base. These models use clustering techniques to group data in subsets of similarity in order to simplify fuzzy systems' rule base. In this work a classification model, and a NARX model were used, which can use past data as inputs (including past sales data). Artificial neural networks consist of an inter-connection of a number of neurons that try to resemble the way the human brain works. There are many varieties of connections under study, however, here it was used one type of network, which is called multilayer perceptron.

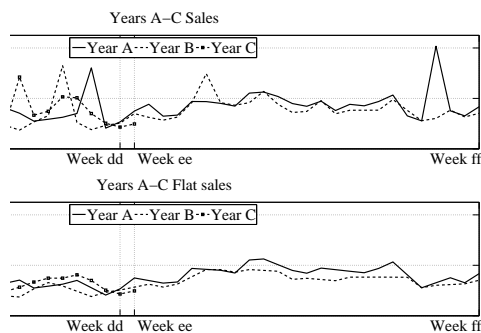


Figure 1: Comparison of real sales with flat sales per year

Neuro-fuzzy modeling, refers to the way of applying various learning techniques developed in the neural network literature to fuzzy modeling or a fuzzy inference system. ANFIS use a feed forward network to search for fuzzy decision rules that perform well on a given task. Using a given input-output data set, the system creates a FIS whose membership function parameters are adjusted using a back-propagation algorithm alone or a combination of a back-propagation algorithm with a least-squares method.

III. PREPROCESSING OF SALES DATA

One of the goals when building prediction models is the ability to use them on the prediction of several different periods. For that, they need to be sufficiently generic and its inputs robust enough so they can translate the system's dynamics effectively. For this purpose, it's necessary that the inputs are constructed in a coherent manner with a logic that sustains the numerical values that they have. Due to confidentiality restrictions none of the timespan can be associated to real years, months or specific days (such as known holidays).

A. Period definition

For the period definition, the available data in a first approach was weekly sales data from week aa to week $aa+44$, named ff from year A to B , and from week aa to week $aa+22$, named ee , of year C . The objective of this work is forecasting year C sales. For that purpose, the models are trained using data from a certain period of year A and B to predict the same period of year C . After defining the periods of forecasting, daily sales data is used in the modeling and forecasting phase.

The approach chosen to deal with period selection was to select three different forecasting periods, starting from a stationary period (no disturbances) and evolving to gradually more complex (disturbed) periods. The stationarity of a sales curves means a sales pattern without the effect of monthly seasonality, yearly seasonality and promotions. In Fig. 1 is presented the comparison between the real weekly sales curve with the flat curve, without the previous effects. From this figure is possible to compute the three forecasting periods desired. As the real curve from weeks aa to bb has a similar dynamic than the flat, it means that it's a period without major events and, thus, stationary. If we extend the period to weeks cc there is an inclusion of some disturbances to this

TABLE I: WEEKLY SEASONALITY

Week day	Mon	Tue	Wed	Thu	Fri	Sat	Sun
ws	0	-0.1	-0.2	-0.12	0	1	0.8

period. Furthermore, if the period is even more extended until weeks dd , it is defined a period plenty of disturbances, which dynamics are translated by a non-stationary behavior instead of a stationary with disturbances behavior. In this sense, the periods are defined as: **Stationary period:** From weeks aa to bb , 6 weeks, 42 days per year, 126 days in total; **stationary period with disturbances:** From weeks aa to cc , 9 weeks, 63 days per year, 189 days in total; **non-stationary period:** From weeks aa to dd , 20 weeks, 140 days per year, 420 days in total.

B. Feature construction

The goal of feature construction is to obtain features that accurately represent the effects that they have in sales. For that, one needs to understand its effect, and then have a logical approach to its mathematical definition. The main attributes that influence sales are the **weekly seasonality** (ws), **monthly seasonality** (ms), **purchasing power of customers** (pw), **promotions** (p) and **holidays or festive days** (h).

1) *Weekly seasonality* (ws): The weekly seasonality could be compared to a distribution of sales during the week. It is a pattern that describes sales during the several days of the week. There is a peak on weekend sales, which starts to raise from wednesday, and declines until tuesday.

The input started to be constructed as a normalized [0 1] distribution, being saturday 1 and wednesday 0, but after some adaptations, the input resulted as presented in Table I. These adaptations were done based on a greedy heuristic, developed for this feature. As it is a pattern that will remain constant, unless significant political measures occur, such as saturdays become working days as well, which may happen; this type of seasonality will have minor changes through the years. The resulting input is presented on the following table.

2) *Monthly seasonality* (ms): The monthly seasonality refers to the way people spend money during a month period. Being used to receive wages at the end of the month, usually the last weekend of a month and the first weekend of the next (weekends after wages - WAW) are the weekends where customers are more willing to spend. There is also an addition to this trend, as in the weekend before customers receive their wages (weekend before wages - WBW) they have less money, which has the consequence of being less willing to spend money. So there is contention of expenses and sales on those weekends tend to be lower than on a regular weekend.

The values given to this type of seasonality are represented on Table II, presented next. The logic behind its construction was the multiplicative effect these days have on sales. It was built comparing the values of sales on the intended weekends with the average of a regular weekend. The first group of numbers concerns to the weekend of contention of expenses, and the last to the expected increase in sales.

TABLE II: MONTHLY SEASONALITY

<i>m.s</i>	WBW		WAW	
	Sat	Sun	Sat	Sun
	0.94	0.76	1.27	1.05

3) *Purchasing power of costumers (pw)*: From daily sales analysis, it was clear that despite different years having the same pattern, there was an offset between the curves, where sales have been decreasing along the years.

In that sense it was needed to construct an input that would account for this influence. It was named purchasing power, although it doesn't have a direct relation with the purchasing power definition, and the goal was to build a vector of inputs, which values would be constant during each year, relating years *B* and *C* overall sales behavior with year *A*. In that sense, the input for year *A* was zero. Its construction was made through the analysis of internal documentation for the years *A* and *B* (10%), and assumed for the forecasting year (26% from year *A* to *C*).

4) *Promotions (p)*: Concerning the promotions, there are of three types. Type 1 (p_1) are transversal promotions discounts spendable in future sales that last 2 or 3 days. There are several of this type of promotions in every year. Type 2 promotions (p_2) only happened once in year *C*, the forecasting year. The difference is that, instead of the transversal discount, the customer has to spend multiples of a certain amount to have access to the same discount. The third type of promotions, named promotions of type 3 (p_3), are promotions equal to p_1 but only applied to a category (a part) of a business unit, instead of being transversal. There is also only one promotion of this type, in year *C*. This type of promotions is announced two days before its beginning in order to reduce the decrease on sales that happens in between.

The approach for the construction of this parameter was similar to the monthly seasonality. It was compiled the sales value of the peaks of the promotion compared to the average of the corresponding regular weekday (without the effect of promotions) sales. The value computed was the multiplicative factor in sales due to promotions compared to the same regular weekday. This procedure was also adopted in the 2 days before promotions. In that way, the input for the type 1 promotions, p_1 , was constructed as a vector of ones, with the values of Table III whenever there was a promotion. The p_1 present in the forecasting period is slightly different, as consists of 3 days, where the first is a holiday, and the last is a holiday where people tend to spend in family as is described in the next section. Due to that it was modeled as a 2 day promotion on friday and saturday. The definition of the p_2 , the first in the prediction period, was slightly different. Although the type of discount was similar, this promotion lasted for a week, in opposition to the type 1 and 3. The approach taken was to compute the average increase in sales of all days of the type 1 promotion, i.e., the average of all the values of corresponding to the training set in Table III. By doing this, the average effect of a p_1 was computed. Then the attribute was constructed with 40% (due to an assumed expectation of lower affluence) of this value for all days of promotion. The type 3 promotion, p_3 , was modeled in a slightly different way. The effect of the average increase of a p_1 promotion were multiplied by 0.2,

TABLE III: PROMOTION INPUT

Promotion	2 days of active promotion
p_1 year <i>A</i>	[3.16 3.05]
p_1 year <i>B</i>	[2.97 3.13]
p_1 year <i>B</i>	[3.08 3.25]
p_2 year <i>C</i>	[3.11 3.11] × 0.4
p_1 year <i>C</i>	[3.07 3.13]
p_3 year <i>C</i>	[1.42 1.43]

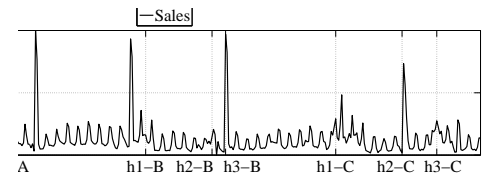


Figure 2: Events related with holidays

TABLE IV: TYPE 1 EFFECT

Year	Monday	Tuesday (event day)	Wednesday
<i>A</i>	1.37	1.33	1.51
<i>B</i>	1.14	1.22	1.01
<i>C</i>	1.26	1.28	1.25

the expected value of the weight of the category in discount in the days of promotion. In that sense, the resulting input of this promotion would be $p_3 = [1 + (p_1 - 1) \times 0.2]$. Next is presented Table III, which shows the input values.

5) *Holidays or festive days*: Finally, the last effect taken in account was the existence of holidays or festive days. These are of three types: a holiday always on the same day of the week, h_1 ; a combination of two holidays, on friday and sunday, which affect the hole previous week, h_2 ; and a combination of two holidays always on the same day (different days of the week in different years), h_3 . In Fig. 2 are represented all the effects related with this input.

Type 1: In fact, this event is not a holiday (H), it's a day where employees are allowed to skip work. Due to that, it might implicate going to a major commercial surface and being exposed to the retailer products. From Fig. 2 observation, the main effect is avoiding the sales decrease, delaying the regular week dynamics. In that sense it was compiled using the multiplicative effect this input has on the weekday and its neighborhood of the event. The values are presented in Table IV.

Type 2: This type of holidays is a combination of 2 holidays but has an effect on a hole week. It is period marked by contention due to the facts associated with it. The week ends with holidays on friday and sunday. Specially on sunday, families tend to gather and spend the day together. Being an important holiday, in years *A* and *B*, stores were only partially opened (half day), which had the consequence of lowering sales in those days. Although sunday is an important day, the hole week has a different behavior. As before, the rational behind the definition of the hole week as input, was the quotient between sales those days and average sales for the same weekday, without promotions effect. The prediction input was slightly different, as it wasn't the average of the effect on

TABLE V: TYPE 2 EFFECT

Year	Mon	Tues	Wed	Thu	Fri (H)	Sat	Sun (H)
A	1.11	1.13	1.34	1.50	1.48	1.09	0.47
B	0.95	1.10	1.01	1.31	1.39	0.81	0.42
C	1.92	1.70	1.66	1.64	1.68	2.42	2

the previous years for one of the days. In year *C* there was a p_1 on the weekend, beginning on friday and ending on sunday, which means that stores weren't partially closed on sunday. In that sense, for this day, as the previous years shape a partially closed day, the input was as if there was no effect, as if it was a regular sunday. This approach was chosen for two reasons. Firstly, it's impossible to know the effect of a open sunday holiday, as the data doesn't show it. Secondly, there is a p_1 promotion on that weekend and sunday was the last day of promotion, which may be sufficient to counter the possible decrease that a sunday holiday of this type may have in sales. In that sense, the input is presented in Table V. This approach was already mentioned for the promotions.

Type 3: This is an effect cause by a combination of two holidays. This holidays have 5 days in between, which means that they form a week if the days between are considered, which was the case. The approach used to build this attribute was similar to the remaining, having some minor changes.

In years *A* and *B* both holidays have a completely different behavior, which makes the definition of this attribute very difficult to accomplish. This has concern to politics in the company as well because, as in the Type 2 holidays, where shops closed on sunday afternoon in year *A* and *B* and then were opened in year *C*; here, for instance, on the holiday of the end of the week of year *A* shops did close on the afternoon (sales break down), whereas in years *B* and *C* they were opened. Also, the first holiday of the week in year *B* was the day right after the Type 2 sunday (holiday), when shops closed in the afternoon, leading to an increase in sales.

In addition to these facts, both holidays have a fixed day, which, in comparison with Type 1 and 2, is worse for input construction, because it means that they move around weekdays during the years. And, as it was possible to see throughout the section, sales have a high dependence on weekdays, and the fact that these holidays change their weekday depending on the year, makes defining its influence through training very difficult.

The procedure to the construction of this input was to define a quotient between the multiplicative effect on sales each day. The only points that were not averaged, were the ones where in one of the years was a promotion (year *B*) and where the stores were partially closed (year *A*). Those values were chosen to be the same as the year *A* values, in the first case; and the same as the values in year *B*, in the second case. Finally, as there was intense promotional activity in that week, those values were multiplied by 2. Table VI presents the input vales.

IV. INTELLIGENT MODELING FOR SALES FORECASTING

After developing the inputs, the models were obtained. There were five models applied to each forecasting horizon:

TABLE VI: TYPE 3 HOLIDAYS INPUT

Year	Day1(H)	Day2	Day3	Day4	Day5	Day6	Day7(H)
A	0.91	0.88	0.88	0.91	1.05	1.21	0.65
B	1.01	0.83	0.78	0.73	0.62	3.08	3.25
C	0.96	0.85	0.83	0.82	0.84	1.21	1

Fuzzy classification models, fuzzy NARX models (FNARX), feedforward classifications neural networks, NARX networks (NNNARX) and ANFIS. Each model was trained using the pervious section's periods and inputs. Concerning the fuzzy models, different cluster (C) structures were compared and different delays for the NARX. For neural networks different combinations of hidden-layers (HL) and neurons (N) were balanced, and different delays for the NARX. For the ANFIS, only in one period different numbers of membership functions (MF) were analyzed, as for the longer periods, due to computational efforts, it was only possible to perform with 2 MF.

For the fuzzy models, the fuzziness exponent was set to 2; the termination tolerance to 0.01; the seed to $sum(100*clock)$; the antecedents were antecedent membership functions and the consequents estimated with locally weighted Least-Squares. The clustering algorithm was chosen to be the Fuzzy C-means. For the neural networks, the number of training epochs and training algorithm used were 1000 training epochs and Levenberg-Marquardt algorithm, respectively. For the ANFIS, the number of training epochs was set to 20 and the membership functions used were Gaussians. A summary of the parameters for all the models in each specific period, is resented in Table VII. For the stationary period the delays in the FNARX an NNNARX were of [7,1,3,4] and [11 for all] for the $[s,ws,ms,pw]$ inputs, respectively. Concerning the stationary period with disturbances, the delays were of [9,3,5,1,3,1] and [11 for all] for the $[s,ws,ms,pw,h,p]$ inputs, respectively. For the last period, it was of [7,1,5,1,14,1] and [10 for all] for the $[s,ws,ms,pw,h,p]$ inputs, respectively.

V. RESULTS AND DISCUSSION

This section is divided by forecasting period and only the best forecast is presented in a figure. The performance criteria used were the variance accounted for, $VAF_i = \left(1 - \frac{var(y_i - \hat{y}_i)}{var(y_i)}\right) \times 100\%$; and the root mean square error, $RMSE = \sqrt{\frac{\sum_{i=1}^n (x_{1,i} - x_{2,i})^2}{n}}$.

A. Stationary period

The models' performance for the stationary period are presented in Table VIII and the best model forecast is presented in Fig. 3. As it is possible to observe in Fig. 3 and Table VIII, the fuzzy classification model, which had the worse performance of all the models in training, presents the best test results. The main differences between the forecast and target are a discrepancy in the beginning of the period, some irregular peaks during weekdays and a general offset between both curves. The first may have to due with a discounts season that usually happens in that season but, as can be seen in previous years, that effect is'n visible and wasn't shaped in testing due to the lack of importance. The majority of the

TABLE VII: PARAMETERS OF THE MODELS FOR EACH PERIOD

Type of model	Structure for each period		
	Stationary period	Stationary period with disturbances	Non-stationary period
Fuzzy Classification	17 C	19 C	8 C
Fuzzy NARX	2 C	3 C	2 C
NN Feedforward	1 HL - 10 N	8 HL - 9 N	8 HL - 2 N
NN NARX	1 HL - 5 N	6 HL - 1 N	6 HL - 2 N
ANFIS	4 MF	2 MF	2 MF

TABLE VIII: PERFORMANCE PER NUMBER OF CLUSTERS FOR THE CLASSIFICATION MODEL - STATIONARY PERIOD

Model	VAF		RMSE	
	Train	Test	Train	Test
Fuzzy Class.	91.16%	84.90%	8.36×10^4	2.29×10^5
Fuzzy NARX.	92.60%	N/S	7.44×10^4	4.99×10^5
Feedforward NN	91.79%	48.83%	8.02×10^4	3.64×10^5
NARX NN	67.67%	59.93%	1.81×10^5	2.64×10^5
ANFIS Class.	92.30%	81.31%	7.84×10^4	1.50×10^5

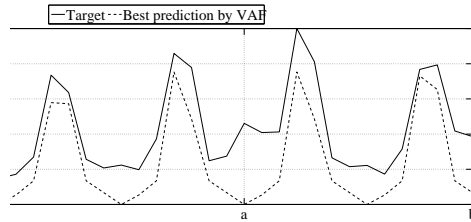


Figure 3: Sales forecasting with the fuzzy classification model - Stationary period

TABLE IX: PERFORMANCE PER NUMBER OF CLUSTERS FOR THE CLASSIFICATION MODEL - STATIONARY PERIOD WITH DISTURBANCES

Model	VAF		RMSE	
	Train	Test	Train	Test
Fuzzy Class.	95.64%	54.42%	1.06×10^5	2.41×10^5
Fuzzy NARX.	96.26%	N/S	9.02×10^4	3.08×10^5
Feedforward NN	60.42%	N/S	3.77×10^4	2.82×10^6
NARX NN	19.05%	N/S	3.40×10^5	3.95×10^5
ANFIS Class.	96.13%	N/S	9.55×10^4	3.85×10^5

effects on the middle of the week seem random, although point a is precisely the beginning of the month. In that sense, it could be introduced as input. But from training data, this effect is not visible, thus, it wouldn't be expected to happen. Point b is also an exception as it was a special day that wasn't accounted due to the fact that in the only year that this effect was visible was coincident with the h_1 promotion.

B. Stationary period with disturbances

The models' performance for the stationary period with disturbances are presented in Table IX and the best model forecast is presented in Fig. 4. The only model that performed well enough was, once again, the fuzzy classification model. In Fig. 4 it is possible to observe that the lower performance has to do with the added weeks, where there are several effects that couldn't be captured by the system. The p_2 promotion (points b

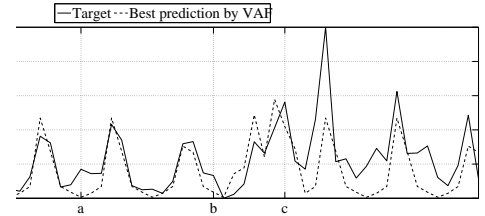


Figure 4: Sales forecasting with the fuzzy classification model - stationary period with disturbances

TABLE X: PERFORMANCE PER NUMBER OF CLUSTERS FOR THE CLASSIFICATION MODEL - NON-STATIONARY PERIOD

Model	VAF		RMSE	
	Train	Test	Train	Test
Fuzzy Class.	92.98%	64.41	1.82×10^5	3.15×10^5
Fuzzy NARX.	92.35%	N/S	1.47×10^5	4.58×10^5
Feedforward NN	47.97%	N/S	3.49×10^5	4.75×10^5
NARX NN	5.48%	N/S	5.16×10^5	1.51×10^6
ANFIS Class.	93.28%	N/S	1.61×10^5	8.05×10^5

to c) is badly captured, only the part aligned with the h_1 (point c)) is minimally accurate. The biggest error comes after, on the final weeks of the period where no event is defined, due to the fact that on the training set none happens on those weeks in previous years.

C. Non-stationary period

The models' performance for the non-stationary period are presented in Table X and the best model forecast is presented in Fig. 5. In this period, the best model was, once again, the fuzzy classification system. The higher VAF of this period's forecast means that the addition made to this period has a better forecast than the one presented in the stationary period with disturbances. In fact, the model presents the same failures as the stationary and stationary with disturbances period, in what capturing the system dynamics is concern. In addition to that, it has also some difficulties in capturing event h_3 , which was already expected. The h_2 effect is not possible to discuss due to a combination of that event with p_1 , which the system was able to capture accurately. Concerning the p_1 and p_3 , the system is extremely accurate on its forecast. Concerning the p_1 , and comparing with the retailer's forecast (the only type of forecast made by the retailer), is important to mention that the model had an error of 1.7% of the total promotion, while the retailer had an error of 30%. This is a major improvement.

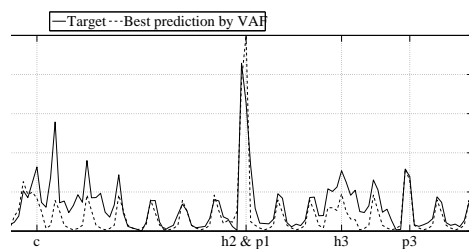


Figure 5: Sales forecasting with the fuzzy classification and NARX model - Non-stationary period

VI. CONCLUSION

This work addressed the problem of sales forecasting, by applying soft, or intelligent, computing techniques to a retailer. Firstly, the approach to the problem was defined, selecting the periods to forecast and which features to use in each period. Then, different modeling techniques were applied and the models for each technique were obtained. Finally, the forecasting results were achieved for each horizon of prediction.

For the five models applied to the problem, only the fuzzy classification is applicable to the problem, achieving accurate forecasts of the stationary trend and some well defined events. Specially for the stationary period, the performance was superior than for the remaining periods. The remaining models are not applicable. The reasons for not having performances as high as on the first period have to do with exceptional events that either weren't present in training data and, therefore the model couldn't learn its impact; or were present in training but not in the way as it happened in the test year. So, although the model had knowledge about the impacts of these events, it didn't had knowledge about the precise circumstances in which these events would affect the system. The first examples are, for instance, the three weeks after the p_2 promotion, where there is an increase in sales and, on previous years, that didn't happen and it wasn't predictable to happen in year C . It is also the case of the p_2 promotion, which is a promotion never made before. For the second case there is the week of the h_3 holidays, when although there was knowledge about past years, the fact that these holidays are movable, in addition with a strong promotional activity made this events unpredictable. On the other hand, one major conclusion that can be drawn is the accurate forecast of the p_1 and p_3 promotions. On the two promotions of this type in testing, the sales value estimations were very accurate.

Finally, an important conclusion is that the best model improves by far the actual forecasting existing in the company analyzed. In the future, this tool can bring major benefits.

ACKNOWLEDGEMENTS

This work was supported by Strategic Project, reference PESt-OE/EME/LA0022/2011, through FCT (under the Unit IDMEC - Pole IST, Research Group IDMEC/LAETA/CSI). This work is also supported by the FCT grant SFRH/BPD/65215/2009, Fundação para a Ciência e a Tecnologia, Ministério da Educação e Ciência, Portugal. The authors would also like to thank SONAE SR and more specifically Eng. Hugo Alexandre and his team, for providing all the

information needed and for all the support given throughout the project.

REFERENCES

- [1] F. Chen and T. Ou, "Sales forecasting system based on gray extreme learning machine with taguchi method in retail industry," *Expert Systems with Applications*, vol. 38, no. 3, pp. 1336 – 1345, 2011.
- [2] I. Alon, M. Qi, and R. J. Sadowski, "Forecasting aggregate retail sales: A comparison of artificial neural networks and traditional methods," *Journal of Retailing and Consumer Services*, pp. 147–156, 2001.
- [3] T. Xiao and X. Qi, "Price competition, cost and demand disruptions and coordination of a supply chain with one manufacturer and two competing retailers," *Omega*, vol. 36, no. 5, pp. 741 – 753, 2008.
- [4] A. A. Levis and L. G. Papageorgiou, "A hierarchical solution approach for multi-site capacity planning under uncertainty in the pharmaceutical industry," *Computers and Chemical Engineering*, vol. 28, no. 5, pp. 707 – 725, 2004.
- [5] G. E. P. Box and G. Jenkins, *Time Series Analysis, Forecasting and Control*. Holden-Day, Incorporated, 1990.
- [6] S. W. Makridakis, S. and V. McGee, *Forecasting: Methods and Applications, 2nd edn.* New York, NY, USA: John Wiley & Sons, Chichester, 1983.
- [7] A.-C. Cheng, C.-J. Chen, and C.-Y. Chen, "A fuzzy multiple criteria comparison of technology forecasting methods for predicting the new materials development," *Technological Forecasting and Social Change*, vol. 75, no. 1, pp. 131 – 141, 2008.
- [8] C.-W. Chu and G. P. Zhang, "A comparative study of linear and nonlinear models for aggregate retail sales forecasting," *International Journal of Production Economics*, vol. 86, no. 3, pp. 217 – 231, 2003.
- [9] M. J. C. Hu, "Application of the adaline system to weather forecasting," E. E. Degree Thesis, Stanford Electronic Lab, Tech. Rep., 1964.
- [10] G. Zhang, B. E. Patuwo, and M. Y. Hu, "Forecasting with artificial neural networks:: The state of the art," *International Journal of Forecasting*, vol. 14, no. 1, pp. 35 – 62, 1998.
- [11] J. Deppisch, H.-U. Bauer, and T. Geisel, "Hierarchical training of neural networks and prediction of chaotic time series," *Physics Letters A*, vol. 158, no. 1 - 2, pp. 57 – 62, 1991.
- [12] E. M. Azoff, *Neural Network Time Series Forecasting of Financial Markets*, 1st ed. New York, NY, USA: John Wiley & Sons, Inc., 1994.
- [13] D. Srinivasan, A. Liew, and C. Chang, "A neural network short-term load forecaster," *Electric Power Systems Research*, vol. 28, no. 3, pp. 227 – 234, 1994.
- [14] J. Ruiz-Suárez, O. Mayora-Ibarra, J. Torres-Jiménez, and L. Ruiz-Suárez, "Short-term ozone forecasting by artificial neural networks," *Advances in Engineering Software*, vol. 23, no. 3, pp. 143 – 149, 1995.
- [15] S. Y. Kang, "An investigation of the use of feedforward neural networks for forecasting," Ph.D. dissertation, Kent, OH, USA, 1992, uMI Order No. GAX92-01899.
- [16] Z. Tang and P. A. Fishwick, "Feedforward neural nets as models for time series forecasting," *INFORMS Journal on Computing*, pp. 374–385, 1993.
- [17] J. M. P. Menezes, Jr. and G. A. Barreto, "Long-term time series prediction with the narx network: An empirical evaluation," *Neurocomput.*, vol. 71, no. 16-18, pp. 3335–3343, Oct. 2008.
- [18] P. Dash, A. Liew, S. Rahman, and S. Dash, "Fuzzy and neuro-fuzzy computing models for electric load forecasting," *Engineering Applications of Artificial Intelligence*, vol. 8, no. 4, pp. 423 – 433, 1995.
- [19] A. Al-Anbuky, S. Bataineh, and S. Al-Aqtash, "Power demand prediction using fuzzy logic," *Control Engineering Practice*, vol. 3, no. 9, pp. 1291 – 1298, 1995.
- [20] R. Kuo, P. Wu, and C. Wang, "An intelligent sales forecasting system through integration of artificial neural networks and fuzzy neural networks with fuzzy weight elimination," *Neural Networks*, vol. 15, no. 7, pp. 909 – 925, 2002.
- [21] P.-C. Chang, Y.-W. Wang, and C.-H. Liu, "The development of a weighted evolving fuzzy neural network for pcb sales forecasting," *Expert Systems with Applications*, vol. 32, no. 1, pp. 86 – 96, 2007.

Transmission Network Expansion Planning under Uncertainty using the Conditional Value at Risk and Genetic Algorithms

Hugo R. Sardinha, João M. C. Sousa, Carlos A. Silva
 Technical University of Lisbon, Instituto Superior Técnico
 Dept. of Mechanical Engineering, CIS, IDMEC, LAETA
 Lisbon, Portugal

Daniel Delgado, João Claro
 Universidade do Porto, Faculdade de Engenharia
 INESC Porto, Rua Dr. Roberto Frias, 378
 4200-465 Porto, Portugal

Abstract—The aim of this work is to study the Transmission Network Expansion Planning (TNEP) problem considering uncertainty on the demand side. Such problem consists of deciding how should an electrical network be expanded so that the future demand is ensured. We expanded the power transport problem formulation so that power losses are included in the objective function. Uncertainty is included through stochastic programming based on scenario analysis; different degrees of uncertainty are considered. Further, an explicit risk measure is added to mathematical model using the Conditional Value at Risk (CVaR). Weighting the relative importance of minimizing expansion and operational costs against the value of the CVaR simulates the attitude of the investor towards risk and shows to be of significant importance when planning the future. The problem was optimized using Genetic Algorithms. This work provided insight on how investment decisions change when considering several levels of uncertainty and risk aversion, in an extended formulation of the TNEP problem.

Keywords—Transmission Network Expansion Planning; Genetic Algorithms; Uncertainty; Risk Analysis.

I. INTRODUCTION

The prime objective of the Transmission Network Expansion Planning (TNEP) [1] problem is to decide how should a power transmission network be expanded in order to supply a forecast value (or values) of the demand.

Future uncertainties are such a challenging issue for the various prediction methods that one must acknowledge that long-term forecasts might, and most likely will, be wrong [2]. In order to mitigate the effect of uncertainty, building not only one but several scenarios has proved to be a technique that, despite its greater computational effort, presents an reliable method to tackle the ambiguities of the future. Some of the most commonly uncertainties studied in the TNEP problem relate to: deliberate attacks upon the grid [1], [3], capacity failing of the transmission lines [4], and demand uncertainty [5]. The scenario analysis in the above works is implemented using stochastic programming [4]. Despite the usefulness of stochastic programming and scenario analysis, these approaches do not provide a risk assessment method. The work developed in [5] evaluates risk using fuzzy techniques after the optimization is done for each scenario individually,

and so is not incorporated in the cost function. The drawback of this approach is that not including risk measure in the mathematical model conditions the number of scenarios that can be tested mainly to the difficult interpretation of the individual results of each scenario [3]. In this work we aim to implement a risk-based stochastic formulation of the TNEP problem that considers the concepts of *Value at Risk (VaR)* and *Conditional Value at Risk (CVaR)*.

In the business and finance sectors, the VaR summarizes the worst expected loss over a target horizon within a given confidence interval and CVaR is a measure which could be defined as the expected value of the losses worse than VaR, over the same target horizon [6]. In the TNEP problem the losses that were just referred, concern the operational costs for the different scenarios (namely generation and curtailment), under each expansion plan.

The paper is organized as follows. Section 2 describes the modeling of TNEP. Emphasis is made on modeling with uncertainty. The risk analysis used in the paper are described in Section 3. Section 4 described the genetic algorithm applied to solve the TNEP problem. The obtained results are presented and discussed in Section 5, and finally, Section 6 presents the conclusions.

II. MODELING

A. Loss Free Model

The TNEP problem is a large combinatorial problem, as many possible configurations of the network may satisfy the demand, and more importantly might have very similar or equal costs. A common approach to tackle the problem is to use the DC model formulation for the power flow equations.

Even with the simplifications considered in the DC-Model the TNEP problem constitutes a large combinatorial, non-polynomial, multi-dimensional problem, that cannot be solved either without employing further simplifications, or heuristic and meta-heuristic approaches. The classical DC-Model for the TNEP problem is presented below.

$$\min_{\theta, g, n} \sum_{\forall (i,k) \in \Omega} c_{ik} n_{ik} + \sum_{\forall i \in \Omega_g} c_{g_i} p_{g_i} \quad \text{s.t.} \quad (1)$$

$$-\sum_{k \neq i} f_{ik} + p_{g_i} = d_i \quad (2)$$

$$f_{ik} - b_{ik}(n_{ik}^o + n_{ik})(\theta_i - \theta_j) = 0 \quad (3)$$

$$|f_{ik}| \leq (n_{ik}^o + n_{ik})\overline{f_{ik}} \quad (4)$$

$$0 \leq p_{g_i} \leq \overline{p_{g_i}} \quad (5)$$

$$0 \leq n_{ik} \leq \overline{n_{ik}} \quad (6)$$

where n_{ik} is integer, θ_i is unbounded, (1) is the cost function divided in two parcels, the first relating to expansion costs and the second to operational costs, (2) is the flow balance constraint in each node network, (3) is the flow calculation formula, and (4)-(6) are the capacity constraints.

B. DC Model with power losses

The inclusion of power losses in a non-linear manner in the TNEP problem has already been presented in [7] and results in changes to (2) and (4) which can now be written as:

$$-\sum_{k \neq i} (f_{ik} + \frac{1}{2}h_{ik}) + p_{g_i} = d_i \quad (7)$$

$$|f_{ik}| + \frac{1}{2}h_{ik} \leq (n_{ik}^o + n_{ik})\overline{f_{ik}} \quad (8)$$

where the losses h_{ik} are defined as:

$$h_{ik} = g_{ik}\theta_{ik}^2 \quad (9)$$

C. DC Model with load curtailment

This paper introduces load curtailment as measure of how much active power is left unsupplied. This is an important variable when considering uncertainty, since the unexpected rise of the demand might lead to a shortage of power transmission capability.

One must notice how the cost associated with unsupplied power changes the problem in conceptual terms. If the cost of load curtailment is low, then this would pose another decision for the investor to make, whether or not to expand the network further satisfying a higher percentage of the total demand or if not leaving a higher percentage of the demand unsupplied. On the other hand if the the cost of the load curtailment is extremely high this would cause the solutions that consider curtailed load to be extremely costly. Practically, this means that considering high curtailment costs is equivalent to search for a solution where all of the demand is met.

The model considering load curtailment and power losses simultaneously changes the problem cost function, (1), and the flow balance (7), into the following:

$$\min_{\theta, g, n, r} \sum_{\forall (i, k) \in \Omega} c_{ik}n_{ik} + \sum_{\forall i \in \Omega_g} c_{p_{g_i}}p_{g_i} + \sum_{\forall i \in \Omega_d} c_{r_i}r_i \quad (10)$$

$$-\sum_{k \neq i} (f_{ik} + \frac{1}{2}h_{ik}) + p_{g_i} + r_i = d_i \quad (11)$$

D. Model with uncertainty

Deterministic models can be transformed into stochastic optimization models that take into account the randomness of the stochastic variables and these models can be solved using stochastic programming techniques. The stochastic model that considers power losses, load curtailment and uncertainty is:

$$\min_{\theta, g, n, r} \sum_{\forall (i, k) \in \Omega} c_{ik}n_{ik} + \sum_{\lambda \in \Lambda} \Pi(\lambda) \left(\sum_{\forall i \in \Omega_g} c_{p_{g_i}}p_{g_i}^\lambda + \sum_{\forall i \in \Omega_d} c_{r_i}r_i^\lambda \right) \quad (12)$$

s.t.

$$-\sum_{k \neq i} (f_{ik}^\lambda + \frac{1}{2}h_{ik}^\lambda) + p_{g_i}^\lambda + r_i^\lambda = d_i^\lambda \quad (12)$$

$$f_{ik}^\lambda - b_{ik}(n_{ik}^o + n_{ik})(\theta_i - \theta_j) = 0 \quad (13)$$

$$h_{ik}^\lambda = g_{ik}(\theta_{ik}^\lambda)^2 \quad (14)$$

$$|f_{ik}^\lambda| + \frac{1}{2}h_{ik}^\lambda \leq (n_{ik}^o + n_{ik})\overline{f_{ik}} \quad (15)$$

$$0 \leq p_{g_i}^\lambda \leq \overline{p_{g_i}} \quad (16)$$

$$0 \leq n_{ik} \leq \overline{n_{ik}} \quad (17)$$

where n_{ik} is integer, θ_i^λ is unbounded, λ is a scenario, and $\Pi(\lambda)$ is the probability of each scenario. The model given above shows that each expansion plan is evaluated for all possible scenarios.

However, in [8], stochastic programming in itself does not rule out that riskier options are chosen considering all plausible scenarios. In fact, this stochastic formulation alone is considered to be a *Risk-Neutral* approach when dealing with uncertainty as pointed out by [1]. To address this issue the following subsection describes the risk measure used in this work, its relation to scenario analysis and stochastic programming and its inclusion in the mathematical model.

III. RISK ANALYSIS

One of the major purposes of this work is to assess investments cost under uncertainty considering an explicit risk measure in the mathematical model. The choice then falls on how to quantify risk and the investor's respective risk attitude. In order to do so effectively, a measurement is needed that provides reliable assessment on the relative risk of several different solutions for set of plausible scenarios.

A. Conditional Value at Risk

The *Conditional Value at Risk* has proven to be an useful tool in assessing risk due to its linearity and conservativeness [9]. Moreover, CVaR has been reported to outperform other risk measurements as it can readily be incorporated into any optimization problem as using the following formula [9], [10] as:

$$\tilde{F}_\varphi(\omega_\lambda, \xi) = \xi + \frac{1}{m(1-\varphi)} \sum_{\lambda=1}^m \omega_\lambda \quad (18)$$

and the CVaR optimization problem as:

$$\min_{\xi, \omega_\lambda} \tilde{F}_\varphi(\omega_\lambda, \xi) \quad (19)$$

s.t.

$$\omega_\lambda \geq 0 \quad (20)$$

$$\omega_\lambda \geq f(\mathbf{x}, y_\lambda) - \xi \quad (21)$$

where m is the number of scenarios, \mathbf{x} is the variable concerning the option to be taken for the project and y_λ the value of the random variable y in scenario λ . In addition, for any solution \mathbf{x} and a confidence level φ , VaR is the value of ξ such that the probability of the loss not exceeding ξ is φ [11].

To solve the TNEP problem. It is important to notice that what Rockafellar defines in [9] and [10] as the losses function $f(\mathbf{x}, y_\lambda)$, relates in the TNEP problem, to the cost of a given plan after uncertainty clears, i.e., the cost for a given scenario. Minimizing the CVaR for a given expansion in the TNEP problem can then be described by the model below.

$$\min_{\xi} \text{CVaR} \quad (22)$$

s.t.

$$\omega_\lambda \geq 0 \quad (23)$$

$$\omega_\lambda \geq \left(\sum_{\forall(i,k) \in \Omega} c_{ik} n_{ik} + \sum_{\forall i \in \Omega_g} c_{p_{g_i}} p_{g_i}^\lambda + \sum_{\forall i \in \Omega_d} c_{r_i} r_i^\lambda \right) - \xi \quad \forall \lambda \in \Lambda \quad (24)$$

Notice that, in our model we aim to include the risk attitude of the investor. The CVaR in itself does not provide information about the attitude of the investor, it provides information about the investment necessary to supply the demand under a set of possible scenarios with a certain degree of confidence. To include the risk attitude in the objective function the TNEP problem is expanded to include the CVaR, and weights were established between the stochastic formulation and the CVaR, to reflect the relative importance of minimizing each one.

B. Stochastic Model with Risk Aversion

The full optimization problem is presented below:

$$\min_{\theta, g, n, r} (1 - \beta) \left[\sum_{\forall(i,k) \in \Omega} c_{ik} n_{ik} + \sum_{\lambda \in \Lambda} \Pi(\lambda) \left(\sum_{\forall i \in \Omega_g} c_{p_{g_i}} p_{g_i}^\lambda + \sum_{\forall i \in \Omega_d} c_{r_i} r_i^\lambda \right) \right] + \beta(\text{CVaR}) \quad (25)$$

s.t.

$$-\sum_{k \neq i} (f_{ik}^\lambda + \frac{1}{2} h_{ik}^\lambda) + p_{g_i}^\lambda + r_i^\lambda = d_i^\lambda \quad (26)$$

$$f_{ik}^\lambda - b_{ik} (n_{ik}^o + n_{ik}) (\theta_i - \theta_j) = 0 \quad (27)$$

$$h_{ik}^\lambda = g_{ik} (\theta_{ik}^\lambda)^2 \quad (28)$$

$$|f_{ik}^\lambda| + \frac{1}{2} h_{ik}^\lambda \leq (n_{ik}^o + n_{ik}) \overline{f_{ik}^\lambda} \quad (29)$$

$$0 \leq p_{g_i}^\lambda \leq \overline{p_{g_i}^\lambda} \quad (30)$$

$$0 \leq n_{ik} \leq \overline{n_{ik}} \quad (31)$$

$$\omega_\lambda \geq 0 \quad (32)$$

$$\omega_\lambda \geq \left(\sum_{\forall(i,k) \in \Omega} c_{ik} n_{ik} + \sum_{\forall i \in \Omega_g} c_{p_{g_i}} p_{g_i}^\lambda + \sum_{\forall i \in \Omega_d} c_{r_i} r_i^\lambda \right) - \xi \quad \forall \lambda \in \Lambda \quad (33)$$

with n_{ik} integer and θ_i^λ unbounded. In the objective function the stochastic formulation presented earlier and the CVaR are weighted by the parameter β . Such Parameter reflects the attitude towards risk of the investor. The the higher the β is, the more averse to risk the investor. Notice that for $\beta = 0$ the objective is reduced to the one of the stochastic formulation and so, according to [1], the investor is *Risk-Neutral*. Therefore, an investor whose attitude towards risk is very high will have a value of β very close to one. In this work we will employ a variety of values of β to study different levels of risk aversion.

IV. GENETIC ALGORITHMS IN TNEP

GA belong the set of evolutionary algorithms (EA), that due to their population-based inherent nature, are able to tackle problems with a high degree of complexity [12]. For the TNEP problem an integer encoding is chosen that reflects the number of lines in the connection that such entry of the chromosome relates to, as done by Gallego in [13].

However, this information alone can only provide information on the expansion cost of the solution. In order to evaluate operational costs, namely generation and curtailment an augmented version of the common Optimal Power Flow problem was also derived in [7]. Possible load curtailment is considered at every demand node by the inclusion of a high cost generator and the full augmented OPF is presented below. One must notice that if the lossless model is to be tested the

term G is dropped.

$$\min_{\theta, P_g, P_r} \sum_{\forall i \in \Omega_g} \Gamma(P_{g_i}) + \sum_{\forall r \in \Omega_d} \Gamma(P_{r_i}) \quad (34)$$

$$\text{s.t.} \\ - \sum_{i \neq k} \left(F_{ik} + G_{ik} \frac{\theta_{ik}^2}{2} \right) + P_{g_i} + P_{r_i} = D_i \quad (35)$$

$$F_{ik} = -B_{ik} \theta_{ik} \quad (36)$$

$$|F_{ik}| + G_{ik} \frac{\theta_{ik}^2}{2} - \bar{F}_{ik} \leq 0 \quad (37)$$

$$0 \leq P_{g_i} \leq \bar{P}_{g_i} \quad (38)$$

$$\theta_r = 0 \quad (39)$$

The GA then performs a series of iterative computations in order to evolve a population of individuals (possible solutions), using the principle of *survival of the fittest*. These steps are the following: 1) Initialize the population; 2) Evaluate each chromosome; 3) Selection; 4) Crossover; 5) Mutations; 6) Replacement of the old population by the new; 7) Back to 2) until the termination criteria is met.

1) *Evaluation*: Operational costs are calculated through the augmented version of the OPF. Performing risk analysis is then possible minimizing the CVaR. Notice that if uncertainty is not considered then the cost evaluations consists in running the OPF once for the demand profile of case at study, since there are no scenarios and no possible risk.

2) *Selection*: Selection is a fitness based method, used with the purpose of choosing the most suited chromosomes in the population to form new individuals.

3) *Crossover*: Two individuals are selected from the population (applying two times the chosen selection operator) and are then recombined with a probability p_c , creating two new individuals. This is done by generating a random number $r \in [0, 1]$. If $r \leq C_r$, the two individuals are combined through crossover. The method chosen in this work is the two-point crossover.

4) *Mutation*: This operator selects an individual from the population with probability M_r and randomly changes one of its alleles. Having the chromosome integer variables, this consists in randomly choose one of the values possible for that variable.

5) *Replacement and Elitism*: Replacement is the process by which the new individuals, created with the above operators, are introduced in the population. There are cases when the fittest individual in the population is replaced by an individual with lower fitness. Therefore, the elitism reintroduces n_c copies of the best individual into the population.

V. RESULTS

A. Deterministic approach

The network studied in this section is one of the most studied network configurations and was created specifically for the TNEP problem. [14] This network has been the subject of various studies namely the ones presented in [14] [15] and [7]. This network consists on 3 generation nodes with a total

TABLE I
LINE DATA FOR GRAVER'S EXAMPLE

Corridor	R (pu)	X (pu)	Capacity	Cost(\$*10 ³)
1-2	0.10	0.40	100	40
1-3	0.09	0.38	100	38
1-4	0.15	0.60	80	60
1-5	0.05	0.20	100	20
1-6	0.17	0.68	70	68
2-3	0.05	0.20	100	20
2-4	0.10	0.40	100	40
2-5	0.08	0.31	100	31
2-6	0.08	0.30	100	30
3-4	0.15	0.59	82	59
3-5	0.05	0.20	100	20
3-6	0.12	0.48	100	48
4-5	0.16	0.63	75	63
5-6	0.15	0.61	78	61

TABLE II
BUS DATA FOR GRAVER'S EXAMPLE

Bus	D_i (MW)	\bar{P}_{g_i} (MW)	c_{g_i} €/MW
1	80	150	10
2	240		
3	40	360	20
4	160		
5	240		
6	0	600	30

capacity of 1100 MW, 5 demand nodes with a total demand of 760 (MW), and 15 different possible connections most of them with different line characteristics. Each entry of the chromosome corresponds to the listing of connection presented in Table I, and the constraints concerning generation capacity and the demand profile of the network are presented in Table II. In order to validate our results we will begin by employing a deterministic model, namely considering and neglecting losses.

At this stage, and to have comparable results, we considered that no curtailment was possible and so, the cost of unsupplied load is very high to penalize solutions unable to supply all the demand. Notice that when using a meta-heuristic approach the inclusion of the load curtailment a more natural formulation of the problem, since during the solution-space search the random inherent characteristics of meta-heuristic methods might find solutions where is impossible to supply all the demand. Should this occur, considering load curtailment in the mathematical model works as a penalty to the objective function rather than a possible operational cost.

Below, Tables III and IV present the results yielded by our GA when losses were neglected and considered, respectively. From these results we notice that in both cases the GA were able to find the best solution proposed thus far by any study.

Table V shows statistical results and the genetic operators with which the solutions were obtained.

B. Stochastic Cases

In this section, the optimization problem tackled through the GA is the one described from (25) to (33). For this purpose 30 scenarios were built randomly with a normal distribution and standard deviations of: 0.1, 0.2 and 0.3 from the mean value. Probabilities for each scenario were considered to be

TABLE III
 EXPANSION PLAN FOR GRAVER 6-BUS - LOSSES NEGLECTED

Method	Corridor	Number of Lines	Expansion Cost(10 ³ €)
Heuristic [14]	4-6	2	130
	3-5	2	
	2-3	1	
Genetic [13]	4-6	3	110
	3-5	1	
Improved Heuristic [7]	4-6	3	110
	3-5	1	
Proposed Genetic	4-6	3	110
	3-5	1	

 TABLE IV
 EXPANSION PLAN FOR GRAVER 6-BUS - CONSIDERING LOSSES

Method	Corridor	Number of Lines	Expansion Cost(10 ³ €)
MILP [15]	4-6	2	140
	3-5	1	
	2-6	2	
Improved Heuristic [7]	4-6	2	130
	3-5	1	
	2-6	1	
	2-3	1	
Proposed Genetic	4-6	2	130
	3-5	1	
	2-6	1	
	2-3	1	

equal, and Risk Attitude (β) was considered to have values of: 0; 0.25; 0.5; 0.75 and 1.

In order to consider a cost of curtailed load that will allow the investor to choose between curtailed load for a subset of scenarios and further network expansion we employ a method used by Van Mieghen in [16] where such cost is based on the concept of *Critical Fractile* (C_f). The *Critical Fractile* expresses the optimal service probability and depends on unit cost to unit return [16] or in TNEP, unit cost to unmet unit penalty. Practically it means that if the value of C_f is set a priori, differently for each demand node, it will also impose a different value of c_{r_i} for each demand node. To transpose these concepts from the work of Van Mieghen to the TNEP problem, we propose a curtailment cost based not only on the Critical Fractile but also on the average line cost and capacity as follows:

$$c_{r_i} = \frac{\bar{c}/\bar{F}}{1 - C_f} \quad (40)$$

$$C_{f_i} = 0.5 \quad \forall i \in \Omega_d \quad (41)$$

where \bar{c} is the average cost, \bar{F} the average transmission capability. Fig. 1 shows the evolution of the cost function value as the risk aversion and standard deviation vary.

Notice how a standard deviation of 0.3 yields a much costlier solution, specially for higher degrees of Risk Aversion. This results show how for medium networks the effect of uncertainty can be extremely constraining, specially when many nodes have different mean values of demand. Secondly we present in Table VI the configurations that yielded the above costs.

 TABLE V
 GENETIC PARAMETERS AND STATISTIC RESULTS FOR GRAVER'S NETWORK

Assumption	P_z	M_r	C_r	Mean €*10 ⁵	Std Dev €*10 ⁵	Min €*10 ⁵
No Loss	150	0.04	0.9	1.4453	0.1935	1.2668
Loss	100	0.05	0.9	1.5519	0.1756	1.4716

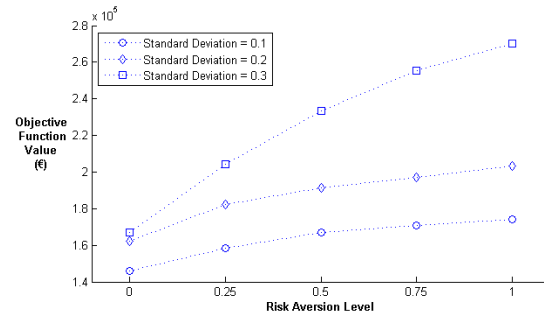


Figure 1. Results for Graver's Network under Uncertainty

Here we see that the solutions found for smaller values of standard deviations are in fact very similar to the ones obtained under the lossless-line assumption. Notice however, that now we considered possible curtailment and so decision of considering load which is not supplied is possible contrarily to before. It is also interesting to notice how the the connections built with an increasing degree of uncertainty and with an increasing level of risk aversion are in fact reinforcements of the configurations achieved before, meaning that for this particular case there is a set of connections which is extremely important when expanding the network.

Nevertheless, Fig.1 shows only the objective function value considering different values of standard deviation and risk aversion. Here would also be interesting to present how expansion costs and the risk measure evolve with the given varying parameters. Figs.2 and 3 show such evolutions.

As one can see, for any degree of uncertainty, we observe a decreasing in the CVaR value as risk aversion increases. An expected result as risk becomes more important to minimize when comparing to the expansion costs that, as also observable from Fig.2 increase as the aversion towards risk is higher.

Also these evolutions show that for some risk aversion levels (namely $\beta = 0.75$ and $\beta = 1$) the values of both expansion costs and CVaR are constant even though the value of the objective function in Fig.1 increases. This is explained by the different weights present in the objective function for different levels of risk aversion which let us conclude that even with an increasing aversion towards risk there was no solution that could further decrease the value of CVaR.

VI. CONCLUSIONS

This paper studies the Transmission Network Expansion Planning problem considering uncertainty on the demand side. Uncertainty is included considering scenario analysis. An explicit risk measure is incorporated in the mathematical model using the Conditional Value at Risk (CVaR). The problem

TABLE VI
GA GRAVER'S NETWORK

σ	Corridor	β				
		0	0.25	0.5	0.75	1
0.1	4 - 6	3	3	2	2	2
	3 - 5	1	1	1	1	1
	2 - 6	0	0	2	2	2
0.2	4 - 6	3	2	2	2	2
	3 - 5	1	1	2	2	2
	2 - 6	0	2	2	2	2
0.3	4 - 6	1	2	2	2	2
	3 - 5	1	1	2	2	2
	2 - 6	2	2	2	3	3

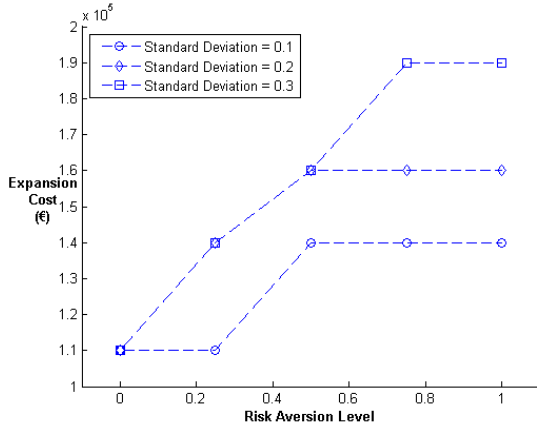


Figure 2. Expansion Costs for Graver's Network under Uncertainty

is optimized using genetic algorithms. Our results present concrete values for investment, ranging from a slightly risk-averse investor to an extremely risk-averse one. These results show that the variation in investment is steeper between a risk-neutral investor and a slightly-averse investor, since in the former no importance is given to the Conditional Value at Risk. We noticed that, even if the value of the cost function increases, certain levels of aversion yield the same expansion plan, meaning that in fact for this problem only a subset of risk attitudes of those considered are relevant to the study. From this perspective, this work also presents information on which risk aversion levels are enough to study risk attitude in TNEP, and in general values for $\beta = \{0, 0.5, 1\}$ show satisfactory differences that provide reliable information on how investment will increase with risk aversion. Another aspect of employing a risk analysis in TNEP is the cost of curtailed load. An increasing aversion towards risk was observed when a higher investment is needed.

ACKNOWLEDGEMENTS

This work was supported by Strategic Project, reference PEst-OE/EME/LA0022/2011, through FCT (under the Unit IDMEC - Pole IST, Research Group IDMEC/LAETA/CSI), and by the ERDF - European Regional Development Fund through the COMPETE Programme (operational programme for competitiveness) and by National Funds through the FCT - Fundação para a Ciência e a Tecnologia (Portuguese Foundation for Science and Technology) within project Flexible Design of Networked Engineering Systems / PTDC/SEN-ENR/101802/2008.

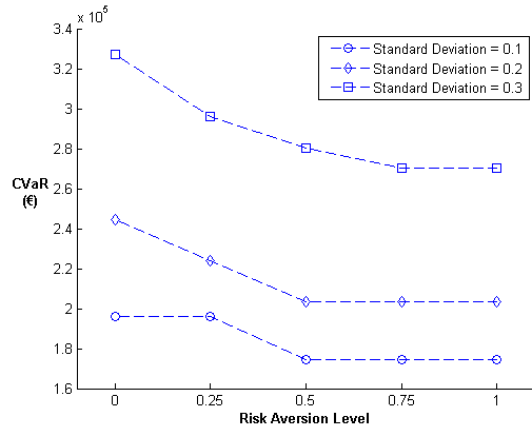


Figure 3. Conditional Value at Risk for Graver's Network under Uncertainty

REFERENCES

- [1] N. Alguacil, M. Carrión, and J. M. Arroyo, "Transmission network expansion planning under deliberate outages," *Electrical Power and Energy Systems*, vol. 31, pp. 553–561, 2009.
- [2] B. Kermanshah, "Recurrent neural network for forecasting next 10 years loads of nine japanese utilities," *Neurocomputing*, vol. 23, pp. 125 – 133, 1998.
- [3] J. M. A. M. Arroyo, N. Alguacil, and M. Carrión, "A risk-based approach for transmission network expansion planning under deliberate outages," *IEEE Transactions on Power Systems*, vol. 25, pp. 1759–1766, 2010.
- [4] J. Alvarez, K. Ponnambalam, and V. H. Quintana, "Transmission expansion under risk using stochastic programming," in *9th International Conference on Probabilistic Methods Applied to Power Systems*, 2006.
- [5] P. Maghouli, S. H. Hosseini, M. O. Buygi, and M. Shahidehpour, "A scenario-based multi-objective model for multi-stage transmission expansion planning," *IEEE Transactions on Power Systems*, vol. 26, pp. 470–477, 2011.
- [6] J. Claro and J. P. de Sousa, "A multiobjective metaheuristic for a mean-risk multistage capacity investment problem," *Journal of Heuristics*, vol. 16, pp. 85 – 115, 2010.
- [7] E. J. de Oliveira, I. C. da Silva Jr, J. M. A. L. R. Pereira, and S. C. Jr, "Transmission system expansion planning using a sigmoid function to handle integer investment variables," *IEEE Transactions on Power Apparatus and Systems*, vol. 20, pp. 1616 – 1621, 2005.
- [8] V. Miranda and L. M. Proença, "Probabilistic choice vs risk analysis - conflicts and synthesis in power system planning," in *20th International Conference on Power Industry Computer Applications*, 1997.
- [9] R. T. Rockafellar and S. Uryasev, "Conditional value-at-risk for general loss distributions," *Journal of Banking & Finance*, vol. 26, pp. 1443 – 1471, 2002.
- [10] R. T. Rockafellar and S. Uryasev, "Optimization of conditional value-at-risk," *Journal of Risk*, vol. 2, pp. 21–41, 2000.
- [11] C. Lim, H. D. Sherali, and S. Uryasev, "Portfolio optimization by minimizing conditional value-at-risk via nondifferentiable optimization," *Computational Optimization and Applications*, vol. 46, pp. 391 – 415, 2010.
- [12] C. A. Coello, G. B. Lamont, and D. A. V. Veldhuizen, *Evolutionary algorithms for solving multi-objective problems*. Springer, 2007.
- [13] R.A.Gallego, A. Monticelli, and R. Romero, "Transmission system expansion planning by an extended genetic algorithm," in *IEE Proceedings online*, 1998.
- [14] L. Graver, "Transmission network estimation using linear programming," *IEEE Transactions on Power Apparatus and Systems*, 1970.
- [15] N. Alguacil, A. L. Motto, and A. J. Conejo, "Transmission network expansion planning: A mixed-integer lp approach," *IEEE Transactions on Power Systems*, 2003.
- [16] J. A. V. Mieghem, "Risk mitigation in newsvendor networks: Resource diversification, flexibility, sharing, and hedging," *Management Science*, vol. 53, pp. 1269–1288, 2007.

General Framework for Context-Aware Recommendation of Social Events

Wolfgang Beer, Walter Hargassner
Software Competence Center Hagenberg GmbH
Softwarepark 21, Austria
Hagenberg, Austria
{wolfgang.beer; walter.hargassner}@scch.at

Christian Derwein, Sandor Herramhof
Evtntogram Labs GmbH
Leonfeldner Strasse 328
Linz, Austria
{sandor; chris}@evntogram.com

Abstract—Modern e-commerce systems offer a multitude of products and services in global marketplaces. The modern consumer is therefore overwhelmed by millions of options, variants and choices of products and services. With the rise of global marketplaces with their huge amount of items, recommendation systems became the basis for modern e-commerce systems. The traditional approaches for implementing recommendation engines, such as content and collaborative filtering, solve the challenge of calculating a recommendation set of items for a given user. While these traditional approaches cope well with large sets of static user and item information, they lack a general approach for including highly dynamic context-information. As the e-commerce market swiftly changes to mobile computing platforms, such as smartphones and tablets, the use of context-information for generating item recommendations is of great interest. In this work, we propose a concept for a general framework for the implementation of such context-aware recommendation engines, specifically for mobile platforms.

Keywords—context awareness; context aware recommendation; decision support; recommendation system;

I. INTRODUCTION

The modern consumer is overwhelmed with options and choices. Global marketplaces, such as ebay, Amazon, Apple iTunes or Google Play, offer millions of different products and services in hundreds of different categories. These categories span a wide spectrum of product families from traditional hardware to software and mobile apps, ebooks, electronics, video and music streaming or even food. Today global marketplaces offer unlimited possibilities to publish and instantly deliver all kinds of products and services. While the publishing and delivery of products and services is getting easier for companies, it is difficult to uniquely present a specific product to customers. According to the huge number of products available in global marketplaces and the consumers limited time and motivation to check all similar products, recommendation engines are of crucial interest for modern consumers. Recommendation systems, such as the product recommendation at Amazon or ebay, are already present for several years. Without traditional recommendation systems, the consumer soon gets lost within the huge amount of available products. To counter that, global marketplaces soon recognized the need for transparent

product recommendation within their systems. In 2006 the Netflix Prize competition was initiated with a 1 million dollar prize for achieving a ten percent or more improvement of Netflix's video recommendation algorithm. The training set that Netflix published for the price competition contained around 100 million ratings from about 500.000 anonymous customers on 17.000 videos. The contest attracted 48.000 competing teams from 182 different countries. The winning team (BellKor) from AT&T Research Labs (made up of Bob Bell and Chris Volinsky, from the Statistics Research group in AT&T Labs, and Yehuda Koren) was able to improve the performance of Netflix's recommendation algorithm by 8.43 percent. So it is obvious that traditional recommendation systems play an important role in modern consumer markets. On the other side many interesting aspects of recommendation systems have not been fully addressed by the research community so far. Bell et al. identified several such research aspects during their work on the Netflix prize competition [1]. One of these aspects, which we will also address in this work, is the relation of temporal effects and the realization that parameters describing the data are not static but dynamic functions. So the client-centric view on recommendation systems much depends on the consumer's actual context. Client-centric recommendation system approaches, such as implementations on smartphones and mobile devices, should focus on the user's demands in a tight relation to the users actual situation. So for a user the context-related dimensions time, location, weather, activity and companions play a major role in any decision. Bell et al. also identified that a combination and blending of several quite simple recommendation approaches often result in excellent recommendations. In this work, we also argue that building a framework for blending of multiple dimensions, containing context-related information such as time and distance and linked data information, can lead to reliable and customizable client-centric recommendation models.

Section II gives a short overview on state-of-the-art in recommendation systems and related work on how to introduce context-awareness in recommendations. Section III focuses on the requirements a general framework for context-aware recommendation systems has to fulfill. Section IV gives an

abstract overview on our approach for introducing context-information in traditional recommendation methods and section V defines a practical software architecture to implement our approach. Section VI concludes with an application case study that introduces context-aware recommendation to the domain of social events.

II. RELATED WORK

The importance of context-awareness in software systems has been discussed by research communities in many different application domains, including ubiquitous and pervasive computing, mobile computing, e-commerce, information retrieval, marketing and management as well as in several engineering disciplines. The term context-aware software was first used in the Xerox PARC research project PARCTAB in 1994 [2]. In this work, the term was defined and used for software that is able to adapt according to its actual location, the collection of nearby people, hosts and accessible devices. Also the possibility to track the changes of context information over time, in other words to store historic context information, was mentioned. Over the years, different research groups enriched this basic definition of context and context-aware software. Brown et al. [3], for example, widened the scope of context information to temperature, time, season and many other factors. Due to the fact that the number of context information factors is nearly unlimited, the definition of context by Anhind K. Dey is one of the most commonly used:

Context is any information that can be used to characterize the situation of an entity. An entity is a person, place, or object that is considered relevant to the interaction between a user and an application, including the user and application themselves. [4]

This definition of context specifies that context contains any kind of information about an entity in order to understand its situation. So context information is not limited to location information, but could also mean information about the social situation of a person or the persons mood. Usually, such a sort of context information is hard to collect, but there are a reasonable number of research projects that try to collect even this kind of information. An interesting fact about the above definition of context is that Dey identifies three base classes that classify all objects: person, place and object. This kind of classification has practical reasons but is also fixed to a location-dependent view of context information. Over the last ten years several architectures and implementations of software middleware frameworks were published that emphasised the aggregation and interpretation of context-information [5].

In addition to context-acquisition, processing and interpretation, traditional algorithms for designing recommendation systems need to be considered. Traditional recommendation systems take a set U of users and a set of products (items) P ,

which should be recommended to a user. A recommendation system then provides an utility function f that measures the relevance of a product out of set P to a given user. This utility function f ($f : U \times P \rightarrow R$, where R is an ordered set of numbers) assigns a number to each item (or even to a compound set of items) in a way that captures the relevance or preference of an user. The objective of recommendation systems is to find or learn this utility function f . Function f is used to predict the relevance of items out of P and of new appearing items with similar attributes. In the literature different approaches exist for finding a function f by using an available dataset. Traditional recommendation approaches are distinguished into two major strategies: content filtering and collaborative filtering.

A. Content Filtering

The content filtering approach creates profiles for each item and user, in order to characterize and compare its nature [6]. Each profile contains a specific set of attributes, which can be used to compare objects. For example, a restaurant could have a cuisine attribute, describing the type of food it offers, a location attribute, a vegetarian tag, and so on. A recommendation function f chooses items that are similar to items the user has already chosen or rated before. The utility function compares the user's profile and calculates the similarity of a user profile with the available items. Therefore, the user profile allows the recommendation engine to create a list of items that could fit to a given user profile. Many implementations of this approach additionally refer to Linked Data information, such as RDF stores and Semantic Web repositories, to classify and search systematically for related information.

B. Collaborative Filtering

In collaborative filtering approaches, the recommendation function chooses items that were preferred by other users with similar attributes. So collaborative filtering approaches depend on either explicit or implicit user ratings of items. By rating different items a user can feed explicit ratings into the recommendation engine, while implicit feedback is collected by the system through the analysis of the users behaviour (previous purchases, navigation path, search terms, ...). Collaborative filtering is domain-free, which means that it can be applied to any application area and to different data aspects, which could be hard to formulate into an explicit profile. Collaborative filtering is more accurate than content filtering [6], but has the challenge of starting without any initial data sets (cold start problem). It is not directly possible to address new users or objects for which the system has no initial data set available. Popular collaborative filtering methods are neighborhood methods and latent factor models. The Pearson's correlation coefficient $sim(u, v)$ is often used to calculate the popular neighborhood method kNearest Neighbor, in order to measure the similarity between the



Figure 1. General approach for estimating the overall relevance of items for a given user in multiple dimensions

target user u , and a neighbor v . The symbol \bar{r}_u corresponds to an average rating of user u and P denotes the set of products or items.

$$sim(u, v) = \frac{\sum_{i \in P} (r_{u,i} - \bar{r}_u)(r_{v,i} - \bar{r}_v)}{\sqrt{\sum_{i \in P} (r_{u,i} - \bar{r}_u)^2} \sqrt{\sum_{i \in P} (r_{v,i} - \bar{r}_v)^2}} \quad (1)$$

Another method uses association rules to explicitly model the dependency and similarity of items. So a rule could e.g. be: when a customer buys ItemA and buys ItemB, then the rule recommends to buy ItemC. One of the most widespread methods for calculating latent factors is matrix factorization, which is described in detail in [6]. Most of the modern recommendation systems use a combination (hybrid approach) of content filtering and collaborative filtering approaches to further improve the accuracy of recommendations. Beside these traditional approaches for implementing recommendation algorithms, several groups are working on the challenge of customizing recommendations and to build flexible recommendation queries. REQUEST: a query language for customizing recommendations was published by Adomavicius et. al. in 2011 [7], which promotes a custom query language to build flexible and customized recommendation queries based on multidimensional OLAP-cubes. Several contributions have been made by research groups that built various application scenarios for context-aware recommendation systems, ranging from tourism [8], restaurants [9], or even people (e.g. glancee.com).

III. FRAMEWORK REQUIREMENTS

Within this section we would like to discuss requirements a general framework for implementing context-aware recommendation systems has to fulfill. To discuss each requirement in detail would exceed the scope of our work,

so we focus on several requirements that had a high priority for our use-case in VI.

A. Flexible and dynamic customization

A client-centric view on the recommendation process demands for a flexible user interface to enable the customization and fine tuning of recommendation impact factors for non-technical users. So the users should be able to control the learning and recommendation process at a most fine grain level, while the configuration and presentation should be on an abstract and understandable level. The user should be able to specify a variable number of impact factor dimensions and even to add custom defined impact factors. The framework should normalize all the chosen impact factors and automatically provide a list of recommended items that is sorted according to the weighted sum of normalized impact factors.

B. Temporal aspect

Temporal aspects [10] deal with the change of the context and with the change of the content profiles over a timeline. A recommendation framework has to consider the fact that the importance of specific datasets may change over time. It makes a big difference, if a person has bought an item yesterday or 10 years ago. A general framework has to cope with this varying impact.

C. Transparency

To raise the users confidence in recommendations, it is of crucial importance to give immediate and transparent feedback on recommendations. The recommendation framework has to provide a human understandable explanation for a given recommendation set. Sundaresan, from ebay research, published a great article about the 6 questions you have to

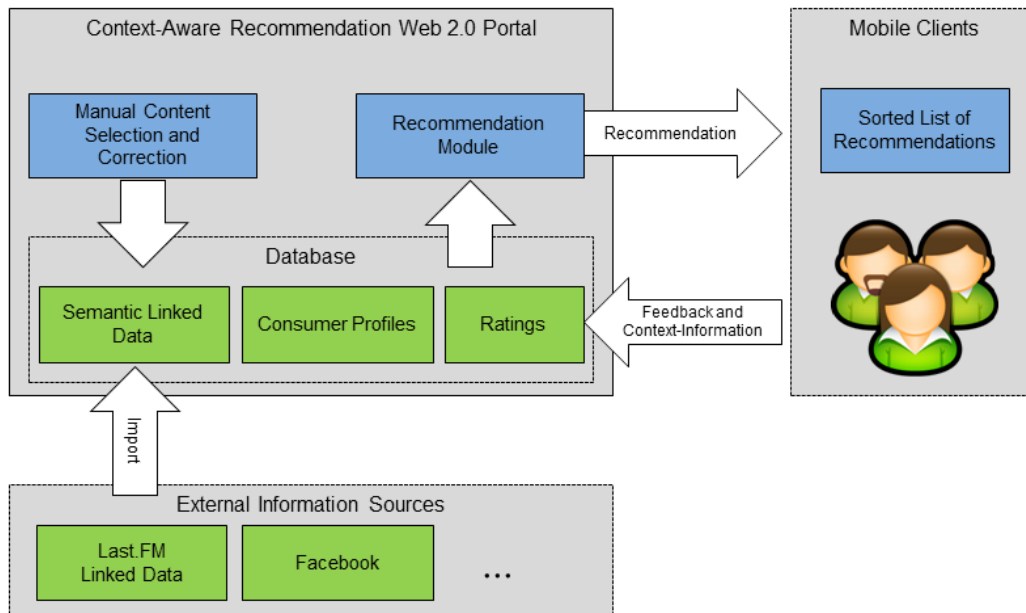


Figure 2. General software architecture for the implementation of a context-aware recommendation system

address during the design and implementation of recommendation engines [11] (What, Where, When, Why, Who and How). He also points out that recommendation engines that address the transparency aspect (the Why question), offer a better conversion rate in e-commerce applications. There are several user studies that clearly show that addressing the transparency aspect improves the performance of recommendation engines [12].

D. Performance

In order to provide recommendations for mobile applications that consider the actual context of a mobile user, it is necessary to deliver immediate results. Recommendations that consider the location and activity of an user, have to react in time to provide recommendations in the specific situation, when a user needs them. As actual recommendation approaches harvest and analyse a huge amount of data, this requirement is critical for every implementation.

E. Quality

As users are implicitly benchmarking recommendation engines according to the quality of recommendations they are able to provide, it is necessary for a general framework to provide a standard approach for evaluating the quality of recommendation engines. A framework has to provide implicit and explicit quality evaluations, which means that the framework constantly evaluates the quality of results by using test data sets, as well as to explicitly ask the users for quality feedback.

IV. APPROACH

To implement a general framework for context-aware recommendation systems for mobile applications it is necessary to define the impact of context related, dynamic information on the recommendation of items for users. Compared to the traditional recommendation approaches, which were already discussed in Section II, we combine these traditional collaborative filtering approaches with user related context-information. For each application scenario there exists a collection of context aspects that are relevant for a recommendation in a certain situation. While the location information might not be relevant for recommending books in an online bookshop, it is of crucial importance for the recommendation of nearby restaurants. Each dimension of a given context, such as location, weather or even companions is represented through an impact function. An impact function defines the influence of one dimension of a given context on the overall relevance for a given user. All impact functions are of the given form

$$f_i : U \times P \times C \rightarrow R$$

where U represents the set of users, P the set of products and C a dimension of a given context (e.g. location, number of nearby friends, ...). The weighted sum of all normalized impact functions results in an overall relevance for a product p , a given user u and context c , where w_i represents a weight, that the end user defined for a specific dimension of the context:

$$f(u, p, c) = \sum_{i < P} f_i(u, p, c) w_i(c) \quad (2)$$

A general framework for context-aware recommendation systems has to offer the basis for customizable recommendation engines, that consist of a variable and dynamic set of impact functions that can either be predefined by the framework (e.g. aspects such as distance, user ratings, history, friends, ...), or explicitly defined by users. Furthermore, the users are able to dynamically define and adapt the weight of different impact functions according to their preferences, which is shown in Fig. 1.

As Fig. 1 shows, the customized recommendation system within this example contains six different impact functions. Each of these impact functions calculates the relevance of an item for a given user for a specific dimension of a given context, such as distance, friends (companions), genre, ratings, prices or artist. The general framework is not limited to these six impact functions. The designers of recommendation systems should provide a domain-specific set of additional functions, in order to improve the quality of recommendations for the users in different application domains. The radar chart in the lower left corner of Fig. 1 visualizes the weight an individual user defined for a given set of impact functions. Each user specifies the personal weight of each dimension of the context. Another important feature of this approach is, that each of the impact functions can be defined and calculated by using completely different strategies. While the distance impact function could be a simple spatial query, the rating impact function could be implemented as traditional collaborative filtering approach.

V. SYSTEM ARCHITECTURE

The general software architecture for context-aware recommendation systems, that implements the approach in section IV is divided into a client-server model, that implements several subsystems. As it is shown in Fig. 2, the server defines all necessary subsystems for data access and third-party information retrieval, user interfaces for manual content selection and correction, as well as the recommendation module. The server database contains a matrix of given ratings, user and product profiles as well as additional semantic information. All additional semantic data can be accessed by using semantic web standards and query languages, such as RDF and SPARQL. The purpose of accessing these sources of semantic information is to receive additional item-based similarity measurements that are used in combination with the traditional collaborative filtering result. External sources of semantic information, such as Facebook or Last.FM, are either directly imported and duplicated, or directly accessed through a defined service interface. The decision if an external information source is either imported or directly accessed depends on the third-parties' service level agreements.

The recommendation module is responsible for calculating the recommendation approach in section IV and to communicate the resulting product ratings to the clients. The client-server communication is implemented as a lightweight REST (Representational state transfer) service approach. On the client-side, a local application is visualizing the resulting list of recommendations and is collecting the necessary context information in combination with the user's feedback on the given recommendations.

VI. USE-CASE: EVNTOGRAM

The following use-case was selected out of a running project in cooperation with EVNTOGRAM, which is a platform operator for personalized and context-sensitive recommendation of social events. The philosophy of EVNTOGRAM is to analyze the users' habits and activities, as well as their social interaction, in order to offer personalized and context-aware recommendations for social events, specifically in the domain of music events, such as concerts and music festivals. The general framework, explained in section IV and section V, helps to include various context-dimensions into the calculation of the relevance of an event for a given user. EVNTOGRAM records these context-dimensions, such as the users' activities, social interaction, music listening habits and individual ratings, in order to sort a list of music events according to the calculated relevance, as it is shown in Fig. 3. In a first prototype EVNTOGRAM is trying to find out which subset of context-dimensions is providing good recommendations for the users. In that sense 'good' means the feedback the user is providing for a given ordering of items.

VII. CONCLUSION

In this work, we propose a general approach as well as a general software architecture for the implementation of context-aware recommendation systems was presented. The approach as well as the framework offers high flexibility according to the definition and configuration of new impact functions, which influence the recommendation of items for given users. The framework is domain-free, which means that this approach can be implemented and adapted for different application domains. The context-aware recommendation of items of all kind, ranging from products in e-commerce to activities and services in sport and fun will get much attention in future software development. We think that a general framework for designing and implementing such recommendation systems for different application domains is of great importance. The next steps within our work will be to gather empirical feedback from the community within the given use-case of recommending music related events.

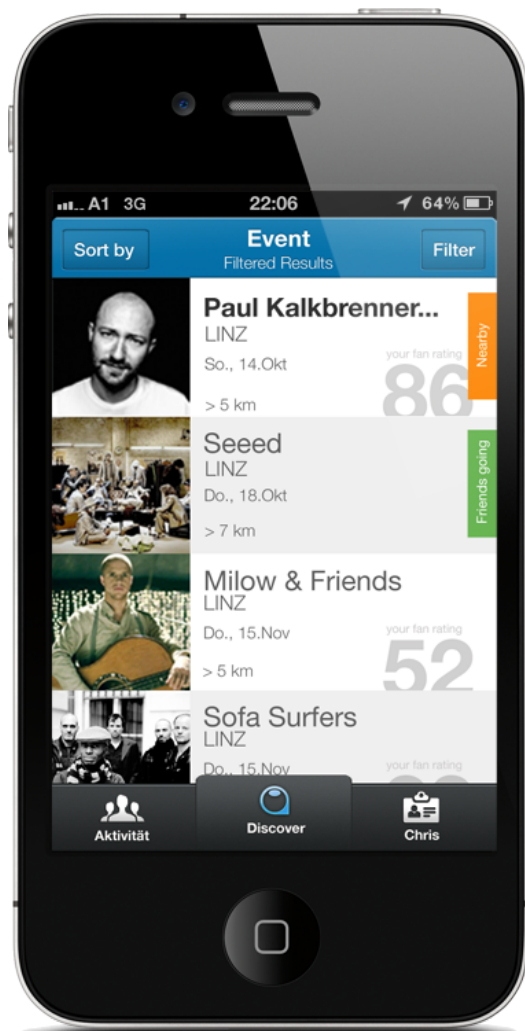


Figure 3. EVNTOGRAM Music Event Recommendation App

REFERENCES

- [1] R. M. Bell, Y. Koren, and C. Volinsky, "The bellkor solution to the netflix prize," [retrieved: jan. 2013]. Available: <http://www2.research.att.com/volinsky/netflix/ProgressPrize2007BellKorSolution.pdf>
- [2] B. Schilit, N. Adams, and R. Want, "Context-aware computing applications," in *Mobile Computing Systems and Applications*, 1994. WMCSA 1994. First Workshop on Mobile Computing Systems and Applications. IEEE, 1994, pp. 85–90.
- [3] P. J. Brown, J. D. Bovey, and X. Chen, "Context-aware applications: From the laboratory to the marketplace," *IEEE Personal Communication*, vol. 4, no. 5, Oct. 1997, pp. 58–64.
- [4] A. Dey and G. Abowd, "Towards a better understanding of context and context-awareness," in *CHI 2000 Workshop on The What, Who, Where, When, and How of Context-Awareness*, 2000.
- [5] W. Beer, V. Christian, A. Ferscha, and L. Mehrmann, "Modeling context-aware behavior by interpreted eca rules," *Euro-Par 2003 Parallel Processing*, 2003, pp. 1064–1073.
- [6] Y. Koren, R. Bell, and C. Volinsky, "Matrix factorization techniques for recommender systems," *IEEE Computer*, vol. 42, no. 8, Aug. 2009, pp. 30–37.
- [7] G. Adomavicius, A. Tuzhilin, and R. Zheng, "Request: A query language for customizing recommendations," *Info. Sys. Research*, vol. 22, no. 1, Mar. 2011, pp. 99–117.
- [8] W. Beer and A. Wagner, "Smart books: adding context-awareness and interaction to electronic books," in *Proceedings of the 9th International Conference on Advances in Mobile Computing and Multimedia, MoMM '11*. New York, NY, USA: ACM, 2011, pp. 218–222.
- [9] V.-G. Blanca, G.-S. Gabriel, and P.-M. Rafael, "Effects of relevant contextual features in the performance of a restaurant recommender system," in *In RecSys11: Workshop on Context Aware Recommender Systems (CARS-2011)*, 2011.
- [10] Y. Koren, "Collaborative filtering with temporal dynamics," in *Proceedings of the 15th ACM SIGKDD international conference on Knowledge discovery and data mining, KDD '09*, New York, NY, USA: ACM, 2009, pp. 447–456.
- [11] N. Sundaresan, "Recommender systems at the long tail," in *Proceedings of the fifth ACM conference on Recommender systems*, ser. *RecSys '11*, New York, NY, USA: ACM, 2011, pp. 1–6.
- [12] R. Sinha and K. Swearingen, "The role of transparency in recommender systems," in *CHI '02 extended abstracts on Human factors in computing systems*, ser. *CHI EA '02*. New York, NY, USA: ACM, 2002, pp. 830–831.

Collective Intelligent Management of Freight Trains' Flow

Boris Davydov

Institute of Natural Science
Far Eastern State Transport University
Khabarovsk, Russian Federation
e-mail: dbi@rambler.ru

Abstract—The paper describes method and criteria for assessing the quality of freight trains' traffic dispatching. The main idea is to make the maximum profit for the rail operator through the compromising decisions between regional (commercial) and local traffic dispatchers. We use results of the game theory and the operations research method (AHP) to find optimal trains' traffic adjustments. The game model of joint decision making is used to overcome the internal conflict between dispatchers. It is helpful to use the increment of local profit as a criterion for assessing the quality of traffic controller's decisions. We also describe the modified AHP method oriented for the efficient on-line management. We present an example of the hierarchy model and results of the decisions efficiency assessment for the typical situation of freight trains traffic. Rational use of computing abilities of the decision support tools together with collective intelligence allow to increase quality of decisions on settlement difficult conflicts between trains.

Keywords—Trains' traffic; real-time management; railway dispatching; optimal decision making; transportation economics

I. INTRODUCTION

The main function of the operative train traffic management is solving two problems. The first problem is how to organize the best transportation service for consumers (passengers, cargo owners). First of all, the management provides high passenger trains' punctuality. The second condition is meeting the requirements of railroad operator in getting profit from the transportation process realization. This is mainly attained by the rational organization of the freight trains stream passing.

The need for operational management arises owing to disturbances which are caused by repair breaks, technical failures and errors of operational personnel. Failures are characterized by a high variety of variants and there are many ways of their elimination. Besides, it is known that information about railroad situation is often incomplete. This leads to the adoption of the optimum decision whose result is overcoming of an arising problem..

The analysis of the researches and developments in the related field allows us to make the following conclusion: nowadays it is impossible to make the full automation in real time for train traffic. The effective way to solve the problem is to take the decision through the man-machine dialogue.

Numerous researches all over the world are devoted to the optimization problem and to effective management of railway traffic. The present work carries out the analysis of

the joint passenger/freight traffic effective management with the use of intelligent computer support.

We formulate an optimization problem in which at least two agents – regional and section traffic manager – control trains movement. Regional dispatcher (RD) objective is to maximize the line productivity, sometimes without taking the local section effectiveness into account. Regional dispatcher is given the authority to control the trains set repositioning. Section dispatcher (SD) has the opportunity to improve the operations by prescribing the rational headways and by solving the local conflicts. There are many cases when infrastructure managers are involved into the decision making process.

The developed model of the interacting parties gives the opportunity to provide the cooperative way to resolve the working conflict between RD and SD and to take the optimal decisions by using the analytic hierarchy process (AHP).

The paper is structured as follows: Section II presents the specificity of trains' traffic operative management on the main railways. In Section III, we present the overview of the methods of conflicts resolution to the trains' movement in the railway section. Section IV describes the modes of operation and economic performance criteria of the railway. We also show the conflict solution algorithm that uses the game theoretic approach. In Section V, we present the trains' control model, based on the analytical hierarchy process (AHP-approach). Algorithm, based on AHP, delivers agreed decisions of rail managers. An example of using AHP-model are presented in Section VI, show the effectiveness of the proposed approach. The paper ends with conclusions, the main one being the following. The hierarchy model and man-machine dialogue promotes adoption of effective decisions and the subsequent fine adjustments.

II. BACKGROUND

Many of conventional main railways (Russian, American, Chinese etc.) are characterized by intensive joint passenger and freight traffic with prevalence of a freight segment. The basis of freight traffic is heavy trains. Dense railway system with the intensive passenger flows, similar to European railroads, is available only in nearest areas of the large cities. All the above define the specificity of trains' traffic operative management on the main railways. There are many differences in the passenger and freight rail line traffic dispatching. First of all, passenger traffic requires high micro-punctuality. It is not true for the conventional freight

trains traffic. Railway operative planners often do not take these differences into consideration. Nonoptimal adjustments and economical losses are the consequences of this incomprehension.

III. OVERVIEW OF THE RELATED LITERATURE

Many authors consider the problem of conflict resolution in real-time on the railroads [1-4]. Most of them use the determined modeling of the railway traffic. This approach allows accurate predicting of the future evolution of the traffic on the basis of the actual train positions and speeds, signaling and safety system constraints. Computerized supporting system operates with accurate input data. If input data is incomplete or indistinct, it is unlikely that the solutions provided by the DSS will be effective. It is known that the additional real-world constraints such as commercial interests and human behaviors are not taken into attention by the support tools. It is necessary to remove this fundamental disadvantage by the use of professionals' experience and intuition.

Criteria of a freight trains' traffic control is different from the passenger one. There are a few works devoted to this topic [5-8]. The works mentioned do not demonstrate the adequate formulation of economic quality indicator of dispatching. This paper gives a novel economic model and indicator which enables to make effective freight traffic adjustments.

There are many works in the field of collective decisions making [9, 10]. Most of them describe the approaches which demand much time for the problem analysis. Up to now, there are a few works devoted to the collective decision-making whose purpose is intellectual support of real-time transportations management. These researches show that it is effective to resort to the possibilities of the analytical hierarchy process (AHP) for operative personnel viewpoints coordination. A wide range of AHP problems and applications has been described in edited volumes and books (e.g., [11-13]). Some of them [14-18] are devoted to aggregating individual judgments. But a fast coordination approach is not known to be effective in wide practice. This work contributes to fill the gap between theory and practice of train operative management by the human and machine intelligent interaction.

IV. TRAINS' TRAFFIC OPTIMIZING CRITERIA

Trains' traffic on conventional rail lines - from the point of view of operative management - is divided into two segments. Trains of the passenger segment are defined by the highest priority. Their passing through the railway section is carried out by using any resources (free ways, additional fuel, etc.) when failure occurs. Unlike passenger trains the stream of the freight trains can move more economically. Therefore the first stage of formulating the optimization problem for the traffic control area is to set the specific criteria: punctuality of trains' movement, section throughput or local economic efficiency.

The failures sharply change movement conditions of the rail section. In these cases the dispatching personnel ought to repair the schedule to provide minimum losses of the

throughput and the expenses. Modified operative train schedule for a section movement is under construction in a real time. The choice of the best variant from a number of possible decisions is being represented as the optimization problem. The losses of the throughput and expenses may serve as the criteria for optimization.

The provision of rational modes of trains' traffic on a railway section is an important component of an operative management. On the one hand, the management should "construct" a chain of train-units to minimize conflicts between trains. This purpose is reached by transmitting commands to locomotives. These commands correspond to the developed dispatching plan. On the other hand, each train may be regarded as an independent unit and its movement should be optimal. Both degree of safety and power efficiency may be used here as criteria for a traffic optimality.

Cost-effective traffic management is the choice of adjusting actions that is aimed at providing the minimum economic losses caused by train delays. The optimization criterion is needed in order to solve the problem of searching the ways of effective process management. In this case the most efficient development of the process is expected. Economical indexes and reliability rate are usually used as criteria of the industrial processes flow and systems operating.

Fundamental criteria of the railway functioning quality are the following:

- operational safety;
- railway section capacity;
- economic effectiveness of handling trains along the section.

First of all, the capacity criterion is used in those sections which are characterized by the large volume of passenger and freight traffic. There are few possibilities for an operating cost saving under the heavy traffic.

The quality of movement of the passenger trains or group of trains is determined by the degree of correspondence of the real timetable (stations arrival and departure times) to the normative (scheduled) timetable. Assessment of passenger timetable is given by the train operating reliability index [17].

Punctuality as the requirement to the freight services movement recedes into the background. The main issue is prevention of unplanned stops, slowdowns of trains and therefore the loss of time and energy. The trains' trajectories on a railroad section can be chosen rather arbitrarily. This flexibility is particularly important in situations where you need to prevent future failure of movement or propagation of an already existing fault in the chain of trains. The optimization problem solution allows assigning such schedule to each train that will minimize the losses of time and energy on the entire packet of trains.

The following optimization criteria are appropriate for adjusting the timetable of freight traffic:

- best utilization of train operating productivity – ensuring maximum volume of freight and empty cars traffic;
- cost-effective operating in the period of weak traffic.

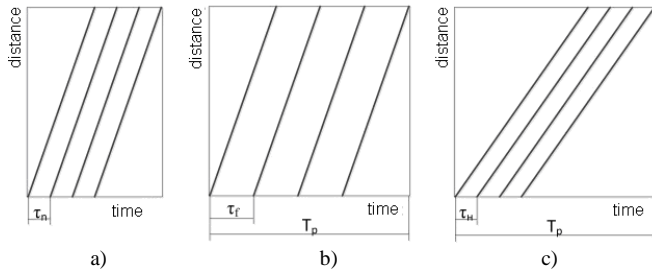


Figure 1. Schedule's fragments: a) normative; b) sparse timetable; c) enhanced travel times

The first criterion is used when traffic volume is approaching to the theoretical capacity of the railway as a limit. Cost minimization comes to the background during these periods. This operation mode of the railroad is called **extensive**.

Economical mode is established when the flow density of freight trains falls. During this period traffic controllers can use non-standard (decelerated) schedules for one or more trains which allow large energy savings. Variants of the train timing for the above mentioned section operations are shown on Figure 1. Regional traffic operator specifies one of these modes for every up-coming hour.

Regional traffic operator organizes and controls the functioning of extensive segment of trains' stream. Local dispatcher controls the efficient trains' movement. It is a basis for the collective management paradigm.

Best economic effect can be obtained using a rational combination of trains N^{ext} that represents an extensive segment and trains N^{econ} with economy movement. The train traffic separation into two segments can be viewed as a game problem the aim of which is to mitigate the conflict between the managers [18].

We suggest a new economic efficiency criterion, which is used to find a decision for trains' traffic regulation. It is helpful to use the increment of local profit ΔB as a criterion for assessing the quality of traffic controller's decisions who regulates the freight trains flow on the section [19]:

$$\Delta B = \Delta I - \Delta E ,$$

where ΔI is the change of an operator company's income because of the realized adjustment;

ΔE is the additional expenses for making the adjustment.

The optimal variant is chosen from the range of feasible decisions according to the maximum of efficiency function: $\Delta B \rightarrow \max$.

The area of the solutions for the ratio choice of N^{ext} and N^{econ} in the flow of freight trains is shown on the Edgeworth-Bowley diagram (Figure 2). The diagram includes all possible combinations of the decisions in the game – i. e. shares of economical (N^{econ}) and fast (N^{ext}) freight trains in the aggregate flow. Coordinates (a_{10}, b_{10}) are valid for the strategy of the fast (extensive) segment.

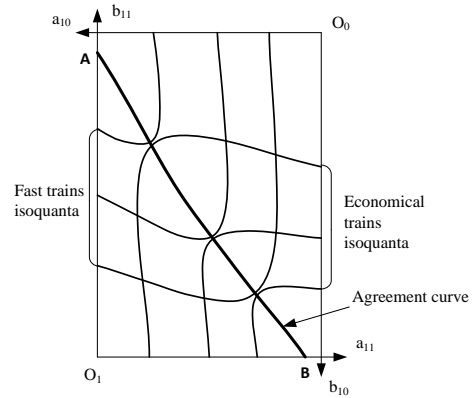


Figure 2. Edgeworth-Bowley diagram for the variants of the train traffic management strategy

The method of choosing a compromising decision which meets the condition of maximum corporation gain is given by Kolemaev [20]. It is shown that the optimal decisions according to Pareto principle are located on the contractual curve. This curve (AB line) is shown on the Edgeworth-Bowley diagram.

The choice of a decision lying on the AB is accompanied by severe competition between the parties. More mild interaction and cooperation between the players occur when the source point is chosen beyond this curve. The moving from this point along the line of equal output (isoquantum) provides way of increasing the second player gain without influence on the interests of the first player. Figure 2 shows the isoquanta which is corresponded with the game tactics of the each game participant.

We should note that this feature allows dispatchers to find the optimal decision without the players' participation. This means that the dispatchers elaborate compromising decision on defining the structure of the trains flow in the majority of typical situations.

The sizes of the extensive and economical segments obtained through the game analysis are used further as the local priorities of the second level when calculating the resultant vector of the optimizing problem.

V. MODEL OF THE FREIGHT TRAINS' MANAGEMENT

We formulate an optimization problem in which two agents control the trains' movement. The objective of one of them (regional traffic dispatcher - RD) is to maximize the line productivity, at the same time without taking the local section effectiveness into account. RD is given the authority to control the trains pool repositioning. Another one (section dispatcher - SD) has the possibility to improve the operations by the rational headways prescriptions and passing trains over a section. This means that trains can travel on less than maximum velocity to minimize fuel consumption. The suggested approach in comparison with the traditional dispatching approach is a potentially cost-effective technique for the control of trains' movement in a real environment.

Operation decisions on traffic management are often made under the conditions of shortage of information and time. In complicated and non-standard situations two or

more dispatchers participate in the decision making. The majority of factors involved in the optimization task are defined indistinctly and there is a discrepancy in how different people evaluate their influence on the traffic.

Operation decisions on traffic management are often made under the conditions of shortage of information and time. In complicated and non-standard situations two or more dispatchers participate in the decision making. The majority of factors involved in the optimization task are defined indistinctly and there is a discrepancy in how different people evaluate their influence on the traffic.

The choice of priority resolution among a row of alternative variants given poorly formalized or insufficient information about the subject is made through employing the analytical hierarchy process (AHP by T. Saaty [12]). The basic framework is a benefit/cost analysis. The last mentioned is used as a priorities-determining method in relation to the operational constraints, specialties, actors and their preferences.

This paper presents an attempt to employ the AHP method in the problem of taking rational decisions on-line which are adopting in current conditions. The dispatcher who operates the freight trains traffic resolves several heterogeneous optimization tasks simultaneously. He has little time to think out each decision thoroughly. Therefore the algorithm of his dialogue with the computer system which prompts the variants of adjusting actions and evaluates their efficiency must be maximally simplified.

Analytical hierarchy process formulates a problem which should be decomposed into elements belonging to different hierarchical levels. Level I present the general goal (the choice of an optimal variant) and it is called the focus of the problem. Level II (the subgoal level) comprises the row of the scenarios which includes both extensive (fast) and economy segments of train movement. The lower level (the level of politics) – covers the variants of the resolutions which are compared with each other.

The hierarchy of the operating process of freight trains focuses either on volume of the traffic passed or on profits of shipping operations (Figure 3). The weights of the variants are defined on the basis of judgments of persons (or group of people) when using AHP method. They make a decision by the way of determination the mutual priorities of the elements of the hierarchy.

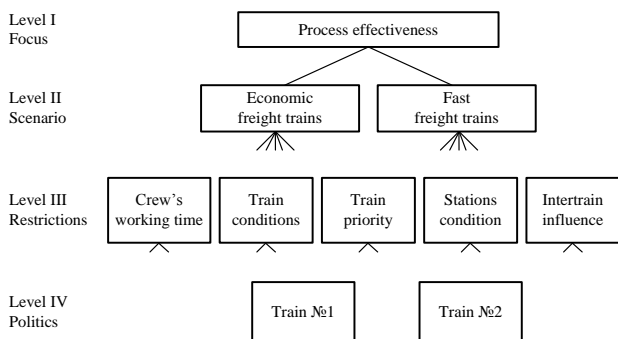


Figure 3. Hierarchy of the freight train traffic management

These people (experts) make use of their knowledge, experience and intuition to define the weights of the elements of the lower level with respect to the criteria of higher level. They employ the method of pair comparison which provides the numerical evaluations of the judgments.

The priority of each policy, i.e., choice of the decision variant, is determined through employing the procedure of synthesis of multiple judgments. This procedure is based on the weighing formula which gives relative weights Y_i of each variant:

$$Y_i = \sum_n \overline{x_{jk}} \cdot \overline{x_k}$$

where n – number of criteria;

$\overline{x_{jk}}$ - local priority of j policy (lower level);

$\overline{x_k}$ - local priority of k criterion (upper level).

Hierarchy analysis allows us to outline the ways of relieving of the internal conflict within the system. In order to achieve this, the degree of influence of each actor on the process is determined according to the AHP technique. The results of modeling and the outcomes of real situations are also compared. This helps to substantiate compromise resolutions of the problem.

When process deviates the standard condition there is a need of intervention of the dispatcher. These regulations may be an unplanned stopping of a freight train or its new scheduled departure from the station. It also may be a passing priority change of consecutive freight trains.

Selection of a specific train which would provide the best result is more complicated problem. It is reasonable to resolve this optimization problem with the help of modified hierarchy model.

The analysis shows that the hierarchy of the train traffic management coincides with the inverse AHP. Such process models the desirable future; this allows us to define the priorities of the policies – operations decisions which lead to the achievement of the desired resolution.

The type of criterion for the forthcoming period is set by the Chief (regional) dispatcher. This period may comprise 3 or 6 hours; in certain cases it may be diminished to 1 hour. The scenario of the train passing process (Level II) implies rational combination of freight trains which are let through at an accelerated pace and the trains of economic (standard, decelerated) movement. The schedule of the latter trains is established in the way to obtain maximum saving of electricity or fuel. It is obvious that the mode of economical passing is reasonable during the slump in the intensity of the traffic.

Revenues from shipping operations decrease due to little number of trains when the saving regime is employed. Nevertheless additional profit can be obtained at this period due to significant decrease in operational costs.

The trains, one of which requires such a regulation, are considered as the variants of decision (Level IV). Train dispatcher chooses the criterion for evaluation of the weight of each decision (Level III) in every specific situation. If the problem is connected with the need for stop at the station the

priority will be given to the train whose service is the most urgent. Dispatcher expresses his understanding through filling the table of pair comparison.

Standard AHP consider the structure of the hierarchy unchanged during the whole period of analysis. The number of criteria for each level of hierarchy is representative to cover all the variants of situations which can occur on the section. The size of pairwise matrix proves to be large which leads to substantial expenditures of experts' time and effort.

The suggested specialized model differs from the traditional model in the following way. The structure of the hierarchy is not fixed. It changes depending on the situation in the section under operation. These changes are caused by rapid and uncontrolled restrictions. The choice of the suitable criterion corresponding to a situation is made. Commercial priority may be of the most importance for one train and technical condition is suited to others. Dispatcher has the information about the restrictions which take place. Therefore it is reasonable to charge them with the selection of the type of problem (restriction) which is taken into consideration in each specific situation. The dispatcher makes the choice through entering the corresponding indication in the adviser-program. The chosen restriction is used then as a criterion for comparison of trains. This algorithm corresponds with the logic usually employed by dispatcher. The volume of man-computer interactions is minimal.

VI. EXAMPLE OF THE DISPATCHING HIERARCHY MODEL UTILIZATION

As an example of the modified AHP method, we show one of typical problems on decision-making on a overcome of an unplanned obstacle to movement of a stream of trains. The restriction makes the train dispatcher stop one of the freight trains at a station. Rational decision is to select the train whose stop will cause minimal losses.

The choice is made among three freight trains. Train 1 is a container train with low weight but an extremely large length (100 cars). Two other trains have small length; one of them is a heavy haul train (6,000 tones), the other is of medium weight. The restriction is the length of the tracks at the some stations. Station M is the only station where the length of the tracks allows stopping the long train.

Table 1 shows the source data used in decision making and the results of analysis for the situations with intensive and weak train traffic. The first rational decision (weak flow) is to stop the train №3; the opposite adjustment (intensive flow) is to stop the train №1.

TABLE I. SOURCE DATA AND RESULTS OF ANALYSIS FOR THE DECISION ABOUT AN UNPLANNED STOP OF THE FREIGHT TRAIN

Trains	Com- mercial value	Length of train	Additional expenses for stop	Priority	
				Intensive flow	Weak flow
№1	1.0	1.0	30	3	1
№2	0.5	0.7	100	2	3
№3	0.9	0.7	60	1	2

In the latter case the commercial interest to deliver containers in time will not be breached. Expenditures on passing the trains through will also be lower.

Real testing of the presented methodology was carrying out on the Transsiberian main rail line. It is shown the 10 percent reduction of unplanned freight trains stops and up to 8 percent energy economy.

CONCLUSIONS

We presented a new technique of realization of traffic control of freight trains' operative management which is based on economic basis. The criterion of economic efficiency to make optimum adjustments into trains' traffic was formulated.

We also offered game approach for selection of the compromise dispatching decision. It will be effective for the short time traffic planning. The hierarchy model and man-machine dialogue promote adoption of effective decisions and the subsequent fine adjustments.

The developed modification of AHP allows making a compromise decisions on regulation of a freight stream through dialogue between heads of control center. Dialogue is implemented rationally with attraction of computer abilities and hierarchy model.

The number of interactions of train dispatcher with the computerized "adviser" is minimized due to game approach. In ordinary cases dispatcher need to execute only two choice operations for each pair of trains: type of problem and local priority of trains.

Real testing of the economical supported dispatching on the Russian main rail lines show the 10 percent reduction of unplanned freight trains stops and great energy economy.

The reported study was partially supported by RFBR, research project № 12-08-98513-p_vostok_a.

REFERENCES

- [1] A. D'Ariano, F. Corman, D. Pacciarelli, and M. Pranzo, Reordering and Local Rerouting Strategies to Manage Train Traffic in Real Time, *Transportation Science*, Vol. 42, No. 4, November 2008, pp. 405-419
- [2] M. J. Dorfman and J. Medanic, Scheduling trains on a railway network using a discrete event model of railway traffic, *Transportation Research, Part B*, 2004, 38, pp. 81-98
- [3] X. Delorme, Modelisation et resolution de problemes lies a l'exploitation d'infrastructures ferroviaires, PhD thesis, University of Valenciennes et du Hainaut Cambresis, 2003
- [4] V. A. Ivnitkiy and A. A. Poplavskiy, The problem of transition to the informational-managing regime in the system of the transportation process operational management, *Vestnik VNIIZhT*, vol.1, 2007, pp. 15-21 (in russian).
- [5] T. Richter, Systematic analysis of transit freight train Performance, / 4th Int. seminar on Railway Operations Modeling and Analysis, Book of abstracts, Rome, Feb. 2011, p. 35
- [6] M. Carey, and I. Crawford, Scheduling trains on a network of busy complex stations, *Transportation Research, Part B*, 41 (2): 2007, pp.159-178
- [7] B. D.Nikiforof, E. M.Tishkin, V. M.Makarov, and V. S.Klimanov, Trains' traffic management on the railway direction of transportation, *Railway transport*, vol.2, 1982, pp. 17-24 (in russian).

- [8] V. A. Ivnit'skiy, Speed outstanding risk of freight trains due to technical failures, *Vestnik VNIIZhT*, vol.1, 2012, pp.33-37 (in russian).
- [9] O. Meixner, Fuzzy AHP Group Decision Analysis and its Application for the Evaluation of Energy Sources, *Proceedings of the International Symposium on the Analytic Hierarchy Process*, 2010, pp. 114-119.
- [10] L. Mikhailov, Group prioritization in the AHP by fuzzy preference programming method, *Computers & Operations Research*, 31., 2004, pp. 293-301.
- [11] G. S. Maltugueva and A.U. Yurin, The algorithm of collective choice on the basis of the generalized rankings for decision-making support, *Modern technologies. System analysis. The simulation*, vol.3, 2009, pp.57-62 (in russian).
- [12] T. L. Saaty and L. Vargas, *Models, Methods, Concepts and Applications of the Analytic Hierarchy Process*, Kluwer, Boston, MA., 2000, 381 p.
- [13] E. Forman and S. Gass, The analytic hierarchy process: an exposition, *Operations Research*, Vol. 49, 2001, pp. 469-486.
- [14] E. Forman and K. Paniwati, Aggregating individual judgments and priorities with the analytical hierarchy process, *European Journal of Operational Research*, Vol. 108., 1998, pp. 165-169.
- [15] A. Shahin and M. A. Mahbod, Prioritization of key performance indicators. An integration of analytical hierarchy process and goal setting, *International Journal of Productivity and Performance Management*, Vol. 56 No. 3, 2007, pp. 226-240.
- [16] K. Suryadi, Empirical Experience on Combining AHP with Non-ANP Decision Models in Managing Cross Functional Conflict, *Proceedings of the International Symposium on the Analytic Hierarchy Process*, 2007. pp. 183-191.
- [17] A. P. Kovalev, The timetable reliability and passenger trains speed volume estimation, *Railway Transport, Russia*, 2006, №5, pp. 42-45 (in russian).
- [18] B. I. Davydov, V. I. Chebotarev, The gaming solving of the problem of trains' traffic dispatching, *Transport Bulletin, Russia*, 2007, №10, pp. 37-39 (in russian).
- [19] B. I. Davydov, Economically effective trains traffic management, *Railway Economic, Russia*, 2012, №3, pp. 28-37 (in russian).
- [20] *Mathematical methods and models of the operations research*, ed. by V. Kolemaev, UNITI-DANA, Moscow, 2008, 350 p.

Infomobility and Vehicle Routing Problem

Transportation Models of goods

Giuseppe Salvo, Luigi Sanfilippo

Technology and Economy of Transport

University of Palermo

Palermo, Italy

giuseppe.salvo@unipa.it; luigi.sanfilippo@unipa.it

Abstract—The research of optimization techniques in the system of goods distribution from warehouses to final users (vehicle routing problem), made considerable savings on the total cost of transport and, consequently, on the final cost of goods, and produced the models applicable to other operating environments (e.g., transport for disabled people, school, municipal waste collection). The analysis conducted on the different models developed under the VRP highlights the support that these models can give on the infomobility of goods.

Keywords—*Infomobility of goods; Model of Vehicle Routing Problem; Models of DRAI; Logistic Operator; Multimodal Transport Operator; Transport of goods*

I. INTRODUCTION

The distribution of goods, delivery to a clients set or pick up of goods by one or more deposits, made with suitable transport, causes many problems. In particular, transport takes place in urban areas, deposits are located in the peripheral areas (suburban); customers are all in the urban area and vehicles used are mainly by road. In pick-up and delivery of goods lie the problems of vehicle routing and scheduling.

In fact, the adoption of standard operating procedures which make extensive use of vehicle techniques routing allow sizing of fleet and driving staff, with positive effects on business management. On the other hand the reduced availability of time on the part of customers to receive the goods requires a careful scheduling of deliveries.

The solution of a transporting goods problem in a predetermined time interval requires the determination of a trips set, all with original and final destination at the depot and carried out by various vehicles of the fleet, so as to meet the demands of customers, respecting operational service constraints and minimizing the overall cost for the transport.

In recent years, thanks to the numerous technological advances, the Vehicle Routing Problem (VRP) [9] has been an active area of Operational Research. New approaches, new models and faster solution algorithms were developed as a result of more accurate techniques, (e.g., Asymmetric Vehicle Routing Problem AVRP [9]; Capacitated Vehicle Routing Problem CVRP [9]; Traveling Salesman Problem TSP [14]; Green Vehicle Routing Problem G-VRP [1]). The

application of these approaches for solving vehicle routing problems is very useful in solving various problems (e.g., transport services disabled, school buses, on-demand, etc.). Much still needs to be done to determine the extent how the traffic information can help operators to solve logistical problems of routing and scheduling.

Development of Operations Research models increasingly specialized is accompanied with proliferation of devices that, using information technology and communications (ITC), are able to expand the user's knowledge, leading to better decisions. As part of the transport activity, this involves, e.g., the knowledge of the congestion state of the network, the possibility of modifying in real time the route according to the changed conditions of the road network, the possibility, on the part of the customer to monitor the arrival of the goods pending. The availability of extensive and detailed information occurs affecting the structures of the VRP algorithms, giving origin to a continuous "loop".

The objective of this work is to analyze the interaction in the transport of goods, between mobile information systems (e.g., devices, information technologies, communication protocols, etc.) and VRP models available in the literature.

To this end, in Section II, it will be taken into account the needs of logistics operators to see how goods transportation changed and what are new requirements, passing in review the main traffic service and their usefulness in the transport of goods.

In Section III, we will analyze the mathematical models for the transport of goods. In particular, we will focus on the problems DRAI (Dynamic Routing And Inventory), collection and delivery of goods, giving a classification of variable according to topology, type of goods, demand, kinds of decision, constraints/objectives, costs, solving approach. It will also analyze some of VRP models that offer the advantages of lower costs and better management of transport, in order to verify whether these models have among the explicit variables elements infomobility.

In Section IV, we will comment on the analysis results, formulating hypotheses, for the integration of the already known models with the explicit variables related to the

availability of information on the road network state, and monitoring of the fleet.

II. THE NEEDS OF LOGISTICS OPERATORS

The factor which has made necessary a different approach toward the transport activities are:

- **Compression of time in the supply chain.** The shortening of the transfer of information within the chain has highlighted the relative slowness of the process of physical transfer of goods. It is obvious that effort have been focused on this process to make it faster and more reliable.
- **Control of the transport process.** In the effort of reduction in transit times in the supply chain, strict control of goods has become an inevitable requirement. Satellite vehicle positional system, system for the control in various links in the chain of the specific goods (tracking and tracing), systems for continuous communication with various units are indispensable tools today.
- **Dissemination of outsourcing logistics and evolution of operators.** The assignment to third parties by companies of their logistics activities has created a new market of the logistics operators. So in most cases not more carriers that perform the simple activity from origin to destination, but logistic operators can manage with tools, reality quite complex, requiring the ability to integrate with various systems of the client companies or other actors in the world of transport (customs, ports, etc.).
- **Diffusion of the Internet.** Even in the transport sector, as in many areas Internet has opened up new opportunities that require ability to adapt to the new technologies. The e-commerce further strengthens the compression of time, but it also poses considerable problems of reorganization to reach a new market in a competitive way. The availability of portals (market places) dedicated specifically to the various modes of transport offers new tools to operate more efficiently.

The modern production processes resulted in a significant increase in demand for logistics and is more frequent in the case of manufacturing companies that make outsourcing, relying on established companies or applying spin-off of the business that deals with the logistics. Cost, time and quality are the basis of service, but the primary factor of success for a logistic enterprise is a service "tailored" to the customer. To be able to offer a service "ad hoc" we need a particular focus on the Human Resources, on the *Information and Communication Technology* (ICT). In particular, for logistic operators that operates as MTO (*Multimodal Transport Operator*), the availability of effective ICT tools to communicate with customers and other transport operators has a real strategic value [11].

Most of the "traditional" problems in the transportation of goods derive from the need to maintain continuous contact workers with staff on board, with customers and suppliers, as well as databases and service companies such as customs, insurance companies and banks. This also means a wide and full cooperation between all actors in the supply chain such as intermodal shipping companies, intermodal operators, terminal operators and transport providers (land/sea/air) for the exchange of all data of transport fundamentals to handle the shipping [13]. An adequate system of telecommunications is the support for the exchange of electronic documents to allow the tracking and control of shipments to foster the development of a "just-in-time" ensuring effective efficiency of the logistics cycle considerably higher than that now obtainable [8].

The use of telecommunications networks, Internet and the introduction of the exchange data electronically help to pursue some primary objectives as:

- Reduction in production of paper documents;
- Reduction in time sorting the delivery documents;
- Reduction in procedural costs;
- Acceleration in cash flows;
- Reduction in errors and misinterpretations;
- Reduction in time and costs of storage;
- Information about the products location during transport;
- Optimization in use of means of transport;
- Information and documents;
- Contribution to the creation of statistical data on transport at national / international level.

Therefore, it is essential providing a flow of information to ensure the fulfillment of the objectives listed above with particular reference to traceability of load, timely communication with forecast delivery date, and billing system on computer, agreed with customer, clear and standardized [12]. The same exchange of information must be provided by operator intermodal to its customers assuring certainty and timeliness in supply data using both mainframes and operating systems on a PC.

Only upon reaching these goals the intermodality will expand its incidence rate in the world of transport and reducing the negative weight of some serious infrastructure.

Several studies conducted in Europe (Davies, et al. [4] and Golob and Regan [7]) have examined the effects of the use of ICT in transport processes of goods, in the field of e-commerce in particular is analyzed the influence of the use of technology information and communication technologies (ITC) on the organization of transport. In particular, the use of seven technologies:

1. Satellite or radio based communication (S/RC);
2. AVL technologies;
3. AVI systems, including PrePass transponders;
4. EDI;
5. Vehicle maintenance software (VMS);
6. Routing and scheduling software (R/SS);

7. CB radio (CBR).

This analysis was based on the results of a survey of transport operators with the aim of:

- a) Exploring the extent to which ICT is used by businesses.
- b) Checking that the transporters believe it is important to use the ITC.
- c) Identifying the efficiency of the fleet in terms of return empty running.
- d) Identifying sources of backloads.
- e) Analyzing the methods used to find backloads.
- f) Identifying the benefits and barriers to the view of the drivers' trade in goods.

A first major finding from the survey, confirmed by a similar study conducted on a sample of transport companies of southern Italy, address the issue of management of empty running and significant impact on the total cost of transport. Less than 5% of companies are part of a network for the exchange of transport orders that allows them to reduce the distances with empty vehicles. The investigation demonstrated how ICT, although recognized as an important tool, is only partly used to support technical activities (planning vehicle routing, vehicle tracking, vehicle telematics) and how the perception of the informatics support is only limited to accounting matters.

III. MATHEMATICAL MODELS FOR TRANSPORT OF GOODS

A. Problems DRAI

The logistics distribution, namely organization and implementation of physical distribution of goods, must also include, for example, the management of possible intermediate storage, handling from warehouse to vector and vice versa, the bargaining of times and modes of delivery goods to the customer. Mathematical models for this kind of issues must give a description integrated to whole process of physical distribution and consider, in addition to transport costs, other logistical costs such as those related keeping goods in the warehouse (*inventory costs*) and materials handling (*handling costs*). These models are described by Tinarelli [25], in case of single destination, and in Anily and Federgruen [26], in case of multiple destinations. Below, will be considered models that refer to problems characterized by at least the following three aspects:

- The need to define the paths that must be followed by the transport of goods;
- The existence of costs related to the quantity or value of the goods in question;
- The presence of dynamic aspects that require repeated decisions during a given time interval.

The problems that fall within the context defined will be referred to here after as problems DRAI (Dynamic Routing and Inventory). The problem DRAI, concern how to manage the supply of customers geographically distributed during a given time interval, considering issues relating to both the

transport and the management of the warehouses. DRAI's in problems, it is assumed that the transport takes place via rubber and that time departure, loads and locations are subject to decision. It is also supposed that deployment task rather than collection occurs. In the context defined above, decision makers that make a problem DRAI must answer at least the following questions:

- When the shipments are made, in other words, when you have to load the vehicles and when they are visited customers;
- How much load in each vehicle and how much deliver to each customer;
- Which path should be followed by each vehicle to serve its customers.

The literature has lots of articles speaking about *Pick up and Delivery* (PD), especially if the application is affected by conditions of uncertainty, in terms of geographical location of customers and/or terms of the amount of goods required. Interesting problems of PD are analyzed by Savelsbergh and Sol [18]. A classification of DRAI problems in literature is described in Table 1.

TABLE I. CLASSIFICATION OF DRAI PROBLEM

Topology			
<i>Distribution Structure</i>	one to many	many to many	
Types of goods			
<i>Number</i>	one	many	
Demand			
<i>Knowledge</i>	known	uncertain	unknown
<i>Variability in time</i>	constant	variable	
<i>Distribution</i>	uniform	not uniform	
Kinds of Decisions			
<i>Domain</i>	time	frequency	
Constraints / Objectives			
<i>Vehicle capacity</i>	equal	different	
<i>Storage capacity</i>	infinite	over	
<i>Storage capacity customers</i>	infinite	over	
<i>Number of vehicles</i>	known	decision variable	non-binding
Cost			
<i>Warehouse</i>	conservation	lost sales	shuffle
<i>Transport</i>	fixed	proportional to the distance	proportional to number of stops
Solving Approach			
<i>Decomposition</i>	time	regions - routes	
<i>Grouping</i>	time	frequency	position
<i>Models / Algorithms</i>	exact	approximate	

B. Models of DRAI

The models considered here are well suit to problems where demand is almost constant or varies slowly over time. There are two dominant schools that study the models in the frequency domain. The first of these is the so-called *Continuous Approximation (CA)*, while the second refers to the *Fixed-Partition Policies (FPP)*.

Both schools are based on some of the following results, which allow the assessment (asymptotically) the length of paths.

1. Assuming it is worth the triangle inequality, minimum length Z of a closed path that from the central warehouse allows you to visit all customers in a particular region satisfies (1).

$$\max \left\{ L^*(N), \frac{2}{|N|} \sum_{i \in N} d_i \right\} \leq Z \leq \min_{i \in N} d_i + L^*(N) \leq d_i + L^*(N) \tag{1}$$

where N is the set of customers to visit, d_i is the distance of the client from the warehouse and $L^*(N)$ is the minimum length of a Hamiltonian path between customers in N .

2. If the set customers is partitioned according to any policy RP in R regions each, that containing q customers, the minimum value Z^{RP} of the lengths sum of the paths of customer visit, meets (2).

$$\frac{2}{|q|} \sum_{i \in N} d_i \leq Z^{RP} \leq \frac{2}{|q|} \sum_{i \in N} d_i + 2 d_{max} + \sum_{j \in R} L^*(N(j)) \tag{2}$$

where $N(j)$ is the set of customers in region j .

If the distance between any pair of customers is Euclidean, whatever policy of partition RP , (3) is true

$$\sum_{j \in R} L^*(N(j)) \leq L^*(N) + \frac{3}{2} P^{RP} \tag{3}$$

where P^{RP} is the length of perimeters of regions in which it was divided the area containing all customers to visit.

If the distance between any pair of customers is Euclidean and they are distributed on a compact region of the plane at random and independent, (4) is the result on the asymptotic length.

$$\lim_{|N| \rightarrow \infty} \frac{L^*(N)}{\sqrt{|N|}} = \beta \tag{4}$$

where β is a constant that dependent on the law of random distribution of customers.

In the case of Euclidean distances, if there are policies for which the term PRP increases with order less than O

($|N|$), the above observations allow us to affirm that the sum of the lengths of shortest paths that cover all customers with probability 1, asymptotically (5).

$$\lim_{|N| \rightarrow \infty} Z^{RP} = \frac{2|N|}{q} E(d) \tag{5}$$

where $E(d)$ is the average distance of customers from the warehouse.

The length of the minimum Hamiltonian path, which covers all customers grows with the square root of the number of the same, while, if it is determined the maximum number of clients per path, the sum of the lengths of multiple paths necessary to cover the totality of customers grows linearly.

C. 9.4.2 The Continuous Approximation

This class of models offers a hierarchical approach to DRAI problems solving. The basic principle is that many specific data can be neglected, retaining the ability of analytical model to provide useful solutions. The discrete data, when sufficiently numerous, may be approximated by continuous functions so as to develop simple (but plausible) models. The solution process is to define a cost function to be minimized. This includes all relevant costs along the distribution cycle, which can be summarized as follows:

- Physical handling of goods: transport in strict sense, preparation and packaging of the lots to be dispatched;
- Storage: cost of renting facilities dedicated to storage, cost related to expectation of goods.

The cost function under realistic conditions (such as economies of scale in goods flow) is a concave function. Concave functions have many local optima, which makes it difficult to determine the global optimum. Two important consequences of the concavity are: justifies the use of the approximation by continuous functions, and leads to solutions of "all or nothing". The main hypotheses underlying the Continuous Approximation approach are: the demand varies slowly with time, the geographical distribution of consumers varies slowly in space, the total cost can be expressed as the sum of costs of small components (disjoint) of the total region.

An extensive review of the literature on Continuous Approximation is provided by Langevin, et al. [16] and Federgruen and Simchi-Levi [19].

D. The Fixed-partition policies

Baseline scenario for the Fixed-partition policies, are as follows:

- Topology: one to many, with Euclidean distances approximately;
- Question: constant over time and uniform in space;
- Constraints: both on the capacity of vehicles on their number;

- Inventory costs: storage (possibly different depending on the customer), fixed or reorder;
- Transport costs proportional to the length of the routes, fixed costs;
- Solutions: heuristics, asymptotically optimal of the number of customers.

Φ is the set of all policies FPP. Determine a strategy that minimizes the cost Φ respecting the constraints defined above is clearly NP-hard, since it must still determine the minimum Hamiltonian circuits. But taking advantage of structural properties the cost average value expression over the long term is shown that it is possible to define, without having to determine simultaneously Hamiltonian paths and frequency of clients access, a partition in regions, with probability 1, asymptotically optimal in the number of customers.

Instead of *Fixed-Partition Policies* spoken Anily and Federgruen [28] and Bramel [20].

E. Problems Routing and Scheduling in the distribution of goods

Below, we describe different characteristics of the problems routing and scheduling freight, considering key components of this problem - road network, customers, stores and vehicles - various operational constraints that may be imposed in construction of travel, and finally, possible objectives to be pursued in the optimization. The road network used for the transport, normally is described by a graph whose edges represent road sections passable and whose vertices correspond to remarkable points of the network, i.e., at intersections and at points where they are localized customers and deposits. Each customer is characterized by:

- Vertex of road graph;
- Amount of goods, possibly of different types, which must be delivered and / or collection;
- Intervals of time, also referred to as time windows, in which can be served;
- Time loading and unloading;
- Any subset of vehicles that can be used to serve him.

If you cannot fully meet the demand of transport associated with all customers, some of them or are not served or are only partially. To this end are generally defined priority levels of service between customers. The travels for customers service have origin and destination in one or more deposits located in the vertex of the road graph.

The number and types of vehicles of each deposit, as well as the amount of goods that each store is capable of treating, may depend on the deposit. The transportation of goods is made using a fleet of vehicles that can be fixed or variable in size. The truck drivers are subject to restrictions of trade union different.

Other limitations are given by Erdogan and Miller-Hooks [1] in Green Vehicle Routing Problem. The G-VRP seeks to find at most m tours, one for each vehicle, that

starts and ends at the depot, visiting a subset of vertices including AFSs when needed such that the total distance traveled is minimized. Vehicle driving range constraints that are dictated by fuel tank capacity limitations and tour duration constraints meant to restrict tour durations to a pre-specified limit T_{max} , apply.

Travel must meet a number of operational constraints, arising from the nature of the transport operation, the quality of the desired service and employment contracts of staff. In any moment the quantity of goods loaded on each vehicle may exceed the respective load capacity. The travel can include both pick-up and delivery of goods, or only one of these activities. The visit to the customer must be made within relevant time windows or can also be defined as a maximum total duration of journey. To this end, a complete graph whose vertices are the vertices of network corresponding to and deposits is defined, starting from the road network. For each pair of vertices i and j of the graph, there is an arc whose cost c_{ij} is the cost of the shortest path, in terms of distance or travel time, between the two vertices, measured on the original road network. In some cases the problem does not explicitly refer to a road network: the vertices (customers and deposits) are determined exclusively by their coordinates in a plane and the costs c_{ij} of the graph are defined by the Euclidean distance between the vertices i and j . These problems, known as Euclidean problems are obviously symmetrical and have the property of triangularity. The objectives that can be pursued in the solution of a problem of freight transport are numerous, including:

- Minimization of the total cost of transport (depending on the total distance traveled and/or time travel) and the fixed costs associated with the use of vehicles and crews;
- Minimization of vehicles numbers and/or drivers necessary;
- Balancing of the various paths from the point of view of the distance traveled or the workload associated;
- Minimization of the penalties associated with non- or partial service to customers.

Extensive surveys on the problems of vehicle routing and scheduling were presented by Laporte [24], Fisher [17], and Toth and Vigo [10] [14]. An annotated bibliography of these problems has been proposed by Laporte [15]. There are also available studies on the subject of comprehensive volumes such as Toth and Vigo [9].

Methods of solution metaheuristics for the standard version of the VRP were compared by Bianchessi and Righini, [5], in particular Tarantilis, et al. [6] analyzing various models (Type of moves employed; Intermediate infeasible solutions; Solution-attributes stored in tabu list; Tabu tenure; Diversification; Intensification).

Definitions and formulations of the performance in distribution, or rather about effectiveness (that extent they are satisfied with the goals of rapid deployment) and equity,

(ie the extent to which all recipients receive a similar service), are discussed by Huang, et al. [2]. They demonstrated that the efficiency is the total travel time for selected routes, the efficacy is the measure of which calculates the speed and sufficiency of deliveries, the equity is the measure the spread in service level across nodes.

R. Bachmann and Langevin [3] developed an algorithm with few data (cost of delivering a load to each store and cost per stop in that region); this algorithm provides a viable solution and considers the decrease in capacity of trailers.

F. Models and exact algorithms for the VRP

The *Asymmetric Capacitated Vehicle Routing Problem* (ACVRP) is linked to *Bin Packing Problem* (BPP), which requires to determine the minimum number of identical containers (bins), each with capacity D, necessary to contain a given set of objects, the j-th of which is characterized by a non-negative weight d_j .

It is known in fact that in the particular case where $c_{ij} = 0$ for all $(i, j) \in A, i \neq j, i \neq 0$, and $c_{0j} = 1$ for all $j \in V \setminus \{0\}$, and ACVRP equivalent to BPP. Note that if the value of the optimal solution of the BPP associated to ACVRP (from (6) to (12)) is greater than K, the ACVRP have no solution. A linear programming model for whole ACVRP can be obtained using $(n + 1)^2$ x binary variables, one for each arch of the complete graph. The variable x_{ij} takes the value 1 if and only if the arch (i, j) and in the optimal solution assumes value 0 otherwise. For each $S \subseteq V \setminus \{0\}$, and $\sigma(S)$ the minimum number of vehicles needed to serve all customers in S, i.e., the value of the optimal solution of the BPP with set of objects S. Note that $\sigma(V \setminus \{0\}) \leq K$. It therefore has the following formulation:

$$z = \min \sum_{i \in V} \sum_{j \in V} c_{ij} x_{ij} \tag{6}$$

$$\sum_{i \in V} x_{ij} = 1 \quad \forall j \in V \setminus \{0\} \tag{7}$$

$$\sum_{i \in V} x_{i0} = K \tag{8}$$

$$\sum_{j \in V} x_{ij} = 1 \quad \forall i \in V \setminus \{0\} \tag{9}$$

$$\sum_{j \in V} x_{i0} = K \tag{10}$$

$$\sum_{i \in S} \sum_{j \in S} x_{ij} \geq \sigma(S) \quad \forall S \subseteq V \setminus \{0\} \quad S \neq \emptyset \tag{11}$$

$$x_{ij} \in \{0, 1\} \quad \forall i, j \in V \tag{12}$$

G. Lower bounds and exact algorithms

Being the TSP a relaxation of VRP, it is evident that any lower bound valid for TSP is also valid for VRP. Considering the symmetric version of the problem is possible to perform a relaxation which requires the computation of a spanning tree of minimum cost (*Shortest*

Spanning Tree, SST) of undirected graph in place of arborescence. A "lower bound" alternative is given by the cost of the same SST on the graph G plus the cost of the K cost arcs. A second type of "lower bound" for ACVRP considering the graph extended, oriented and complete.

Thoth and Vigo [14], Fischetti, et al. [21] Cornuejos and Harche, [23], and Fisher [22] presented review that offer relaxations of the Lower bounds and exact algorithms.

H. The method of Clarke-Wright

The algorithm of Clarke-Wright [9] is one of the first attempts to solve VRP with capacity constraints (CVRP). The algorithm starts from a solution no admissible where every guest is served in a different journey. Trips are then iteratively combined considering the saving s_{ij} (13), in terms of cost of travel, which can be achieved by serving two customers in one trip instead of leaving them in two separate trips.

$$s_{ij} = c_{0i} + c_{i0} + c_{0j} + c_{j0} - (c_{0i} + c_{ij} + c_{j0}) = c_{i0} + c_{0j} - c_{ij} \tag{13}$$

Depending on the construction method of travel, it obtain two distinct versions of the algorithm (sequential and parallel), but in both cases the pairs of customers are taken into account for the possible union of travel which contain them to decreasing values of saving associated with them.

The sequential version of the algorithm of Clarke and Wright builds a trip at a time, adding a new customer at the beginning or at the end of the trip, as long as no other customer can be inserted without violating the constraint on the ability or has reached the end of List of saving.

The most widespread version of the algorithm of Clarke and Wright is parallel, where the list of saving is examined only once, and if both the couple's current customers are at the beginning or at the end of two trips and if the union of the two trips is eligible for the capacity constraint, the travel to which customers belong are merged into one trip, as long as the list of saving is not full. One can change the algorithm of Clarke and Wright in order to consider operational constraints also extremely complex, just merely do the unions of travel leading to a new journey admissible.

I. The algorithm of Fisher and Jaikumar

Fisher and Jaikumar [9] proposed an algorithm for CVRP based on a reformulation of the problem as a *Generalized Assignment Problem* (GAP) non-linear, which determines an allocation of eligible customers to a number of trips and the objective function which takes into account the cost of sequencing customers in each trip. In the approach proposed, the non-linear the objective function is approximated by a linear function. The method of solution is of the type called a *cluster-first-route-second* and is decomposed into two phases.

In the first phase, customers are partitioned into subsets (clusters), eligible from the point of view of capacity constraint, solving a GAP with the objective function

linearized. During the second stage, the final solution is obtained by sequencing of the customers of each subset using an algorithm (from (14) to (17)) for the resolution of TSP.

$$\min \sum_{k=1}^k f(y_k) \tag{14}$$

$$\sum_{i \in V \setminus \{0\}} d_i y_k \leq D \quad k=1, \dots, K \tag{15}$$

$$\sum_{k=1}^k y_k = 1 \quad \forall i \in V \setminus \{0\} \tag{16}$$

$$y_{ik} \in \{0,1\} \quad i \in V \setminus \{0\}, k=1, \dots, K \tag{17}$$

where $y_{ik} = 1$ if and only if the i customer is assigned to the subset k and $f(y_k)$ is the cost of sequencing optimal customer assigned at the k trip, that is, the value of the optimal solution of TSP associated with the vertices of the subset $N_k = \{ i \mid y_{ik} = 1 \} \cup \{0\}$. The focus of the algorithm is constituted by the construction of the linear objective function nonlinear $f(y_k)$.

A possible way to construct this approximation is based on the determination of K customers (or points) *seed* the, i_1, \dots, i_K , associated with vehicles 1, ..., K . The γ_{ik} coefficients are calculated as the insertion cost of customer on journey from warehouse to seed i_k and back. Due to the strong influence of seed on the placement of customers to different subsets made by the GAP, the choice of the set of seed is an extremely delicate phase heuristic Fisher and Jaikumar.

J. Finishing techniques based on local search

The solutions obtained by heuristic algorithms can often be improved using post-optimization procedures (called *local search*) based on movements of customers or exchanges of arcs. The algorithms of local search iteratively evaluate eligibility and cost of all solutions of the surroundings of the current solution, saving the best feasible solution found. If the cost of the best solution of the surroundings is lower than the current solution, it runs the transfer or exchange associated with it and it becomes the new current solution.

The algorithm terminates when no solution of the surroundings current has lower cost than the current. The difference between current and new solution cost (18) is easily obtained considering only arcs removed from the current solution and those inserted in the new solution.

$$\Delta_{ab}^i = (c_{\pi(a)a} + c_{a\sigma(a)} + c_{b\sigma(b)}) - (c_{\pi(a)\sigma(a)} + c_{ab} + c_{a\sigma(b)}) \tag{18}$$

The procedures of local search easily are generalized so as to consider displacements of more than two clients or exchanges of more than two arcs. These generalizations produce better solutions.

IV. CONCLUSIONS AND FUTURE WORK

Highlighting the interaction of ITS and goods transportation was essential to analyze the needs of logistics operators and the primary objectives that they pursue, describing goods transportation models in order to identify the main problems of the operators (DRAI; VRP). Defining a wide scenery of the models in the literature was useful for making a classification according to the following parameters: topology, type of goods, demand, kinds of decision, constraints/objectives, costs, solving approach.

During the study, we analyzed models for goods transportation that interacted with ITS. These models have shown that the implementation of ITS not only reduces costs, but also facilitates an efficient organization and management of goods. Further studies could be developed to identify the extent to which the use of certain instruments of ITS vary some elements of a supply chain.

A future work could include the study of fleet management, understood as tracking and tracing of vehicles that usually use the following services:

- Mobile terminals management;
- Fleet management and their list;
- Management of the position requests for terminal or fleet;
- Visualization of the terminal position on the map;
- Management of the terminal lists of a specific fleet;
- The introduction of this elements as decision variables in the VRP, would achieve more accurate results.

In particular, it seem to be a priority:

1. Knowledge of road network portion passable in function of the geometric characteristics vehicle and emissions into the atmosphere of own engine;
2. Monitoring of average speeds along the network arcs used in the assigned itinerary to update the generalized cost of transport (at least for the travel time);
3. Possibility to reserve the use of spaces for parking dedicated to the loading / unloading of goods, so as to reduce the search time of parking, to reduce the delay on the current traffic produced by illegal parking, and ultimately, reduce the crew of each vehicle.

The use of mathematical models of routing and scheduling that considers the variables described above, could yield further improvements in business management.

REFERENCES

[1] S. Erdogan and E. Miller-Hooks, "A Green Vehicle Routing Problem," *Transportation Research Part E*, vol. 48, pp. 100-114, January 2012;

[2] M. Huang, K. Smilowitz, and B. Balcik, "Models for relief routing- Equity, efficiency and efficacy," *Transportation Research Part E*, vol. 48, pp.2-18, January 2012;

- [3] R. Bachmann and A. Langevin, "A vehicle routing cost evaluation algorithm for the strategic analysis of radial distribution networks," *Transportation Research Part E*, vol. 45, January 2009;
- [4] I. Davies, R. Mason, and C. Lalwani, "Assessing the impact of ICT on UK general haulage companies," *International Journal of Production Economics*, vol. 106, pp. 12-27, March 2007;
- [5] N. Bianchessi and G. Righini, "Heuristic algorithms for the vehicle routing problem with simultaneous pick-up and delivery," *Computers & Operations Research*, vol. 34, pp. 578-594, February 2007;
- [6] C.D. Tarantilis, G. Ioannou, and G. Prastacos, "Advanced vehicle routing algorithms for complex operations management problems," *Journal of Food Engineering*, vol. 70, pp. 455-471, October 2005;
- [7] F. Golob Thomas and C. Regan Amelia, "Trucking industry adoption of information technology- a multivariate discrete choice model," *Transportation Research Part C: Emerging Technologies*, vol. 10, pp. 205-228, June 2002;
- [8] R. Danielis, "Domanda di trasporto merci e preferenze dichiarate," Franco Angeli, Milano 2002;
- [9] P. Thot and D. Vigo, "Vehicle Routing Problem," SIAM monographs on discrete mathematics & applications, Philadelphia, 2002;
- [10] P. Thot and D. Vigo, "Models, relaxation and exact approaches for the capacited Vehicle Routing Problem," *Discrete Applied Mathematics*, vol. 123, pp.487-512, 2002;
- [11] Ministers of Transport (ECMT), European Commission (EC), "Terminology on combined transport, United Nations, New York and Geneva," 2001;
- [12] Politecnico di Milano - Dipartimento di Economia, "Indagine sull'Evoluzione Strutturale delle Imprese della Logistica in Italia," Assologica, 2001;
- [13] O. Baccelli, "La Mobilità delle Merci in Europa: Potenzialità del Trasporto Intermodale," Egea, 2001;
- [14] P. Thot and D. Vigo, "Exact Algorithms for Vehicle Routing," in T. Crainc and G. Laporte, Eds. *Fleet Management and Logistic*, 1-33 Kluwer Academic Publisher, Boston, 1998;
- [15] G. Laporte "Vehicle routing," M. Dell'Amico, F. Maffioli, and S. Martello, Eds. *Annotated Bibliographies in Combinatorial Optimization*, Wiley, Chichester, U.K, 1997;
- [16] A. Langevin, P. Mbaraga, and J.F. Campbell, "Continuous approximation models in freight distribution: an overview," *Transportation Research B*, vol. 30, pp. 163-188, 1996;
- [17] M.L. Fisher, "The Vehicle routing," in M.O. Ball, T.L. Magnanti, C.L. Monna, and G.L. Nemhauser, editor *Network Routing*, Vol. 8 *Handbooks in Operation Research and Management Science*, pp 1-33, North-Holland, Amsterdam, 1995;
- [18] M.W.R. Savelsbergh and M. Sol, "The general pickup and delivery problem," *Transportation Science*, vol. 29, pp. 17-29, 1995;
- [19] A. Federgruen and D. Simchi-Levi, "Analysis of Vehicle Routing and Inventory Routing Problems," in *Handbooks in Operations Research and Management Science*, M. Ball et al., Eds. 297-371, North Holland, Amsterdam, 1995;
- [20] J. Bramel and D. Simchi-Levi, "A location based heuristic for general routing problems," *Operations Research*, vol. 43, pp. 649-660, 1995;
- [21] M. Fischetti, P. Thot, and D. Vigo "A Branch-and-Bound Algorithm for the Capacited Vehicle Routing Problem on direct graphs," *Operation Research* 42(5), pp 846-859, 1994;
- [22] M.L. Fisher, "Optimal Solution of Vehicle Routing Problem Using Minimum k-Trees," *Operation Research* 42(4), pp 626-642, 1994;
- [23] G. Cornuejos and F.Harche, "Polyhedral Study on the Capacitated Vehicle Routing Problem," *Mathematical Programming* 60(1), pp 21-52, 1993;
- [24] G. Laporte, "The Vehicle routing problem: An Overview of Exact and Approximate Algorithms," *European Journal of Operational Research* 59, pp 345-358, 1992;
- [25] G.U. Tinarelli, "La gestione delle scorte nelle imprese commerciali e di produzione," Etas Libri, Milano 1992;
- [26] S. Anily and A. Federgruen, "One warehouse multiple retailer systems with vehicle routing costs," *Management Science*, vol. 36, pp. 92-114, 1990.

Overcoming the Condorcet's Border in Collective Intelligence Systems

Vladislav Protasov, Zinaida Potapova
Center of Computing for Physics and Technology
Moscow, Russia
protvld@gmail.com, zinaida.potapova@gmail.com

Eugene Melnikov
Center of Computing for Physics and Technology
Moscow, Russia
apinae1@gmail.com

Abstract – The paper presents a new approach of solving intellectual problems by means of collective intelligence. The essence of the approach is combination of two principles: Condorcet's principle of the jury and evolutionary coordination, based on reciprocal evaluation among intellectual agents. This method exploits both generative and evaluative abilities of the agents and allows to eliminate so called Condorcet's border, which means that for obtaining correct solution every expert must make correct decision with probability greater than 0.5. The paper also observes the conditions that guarantee correct solution obtainment.

Keywords – *collective intelligence; genetic algorithm; coordination; generation; evaluation.*

I. INTRODUCTION

In October 2010 in the "Science" magazine (USA) employees of the Center for Collective Intelligence of the Massachusetts Institute of Technology headed by Pr. Thomas V. Malone published the first English language paper that proved the effect of excess of the collective Intelligence Quotient value over both group average and maximum individual IQ values [1]. The factor was identified that determines the successfulness of solution in intelligent groups. It was called the C-factor (collective factor). The factor analysis approved the existence of the only significant component for all collective activities. This component is the C-factor.

The analysis of these experiments has provided two conclusions: first of all, the collective component, that defines group intelligence potential, exists, secondly, it can be evaluated objectively.

There are also a huge number of well-known crowdsourcing application success stories [2], based on the application of Condorcet's jury theorem [3]. The intellect gain effect during expert group work takes place due to several reasons. In the first case (Malone's) it is defined mainly by the "legislative" component. It means that at the first step some solutions are generated and during further discussion they are combined by the collective intelligence of the group into a collective solution. In the case of crowdsourcing the process often consists of only the first step – ideas generation, and if every expert has a probability of correct solution $G_P > 0.5$, then at a great number of experts the probability of the collective solution correctness tends to 1. If for every expert $G_P < 0.5$, then the probability tends to 0, which is a big problem in application of crowdsourcing.

Most papers upon collective intelligence refer the Condorcet's principle [4]. This paper provides an approach of eliminating the Condorcet's constraint of 0.5. First of all, the method will be introduced and explained. After that there will be a computer experiments report. In the end goes the definition of the condition that must hold in order to obtain correct result.

In this paper, basic principles that are related to the algorithm are discussed in Section II, while Section III describes the method itself. Section III deals with theoretical and experimental substantiation of the method. Last section provides the conclusion.

II. QUICK VIEW UPON THE BASIC PRINCIPLES

The Condorcet's jury theorem assumes that a group of individuals wishes to reach a decision by a majority vote. One of the two outcomes of the vote is correct, and each voter has a probability p of voting for the correct decision. The theorem contends that if $p > 0.5$ then with increasing the number of voters the probability of obtaining the correct solution tends to 1; in other hand, if $p < 0.5$ then with increasing the number of voters it tends to 0.

This means, for a jury group making a decision between two alternatives, if their $p > 0.5$ then a large group will make correct decision with higher probability than a small one, but if their $p < 0.5$ then one expert will make correct decision much more probably than a group.

Another approach that lies on the foundation of this paper is Genetic Algorithms (GA) [5]. Its basis is rather simple. Each solution is assumed as a biologic individual that has a genotype (sequence of bits that encodes the set of its characteristics or so called phenotype). The algorithm starts with generation of initial set of individuals (solutions). The correct solution search passes like a biological cycle of population. It consists of three stages that repeat iteratively:

1) *Mutation* of random individuals: each individual subjected for mutation changes random bits of its genotype. Usually only few bits are subjected for change – near 10%.

2) *Natural selection*: each individual has a value of the *fitness function*. Basing on this values some "weak" individuals are eliminated and population decreases, usually on 50%. The selection algorithm may vary.

3) *Crossover*: all individuals divide into pairs and every pair give birth to two children – individuals that incorporate the genotypes of their parents.

These stages run iteratively until the *convergence condition* holds. It may be an obtainment of some fitness

value or end of the population progress (maximal fitness doesn't increase). The individual with the highest fitness is selected as the final solution.

As an example of GA application let's assume a chemical experiment. We need to adjust the volumes of reagents to provide maximal heating of the mixture. The set of volume values represents an individual and is encoded into bits of its genotype. Fitness of each individual (solution) is evaluated by chemical modeling module. Since we have all the data presented in GA model, we can run the algorithm to obtain a rational solution.

III. METHOD OF EVOLUTIONARY SOLUTIONS COORDINATION INTRODUCED

As Malone's experiments proved, in experts' work, based on legislating and voting procedure, the leader effect and conflicts, hidden and evident, considerably worsen effectiveness of the group.

This paper proposes the synthesis of the two approaches that is called by the authors Method of Evolutionary Solutions Coordination (MEC), which has advantages of two methods and considerably compensate their weaknesses.

The method incorporates genetic algorithms (GA) [6], Condorcet's theorem, Tychurin's metasystem transitions theory [7] and collective intelligence systems theory, that is partially presented in this paper.

The method is defined as follows. MEC is an approach of organization of collective work upon a project with predefined objectives and rules of interaction, based on classic GA principles. Experts work is usually organized by the means of a computer network. These are the rules of organization of intellectual agents work and interaction:

- 1) Objectives of the project are defined
- 2) Experts group and their interaction method are selected
- 3) Frame (slots structure) of the project is created
- 4) The first solutions are found, they may be incomplete
- 5) Solutions are exchanged between the experts
- 6) Exit condition is checked; if it's fulfilled, algorithm halts
- 7) New solutions are created from the old ones through crossover
- 8) Some new solutions mutate
- 9) Go to the point 5

According to interaction rules the collective work instructions are developed considering features of certain problem, communication environment, abilities and qualification of the intellectual agents. The scheme of MEC is illustrated on Fig. 1.

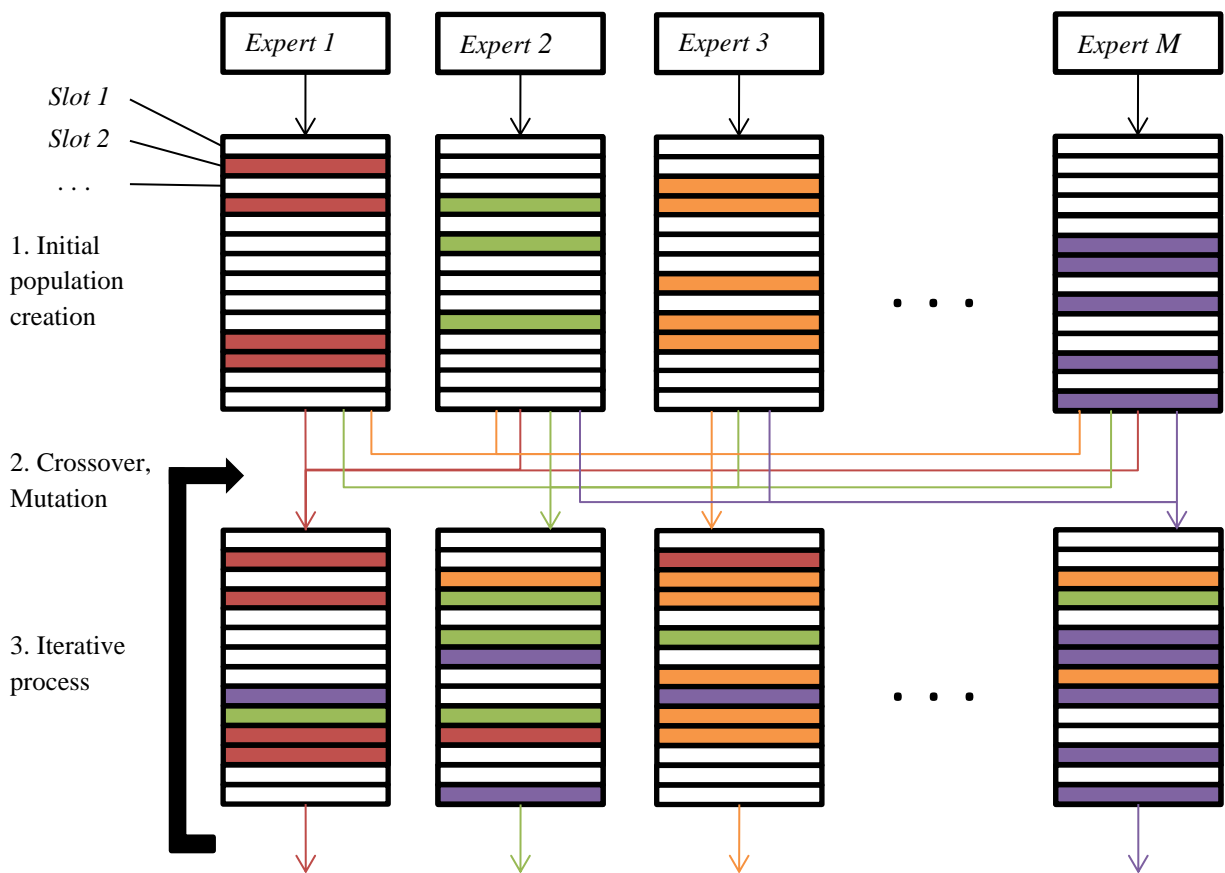


Figure 1. MEC scheme

On the zero iteration experts fill slots of the project according to their knowledge. In Figure 1 these slots are marked with dark rectangles. On the iterations of coordination, each expert checks others' variants and picks some of those that he considers to be the best and fills blank cells of his variant with them. After performing several iterations, the process converges to a population of equally filled solutions. For accelerating the process, it can be adjusted with the Condorcet's rule – a slot is considered as filled, if more than half of experts have made the same decision on it.

Experiments on solving complicated intellectual problems from different creative areas by expert groups have demonstrated the MEC efficiency. With this method high level checkmate problems were successfully solved by collective intelligence, when the group members could not solve the problems individually. A witnesses group effectively restored an identikit, IQ measurement [8] upon verbal Eysenck's tests [9] demonstrated an extremely high intellectual level of the group. There are many papers in Russian that refer to these results [10][11][12][13][14], but they are unknown for English-speaking audience. This paper partially makes up this lack.

Most papers upon negotiation of agents group offer approaches to find some trade-off in preferences of several individuals [15][16]. They use predefined utility functions of the agents to obtain Pareto-optimal solutions. Supposed methods are considered to demonstrate high quality of negotiating in multi-party cases. There are also some papers [17] that describe complex approaches – concluding contracts are defined by utilizing several strategies of negotiation. All these theories aim to obtain a solution in case of multiple preferences of different parties. This signifies that each party has its own assumption upon correct solution. Such circumstances appear not frequently enough on complicated multidimensional problems. In real life situations not every agent can provide a value for each component of the solution. MEC deals with such situations throughout utilization of agents' ability of estimating other agents' solutions. In most cases even if an expert can't provide his own solution of a problem, at least he can express his opinion upon an existing solution.

IV. MODELING THE CALCULATION PROCESS

The main way, considered to explore the proposed method in this paper, is computer modeling. The project, subjected for solving by a group of virtual experts, is meant to consist of K slots that must be filled with correct answers after several stages of coordination according to the vote majority.

Let us draw up a computer model of a slot filling process with applying it to all slots of the project successively. The decision-making process is divided into several stages. The first stage is individual decisions creation, further follow stages of iterative coordination of the solutions by a group of M experts. Let us suppose that on the stage of individual decisions creation every expert gives a correct solution with probability $0 < G_P < 1$, an incorrect solution with probability $0 < G_N < 1$ and with probability $G_V = 1 - G_P - G_N$ he gives no solution. On coordination stages an expert, who didn't make a decision, chooses among other experts' solutions –

correct one with probability E_P , incorrect one with probability E_N – and chooses no solution with probability $E_V = 1 - E_P - E_N$.

All the probabilities are determined with consideration that correctness of solutions can be estimated. It is necessary for building the mathematical model, but in further application it isn't essential – real life problems are not usually provided with fitness function and each solution is estimated by subjective opinion of an expert. And for MEC it isn't matter if the estimation process is formulized or defined by certain expert's opinion.

Moreover, the assumption that correctness of solution is a binary function (correct/incorrect) is also considered only for durable mathematical substantiation. It can be discarded f.e. with application of fuzzy logic (every solution is correct and incorrect with some degrees). All further deductions can be completed with probabilistic functions of correctness. We assume that taking them into consideration is not essential and theoretical substantiation on strict correctness can be propagated to fuzzy functions.

The algorithm of the decision-making process that lies upon the computer model can be easily described on cellular automata language. Let us suppose that experts fill the automata cells basing on the following rules.

Initial state of the cellular automata is determined by G_P and G_N parameters, it is represented by the vector $B_i, i = 1, 2, \dots, M$.

$$B_i = \begin{cases} 1, & 0 < \xi \leq G_P \\ 2, & G_P < \xi \leq G_P + G_N, \\ 0, & \xi > G_P + G_N \end{cases}$$

where ξ is a random number in the interval $(0, 1)$. 1 means that an expert has made a correct decision, 2 means an incorrect decision, 0 – the expert has not made a decision. Mean of the number of ones in the automata equals $M \cdot G_P$, of the number of twos – $M \cdot G_N$, of the number of zeros – $M \cdot G_V$.

The subsequent state C_i of the cellular automata, that imitates solutions coordination process, is filled according to the following rules.

1. If $B_i > 0$, then $C_i = B_i$ (experts have filled their cells and now are waiting for other experts to fill up the cells).
2. If $B_i = 0$, then then the i -th expert uniformly chooses another cell j such that $B_j > 0$ and randomly updates his ξ in the interval $(0, 1)$. Depending on value of ξ he chooses one of three options:
 - 2.1. If $0 < \xi \leq E_P$, then if $B_j = 1$, then on the second state of the expert $C_i = 1$, if $B_j = 2$, then the expert ignores wrong decision and saves 0 to the C_i cell.
 - 2.2. If $E_P < \xi \leq E_P + E_N$, then if $B_j = 1$, then the expert makes wrong decision – he ignores the correct 1 and saves 0 to the C_i . If $B_j = 2$, he saves 2 to the C_i by mistake.

- 2.3. If $\xi > E_P + E_N$, then the expert cannot estimate the B_j cell solution and saves 0 to the C_i .
3. C array is saved to B . If it still has zeros, then proceed from the point 2, otherwise – move to the point 4.
 4. At this stage the group’s solution is defined by the votes majority. If ones dominate, then it’s considered, that the group has made a correct decision. If twos dominate, then the decision is wrong.

Basing on this algorithm, a computer program was developed, that allowed to find G , the probability of making correct decision for one expert in the end of convergent iterative process, according to predefined parameters of the model: G_P, G_N, E_P, E_N , when he use his expert ability of choosing between others’ solutions together with the ability of ideas generation. To find P – the probability of finding correct solution by votes majority in the group of M experts – let us use famous formula, that follows from the Condorcet’s Theorem [3]:

$$P = \sum_{i=0}^{M-1} C_{i, \frac{M-1}{2}}^i G^{M-i} (1 - G)^i \quad (1)$$

One of the research objectives was to explore the dependence of the group intellectual potential upon the model parameters. As the intellectual potential, the function $IP = \frac{1000}{M}$ was considered. It is inversely proportional to the number of experts that have found correct solution with probability $1 - \varepsilon$, where ε is a predefined small value. In our experiments $\varepsilon = 0.001$.

Computer experiments were performed with different values of the parameters G_P and G_N . Their variations are given in the Table I. There are also presented the evaluated values of M (top left corner of a cell) and IP (bottom right corner of a cell) for $\frac{E_N}{E_P} = 2$ and $\frac{E_N}{E_P} = 0.5$. Obviously, the cases where $G_P + G_N > 1$ are impossible. Furthermore, some small values of these parameters where $G_N > G_P$ also give no results because the number of experts M in these cases tends to infinity.

It is shown that intellectual potential of the experts differs by degrees and the legislative component brings a considerable contribution to the intellect structure. Moreover, it is the very thing that allows to overcome the Condorcet’s “border”.

4. Conditions of correct solution obtainment

Basing on the experiments the empirical inequality was defined that bounds up parameters of the model. When it holds, it’s always possible to find M , such that guarantees obtaining correct solution with probability 0.999 for the group:

$$G_P + \frac{E_P G_V}{E_P + E_N} > 0.5 \quad (2)$$

For convenience, in practical applications, the constraint (2) can be deduced to:

$$\frac{E_P}{E_N} > \frac{1-2G_P}{1-2G_P} \quad (3)$$

Here are some consequences of the inequality (3):

1. If experts have low ability of decision generation ($G_P < G_N$), then for obtaining a correct solution it’s necessary for them to have high abilities of evaluation ($E_P > E_N$).
2. If experts have high ability of decision generation ($G_P > G_N$), then for obtaining a correct solution it’s not necessary for the group to have high evaluation abilities ($E_P < E_N$).
3. If experts’ abilities of both generation and evaluation are both low, they cannot obtain a correct solution. Moreover, if the portion of such experts in the expert group increases, then correctness of the group work result decreases.

Convergence of MEC to the correct solution and fulfillment of the inequality (3) in quantitative form were inspected also in condition of normal distribution of the model parameters. Just like in Condorcet’s research, in this paper, basing on computer experiments, it’s deduced that the results obtained in case of normal distribution of parameters in limits of statistical errors, concurred with results of inspection, performed with average values of the parameters.

Let us consider a practical example of the MEC usage. One of the experiments that were made by the authors is an IQ test. The test consists of a set of questions, i.e. 50. Every question is provided with several answers only one of which is correct. There are 10 students (experts) participating in the test solving.

According to the MEC model solution template can be divided into 50 slots – one for a question. On the first iteration of MEC each of 10 students proposes answers for every question he is sure and leaves unanswered those he has doubt with. On the second and other iterations each expert receives a solution of another randomly chosen expert and rates his answers. If some answer of the expert being rated seems more correct that the one which the rater has in susceptible slot then he replaces his old slot value or blank slot with the value of that user. These iterations proceed until all solutions are similar (the students have come into conclusion). Thus, the solution that is left in the solutions population is considered as the most correct one.

On multiple experiments the method demonstrated high increase of the intellect level of real students groups.

V. CONCLUSION AND FUTURE WORK

On the results of the research, the following conclusions were made:

- Simple and efficient iterative method of collective decision-making was proposed and explored.

TABLE I. VALUES OF THE MODEL PROPERTIES

$E_N/E_P = 0.5$									
$G_N \backslash G_P$	0.1	0.2	0.3	0.4	0.5	0.6	0.7	0.8	0.9
0.1	129 7.75	81 12.3	55 18.2	39 25.6	29 34.5	21 4.,6	17 58.8	13 76,9	9 111.1
0.2	535 1.87	233 4.29	127 7.87	81 12.3	55 18,2	37 27,0	27 37.0	21 46.7	-
0.3	-	2147 0.465	531 1.88	233 4.29	129 7.75	81 12.3	55 18.2	-	-
0.4	-	-	-	2143 0.467	533 1.88	235 4.26	-	-	-
$E_N/E_P = 2$									
$G_N \backslash G_P$	0.1	0.2	0.3	0.4	0.5	0.6	0.7	0.8	0.9
0.1	-	-	-	535 1.87	129 7.75	55 18.2	29 34.5	17 58.8	9 111.1
0.2	-	-	-	2145 0.466	233 4.29	81 12.3	39 25.6	21 46.7	-
0.3	-	-	-	-	535 1.87	127 7.87	55 18.2	-	-
0.4	-	-	-	-	2147 0.465	235 4.26	-	-	-

- The conditions were determined, that can guarantee obtainment of correct solution by a group of experts using the Method of Evolutionary Solutions Coordination.
- The experts' competence of legislation and decisions evaluation was engaged together with the ideas generation competence. It helps experts groups to operate more efficiently and eliminate the Condorcet's border.

The obtained results have become the beginning of large research, that is divided into two branches. The first is exploring applications of MEC with creation of different variations of the method and different coordination models. For example, so-called Dynamic Slots variation was developed to apply the method in machine translation. Also MEC was utilized in collaborative text creation and concepts visualization. For all these applications software products were created. The second direction of the related work is improvement of MEC. A considerable part of theoretic research is related to elitist modification of the iterative process. It means that in creation and legislation stages experts' weights differ according to their creative and evaluative skills. Several algorithms were developed for calculating these skills.

Implementation of the coordination process in collective intelligence algorithms opens new fields of application for

information technologies. Not everybody is able to create great solution for certain problem, but comparison of several solutions with picking the most impressive one is a simpler task, and usage of this point gives wide opportunities. In order to apply these concepts in practice we need to discover new models of collective work organization, that, first of all, can be attractive for experts, e.g., in the Wide Web, and in the second, will provide solutions for some actual problems.

ACKNOWLEDGEMENTS

This work was supported by the Russian Foundation for Basic Research, grant #13-07-00958 "Development of the theory and experimental research of a new information technology of self-managed crowdsourcing".

REFERENCES

- [1] Woolley A. W., Chabris C. F., Pentland A., Hashmi N., and Malone T. W. Evidence for a Collective Intelligence Factor in the Performance of Human Groups // Science. 2010. V. 330 pp. 686–688.
- [2] P. Venetis, H. Garcia-Molina, K. Huang, and Polyzotis N. Max Algorithms in Crowdsourcing Environments // April 16–20, 2012, Lyon, France.
- [3] Le Marquis de Condorcet. Essai sur l'application de l'analyse à la probabilité des décisions rendues à la pluralité des voix. 1785. Les Archives de la Revolution Française, Pergamon Press.

- [4] Bachrach Y., Minka T., Guiver J., and Graepel T. How To Grade a Test Without Knowing the Answers | A Bayesian Graphical Model for Adaptive Crowdsourcing and Aptitude Testing // 2012 pp. 1–2.
- [5] Mitchell M. An Introduction to Genetic Algorithms, MIT press //1996. pp. 2–23.
- [6] Kosorukoff A. Human Based Genetic Algorithm // Illinois Genetic Algorithms Laboratory, University of Illinois at Urbana-Campaign. January 2001.
- [7] Turchin V. The phenomenon of science. A cybernetic approach to human evolution // Columbia University Press, New York, 1977.
- [8] Stern W. The Psychological Methods of Intelligence Testing (G. Whipple, Trans.). // Baltimore: Warwick and York.
- [9] Eysenck H. J. The Structure and Measurement of Intelligence. // University of London. Institute of Psychiatry.
- [10] Гузеев В.В. Преподавание. От теории к мастерству. – М.: НИИ школьных технологий, 2009. pp. 261–264
- [11] Кузнецов В.В. Технологии интернет-образования . <http://www.masters.donntu.edu.ua/2006/fvti/grach/library/st2.htm>
- [12] Козленко А.Г. Информационная культура и/или компьютер на уроке биологии.
- [13] Чернухин Ю.В. и Здоровеюшев В.В. Сетевой эволюционно-генетический алгоритм принятия коллективных решений в человеко-машинных системах.
- [14] Затуливетер Ю.С. Информация и эволюционное моделирование. Труды международной конференции «Идентификация и проблемы управления» SICPRO 2000, Москва. pp. 1529-1571.
- [15] Faratin P., Sierra C., and Jennings N.R. Using similarity criteria to make negotiation trade-offs. Proceedings Fourth International Conference on MultiAgent Systems. IEEE Comput. Soc. //2000.
- [16] Ehtamo H., Ketteunen E., and R. Hamalainen, Searching for Joint Gains in Multi-Party Negotiations. European Journal of Operational Research. //2001
- [17] Klein M., Faratin P., Sayama H., and Bar-Yam Y. Negotiating Complex Contracts. Sloan School of Management 3 Cambridge Center, NE20-336. //2007

Measurement and Calibration System of Arrow's Impact Point using High Speed Object Detecting Sensor

Yeongsang Jeong, Hansoo Lee, Jungwon Yu, Sungshin Kim
Department of Electrical Engineering
Pusan National University
Busan, Korea
e-mail: {dalpangi03, hansoo, garden0312, sskim}@pusan.ac.kr

Abstract— Currently, the method used to analyze the manufactured arrow's performance is to use the accumulated impact points of arrow. The impact point of arrow is appeared by shooting the arrow repeatedly with same force to a target paper using a shooting device. The method has some weak points, such as low accuracy, it needs long time to do the experiments because the arrow is shoot in several times, and difficult to digitize between impact points. Therefore, the measuring system for comparing manufactured arrows performance objectively and confirming quality and performance of arrow methodically and a sensor that can measure high-speed-moving object is needed. In this paper, line lasers are placed upper side and left side of a square-shaped frame, and photodiode sensors are installed at the opposite side of line lasers. When fired arrow goes through the square shaped frame, the voltage acquisition device measures the voltage level difference of photodiodes. Impact points of arrow are shown using the data derived by voltage acquisition device. A neural network calibration method is implemented using impact points which are printed out precisely by manufactured grid plate. The calibration method replaces the impact points included errors with precision and high reliability impact points.

Keywords-measuring system; calibration; neural network; impact point; photodiode; arrow

I. INTRODUCTION

Currently, the bow and arrow are used as a tool for hunting, recreation, sports to hobbies. Since 1972, at the Munich Olympics to date, archery rules have been revised and changed drastically. The quality and performance of bow and arrow is needed for not only getting a good score at Olympics but also increasing of customers demand for leisure. Especially, there are plenty of ongoing researches about arrow which has complex manufacturing process and should analyze scientifically, but there are no systems and intuitive numerical data for evaluating [1][2]. The intuitive numerical data means information which can be expressed as coordinate points, such as distance between impact points, two impact point coordinate that has maximum distance, and so on. Generally, the method or reference used to evaluate arrow's quality and performance is to use data based on testimonials by hunters who have used bow and arrow for a long time, by technicians who produce leisure sporting goods,

and by customers. In addition, previous research results through patents have biased technology that optimizes producing process using manufacturing variables. There is testing process for getting performance of arrow. First, attach shooting sheet on target. Second, shoot an arrow repeatedly with changing angles of nock every time. Third, check impact points of arrow and measure how dense they are. The denser of impact point, the better of performance and quality of the arrow. Analyzing impact point of arrow using shooting sheets has some disadvantages, such as low accuracy, should be replaced frequently and periodically, and the difficulty of digitize between impact points. The other way to gather data of arrow's performance is using high-speed camera, but it has also disadvantages that can see only limited angle images, and highly expensive price. For overcoming disadvantages of traditional analyze process, this paper suggest that by using of line laser and photodiode sensors which have high resolution and fast response rate, the measurement of high-speed moving arrows produced good results. By installing photodiode sensors in array formation, it can obtain the voltage level changes in the position to be passed by the arrows in the frame. All data from the photodiode sensors are acquired by Data Acquisition Device (DAQ), produced by National Instruments (NI). Then, they are transferred to Host PC connected by port or slot. This transferred data is shown by LabVIEW program in PC. However, initially appearing impact point of arrow includes errors that occurred by light of line laser and structure of photodiode array. To compensate the errors, this paper suggests calibration method using neural network (NN) [3][4].

The remaining part of the paper is organized as follows: In section 2, we describe about measuring impact point of arrow system. Additionally it describes that previous measuring system which has some drawbacks and theoretical explains about suggested method. Section 3 gives a calibration algorithm using NN. Also it includes experiments and results to proof calibration. Finally, a conclusion is drawn in section 4 with an outlook to future work.

II. MEASURING SYSTEM DESIGN OF ARROW'S IMPACT POINT

In this section, the problems of current used measuring system of arrow's impact point in real manufacturing

company are discussed. And also the solving problem by the proposed novel hardware structure and method of impact point using measuring data are showed.

A. Problems of impact point measuring system

Fig. 1 indicates structure of arrow. It consists of point, insert, shaft, crest line, fletching, and nock. It also can be divided into three parts, each part named arrowhead, shaft of arrow, and feathering. Arrowhead is usually made from stone or metal which is attached to the end, and its role is to penetrate targets substantially. Shaft of arrow is made from composite materials, generally produced in the form of aluminum core wrapping by carbon fiber. Traditionally, feathering is made from feathers. But in modern, it is made from plastic materials. It can prevent shaking of arrow, and also ensure stability of flight.

Due to advance manufacturing process and materials, it is possible to produce arrows which have not only good quality

but also good performance, and increased flight distance and accuracy. Both flight distance and precise accuracy are largely affected by characteristic variables of arrow, such as weight, external diameter, spine, straightness, angle and shape of feathering. According to these characteristic variables, the impact point and flight distance of arrow shows different. Hence, there are plenty of researches and experiments about impact point's density by attaching shooting sheets on target that find out relations between characteristic variable, impact point and flight distance. But in case of measuring arrow's impact points, commercialization of technologies and systems are lacking. And arrow manufacturing company focuses on patents and technologies that optimizing the characteristic variables that occurring in production process. That disproportionate development caused by difficulties of determining objective performance of produced arrow because there is no measuring and classifying system of arrow's impact points, also there are no data numerically represented. Analyzing technology of arrow's impact point density is still in the early stage, and there are only a few available measuring platforms using handwriting and high-speed camera. Handwriting process is shown in Fig. 2b. First, attach shooting sheet on rational distance from target. Second, shoot an arrow repeatedly changing angles of nock every time. Third, check impact points of arrow and measure how dense they are. If impact point of an arrow has high density, then the arrow is determined that it has good quality and performance. But analyzing impact point of arrow using handwriting, there are some disadvantages, such as; low accuracy, it should be replaced frequently and periodically, and it is hard to digitize between impact points. In case of high-speed camera, on the other hands, it can compare arrow's shape while flying to other arrows using obtained video or images, but it can only watch restricted view angles. And it is hard to digitize between impact points, like handwriting. Fig. 2a shows the

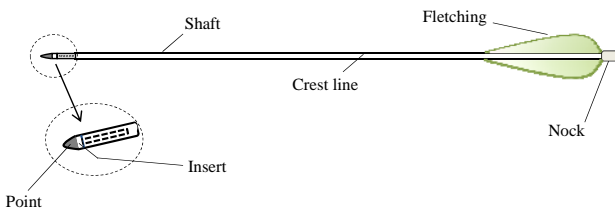
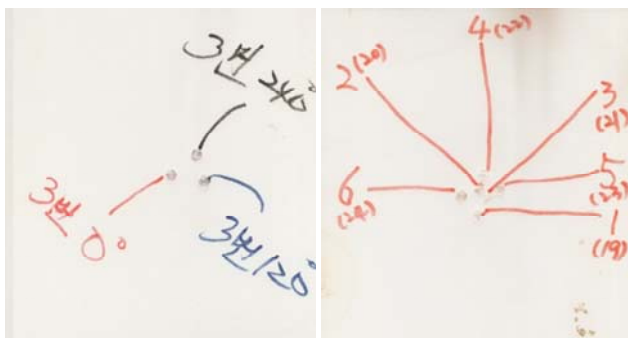


Figure 1. Structure of arrow



(a)



(b)

Figure 2. Arrow shooting environment and test sheet of impact point: (a) Arrow launch pad and shooting environment, (b) Analyzing density of arrow's impact points by handwriting.

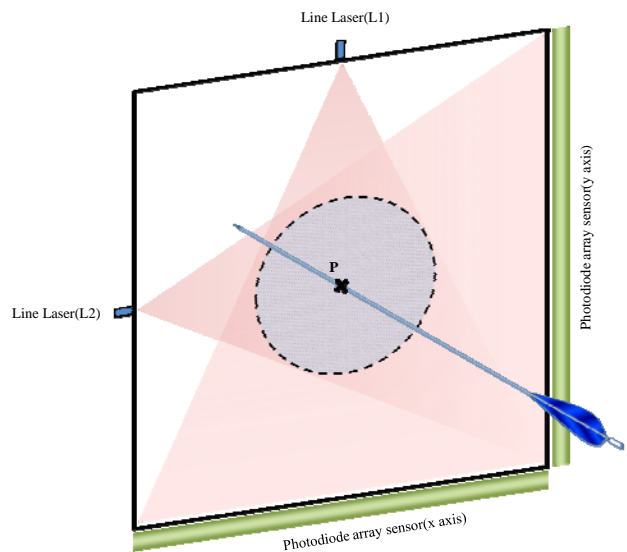


Figure 3. Single frame for measuring arrow's impact point.

pictures of launch pad and shooting experiment environment which are actually used in manufacturing industry. It is about 39 meters far from launch pad to target. And the launch pad can shoot arrow with the same force. Fig. 2b shows the pictures that currently used handwriting impact points of arrow result in manufacturing company.

B. Hardware design for detecting high speed moving object

In order to solve current system problem that using handwriting and high-speed camera, this paper suggests hardware design for measuring impact point using novel structure and sensors. Photodiode sensor is suitable for measuring position of arrow moving in high speed, and considering response sensitivity of photodiode, it is appropriate pair that red light line laser [5][6][7]. The photodiode has 5.6mm diameter, spectral sensitivity is 450~1050nm range. Power consumption of a line laser is 100mW, and the laser straightly emits red light laser with spread 60 degrees because of inner structure consists of small size mirror in the module. Since photodiode is converting device that converts light energy to electrical energy, so photodiode voltage level changes relying on light intensity of line laser. When arrow passes the experimental structure consists of photodiode and line laser, namely the frame, voltage level changes of photodiode can be measured. Based on the measured data, impact point of the arrow can be represented. As shown in Fig. 3, two line lasers installed in L1, L2 position at the single frame, 80 photodiodes on the substrate installed opposite position of line laser. Position of the line laser should be placed in the center of photodiode substrate. And position should be in the form of coordinates, so square-shaped frame is used. The length of one side is 65cm, and each side is exquisitely crafted in right angle.

An arrow has high flight speed, average 250km/h and maximum 300km/h. For obtaining one point of the high-speed arrow, sampling time should be about 5ms to 15ms.

For measuring and dealing with large amount of data, analog input module that have high sampling rate and cover lots of channels relying on number of photodiodes is needed. Therefore, this paper chooses DAQ device, produced by National Instruments, which has high sampling rate and can handling lots of input channels. In order to measure the data that is output from a number of photodiodes, 8:1 Multiplexers(74HC/HCT4051) are used, and the MUX is controlled 3 bit digital signal generated by NI 9401 module. Signals from MUX are connected 20 channels as input using NI 9205 analog input module. The NI 9205 analog input module has maximum 250kS/s on sampling rate, also has 32 analog input channels. 20 channels used in this paper, and 20kS/s for each channel. One channel of NI 9205 connected to output of MUX, and each MUX cover 8 photodiodes. NI cDAQ 9718 8-slot USB chassis performs not only synchronizing NI 9401 and NI 9205 module, but also sending analog signal that input analog signal from NI 9205 to Host PC. Trigger signal occurs when arrow is shot on launch pad then NI-9178 chassis take the signal as input, and acquiring data during 1 second. Due to obtain data for 1 second, the number of acquiring data from one photodiode is 2500. The acquired data is sent by computer bus connected slot or port from DAQ to Host PC. The computer bus performs communication interface between DAQ device and computer for transmitting and receiving commands and acquired data. Fig. 4 shows hardware design of suggested system that starts emitting red light line laser, causes changing voltage level of photodiode, DAQ measures the changes and finally sends the measured signal to Host PC.

C. Impact point expression using voltage level scale

In previous section, the explanation of devised structure for expressing impact point and measuring data generated by photodiode sensor using NI DAQ were described. As shown in Fig. 5, the flowchart present the entire processes from

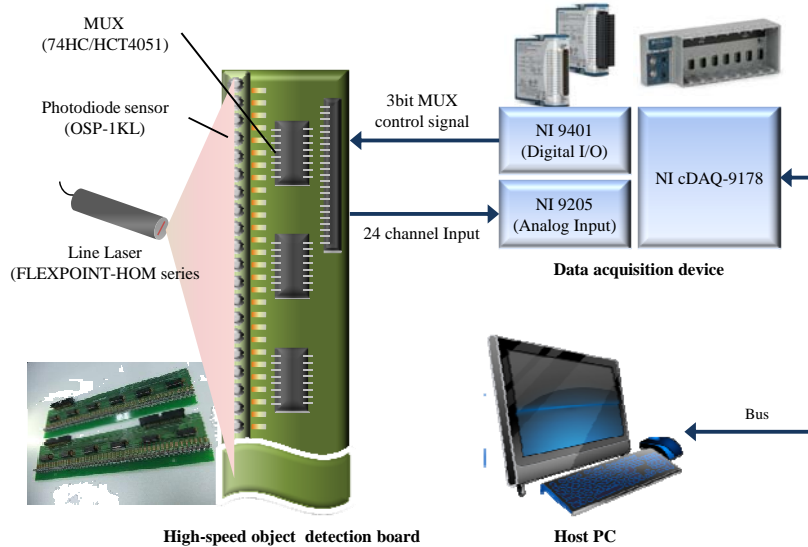


Figure 4. System design of measuring impact point.

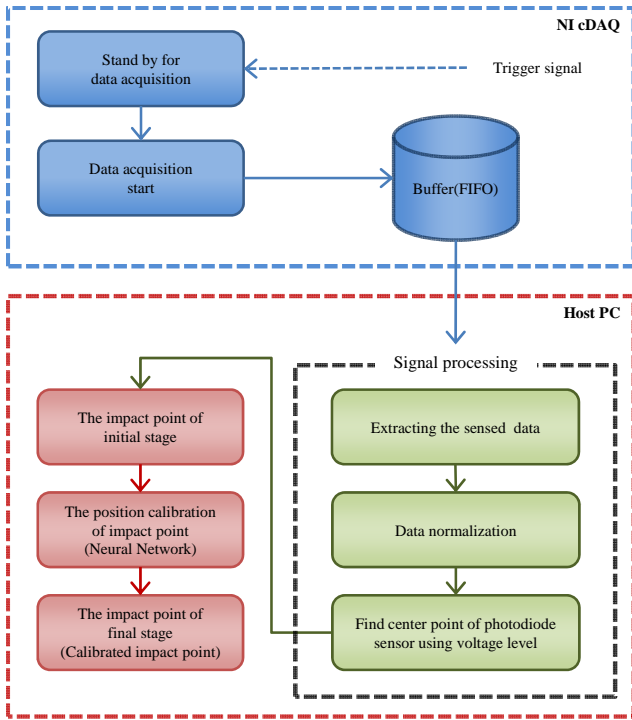


Figure 5. Overview system.

above the single photodiode, then output voltage is dropped at about 0.3V. At the moment of shooting arrow the trigger signal appeared. After the trigger signal, acquiring time begins during 1 second. Due to obtain data for 1 second, the number of acquiring data from one photodiode is 2500. The voltage dropping levels are slightly different each other because of photodiodes sensitivity. And because of line laser spreading angle, 60 degree as mentioned earlier, there are voltage level difference between photodiodes which located center position and photodiodes which located edge of the substrate. The center position of photodiodes has higher voltage level than the edge position ones. In order to make voltage level equivalent, min-max normalization method [8] is used. The extracted data is normalized in Host PC, the normalized data is used for obtaining center point of photodiodes that changing the voltage level because of shade of arrow, finally initial impact point is expressed including errors. Errors that occurring square-shape steel structure for measuring arrow's impact point are calibrated using NN.

If an arrow passes through single frame, shade occurs by the arrow in A, B region that part of photodiode array as shown in Fig. 6. Due to the shade by the arrow, voltage level of photodiode sensor drops. Using the voltage level of the photodiode and its index, center of photodiodes is derived. For finding center point of photodiode shaded by the arrow, equation of finding center of mass [9] is used, and it is represented in,

$$P = \frac{\sum_{i=\alpha}^{\beta} V_i K_i}{V_{total}}, \quad (1)$$

where, K indicates index of the photodiodes. V means dropped voltage level by the shade of arrow, and V_{total} is total dropping voltage level by the shade. The center point of photodiode which shaded by the arrow is shown in Fig. 6. Where M_x is center point of A region, and M_y is center point of B region. In other words, the intersection point of $\overline{L1M_x}$ and $\overline{L2M_y}$ is the impact point of the arrow, represented as Position(x,y).

III. CALIBRATION AND RESULT OF ARROW'S IMPACT POINT USING NEURAL NETWORK

The calibration algorithm for improving precision of measuring arrow's impact point using grid calibration plate is applied. The grid calibration plate has grid points that have 1cm interval each other and the plate attached on single frame. The measuring data before applying calibration algorithm using grid plate at the frame and each grid point that the position of arrow is shown in Fig. 7. In the figure, the measuring data before applying calibration algorithm shows gradually increasing tendency of error through center to edge of frame. Neural network method with back propagation learning is used as calibration algorithm. NNs are systems that are deliberately constructed to make use of some organizational principles resembling those of the human brain. A number of recent reviews have identified a

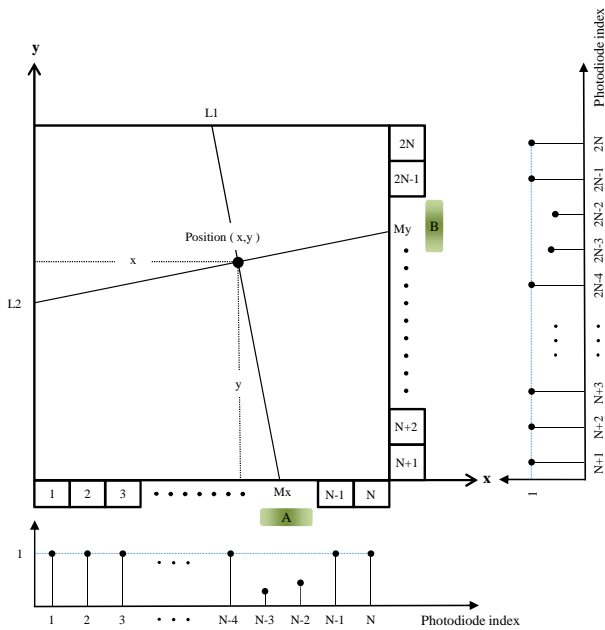


Figure 6. Impact point expression using voltage level scale.

sending measured data to Host PC using NI DAQ to expressing impact point through processing of the transferred signal. When line laser emits light to single photodiode sensor, output voltage of the photodiode is about 0.5V. On the other hands, if some object makes shadow by passing

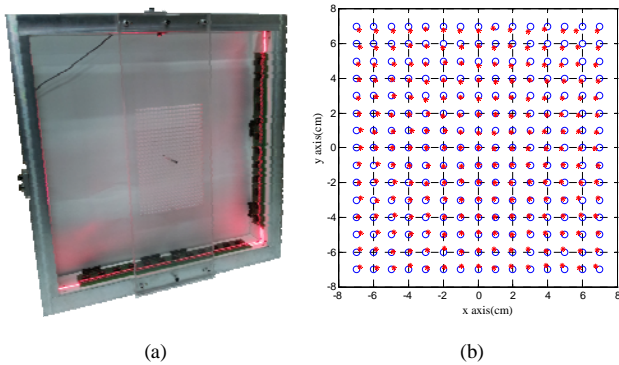


Figure 7. (a) Grid plate installed on the frame, (b) Measuring data of grid point before applying calibration algorithm.

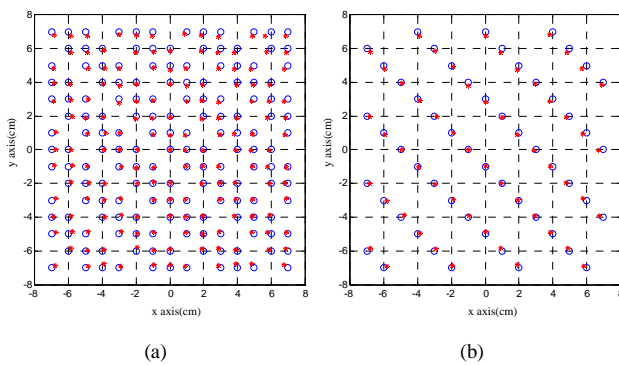


Figure 8. Split of learning: (a) Training data, (b) Test data.

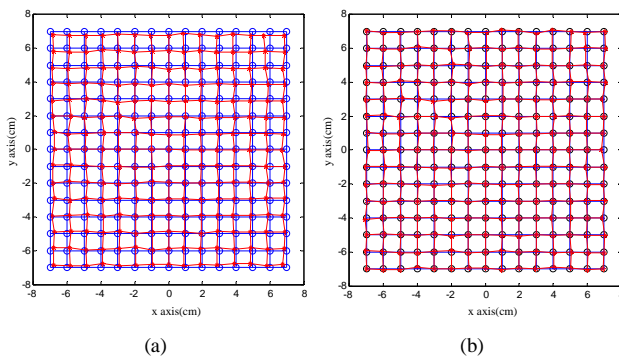


Figure 9. Result of calibrated data using NN: (a) Before calibration, (b) After calibration.

TABLE I. RESULT OF CALIBRATION ALGORITHM

	Training error	Test error
Before calibration	3.172mm	
After calibration	0.544mm	0.617mm

diverse range of adaptive system [10], process optimization [11], pattern matching and classification, function approximation, optimization, vector quantization, and data clustering [12]. Investigations have also been completed in various aspects of calibration and analysis of measurement errors [13][14][15]. The structure of NN is 2-6-2 feed-forward form, and uses Levenberg-marquardt algorithm, and its learning rate is 0.01. The activation function of hidden layer is tangent sigmoid function, and output layer's activation function is linear function. For learning NN, 225 data that measuring at grid plate are classified into 169 training data and 56 test data as shown in Fig. 8.

The result of grid point calibration using NN is shown in Fig. 9 and Table I. It can be found that error is fairly calibrated not only center of frame but edge of frame. And average error is also improved that comparing 3.17mm before calibration to 0.62mm after calibration result. For deriving error, MAE (Mean Absolute Error) method is defined by,

$$MAE = \frac{1}{n} \sum_{i=1}^n \left\| (\hat{x}_i, \hat{y}_i) - (x_i, y_i) \right\| = \frac{1}{n} \sum_{i=1}^n Error, \quad (2)$$

IV. CONCLUSION

This paper suggests that the novel structure can measure impact point of arrow, the sensor can detect high-speed moving object, and the system can represent impact point of the arrow using the voltage level change of photodiode sensor. In order to make measuring system, square-shaped steel frame is produced which length of one side is 65cm, and the photodiode sensor and line laser is attached at the frame. When an arrow passes the frame, NI 9205 device is acquiring voltage level changes of photodiode sensor at any points, and sending the data to Host PC through NI cDAQ-9178. Changing interval is extracted using the voltage level of photodiode sensor, and the impact point of arrow is represented by index and voltage drop size of the photodiode. But the represented impact point includes error due to structure of substrate that designed for detecting high-speed moving object and angle of light emitted by line laser. Therefore, the represented impact point is distorted at this moment. For solving this problem of impact point, calibration method is applied using NN. After calibration, average error is decreasing from 3.17mm to 0.62mm. Now, it can digitize among the impact points, also the result can be used as manufacturing variables that use for performance analyzing with other arrows and also making arrow. Our proposed measurements method is a reflection in the manufacturing process that classifying manufactured arrow characteristics, choosing appropriate arrow for user, and determining quality and performance objectively.

ACKNOWLEDGMENT

This work was supported by the National Research Foundation of Korea (NRF) grant funded by the Korea government (MEST) (No. 2012-0006889).

REFERENCES

- [1] J. W. Yu, H. S. Lee, Y. S. Jeong, and S. S. Kim, "Measuring system for impact point of arrow using mamdani fuzzy inference system," *Journal of Korea Institute of Intelligent systems*, vol. 22, pp. 521–526, August 2012.
- [2] Y. S. Jeong, J. W. Yu, H. S. Lee, and S. S. Kim, "Hardware Configuration and paradox measurement for the determination of arrow trajectory," *Journal of the Korean Society of Manufacturing Technology Engineers*, Vol. 21, pp. 459–464, 2012.
- [3] L. N. Smith, and M. L. Smith, "Automatic machine vision calibration using statistical and neural network method," *Image and Vision Computing*, vol. 23, pp. 887–899, 2005.
- [4] J. H. Lee, and C. W. Kim, "Robust camera calibration using neural network," *IEEE Tecon*, vol. 1, pp. 694–697, 1999.
- [5] J. Yu, and X. Wang, "Velocity and position measurement for projectile using double optical detectors and reflectors," *IEEE conference publications*, pp. 1–4, August 2009.
- [6] H. Kanbe, T. Kimura, and Y. Mizushima, "Silicon avalanche photodiodes with low multiplication noise and high-speed Response," *IEEE Transactions*, vol. ed-23, pp. 1337–1343, 1976.
- [7] S. T. Lu, C. Chou, M. C. Lee, and Y. P. Wu, "Electro-optical target system for position and speed measurement," *IEEE Proceedings A*, vol. 140, pp. 252–256, July 1993
- [8] L. T. Daniel, "Discovering knowledge in data: An introduction to data mining," *Wiley*, New York, 2004.
- [9] B. H. Tonque, and S. D. Sheppard, "Dynamics: Analysis and design of systems in motion," *inter vison*, 2005.
- [10] J. C. Principe, N. R. Euliano, and W. C. Lefebvre, "Neural and adaptive system: Fundamentals through simulations," *Wiley*, New York, 1999.
- [11] E. Westkamper, and T. Schmidt, "Computer-assited manufacturing process optimization with neural networks," *Journal of Intelligent Manufacturing*, vol. 9, pp. 289–294, October 1998.
- [12] Lin. C, and C. S. George, "Neural fuzzy systems : A neuro-fuzzy synergism to intelligent systems," *Prentice- hall*, 1996.
- [13] C. A. Chang, and C. Su, "A comparison of statistical regression and neural network methods in modeling measurement errors for computer vision inspection systems," *Computer ind*, vol. 28, pp. 593–603, 1995.
- [14] C. T. Su, C. A. Chang, and F. C. Tien, "Neural network for precies measurement in computer vision system," *Computers in Industry*, vol. 27, pp. 225–236, 1995.
- [15] L. W. Yu, and X. Kai, "A camera calibration method based on neural network optimized by genetic algorithm," *IEEE International*, pp. 2748–2753, October 2007.

Vision-based Cattle Detection and Localization System in an RGB Color Space

Detection and localization system for cattle shed management

Jieun Kim

Department of IT Convergence
Daegu Gyeongbuk Institute of Science and Technology
Daegu, Republic of Korea
intocosmos@dgist.ac.kr

Woo Young Jung

Department of IT Convergence
Daegu Gyeongbuk Institute of Science and Technology
Daegu, Republic of Korea
wyjung@dgist.ac.kr

Abstract— In this paper, we present an approach to automatic cattle detection and localization system from natural scenes. Cattle shed scene has complex background and various illumination. In this reason, the proposed approach includes object detection method in complex background using active tags and RGB color filtering. In addition, we proposed localization method using image data and RFID data. First, we narrow down the localization range using RFID data. Then, we estimate more accurately the object location using vision-based methods.

Keywords—animal localization; cattle shed surveillance system

I. INTRODUCTION

Robust object localization and object detection method have applications including gaming, security, defense and even medical service.

Recently, domestic stock farmers suffered from highly contagious livestock diseases, such as the Foot-and-mouth disease (FMD). These kind of contagious livestock diseases have often initial symptom of high temperature. For this reason, it is necessary to sense a temperature change of cattle in stock farms. Additionally, we are able to early detect and isolate a cow which has high temperature change through each object localization. This is important because isolation of an ill cattle prevents spread of the disease. Furthermore, we should isolate not only the sick cattle but also a group containing the sick cattle. Previous researches [1] of finding a group containing target object are less accurate in cattle shed. For this reason, we propose a vision-based cattle localization and detection system in stock farm. Our system performs vision-based ill cattle detection and localization, as shown in Fig. 1. Target stock farm is divided into multiple room. We called each room “cattle shed cell” and each cell has unique number as Fig. 1. Each cattle shed cell has one or two cows. Our system has one camera per each axis. Each camera can move horizontally on axis. We utilize the active tag [3] and Radio Frequency Identification (RFID) [4] information and camera images for assistance of object detection. Each active tag works along with temperature sensor. We put active tag and RFID on each cow’s body. In other words, each cow has an

active tag and a RFID chip. When it senses an increase in temperature that is above a given threshold, the tag light associated with the sensor lights up. We detect the active tag and estimate the object’s localization. Then, mobile cameras collect cattle’s image data using object position information.

Object localization and detection systems have two problems. Generally, vision-based object detection system has less accuracy on brightness change. As mentioned earlier, we propose active tag as technical assistance. It has merits and demerits. It helps the systems to achieve high accuracy by detection in dark environment, but it requires checking the batteries periodically. Second, it is difficult to estimate the object’s location in a natural scene by using vision-based methods.

Our localization method has two steps. We localize object cattle using RFID primarily. We narrow down the localization range using RFID location information. Then, we estimate the object’s location using vision-based method.

A common approach is a region-based method, which uses multiple feature or high complexity feature and Adaboost or neural network. [5],[6],[7]. This method needs a diverse training dataset and multi-features require large processing time. Also, the recently proposed camera-based real time mapping for Simultaneous Localization And Mapping (SLAM) [8],[9],[10] is not suitable for stock farm environment.

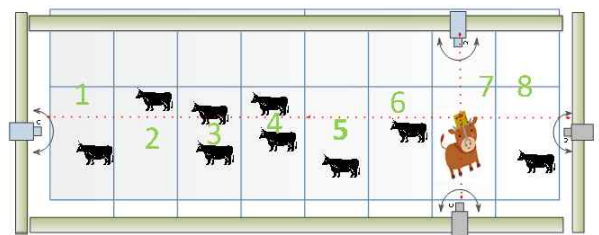


Figure 1. Vision-based ill cattle localization system

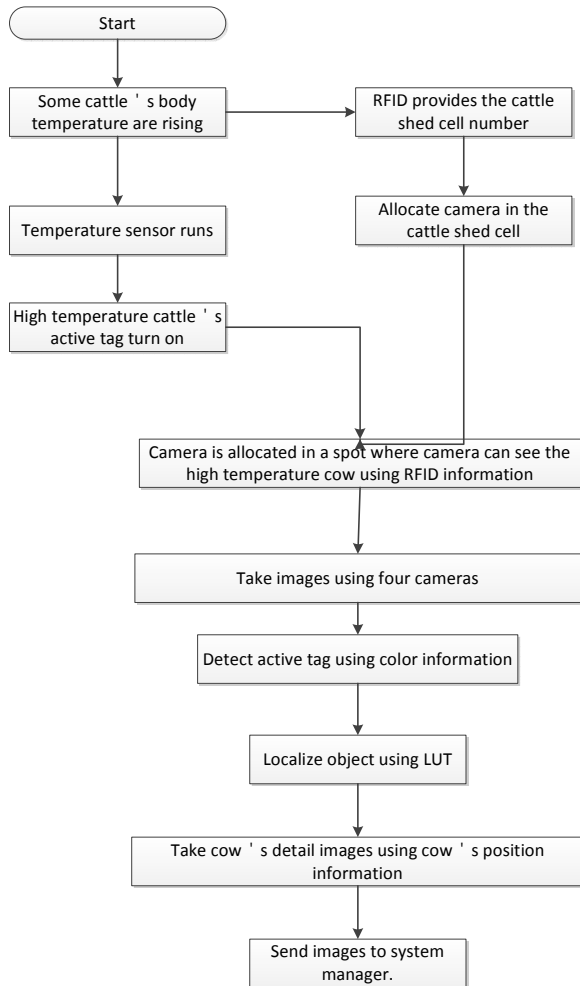


Figure 2. System Flow Chart

II. CATTLE DETECTION AND LOCALIZATION SYSTEM

In this section, we describe our system. We proposed ill cows detection and localization system in stock farms. Fig. 2 shows a system overview. This vision-based system works when the cattle's body temperature rises. If some cattle's temperature rises, the cattle's RFID provides the corresponding shed number. At the same time, the cattle's active tag turns on and four cameras convey the location of the targeted cow using the light Images are captured by these four cameras. An active tag has brighter and clearer color than general object. Accordingly, we detect active tags using color filtering. We make a localization map using color markers as Figs. 4(c), (d) and (e). Also, we estimate the active tag's position using matching LUT (Look-up table). LUTs are trained beforehand. We record the image of the affected cow using the estimated position. Finally, we send images to system administrator. These images are used for cattle shed management service.



Figure 3. Active tag sample

A. Cattle detection in RGB color space

Real datasets in cattle shed have more problems than indoor images. These images are more sensitive to lighting variation. In order to solve the problem, we propose active tags that provide illumination invariant color information. Our active tag is made of LEDs, as shown in Fig. 3. Each cow has one active tag, and each active tag turns on when the cow has high temperature.

Our active tag gives out a red light. Using this simple fact, we perform normalized color filtering to detect active tag. R-band pass filter has high weight.

B. Processing region define method and object localization using color marker and RFID information

A common approach is vision-based probabilistic model [11]. Natural scene includes various color and illumination. For this reason, it is difficult to perform object localization in wide natural scene. In order to solve the problem, we defined processing region using RFID information and color marker as shown in Figs.4 (b). Fig. 4.(d) and (e) show color marker examples. The marker is placed at one meter interval. We make color marker-based localization map as shown in Fig.4 (c). We have absolute position of four cameras. Thus, we estimate active tag position using LUT.

LUTs are trained beforehand using k-means clustering and Euclidean distance. We perform the training using 640 images. In order to overcome various illumination in cattle shed images, these images have two types brightness, such as 0.15klux, 0.3klux.

III. EXPERIMENT RESULT

We have tested our system on real datasets and test datasets. Real datasets are captured at the target cattle shed as shown in Fig. 4 (a), and test datasets take our indoor test-bed as shown in Fig. 5. These images are captured in jpeg RGB colored form in the size of 1600*1200 pixels. The indoor test-bed size is 4 meters * 6meters. We used Intel Xeon 3.2GHz, 16G RAM, Win7, Visual Studio C++ 2008 in all of our computations. Fig. 6 shows the system's GUI.

The test-bed has 1 meter x 1 meter grid, as shown in Fig. 5. Each grid component has unique number. We evaluate the localization system using the grid.

In our research, the performance of object detection is 79.16%. Localization performance is 71.52%. The main reasons of errors are comprised of two categories, as follows.

- Images have various illuminations. Because part of test images is a natural scene, the images have shadows spots and sunny spots. A sunny spot is so much brighter than an active tag. It is difficult to detect an active tag in sunny spots.

- Camera's position and PTZ (Pan, Tilt, Zoom) have errors because four cameras are mobile cameras. To solve this matter, we need to perform camera calibration. Camera calibration reduces error rate, but camera calibration method requires a considerable processing time.

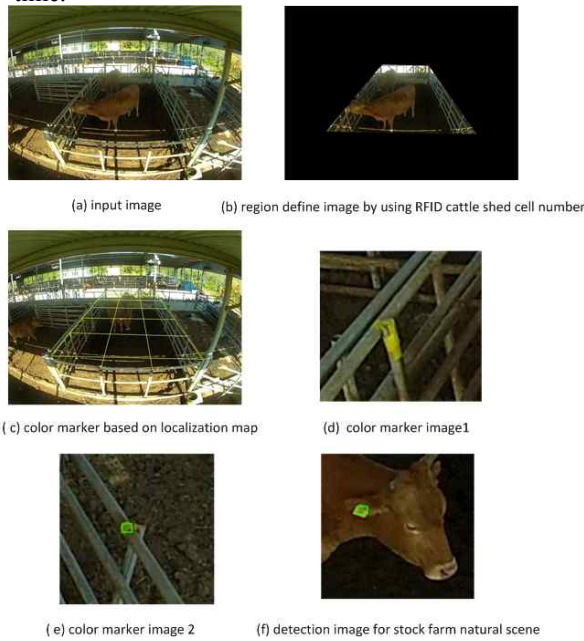


Figure 4. Experiment result in real cattle shed dataset



Figure 5. Indoor Testbed

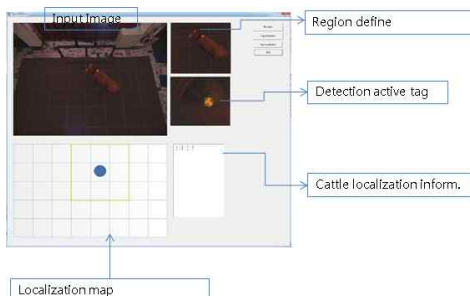


Figure 6. System GUI

IV. DISCUSSION AND FUTURE WORK

In this paper, we proposed object detection and localization in cattle shed. Cattle shed images has complex background and a variety of illumination changes. In illumination changes, the color active tag-based method is used for detection. In addition, our localization method is attractive. The proposed localization method has two steps. First, we estimate rough location using RFID. Then, we localize object using vision-based method. We have tested our approach on a number of real datasets, demonstrated its good capabilities of cattle shed area.

Object detection is difficult in cattle shed because cattle shed images have a lot of image noise. Our future work involves color filtering method and image segmentation method to solve illumination and complex background problem. Also, we need to solve the camera calibration problem. We will continue developing our detection and localization algorithm.

ACKNOWLEDGEMENT

This research was financially supported by the Ministry of Knowledge Economy (MKE), Korea Institute for Advancement of Technology (KIAT) through the Inter-ER Cooperation Projects. No. R0000577

REFERENCES

- [1] M. D. Fresno, "Application of Color Image Segmentation to Estrus Detection". Journal of Visualization, vol.9, no. 2, 2006, pp. 171-178
- [2] D. T. Booth, "Image-based monitoring to measure ecological change in rangeland". Front. Ecol. Environ. vol.6, 2008, pp. 185-190
- [3] M. Sakata, "ALTAIR: automatic location tracking system using active IR-tag". IEEE Conf. Multisensor Fusion and Integration for Intelligent systems, 2003, pp. 299-304
- [4] J. Landt, "The history of RFID". Potentials, IEEE, vol. 24, no. 4, 2005, pp. 8-11
- [5] H. Takahashi. "Region graph based text extraction from outdoor images". In Proc. Third Int'l Conf. Information Technology and Applications (ICITA'05), 2005, pp. 680-685.
- [6] H. Takatsuka, M. Tanaka, and M. Okutomi. "Distribution-based face detection using calibrated boosted cascade classifier". In Proc. 14th Int'l Conf. Image Analysis and Processing (ICIAP'07), 2007, pp. 351-356.
- [7] S. M. Hanif and L. Prevost. "Text Detection and Localization in Complex Scene Images using Constrained AdaBoost Algorithm". ICDAR, 2009, pp.1-5.
- [8] M. Agrawal and K. Konolige "Real-time localization in outdoor environments using stereo vision and inexpensive GPS". Proc. Intl. Conf. Pattern Recog. (ICPR), 2006, pp.1063-1068.
- [9] M. Dissanayake , P. Newman , S. Clark , H. Durrant-Whyte, and M. Csorba "A solution to the simultaneous localization and map building (SLAM) problem". IEEE Trans. Robot. Autom., vol. 17, no. 3, 2001, pp. 229 -241.
- [10] A. Davison "Real-time simultaneous localisation and mapping with a single camera". Proc. Int. Conf. Comput. Vis. (ICCV), 2003, pp. 1403 -1410.
- [11] B.Krose, R. Bunschoten, "Probabilistic localization by appearance models and active vision". Proc. In. conf. Robot. 1999, pp. 2255-2260

Evaluation of Machine Learning Methods in a Rain Detection System for Partial Discharge Data Analysis

Leandro H. S. Silva, Sergio C. Oliveira
 Polytechnic School of Pernambuco
 University of Pernambuco
 Recife - PE, Brazil
 {lhss, scampello}@ecomp.poli.br

Eduardo Fontana
 Department of Electronic and Systems
 Federal University of Pernambuco
 Recife-PE, Brazil
 fontana@ufpe.br

Abstract — Partial discharges (PD) on high voltage insulator surfaces are directly related with the deposition of pollution over the insulators. A complete partial discharge sensor network was previously developed and has been in operation for approximately three years. This system records the PD activity classifying it into four levels. As the PD activity is influenced by the weather conditions the sensor network measures the one hour average temperature and relative humidity. Also a fuzzy inference system was developed to extract the flashover occurrence risk level based on the partial discharge activity recorded. However, a strong rain event can wash the insulators strings almost instantaneously decreasing the risk level. To a correct result interpretation it is important to properly analyze the weather data to detect the rain occurrence. This paper presents a comparison among three approaches for rain detection from humidity and temperature data. The three approaches, Naïve Bayes Classifier, Support Vector Machines and Multilayer Perceptron Neural Network are trained on data gathered by meteorological stations located nearby the PD sensors and used in conjunction with the data obtained by those. Promising preliminary results are presented.

Keywords; *Partial discharges; rain detection; pattern recognition; leakage current; insulators.*

I. INTRODUCTION

The high voltage transmission lines are affected by many problems. One of them is the pollution accumulated over the insulators strings. When combined with high relative humidity the pollution layer becomes a conductive layer. A leakage current flows by this conductive layer causing irregular heating and then humidity evaporation, creating thin dry bands. The increase of electric charges in dry bands borders combined with the high electric field causes partial discharges near these dry bands [1]. The partial discharges phenomenon increases its rate and intensity until a complete discharge, known as flashover, bypassing all insulators causes a failure on the transmission line [2].

One way to avoid the flashover is by removing the pollution layer deposited over the insulator string by washing. However, this is a high cost operation and failures may occur during the procedure.

Aiming to assist the decision regarding the need for maintenance of the insulator string, a sensor network was previously developed to detect and classify partial discharges

according to their frequency of occurrence and intensity [3]. This system comprises an optical sensor coupled to an optical fiber, which transmits the leakage current [4] signal to an electronic processing module, which has also a temperature and a humidity sensor [5]. The collected data are transmitted via satellite and stored in a database.

A fuzzy inference system has been developed in order to extract the flashover risk occurrence. The risk level is incremented and decremented according to the level of partial discharge activity considering its intrinsic relation with relative humidity [6]. The use of a fuzzy system has the advantage of being able to represent uncertainties of natural language, such as, for example, “the insulator string is slightly polluted”.

However, on strong rain events the insulator string is washed ceasing the flashover risk after it. This almost instantaneous risk variation is not reflected on the fuzzy sequential decrement risk level. This work aims to develop a system capable of detecting the instantaneous cleaning of the insulator by strong rains, based on the available humidity and temperature data. The rain detection will make the fuzzy risk classification system more precise and turn the maintenance schedule more robust, reducing costs due to unnecessary washes.

Common electronic rain sensors are only capable of detecting rain in a small surface and are not capable of quantifying the event [7]. Electromechanical rain sensors are capable of easily detecting and quantifying rain. Nevertheless, when installed in outdoor environments this kind of sensor accumulates water, in turn attracting infestation by wasps or bees. The presence of these insects increases the risk for operators of the power transmission company and increases the failure rate of the rain sensor itself once the hives might block the mechanical parts of the sensor.

Temperature and humidity data gathered by the sensor network exhibits a daily regular pattern. This pattern is changed by rain events and a new rain pattern starts to occur. So, a pattern recognition system can be applied to detect the insulator washing by rain. A pattern recognition prototype system was developed based on the reliable data obtained from the Brazilian Institute of Meteorology, INMET, database. This database has humidity and temperature information as also the amount of rain precipitation per hour.

This paper compares three approaches for the rain detection system proposed: Naïve Bayes Classifier, Support Vector Machine (SVM) and Multilayer Perceptron Neural Network (MLP). After this analysis, the MLP was applied in a data set gathered by the partial discharge sensor network and visual inspections were realized to ensure empirically the rain detection success.

The following sections are organized as: Section 2 describes the satellite sensor system network; Section 3 describes the used data sets and the rain pattern; Section 4 discuss the concepts of each approach for rain detection; Section 5 describes the methodology used in this work; Section 6 presents the results and finally, the conclusions and final considerations are in Section 7.

II. SATELLITE SENSOR SYSTEM NETWORK

The satellite network is composed by six nodes operating and it has been in operation for three years in the Northeast region of Brazil. Each node is composed by an optical sensor, an electronic processing module and a satellite transmission modem [3], as illustrated in Fig. 1.

Each hour the sensor node transmits the partial discharges activities, average temperature and average humidity. The partial discharge activity is classified into four current ranges named N1 to N4, which are related to current pulses larger than 5, 10, 20 and 40 mA, respectively [3].

The information gathered by each sensor is organized into two 64-bit packets and transmitted via satellite each half hour. After reception the data are stored in a database. The access to this database is provided by the ADECI (from their initials in Portuguese – Electric Performance Evaluation on Insulator Strings) system. Only identified employees of CHESF (the generation and distribution company in the Northeast region of Brazil) can access the information.

III. DATA SETS AND RAIN PATTERN

The temperature and humidity have an almost regular daily behavior. During the day, the temperature is high and the humidity is low; at night the temperature falls down and the humidity goes up. During rain events this behavior is modified because the rain causes an immediate increase in humidity and decrease in temperature. This behavior can be seen in Fig. 2 – at rain events the temperature falls down and the humidity goes up. This behavior is better observed in heavy rain events than in light rains.

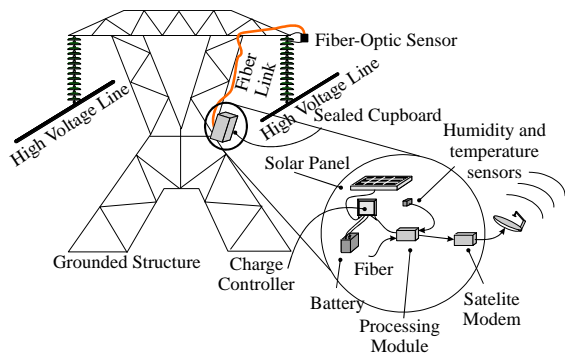


Figure 1. Sensor node for partial discharge monitoring.

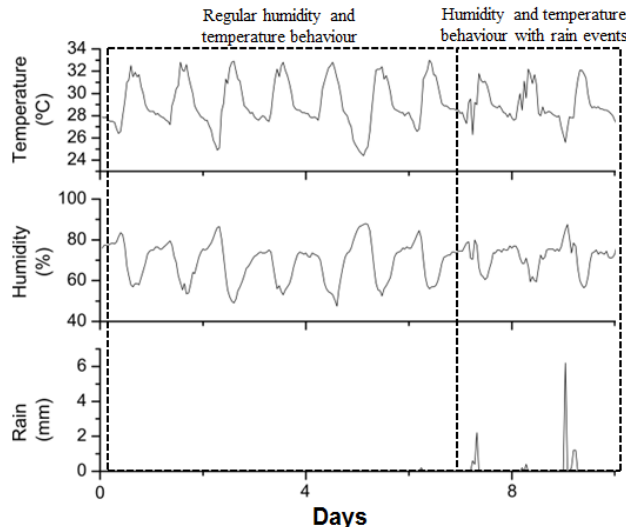


Figure 2. Plots of temperature and humidity patterns.

The INMET meteorological stations data contain average temperature and humidity as also the amount of rain precipitation in millimeters per hour. Linear interpolations were used to complete the series on every data missing less than 5 hours. When the time period of the missing data was larger than 5 hours, data for the full day were excluded from the database.

The INMET database was used to train each detection rain model for further use on ADECI bases. Fig. 3 shows the sensor network topology and each node of the nearest INMET meteorological station. Although each sensor node has a near INMET station, the distance between them is about tens of kilometers and a rain in the INMET station does not imply a rain in the nearest ADECI sensor location.

The data set was organized on day-long vectors as show in Table I. T0 to T23 represents the temperatures for the 24 hours as well as U0 to U23 represent humidity values. If the day has a total rain precipitation larger than 1 mm, the day is classified as rainy. Otherwise it is classified as no rain.

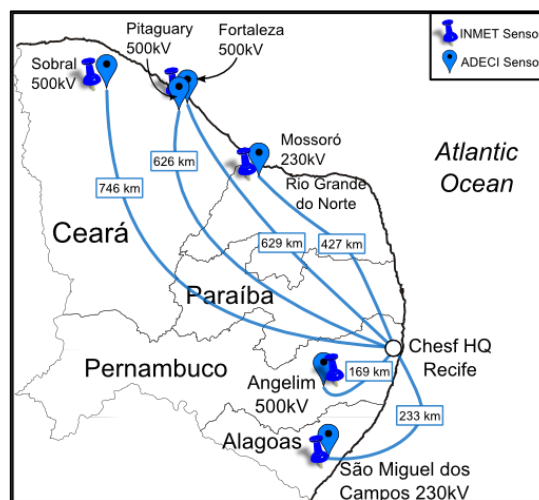


Figure 3. Sensor node and INMET station location.

TABLE I. DATA SET ATTRIBUTES AND CLASS.

Attributes						Class
T0	...	T23	U0	...	U23	[rain / no rain]

IV. APPLIED TECHNIQUES

A. Naïve Bayes Classifier

A Naïve Bayes Classifier [8] is a supervised-learning statistical technique. A vector x represents m features (x_1, x_2, \dots, x_m) , in this work, each dimension of vector x comprehends an attribute of the database. The a posteriori probability of having rained in a specified day can be calculated using Bayes theorem as

$$P(rain|x) = \frac{P(rain)P(x|rain)}{P(x)}. \tag{1}$$

In (1), $P(x)$ is the probability of x occurring in the data set and $P(x|rain)$ is the likelihood probability of x occurring in the “rain” class.

By using the naïve assumption, i.e. the attributes are conditionally independent, the likelihood probably of $P(x|rain)$ is

$$P(x|rain) = \prod_{i=1}^m P(x_i|rain). \tag{2}$$

It means that under the naïve assumption, the conditional distribution over the “rain” class can be expressed as

$$P(rain|x) = \frac{1}{Z} P(rain) \prod_{i=1}^m P(x_i|rain), \tag{3}$$

where Z , the evidence, is a scaling factor dependent only on the features of the x vector.

All the Naïve Bayes Classifier parameters (the class prior and feature probability distributions) can be approximated with relative frequencies from the training set. In this work the continuous values associated with each class were considered to have a Gaussian distribution.

B. Multilayer Perceptron Neural Network

The MLP [9] is an artificial neural network whose architecture is based on multiple layers of neurons: an input layer, one or more hidden layers and an output layer. The number of hidden layers can be changed depending on the application.

Each neuron can be seen as an element with inputs, weights, one activation function and the output signal. The output signal of each neuron is given by

$$y_j = f \left(\sum_{i=1}^n x_{ji} w_{ji} \right), \tag{4}$$

where, y_j is the output signal of the j neuron, x_{ji} is the i th entry of the j neuron, w_{ji} is the i th weight of the j neuron and f is the activation function. In this work the sigmoid function was used as activation function [9]. The signal is propagated from the input layer to the output layer – where the classifier result is available.

The training of a MLP consists on the weights adjusts. The objective is to train the MLP network to achieve a balance between the ability to respond correctly to the input patterns used for training and the ability to provide good results for other similar inputs, i.e. train the network to be capable of performing generalization. For this task, the classic backpropagation algorithm was used to realize the training of the neural network [9].

C. Support Vector Machine

The SVM [10] is a statistically robust learning method in which the training process consists into finding an optimal hyperplane which maximizes the margin between two classes of data in the kernel induced feature space.

Given an input data of n samples $x_i (i = 1, \dots, n)$ classified into two classes. Each one of the classes associated with labels are $y_i = +1$ for the positive class (rain) and $y_i = -1$ for the negative class (no rain), respectively. For linear data, it is possible to determine the hyperplane

$$f(x) = xw + b = 0, \tag{5}$$

where w an M -dimensional vector and b is a scalar. This separating hyperplane should satisfy the constraints

$$\begin{aligned} x_i w + b &\geq 1, \text{ if } y_i = +1 \\ x_i w + b &\leq -1, \text{ if } y_i = -1 \end{aligned} \tag{6}$$

Furthermore, as the SVM searches for an optimal hyperplane, the margin width between the support vectors and the optimum hyperplane must be maximized, as showed in Fig. 5. The margin is calculated as

$$2 \cdot d = \frac{2}{\|w\|}, \tag{7}$$

so $\|w\|$ must be minimized.

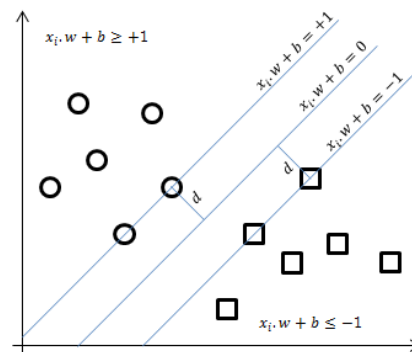


Figure 4. Support Vectors and separating hyperplane.

There is also the introduction of positive slack variables ξ_i , to measure the distance between the margin and the vectors x_i , which means that some mistakes can be tolerated. The optimal hyperplane separating the data can be obtained by solving the optimization problem

$$\min \frac{1}{2} \|w\|^2 + C \sum_{i=1}^M \xi_i, \tag{8}$$

subject to

$$y_i(x_i \cdot w + b) - 1 + \xi_i \geq 0 \tag{9}$$

The constraints aim to put the instances with positive label at one side of the margin of the hyperplane, and the ones with negative labels at the other side. C is the cost parameter, with is a positive constant specified by the user.

The optimization problem of the SVM is usually solved by introducing the Lagrangian multipliers α_i , transforming the problem on the dual quadratic optimization.

SVM can also be used to classify nonlinear problems. By using a nonlinear mapping function, called Kernel function, the original data are mapped into a high-dimensional feature space, where the linear classification is possible. There are different Kernel functions used in SVMs, such as linear, polynomial, sigmoidal and Gaussian RBF. The selection of the better Kernel function is very important, since this function will define the feature space in which the training set examples will be classified [10].

V. METHODOLOGY

A. Experiments to setup parameters

At first, some experimental arrangements were made in order to evaluate the best set up parameter for the ANN MLP and for the SVM.

For the used ANN MLP the numbers of hidden layers were limited in two. The tested topologies are showed in the Table II. There are two MLP output neurons, one indicates the “rain” class and the other indicates the “no rain” class. The validation set, necessary to avoid overfit was generated by selecting randomly 30% of the normalized complete data set.

TABLE II. EXPERIMENTAL ARRANGEMENT FOR MLP.

Neuron quantity	
First hidden layer	Second hidden layer
10	0
20	0
30	0
40	0
5	5
10	10
20	20
30	30

For the SVM, four kernel functions were tested: radial basis, linear, sigmoid and polynomial. For each kernel

function the C parameter assumed respectively 1, 5, 10 and 30. The ϵ parameter was fixed in 0.001. And for the Naïve Bayes Classifier a gaussian distribution function was assumed.

The test method for all experiments was the stratified cross-validation 5-fold. For the MLP the experiment was repeated twenty times. One INMET database (near São Miguel dos Campos) was used to evaluate the best setup parameter for the techniques.

The metrics used to compare the three techniques are the TP (True Positive) rate and the F-Measure. The F-Measure is an accuracy evaluation which considers the precision generating an overall score about the classifier. For this application, the TP of no-rain class is a very important measure, and this rate must be maximized. A false positive for the rain class will cause a decrease of the risk level of a flashover and the prediction system can miss the flashover event because of this false positive rain detection.

B. Experiments to evaluate the training applied in other data bases

With the best setup parameters, all three techniques were trained with the data from São Miguel dos Campos INMET station and the trained models were applied in all others INMET stations.

The main objective was to evaluate if a training realized on one station could be applied to another one. The geographic limits of the training and the influence of the climate were also investigated.

C. Results on ADECI data

The trained models were applied on ADECI databases aiming to verify if the rain detection was satisfactorily.

The analysis of these experiments could not be measured in mathematical ways because the ADECI data does not include the rain information. Instead careful visual inspections were made to identify the temperature and humidity behavior changes in order to qualitatively verify the results obtained.

VI. RESULTS

A. Evaluation of setup parameters

Table III presents the results for the Naïve Bayes Classifier. There are no parameters to adjust on this classifier.

The Naïve Bayes Classifier achieve TP rate over 0.5 for both classes. However, the FP (false positive) rate of the “no-rain” class is still high for the application (the FP for the “no rain” class is 0.227). The high result of FP “no rain” is a bad issue as it can lead to unnecessary maintenance action for insulators wash.

Table IV presents the results for all ANN MLP topologies experimented.

TABLE III. EXPERIMENTAL ARRANGEMENT FOR NAÏVE BAYES CLASSIFIER.

TP rate “rain”	TP rate “no-rain”	F-Measure “rain” class
0.807	0.798	0.746

TABLE IV. RESULTS FOR ANN MLP.

Topology (as in Table II)	TP rate "rain" class	TP rate "no-rain" class	F-Measure "rain" class
10, 0	0.802 (0.047)	0.873 (0.020)	0.790 (0.016)
20, 0	0.793 (0.049)	0.877 (0.022)	0.788 (0.016)
30, 0	0.784 (0.049)	0.878 (0.021)	0.783 (0.016)
40, 0	0.784 (0.049)	0.878 (0.021)	0.783 (0.016)
5, 5	0.810 (0.050)	0.866 (0.025)	0.791 (0.016)
10, 10	0.810 (0.051)	0.869 (0.024)	0.792 (0.017)
20, 20	0.814 (0.049)	0.867 (0.022)	0.793 (0.016)
30,30	0.812 (0.051)	0.867 (0.022)	0.793 (0.018)

In order to choose the best topology for the ANN MLP, statistical tests were made. With the Shapiro Wilk test, all samples follow the normal distribution, and with the F test, all samples have the same variance. So, the T-Student test was applied to evaluate the best topology with statistical significance. The result of the T-Student test proves that there is no statistical difference between the topologies. So, the topology with fewer neurons in one layer was chosen. As shown in the highlighted cells in Table IV the results of the ANN MLP were better than those of the Naïve Bayes Classifier.

Table V presents the results for the SVM. In this table, only the best results for each kernel function are presented.

As the SVM classifier presents a unique solution, the set of parameters that resulted on the highest F-Measure was chosen (Radial Basis kernel function and C equals 10.0).

The results obtained with training and execution of the classifiers within the same database shows that the rain pattern recognition is possible.

TABLE V. RESULTS FOR SVM.

Kernel Function	C	TP rate "rain"	TP rate "no-rain"	F-Measure "rain"
Linear	1	0.758	0.896	0.781
	5	0.754	0.880	0.767
	10	0.754	0.880	0.767
Polynomial (3 degree)	1	0.256	0.973	0.393
	5	0.575	0.929	0.676
	10	0.643	0.916	0.717
Radial Basis	1	0.720	0.910	0.766
	5	0.749	0.889	0.777
	10	0.758	0.902	0.785
Sigmoidal	1	0.671	0.921	0.741
	5	0.744	0.905	0.778
	10	0.754	0.905	0.784

B. Evaluation of trainig applied in other databases

Each classifier was trained with the data from the São Miguel dos Campos INMET station and applied in all others INMET stations. The parameter set used for the ANN MLP and for the SVM were the ones chosen in the previous section. The results for the Naïve Bayes Classifier, ANN

MLP and SVM methods are presented on Tables VI, VII and VIII, respectively.

TABLE VI. NAÏVE BAYES CLASSIFIER TRAINED WITH SÃO MIGUEL DOS CAMPOS INMET STATION.

Data Base used for Evaluation (INMET station)	Naive Bayes Classifier		
	TP rate "rain" class	TP rate "no-rain" class	F-Measure "rain" class
Sobral	0.585	0.720	0.385
Fortaleza	0.033	1.00	0.065
Mossoró	0.203	0.989	0.316
Angelim	0.995	0.060	0.522

TABLE VII. ANN MLP TRAINED WITH SÃO MIGUEL DOS CAMPOS INMET STATION.

Data Base used for Evaluation (INMET station)	ANN MLP		
	TP rate "rain" class	TP rate "no-rain" class	F-Measure "rain" class
Sobral	0.830 (0.041)	0.895 (0.020)	0.823 (0.024)
Fortaleza	0.856 (0.058)	0.887 (0.027)	0.832 (0.025)
Mossoró	0.842 (0.045)	0.883 (0.023)	0.821 (0.014)
Angelim	0.835 (0.043)	0.887 (0.020)	0.820 (0.016)

TABLE VIII. SVM TRAINED WITH SÃO MIGUEL DOS CAMPOS INMET STATION.

Data Base used for Evaluation (INMET station)	SVM		
	TP rate "rain" class	TP rate "no-rain" class	F-Measure "rain" class
Sobral	0.585	0.880	0.523
Fortaleza	0.366	0.981	0.506
Mossoró	0.270	1.000	0.423
Angelim	0.967	0.599	0.705

The Naïve Bayes Classifier presented unstable results. In the Fortaleza INMET station, only 3.3% of the examples of the "rain" class were correctly classified. But in the Angelim INMET station, the result was the opposite: only 6.0% of the "no-rain" class was classified correctly. A possible reason for this is the climate difference between these stations. Fortaleza has a tropical climate, with average temperature over 25°C and there is almost no rain in the second semester of the year. Angelim is a mountain region with a mesothermal climate and average temperature of 20°C. This is a strong clue that this classifier is sensible to climate differences.

The SVM presented a result similar to the Naïve Bayes Classifier; however, the result of SVM was better than the previous one. But the result analysis for the SVM indicates that this classifier is also sensible to climate differences. In fact, these results mean that the used kernel function is

sensitive to the climate difference, i.e, the kernel was not able to provide a linear separation between the ‘rain’ and ‘no-rain’ class with the gathered data in all stations.

The ANN MLP was able to identify more assertively the pattern of rainfall in all other databases. This means that the power of generalization of this classifier acted more efficiently.

Comparing the three classifiers, the ANN MLP presented better results. The selected INMET stations are located in different climates. It implies differences on the mean values of temperature and humidity between the databases. This difference affects the Naïve Bayes Classifier, since the means and standard deviations (parameters of the Gaussian distribution) in the training can be very different in test dataset. This same influence affects the SVM, since this technique finds a unique hyperplane solution which separate booth classes, and the power of generalization depends on the parameter. Some variation experiments need to be done in order to evaluate the SVM. The ANN MLP also finds a hyperplane solution which separates booth classes. The solution might not be the optimum, but in this case it presented the higher generalization power.

C. Evaluation on ADECI data

The ADECI data does not include the information about the amount of rain, so, a visual analysis was made in order to verify results. Once the MLP presents better results only this strategy was applied on ADECI databases.

Fig. 5 shows the result of the ANN MLP trained with the data from São Miguel dos Campos INMET station and

applied in the São Miguel dos Campos ADECI station. The result of the ANN MLP is a binary neuron indicating class “rain” (one) and “no rain” (zero). As can be seen in Fig. 5, the rain pattern was successfully recognized in some data subsets. The visual analysis of the rain pattern matches with the previous patterns in Fig. 2.

There are some possible rain events not successfully recognized. These events are marked in Fig. 5. But, for every rain detected the visual analysis of temperature and humidity suggests a rain event.

If a rain is not properly detected, as showed on highlighted areas of Fig. 5, the risk level will not be reset. If the risk level before the rain event was high enough to require a schedule maintenance, this maintenance will happen, even with the insulator rain wash, causing an unnecessary spending by the electric company. But some rain events were detected, and in these cases the maintenance schedule could be reprogrammed with this new information. It is not possible to quantify the rain detection efficiency but visually it is possible to verify that approximately 66% of rain events in Fig. 5 were properly detected.

Furthermore, during a rain event, naturally there is an increase in the activity rate, mainly N1 as can be seen in the last rain detection, marked in Fig. 5. This activity increase causes an increment in the risk level leading to wrong interpretations. With the proper rain detection, the activity increase can be related to the rain event and the risk level is not increased.

Fig. 6 shows the result of the same ANN MLP applied in the Mossoró ADECI station.

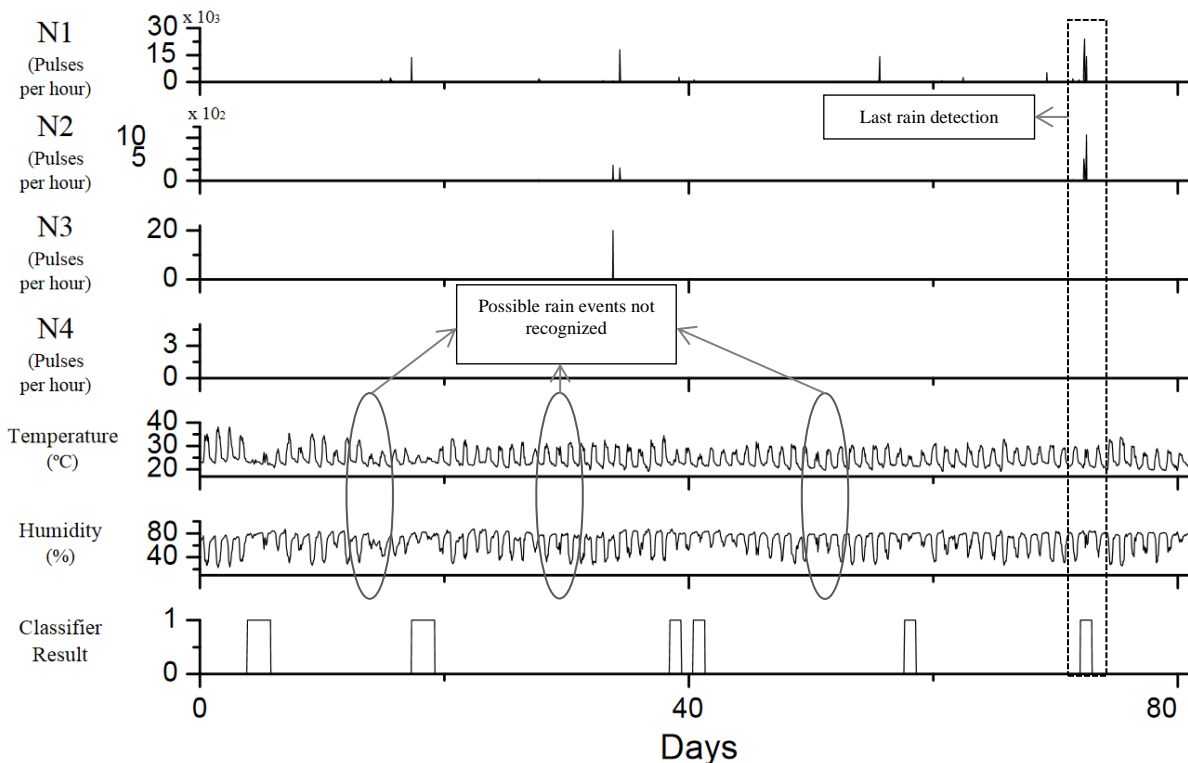


Figure 5. Application of ANN MLP in São Miguel dos Campos ADECI station.

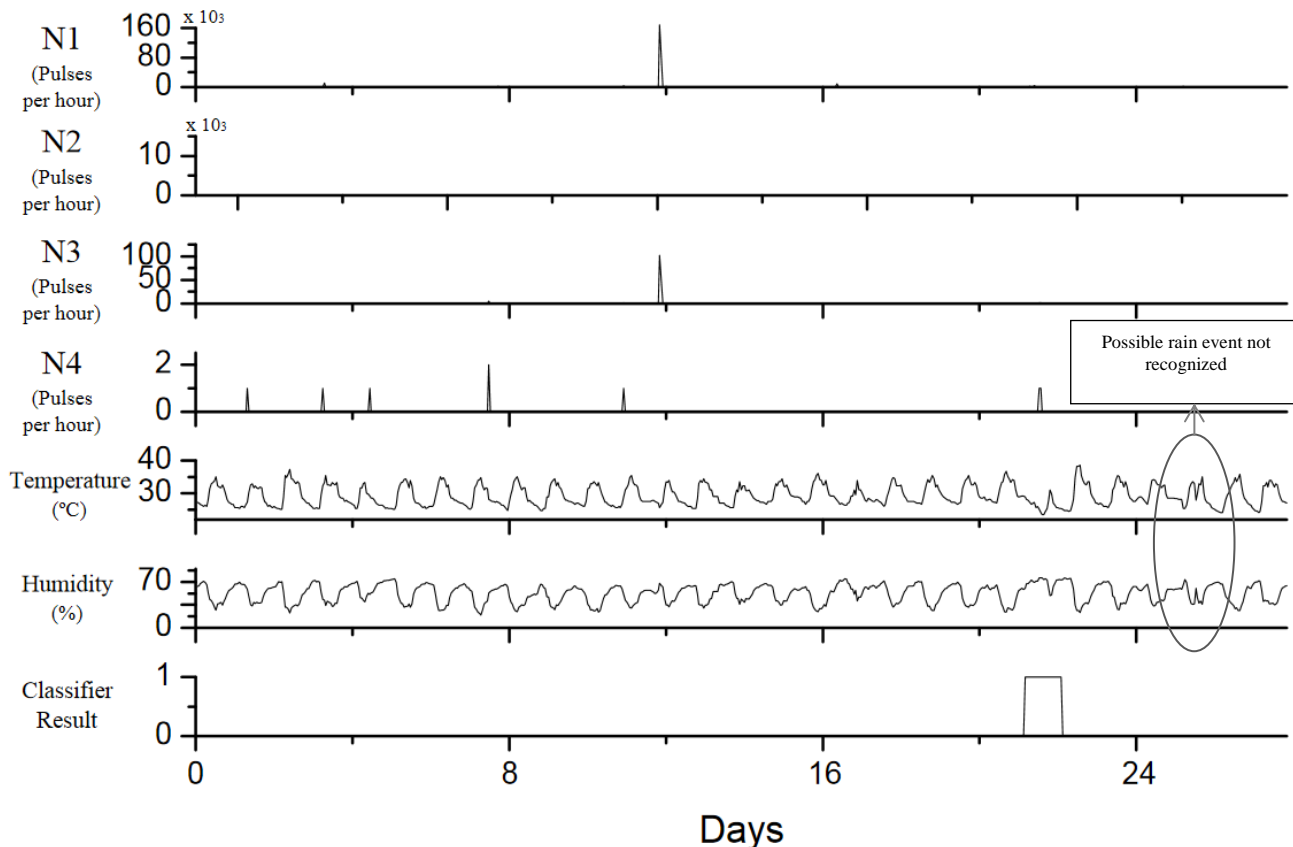


Figure 6. Application of ANN MLP in Mossoró ADECI station.

A clear rain pattern was successfully recognized, but the visual analysis also suggests that some rain events were not successfully recognized. The general visual analysis suggests that the false negative rain rate was higher in Mossoró ADECI station than in São Miguel dos Campos ADECI station. The efficiency decrease observed to Mossoró ADECI station suggests that it decreases with distance, indicating that one single model can not be used to analyze all network nodes.

VII. CONCLUSION AND FUTURE WORK

This work presented an initial attempt to detect rain with relative humidity and temperature obtained from the partial discharges satellite sensor network. Preliminary results show that it is possible to detect rain events and use them to improve the flashover risk classification.

The initial tests were performed on the reliable data from INMET meteorological stations in the Northeast Region of Brazil. Three techniques were applied: Naïve Bayes Classifier, ANN MLP and SVM.

All three techniques presented acceptable results when tested on data from the same base. However, when the three classifiers were trained with data from one station and applied in the others INMET stations, only the ANN MLP presented acceptable results. The main reason for this is the different climates between each station, so the generalization ability of the classifier is an important feature.

The ANN MLP trained with the São Miguel dos Campos INMET station was applied in data sets from ADECI database (obtained from the sensor network). Two ADECI stations were used to evaluate the ANN MLP. The rain pattern was successfully recognized in this database, however some false negatives were visually observed.

The result of this work will improve the maintenance schedule system. Without the rain detection attribute, when a rain event occurs, the initial humidity increase causes a PD activity increase rising the risk of a flashover in the prediction system. With the addition of the rain detection attribute, this effect will not be taken into account and after the rain event, the flashover risk can be reset because the insulator string was washed.

Future works aims to evaluate the threshold of rain precipitation, in millimeters, used to label the day as a rainy day and use larger data sets to evaluate the techniques. Data sets from different locations will also be used in order to test the climate characteristics influence on the proposed approach to rain detection and define the borders where the same model can be applied.

Another improvement on the system is to split the days in mornings and nights because rain events during mornings cause a greater change in the temperature/humidity behavior than on nights.

ACKNOWLEDGMENT

The authors thank CHESF.

REFERENCES

- [1] M. G. Danikas, "The definitions used for partial discharge phenomena," IEEE Transactions on Electrical Insulation, vol. 28, no. 6, pp. 1075-1081, 1993.
- [2] E. O. Abdelaziz, M. Javoronkov, C. Abdeliziz, G. Fethi, and B. Zohra, "Prevention of the interruptions due to the phenomena of the electric insulators pollution," Control, Communiation and Signal Processing, 2004. First International Symposium on, pp. 493-497, 2004.
- [3] R. a de Lima et al., "Remote monitoring of the degree of pollution of high voltage insulator strings via satellite with a sensor system network," 2010 IEEE Sensors, Nov. 2010, pp. 1113-1117.
- [4] E. Thalassinakis and C. G. Karagiannopoulos, "Measurements and interpretations concerning leakage currents on polluted high voltage insulators," Meas. Sci. Technol, vol. 421, pp. 421-426, 2003.
- [5] E. Fontana, S. C. Oliveira, F. J. Cavalcanti, R. B. Lima, J. F. Martins-Filho, and E. Meneses-Pacheco, "Novel Sensor System for Leakage Current Detection on Insulator Strings of Overhead Transmission Lines," vol. 21, no. 4, pp. 2064-2070, 2006.
- [6] H. O. de Lima, S. C. Oliveira, and E. Fontana, "Flashover risk prediction on polluted insulators strings of high voltage transmission lines," 11th International Conference on Intelligent Systems Design and Applications, Nov. 2011. pp. 397-401.
- [7] K. N. Choi, "Omni-directional rain sensor utilizing scattered light reflection by water particle on automotive windshield glass," in 2011 IEEE Sensors Proceedings, 2011, pp. 1728-1731.
- [8] R. Duda, P. Hart, and D. Stork, Pattern Classification. Wiley-Interscience; 2 edition (October 2000), 2000, p. 654.
- [9] S. Haykin, Neural Networks: A Comprehensive Foundation. PTR Upper Saddle River, NJ, USA, Prentice Hall, 1994.
- [10] A. Christmann and I. Steinwart, Support Vector Machines, Springer. New York, NY: Springer New York, 2008.